Measurement and modellingof pharmaceutical bioconcentration in an aquatic invertebrate, Gammarus pulex.

Miller, Thomas Henry

Awarding institution:
King's College London

Measurement and modelling of pharmaceutical bioconcentration in an aquatic invertebrate, *Gammarus pulex*.

Doctoral Thesis in Environmental Toxicology

Author:

Thomas Henry Miller, MSc, BSc(Hons), AMRSC

Supervisors:

Dr Leon P. Barron

Dr Nicolas R. Bury

Dr Stewart F. Owen

Faculty:

Life Sciences and Medicine

King's College London
Academic Year 2016/2017

Dedicated to the memory of my Grandfather Henry Joseph Miller (1921-2011) and my Grandmother Irene Ethel Miller (1920-2015).

Acknowledgements

First and foremost I would like to thank my supervisors Dr Leon Barron, Dr Nicolas Bury and Dr Stewart Owen. The commitment, advice, support and guidance they have all shown throughout my time as a PhD student has been beyond extraordinary. I would also like to thank Dr Rebecca Brown for her guidance during the earlier stages of my research. I thank the BBSRC and AstraZeneca for funding this studentship and providing me with the opportunity to achieve my goal of becoming an independent researcher in a subject I have enjoyed since I was a child. I must also thank one of my dearest friends and soon to be Dr Kelly Munro. She is truly one of a kind and I do not think I would have achieved as much as I have without her support over the past four years. The path I have taken here today has only been possible with the help, support and love of so many that I could not possibly mention all and give them proper credit in this small acknowledgement. However, I would especially like to mention my undergraduate and post-graduate project supervisors Dr Carl Hall, Dr George Zouganelis and Dr Darren Gowers. I would like to thank my parents for their continued support. I will never be able to show how much I have appreciated what they have done for me. I would like to thank my closest friends David Chesterman Taylor, James Boyce and James Going for all the good times that have kept me sane over the past years. I would also like to give a special mention to Jack Curl who had it not been for his motivation and help during my A-level exams, I may not be where I am today. Finally, I would like to thank the rest of my friends and family and I must apologise that I have not named you all, but I am truly thankful for all of you.

“I’ll never forget what this wise man told me

‘The most brutal teacher of all is experience, you'll see

But in return, you learn, my God do you learn’”

Relentless,
James Teyler, Worthwhile,
Excerpt from C.S. Lewis

List of Abbreviations

Acronym	Definition
3Rs	Replacement, reduction and refinement
ABC	ATP-binding cassette transporter
AC	Alternating current
AED	Anti-epileptic drug
AFW	Artificial freshwater
ANN	Artificial neural network
ANOVA	Analysis of variance
API	Active pharmaceutical ingredient
ASE	Accelerated solvent extraction
ASTM	American society for testing and materials
ATP	Adenosine triphosphate
BA	Backwards algorithm
BAF	Bioaccumulation factor
BAP	Best aquaculture practice
BAT	Best available techniques
BCF	Bioconcentration factor
BMF	Biomagnification factor
BOD	Biochemical oxygen demand
BP	Backpropagation
CERI	Chemicals evaluation and research institute
CID	Collision induced dissociation
CPM	Counts per minute
CRM	Charged residue model
CSA	Chemical safety assessment
CSO	Combined sewer overflow
CYP	Cytochrome P450
DC	Direct current
DDT	Dichlorodiphenyltrichloroethane
DEA	deethylatrazine
DEFRA	Department for environment, food and rural affairs
DET	N,N-diethyltryptamine
DIA	deisopropylatrazine
DLI	Direct liquid injection
DOM	Dissolved organic matter
DPM	Disintegration per minute
E2	Estradiol
E3	Estriol
EC_{50}	Concentration to effect 50 % of the population
ECETOC	European centre for ecotoxicology and toxicology of chemicals
ECHA	European chemicals agency
EE2	Ethinylestradiol
EMA	European medicines agency
ENCE	United nations economic commission for Europe
EQSD	Environmental quality standards
ERA	Environmental risk assessment
ESI	Electrospray ionisation

Acronym	Definition
EU	European Union
EUWFD	European Union water framework directive
FA	Forwards algorithm
FRET	Förster resonance energy transfer (FRET)
GA	Genetic algorithm
GC	Gas chromatography
GCD	Conjugate gradient descent
GRNN	Generalised neural network
GSD	Genetic selected descriptor
HE	High energy
HETP	Height equivalent theoretical plate
HLB	Hydrophilic-lipophilic balance
HP	Hydroxypropranolol
HP-GLU	Hydroxypropranolol glucuronide
HPLC	High performance liquid chromatography
HP-SULPH	Hydroxypropranolol sulphate
HRMS	High resolution mass spectrometry
IEM	Ion evaporation model
LC	Liquid chromatography
LC_{50}	Lethal concentration to 50 % of the population
$LC\text{-}MS^n$	Tandem mass spectrometry
LE	Low energy
LLE	Liquid-liquid extraction
LOD	Limit of detection
LOEC	Lowest observed effect concentration
LogD	Logarithm of the octanol-water distribution coefficient
LogP	Logarithm of the octanol-water partition coefficient
LogS	Logarithm of water solubility
LOQ	Limit of quantification
LSC	Liquid scintillation counting
MAE	Microwave assisted extraction
MDR	Multidrug resistance
MeCN	Acetonitrile
MEF	Metabolite enrichment factor
MeOH	Methanol
MLP	Multilayer perceptron
MRM	Multiple reaction monitoring
MS	Mass spectrometry
MXR	Multi-xenobiotic resistance
NSAID	Non-steroidal anti-inflammatory drug
OECD	Organisation for economic cooperation and development
OSPAR	The Convention for the Protection of the Marine Environment of the North-East Atlantic
PAH	Polyaromatic hydrocarbon
PBDE	Polybrominated diphenyl ether
PBT	Persistent, bioaccumulative and toxic

Acronym	Definition
PCB	Polychlorinated biphenyl
PEC	Predicted environmental concentration
PES	Polyethersulfone
pH	Negative logarithm of the hydrogen ion concentration
pK_a	Acid dissociation constant
PLE	Pressurised liquid extraction
PLS	Partial least squares
PMT	Photomultiplier tube
PNEC	Predicted no effect concentration
POCIS	Polar organic chemical integrative sampler
POP	Persistent organic pollutant
PPB	Parts per billion
PPCP	Pharmaceutical and personal care products
PPM	Parts per million
PPT	Part per trillion
PROP	Propranolol
PSD	Passive sampling device
PuLE	Pulverised liquid extraction
QSAR	Quantitative structure activity relationship
QSPR	Quantitative structure property relationship
RBF	Radial basis function
REACH	Registration, evaluation, authorisation and restriction of chemicals
RF	Radiofrequency
RSD	Relative standard deviation
RTD	Retention time descriptor
S/N	Signal-to-noise ratio
SD	Standard deviation
SDS	Safety data sheet
SE	Standard error
SIL-IS	Stable isotope labelled internal standard
SLC	Solute carrier family
SMILES	Simplified molecular input line entry systems
SPE	Solid phase extraction
SPMD	Semi-permeable membrane device
SPME	Solid phase microextraction
SRM	Single reaction monitoring
SRT	Solids retention time
SS	Suspended solids
SSRI	Selective serotonin reuptake inhibitor
SVM	Support vector machines
TEP	Transepithelial potential
TOF	Time-of-flight
TPSA	Topological polar surface area
UPLC	Ultra-performance liquid chromatography
USEPA	United States environmental protection agency
UV	Ultraviolet
WWTP	Wastewater treatment plant

List of Figures

Chapter 1

Chapter 2

Chapter 3

Chapter 4

Chapter 5

Chapter 6

List of Tables

Chapter 1

Chapter 2

Chapter 3

Chapter 4

Chapter 5

Chapter 6

List of Publications

1. Miller, T.H., Bury, N.R., Owen, S.F., & Barron, L.B. (2017). Uptake, biotransformation and elimination of selected pharmaceuticals in a freshwater invertebrate measured using liquid chromatography tandem mass spectrometry. *Chemosphere*, 183, 389-400.
2. Vidaki, A., Ballard, D., Aliferi, A., Miller, T.H., Barron, L.P., & Syndercombe Court, D. (2017). DNA methylation-based forensic age prediction using artificial neural networks and next generation sequencing. *Forensic Science International: Genetics*, 28, 225-236.
3. Miller, T.H., Baz Lomba, J.A., Harman, C., Reid, M.J., Owen, S.F., Bury, N.R., Thomas, K.V. and Barron, L.P. (2016). The first attempt at non-linear *in silico* prediction of sampling rates for polar organic chemical integrative samplers (POCIS). *Environmental Science & Technology,* 50(15), 7973–7981.
4. Gómez-Canela, C., Miller, T. H., Bury, N. R., Tauler, R., & Barron, L. P. (2016). Targeted metabolomics of *Gammarus pulex* following controlled exposures to selected pharmaceuticals in water. *Science of the Total Environment*, 562, 777-788.
5. Miller, T. H., McEneff, G. L., Stott, L. C., Owen, S. F., Bury, N. R., & Barron, L. P. (2016). Assessing the reliability of uptake and elimination kinetics modelling approaches for estimating bioconcentration factors in the freshwater invertebrate, *Gammarus pulex*. *Science of the Total Environment,* 547, 396-404.
6. Bade, R., Bijlsma, L., Miller, T. H., Barron, L. P., Sancho, J. V., & Hernández, F. (2015). Suspect screening of large numbers of emerging contaminants in environmental waters using artificial neural networks for

chromatographic retention time prediction and high resolution mass spectrometry data analysis. *Science of the Total Environment*, 538, 934-941.

7. Schnell, S., Bawa-Allah, K., Otitoloju, A., Hogstrand, C., Miller, T. H., Barron, L. P., & Bury, N. R. (2015). Environmental monitoring of urban streams using a primary fish gill cell culture system (FIGCS). *Ecotoxicology and Environmental Safety*, 120, 279-285.
8. Munro, K., Miller, T. H., Martins, C. P., Edge, A. M., Cowan, D. A., & Barron, L. P. (2015). Artificial neural network modelling of pharmaceutical residue retention times in wastewater extracts using gradient liquid chromatography-high resolution mass spectrometry data. *Journal of Chromatography A*, 1396, 34-44.
9. Miller, T. H., McEneff, G. L., Brown, R. J., Owen, S. F., Bury, N. R., & Barron, L. P. (2015). Pharmaceuticals in the freshwater invertebrate, *Gammarus pulex*, determined using pulverised liquid extraction, solid phase extraction and liquid chromatography–tandem mass spectrometry. *Science of the Total Environment*, 511, 153-160.
10. Miller, T. H., Musenga, A., Cowan, D. A., & Barron, L. P. (2013). Prediction of chromatographic retention time in high-resolution anti-doping screening data using artificial neural networks. *Analytical Chemistry*, 85(21), 10330-10337.

List of Conference Presentations

1. Miller, T.H., Gallidabino, M., Bury, N.R., Owen, S.F., & Barron, L.B. (2017). Investigating the application of artificial neural networks to predict the bioconcentration of xenobiotics in fish and invertebrates. **Platform**. 2017 SETAC Europe 27th Annual Meeting (Brussels).
2. Miller, T. H., McEneff, G. L., Brown, R. J., Owen, S. F., Bury, N. R., & Barron, L. P. (2016). Bioconcentration and biotransformation of selected pharmaceuticals in the freshwater amphipod, *Gammarus pulex*. **Platform**. 2016 SETAC Europe 26th Annual Meeting (Nantes).
3. Miller, T.H., Baz Lomba, J.A., Harman, C., Reid, M.J., Owen, S.F., Bury, N.R., Thomas, K.V. and Barron, L.P. (2016). *In silico* prediction of sampling rates for polar organic chemical integrative samplers (POCIS) **Platform**. 2016 SETAC Europe 26th Annual Meeting (Nantes).
4. Miller, T. H., McEneff, G. L., Brown, R. J., Owen, S. F., Bury, N. R., & Barron, L. P. (2015). Determination of pharmaceutical residues in the freshwater invertebrate, *Gammarus pulex*, using agitated solvent extraction, solid phase extraction and liquid chromatography tandem mass spectrometry. **Platform**. SETAC Europe 25th Annual Meeting (Barcelona).
5. Miller, T. H., McEneff, G. L., Brown, R. J., Owen, S. F., Bury, N. R., & Barron, L. P. (2015). The uptake and elimination of selected pharmaceuticals in the aquatic invertebrate, *Gammarus pulex*. **Poster**. SETAC 25th Annual Meeting (Barcelona).
6. Miller, T. H., McEneff, G. L., Brown, R. J., Owen, S. F., Bury, N. R., & Barron, L. P. (2014). Determination of pharmaceutical residues in the fresh water invertebrate, *Gammarus pulex*, using agitated solvent extraction,

solid phase extraction and liquid chromatography tandem mass spectrometry. **Platform**. RSC Analytical Research Forum (London).

7. Miller, T. H., McEneff, G. L., Brown, R. J., Owen, S. F., Bury, N. R., & Barron, L. P. (2014). Determination of pharmaceutical residues in the fresh water invertebrate, *Gammarus pulex*, using agitated solvent extraction, solid phase extraction and liquid chromatography tandem mass spectrometry. **Poster**. SETAC Europe 24th Annual Meeting (Basel).
8. Miller, T. H., Musenga, A., Cowan, D. A., & Barron, L. P. (2013). Post-analysis prediction of drug retention time in gradient liquid chromatography-high resolution mass spectrometry data using artificial neural networks. **Poster**. EMCDDA Testing the Waters: first international multidisciplinary conference on detecting illicit drugs in wastewater (Lisbon).

Contents

Abstract

The aim of this work was to understand the bioconcentration potential of pharmaceuticals in a freshwater invertebrate. The novelty of this work lies in several parts of which the most important was that a computational model was developed to successfully predict bioconcentration in invertebrates, which has not been achieved previously. For the first time, a developed analytical method using liquid chromatography tandem mass spectrometry (LC-MS/MS) was used to determine the occurrence of pharmaceuticals in *Gammarus pulex* across several tributaries of the River Thames (London, UK). The occurrence reached low level ng g^{-1} concentrations and indicated that further experiments were needed to determine the accumulation potential.

Toxicokinetic exposures were performed to characterise the bioconcentration potential of 16 pharmaceuticals. The determined bioconcentration factors (BCFs) remained below regulatory thresholds indicative of bioaccumulation, which contrasted field-derived bioaccumulation factors that would have triggered regulatory guidelines. However, the standardised models employed for kinetic BCF estimation were evaluated and it was found that model assumptions concerning the uptake rate constant were not reliable, leading to extremely important implications for regulatory bodies. In addition, the developed LC-MS/MS method determined phase I and phase II metabolites in *G. pulex,* indicating that these organisms are capable of extensive biotransformation of pharmaceuticals.

To further understand uptake mechanisms such as passive diffusion, a modelling approach using artificial neural networks were developed to characterise the uptake of pharmaceuticals onto passive sampling devices. No previous investigations have aimed to predict uptake onto polar organic chemical

integrative sampler devices and this work represented the first of its kind. The passive sampling models demonstrated good predictive accuracy at a fraction of the cost and time required by experimental measurements. Furthermore, the modelling gave mechanistic insight into molecular descriptors that were related to uptake onto passive samplers. The modelling approach was extended to predict bioconcentration of pharmaceuticals in fish and *G. pulex* using data from the literature and data determined from the toxicokinetic experiments presented here. Interestingly, the fish-based model could not be used to predict the invertebrate data. This indicated that either the class of compounds (pharmaceuticals) or the fish-to-invertebrate bioconcentration data could not be cross predicted. Thus, a standalone model was developed for the invertebrates and showed good predictive accuracy for this species. Overall, the work presented herein has achieved novel impact to address the lack of knowledge concerning bioconcentration in invertebrates.

Keywords: pharmaceuticals, occurrence, bioconcentration, ANN, toxicokinetic

Chapter 1 Review of literature concerning pharmaceuticals in the aquatic environment.

1.1 Overview of xenobiotics in the environment

Continued anthropogenic activities that introduce millions of tonnes of chemicals into the environment are a growing cause for concern [1]. Research into the field of ecotoxicology has become a priority among various scientific and governmental bodies, in which their main efforts have been to investigate the occurrence and fate of xenobiotics from a variety of sources including industry, hospital/veterinary waste, domestic waste, agricultural and livestock farms thus far. The potential risk of these chemicals is characterised by hazard criteria which can be used to classify priority pollutants, such as persistence, bioaccumulation and toxicity (PBT). Compounds may persist in the environment for days to years before they are degraded and they have the ability to accumulate in an organism even across trophic levels. Therefore, they may have an associated toxicity to exposed biota. The aquatic environment is exposed via several sources including the continual contribution of contaminants from waste water effluents as well as the input from the terrestrial environment where contaminants are cycled into aquatic environments (i.e. surface run-off). Therefore, these contaminants can be termed ‘pseudo-persistent’ due to their continual input which leads to chronic exposures of biota over their entire life cycle which may have further implications for toxicity and transfer between trophic levels [2].

Contaminants are subject to a complex pathway of interactions when exposed in the environment, which will be discussed in later sections. This creates difficulty in fully understanding the resultant risk to the environment. This highlights the importance of research into their fate and occurrence, but also the acute and chronic toxicity as single compounds and mixtures. The strategies to

deal with pollutants in environmental matrices can be broadly characterised into environmental risk assessment and environmental risk management, which allow the mapping of fate and effects with monitoring and control for those compounds deemed the most hazardous. This topic has not only gained attention from researchers but also from governmental agencies that have published legislation and guidelines for controlling the mass of pollutants that are introduced into the environment. Among the numerous classes of compounds that exist today there is one particular set that have been termed pharmaceutically active compounds (PhAC) which can be defined as compounds which are used for health or cosmetic purposes and are not limited to human application [2]. These compounds have been described as emerging contaminants and thus research efforts are required to understand the potential environmental risks posed by this class of compounds.

1.2 Sources of PhACs in the environment

As mentioned above there are many routes that can lead to the entry of PPCPs into the environment. The largest identified route of contamination is currently via consumption and excretion or topical use of PhACs by the general population. Figure 1.1 summarises the various routes of entry of PhACs into the environment, adapted from [3].

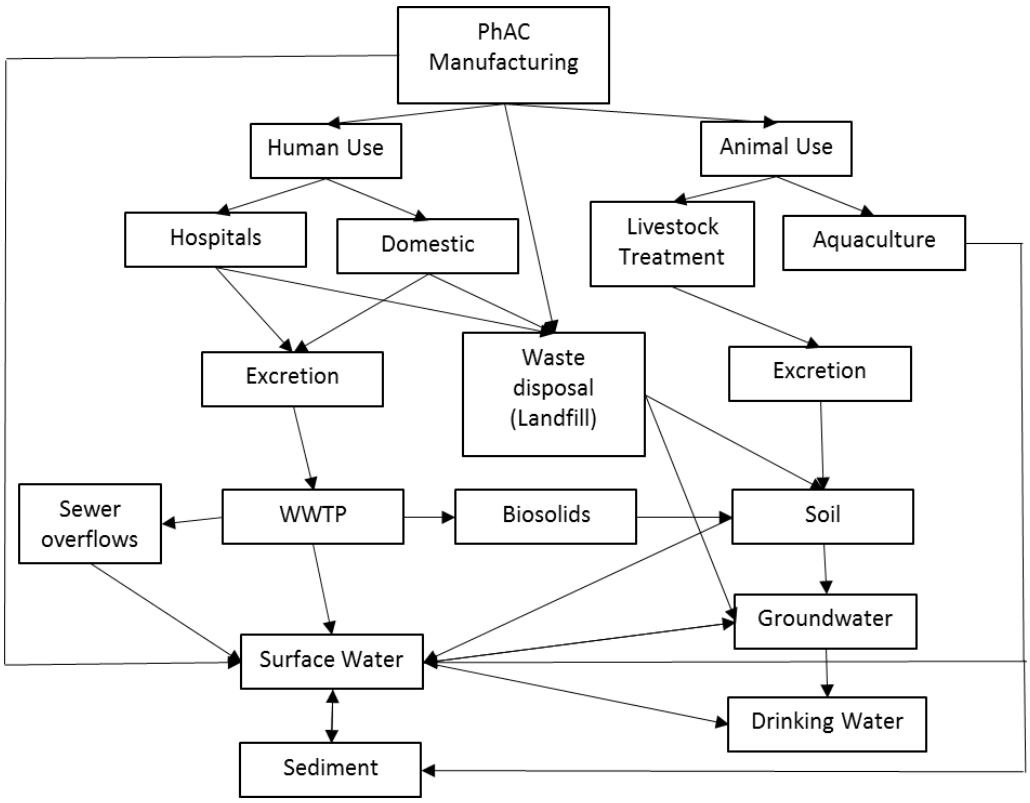

Figure 1.1: Schematic overview of the major routes of PhACs into terrestrial and aquatic environments. Figure adapted from [3]

1.2.1 PhAC manufacturers

Industry waste could be considered a source contributing to contamination but due to various legislation and guidelines from environmental protection agencies as well as the good management practice, it is considered to have a relative minor contribution [4]. This may be true for Europe and North America but recent studies in Asian regions have revealed that production plants in India had effluents containing up to 31 mg L^{-1} of ciprofloxacin, a synthetic fluoroquinolone antibiotic [5]. This is a cause for concern as many PhACs are found at much lower concentrations, often in the ng L^{-1} range. It should also be noted that compounds in the mg L^{-1} range are often used in acute toxicity assays to determine lethal concentrations to 50% of the population (LC_{50}). A production plant from China that manufactured contraceptives was found to contain up to 51 ng L^{-1} of ethinylestradiol (EE2) in effluents which is high enough to cause

detrimental effects to aquatic organisms [6, 7]. The reason for such high concentrations could be due to lower enforcement of legislation and regulations when compared with more developed countries. For example, it was reported that a local authority, in the Indian region referred to above, identified 40 dumping sites of industrial waste [8].

1.2.2 Hospitals

The use of antibiotics among other pharmaceuticals at hospitals could be a significant point source of PhAC contamination in the environment. Wastewater effluents from hospitals often have no preliminary treatment and is directly fed into municipal sewerage systems, which may lead to a high input of antibiotics. A study of five hospitals in New Mexico revealed untreated effluents contained six antibiotics ranging from 0.3 – 35 μg L^{-1}, this value is generally the range that other classes of antibiotics are found within hospital effluents from different countries [8-11]. It is not only antibiotics that are input from hospitals, many different classes of PhACs such as cytostatics, anti-epileptic drugs (AEDs), analgesics, beta-blockers, lipid regulators and barbiturates have been quantified in hospital wastewater effluents, ranging from ng - μg L^{-1} [12, 13].

1.2.3 Veterinary practices & agriculture

Veterinary practices lead to antibiotics and other pharmaceuticals excreted from animals which are can be leached into soilaffecting terrestrial environments and also lead to the contamination of groundwater sources or alternatively may be washed into surface waters via surface run-off affecting aquatic environments [14]. Manure and bio-solid sludge are often used in agriculture to fertilise fields for crop growth, these solids may be contaminated with PhACs and thus can enter aquatic and terrestrial environments as mentioned

above [15]. These compounds can often reach up to mg kg^{-1} concentrations [16, 17]. Prophylactic antibiotics are commonly used in animal husbandry to prevent disease due to often poor housing conditions, they are given to both healthy and unhealthy animals,thus accounting for another source of PPCP contamination in the environment. In addition to terrestrial agriculture that is a source of contamination, aquatic farming (aquaculture) use antibiotics which leads to the direct emission of PPCPs into surface waters and sediments, which can also lead to ground water contamination [18].

1.2.4 Unused Medication

PhACs may be produced in quantities that reach several thousand tonnes per annum, which are distributed to hospitals, pharmacies and veterinary practices. Often these compounds that are prescribed or bought over the counter will be taken by an individual at home, and is the reason that domestic use of PhACs account for the largest contributor of environmental contamination. The disposal of expired or unused PhACs also contributes to the contamination of the environment; a survey in the United States (US) reported that 35.4% of people flushed medication down the toilet/sink [19]. A more recent survey in the United Kingdom (UK) reported only 11.5% are disposed of down the toilet/sink [20], this could be due to better awareness of disposal methods but as the sample sizes were small in the surveys (n = <500) it may not represent true disposal patterns. Whilst, PhACs may not necessarily be flushed down the drain in the majority of cases, other responses showed that the main route of disposal is the bin. This does not avert the problem as waste will most likely be transported to landfill sites where they can enter the environment directly through either leaching or surface run-off.

1.2.5 Combined sewer overflows (CSOs)

During periods of heavy precipitation the capacity of sewers can often be exceeded, to alleviate this overload many sewerage systems have CSOs. These systems therefore allow the overflow of rainwater and municipal wastewaters leading to direct emission into surface waters without any treatment. Thus, leading to potentially a great source of contamination in aquatic environments. It is considerably difficult to quantify the input of CSO related PPCPs, but a recent study correlated that increased rainfall lead to an increased input of caffeine into a lake in Switzerland [21]. Caffeine was suitable as a CSO marker due to the high removal efficiency of the compound from sewage at wastewater treatment plants, which allowed accurate determination of caffeine input from CSOs [21].

1.2.6 Wastewater treatment plants (WWTPs)

The implication that a pharmaceutical that is used may end up in sewage, provides a significant route of entry for PhACs into the environment. Urban areas will generally not discharge wastewater directly to the environment, and most are subject to sewage treatment at WWTPs. These plants will receive influent from the area they service known as a catchment area. The incoming water may be contaminated with PPCP residues which will undergo treatment before they are input into surface waters. However, the efficiency treatment process is variable for different compounds iand complete removal is not often achieved for many PhACs.

1.3 WWTP Removal efficiency

Removal of contaminants is often incomplete by WWTPs and the efficiency of the removal process is dependent on several factors, the first of which is the type of treatment stages used. Primary treatment involves the removal of suspended solids by sedimentation/flocculation units but does not remove dissolved solids. Secondary treatment can involve a biological process which is dependent on the use of microbial populations to remove organic matter. These biological treatments can be separated into eitherof suspended growth processes (activated sludge/oxidation ditches) or attached growth processes (trickling filters/biotowers). Tertiary treatments can involve ozonation, membrane filtration or the addition of ferric/aluminium salts [22]. Outcomes of tertiary treatment depend on the type of treatment in place; suspended solids are removed from the activated sludge stage (membrane filtration, ferric/aluminium salts), remaining PhACs from the secondary treatment are oxidised (ozonation) or further biological treatment is used for nutrient removal (ammonia and phosphorus). After the secondary treatment and if there is no tertiary treatment the effluent may undergo a disinfection stage to reduce microbial populations by chlorination or ultraviolet (UV) radiation before discharge into surface waters [23].

There are many factors that influence the removal of PPCPs such as the type treatment stages a WWTP uses, biochemical oxygen demand (BOD), total suspended solids (SS), solids retention time (SRT), pH, temperature and the type of compounds present in the influent. Due to the variety of classes that encompass PhACs there is a great range in physicochemical properties exhibited. Properties such as hydrophobicity that are quantified via the partition coefficient (log*P)* and distribution coefficient (log*D)* influence the sorption mechanisms. As mentioned in the previous section, the primary and secondary

WWTP stages will have suspended solids present that may sorb PPCPs via hydrophobic interactions, this sorption will effectively remove certain PPCPs from the aqueous phase of the influent. However, sorption to suspended solids can result from more than a single type of interaction and can be the result of a mixture of interactions such as ionic exchange, cation bridging, complexation, Van der Waals and hydrophilic interaction [24].

Another important consideration of influent in WWTPs is the dissolved organic matter (DOM) which is primarily acidic in nature but will vary from plant to plant [25]. It may be expected that hydrophobic compounds would sorb to the sludge and be removed during primary/secondary treatment but DOM provides an alternate pathway for hydrophobic compounds to remain in the aqueous phase, thus lowering their removal efficiency and allowing for input to aquatic environments [26]. The microbial populations in the activated sludge treatment may remove PPCPs by biodegradation of the compound, one study showed that biodegradation of PPCPs can account for up to 80% removal from WWTP influents [27]. However, studies often measure only the reduction of the parent compound which does not necessarily indicate that the compound has undergone biodegradation, it may be present as a metabolite or biotransformed product which is not often determined.

SRT is a very important variable during wastewater treatment, it is defined as the length of time in days that the activated sludge is in contact with the wastewater. A high SRT means that microbial populations will be well established and consist of range of microorganisms which may allow for a higher removal efficiency. Generally, a higher removal efficiency has been observed with SRTs of at least 10 days (approximately 95% or above), but is not always true for some

pharmaceuticals such as diclofenac and carbamazepine which have demonstrated low removal [28].

1.4 Occurrence of PhACs in the aquatic environment

The occurrence of PhACs in the environment and their concentrations within organisms depend on a broad range of factors such as temperature, pH, season, removal efficiency at WWTPs, usage patterns, physicochemical properties of the compounds and the physiological characteristics of organisms (discussed in later sections). As mentioned above, removal efficiency is a predominant factor that will affect occurrence of contaminants in surface waters. Therefore, a high removal efficiency is often desirable but a high rate of removal may not be sufficient to reduce the input of contaminants into the environment.

This has been observed, with the non-steroidal anti-inflammatory drugs (NSAIDs) that are often detected at high concentrations relative to other PhACs in influent. This class of pharmaceuticals are usually over-the-counter and can be sold in amounts reaching up to 1,000 tonnes per annum [29]. Removal is often >90%, but they are still released at relatively high concentrations from WWTPs due to the daily loads in wastewater resulting from high usage rates. Usage patterns are important as they can explain trends for occurrence of PhACs, such as seasonal trends associated with macrolide antibiotic use [30]. One study showed that the daily usage of macrolides, sulphonamides and trimethoprim was correlated with daily variations from composite samples within a WWTP [31]. Furthermore, removal does not indicate that the compound has been mineralised. The compound may exist as a biotransformed product, which are often not determined during environmental monitoring campaigns.

1.4.1 Occurrence in surface waters

The occurrence is surface waters will be predominantly a result of the input through wastewater. However, abiotic and biotic degradation will also influence the concentration of contaminants in surface waters. In addition to degradative processes, the removal of contaminants in the water phase due to their sorption to sediments will also have a role in the concentrations of contaminants that are quantified. Monitoring of surface waters will often involve composite sampling where a set volume of water is collected over a specified time period or point sampling where samples are taken at a single point in time. Whilst composite sampling mitigates the limitation of temporal fluctuations in contaminant concentrations both sampling techniques are still limited by this and thus may not accurately reflect surface water concentrations [32]. Furthermore, these techniques are also limited as they require high-volume sampling frequency. An alternative sampling technique is the use of passive sampler devices (PSDs). These samplers contain a sorbent material which acts as a ‘sink’ for the accumulation of contaminants in surface waters [32]. PSDs enable the integration of temporal fluctuations of contaminant concentrations. Thus, they can be used to assess temporal and spatial trends with a low sampling frequency [33].

Table 1.1: Example of occurrence data for pharmaceuticals determined in surface waters.

		Mean Concentration (µg L^{-1})			Mean	Maximum Concentration (µg L^{-1})		
Compound	Class	Influent	Effluent	Surface Water	Removal (%)	Influent	Effluent	Surface Water
Diclofenac	NSAID	1.854	1.028	0.185	45	181.000	24.256	18.740
Carbamazepine	TCA	0.637	0.498	0.409	22	2.600	67.715	11.561
Ibuprofen	NSAID	12.005	1.363	0.240	89	373.110	95.000	303.000
Sulfamethoxazole	Sulfonamide	2.333	0.238	0.120	90	309.000	24.800	29.000
Naproxen	NSAID	3.380	0.514	0.119	85	551.960	39.300	12.300
Estrone	Estrogens	0.219	0.073	0.039	67	129.000	32.980	5.000
Estradiol	Estrogen	0.359	0.019	0.005	95	3.000	0.082	0.012
Ethinylestradiol	Estrogen	0.032	0.027	0.143	16	140.000	5.040	5.900
Estriol	Estrogen	0.226	0.226	0.010	0	110.700	83.430	0.480
Trimethoprim	Antibiotic	0.768	0.879	0.071	-	162.000	95.100	13.600
Paracetamol	NSAID	35.902	3.492	0.331	90	1200.000	280.000	37.000
Clofibric acid	Lipid regulator	0.568	0.049	0.068	91	61.000	3.290	7.910
Ciprofloxacin	Quinolone	1.784	185.855	20.509	-	160.000	31000.000	2500.000
Ofloxacin	Quinolone	0.201	0.406	0.208	-	20.200	160.000	10.000
Norfloxacin	Quinolone	0.458	7.487	0.061	-	16.500	420.000	4.700
Aspirin	NSAID	88.385	8.863	1.773	90	1731.000	193.000	20.960

Table adapted from [34]

Example occurrence data of PPCPs around the world is presented in Table 1.1, these 16 compounds are the only PhACs that have been detected in all 5 UN regions [34-41]. Depending on the location, surface concentrations of PPCPs ranged from up to 2500 μg L^{-1} for the antibioitc ciprofloxacin. It might be expected that over-the-counter pharmaceuticals, like the non-steroidal anti-inflammatory drugs (NSAIDs), reach higher concentrations in surface water due to their high usage consumptions [29]. However, the quantification of these pharmaceuticals can also be influenced by the proximity to WWTPs. Other antibiotics such as amoxicillin has been detected at relatively high concentrations reaching up to 622 ng L^{-1} in the River Taff, U.K. The authors of this study, noted that the high concentration of amoxicillin was due to the close proximity of a WWTP. Further downstream the concentration had decreased below the limit of detection (LOD) [35]. Similarly, from Table 1.1 effluent concentrations of PhACs are usually much higher than surface water concentrations. Thus, suggesting that high risk areas for adverse effects could be areas that surround WWTP outfalls [23].

The reduction in concentration downstream is likely to be a result of dilution, sorption, biodegradation, photodegradation and bioaccumulation [42, 43]. Photodegradation can be direct or indirect where half-lives can vary depending on the presence of other substances such as humic acids, nitrate and Fe(III) [44]. In addition, ionic speciation of the compound can increase photodegradation, where deprotonation can increase electron densities favouring electrophilic attack by reactive oxygen species [44, 45]. Biodegradation is also variable and is a result of the degradation by microbial populations in the WWTP and surface waters. A major limitation of monitoring occurrence is that methods do not often target transformation products. Therefore, the reduction of the

precursor compound may not indicate removal and these transformation products might potentially be more toxic [46]. As mentioned previously, compounds can also vary in line with seasonal trends thus the sampling times of monitoring studies may also influence reported concentrations. Interestingly, diclofenac was reported to reach high concentrations (700 - 4400 ng L^{-1}) in Pakistan. This region has had severe ongoing socioeconomic consequences due to the collapse of several vulture species through the use of diclofenac by livestock farmers [47]. This may suggest that surface run-off and leaching is leading to high input into surface waters, among other potential sources. Furthermore, the compound diclofenac has also been observed to have low removal rates in WWTPs, often <40 % [48]. As summarised, the occurrence of PhACs in surface waters is a mixture of complex interactions that requires the determination by monitoring campaigns to assess the potential risk posed by these emerging contaminants.

1.4.2 Occurrence in aquatic biota

Currently, the occurrence of PhACs in biota is under reported with most focus on the occurrence in fish in contrast to invertebrates. To the authors' knowledge, a total of 43 publications have reported PhAC (with the exception of endocrine disruptors) occurrence data in aquatic biota. This is of critical importance as surface water concentrations may not translate well into biota concentrations due to the number of interactions in the environment (temporal fluctuations, bioavailability, physiological characteristics etc.).

Table 1.2: Occurrence data of pharmaceuticals determined in fish and invertebrates. Concentration for solid samples is ng g^{-1} and for liquid samples is ng mL^{-1}.

Compound	Concentration	Sample Type	Organism	Location	
diclofenac	6.0-95.0	Bile	Bream	Finland	[49]
	44.0-148.0	Bile	Roach	Finland	[49]
	2.2-20.0	Plasma	Trout	Sweden	[52]
	<LOD-16.1	Whole-body	Mussel	Italy	[60]
	<LOD-12.4	Whole-body	Invert	Spain	[50]
	4.1-8.8	Homogenate	Fish	Spain	[51]
naproxen	6.0-32.0	Bile	Bream	Finland	[49]
	11.0-103.0	Bile	Roach	Finland	[49]
	33.0-46.0	Plasma	Trout	Sweden	[52]
ibuprofen	16.0-34.0	Bile	Bream	Finland	[49]
	15.0-26.0	Bile	Roach	Finland	[49]
	5.5-102.0	Plasma	Trout	Sweden	[52]
	<LOD-9.4	Whole-body	Mussel	Italy	[60]
	<LOD-183.0	Whole-body	Invert	Spain	[50]
carbamazepine	0.3-1.0	Plasma	Trout	Sweden	[52]
	1.3-5.3	Whole-body	Mussel	USA	[53, 56]
	17.9	Liver	Fish	Spain	[51]
cilazapril	<LOQ-0.7	Plasma	Trout	Sweden	[52]
diltiazem	<LOQ-0.9	Plasma	Trout	Sweden	[52]
	<LOD-0.1	Whole-body	Mussel	USA	[53, 56]
haloperdiol	<LOQ-1.2	Plasma	Trout	Sweden	[52]
ketoprofen	15.0-107	Plasma	Trout	Sweden	[52]
levonorgesterol	<LOQ-12.0	Plasma	Trout	Sweden	[52]
meclozine	<LOQ-0.7	Plasma	Trout	Sweden	[52]
memantine	<LOQ-2.3	Plasma	Trout	Sweden	[52]
oxazepam	0.4-0.7	Plasma	Trout	Sweden	[52]
risperidone	0.4-2.4	Plasma	Trout	Sweden	[52]
sertraline	<LOQ-1.2	Plasma	Trout	Sweden	[52]
	<LOD-5.5	Whole-body	Mussel	USA	[53, 56]
	<LOQ-4.2	Brain	Fish	USA	[58]
tramadol	1.1-1.9	Plasma	Trout	Sweden	[52]
verpamil	<LOQ-0.7	Plasma	Trout	Sweden	[52]
trimethoprim	<LOQ-9.2	Whole-body	Mussel	Ireland	[54]
fluoxetine	<LOQ-79.1	Whole-body	Mussel	USA	[55]
	<LOQ-1.6	Brain	Fish	USA	[58]
norfluoxtine	<LOQ-3.6	Brain	Fish	USA	[58]
sulfamethazine	<LOD-430.0	Whole-body	Mussel	USA	[53, 56]
caffeine	<LOD-140.0	Whole-body	Mussel	USA	[53, 56]
diphenhydraine	<LOD-11.0	Whole-body	Mussel	USA	[53, 56]
	0.04-0.07	Muscle	Bream	Germany	[57]
methylprednisolon	<LOD-210.0	Whole-body	Mussel	USA	[53, 56]
amitriptyline	<LOD-6.2	Whole-body	Mussel	USA	[53, 56]
enrofloxacin	<LOD-12.0	Whole-body	Mussel	USA	[53, 56]
atenolol	<LOD-13.0	Whole-body	Mussel	USA	[53, 56]
norsertraline	1.7-3.3	Muscle	Bream	Germany	[57]
	0.2-6.1	Brain	Fish	USA	[58]
diazepam	23.0-110.0	Liver	Flatfish	USA	[59]
nimesulide	3.0-6.0	Whole-body	Mussel	Italy	[60]
citalopram	0.8	Homogenate	Fish	Spain	[51]
venlafaxine	0.6	Homogenate	Fish	Spain	[51]
carazolol	3.8	Homogenate	Fish	Spain	[51]
propranolol	4.2	Homogenate	Fish	Spain	[51]
salbutamol	2.6	Homogenate	Fish	Spain	[51]

Example data on occurrence in both fish and invertebrates is presented in Table 1.2 [49-60]. The concentration of PPCPs ranged from <LOD-430 ng g^{-1} (sulfamethazine) for tissue analysis and <LOQ-148 ng mL^{-1} (diclofenac) for plasma/bile measurements. A majority of the PPCPs were detected below three figure concentrations (0-100 ng mL^{-1} or ng g^{-1}) with higher concentrations generally occurring with high consumption compounds such as ibuprofen (183 ng g^{-1}), diclofenac (148 ng mL^{-1}) and caffeine (140 ng g^{-1}). Factors that affect the occurrence of PPCPs in biota are further discussed in Section 1.6 that details uptake and elimination processes in bioaccumulation.

As pharmaceuticals undergo significant metabolism, it is possible that biotransformed products might be present at higher concentrations. This is a key consideration as transformation products might be more toxic than precursors, such as prodrugs where the metabolite is the biologically active compound. As mentioned previously with surface water measurements, current analytical methods often do not target biotransformation products. This can be explained in part by the lower availability of reference standards for confirmation and quantification of these types of compounds. Furthermore, the complexity of biological matrices to determine both precursor and biotransformed compounds is very analytically challenging [61]. Thus, this is likely to account for the low number of studies focussed on PPCP occurrence in biota. As the occurrence of PPCPs is understudied it is essential that methods are developed to analyse these compounds in biota. Furthermore, future studies are needed to address the uptake, metabolism and elimination of pharmaceuticals in biota to ensure that risk assessment is reliably determined.

1.5 Instrumental techniques for analysis of environmental samples

The determination of trace PPCP residues in complex media, such as sewage influent or a biological matrix requires instrumental techniques and methodologies that are accurate, selective, sensitive and precise. Occurrence, especially for PPCPs, is most commonly determined by liquid chromatography coupled to mass spectrometry (LC-MS) which enables the determination of compounds at trace levels (ng - µg) without required chemical derivitisation. Other techniques used to measure occurrence can also involve gas chromatography coupled to MS. However, this type of technique is usually used with more volatile hydrophobic organic contaminants such as phthalates [62]. Polar compounds such as pharmaceuticals will usually require derivitisation before they can be analysed by GC-MS [63]. Therefore, LC-MS is the technique of choice for more polar compounds.

As the complexity of environmental samples can hinder the performance of these techniques, a sample preparation methodology can be used to pre-concentrate the analytes and clean-up interfering matrix components. Sample preparation methods can involve techniques such as protein precipitation, solid-phase extraction (SPE) and liquid-liquid extraction (LLE). In addition to occurrence studies, these methods and techniques can also be used to study the bioaccumulation and effects of environmental contaminants. Furthermore, bioaccumulation studies can also involve the use of liquid scintillation counting (LSC) to measure activity of radiolabelled compounds to determine the bioaccumulation potential of a contaminant.

1.5.1 Liquid scintillation counting (LSC)

Liquid scintillation counting is a technique that is used to detect the radioactivity of a sample and can be used to quantify the amount of radionuclide for alpha and beta particle emitters. Typically, a sample that contains radionuclides is dissolved in a solution known as a liquid scintillation cocktail. This cocktail contains a scintillator (fluor) and solvent. The fluor will exhibit scintillation (re-emission of energy as photons) when it is excited which will then be detected by a photomultiplier tube and counted as disintegrations per minute (DPM) [64]. In a sample, a radionuclide will typically decay through the emission of either beta or alpha particles due to nuclear instability. These particles will transfer energy to the solvent molecules through excitation of the π-cloud in aromatic solvent molecules leading to singlet states. The solvent molecules serve to transfer this energy to the fluor, which once excited will emit the absorbed energy through the emission of photons. The solvent molecules have a low quantum efficiency resulting in a low probability to release energy as photons. Therefore, they are efficient at transferring energy to other solvent molecules and eventually the fluor. The transfer between solvent molecules has two proposed mechanisms. First the energy is transferred by a non-radiative process such as seen with Forster resonance energy transfer (FRET) [65]. The second is that solvent molecules form an excimer and then dissociate so that the previously unexcited molecule becomes excited [66, 67]. The flour will trap the energy transfer so that solute-solvent excitation does not occur. In most cases an additional fluor is used which re-emits photons at a different wavelength enabling detection by the PMT.

1.5.2 High performance liquid chromatography (HPLC)

Chromatography, a technique for analysis has existed since the beginning of the 20th century [68]. In chromatography, two important components referred to as the mobile phase and stationary phase are used to separate a mixture of compounds. The mobile phase can either be a liquid or gas. The stationary phase, depending of the physicochemical properties of the compound, will hinder the movement of the analyte in the mobile phase. It was not until the 1960s that HPLC was developed; revolutionising the field of separation science [69]. This technique, as the name suggests, involves the use of a high pressure to pump mobile phase (liquid) through a column containing the stationary phase leading to greater efficiency and hence improved separations. The efficiency seen in chromatographic separation can be represented by theoretical plates. These plates can also be described by the van Deemter equation [70] which relates column efficiency to flow rate and mass transfer kinetics (Equation 1.1).

$$H = A + \frac{B}{\mu} + C.\mu \qquad (1.1)$$

Where, A is eddy diffusion, B is longitudinal diffusion, C is the resistance to mass transfer and μ is the flow rate. The resistance to mass transfer is the reciprocal of mass transfer coefficient, thus larger mass transfer coefficients will lead to smaller C terms and improve efficiency. The A term in the equation describes the eddy diffusion, also referred to as the multiple flow path, which arises from the particles that are used in the stationary phase. This process is independent of flow rate and is proportional to particle size and packing factor

The longitudinal diffusion term describes the molecular diffusion at the front and the end of the eluting band of molecules, as the molecules become more dispersed the efficiency is lowered which also leads to band broadening.

This term is inversely proportional to the mean flow rate, therefore by increasing the flow rate the effect of molecular diffusion is reduced [71]. Expansion of the van Deemter equation into its explicit form is given in Equation 1.2 [72].

$$H = 2\lambda D_p + \frac{2\gamma D_m}{\mu} + \frac{f_1(k')D_p{}^2}{D_m} + \frac{f_1(k')D_f{}^2}{D_s} \cdot \mu \qquad (1.2)$$

Where, $f_1(k')$ is a constant, D_m is the diffusion coefficient in the mobile phase, D_s is the diffusion coefficient in the stationary phase, D_f is the film thickness, γ is an obstruction factor, λ is a packing factor and D_p is the particle size. The expanded resistance to mass transfer term is separated into the mass transfer concerning the stationary and mobile phase. As expected larger diffusion coefficients will lead to a smaller C term, thus improving efficiency. Larger particle diameters will increase the C term leading to decreased efficiency. The decreased efficiency is a result of stagnant mobile phase in the pores of the particle where large particle sizes will result in increased diffusion distance. The same explanation can also be attributed to film thickness of the stationary phase.

1.5.3 Mass spectrometry (MS)

Mass spectrometry is a technique that measures the mass-to-charge ratio (m/z) of an ion. The measurement of the ion is achieved through either the use of a magnetic field (magnetic sector instruments) or electric field (time-of-flight, quadrupole, orbitrap, ion trap, electric sector instruments) or a combination of both (sector and fourier transform ion cyclotron resonance instruments). In basic mass spectrometers (sector instruments) the sample containing the analyte to be ionised will be accelerated by an electric field where the ions will enter a magnetic field and separate based on their m/z, by varying the strength of the magnetic

field a full spectrum of the analytes in a sample will be produced. The kinetic energy of an ion can be explained by Equation 1.3 below.

$$e.E = \frac{1}{2}mv^2 \quad (1.3)$$

Where, e.E is the kinetic energy (e, charge on the ion, E, electric field potential), m is the mass of the ion and v is the velocity of the ion. This equation can be rearranged to show that both the magnetic field and electric field can be varied to detect different ions (Equation 1.4).

$$\frac{m}{e} = \frac{H^2r^2}{2E} \quad (1.4)$$

Where, *H* is the applied magnetic field and *r* is the radius. Thus, by increasing or decreasing either the magnetic of electric field the m/z detected is different. Heavier ions or ions with low charges will move in a wider radius whereas lighter or more highly charged particles will move in a smaller radius, the motion of these ions will thus determine whether they reach the detector or collide with the walls of the mass analyser. This equation also shows that if a particle had a +2 charge the mass that is detected would be half of its true value [73].

1.5.3.1 Quadrupole mass spectrometry

As mentioned above the electric or magnetic field can be manipulated to detect ions of specific m/z values. The quadrupole mass analyser consists of four rods that have an applied direct current (DC) voltage and alternating current (AC) voltage of a radiofrequency (RF) range. The rods are placed parallel to each other in the X and Y plane, where the ions will travel along the Z-axis. By varying the applied voltage only specific ions of a single m/z value may pass along the quadrupoles whilst all others follow an unstable trajectory and collide into the

poles. The applied voltages are described by two equations of which one applies to the rods on the X axis and one to the rods on the Y axis (Equation 1.5 and 1.6) [74].

$$x = \cup + V_o \cos(\omega t) \tag{1.5}$$

$$y = -\cup - V_o \cos(\omega t) \tag{1.6}$$

Where, ∪ is the DC potential, V is the AC potential, ω is the angular frequency of the AC potential and t is time. As shown the rods on the X plane have a positive DC potential with a varying AC potential and the Y rods have a negative DC potential with an applied AC potential (Figure 1.2).

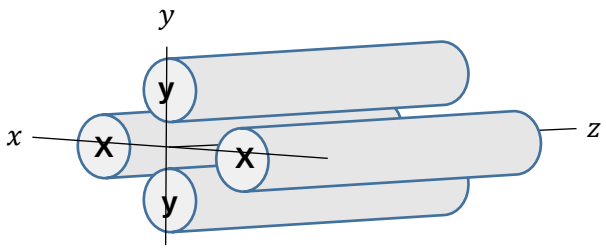

Figure 1.2: Configuration of the rods in a quadrupole mass analyser. The flight path of the gas phase ions is along the z-axis.

These rods have a bias so that simply the X rods are more positive and the Y rods are more negative until the potential of the AC voltage is high enough to reverse the charge on the rods. If the individual pairs of rods are taken into account separately, then once the potentials are applied the ions will be focused along the Z plane by the positive DC and will be focused and defocused by the changing AC potential. The effect is also time dependent so that if the AC potential has a high frequency then the ions will tend to only 'feel' an average potential or if the ion is heavy as described previously, the radius of motion will be larger so that the smaller amount of time the rods are negative will have little effect on heavy ions thus their trajectory will remain stable. Alternatively, if the ion

is light the force exerted by the varying AC potential when it is negative may be sufficient to cause the ion to follow an unstable trajectory and collide with the rods, thus the X rods are known as a high pass mass filter. The Y rods will have an equal potential to the X rods but will be the opposite sign, so the waveforms are 180^{o} out of phase. As the larger ions only feel an average of the applied potential and these rods are negatively bias, they will follow an unstable trajectory. However, a light ion will be focused and defocused continually so that overall the path is stable and the ions are detected. There is a critical point at a specific DC and AC potential in each X-Z and Y-Z plane that will determine if an ion will pass through or be removed as a neutral upon collision with the rod. For an ion to reach the detector in a quadrupole mass analyser, the ion must be of a specific m/z so that it is not too light to go below the critical point in the high pass mass filter and not to heavy that it is above the critical point in the low pass mass filter. Thus, if an AC:DC ratio of potentials is optimised, a point at which only one atomic mass unit can pass through the rods is obtained.

Mass analysers can be coupled to together to form what is known as tandem mass spectrometry (MS^{n}). Tandem mass spectrometry is a very selective and sensitive technique enabling both accurate and reliable determination of trace concentrations of analytes. In quadrupole analysis the most common type of mass spectrometer is a triple quadrupole, where the sample will be ionised and enter the first quadrupole. Here in the first mass analyser usually parent ions are detected which are then accelerated to the second mass analyser which acts a collision cell, this causes collision induced dissociation (CID) of the parent molecules so that fragmented ions or product ions are produced. These product ions are then detected by the third quadrupole. The fragmentations are known as transitions, a specific parent ion will fragment to a specific product ion, so the

operator can perform single or multiple reaction monitoring (SRM/MRM). This allows the monitoring of single or multiple transitions which in turn allows quantification and confirmatory determination of selected analytes.

1.5.4 Liquid chromatography-mass spectrometry

The coupling of liquid chromatography to mass spectrometry is perhaps one of the most powerful instrumental techniques for target/non-target analysis, structure elucidation and confirmation. As described previously, it allows the separation of complex mixtures which can subsequently be analysed for identification of the analytes in the sample. The coupling of LC to MS was particularly difficult as the flow rate from the HPLC translated into gas flow rates that were far too high to be able to maintain the high vacuum required for mass analysers. Many different types of interfaces were produced to overcome this problem such as direct liquid introduction (DLI), moving belt interface and thermospray which had moderate success in laboratory application. The major revolutionary interface in LC-MS that overcame the previous problems encountered with other interfaces was known as electrospray ionisation (ESI) developed by Fenn et al., [75]. This ion source was a soft ionisation technique meaning that there was less fragmentation in source so parent ions would be detected, molecular ions could also be produced that would be beyond the operating mass range associated with a particular mass analyser (multiple charged ions). These sources could only be used with low flow rates at first but were then modified to include a nebuliser gas which aided with desolvation of the effluent allowing flow rates from the LC of up to 1 mL min^{-1}.

The ESI source directly introduces the LC eluate via a capillary that has a very high potential applied to the tip. As the liquid passes this tip it is sprayed into

a mist where small droplets become charged [76]. Droplets are emitted from the capillary tip due to the formation of a Taylor cone by the balance of the electrostatic potential and the surface tension of the effluent. The potential acts to ‘pull’ the liquid from the capillary tip to the ground plate, counter to this force is the surface tension which acts to minimise the surface area of the liquid by opposing the pull of the electrostatic force. Upon the applied potential a point is reached where the electrostatic force and the surface tension are equal to one another and thus a Taylor cone is formed. If the threshold potential of the capillary is exceeded the balance between the forces is disrupted and thus droplets are ejected from the Taylor cone [77].

Two models exist that explain the formation of charged analytes from the charged droplet which are known as the ion evaporation model (IEM) and the charge residue model (CRM) [78]. In the first model after the formation of the Taylor cone and emission of charged droplets, as the droplet size decreased the charge density on its surface would become sufficiently high to overcome the surface tension forces of the droplet so that an ion would be ejected from the droplet and into a gaseous phase ion. The CRM proposed that as the droplet decreases in size due to evaporation the charge density on the droplet increases until a point is reached known as the Rayleigh limit whereby the ions on the surface of the droplet become so close their repulsion causes a process known as coloumbic explosion [79]. This process repeats constantly until a droplet contains a single analyte ion. The coloumbic explosion occurs in both models but the difference is that the IEM describes that before a droplet can become so small to only contain one analyte, desorption of a single analyte will occur from a larger droplet. Much debate has occurred over which mechanism is responsible for ion formation in ESI-MS and there is evidence for both mechanisms occurring. It was

suggested that IEM occurs for lower molecular weight analytes whereas CRM ion formation occurs with large molecular mass compounds [80]. This is perhaps due to the fact that a molecule increases in size, the energy required for the ion to desorb from the droplet is not reached.

1.5.5 Sample preparation

One key aspect to the development of analytical workflows to determine the impact of environmental contaminants is sample preparation. As environmental samples are complex matrices which include biological tissues, soil, surface water and biosolids, it is essential to sample preparation that allows the clean-up of the sample and pre-concentration of the analytes. There are numerous sample preparation techniques with the most common employing protein precipitation, solvent extraction and solid-phase extraction (SPE) [81]. Protein precipitation usually involves the uses of organic solvents such as acetonitrile which precipitate proteins out of solution due to the low solubility of the proteins in these hydrophobic solvents. Weak acids such as acetic acid can also be added to a biological sample which disrupts protein binding to analytes such as pharmaceuticals.

Liquid extractions also involve the use of organic solvents due to the high solubility of organic compounds. Liquid extractions can involve liquid-liquid extractions (LLE) where two immiscible solvents are used to extract analytes into one of the phases. Microwave-assisted extraction (MAE) is the use of microwave radiation to heat a solvent and improve extraction efficiency of a sample. Another comparable technique is pressurised liquid extraction (PLE) or also known as accelerated solvent extraction (ASE) which uses high pressure to alter the boiling point (increases) of a solvent so that higher temperatures can be used during extraction. The increase of temperature and pressure raises the solvent to near

their supercritical region leading to improved extraction efficiencies. The increased temperature of both MAE and PLE enables greater extraction efficiencies as penetration of the sample with the solvent and diffusion of the analyte out of the sample is increased [82]. Several factors can affect solvent extractions but of greater importance is the choice of solvent [83] and the temperature [84]. A solvent or mixture of solvents can be used to take advantage of the physicochemical properties of the analyte. Temperature is critical for compounds that may be thermolabile and degrade during extraction.

One of the most used sample clean-up and pre-concentration techniques is SPE. This technique allows clean-up by removing interfering matrix components whilst retaining analytes [85]. SPE also pre-concentrates analytes as it is possible to use very large samples volumes (up to 20 L). However, sample volumes used are typically < 1 L. SPE involves a cartridge that contains a sorbent material such as C_8. The sample solution is passed through a conditioned cartridge in a loading phase where the sorbent retains the analyte whilst matrix components pass through and go to waste. However, the sorbent may also retain some undesirable matrix components that can interfere with the instrumental analysis. Thus, a wash phase is used that uses a 'weak' solvent to remove the interferences whilst not affecting the retention of the analytes. After the wash step, the analytes are eluted with an organic solvent and then dried down under nitrogen and reconstituted in a small volume (e.g. 50 to 1000 μL) for analysis. The main factor to influence the extraction and recovery in SPE will be the sorbent material. Many environmental applications use a dual mode copolymer known as hydrophilic-lipophilic balance (HLB) which can retain both polar and non-polar compounds through Van der Waals forces, π-π interactions and hydrogen

bonding. Retention can also be through ionic interactions in ion exchange sorbents, which can be useful for compounds that are ionised.

Another factor that can affect SPE efficiency is the sample volume, where larger volumes lead to breakthrough, where recovery is low and not reproducible [86]. The wash and elution solvents are also important as it can lead to the loss of analyte and increase the remaining matrix components after the procedure. As a final point, the pH of the sample when loading can be important for retention on ion exchange cartridges or for compounds that are ionisable such as pharmaceuticals. Whilst sample preparation is important for environmental applications, due to the complexity of samples interfering components will inevitably remain and can affect the instrumental analysis. Therefore, it is important to characterise the extraction efficiency and any matrix effects to ensure reliable analysis.

1.6 Accumulation of PPCPs in aquatic biota

The uptake and elimination of contaminants in biota can be quantified using a ratio that represents either the bioconcentration, bioaccumulation or biomagnification of a selected compound. Bioconcentration has been defined as the uptake of contaminants from only the exposure medium (freshwater/sediment) and is represented by the bioconcentration factor (BCF). Bioaccumulation and biomagnification relate to the accumulation through both the exposure medium and the diet of organism. Where, biomagnification quantifies the accumulation across trophic levels in contrast to a single organism. These two processes are quantified by the bioaccumulation factor (BAF) and biomagnification factor (BMF). These factors thus provide a quantitative measure of the accumulation potential useful in a regulatory context. However, these factors can be influenced by several variables that will be discussed further.

1.6.1 Uptake pathways

The uptake pathways are depicted simplistically in Figure 1.3 [87, 88]. Membranes that are specialised for transport such as those found in the gills and digestive tracts of aquatic organisms are constantly exposed to contaminated surface waters which leads to the possibility that PPCPs will be transported into the organisms by a process such as diffusion or carrier-mediated transport. Specialised sensory organs such as lateral lines in fish or olfactory/optic cells can also affect accumulation of pollutants of contaminants leading to localised areas of within organisms containing high concentrations of xenobiotics [89].

1.6.1.1 Accumulation through gill uptake

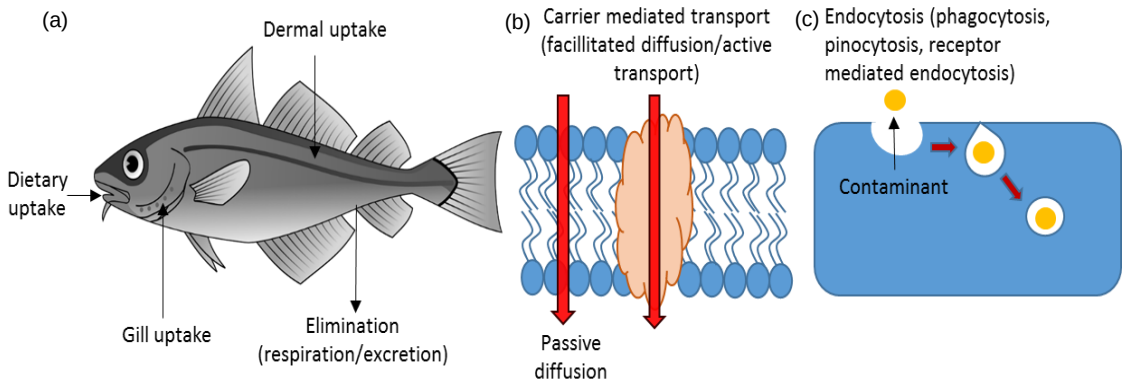

Figure 1.3: Accumulation pathways in fish, (a) the uptake and elimination routes (b) the uptake pathways across epithelia tissue (i.e. gill) (c) transport through vesicles into the cell (endocytosis).

Gill transport is likely to be a major mechanism of PPCP accumulation. Early work with gill tissue investigated log*P* with uptake rate, and it was determined that over a defined log*P* range the uptake increased. However, after a specific point was met, the uptake began to decrease. It was found that when log*P* when plotted against uptake rate a sigmoid curve was fitted. Based on passive diffusion, the reason for such an observation is that compounds with a low log*P* would be insoluble in lipid thus not able to penetrate biological

membranes. Compounds with high log*P* would essentially become ‘stuck’ in the lipid layer and would not be released into the blood or other compartments [90]. As PPCPs usually have a moderate range of log*P* (e.g. 0-5), they will most likely accumulate through passive diffusion. However, as many exist in an ionisable form it is possible that carrier-mediated transport, in the form of either facilitated diffusion or active transport could also account for uptake.

Mechanisms of drug absorption is usually based on lipophilicity and is thought to be the dominant mechanism of transport across memebranes. However, carrier-mediated transport may play a more important role than previously thought [91]. Xenobiotics may act a substrate for various families of transporters such as the solute carrier family (SLCs). These SLCs have been isolated in fish gill cells which are considered the primary organ for contaminant uptake in aquatic organisms [92-94]. Furthermore, SLCs can recognise multiple substrates such as ionic and non-ionic organic compounds and thus provide a pathway for non-specific substrate transport [91]. Characterisation of transporters is limited with perhaps the greatest coverage in humans. However, conservation of transporters across taxonomic groups may underpin identification from well-studied model organisms. For example the SLC22 family of transporters (organic anionic/zwitterionic/cationic transporters) which is involved with the transport of many pharmaceuticals has homologs found in *Drosophila* and *C. elegans* [95].

Localised accumulation of tributyltin in the brain of fish suggested specific tissue accumulated this organometal. This data may indicate that that passive diffusion may not account for the uptake [89, 91]. A study on the concentration of the β-blocker propranolol in fish plasma showed that at a relatively high exposure concentration (10 mg L^{-1}) the concentration in the fish plasma exceeded that of the exposure media that may also indicate active transport of this pharmaceutical

[96]. The epithelial tissues that make up the gills are involved heavily in ion transport systems for ion regulation and osmoregulation in aquatic organisms, and have been noted to accumulate toxic heavy metal ions via these transport mechanisms [97].

The uptake of acidic organic chemicals was shown to decrease as the pH of the environment increased indicating that the ionised form was accumulated at a lower rate to the neutral form. This data demonstrates the idea that crossing hydrophobic membranes is unlikely for ionised compounds. However, authors noted that the change in the fraction of the ionised species compared with the increase in the pH did not decrease the uptake rates proportionately, thus indicating that even in a compounds ionised form it still accumulates [98]. Release of ammonia and carbon dioxide across the gill structures will affect the pH of the interphase layer compared with that of the bulk solution, thus an underestimate of uptake is likely as the compounds that would be expected to be ionised may remain neutral. It is also a possibility that organic ions such as pharmaceuticals may be able to partition directly into across the membrane depending on their lipophilicity or accumulate into tissue by paracellular transport at cell junctions [98].

The equilibrium of a predominantly ionised compound outside the gill will shift towards the formation of neutral species as the neutral fraction diffuses across the membrane [98]. Therefore, this equilibrium process suggests another mechanism for uptake of ionisable compounds. The potential across the membrane may also have an effect on the efficiency of uptake. Diffusion is dictated by electrochemical gradients where the PPCP will move down the gradient into the epithelial tissue. However, the potential of the membrane may setup a gradient that will oppose or enhance the chemical gradient depending on

the ions involved, thus known as the Nernst potential [99]. Transepithelial electric potentials (TEP) have been demonstrated to vary on a species basis and are found to be positive to negative thus affecting uptake and extrusion of various ions [97]. These potentials are also varied depending on the aquatic environment (salt-water or freshwater) as salt-water will have increased ionic strength, thus affecting ionic transporters.

1.6.1.2 Dermal and digestive tract accumulation

Trophic transfer and feeding (biomagnification/bioaccumulation) is another route for uptake as the digestive tract will contain assimilated food that may be contaminated with PPCPs (or other contaminants). Thus, accumulation of PPCPs through the diet and trophic levels can occur. Sorption of contaminants to sediment may also enter digestive tracts of some aquatic organisms through feeding. Sorption is an important consideration when studying the effects of uptake, as PPCPs have the potential to adsorb to exoskeletons and scales which could then diffuse through and accumulate in tissues. Studies have estimated between 10-50 % of absorption of contaminants is by dermal absorption in fish [100, 101]. To understand this potential the structure of both fish dermal layers as with invertebrate exoskeleton must be considered.

Teleost fish scales consist of a mineral layer known as hydroxyapatite containing ionic groups such as phosphate, which is interwoven with type 1 collagen fibres, containing alkylated amino groups, carbonyl and carboxylic acid groups [102-104]. The phosphate groups have been noted to complex with metal ions in the aqueous phase and that the amino groups play an important part of sorption [102]. The hydroxyapatite layer in fish scales has been determined to have a porous structure therefore the possibility for molecules to penetrate and absorb into epithelial tissue exists. However, this will be limited by the diffusivity

of the compounds in these pores which may account for the lower estimate of dermal absorption reported [103]. Estimates were reported for different sizes of fish and the variability could also be the result of surface area to volume of the organism. Furthermore, some estimates were based on models developed on mammals which may not be suitable to assess dermal absorption in fish [100, 105]. A subcutaneous layer of fat in fish also exists which could have storage capacity for organic contaminants [100].

Invertebrate organisms have an exoskeleton which consists of chitin, or more specifically N-acetyl-glucosamine [106]. Early work with chitin involved dichlordiphenyltrichloroethane (DDT) sorption capacity, the authors noted that when compared with cellulose, which is structurally similar to chitin, there was no sorption of DDT. Thus, the authors concluded that the amino groups in chitin would be responsible for the sorption of DDT [107]. Later experiments determined that sorption of lindane to chitin was through hydrophobic and electrostatic interactions and decreased with increasing temperature owing to an increase in energy of the solute to overcome intermolecular forces. The authors also noted that sorption was split into two categories; one that was reversible (i.e. sorption-desorption) and a second that was resistant to desorption. The effect of salinity on this desorption resistance showed that as the ionic strength increased the resistant mode became more favourable. This could be due two reasons, firstly that ions will effectively reduce the hydration of sorbent surface making sorption more favourable. Secondly, an increase in adsorbed cations from the seawater will allow more specific electrostatic interactions to occur. It is also possible that inorganic salt concentration could effectively begin to ‘salt-out’ hydrophobic molecules causing them to aggregate with chitin molecules [106, 108].

Although these studies described above have not been conducted with PPCPs, pharmaceuticals that contain multiple ionisable sites and varying degrees of hydrophobicity may undergo biosorption, particularly as electrostatic interactions might be more important in determining sorption than hydrophobicity [109]. Sorption to animals is not often a considered aspect in bioconcentration studies. If the compound is adsorbed to the animal then it may be prevented from accumulating in the organism internally. However, sorption is important in bioaccumulation where bound contaminants may enter into the digestive tract of higher trophic level organisms.

1.6.2 Models of accumulation

To determine the accumulation of a xenobiotic in the aquatic environment, models were developed that described the uptake of compound into an organism. These model described variables such as chemical fugacity, metabolism, respiration, fish weight, gill flow rate, diffusion resistance and permeation resistance among others [110-112]. Early models were used to determine hydrophobic organic contaminants and organometals in fish [113]. Other models have tried to predict bioconcentration from using physicochemical properties such as log*P* and log*S* based off of linear regressions estimates using a training set of compounds [114, 115].

The importance of determining the potential of a compound to accumulate in an organism is crucial to assess the risk in the environment. Therefore, several technical guidance documents have been released including the American Society for Testing and Materials (ASTM) 1993, European Centre for Ecotoxicology and Toxicology of Chemicals (ECETOC) 1996 and Organisation for Economic Co-operation and Development (OECD) 1996 to experimentally determine bioconcentration/bioaccumulation [116]. However, the most generally

applied guidance document to determine BCF/BAF is the OECD 305 bioaccumulation in fish: aqueous and dietary exposure [117]. The determination of BCF using this document can involve kinetic estimation where the ratio of the uptake rate constant (k_1) and the elimination rate constant (k_2) are used to estimate the BCF. Alternatively, steady-state measurement (concentration no longer increases in the animal) can be used to estimate the BCF where the concentration of compound in the organism is divided by the concentration in the water.

The advantage of steady-state measurements is the simplicity in determining BCFs. However, the time to reach steady-state can be considerable, thus if steady state is not reached a BCF cannot be determined. Extension of the experiment length is also undesirable as they are resource intensive (cost, time and labour). Therefore, the kinetic measurements offer a solution to this limitation but as they use iterative algorithms (Levenberg-Marquardt) another source of error is introduced in the estimation of BCFs. Currently, the models that have been developed describe only the accumulation potential of a contaminants in fish. Models that describe accumulation in invertebrates do not exist. Therefore, the application of fish uptake models to the invertebrate phyla remains understudied. In addition, contaminants used to develop models have predominantly been neutral hydrophobic contaminants. Thus, whether these models are suitable to describe the accumulation of amphoteric and ionisable PPCPs is a current knowledge gap.

1.6.3 Factors influencing bioaccumulation

The accumulation of contaminants can be affected by numerous factors including bioavailability, metabolism, water chemistry, growth and excretion. Sorption is important in understanding the bioavailability of the PPCPs to

organisms, and the idea of non-reversible desorption is also a factor for consideration. If a compound is adsorbed to sediment particle, particularly the desorption-resistant fraction will be unavailable to accumulate in organisms which is more likely to be advantageous in benthic organisms. As demonstrated with the hydrophobic organic compound phenanthrene, there was desorption-resistant fraction and the sediment bioaccumulation factor for the resistant fraction of phenanthrene was two times lower than the reversible fraction [118]. Furthermore, the association of contaminants to DOM such as humic acids may also reduce the bioavailability of the compound to accumulate in biota [119].

We must also consider the efflux and removal of PPCPs from organisms to understand the accumulation potential. As mentioned above gradients of electric potential and chemical concentration can oppose each other increasing the extrusion of organic ions that are accumulated in the cell and may also prevent further uptake from the outside environment. Proteins known as the multidrug resistance (MDR) transporters consisting of the proteins from the ATP binding cassette (ABC) superfamily can also affect accumulation. This superfamily of proteins are found in aquatic species and are termed multi-xenobiotic resistant MXR transporters, these proteins have a very wide spectrum of substrate affinities which is very advantageous for removing toxic xenobiotics and as these are driven by active transport it counters passive diffusion [120].

Accumulation of compounds is also affected by numerous biotic factors. Studies suggest that strategies and traits specific to different taxonomic groups, for example life cycle and reproduction, will affect the sensitivity of the organism to the pollutant [121]. The habitat choice will determine the accumulation as benthic organisms will come into contact with sediment which could contain more hydrophobic compounds associated with high uptake potentials. There is the

metabolic rate which determines the nutrient requirement indicating that organisms that feed frequently might have a higher exposure to pollutants. The type of integument of the organisms whether the species is soft bodied or hardened with heavily deposited inorganic salts will influence the permeability of the compound and whether the compound is lost to moulting cycles [122]. The type of lipid and the lipid content will affect accumulation predominantly through hydrophobic effects, in combination with the variety of physico-chemical properties it is apparent that there is a complex network of interactions that influence the occurrence of PPCPs in biota [123]. The biochemical activity inside the organism (xenometabolism) may also have a profound effect on accumulation as one species may be able to efficiently remove the compound in comparison to another [124]. This will be determined by conservation of Phase 1 and Phase 2 metabolic enzymes such as cytochrome P450 (CYP). Currently, xenometabolism is understudied in assessing the accumulation potential. Models to determine bioconcentration do not often take biotransformation into account. Thus, the potential of non-target organisms to biotransform PPCPs is not well known. This is especially so for invertebrates where conservation of metabolic enzymes is not well characterised.

In an exposure study, five pharmaceuticals were measured across two test species which had very similar order of accumulation but at very different concentrations [125]. *In G. pulex* fluoxetine was shown to have a BCF value of 185,900 in comparison to *N. Glauca* which was measured at 1.387. The reason for such a difference was explained in part by the different exposure pH values, as fluoxetine would have been more ionised in the *N. glauca* exposure than in the *G. pulex* exposure. However, three other compounds had higher BCFs in *G. pulex* although the influence of pH would have been minimal. This further

demonstrates species differences in uptake and depuration rates and may have been further explained by biotransformation [125]. The authors of this paper also noted that they found no relationship between lipid content and BCF which was also indicated in two other studies where uptake was unrelated to lipid content, although it was shown in one of the investigations that chlorpyrifos uptake correlated well with the water permeability of the organism [125-127]. Fluoxetine has also been studied in *Oryzias latipes* with reported BCF values ranging from 74 – 260 depending on the pH, in which it is shown to increase as the compound becomes less ionised. In both investigation the authors also noted that the metabolite of fluoxetine, norfluoxetine, was measured at a higher concentration than the parent compound and it was noted that a longer exposure study may in turn reduce the apparent uptake rate of the parent as it is metabolised into norfluoxetine. [128, 129]. The pH influence on BCFs indicates the potential for water chemistry to affect accumulation.

Other abiotic factors may also affect accumulation such as temperature which was demonstrated to increase determined BCFs [130]. Seasonal variation in BCFs can also occur where a mixture of factors can have influence such as dilution of contaminant levels in surface waters and temperature of the water [131]. Furthermore, the physico-chemical properties of the compound itself can affect accumulation through its ionisability, hydrophobicity, molecular size and solubility among other factors. It is also important to note that these influences do not occur individually and thus it is a complex interaction between numerous biotic and abiotic factors that determine the accumulation potential of a compound. Therefore, accurate modelling and prediction of accumulation such as BCF estimation might be limited especially in the field.

1.7 Ecotoxicological importance of invertebrates

Invertebrates are critical to understand the impact of environmental contaminants. This phylum is the largest and most diverse to exist with many species not yet identified [132]. They are of crucial importance to ecosystem services, the most well-known of which is insect pollination [133]. These organisms also constitute important roles in food webs where adverse effects to this group of animals could have detrimental effects to ecosystem function [134]. These organisms can be used to understand the impact of environmental contaminants through bioaccumulation and toxicity studies where they serve as useful indicators of adverse effects.

The relative sensitivity of aquatic invertebrates and vertebrates to environmental stressors can vary widely. For example, invertebrates have been shown to be more tolerant to ammonia than fish [135], fish were shown to be relatively less sensitive to metal contaminated sediments than invertebrates [136] and there were varying sensitivities between invertebrates and vertebrates when exposed to thirteen different chemicals [137]. However, even with differing sensitivities, a majority of ecotoxicological assessments are performed with fish where invertebrates are understudied. Thus, it is crucial that we extend studies to the invertebrate phyla to address the current paucity of research in this taxanomic group [138]. Furthermore, responses of invertebrates to environmental pollutants can be used to understand read-across to other vertebrate animals [139]. This is especially important for the replacement of fish species as defined by the policy of replacement, reduction and refinement (3Rs) in animal testing. The use of invertebrates as environmental indicators has involved assessment of endpoints including mortality and sub-lethal endpoints such as the inhibition of feeding among other behavioural and physiological responses [140-143].

The majority of invertebrate regulatory testing involves *Daphnia magna* and *Ceriodaphnia dubia* where they are involved in acute toxicity assays [144]. However, acute toxicity assays are limited in their environmental relevance where exposures are often several orders of magnitude lower. Thus, the focus of research into toxicity should involve sub-lethal chronic exposures to assess the subtle effects of environmental contaminants such as PPCPs. For example, a bioassay used as a stress indicator for both natural and anthropogenic activity is known as the “Scope for Growth” bioassay which measures the difference between energy intake and metabolic output. This assay had been successfully used for the marine mussel (*Mytilus edulis*) and was also determined as a sensitive bioassay when used with the freshwater amphipod *Gammarus pulex* (*G. pulex*) [145, 146].

1.7.1 *Gammarus pulex*

G. pulex is a freshwater benthic detritivore that feed on decaying organic matter and occupy the bottom most layer of a freshwater habitat, i.e. the interface between the sediment and water. Thus, these species provide an important ecosystem service known as nutrient cycling. This species belong to the *arthropoda* phyla and are sub-classified as *crustacea*, these organisms are segmented and have a cuticle known as an exoskeleton which is formed of calcified chitin, a polymer formed of N-acetylguclosamine.

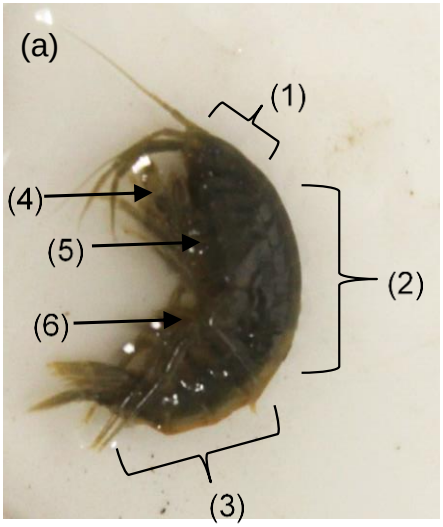

(b)

Image excluded from e-copy as the copyright permission could not be obtained.

Figure 1.4: (a) Gammarus pulex showing (1) the cephalon, (2) pereon, (3) the pleon, (4) the gnathopods, (5) location of the gills and (6) pereopods, pleopods and uropods. (b) Scanning electron micrograph of an arthropod cuticle cross section. Ep is the epicuticle, Ex is the exocuticle, En is the endocuticle and PC shows a pore channel. Figure taken from [150].

These organisms breed throughout the year and will reach sexual maturity within 3-4 months, the juveniles are also found to be much more sensitive to pollutants than the oldest life stage group which further demonstrates that these organisms can be used as very sensitive bioassays for polluted waters [147, 148]. Lipid content of *G. pulex* can vary from ~300-400 µg with males containing a higher lipid content except in cases where gravid females were measured and contained ~550 µg of lipid [149]. The cuticle of *G. pulex* consists of three layers

the epicuticle (outermost), exocuticle (middle) and endocuticle (innermost) below which is the epidermis (Figure 1.4) [150]. The cuticle contains numerous pore channels that contain chitin fibres and cytoplasmic extensions which terminate below the epictuicle layer or at the surface of the epicuticle [151]. The epicuticle layer can be further subdivided into additional layers such as the cement layer, wax layer and cuticulin layer [152]. However, the exact composition of these layers has not been characterised. It is proposed that the cuticulin layer is a formed of an unknown lipoprotein [153]. The epicuticle is also perforated with pore canals which allow secretions when modifying the exoskeleton during moult cycles [150]. The exoskeleton of arthropods must be shed after periods of growth which consists of five stage (A-E) which are further subdivided into A1, A2, B2, B1, C1, C2 and C3 (post-molt stage); C4 (intermolt stage) D0, D1', D1'', D1''', D2, D3, and D4 (pre-molt stage); finally the ecdysis of the cuticle, E [151]. The moult cycle is important when considering ecotoxicological effects as the uptake and depuration may change as certain physiological characteristics of the crustaceans will change such as the calcium concentration and pH value of the haemolymph [151]. In addition to pH alterations, it has also been suggested that CYP expression is increased during post-moult stages where the high levels of the hormone ecdysone (responsible for moulting) is required to be reduced through metabolism [154]. These organisms have been used by several researchers to investigate mortality, sub-lethal effects, bioaccumulation and more recently metabolism of environmental contaminants including PPCPs [140-143, 155-157]. Demonstrating the suitability of these organisms for use in ecotoxicological application.

1.8 Regulation and legislation

To mitigate the risks posed by environmental contaminants a number of governmental bodies have released regulatory and legislative guidance documents. Of this legislation, the Registration, Evaluation, Authorisation and Restriction of Chemicals (REACH) is the main document to assess environmental risk across the European Union (EU) [158]. A stipulation of REACH is that any chemical that is manufactured in excess of 10 tonnes per annum requires a chemical safety assessment (CSA). These CSAs involves the persistent, bioaccumulative and toxicity (PBT) testing. As the name suggests chemicals are tested to determine if a chemical; persists in the environment usually determined by a half-life, bioaccumulates in an organism determined by a BCF or BAF and whether it is toxic to organisms that are exposed to it determined by effect concentrations such as the EC_{50} or LC_{50}.

During the assessment a compound may be classed persistent and bioaccumulative (P/B) or very persistent and bioaccumulative (vPvB). If a manufacturer determines that their chemical fulfils the criteria of PBT testing then they must perform an emission characterisation and minimise exposures through-out the lifecycle of the chemical. The emission characterisation aims to identify and estimate the emission of a chemical into the environment. Secondly, it aims to identify routes of exposure to humans and the environment. The emission characterisation forms the basis of the risk characterisation and management measures. This involves minimising the emissions from a specific use, communicate safety data sheets (SDS) to end-users, containment of the substance, trained personnel to handle the chemical, control technologies and characterising direct exposure risk by establishing exposure thresholds. Substances identified as B/P or vPvB are also prioritised to be phased out of

manufacture where technically and economically viable substitutions are available. Additionally, if a substance has fulfilled the PBT criteria it can be subject to being placed on the candidate list for substances of very high concern (SVHC) by the European Chemicals Agency (ECHA).

Substances defined as SVHC are subject to authorisation so that the risks posed are controlled and prioritised for replacement. Alternatively, the substance can be placed under restriction where the manufacture, placing on the market or use is restricted or banned completely. Substances fulfilling the PBT assessment may also overlap with substances identified by the United Nations Economic Commission for Europe (ENCE) Protocol for Persistent Organic Pollutants (POPs) [159]. This protocol bans the production and use of selected substances where others are scheduled for bans at a later date. The protocol addresses the control and reduction of emissions POPs including waste from banned substances.

The Convention for the Protection of the Marine Environment of the North-East Atlantic (OSPAR) is a legislative body that regulates international environmental protection [160]. This body regulates the emission of hazardous or radioactive substances and the emission of off-shore industrial chemicals and oil from the oil and gas industry. The body aims to achieve this by monitoring environmental emissions, phase out use of hazardous substances, develop best available techniques (BAT) and best environmental practice (BAP). This body also has a List of Chemicals for Priority Action which was the first to include a pharmaceutical among legislative bodies that was clotrimazole in 2002 [161]. This substance only fulfils the P and T assessment set by REACH but fulfils all the PBT criteria set by OSPAR itself.

In addition to OSPAR for the protection of aquatic environments is the EU Water Framework Directive (WFD) [162]. The directive aims to assess the ecological and chemical status of surface waters and groundwater. The framework sets out environmental thresholds for specific pollutants named on the list of Priority Substances. This required EU member states to take action to meet standards set out by Environmental Quality Standards Directive (EQSD). In addition to the Priority Substances List, the WFD also has a Watch List where compounds are required to be monitored across a range of surface waters to assess the potential impact on the environment. The Watch List included three pharmaceutical compounds, a NSAID and two hormones; diclofenac, 17-Beta-estradiol (E2), and 17-Alpha-ethinylestradiol (EE2) [163]. Pharmaceuticals are a unique case for legislation and assessment of environmental risks.

REACH does not cover pharmaceutical compounds. Instead they are covered by the European Medicines Agency (EMA) [164]. The EMA requires ERA for pharmaceutical products which Phase I and Phase II testing. Phase I involves the estimation of exposure through standard testing approaches such as PBT. Phase II involves the fate and effects of pharmaceuticals which are often characterised by OECD technical guidance documents. However, pharmaceuticals intended for veterinary use do not require PBT testing until Phase II. The outcome of the ERA will involve standard approaches such as minimising emissions to the environment, appropriate labelling for disposal methods and other appropriate risk mitigation measures. The ERA involves criteria that will trigger the next level of assessment, but if they are not fulfilled the ERA stops. Thus, for example if Phase I testing concludes a substance is not PBT no further assessments are carried out. However, as these tests are preliminary they do not fully investigate routes of exposures, metabolite products

or chronic toxicity. This presents a problem as the risk posed by pharmaceuticals may not properly be characterised due to poor quality ERAs. In addition to this, pharmaceuticals intended for human use cannot be rejected for market placement regardless of the outcome of an ERA. Thus, it is essential that pharmaceutical risk to the environment requires a focus of research effort to understand the potential for adverse outcomes.

1.9 Quantitative structure activity relationship (QSAR) models

Modelling has become an important aspect in environmental science due to the complexity of the environment and the number of factors that may affect one aspect, for example bioaccumulation [165]. Modelling approaches can involve the linear or non-linear prediction or classification of a desired output function such as toxicity. QSAR models involve the use of multiple input variables which are often molecular descriptors covering a range of chemical compounds. These inputs can cover physico-chemical properties, constitutional, topological (2-D) and geometrical descriptors (3-D). Where selection of descriptors involves some form of pre-processing which can include normalisation (zero/near zero variance), transformation, centering and scaling to reduce descriptor redundancy and improve modelling. Input pre-treatment can also include feature selection such as stepwise or genetic algorithms to identify important descriptors in the modelling approach.

The modelling makes use of either linear or non-linear regression algorithms where non-linear methods are usually accomplished *in silico* [166]. These non-linear algorithms can include artificial neural networks (ANN) [167], support vector machines (SVM) [168], partial least squares (PLS) [169] and tree-based models [170]. Many QSAR models will use two data subsets referred to as the training and validation data. The training data is used to build and develop

the models whilst the validation data is used to test and validate the model. QSARs can be used in categorical classifications or in quantitative predictions depending on the application required. In addition to predictive and categorical applications, developed QSARs can also be used to mechanistically interpret the descriptor-output relationship. Thus, QSARs are both useful and important in understanding complex processes [171].

1.9.1 Artificial neural networks (ANNs)

One computational model that has been established is ANNs. These models map input data to an output or to multiple outputs. The mapping of the input-output relationship is achieved through means of a hidden layer. This layer contains hidden nodes which are connected to both input and output variables (Figure 1.5).

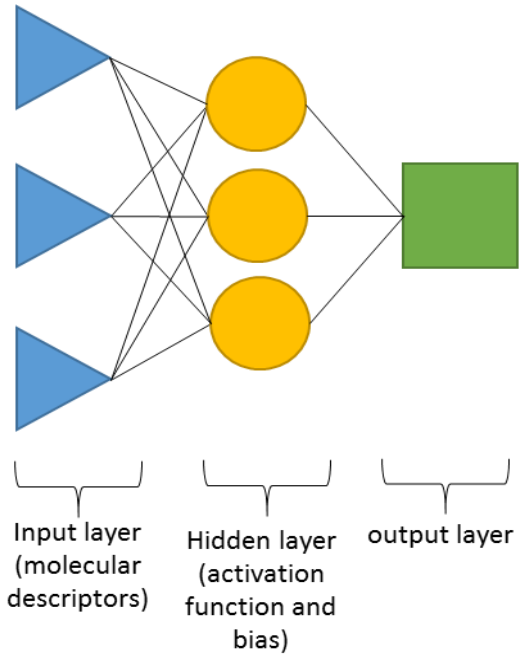

Figure 1.5: Schematic representation of an ANN with 3 inputs, a single hidden layer (3 nodes) and a single output.

The connections between the layers are referred to as neurons which have an individual weight applied. The weight on a neuron can change over time as the model learns. The weight associated with an input neuron will then be converted into an output by means of an activation function on the hidden node. The output activation will be a function of the input neuron weights and bias that is applied. The learning process used to model the data will depend on the type of ANN used such as multi-layer perceptrons (MLP) [172], probabilistic neural networks (PNN) [173] and radial basis function (RBF) networks [174].

MLPs are perhaps the most well-known and are trained using gradient descent algorithms. Gradient descent can be visualised by a plot of an error surface of two or more variables against a loss function [175]. The gradient descent aims to descend down the gradient of the error surface to reach the global minimum, analogous to a ball rolling down a valley. The most popular gradient descent method in MLPs is backpropagation (BP) where the training is recursive [176]. Backpropagation similar to other methods of gradient descent operates by minimising the loss function (usually a quadratic loss function, i.e. mean squared error) using a gradient vector [177]. The gradient vector is calculated and the variables are changed (weights and bias) to decrease the loss function. The change in the variables can be controlled by other variables known as hyper parameters which include the epoch number, learning rate, and momentum [178]. The epoch number is related to the number of iterations the backpropagation uses to reduce the cost function of the network. Learning rates can be small indicating that small changes in weights and bias will take place, thus learning can be slow but more accurate and *vice versa*. Momentum indicates that if the direction of the gradient descent continues to decrease the loss function

the algorithm will start to ‘jump’ further in the same direction thus reducing the time that learning will take.

Backpropagation as a form of gradient descent is powerful for error minimisation but does have limitations. Firstly, the initial weights and biases on the neurons may start a great distance from the global minima, thus training can be slower and shower poorer performance. Secondly, the gradient descent can get stuck in local minima as the error surface of the cost function can be quite complex [176]. Whilst, ANNs offer a very powerful modelling approach to complex processes the main limitation that are associated with ANNs is that they are quite susceptible to overfitting/overtraining [179]. Thus, the model will lose generalisability and predictive power. To avoid this, the training data should be as large reasonably possible, the network architecture (hidden layers and nodes) should be kept as small as possible and test data should also be large to validate the generalisability of the model. A final step to prevent overfitting is a method known as regularisation. Regularisation can include a weight decay which applies a bias to the cost function so that small weight changes or reducing the cost function is favoured during the learning process (depending on the value of the bias) [180]. The smaller weights on the neurons means that changes in a minority of the inputs will not alter the output significantly. Thus, a regularised model does not learn the noise in the data. In contrast, large weights on neurons may change considerably between input data, thus the output will also vary significantly.

In summation, the model will learn general trends across all the data whilst reducing the impact of individual irregular data points thus enabling better generalisation of the actual underlying process that is modelled. Furthermore, this form of regularisation also prevents the algorithm getting stuck in local minima and thus models become more repeatable. The most common and simple form

of regularisation is known as early stopping [181]. As mentioned previously, for QSARs models are split into two subsets (training and validation). However, in the case of ANNs it is often split into three subsets which are the training, verification and test subsets. The verification subset is supervised and used to select the hyper parameters to develop the model but is also used in early stopping. The training of the network is continued across a number of epochs. As the model learns the verification and training error should gradually decrease. However, as training is continued the verification subset error will suddenly increase whilst the training error continues to decrease thus indicating overtraining. Therefore, the training is stopped as this point is reached to prevent overfitting. Whilst ANNs are susceptible overfitting they are an extremely powerful tool in classification and regression of very complex processes as shown in Section 1.9.2.

1.9.2 Applications of QSARs in the environment

As mentioned previously, QSAR modelling approaches are very powerful for understanding complex processes and have a predictive capability that makes their use in environmental sciences suitable. QSARs in environmental sciences have seen application in aquatic toxicity (acute) [182], sorption in soil [183], chromatographic retention behaviour [184], persistence [185], log*P* estimations [186], WWTP performance [187] and bioaccumulation [188]. The applications are wide ranging and have become increasingly popular due to the number of advantages they offer in environmental sciences. They can interpret complex processes to give a mechanistic understanding. They are less resource intensive than using experimental determinations and also reduce the need for testing which is ethically important for experiments that involve animal use. Under REACH alone it has been suggested that 54 million vertebrate animals will be

tested costing an estimated €9.5 billion [189]. Furthermore, the number of chemicals on the market that require ERAs are likely to reach into the hundreds of thousands. Therefore, with the number of chemicals to be tested, animals used and the cost of ERAs, it is possible that QSARs are potentially the only feasible route to prioritise and assess chemical risks in the environment. Furthermore, the predictive ability of models is also valuable to regulators. For example, the use of QSARs have been supported by regulatory bodies such as REACH [190] and the US EPA [191].

QSARs in certain cases have been used to substitute experimental data when it has not been technically possible to perform tests [192]. However, in the majority of cases experimental data is used whilst QSARs supplement experimental measurements in a weight-of-evidence approach. The preference of regulators to use experimental data stems from the reliability of QSARs. The reason is that QSARs are often built on a relatively small number of cases, thus the applicability domain of the model will be relatively narrow. Extrapolations outside of this domain leads to greater uncertainty when a model is used to predict for a compound with no previously available data. Whilst this limitation is critical for ERA, there are technical guidance documents (OECD) available that can be used to ensure models are reliable and validated. The use of ANNs for QSAR applications in environmental toxicology is extremely limited with few studies that have used ANNs to predict toxicity [193-195] and bioconcentration factors [196]. However, these studies have all been limited in the number of training and test cases used. With QSARs becoming more popular in environmental toxicology, the use of ANNs holds great potential as they have been recognised as more powerful tools when compared to classical regression models [193].

1.10 Aims and Objectives

The previously described sections have identified several knowledge gaps in environmental toxicology. Currently understanding is limited with regards to whether pharmaceuticals are accumulative within aquatic biota and this accumulation potential is particularly limited with regards to invertebrates.

The aim of this work is to further the understanding of the extent of pharmaceutical bioconcentration in a freshwater invertebrate, *G. pulex*, with the view towards modelling this *in silico*. To this end, the objectives of the work are:

(a) To develop a reliable analytical method for the determination of PhAC occurrence in whole invertebrate specimens and surrounding surface waters;

(b) To characterise the uptake and depuration kinetics for a selection of PhACs and to determine their bioconcentration factors in *G. pulex;*

(c) To characterise and determine the pathways and extent of metabolism for selected PhACs

(d) To model and predict the uptake of PhACs and other emerging environmental contaminants in fish, invertebrates and moderate hydrophilicity passive sampler sorbent chemistries using ANNs (to be potentially used as a surrogate for *G. pulex*);

The work presented herein, addresses several knowledge gaps related to the occurrence, toxicokinetics and bioaccumulation of PhACs in aquatic invertebrates that has allowed further assessment of the potential of PhACs to pose a risk in the environment. Specifically, the development and use of an analytical method to determine the occurrence of pharmaceuticals in a freshwater invertebrate within the UK has not been previously reported. Furthermore, critical

assessment of models currently used to determine pharmaceutical toxicokinetics and bioconcentration were shown to be unreliable due to non-observance of model assumptions. Finally, the work presents novel *in silico* modelling of accumulation for pharmaceuticals and other organic micropollutants in passive sampling devices and a freshwater invertebrate.

1.11 References

1. Schwarzenbach, R.P., T. Egli, T.B. Hofstetter, U. Von Gunten, and B. Wehrli, Global water pollution and human health. *Annual Review of Environment and Resources*, 2010. **35**: p. 109-136.
2. Daughton, C.G. and T.A. Ternes, Pharmaceuticals and personal care products in the environment: agents of subtle change? *Environmental health perspectives*, 1999. **107**(Suppl 6): p. 907.
3. Boxall, A.B., The environmental side effects of medication. *EMBO reports*, 2004. **5**(12): p. 1110-1116.
4. Kümmerer, K., *Pharmaceuticals in the environment: sources, fate, effects and risks*. 2008: Springer Science & Business Media.
5. Larsson, D.J., C. de Pedro, and N. Paxeus, Effluent from drug manufactures contains extremely high levels of pharmaceuticals. *Journal of hazardous materials*, 2007. **148**(3): p. 751-755.
6. Cui, C., S. Ji, and H. Ren, Determination of steroid estrogens in wastewater treatment plant of a controceptives producing factory. *Environmental monitoring and assessment*, 2006. **121**(1-3): p. 409-419.
7. Kime, D. and J. Nash, Gamete viability as an indicator of reproductive endocrine disruption in fish. *Science of the Total Environment*, 1999. **233**(1): p. 123-129.
8. Larsson, D.J. and J. Fick, Transparency throughout the production chain—a way to reduce pollution from the manufacturing of pharmaceuticals? *Regulatory Toxicology and Pharmacology*, 2009. **53**(3): p. 161-163.
9. Gómez, M.J., M. Petrović, A.R. Fernández-Alba, and D. Barceló, Determination of pharmaceuticals of various therapeutic classes by solid-phase extraction and liquid chromatography–tandem mass spectrometry

analysis in hospital effluent wastewaters. *Journal of Chromatography A*, 2006. **1114**(2): p. 224-233.

10. Martins, A.F., T.G. Vasconcelos, D.M. Henriques, C.d.S. Frank, A. König, and K. Kümmerer, Concentration of ciprofloxacin in Brazilian hospital effluent and preliminary risk assessment: a case study. *Clean–Soil, Air, Water*, 2008. **36**(3): p. 264-269.
11. Kosma, C.I., D.A. Lambropoulou, and T.A. Albanis, Investigation of PPCPs in wastewater treatment plants in Greece: occurrence, removal and environmental risk assessment. *Science of the Total Environment*, 2014. **466**: p. 421-438.
12. Lenz, K., S. Mahnik, N. Weissenbacher, R. Mader, P. Krenn, S. Hann, G. Koellensperger, M. Uhl, S. Knasmüller, and F. Ferk, Monitoring, removal and risk assessment of cytostatic drugs in hospital wastewater. *Water Science and Technology*, 2007. **56**(12): p. 141-149.
13. Verlicchi, P., M. Al Aukidy, A. Galletti, M. Petrovic, and D. Barceló, Hospital effluent: investigation of the concentrations and distribution of pharmaceuticals and environmental risk assessment. *Science of the total environment*, 2012. **430**: p. 109-118.
14. Kemper, N., Veterinary antibiotics in the aquatic and terrestrial environment. *Ecological indicators*, 2008. **8**(1): p. 1-13.
15. Sabourin, L., A. Beck, P.W. Duenk, S. Kleywegt, D.R. Lapen, H. Li, C.D. Metcalfe, M. Payne, and E. Topp, Runoff of pharmaceuticals and personal care products following application of dewatered municipal biosolids to an agricultural field. *Science of the Total Environment*, 2009. **407**(16): p. 4596-4604.

16. McClellan, K. and R.U. Halden, Pharmaceuticals and personal care products in archived U.S. biosolids from the 2001 EPA national sewage sludge survey. *Water Research*, 2010. **44**(2): p. 658-668.

17. Walters, E., K. McClellan, and R.U. Halden, Occurrence and loss over three years of 72 pharmaceuticals and personal care products from biosolids–soil mixtures in outdoor mesocosms. *Water Research*, 2010. **44**(20): p. 6011-6020.

18. Björklund, H., C. Råbergh, and G. Bylund, Residues of oxolinic acid and oxytetracycline in fish and sediments from fish farms. *Aquaculture*, 1991. **97**(1): p. 85-96.

19. Kuspis, D. and E. Krenzelok, What happens to expired medications? A survey of community medication disposal. *Veterinary and human toxicology*, 1996. **38**(1): p. 48-49.

20. Bound, J.P., K. Kitsou, and N. Voulvoulis, Household disposal of pharmaceuticals and perception of risk to the environment. *Environmental toxicology and pharmacology*, 2006. **21**(3): p. 301-307.

21. Buerge, I.J., T. Poiger, M.D. Müller, and H.-R. Buser, Combined sewer overflows to surface waters detected by the anthropogenic marker caffeine. *Environmental science & technology*, 2006. **40**(13): p. 4096-4102.

22. Suárez, S., M. Carballa, F. Omil, and J.M. Lema, How are pharmaceutical and personal care products (PPCPs) removed from urban wastewaters? *Reviews in Environmental Science and Bio/Technology*, 2008. **7**(2): p. 125-138.

23. Batt, A.L., I.B. Bruce, and D.S. Aga, Evaluating the vulnerability of surface waters to antibiotic contamination from varying wastewater treatment plant discharges. *Environmental pollution*, 2006. **142**(2): p. 295-302.

24. Tolls, J., Sorption of veterinary pharmaceuticals in soils: a review. *Environmental science & technology*, 2001. **35**(17): p. 3397-3406.

25. Imai, A., T. Fukushima, K. Matsushige, Y.-H. Kim, and K. Choi, Characterization of dissolved organic matter in effluents from wastewater treatment plants. *Water Research*, 2002. **36**(4): p. 859-870.

26. Katsoyiannis, A. and C. Samara, The fate of dissolved organic carbon (DOC) in the wastewater treatment process and its importance in the removal of wastewater contaminants. *Environmental Science and Pollution Research-International*, 2007. **14**(5): p. 284-292.

27. Jim, T.Y., E.J. Bouwer, and M. Coelhan, Occurrence and biodegradability studies of selected pharmaceuticals and personal care products in sewage effluent. *Agricultural water management*, 2006. **86**(1): p. 72-80.

28. Clara, M., N. Kreuzinger, B. Strenn, O. Gans, and H. Kroiss, The solids retention time—a suitable design parameter to evaluate the capacity of wastewater treatment plants to remove micropollutants. *Water research*, 2005. **39**(1): p. 97-106.

29. Dietrich, D.R., S. Webb, and T. Petry, *Hot spot pollutants: Pharmaceuticals in the environment*. 2005: Academic press.

30. McArdell, C.S., E. Molnar, M.J.-F. Suter, and W. Giger, Occurrence and fate of macrolide antibiotics in wastewater treatment plants and in the Glatt Valley Watershed, Switzerland. *Environmental Science & Technology*, 2003. **37**(24): p. 5479-5486.

31. Göbel, A., A. Thomsen, C.S. McArdell, A. Joss, and W. Giger, Occurrence and sorption behavior of sulfonamides, macrolides, and trimethoprim in activated sludge treatment. *Environmental science & technology*, 2005. **39**(11): p. 3981-3989.

32. Vrana, B., I.J. Allan, R. Greenwood, G.A. Mills, E. Dominiak, K. Svensson, J. Knutsson, and G. Morrison, Passive sampling techniques for monitoring pollutants in water. *TrAC Trends in Analytical Chemistry*, 2005. **24**(10): p. 845-868.

33. Lohmann, R., K. Booij, F. Smedes, and B. Vrana, Use of passive sampling devices for monitoring and compliance checking of POP concentrations in water. *Environmental Science and Pollution Research*, 2012. **19**(6): p. 1885-1895.

34. aus der Beek, T., F.-A. Weber, A. Bergmann, S. Hickmann, I. Ebert, A. Hein, and A. Küster, Pharmaceuticals in the environment—Global occurrences and perspectives. *Environmental Toxicology and Chemistry*, 2016. **35**(4): p. 823-835.

35. Kasprzyk-Hordern, B., R.M. Dinsdale, and A.J. Guwy, The occurrence of pharmaceuticals, personal care products, endocrine disruptors and illicit drugs in surface water in South Wales, UK. *Water Research*, 2008. **42**(13): p. 3498-3518.

36. Kim, J.-W., H.-S. Jang, J.-G. Kim, H. Ishibashi, M. Hirano, K. Nasu, N. Ichikawa, Y. Takao, R. Shinohara, and K. Arizono, Occurrence of pharmaceutical and personal care products (PPCPs) in surface water from Mankyung River, South Korea. *Journal of Health Science*, 2009. **55**(2): p. 249-258.

37. da Silva, B.F., A. Jelic, R. López-Serna, A.A. Mozeto, M. Petrovic, and D. Barceló, Occurrence and distribution of pharmaceuticals in surface water, suspended solids and sediments of the Ebro river basin, Spain. *Chemosphere*, 2011. **85**(8): p. 1331-1339.

38. Yoon, Y., J. Ryu, J. Oh, B.-G. Choi, and S.A. Snyder, Occurrence of endocrine disrupting compounds, pharmaceuticals, and personal care products in the Han River (Seoul, South Korea). *Science of the Total Environment*, 2010. **408**(3): p. 636-643.

39. Feitosa-Felizzola, J. and S. Chiron, Occurrence and distribution of selected antibiotics in a small Mediterranean stream (Arc River, Southern France). *Journal of Hydrology*, 2009. **364**(1): p. 50-57.

40. Scheurell, M., S. Franke, R. Shah, and H. Hühnerfuss, Occurrence of diclofenac and its metabolites in surface water and effluent samples from Karachi, Pakistan. *Chemosphere*, 2009. **77**(6): p. 870-876.

41. Peng, X., Y. Yu, C. Tang, J. Tan, Q. Huang, and Z. Wang, Occurrence of steroid estrogens, endocrine-disrupting phenols, and acid pharmaceutical residues in urban riverine water of the Pearl River Delta, South China. *Science of the total environment*, 2008. **397**(1): p. 158-166.

42. Fick, J., H. Söderström, R.H. Lindberg, C. Phan, M. Tysklind, and D. Larsson, Contamination of surface, ground, and drinking water from pharmaceutical production. *Environmental Toxicology and Chemistry*, 2009. **28**(12): p. 2522-2527.

43. Watkinson, A., E. Murby, D. Kolpin, and S. Costanzo, The occurrence of antibiotics in an urban watershed: from wastewater to drinking water. *Science of the total environment*, 2009. **407**(8): p. 2711-2723.

44. Chen, Y., K. Zhang, and Y. Zuo, Direct and indirect photodegradation of estriol in the presence of humic acid, nitrate and iron complexes in water solutions. *Science of the Total Environment*, 2013. **463**: p. 802-809.

45. Vasconcelos, T.G., D.M. Henriques, A. König, A.F. Martins, and K. Kümmerer, Photo-degradation of the antimicrobial ciprofloxacin at high pH: identification and biodegradability assessment of the primary by-products. *Chemosphere*, 2009. **76**(4): p. 487-493.

46. Dodard, S.G., A.Y. Renoux, J. Hawari, G. Ampleman, S. Thiboutot, and G.I. Sunahara, Ecotoxicity characterization of dinitrotoluenes and some of their reduced metabolites. *Chemosphere*, 1999. **38**(9): p. 2071-2079.

47. Markandya, A., T. Taylor, A. Longo, M. Murty, S. Murty, and K. Dhavala, Counting the cost of vulture decline—an appraisal of the human health and other benefits of vultures in India. *Ecological economics*, 2008. **67**(2): p. 194-204.

48. Heberer, T., Occurrence, fate, and removal of pharmaceutical residues in the aquatic environment: a review of recent research data. *Toxicology letters*, 2002. **131**(1): p. 5-17.

49. Brozinski, J.-M., M. Lahti, A. Meierjohann, A. Oikari, and L. Kronberg, The anti-inflammatory drugs diclofenac, naproxen and ibuprofen are found in the bile of wild fish caught downstream of a wastewater treatment plant. *Environmental science & technology*, 2012. **47**(1): p. 342-348.

50. Huerta, B., A. Jakimska, M. Llorca, A. Ruhí, G. Margoutidis, V. Acuña, S. Sabater, S. Rodriguez-Mozaz, and D. Barcelò, Development of an extraction and purification method for the determination of multi-class pharmaceuticals and endocrine disruptors in freshwater invertebrates. *Talanta*, 2015. **132**: p. 373-381.

51. Huerta, B., A. Jakimska, M. Gros, S. Rodríguez-Mozaz, and D. Barceló, Analysis of multi-class pharmaceuticals in fish tissues by ultra-high-performance liquid chromatography tandem mass spectrometry. *Journal of Chromatography A*, 2013. **1288**: p. 63-72.

52. Fick, J., R.H. Lindberg, J. Parkkonen, B.r. Arvidsson, M. Tysklind, and D.J. Larsson, Therapeutic levels of levonorgestrel detected in blood plasma of fish: results from screening rainbow trout exposed to treated sewage effluents. *Environmental science & technology*, 2010. **44**(7): p. 2661-2666.

53. Klosterhaus, S.L., R. Grace, M.C. Hamilton, and D. Yee, Method validation and reconnaissance of pharmaceuticals, personal care products, and alkylphenols in surface waters, sediments, and mussels in an urban estuary. *Environment international*, 2013. **54**: p. 92-99.

54. McEneff, G., L. Barron, B. Kelleher, B. Paull, and B. Quinn, A year-long study of the spatial occurrence and relative distribution of pharmaceutical residues in sewage effluent, receiving marine waters and marine bivalves. *Science of the Total Environment*, 2014. **476**: p. 317-326.

55. Bringolf, R.B., R.M. Heltsley, T.J. Newton, C.B. Eads, S.J. Fraley, D. Shea, and W.G. Cope, Environmental occurrence and reproductive effects of the pharmaceutical fluoxetine in native freshwater mussels. *Environmental Toxicology and Chemistry*, 2010. **29**(6): p. 1311-1318.

56. Dodder, N.G., K.A. Maruya, P.L. Ferguson, R. Grace, S. Klosterhaus, M.J. La Guardia, G.G. Lauenstein, and J. Ramirez, Occurrence of contaminants of emerging concern in mussels (Mytilus spp.) along the California coast and the influence of land use, storm water discharge, and treated wastewater effluent. *Marine pollution bulletin*, 2014. **81**(2): p. 340-346.

57. Subedi, B., B. Du, C.K. Chambliss, J. Koschorreck, H. Rüdel, M. Quack, B.W. Brooks, and S. Usenko, Occurrence of pharmaceuticals and personal care products in German fish tissue: a national study. *Environmental science & technology*, 2012. **46**(16): p. 9047-9054.

58. Schultz, M.M., E.T. Furlong, D.W. Kolpin, S.L. Werner, H.L. Schoenfuss, L.B. Barber, V.S. Blazer, D.O. Norris, and A.M. Vajda, Antidepressant pharmaceuticals in two US effluent-impacted streams: occurrence and fate in water and sediment, and selective uptake in fish neural tissue. *Environmental science & technology*, 2010. **44**(6): p. 1918-1925.

59. Maruya, K.A., D.E. Vidal-Dorsch, S.M. Bay, J.W. Kwon, K. Xia, and K.L. Armbrust, Organic contaminants of emerging concern in sediments and flatfish collected near outfalls discharging treated wastewater effluent to the Southern California Bight. *Environmental Toxicology and Chemistry*, 2012. **31**(12): p. 2683-2688.

60. Mezzelani, M., S. Gorbi, Z. Da Ros, D. Fattorini, G. d'Errico, M. Milan, L. Bargelloni, and F. Regoli, Ecotoxicological potential of non-steroidal anti-inflammatory drugs (NSAIDs) in marine organisms: Bioavailability, biomarkers and natural occurrence in Mytilus galloprovincialis. *Marine environmental research*, 2016. **121**: p. 31 - 39.

61. Huerta, B., S. Rodríguez-Mozaz, and D. Barceló, Pharmaceuticals in biota in the aquatic environment: analytical methods and environmental implications. *Analytical and bioanalytical chemistry*, 2012. **404**(9): p. 2611-2624.

62. Fromme, H., T. Küchler, T. Otto, K. Pilz, J. Müller, and A. Wenzel, Occurrence of phthalates and bisphenol A and F in the environment. *Water research*, 2002. **36**(6): p. 1429-1438.

63. Ternes, T.A., Occurrence of drugs in German sewage treatment plants and rivers. *Water research*, 1998. **32**(11): p. 3245-3260.

64. Johnson, P., P. Rising, T. Rising, M. Crook, P. Johnson, and B. Scales. *Liquid scintillation counting*. in *Symposium on liquid*. 1972. Citeseer.

65. Voltz, R., G. Laustriat, and A. Coche, FLUORESCENCE-MECANISME DU TRANSFERT DENERGIE DANS LES SCINTILLATEURS LIQUIDES. *COMPTES RENDUS HEBDOMADAIRES DES SEANCES DE L ACADEMIE DES SCIENCES*, 1963. **257**(7): p. 1473-&.

66. Birks, J., Energy transfer in organic phosphors. *Physical Review*, 1954. **94**(6): p. 1567.

67. Birks, J. and J. Conte. *Excimer Fluorescence. XI. Solvent-Solute Energy Transfer*. in *Proceedings of the Royal Society of London A: Mathematical, Physical and Engineering Sciences*. 1968. The Royal Society.

68. Tsvet, M., Physical chemical studies on chlorophyll adsorptions. *Ber. Dtsch. Bot. Ges*, 1906. **24**: p. 316-323.

69. Giddings, J., Comparison of the Theoretical Limit of Separating Ability in Gas and Liquid Chromatography. *Analytical Chemistry*, 1964. **36**(10): p. 1890-1892.

70. Van Deemter, J.J., F. Zuiderweg, and A.v. Klinkenberg, Longitudinal diffusion and resistance to mass transfer as causes of nonideality in chromatography. *Chemical Engineering Science*, 1956. **5**(6): p. 271-289.

71. Knox, J.H. and H.P. Scott, VII. International symposium on column liquid chromatographyB and C terms in the Van Deemter equation for liquid chromatography. *Journal of Chromatography A*, 1983. **282**: p. 297-313.

72. Scott, R.P., Principles and practice of chromatography. *Chrom-Ed Book Series*, 2003. **1**.

73. Faust, C.B., *Modern chemical techniques*. 1992: Royal Soc. of Chemistry, Educ. Divn.

74. Henchman, M. and C. Steel, Understanding the quadrupole mass filter through computer simulation*. J. Chem. Educ*, 1998. **75**(8): p. 1049.

75. Yamashita, M. and J.B. Fenn, Electrospray ion source. Another variation on the free-jet theme*. The Journal of Physical Chemistry*, 1984. **88**(20): p. 4451-4459.

76. Abian, J., The coupling of gas and liquid chromatography with mass spectrometry*. Journal of mass spectrometry*, 1999. **34**: p. 157-168.

77. Wilm, M.S. and M. Mann, Electrospray and Taylor-Cone theory, Dole's beam of macromolecules at last? *International Journal of Mass Spectrometry and Ion Processes*, 1994. **136**(2-3): p. 167-180.

78. Iribarne, J. and B. Thomson, On the evaporation of small ions from charged droplets*. The Journal of Chemical Physics*, 1976. **64**(6): p. 2287-2294.

79. De La Mora, J.F., Electrospray ionization of large multiply charged species proceeds via Dole's charged residue mechanism*. Analytica chimica acta*, 2000. **406**(1): p. 93-104.

80. Nguyen, S. and J.B. Fenn, Gas-phase ions of solute species from charged droplets of solutions*. Proceedings of the National Academy of Sciences*, 2007. **104**(4): p. 1111-1117.

81. Huie, C.W., A review of modern sample-preparation techniques for the extraction and analysis of medicinal plants*. Analytical and Bioanalytical Chemistry*, 2002. **373**(1): p. 23-30.

82. Kaufmann, B. and P. Christen, Recent extraction techniques for natural products: microwave-assisted extraction and pressurised solvent extraction. *Phytochemical analysis*, 2002. **13**(2): p. 105-113.

83. Mol, H.G.J., R.C.J. van Dam, and O.M. Steijger, Determination of polar organophosphorus pesticides in vegetables and fruits using liquid chromatography with tandem mass spectrometry: selection of extraction solvent. *Journal of Chromatography A*, 2003. **1015**(1–2): p. 119-127.

84. Thoo, Y.Y., S.K. Ho, J.Y. Liang, C.W. Ho, and C.P. Tan, Effects of binary solvent extraction system, extraction time and extraction temperature on phenolic antioxidants and antioxidant capacity from mengkudu (Morinda citrifolia). *Food Chemistry*, 2010. **120**(1): p. 290-295.

85. Hennion, M.-C., Solid-phase extraction: method development, sorbents, and coupling with liquid chromatography. *Journal of chromatography A*, 1999. **856**(1): p. 3-54.

86. Bielicka-Daszkiewicz, K. and A. Voelkel, Theoretical and experimental methods of determination of the breakthrough volume of SPE sorbents. *Talanta*, 2009. **80**(2): p. 614-621.

87. Olson, K.R., H.L. Bergman, and P.O. Fromm, Uptake of Methyl Mercuric Chloride and Mercuric Chloride by Trout: A Study of Uptake Pathways into the Whole Animal and Uptake by Erythrocytes in vitro. *Journal of the Fisheries Research Board of Canada*, 1973. **30**(9): p. 1293-1299.

88. Granmo, Å. and S. Kollberg, Uptake pathways and elimination of a nonionic surfactant in cod (Gadus morrhua L.). *Water Research*, 1976. **10**(3): p. 189-194.

89. Rouleau, C., Z.-H. Xiong, G. Pacepavicius, and G.-L. Huang, Uptake of waterborne tributyltin in the brain of fish: axonal transport as a proposed

mechanism. *Environmental science & technology*, 2003. **37**(15): p. 3298-3302.

90. McKim, J., P. Schmieder, and G. Veith, Absorption dynamics of organic chemical transport across trout gills as related to octanol-water partition coefficient. *Toxicology and applied pharmacology*, 1985. **77**(1): p. 1-10.

91. Dobson, P.D. and D.B. Kell, Carrier-mediated cellular uptake of pharmaceutical drugs: an exception or the rule? *Nature Reviews Drug Discovery*, 2008. **7**(3): p. 205-220.

92. Cooper, C.A., M. Shayeghi, M.E. Techau, D.M. Capdevila, S. MacKenzie, C. Durrant, and N.R. Bury, Analysis of the rainbow trout solute carrier 11 family reveals iron import ⩽ pH 7.4 and a functional isoform lacking transmembrane domains 11 and 12. *FEBS Letters*, 2007. **581**(14): p. 2599-2604.

93. Kurth, D., W. Brack, and T. Luckenbach, Is chemosensitisation by environmental pollutants ecotoxicologically relevant? *Aquatic Toxicology*, 2015. **167**: p. 134-142.

94. Fardel, O., E. Kolasa, and M. Le Vee, Environmental chemicals as substrates, inhibitors or inducers of drug transporters: implication for toxicokinetics, toxicity and pharmacokinetics. *Expert Opinion on Drug Metabolism & Toxicology*, 2012. **8**(1): p. 29-46.

95. Eraly, S.A., J.C. Monte, and S.K. Nigam, Novel slc22 transporter homologs in fly, worm, and human clarify the phylogeny of organic anion and cation transporters. *Physiological genomics*, 2004. **18**(1): p. 12-24.

96. Giltrow, E., P.D. Eccles, M.J. Winter, P.J. McCormack, M. Rand-Weaver, T.H. Hutchinson, and J.P. Sumpter, Chronic effects assessment and

plasma concentrations of the β-blocker propranolol in fathead minnows (Pimephales promelas). *Aquatic toxicology*, 2009. **95**(3): p. 195-202.

97. Evans, D.H., P.M. Piermarini, and W. Potts, Ionic transport in the fish gill epithelium. *Journal of Experimental Zoology*, 1999. **283**(7): p. 641-652.

98. Erickson, R.J., J.M. McKim, G.J. Lien, A.D. Hoffman, and S.L. Batterman, Uptake and elimination of ionizable organic chemicals at fish gills: I. Model formulation, parameterization, and behavior. *Environmental toxicology and chemistry*, 2006. **25**(6): p. 1512-1521.

99. Ackerman, M.J. and D.E. Clapham, Ion channels—basic science and clinical disease. *New England Journal of Medicine*, 1997. **336**(22): p. 1575-1586.

100. Nichols, J.W., J.M. McKim, G.J. Lien, A.D. Hoffman, S.L. Bertelsen, and C.M. Elonen, A physiologically based toxicokinetic model for dermal absorption of organic chemicals by fish. *Toxicological Sciences*, 1996. **31**(2): p. 229-242.

101. McKim, J.M., J.W. Nichols, G.J. Lien, A.D. Hoffman, C.A. Gallinat, and G.N. Stokes, Dermal absorption of three waterborne chloroethanes in rainbow trout (Oncorhynchus mykiss) and channel catfish (Ictalurus punctatus). *Toxicological Sciences*, 1996. **31**(2): p. 218-228.

102. Nadeem, R., T.M. Ansari, and A.M. Khalid, Fourier Transform Infrared Spectroscopic characterization and optimization of Pb (II) biosorption by fish (Labeo rohita) scales. *Journal of Hazardous Materials*, 2008. **156**(1): p. 64-73.

103. Ikoma, T., H. Kobayashi, J. Tanaka, D. Walsh, and S. Mann, Microstructure, mechanical, and biomimetic properties of fish scales from Pagrus major. *Journal of Structural Biology*, 2003. **142**(3): p. 327-333.

104. Ikoma, T., H. Kobayashi, J. Tanaka, D. Walsh, and S. Mann, Physical properties of type I collagen extracted from fish scales of Pagrus major and Oreochromis niloticas*. International Journal of Biological Macromolecules*, 2003. **32**(3): p. 199-204.

105. Poet, T.S., R.A. Corley, K.D. Thrall, J.A. Edwards, H. Tanojo, K.K. Weitz, X. Hui, H.I. Maibach, and R.C. Wester, Assessment of the percutaneous absorption of trichloroethylene in rats and humans using MS/MS real-time breath analysis and physiologically based pharmacokinetic modeling*. Toxicological Sciences*, 2000. **56**(1): p. 61-72.

106. Santana-Casiano, J.M. and M. Gonzalez-Davila, Characterization of the sorption and desorption of lindane to chitin in seawater using reversible and resistant components*. Environmental science & technology*, 1992. **26**(1): p. 90-95.

107. Lord, K., The sorption of DDT and its analogues by chitin*. Biochemical Journal*, 1948. **43**(1): p. 72.

108. González-Dávila, M., J. Santana-Casiano, and J. Perez-Pena, Partitioning of hydrochlorinated pesticides to chitin in seawater: Use of a radial-diffusion model to describe apparent desorption hysteresis*. Chemosphere*, 1995. **30**(8): p. 1477-1487.

109. Keiluweit, M. and M. Kleber, Molecular-level interactions in soils and sediments: the role of aromatic π-systems*. Environmental science & technology*, 2009. **43**(10): p. 3421-3429.

110. Thomann, R.V., Bioaccumulation model of organic chemical distribution in aquatic food chains*. Environmental science & technology*, 1989. **23**(6): p. 699-707.

111. Clark, K.E., F.A. Gobas, and D. Mackay, Model of organic chemical uptake and clearance by fish from food and water. *Environmental science & technology*, 1990. **24**(8): p. 1203-1213.

112. Veith, G.D., D.L. DeFoe, and B.V. Bergstedt, Measuring and estimating the bioconcentration factor of chemicals in fish. *Journal of the Fisheries Board of Canada*, 1979. **36**(9): p. 1040-1048.

113. Norstrom, R., A. McKinnon, and A. DeFreitas, A bioenergetics-based model for pollutant accumulation by fish. Simulation of PCB and methylmercury residue levels in Ottawa River yellow perch (Perca flavescens). *Journal of the Fisheries Board of Canada*, 1976. **33**(2): p. 248-267.

114. Spacie, A. and J.L. Hamelink, Alternative models for describing the bioconcentration of organics in fish. *Environmental Toxicology and Chemistry*, 1982. **1**(4): p. 309-320.

115. Schüürmann, G. and W. Klein, Advances in bioconcentration prediction. *Chemosphere*, 1988. **17**(8): p. 1551-1574.

116. Garg, R. and C.J. Smith, Predicting the bioconcentration factor of highly hydrophobic organic chemicals. *Food and Chemical Toxicology*, 2014. **69**: p. 252-259.

117. OECD, *Test No. 305: Bioaccumulation in Fish: Aqueous and Dietary Exposure*. OECD Publishing.

118. Lu, X., D.D. Reible, J.W. Fleeger, and Y. Chai, Bioavailability of desorption-resistant phenanthrene to the oligochaete Ilyodrilus templetoni. *Environmental Toxicology and Chemistry*, 2003. **22**(1): p. 153-160.

119. Freidig, A.P., E.A. Garicano, F.J. Busser, and J.L. Hermens, Estimating impact of humic acid on bioavailability and bioaccumulation of hydrophobic

chemicals in guppies using kinetic solid-phase extraction. *Environmental Toxicology and Chemistry*, 1998. **17**(6): p. 998-1004.

120. Smital, T., T. Luckenbach, R. Sauerborn, A.M. Hamdoun, R.L. Vega, and D. Epel, Emerging contaminants—pesticides, PPCPs, microbial degradation products and natural substances as inhibitors of multixenobiotic defense in aquatic organisms. *Mutation Research/Fundamental and Molecular Mechanisms of Mutagenesis*, 2004. **552**(1): p. 101-117.

121. Rubach, M.N., D.J. Baird, and P.J. Van den Brink, A new method for ranking mode-specific sensitivity of freshwater arthropods to insecticides and its relationship to biological traits. *Environmental Toxicology and Chemistry*, 2010. **29**(2): p. 476-487.

122. Keteles, K. and J. Fleeger, The contribution of ecdysis to the fate of copper, zinc and cadmium in grass shrimp, Palaemonetes pugio Holthius. *Marine Pollution Bulletin*, 2001. **42**(12): p. 1397-1402.

123. Rubach, M.N., R. Ashauer, D.B. Buchwalter, H.J. De Lange, M. Hamer, T.G. Preuss, K. Töpke, and S.J. Maund, Framework for traits-based assessment in ecotoxicology. *Integrated environmental assessment and management*, 2011. **7**(2): p. 172-186.

124. Rust, A.J., R.M. Burgess, B.J. Brownawell, and A.E. McElroy, Relationship between metabolism and bioaccumulation of benzo[α]pyrene in benthic invertebrates. *Environmental Toxicology and Chemistry*, 2004. **23**(11): p. 2587-2593.

125. Meredith-Williams, M., L.J. Carter, R. Fussell, D. Raffaelli, R. Ashauer, and A.B. Boxall, Uptake and depuration of pharmaceuticals in aquatic invertebrates. *Environmental pollution*, 2012. **165**: p. 250-258.

126. Buchwalter, D., J. Jenkins, and L. Curtis, Respiratory strategy is a major determinant of [3H] water and [14C] chlorpyrifos uptake in aquatic insects. *Canadian Journal of Fisheries and Aquatic Sciences*, 2002. **59**(8): p. 1315-1322.

127. Ramirez, A.J., R.A. Brain, S. Usenko, M.A. Mottaleb, J.G. O'Donnell, L.L. Stahl, J.B. Wathen, B.D. Snyder, J.L. Pitt, and P. Perez-Hurtado, Occurrence of pharmaceuticals and personal care products in fish: results of a national pilot study in the United States. *Environmental Toxicology and Chemistry*, 2009. **28**(12): p. 2587-2597.

128. Paterson, G. and C.D. Metcalfe, Uptake and depuration of the anti-depressant fluoxetine by the Japanese medaka (Oryzias latipes). *Chemosphere*, 2008. **74**(1): p. 125-130.

129. Nakamura, Y., H. Yamamoto, J. Sekizawa, T. Kondo, N. Hirai, and N. Tatarazako, The effects of pH on fluoxetine in Japanese medaka (Oryzias latipes): Acute toxicity in fish larvae and bioaccumulation in juvenile fish. *Chemosphere*, 2008. **70**(5): p. 865-873.

130. Jimenez, B., C. Cirmo, and J. McCarthy, Effects of feeding and temperature on uptake, elimination and metabolism of benzo (a) pyrene in the bluegill sunfish (Lepomis macrochirus). *Aquatic toxicology*, 1987. **10**(1): p. 41-57.

131. Cheng, C.-Y., L.-L. Liu, and W.-H. Ding, Occurrence and seasonal variation of alkylphenols in marine organisms from the coast of Taiwan. *Chemosphere*, 2006. **65**(11): p. 2152-2159.

132. Mora, C., D.P. Tittensor, S. Adl, A.G. Simpson, and B. Worm, How many species are there on Earth and in the ocean? *PLoS Biol*, 2011. **9**(8): p. e1001127.

133. Prather, C.M., S.L. Pelini, A. Laws, E. Rivest, M. Woltz, C.P. Bloch, I. Del Toro, C.K. Ho, J. Kominoski, and T. Newbold, Invertebrates, ecosystem services and climate change. *Biological Reviews*, 2013. **88**(2): p. 327-348.

134. Mulder, C., Insects affect relationships between plant species richness and ecosystem processes. *Ecology letters*, 1999. **2**: p. 237-246.

135. Arthur, J.W., C.W. West, K.N. Allen, and S.F. Hedtke, Seasonal toxicity of ammonia to five fish and nine invertebrate species. *Bulletin of Environmental Contamination and Toxicology*, 1987. **38**(2): p. 324-331.

136. Kemble, N.E., W.G. Brumbaugh, E.L. Brunson, F.J. Dwyer, C.G. Ingersoll, D.P. Monda, and D.F. Woodward, Toxicity of metal-contaminated sediments from the upper clark fork river, montana, to aquatic invertebrates and fish in laboratory exposures. *Environmental Toxicology and Chemistry*, 1994. **13**(12): p. 1985-1997.

137. Holcombe, G.W., G.L. Phipps, A.H. Sulaiman, and A.D. Hoffman, Simultaneous multiple species testing: acute toxicity of 13 chemicals to 12 diverse freshwater amphibian, fish, and invertebrate families. *Archives of Environmental Contamination and Toxicology*, 1987. **16**(6): p. 697-710.

138. Morley, E.L., G. Jones, and A.N. Radford. *The importance of invertebrates when considering the impacts of anthropogenic noise*. in *Proc. R. Soc. B*. 2014. The Royal Society.

139. Jobling, S., D. Casey, T. Rodgers-Gray, J. Oehlmann, U. Schulte-Oehlmann, S. Pawlowski, T. Baunbeck, A. Turner, and C. Tyler, Comparative responses of molluscs and fish to environmental estrogens and an estrogenic effluent. *Aquatic toxicology*, 2003. **65**(2): p. 205-220.

140. Maltby, L., S.A. Clayton, R.M. Wood, and N. McLoughlin, Evaluation of the Gammarus pulex in situ feeding assay as a biomonitor of water quality:

robustness, responsiveness, and relevance. *Environmental Toxicology and Chemistry*, 2002. **21**(2): p. 361-368.

141. Felten, V., G. Charmantier, R. Mons, A. Geffard, P. Rousselle, M. Coquery, J. Garric, and O. Geffard, Physiological and behavioural responses of Gammarus pulex (Crustacea: Amphipoda) exposed to cadmium. *Aquatic Toxicology*, 2008. **86**(3): p. 413-425.

142. Matthiessen, P., D. Sheahan, R. Harrison, M. Kirby, R. Rycroft, A. Turnbull, C. Volkner, and R. Williams, Use of a Gammarus pulex bioassay to measure the effects of transient carbofuran runoff from farmland. *Ecotoxicology and Environmental Safety*, 1995. **30**(2): p. 111-119.

143. De Lange, H., W. Noordoven, A. Murk, M. Lürling, and E. Peeters, Behavioural responses of Gammarus pulex (Crustacea, Amphipoda) to low concentrations of pharmaceuticals. *Aquatic Toxicology*, 2006. **78**(3): p. 209-216.

144. Baun, A., N.B. Hartmann, K. Grieger, and K.O. Kusk, Ecotoxicity of engineered nanoparticles to aquatic invertebrates: a brief review and recommendations for future toxicity testing. *Ecotoxicology*, 2008. **17**(5): p. 387-395.

145. Maltby, L., C. Naylor, and P. Calow, Field deployment of a scope for growth assay involving Gammarus pulex, a freshwater benthic invertebrate. *Ecotoxicology and Environmental Safety*, 1990. **19**(3): p. 292-300.

146. Widdows, J., P. Donkin, F. Staff, P. Matthiessen, R. Law, Y. Allen, J. Thain, C. Allchin, and B. Jones, Measurement of stress effects (scope for growth) and contaminant levels in mussels (Mytilus edulis) collected from the Irish Sea. *Marine Environmental Research*, 2002. **53**(4): p. 327-356.

147. McCahon, C. and D. Pascoe, Use of Gammarus pulex (L.) in safety evaluation tests: culture and selection of a sensitive life stage. *Ecotoxicology and Environmental Safety*, 1988. **15**(3): p. 245-252.

148. Rubach, M.N., R. Ashauer, S.J. Maund, D.J. Baird, and P.J. Van den Brink, Toxicokinetic variation in 15 freshwater arthropod species exposed to the insecticide chlorpyrifos. *Environmental Toxicology and Chemistry*, 2010. **29**(10): p. 2225-2234.

149. Plaistow, S.J., J.-P. Troussard, and F. Cézilly, The effect of the acanthocephalan parasite Pomphorhynchus laevis on the lipid and glycogen content of its intermediate host Gammarus pulex. *International journal for parasitology*, 2001. **31**(4): p. 346-351.

150. Halcrow, K., The fine structure of the pore canals of the talitrid amphipod Hyale nilssoni Rathke. *Journal of crustacean biology*, 1985. **5**(4): p. 606-615.

151. Roer, R. and R. Dillaman, The structure and calcification of the crustacean cuticle. *American Zoologist*, 1984. **24**(4): p. 893-909.

152. Dennell, R. and S.R.A. Malek, The Cuticle of the Cockroach Periplaneta americana. II. The Epicuticle. *Proceedings of the Royal Society of London. Series B - Biological Sciences*, 1955. **143**(911): p. 239-257.

153. Philogène, B.J. and J. McFarlane, The formation of the cuticle in the house cricket, Acheta domesticus (L.), and the role of oenocytes. *Canadian Journal of Zoology*, 1967. **45**(2): p. 181-190.

154. Aragon, S., S. Claudinot, C. Blais, M. Maïbèche, and C. Dauphin-Villemant, Molting cycle-dependent expression of CYP4C15, a cytochrome P450 enzyme putatively involved in ecdysteroidogenesis in

the crayfish, Orconectes limosus. *Insect biochemistry and molecular biology*, 2002. **32**(2): p. 153-159.

155. Ashauer, R., I. Caravatti, A. Hintermeister, and B.I. Escher, Bioaccumulation kinetics of organic xenobiotic pollutants in the freshwater invertebrate Gammarus pulex modeled with prediction intervals. *Environmental Toxicology and Chemistry*, 2010. **29**(7): p. 1625-1636.
156. Rösch, A., S. Anliker, and J. Hollender, How Biotransformation influences Toxicokinetics of Azole Fungicides in the Aquatic Invertebrate Gammarus pulex. *Environmental science & technology*, 2016.
157. Gómez-Canela, C., T.H. Miller, N.R. Bury, R. Tauler, and L.P. Barron, Targeted metabolomics of Gammarus pulex following controlled exposures to selected pharmaceuticals in water. *Science of The Total Environment*, 2016. **562**: p. 777-788.
158. Commission, E., Regulation (EC) No 1907/2006 of the European Parliament and of the Council of 18 December 2006 concerning the Registration, Evaluation, Authorisation and Restriction of Chemicals (REACH), establishing a European Chemicals Agency, amending Directive 1999/45/EC and repealing Council Regulation (EEC) No 793/93 and Commission Regulation (EC) No 1488/94 as well as Council Directive 76/769/EEC and Commission Directives 91/155/EEC, 93/67/EEC, 93/105/EC and 2000/21/EC. *Official Journal of the European Union* 2006. **OJ L 396**.
159. van der Gon, H.D., M. van het Bolscher, A. Visschedijk, and P. Zandveld, Emissions of persistent organic pollutants and eight candidate POPs from UNECE–Europe in 2000, 2010 and 2020 and the emission reduction

resulting from the implementation of the UNECE POP protocol. *Atmospheric Environment*, 2007. **41**(40): p. 9245-9261.

160. Agreement, O., 3: Strategy of the OPSAR Commission for the Protection of the Marine Environment of the North-East Atlantic 2010-2020 (also called: The North-East Atlantic Environment Strategy). *Offshore Oil and Gas Industry Strategy*, 2010.
161. Porsbring, T., H. Blanck, H. Tjellström, and T. Backhaus, Toxicity of the pharmaceutical clotrimazole to marine microalgal communities. *Aquatic Toxicology*, 2009. **91**(3): p. 203-211.
162. Directive, W.F., Directive 2000/60. *EC of the European Parliament and of the Council of*, 2000. **23**(1).
163. Ronan, J.M. and B. McHugh, A sensitive liquid chromatography/tandem mass spectrometry method for the determination of natural and synthetic steroid estrogens in seawater and marine biota, with a focus on proposed Water Framework Directive Environmental Quality Standards. *Rapid Communications in Mass Spectrometry*, 2013. **27**(7): p. 738-746.
164. Ågerstrand, M., C. Berg, B. Björlenius, M. Breitholtz, B.r. Brunström, J. Fick, L. Gunnarsson, D.J. Larsson, J.P. Sumpter, and M. Tysklind, Improving environmental risk assessment of human pharmaceuticals. *Environmental science & technology*, 2015. **49**(9): p. 5336-5345.
165. Dearden, J.C., QSAR modeling of bioaccumulation. *Predicting chemical toxicity and fate*, 2004: p. 333-355.
166. Devillers, J., Linear versus nonlinear QSAR modeling of the toxicity of phenol derivatives to Tetrahymena pyriformis. *SAR and QSAR in Environmental Research*, 2004. **15**(4): p. 237-249.

167. Agatonovic-Kustrin, S. and R. Beresford, Basic concepts of artificial neural network (ANN) modeling and its application in pharmaceutical research. *Journal of pharmaceutical and biomedical analysis*, 2000. **22**(5): p. 717-727.

168. Czermiński, R., A. Yasri, and D. Hartsough, Use of support vector machine in pattern classification: Application to QSAR studies. *Quantitative Structure-Activity Relationships*, 2001. **20**(3): p. 227-240.

169. Devillers, J., A. Chezeau, and E. Thybaud, PLS-QSAR of the adult and developmental toxicity of chemicals to Hydra attenuata. *SAR and QSAR in Environmental Research*, 2002. **13**(7-8): p. 705-712.

170. Basant, N., S. Gupta, and K.P. Singh, Predicting toxicities of diverse chemical pesticides in multiple avian species using tree-based QSAR approaches for regulatory purposes. *Journal of chemical information and modeling*, 2015. **55**(7): p. 1337-1348.

171. Hansch, C., D. Hoekman, and H. Gao, Comparative QSAR: toward a deeper understanding of chemicobiological interactions. *Chemical reviews*, 1996. **96**(3): p. 1045-1076.

172. Gardner, M.W. and S. Dorling, Artificial neural networks (the multilayer perceptron)—a review of applications in the atmospheric sciences. *Atmospheric environment*, 1998. **32**(14): p. 2627-2636.

173. Specht, D.F., Probabilistic neural networks. *Neural networks*, 1990. **3**(1): p. 109-118.

174. Bishop, C., Improving the generalization properties of radial basis function neural networks. *Neural computation*, 1991. **3**(4): p. 579-588.

175. Bottou, L., *Large-scale machine learning with stochastic gradient descent*, in *Proceedings of COMPSTAT'2010*. 2010, Springer. p. 177-186.

176. Rumelhart, D.E., G.E. Hinton, and R.J. Williams, Learning representations by back-propagating errors*. Cognitive modeling*, 1988. **5**(3): p. 1.

177. LeCun, Y., L. Bottou, Y. Bengio, and P. Haffner, Gradient-based learning applied to document recognition*. Proceedings of the IEEE*, 1998. **86**(11): p. 2278-2324.

178. Bergstra, J. and Y. Bengio, Random search for hyper-parameter optimization*. Journal of Machine Learning Research*, 2012. **13**(Feb): p. 281-305.

179. Tetko, I.V., D.J. Livingstone, and A.I. Luik, Neural network studies. 1. Comparison of overfitting and overtraining*. Journal of chemical information and computer sciences*, 1995. **35**(5): p. 826-833.

180. Rahiman, M.H.F., M.N. Taib, R. Adnan, and Y.M. Salleh. *Analysis of weight decay regularisation in NNARX nonlinear identification*. in *Signal Processing & Its Applications, 2009. CSPA 2009. 5th International Colloquium on*. 2009. IEEE.

181. Prechelt, L., *Early stopping-but when?*, in *Neural Networks: Tricks of the trade*. 1998, Springer. p. 55-69.

182. Cronin, M.T. and J.C. Dearden, QSAR in toxicology. 1. Prediction of aquatic toxicity*. Quantitative Structure-Activity Relationships*, 1995. **14**(1): p. 1-7.

183. Sabljić, A., H. Güsten, H. Verhaar, and J. Hermens, QSAR modelling of soil sorption. Improvements and systematics of log K OC vs. log K OW correlations*. Chemosphere*, 1995. **31**(11): p. 4489-4514.

184. de Lima Ribeiro, F.A. and M.M.C. Ferreira, QSPR models of boiling point, octanol–water partition coefficient and retention time index of polycyclic

aromatic hydrocarbons. *Journal of Molecular Structure: THEOCHEM*, 2003. **663**(1): p. 109-126.

185. Gramatica, P., F. Consolaro, and S. Pozzi, QSAR approach to POPs screening for atmospheric persistence. *Chemosphere*, 2001. **43**(4): p. 655-664.

186. Duprat, A.F., T. Huynh, and G. Dreyfus, Toward a principled methodology for neural network design and performance evaluation in QSAR. Application to the prediction of logP. *Journal of chemical information and computer sciences*, 1998. **38**(4): p. 586-594.

187. Mjalli, F.S., S. Al-Asheh, and H. Alfadala, Use of artificial neural network black-box modeling for the prediction of wastewater treatment plants performance. *Journal of Environmental Management*, 2007. **83**(3): p. 329-338.

188. Gobas, F.A., B.C. Kelly, and J.A. Arnot, Quantitative Structure Activity Relationships for Predicting the Bioaccumulation of POPs in Terrestrial Food-Webs. *QSAR & Combinatorial Science*, 2003. **22**(3): p. 329-336.

189. Rovida, C. and T. Hartung, Re-evaluation of animal numbers and costs for in vivo tests to accomplish REACH legislation requirements for chemicals—a report by the transatlantic think tank for toxicology (t (4)). *Altex*, 2009. **26**(3): p. 187-208.

190. Ahlers, J., F. Stock, and B. Werschkun, Integrated testing and intelligent assessment—new challenges under REACH. *Environmental Science and Pollution Research*, 2008. **15**(7): p. 565-572.

191. Zeeman, M., C. Auer, R. Clements, J. Nabholz, and R. Boethling, US EPA regulatory perspectives on the use of QSAR for new and existing chemical

evaluations. *SAR and QSAR in Environmental Research*, 1995. **3**(3): p. 179-201.

192. Agency, E.C., Guidance on information requirements and chemical safety assessment Chapter R.6: QSARs and grouping of chemicals. 2008.

193. Kaiser, K.L., The use of neural networks in QSARs for acute aquatic toxicological endpoints. *Journal of Molecular Structure: THEOCHEM*, 2003. **622**(1): p. 85-95.

194. Xu, L., J. Ball, S. Dixon, and P. Jurs, Quantitative structure-activity relationships for toxicity of phenols using regression analysis and computational neural networks. *Environmental toxicology and chemistry*, 1994. **13**(5): p. 841-851.

195. Alvarez-Guerra, M., D. Ballabio, J.M. Amigo, R. Bro, and J.R. Viguri, Development of models for predicting toxicity from sediment chemistry by partial least squares-discriminant analysis and counter-propagation artificial neural networks. *Environmental pollution*, 2010. **158**(2): p. 607-614.

196. Fatemi, M., M. Jalali-Heravi, and E. Konuze, Prediction of bioconcentration factor using genetic algorithm and artificial neural network. *Analytica chimica acta*, 2003. **486**(1): p. 101-108.

Chapter 2. The development of a multi-residue LC-MS method for the determination of pharmaceutical residues in *Gammarus pulex*

2.1 Introduction

Research into the field of ecotoxicology arguably began with Rachel Carson in the early 1960's [1]. Research efforts have gained momentum within environmental toxicology to study the effects of a number of anthropogenic contaminants. These contaminants cover several different classes of compounds including synthetic hormones, polychlorinated biphenyls (PCBs), polyaromatic hydrocarbons (PAHs), pharmaceuticals and personal care products (PPCPs) [2-5]. Monitoring studies across the globe have determined the concentrations of these contaminants ranging from low ng L^{-1} to mg L^{-1} depending on the region and legislation in place to reduce contamination and pollution [6-8]. The class of compounds known as PPCPs have been designated as emerging contaminants due to their occurrence and with little understanding of the risk they pose to the environment [9].

Until recently, the only body that recognised the concern of PPCPs was the Oslo-Paris Convention for the Protection of the Marine Environment of the North-East Atlantic (OPSAR). However, due to potential adverse effects in the environment, two PPCPs were added to the 'watch list' of the EU Water Framework Directive which aims to regulate emissions of contaminants/pollutants into bodies of water. The 'watch list,' has no formal regulation for compounds designated under this list. However, they are monitored in surface water so that they may be added to the 'priority list,' if required. The number of compounds in this class is over several thousand and cover a diverse range of physicochemical properties, thus efforts to identify the potential risks

presents a challenge in the field. Furthermore, environmental factors such as temporal flow, dissolved organic matter (DOM) and pH in aquatic matrices may lead to complex interactions between cause and effects [10].

Many investigations to date have only considered surface water concentrations with less attention given to internal concentrations in biota. The measurement of these internal concentrations is now considered key to the understanding and prediction of risk [11]. Few methods have been reported that can determine internal concentrations of pharmaceuticals in biota, with most methods focused on fish tissue and mussels [12]. A study by McEneff et al. [13], determined concentrations of trimethoprim reaching up to 9 ng g^{-1} in marine mussels off the coast of Ireland. Researchers focussing on marine mussels in San Francisco, reported the occurrence of compounds such as carbamazepine (5.3 ng g^{-1}), sertraline (1.4 ng g^{-1}), atenolol (0.3 ng g^{-1}) amitriptyline (0.2 ng g^{-1}) [14]. A report of a similar study along the coast of California showed mean concentrations of pharmaceuticals reaching up to 29 ng g^{-1} dry weight (dw) [15]. Venlafaxine was measured in marine mussels at 2.7 ng g^{-1} dw [16]. Freshwater mussels were observed to accumulate fluoxetine from an effluent channel, reaching a mean measured concentration of 79.1 ng g^{-1} wet weight (ww) [17]. A reason for the small number of investigations into occurrence of pharmaceuticals in biota is that complex biological matrices present a significant analytical challenge for the reliable measurement of trace pharmaceutical residues that may be found in these organisms.

Models that are concerned with uptake and accumulation are often based on hydrophobicity (log*P*) such as early studies involving with non-polar organic chemicals where passive diffusion across membranes was predominant [18-20]. However, these models may fail to prioritise pharmaceuticals based on their

physicochemical properties (polarity, ionisation etc.). Mounting evidence has also suggested that carrier-mediated uptake is also important in accumulation for bioactive compounds such as pharmaceuticals [21, 22]. Thus, occurrence of PhACs in biota may also indicate compounds that have a potential to accumulate and that should be focused on in future investigations [23].

As mentioned above, reported biota occurrence is sparse with a small focus on fish, and to a lesser extent invertebrates. Furthermore, many of the selected invertebrates in monitoring campaigns are collected from estuarine or marine environments with fewer studies focusing on freshwater species [12]. This is important as many sources of PhAC contamination (WWTP, CSOs, agriculture etc.) will primarily enter freshwater environments. In addition, invertebrates are the largest and most diverse group within the *Animalia* kingdom and therefore are of significant importance to prioritise for environmental risk factors that may affect ecosystem services [24]. One particular species that is useful in monitoring campaigns of freshwater habitats is the amphipod *G. pulex*, which is common throughout Europe. This organism is a detritivore that is important for detritus processing in freshwater ecosystems and also serves as an important food source for fish and birds [25, 26]. Therefore, potential adverse effects would be important to identify within this animal. *G. pulex* has already been demonstrated to be a sensitive indicator of pollutants and contaminants in aquatic environments by using behavioural endpoints [27-30]. Pharmaceutical uptake in *G. pulex* has also been observed by Meredith-Williams et al. [31], which examined the kinetics of five pharmaceuticals with the largest BCF observed for the selective serotonin reuptake inhibitor (SSRI), fluoxetine (~185,000). However, multi-residue methods to determine internal concentrations in *G. pulex* are still lacking.

The aim of this chapter was to develop and optimise an analytical LC-MS/MS methodology for the detection and quantification of several pharmaceutical compounds in the selected aquatic invertebrate *G. pulex* using a combination of extraction techniques. Thus, enabling the confirmatory determination of trace pharmaceutical contamination in a freshwater invertebrate. Then the developed method was assessed for application to specimens sampled from several field sites (tributaries of the River Thames) to determine the occurrence of the selected pharmaceutical across the Greater London catchment area. The work herein represents the first study to report the environmental occurrence of pharmaceuticals in a freshwater invertebrate.

2.2 Materials & methods

2.2.1 Reagents, chemicals and consumables

HPLC grade methanol, acetonitrile, acetone, ethyl acetate, dichloromethane and dimethyldichlorosiloxane were purchased from Fischer Scientific (Loughborough, UK). Analytical grade ammonium acetate was sourced from Sigma-Aldrich (Dorset, UK). Propranolol hydrochloride, ketoprofen, diclofenac sodium salt, bezafibrate, warfarin, flurbiprofen, indomethacin, ibuprofen sodium salt, meclofenamic acid sodium salt, gemfibrozil, atenolol, sulfamethoxazole, sulfamethazine sodium salt, furosemide, carbamazepine, nimesulide, (±)-metoprolol (+)-tartrate salt, triclocarban, cimetidine, ranitidine, antipyrin, temazepam, diazepam, fluoxetine, nifedipine and mefenamic acid were all obtained from Sigma-Aldrich (Steinheim, Germany). Trimethoprim, caffeine, and naproxen were ordered from Fluka (Buchs, Switzerland). Stable isotope-labelled standards including carbamazepine-d_{10}, propranolol-d_7, temazepam-d_5 and diazepam-d_5 were ordered from Sigma-Aldrich. Trimethoprim-d_3 and

warfarin-d_5 were ordered from QMX Laboratories (Essex, UK). All pharmaceuticals were of a purity of ≥97 %. Ultra-pure water was obtained from a Millipore Milli-Q water purification system with a specific resistance of 18.2 MΩ.cm or greater (Millipore, Bedford, MA, USA). Stock solutions (1 mg mL^{-1}) were prepared in methanol and stored in silanised amber vials (40 mL). Working solutions were prepared daily in ultra-pure water, as required. All solutions were stored at 4^{o}C and in the dark for optimum stability.

2.2.2 Sample collection and preparation

Gammarid and surface water samples were sourced from eight tributaries of the River Thames, UK. Surface water chemistry (i.e. pH, DO and temperature) was not measured. These were spread across the greater London catchment area and included the River Wandle (Sites 1 and 2), the River Quaggy (Site 3), the River Ravenstone (Site 4), the River Cray (Sites 5 and 6), the River Darent (Site 7) and Beverley Brook (Site 8). The specific locations of the selected sites are shown in Figure 2.1. Adult specimens were collected in September 2012 via the kick sampling netting method and weighed >5 mg ww. Samples were transported back to the laboratory in Nalgene^{TM} flasks containing 500 mL of freshwater obtained from each corresponding sampling site. A bulk sample of *G. pulex* (~ 25 g dw) from Site 1 was used in all analytical method optimisation experiments and was taken six months prior to samples from the same site used for analyte determination. *G. pulex* were wiped free of debris, rinsed immediately with ultra-pure water (n=3) and gently blotted dry before freezing at -20 ^{o}C. A separate 1 L grab sample of surface water at each site was also collected and transported back to the laboratory in 500 mL Nalgene^{TM} flasks. Water samples were also frozen at -20 ^{o}C until analysis. All glassware and glass beads used for extraction were silanised prior to use and on a recurring monthly basis by washing

each vessel with 10 % (*v/v*) dichlorodimethylsilane solution in dichloromethane (n=3) and followed by a sequence of triplicate rinses with each of dichloromethane, methanol and ultrapure water respectively.

Figure 2.1: Location of the field sites were G. pulex were sampled from; site 1 & 2 – River Wandle, site 3 – River Quaggy, site 4 – River Ravensbourne, site 5 & 6 – River Cray, site 7 – River Darent and site 8 – Beverley Brook. Picture inset is the River Cray sampling site 5.

2.2.3 Sample extraction and clean-up

Prior to extraction, frozen *G. pulex* samples were lyophilised at -50 ^{o}C under vacuum for 24 hours and ground to a fine powder. Pulverised liquid extraction (PuLE) was performed on an Ultra-Turrax® tube driver (IKA, Staufen, Germany). The tube driver was used with an extraction vessel for sample homogenisation and extraction. The contents of the extraction tube were agitated at a set rate by means of a rotor located inside the tube. For each analysis, freeze-dried composite sample material from each sampling site (0.1 g, ~ 40 animals) was transferred to a 20 mL extraction tube (IKA) with any necessary spiking carried out directly onto the solid matrix using a 100 µL volume of an appropriate working solution followed by 5 mL of acetonitrile. The working solution solvent

was allowed to evaporate before the addition of the extraction solvent. Two glass beads (diameter 5 mm) were then added to the extraction tube to enable pulverisation of the sample and the tube agitated at 2,500 rotations per minute (rpm) for 5 minutes (optimised). Following extraction and settling, an aliquot of the supernatant (4.5 mL) was diluted to 100 mL with 10 mM ammonium acetate in ultra-pure water (pH 6.5). Solid phase extraction (SPE) was then carried out as in previously published work on a similar selection of compounds [32] on the diluted extract using Oasis HLB cartridges (6 mL, 200 mg, Waters Corp., Hertfordshire, UK). Before loading of the sample, SPE cartridges were first conditioned with 6 mL of methanol and 6 mL of ultra-pure water. After sample extraction, cartridges were then washed with 1 mL ultra-pure water and dried for ~30 min under vacuum. Sample extracts were eluted with 10 mL of 50:50 (*v/v*) ethyl acetate:acetone and dried under pure nitrogen (1.0 bar) and heated at 30 ^{o}C using a TurboVap (Biotage, Uppsala, Sweden). Extract residues were reconstituted in 0.5 mL 90:10 (*v/v*) 10 mM ammonium acetate in water:acetonitrile. Surface water samples (100 mL) were adjusted to pH 6.5 with ammonium acetate (1 mL of a 1 M solution). Water samples then underwent SPE and reconstitution as described above. Any necessary spiking or liquid volume measurements were carried out using positive displacement pipettes (Gilson Microman, Villiers-le-Bel, France).

2.2.4 Instrumental conditions

A previously published chromatographic method for the analysis of PPCPs in soil and sludge was adapted and applied here [32]. Liquid chromatography (LC) was performed on an Agilent 1100 series LC system (Agilent Technologies, Cheshire, UK) using a Waters SunFire C_{18} column (3.5 µm, 2.1 mm x 150 mm, Waters Corp., Milford, MA, USA) with a KrudKatcher^{TM} Ultra guard column (0.1

mm ID, 0.5 µm filter, Phenomenex, Macclesfield, UK) at a flow rate of 0.2 mL min^{-1} and an injection volume of 20 µL. Mobile phases were 90:10 (*v/v*) 10 mM ammonium acetate in water:acetonitrile (A) and 20:80 (*v/v*) 10 mM ammonium acetate in water:acetonitrile (B). The profile followed a linear gradient ramp of mobile phase B which increased to 10 % at 5 min, 35 % at 28 min, 40 % at 35 min, 50 % at 40 min and 100 % at 55 min and was held for a further 7.5 min before returning to initial conditions. Re-equilibration time was 12.5 min resulting in an overall run time of 75 min. Gradient elution temperature was maintained at 45^{o}C. Detection and quantification was carried out with a Waters Quattro triple quadrupole mass spectrometer (Waters Corp., Milford, MA, USA) equipped with an atmospheric pressure interface-electrospray ionisation (API-ESI) source or a photodiode array detector (DAD) G1315B DAD (Agilent) monitoring three UV wavelengths of 220 nm, 254 nm and 270 nm. DAD setting were as follows; a bandwidth of 8 nm, slit width of 4 nm and a response time of 0.4 s. Mass spectrometric (MS) analysis was carried out in selected reaction monitoring (SRM) mode using positive-negative ionisation mode polarity switching. A scan rate of 0.03 min was utilised with a minimum of 15 points per peak measuring ±0.5 mass units for all transitions monitored. Confirmation of the selected compounds was achieved using both retention time and two transitions (MS^2) with the most intense fragment ion transition signal selected for analyte quantification (Table 2.1). MS conditions as well as all SRM transitions are summarised in Tables 2.1 and 2.3 were determined by direct infusion using a syringe pump which delivered 300 µL h^{-1} of analyte solution at a concentration of 1 µg mL^{-1}.

Table 2.1: ESI-MS conditions used during analysis

Electrospray ionisation conditions		
Desolvation temperature (^{o}C)	300	
Source temperature (^{o}C)	100	
Desolvation flow (L h^{-1})	450	
Nebuliser flow (L h^{-1})	90	
Mass spectrometric conditions		
	Positive ion mode	Negative ion mode
Capillary (kV)	3.00	3.00
Extractor (V)	3.0	3.0
Cone (V)	35.0	30.0
RF Lens (V)	0.30	0.40

2.2.5 Method performance characteristics and quality control

Matrix matching was performed for biota to assess method performance. Linearity was determined by measuring the peak area at concentrations from 0.01 to 10 µg g^{-1} for the *G. pulex* (n≥5). Limits of detection (LODs) were estimated as the lowest concentration of analyte which produced a signal-to-noise (S/N) ratio of 3:1. Limits of quantification (LOQs) were estimated as that analyte concentration to give an S/N ratio of 10:1. Both LOD and LOQ were calculated using the S/N ratios of low-level spiked samples (n=6). Instrumental retention time and method precision was carried out for n=6 replicate injections of a biotic sample spiked at 1 µg g^{-1}. Recovery was determined by comparing spiked sample extracts (1 µg g^{-1} for *G. pulex*, n=3) to sample extracts spiked post-extraction (n=3) at the expected final concentration. Control samples were also analysed for background correction purposes, where necessary. The measurement of ion suppression or enhancement in ESI-MS involved the comparison of sample extracts spiked post-extraction to a 100 ng g^{-1} working solution mixture in starting mobile phase A (n=3). The target analytes in both surface waters and biota were quantified based on their peak areas relative to that of an isotopically-labelled

internal standard (100 ng g^{-1}) or, where unavailable, by an external matrix matched calibration curve (n=3). Relative recovery in *G. pulex* was measured following the analysis of spiked biotic samples (analytes and the internal standard at 100 ng g^{-1} each) by comparing the analyte peak areas to that of the internal standard (n=12). Standard and internal standard solutions were prepared daily.

Mobile phase A was injected between samples from each site as well as between matrix-matched standards and controls to minimise the possibility of carry over. Direct infusion of a propranolol standard (1 µg mL^{-1}) was carried out before each batch analysis to ensure that the MS was operating satisfactorily. None of the targeted analytes were detected in any solvents, reagents or ultra-pure water used in this study.

2.3 Results & discussion

2.3.1 Method development

To understand how PhACs may bioconcentrate in biota, a multi-residue method was developed that allowed the trace determination of selected pharmaceuticals in the invertebrate *G. pulex*. A previously published method that allowed multi-residue analysis in biosolids was used as a starting point [33]. The method was applied to a mixture of 41 pharmaceuticals which resulted in an adequate separation of 25 of the compounds (Figure 2.2). However, the remaining compounds were not resolved and co-eluted. As shown in Figure 2.2 three sets of critical peaks from 20 – 35 min were observed to co-elute with each other. Therefore further optimisation was required.

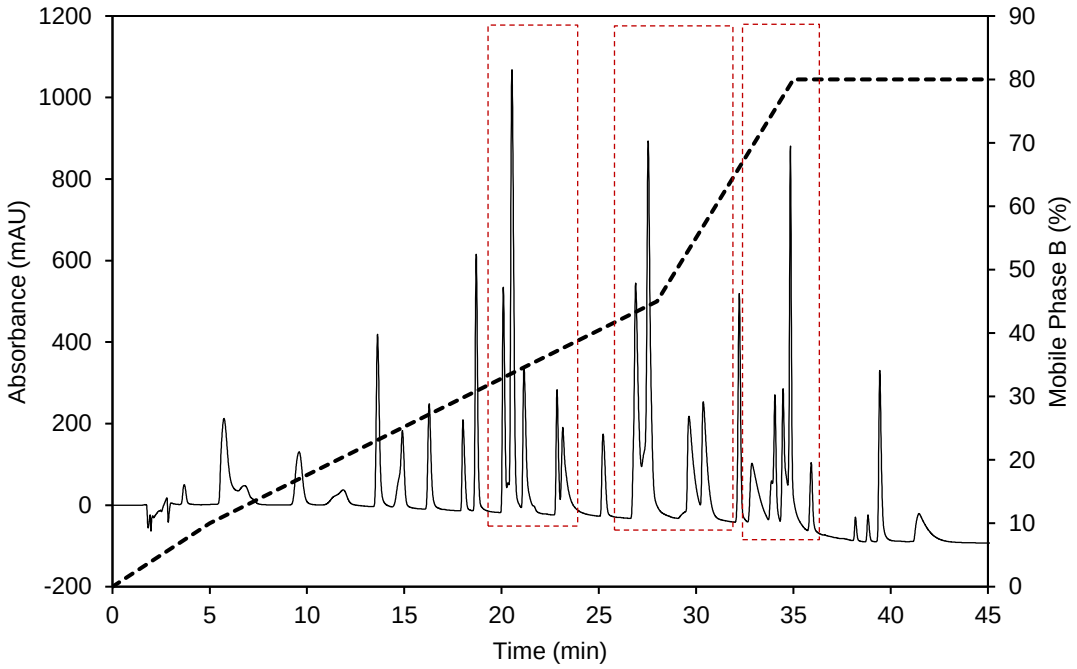

Figure 2.2: Gradient separation of 41 pharmaceuticals from a previously published method used in the analysis of solids (soil and sludge).The dashed line represents the gradient profile of Mobile Phase B (80 : 20 (v/v) of MeCN:10 mM ammonium acetate in H_2O. Dashed line boxes indicate several co-eluting peaks.

2.3.2 Chromatographic gradient and chemical composition

As the base method initially gave a fair separation, only the percentage of the two phases were changed at the time points specified (Materials and Methods). The previous method used a linear ramp between 28 - 35 min of MeCN to 85 %. The decrease in the polarity of the mobile phase would result in more non-polar compounds eluting earlier by reducing hydrophobic interaction with the alkyl chains in the stationary phase.

The percentage of MeCN was lowered at the 28 minute and 35 minute points to improve separation of the later eluting compounds. Method 3 (Figure 2.3c) had the best separation of the compounds eluting after 30 min, in comparison to method 1 which had a slightly higher percentage of MeCN at the 28 and 35 min time intervals (Figure 2.3). The mobile phase of method 1 was less polar between 28 – 35 min, thus more hydrophobic compounds would elute more quickly in comparison to method 3. The early eluting compounds of all the

methods had very similar separations, thus based on the better separation of the late eluting compounds in method 3, this method was taking forward for further development. As shown in Figure 2.3, peak separation in the highlighted box was of importance as several compounds co-eluted thus further methods were focused to separate these compounds.

The decrease in the percentage of MeCN gave the late eluting compounds a better separation at the 35 minute time point. Increasing the polarity of the mobile gradient would increase the retention of these more non-polar (late eluting) compounds through hydrophobic interaction with the C_{18} stationary phase. Therefore, development of method 3 involved further decreasing MeCN to improve the resolution of the late eluting peaks. Method 4 showed an improved separation, which gave a good overall separation with a better resolution of compounds eluting between 30 – 40 min. There were also spurious peaks visible in the chromatogram that did not relate to any retention time observed for the pharmaceuticals in the method. These peaks were found to originate from the lansoprazole and ketotifen fumarate standards, which may have been due to contamination or transformation of the compounds. Therefore, these two standards were removed from standard mixture.

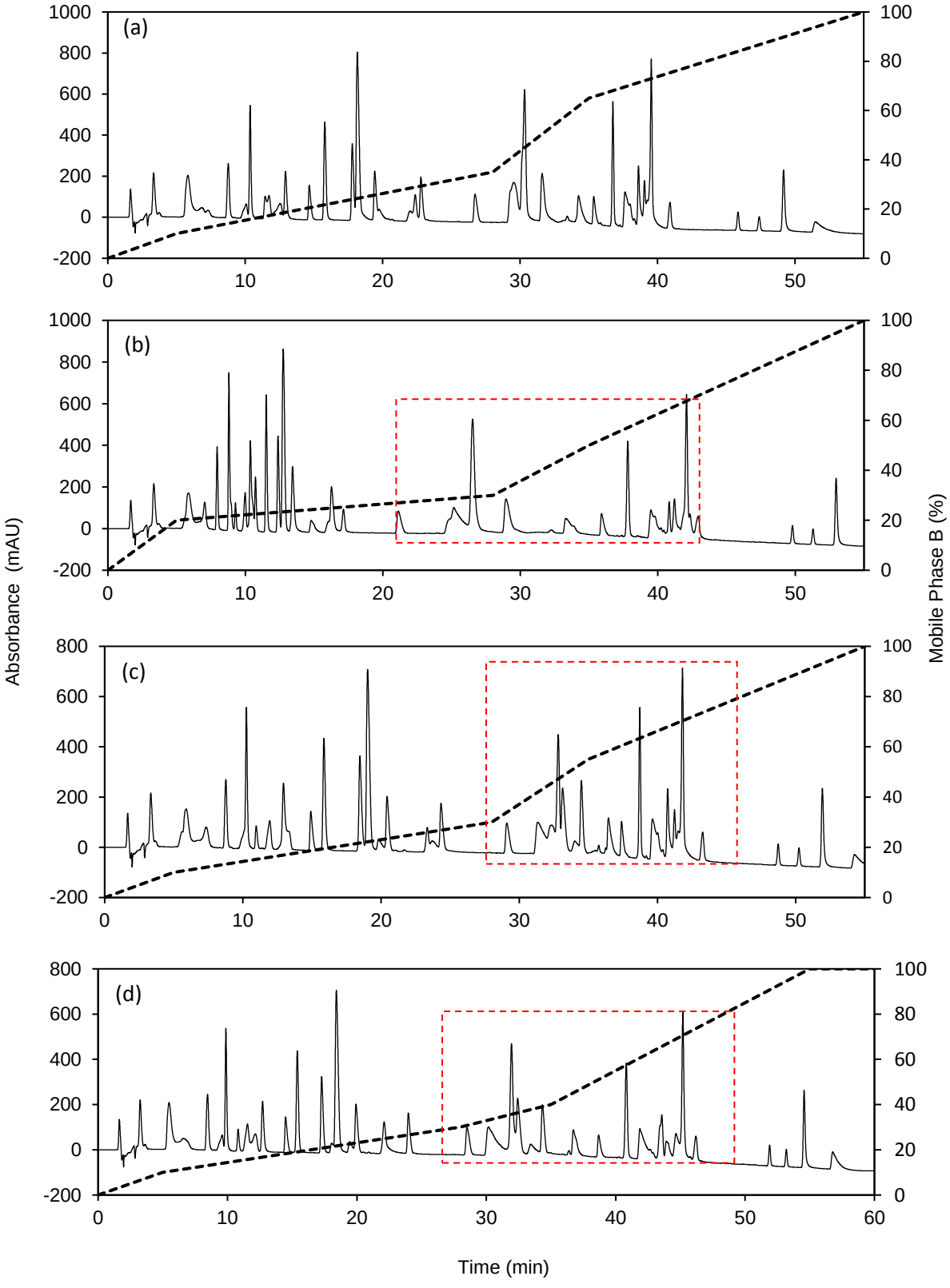

Figure 2.3: Chromatograms of four gradient compositions, (a) method 1, (b) method 2, (c) method 3 and (d) method 4. Dashed line represents the gradient profile of Mobile Phase B (80 : 20) (v/v) of MeCN : 10 mM ammonium acetate in H_2O. Dashed boxes highlight improvement of separation of several species that were co-eluting.

Method 4 was taken for further development with an additional time point at 40 min to resolve the peaks eluting after this time. The MeCN percentage was increased at 40 min from 45 % to 50 % and the best separation achieved was from method 5 (Figure 2.4). The temperature of this method was raised (45 ^{o}C) to increase mass transfer through decreases in mobile phase viscosity and increasing kinetic energy of the molecules involved in diffusion processes. Thus, efficiency was improved resulting in narrower peaks and better resolution of the method. Baseline resolution of all compounds was not considered a necessity, as the method would be transferred to MS. However, where compounds were baseline resolved, peak area was used for quantification as there was less variance associated with this measurement. The labelled chromatogram of all compounds separated by the final method is shown in Figure 2.4. In addition to available occurrence data, the compounds in the mixture were selected to cover a wide range of hydrophobicity (log*P*: -0.11 – 6.82) and included acidic (33 %), basic (53 %) and neutral compounds (14 %). If hydrophobicity is a dominant mechanism of uptake then the compounds selected should provide a wide enough coverage of the chemical space for modelling purposes. A wider range of chemical descriptors are given for the modelled compounds in Chapter 6. Additionally, as PhACs are developed according to Lipinski's rule of 5, the chemical space occupied by these compounds is relatively narrow and well-defined [34]. The sub-classes of the compounds included antibiotics, NSAIDs, TCAs, lipid regulators, beta-blockers and several others which cover various mode-of-actions. Chlorpyrifos was selected as a potential reference compound for use in bioconcentration experiments where it has been previously observed to be accumulative.

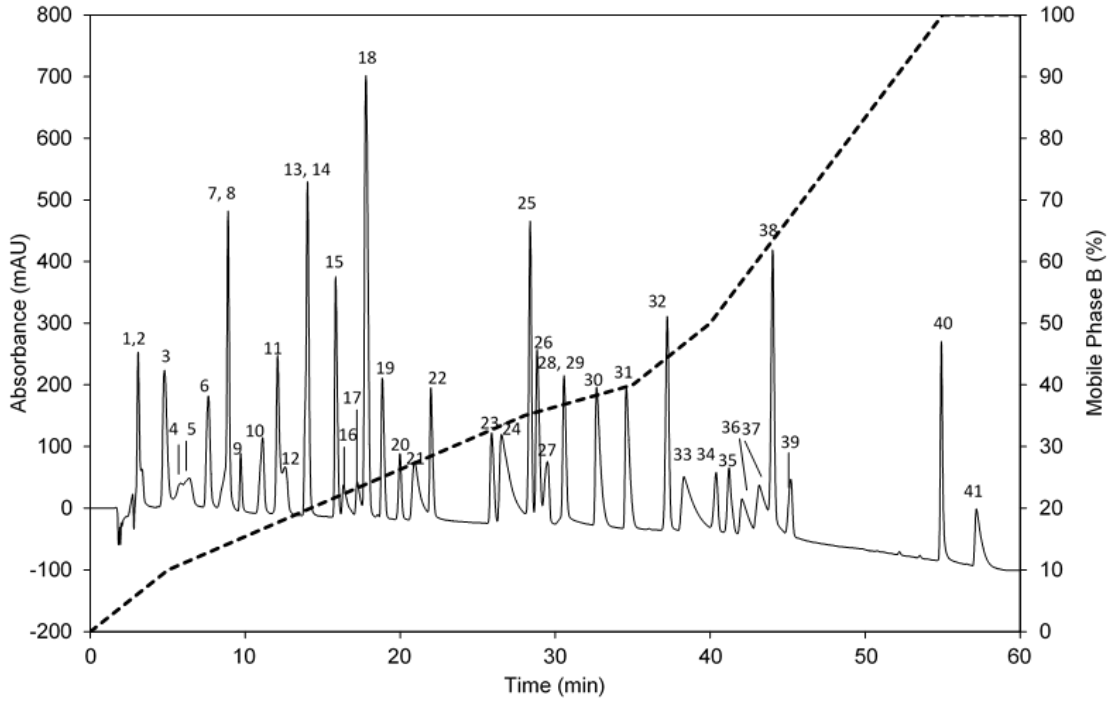

Figure 2.4: Example chromatogram of method 5. 1 - methimazole, 2 – amoxicillin, 3 – salicylic acid, 4 – atenolol, 5 – sulfamethoxazole, 6 – caffeine, 7 – sulfapyridine, 8 – cimetidine, 9 – ranitidine, 10 – sulfamethazine, 11 – sulfaphenazole, 12 – antipyrin, 13 – clofibric acid, 14 – trimethoprim, 15 – furosemide, 16 – metoprolol, 17 – tramadol, 18 – naproxen, 19 – ketoprofen, 20 – chloramphenicol, 21 – warfarin, 22 – bezafibrate, 23 – flurbiprofen, 24 – propranolol, 25 – carbamazepine, 26 – diclofenac, 27 – ibuprofen, 28 – dextromethorphan, 29 – indomethacin, 30 – mefenamic acid, 31 – meclofenamic acid, 32 – temazepam, 33 – nortriptyline, 34 – nimesulide, 35 – nifedipine, 36 – fluoxetine, 37 – amitriptyline, 38 – diazepam, 39 – gemfibrozil, 40 – triclosan and 41 – tamoxifen. Dashed line represents the gradient profile of Mobile Phase B (80 : 20 (v/v) of MeCN : 10 mM ammonium acetate in H_2O. Concentration of all standards were 10 µg mL^{-1}.

2.3.3 Injection volume & column overload

The instrumental response for the chromatographic method was determined using a 7-point calibration ranging from 0.1 - 10 µg mL^{-1} performed in triplicate. The correlation coefficient (R^2) range from 0.8858 (sulfaphenazole) to 0.9999 (temazepam), with only 5 compounds that showed a poor correlation of <0.98. The reason for the poor R^2 with some compounds was due to the higher concentration working solutions (7.5 and 10 µg mL^{-1}). When these points were removed, all compounds showed an increase in the linear response. The observed nonlinear response at the high concentrations can be explained by saturation of the UV detector, which defines the upper limit of the dynamic range.

Therefore, an increase in concentration above a certain threshold will not give a response that is linear. Thus, using the DAD, the dynamic range was from 0.1 to 5 µg mL^{-1}.

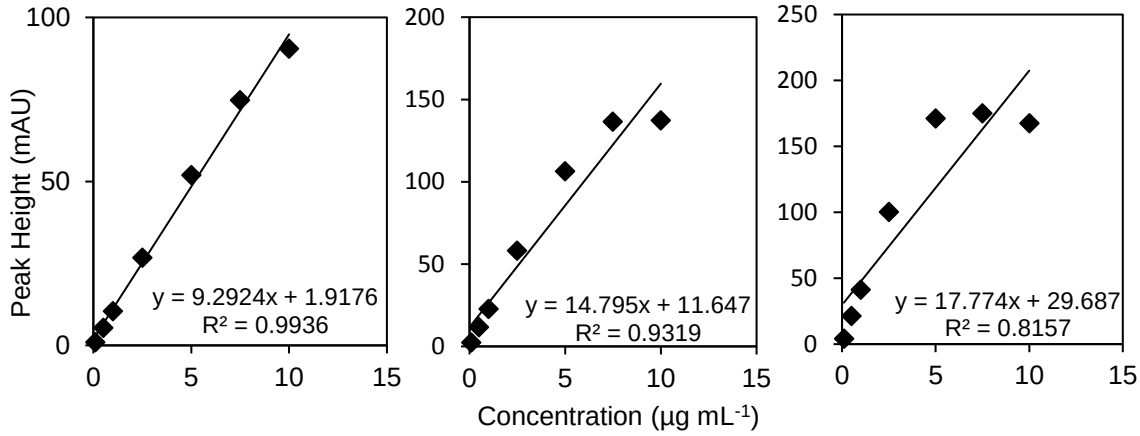

Figure 2.5: Comparison of calibration curves for the compound sulfamethazine when the injection volume is increased, 10 µL (left), 20 µL (centre), 40 µL (right).

The injection volume was also varied to obtain the lower range of sensitivity whilst maintaining a linear response. As shown in Figure 2.5, the 5 µg mL^{-1} standard shows a two fold increase in peak height between the 10 and 20 µL injection volume. However, the 40 µL injection volume did not have the same increase in signal therefore the gain in sensitivity is lower. The linear response was also better using a 10 µL injection for the majority of the compounds; however at this injection volume compounds such as metoprolol and nimesulide were not detected at the lower range of calibration curve, resulting in a loss of sensitivity which was undesirable for the application in trace analysis. At a 40 µL injection volume, band broadening occurred due to column overload, in the example of sulfamethazine the max column load was 150 ng. The band broadening observed could be explained by volume overload as the peaks in the chromatogram have become broader in contrast to mass overload. As the sample is injected in a larger volume longitudinal diffusion is more influential causing the

peak to spread. The resolution has also decreased where compounds such as ibuprofen and diclofenac could not be separated (Figure 2.6). Therefore, it was determined that a 20 µL injection volume was the optimum in terms of sensitivity, resolution and linear response.

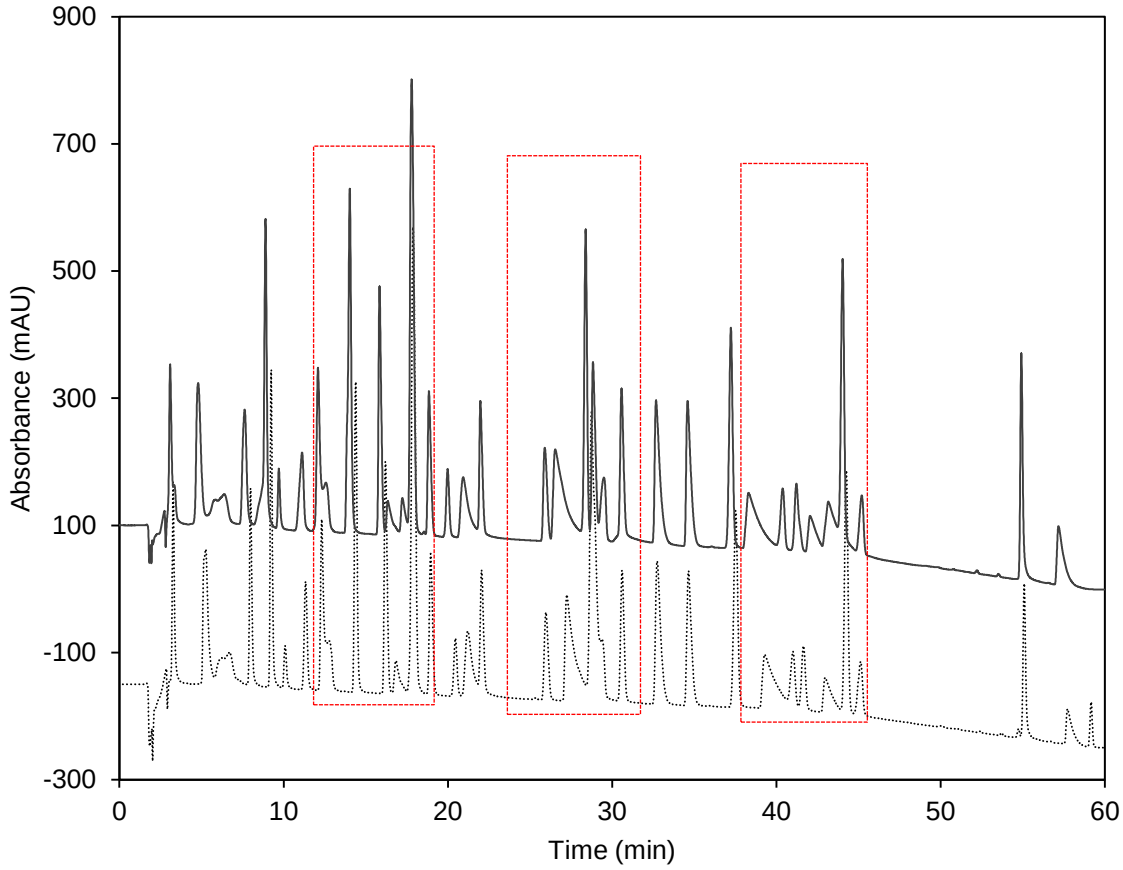

Figure 2.6: Comparison of injection volume on the chromatographic separation of PPCPs. The solid line represents 20 µL injection volume whereas the dashed line indicated the 40 µL injection volume. Dashed boxes indicate areas in the chromatograph where separation has become worse due to volume overload.

2.3.4 Solid phase extraction

Table 2.2: Comparison of recoveries using Oasis HLB SPE cartridges at an acidic, neutral and basic pH (n=6). Compounds spiked at 5 µg mL^{-1}.

Compound	log*P*[a]	Recovery (%) pH 2		SD	Recovery (%) pH 7		SD	Recovery (%) pH 10		SD
Methimazole	-0.11	10	±	1	20	±	7	10	±	3
Atenolol	0.24	63	±	3	61	±	1	65	±	8
Sulfamethoxazole	0.65	105	±	7	123	±	4	53	±	10
Caffeine	0.28	86	±	5	88	±	1	90	±	1
Cimetidine	0.69	60	±	10	67	±	2	76	±	2
Ranitidine	1.86	31	±	3	80	±	5	94	±	7
Sulfamethazine	0.44	61	±	5	83	±	2	74	±	0
Antipyrin	0.72	73	±	13	95	±	1	97	±	3
Sulfaphenazole	1.68	76	±	5	83	±	5	73	±	5
Trimethoprim	1.12	91	±	1	90	±	2	90	±	1
Furosemide	2.35	80	±	5	44	±	3	69	±	8
Metoprolol	1.85	116	±	16	104	±	1	102	±	3
Naproxen	2.98	87	±	3	92	±	3	85	±	9
Ketoprofen	3.12	79	±	4	84	±	3	80	±	7
Chloramphenicol	1.02	118	±	2	119	±	2	114	±	3
Warfarin	3.11	61	±	4	67	±	9	60	±	14
Bezafibrate	3.48	79	±	4	84	±	5	81	±	5
Flurbiprofen	3.82	74	±	5	82	±	6	76	±	13
Propanolol	3.26	85	±	2	78	±	4	67	±	5
Carbamazepine	2.28	79	±	3	83	±	4	77	±	8
Diclofenac	4.48	59	±	4	66	±	10	58	±	14
Ibuprofen	3.37	74	±	2	82	±	2	77	±	12
Indomethacin	4.02	56	±	4	67	±	12	61	±	17
Mefenamic Acid	5.00	38	±	3	57	±	14	53	±	15
Meclofenamic acid	6.02	22	±	0	37	±	12	36	±	14
Temazepam	2.12	74	±	4	79	±	9	70	±	15
Nortriptyline	4.76	77	±	2	54	±	5	0	±	-
Nimesulide	2.70	64	±	3	65	±	10	60	±	12
Nifedipine	3.45	75	±	3	77	±	19	65	±	17
Fluoxetine	4.27	77	±	2	59	±	7	38	±	1
Diazepam	2.74	60	±	2	58	±	12	52	±	14
Gemfibrozil	4.19	51	±	4	60	±	13	55	±	17
Triclosan	5.27	4	±	2	2	±	2	3	±	2
Tamoxifen	6.82	13	±	2	0	±	-	0	±	-
Chlorpyrifos	4.78	4	±	-	0	±	-	0	±	-

[a]*calculated from ACD labs Percepta software*

SPE was performed initially at three pH values (acidic, neutral, and basic) to determine the optimum recovery values of a sample. The pH is an important aspect of SPE, when extracting ionisable compounds. The first eluting compound, methimazole is the most polar pharmaceutical compound in the method and thus was not retained well by the HLB cartridge, as the recovery at every pH remained below 20 %. This compound has two amine functional groups which could be protonated at more acidic pH values and become charged (where HLB cartridges lack an ion exchange groups). The pK_a of methimazole is also 12.37 indicating that a pH below this value will lead to the formation of the protonated species [35]. The histamine H2 receptor antagonists, ranitidine and cimetidine, displayed a better recovery at pH 10. If the pK_a is taken into account at pH 7 and pH 2, these two compounds would be positively charged whereas at pH 10 the compound would remain neutral. The HLB cartridges are a dual phase sorbent containing a hydrophilic N-vinylpyrrolidone and hydrophobic divinylbenzene copolymer. Thus, the sorbent has capacity to retain both polar and non-polar compounds, and therefore neutral species are likely to show improved recoveries in comparison to their charged forms.

The acidic pharmaceuticals (naproxen, flurbiprofen, ibuprofen, ketoprofen, diclofenac, meclofenamic acid and mefenamic acid) showed better recovery at pH 7. However, the acidic pH would be expected to show better recovery of these compounds as they would remain as a neutral species. Furosemide is the only compound that follows this theory as it shows a 40 % improvement in recovery at pH 2 when compared to the recovery at pH 7. The remaining compounds may have undergone acid hydrolysis, thus reducing their recovery. However, it should be noted that a majority of these acidic compounds had an observed recovery that was only between 5-10 % higher at the neutral pH, with the exception of

mefenamic and meclofenamic acid that was 15-20 % higher. These two compounds had a much greater variation in the recovery at pH 7 as shown by the standard deviation.

The later eluting compounds such as triclosan and chlorpyrifos had recoveries below 5 %. The poor recoveries of these compounds may have been due to their log*P*. The low recovery could be due to the reconstitution solvent (mobile phase A) as the solubility of these compounds in water is relatively low (triclosan 1 µg mL^{-1} and chlorpyrifos 2 µg mL^{-1}) [36-38]. With the addition of the other pharmaceuticals in the mixture, it is possible that the low recovery of these compounds was due to reduced solubility into the reconstitution solvent. The elution solvent was relatively strong with a mixture of ethylacetate and acetone (50:50 v/v). Therefore, it was not likely that these compounds remained adsorbed to the SPE cartridge. Furthermore, triclosan has been eluted from HLB cartridges with weaker elution solvents such as methanol [39]. Overall, the neutral pH showed the greatest recovery with an average recovery of 68±6 % compared with the acidic pH (65±4 %) and the basic pH (62±8 %). However, a single factor ANOVA was performed on the recovery means for each pH treatment and indicated that there was no significant difference between the treatment groups (*p*-value = 0.644).

The SPE protocol was repeated at pH 7, but using a reconstitution solvent of water:acetonitrile (70:30 v/v). The change in the reconstitution solvent improved the recovery of 25 compounds in the mixture, with 23 compounds showing a recovery greater than 80% (Figure 2.7). The recovery of triclosan and chlorpyrifos both increased (≥44 %) indicating that the poor recovery from the previous experiment was in part due to a solubility issue. The precision also increased with 25 compounds achieving a SD of less than 10 %. This further

suggested that compound solubility was the reason for poor recovery and the greater variation, depending on the amount of solid residue that re-dissolved after drying down.

Using 30 % acetonitrile in the reconstitution solvent affected the separation of the mixture slightly so that 3 compounds could not be quantified (diclofenac, sulfamethoxazole and chloramphenicol) due to co-elution and the early eluting peaks were also split. The final SPE extract concentrations used in these experiments were 10 µg mL^{-1}, which is a relatively high concentration. Environmentally relevant concentrations were expected to be 10^3 to 10^6 fold lower than this, thus the original reconstitution solvent (Mobile Phase A) was selected. Due to the effect of biological matrices have on instrumental response, the final volume of the reconstitution solution was considered after an LC – MS method was optimised, detailed in Section 2.3.8.

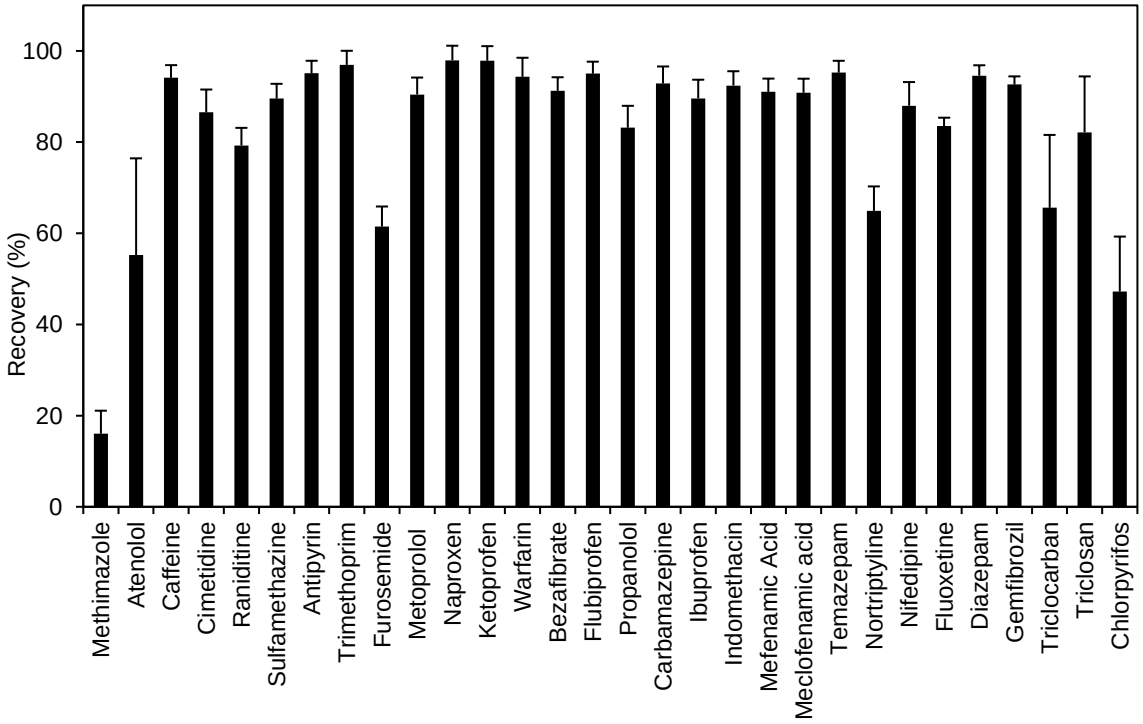

Figure 2.7: Recoveries of PPCPs at a neutral pH using a reconstitution volume of 30:70 (v/v) of MeCN : H_2O (n = 6). Error bars represent standard deviation.

2.3.5 Effect of sorption on ball-mill extraction tubes and glass beads

The sorption of the PPCP mixture during the extraction procedure in the ball-mill tube was characterised by using both unsilanised and silanised glass beads (Figure 2.8*)*. The data demonstrated that the difference between silanised and non-silanised glass beads was minimal for the majority of compounds in the mixture. Although, for some compounds; indomethacin, mefenamic acid, meclofenamic acid, triclocarban, triclosan and chlorpyrifos, there was better recovery using unsilanised glass beads. A possible reason for the better recovery using the unsilanised glass is that silanisation adds alkoxy groups to the silanol groups present on the surface of the glass [40]. Considering that the majority of the compounds had log*P* values greater 3, these compounds are likely to undergo hydrophobic interaction with these alkoxy groups and remain adsorbed to the surface. However, for triclocarban, triclosan and chlorpyrifos the recovery was low regardless of whether beads were silanised or not. Therefore, the main loss of compounds is assumed to be through sorption onto the plastic surface of the extraction tube. However, extraction without the glass beads was not tested.

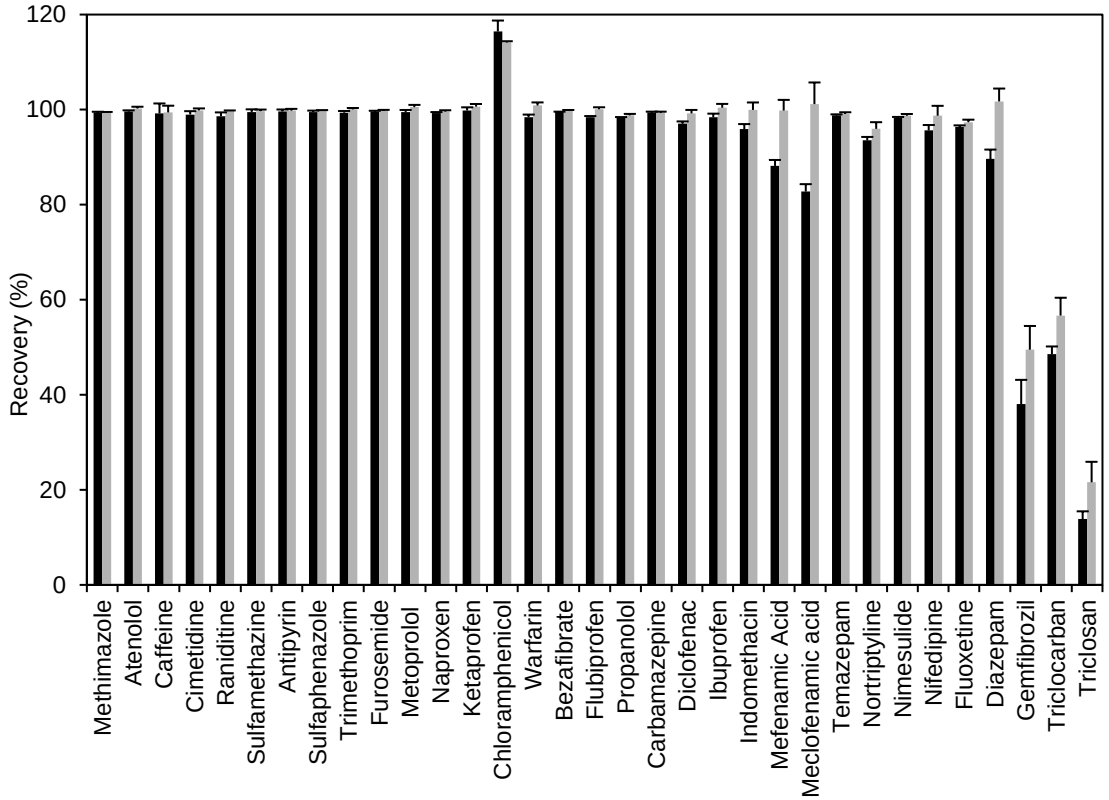

Figure 2.8: Comparison of sorption expressed by recovery for PPCPs used in the extraction procedure (n = 3). Black bars represent silanised glass beads, light grey bars represent unsilanised glass beads. Error bars represent standard deviation.

2.3.6 Liquid chromatography – mass spectrometry

As environmentally relevant concentrations were expected to be at least two orders of magnitude lower than those concentrations using LC-UV, the method was further developed using a triple quadrupole mass spectrometer. This would allow a much greater gain in sensitivity and would also identify compounds by mass transitions for confirmatory analysis.

2.3.7 Direct Infusions and fragmentation pathways

The HPLC-UV method transfer to HPLC-MS/MS first required direct infusions of individual standards (1 µg mL^{-1}), as these compounds eluted from the LC in different gradient compositions each standard was prepared in a solvent mixture that was similar to that point of elution in the LC gradient. The conditions of the mass analyser are displayed in Table 2.1. The fragments monitored are

shown below in Table 2.3 with the collision energy used at each transition. For the confirmation of compounds, a secondary fragment ion was also monitored. However, for certain compounds no secondary ions were produced that was mainly observed in negative ESI mode. A possible reason for this is that many of the acidic compounds may not produce a measureable ion current or that fragmentation yielded anions that are unstable [41]. Triclosan revealed no measurable fragment ions from scanning a mass range of 50-500; however it could be identified by the m/z ratio caused by the isotopic mass differences and peak superposition from the presence of chlorine atoms, ^{35}Cl and ^{37}Cl. When operated in SRM mode, the CID cell (with no collision energy potential supplied) still provided enough internal energy to remove the triclosan molecule.Therefore, no detectable signal was observed for triclosan. Whilst, previous investigation have shown it is possible to monitor a transition from 287>35 [42], it is not good practice due to the commonality of Cl ions with other organic molecules thus leading to reduced selectivity and increased noise. Due to limitations of the software, it was not possible to perform a full scan and SRM scan during a single analysis and thus triclosan was removed from further analysis.

Table 2.3: SRM transitions used for quantification and confirmation (where secondary ions are produced) with the respective collision energies for each compound. Ions determined through direct infusion.

Compound	Collision Energy (eV)	Precursor Ion	*m/z*	Fragment Ion Empirical Formula	*m/z*	Secondary Fragment Ion Empirical Formula	*m/z*
Atenolol	20	$[M + H]^+$	267	$C_{11}H_{12}NO_2$	190	$C_{10}H_9O$	145
Caffeine	21	$[M + H]^+$	195	$C_6H_7N_3O$	138	$C_5H_7N_3$	110
Cimetidine	16	$[M + H]^+$	253	$C_5H_{11}N_4S$	159	$C_4H_9N_2S$	117
Ranitidine	16	$[M + H]^+$	315	$C_5H_{10}N_3O_2S$	176	$C_{11}H_{16}N_2OS$	224
Sulfamethazine	20	$[M + H]^+$	279	$C_6H_8N_3O_2S$	186	$C_6H_{10}N_3$	124
Antipyrin	20	$[M + H]^+$	189	C_7H_4O	104	$C_9H_{10}N_2$	146
Sulfaphenazole	30	$[M + H]^+$	315	$C_6H_8NO_2S$	158	$C_9H_8N_3O_2S$	222
Trimethoprim	20	$[M + H]^+$	291	$C_{14}H_{16}NO_2$	230	$C_5H_7N_4$	123
Furosemide	15	$[M - H]^-$	329	$C_{11}H_{10}ClN_2O_3S$	285	$C_6H_6ClN_2O_2S$	205
Metoprolol	20	$[M + H]^+$	268	$C_6H_{14}NO$	116	$C_8H_{17}NO_2$	159
Naproxen	20	$[M - COOH]^-$	185	$C_{12}H_{10}O$	169	$C_{11}H_9O$	157
Ketoprofen	20	$[M + H]^+$	255	C_7H_5O	105	$C_{15}H_{13}O$	209
Warfarin	20	$[M - H]^-$	307	$C_9H_5O_3$	161	$C_{16}H_{10}O_3$	250
Bezafibrate	20	[M + H]+	362	C_7H_4ClO	139	$C_{18}H_{20}ClNO_2$	316
Flurbiprofen	13	$[M - H]^-$	243	$C_{14}H_{12}F$	199	-	-
Propranolol	20	$[M + H]^+$	260	$C_6H_{14}NO$	116	$C_{10}H_{17}NO_2$	183
Carbamazepine	30	$[M + H]^+$	237	$C_{14}H_{12}N$	194	-	-
Diclofenac	20	$[M - H]^-$	294	$C_{13}H_9Cl_2N$	250	-	-
Ibuprofen	10	$[M - H]^-$	205	$C_{12}H_{15}$	159	-	-
Indomethacin	20	$[M + H]^+$	358	C_7H_4ClO	139	$C_{11}H_{12}NO$	174
Mefenamic acid	15	$[M - H]^-$	240	$C_{14}H_{14}N$	196	-	-
Meclofenamic acid	14	$[M - H]^-$	294	$C_{14}H_{10}ClNO_2$	259	$C_{13}H_{10}ClN$	214
Temazepam	20	$[M + H]^+$	301	$C_{15}H_{12}ClN_2$	255	$C_{16}H_{12}ClN_2O$	283
Nimesulide	14	$[M - H]^-$	307	$C_{12}H_{10}N_2O_3$	229	CH_3O_2S	79
Nifedipine	10	$[M + H]^+$	347	$C_{16}H_{15}N_2O_5$	315	$C_{16}H_{17}NO_3$	271
Fluoxetine	18	$[M + H]^+$	310	$C_{10}H_{14}N$	148	-	-
Diazepam	27	$[M + H]^+$	285	C_8H_9NCl	154	$C_{14}H_{11}N$	193
Gemfibrozil	18	$[M - H]^-$	249	C_8H_9O	121	-	-
Triclocarban	9	$[M - H]^-$	313	$C_6H_5Cl_2N$	162	-	-

2.3.8 Recovery and reconstitution volume

As mentioned above, the reconstitution solvent type affected the recovery of PPCPs due to solubility issues. For this reason the reconstitution volume was also considered. A smaller volume will cause an increase in the concentration of matrix components. Thus, matrix effects are likely to be present to a higher degree than would be observed with a larger reconstitution volume. Matrix effects can either occur as suppression or enhancement of the signal response for analytes. Firstly, overall suppression was observed for a majority of the compounds. Two volumes were investigated 0.5 and 0.1 mL, as shown in Figure 2.9. As expected, the suppression associated with 0.1 mL volumes were much greater than with the 0.5 mL volumes, and matrix effects decreased with

increasing volume. One reason for such matrix effects is that the matrix components affected the droplet formation in the ESI source rather than affecting the gas phase ions. Therefore, the main problem arises from the transfer of analyte from solvent to gas phase ions. This could be due to a number of reasons such as changing the surface tension of the droplet so that more energy is required to overcome the Rayleigh limit or raising the boiling point so that solvent evaporation is less efficient [43]. It is also possible that analytes and matrix components will compete to reach the droplet surface for desorption into a gas phase ion. As described above, negative mode ESI will be likely to have greater matrix effects due to the lower intensity and poorer ionisation efficiency. This is shown as the negative mode analytes (diclofenac, ibuprofen, triclocarban, mefenamic acid, meclofenamic acid) generally have a much higher suppression than compared with compounds detected in the positive mode. There is also a greater matrix effect with compounds that are more hydrophobic, as the later eluting compounds show more suppression even with the largest reconstitution volume. The 0.1 mL volume resulted in the greatest matrix effects and the highest variance associated with each measurement therefore for quantification purposes this volume is less suitable. In comparison, the 0.5 mL volume resulted in similar matrix effects but the variance was much lower.

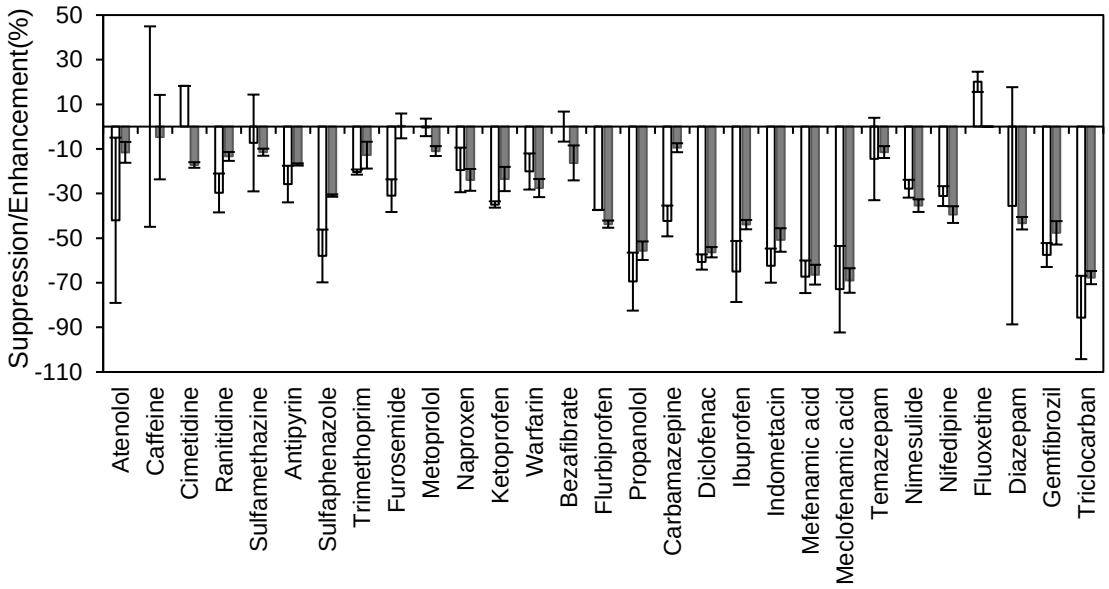

Figure 2.9: Matrix effects of G. pulex on the signal response of selected PPCPs. Positive bars indicate enhancement, negative bars indicate suppression. Dotted bars are the 0.1 mL volume (n = 6), solid bars are 0.5 mL (n = 3) volume. The error bars represent the standard deviation.

The recovery of the method was also determined for the two different reconstitution volumes. Overall, most compounds showed an absolute recovery of 40 – 130 %. Fluoxetine had a recovery that was highly variable as also observed with the matrix effect determination which has been observed in previous studies by other researchers [44, 45]. The more polar analytes and those that were detected in negative mode ESI generally had an observed recovery of ≤ 50 %. As shown in the Figure 2.10, there were several compounds (warfarin, propranolol, temazepam and diazepam) that had lower recoveries with a decreased reconstitution solvent. The standard deviation shown as error bars in Figure 2.10 indicated that recovery was slightly less variable at 0.5 mL when compared to 0.1 mL, as the average standard deviation was 6 % for the 0.5 mL in comparison to 8 % for the 0.1 mL. However, the difference was not statistically significant (*p*-value = 0.306). This indicated the method was slightly more repeatable as the standard deviation remained below 15 % for all compounds

except triclocarban (31 %) and gemfibrozil (21 %). The 0.5 mL volume was decided as the final reconstitution volume.

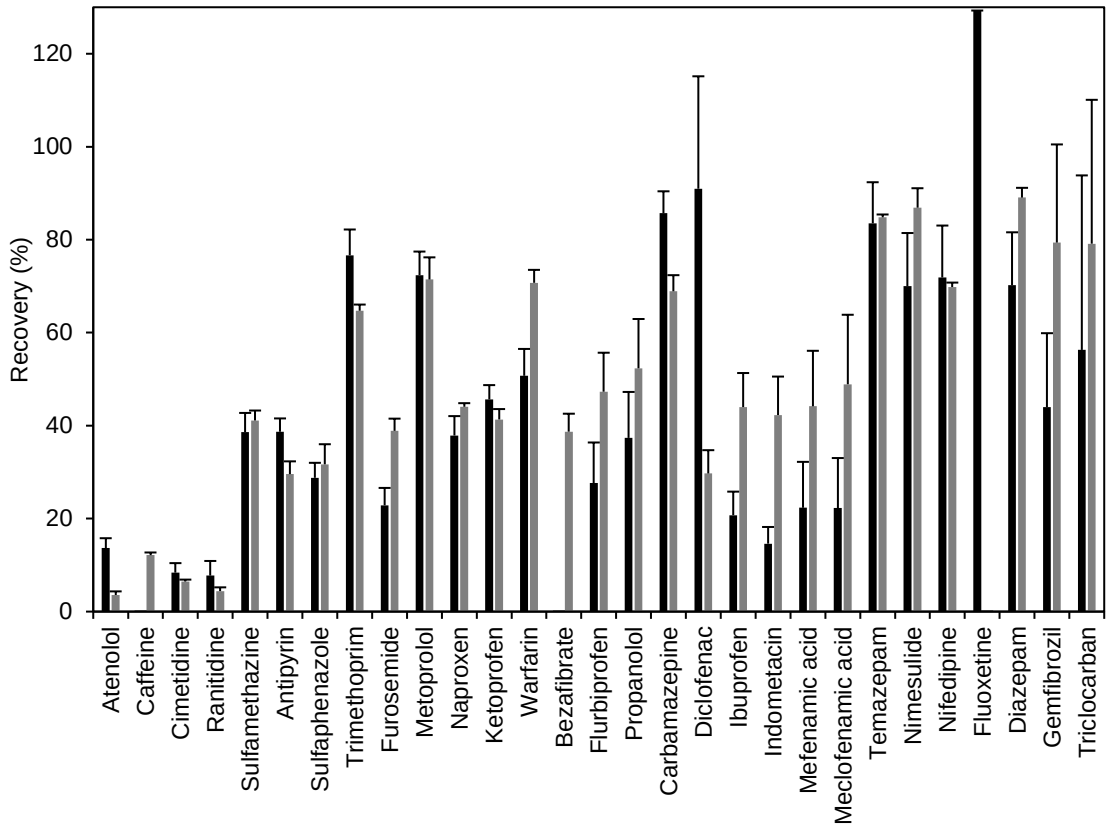

Figure 2.10: The effects of matrix and reconstitution volume on the recovery of selected PPCPs. Error bars represent standard deviation. Black bars are 0.1 mL volume (n = 6), dark grey bars are 0.5 mL volume (n = 3) and light grey bars are 1.0 mL volume (n = 6). Fluoxetine was only measured once in all spiked G. pulex replicates therefore no error bars are displayed

2.3.9 Sample preparation

For the extraction of *G. pulex* samples the sample clean-up procedure involved a protein precipitation step with acetonitrile followed by transfer of the supernatant to a 100 mL volume of buffered (10 mM ammonium acetate) ultra-pure water for loading onto the HLB SPE cartridges. Further clean-up stages were investigated by the addition of a centrifugation step after the protein precipitation and the addition of neutral aluminium oxide. It is desirable to have efficient sample clean-up, as biological matrices contain many macromolecules which may increase signal suppression of the relatively low molecular weight PPCPs [46]. The centrifugation step was added to pellet the proteins and other

solid particles to provide a cleaner extract. The addition of aluminium oxide was used to prevent the co-extraction of lipids, which has been used in previous studies to remove lipid and pigments (chlorophyll) from freshwater bivalves [47]. The removal of lipids from the samples is likely to involve either the retention (sorption) or degradation by peroxidation [48]. This new methodology was compared with the workflow without the additional clean-up stages by assessing recovery, suppression and enhancement (Table 2.4). As shown, overall there was little difference between the suppression and enhancement indicating that matrix components are still interfering with the signal response. However, the recovery and RSD, although only a small difference in some cases, was better with the method without the additional clean-up stages. A single factor ANOVA was performed for the recovery and RSDs which revealed that there was no statistically significant difference between either sample preparation method (p-value 0.124 and 0.054, respectively). Therefore, the additional steps offered no advantage for quantitative purposes and were not included into the finalised analytical method.

Table 2.4: Comparison of sample preparation with centrifugation and Al_2O_3 steps (method A) versus extraction with only MeCN (method B).

	Method A (n = 3)			Method B (n = 3)		
Compound	Supp./Enhanc.	Recovery (%)	RSD	Supp./Enhanc.	Recovery (%)	RSD
Atenolol	10	12	0	-13	4	1
Caffeine	22	48	17	-7	12	1
Cimetidine	-34	4	8	-17	6	0
Ranitidine	-48	0	1	-14	4	1
Sulfamethazine	6	41	1	-12	41	2
Antipyrin	9	65	4	-17	30	3
Sulfaphenazole	-5	32	1	37	32	4
Trimethoprim	-11	62	7	-12	65	1
Metoprolol	-16	66	14	-10	71	5
Ketaprofen	-11	37	4	-24	41	2
Bezafibrate	18	64	7	-17	39	4
Propranolol	-61	30	26	-55	52	11
Carbamazepine	-51	42	2	-10	69	3
Indometacin	-21	33	15	-49	42	8
Naproxen	-23	28	8	-24	44	1
Ibuprofen	-43	23	9	6	44	7
Flurbiprofen	-36	26	14	-44	47	8
Diclofenac	-32	74	5	-56	30	5
Warfarin	-21	56	11	51	71	3
Furosemide	-16	44	1	1	39	3
Mefenamic Acid	-46	25	18	-66	44	12
Gemfibrozil	-44	28	21	-42	79	21
Meclofenamic Acid	-47	25	16	-69	49	15
Nimesulide	-67	26	13	-35	87	4
Triclocarban	-62	34	13	-67	79	31
Temazepam	-16	66	5	-11	85	1
Diazepam	-30	55	11	-43	89	2
Fluoxetine	-	-		-	-	-
Nifedipine	-21	56	9	-39	70	1

Observation of the final reconstituted extract appeared to show an 'oily' red pigment that seemed to form insoluble globules (Figure 2.11). This pigment is likely to be the compound astaxanthin which is a carotenoid pigment often found in *crustacea* [49]. This pigment could also act as a source of signal suppression. Furthermore, the globules could have also potentially acted as a biphasic system in the reconstitution solvent. Thus, the pharmaceutical compounds may have sorbed to the asatxanthin leading to a reduction in the signal response of the determined analytes. A LLE procedure was attempted to remove the compound by using 50:50 hexane:acidified acetonitrile with HCl (aq). After a drying down step, a green pigment remained, however if the acetonitrile was not acidified the pigment remained red indicating that the pigment was not extracted by hexane and had only undergone a reaction such as acid hydrolysis to give the colour change. As the additional steps added no advantages the original method was selected as the optimised sample preparation method.

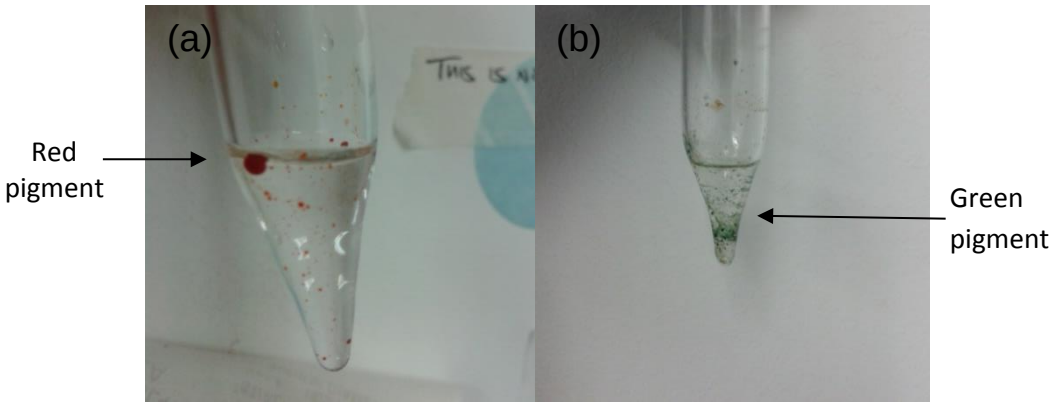

Figure 2.11: Reconstitution after sample extraction and cleanup. (a) followed the normal analytical method showing the red pigment (e.g. astaxanthin). (b) follows the analytical method with a LLE using hexane and acidified acetonitrile leaving behind a green pigment. In both cases the pigment has remained.

2.3.10 Method performance

The method performance was assessed to identify which compounds were suitable for quantification. As few analytical methods to determine PPCPs from aquatic biological matrices exist, a large number of compounds with broad physicochemical properties were assessed with the expectation that several compounds would not pass performance criteria such as linearity, precision, accuracy etc. Table 2.5 shows the in matrix method performance parameters for each compound that was monitored. Overall, the method showed good performance for the selected compounds, retention time precision was ≤0.5 % for all compounds excluding propranolol (1.7 %) which might be expected as this compound has secondary interactions with silanol groups in the stationary phase and can also associate with counter-ions which would lead to variation in retention [50]. All compounds displayed ≥10 points per peak for reliable quantification and retention time measurement. Matrix effects were significant (>50 %) for several pharmaceuticals including triclocarban, propranolol, indomethacin, mefenamic acid, meclofenamic acid and diclofenac. In total 27 compounds were supressed when compared to a working solution (n=3) of equivalent concentration.

Table 2.5: Method performance for 29 selected compounds.

Compound	t_R (min) n=6	Range (ng g^{-1})	Linearity[a] (R^2) n≥5	LOD[b] (ng g^{-1}) n=6	LOQ[c] (ng g^{-1}) n=6	Recovery ±SD[d] (%) n=3	Matrix Effect ±SD[e] (%) n=3
Atenolol	6.3	500 - 10000	0.9543	62	191	30 ± 3	-17 ± 1
Caffeine	8.4	250 - 10000	0.9909	75	194	4 ± 1	-12 ± 5
Cimetidine	10.9	250 - 10000	0.8085	206	687	6 ± 0	-17 ± 1
Ranitidine	13.3	500 - 10000	0.8001	38	145	4 ± 1	-13 ± 2
Sulfamethazine	11.9	25 -10000	0.9987	4	15	41 ± 2	-11 ± 2
Antipyrin	13.8	10 -10000	0.9973	13	43	30 ± 3	-17 ± 1
Sulfaphenazole	12.2	10 -10000	0.9989	11	36	32 ± 4	-31 ± 1
Trimethoprim	16.8	10 -10000	0.9987	2	5	65 ± 1	-13 ± 6
Metoprolol	19.7	10 -10000	0.9992	1	4	71 ± 5	-11 ± 2
Ketoprofen	20.9	10 -10000	0.9976	14	45	41 ± 2	-23 ± 5
Bezafibrate	24.4	10 -10000	0.9807	17	57	39 ± 4	-16 ± 8
Propranolol	30.9	10 -10000	0.9952	13	45	52 ± 11	-56 ± 4
Carbamazepine	31.3	25 - 10000	0.9983	2	6	69 ± 3	-9 ± 2
Indomethacin	32.8	10 -10000 [a]	<0.950	-	-	42 ± 8	-51 ± 5
Naproxen	19.5	75 - 500	0.9861	17	56	44 ± 1	-24 ± 5
Ibuprofen	31.1	500 - 10000	0.9714	111	371	44 ± 7	-44 ± 2
Flurbiprofen	28.1	250 - 10000	0.9625	55	183	47 ± 8	-44 ± 2
Diclofenac	32.6	10 - 10000	<0.950	-	-	30 ± 5	-56 ± 2
Warfarin	22.7	50 - 10000	0.9973	2	6	71 ± 3	-28 ± 4
Furosemide	18.4	10 – 10000[a]	0.9912	14	45	39 ± 3	0 ± 6
Mefenamic acid	35.1	10 -10000 [a]	<0.950	-	-	44 ± 12	-66 ± 4
Gemfibrozil	47.1	10 -10000 [a]	<0.950	-	-	79 ± 21	-48 ± 5
Meclofenamic acid	37.1	10 -10000 [a]	<0.950	-	-	49 ± 15	-69 ± 5
Nimesulide	44.0	25 - 10000	0.9945	3	11	87 ± 4	-35 ± 3
Triclocarban	57.4	100 - 10000	0.9770	9	31	79 ± 31	-68 ± 3
Temazepam	40.2	10 - 10000	0.9930	2	6	85 ± 1	-11 ± 3
Diazepam	46.8	10 - 10000	0.9991	2	5	89 ± 2	-43 ± 3
Fluoxetine	47.9	10 -10000 [a]	<0.950	-	-	ND	ND
Nifedipine	44.4	10 - 10000	0.9985	1	4	70 ± 1	-39 ± 4

[a]Linearity was assessed by a minimum of n=5 points in triplicate
[b]3:1 signal-to-noise ratio with either a 75 ng g^{-1} or 750 ng g^{-1} spiked matrix (n=6).
[c]10:1 signal-to-noise ratio with either a 75 ng g^{-1} or 750 ng g^{-1} spiked matrix (n=6).
[d]determined using a 100 ng g^{-1} pre-extraction spiked sample (n=3)
[e]determined using a 100 ng g^{-1} post-extraction spiked sample (n=3)

Method linearity ranged from R^2 ≤0.9500 to 0.9992. The non-linear responses corresponded to several compounds that were detected in negative ESI (acidic pharmaceuticals) or that were very polar. The polar and acidic pharmaceuticals also displayed relatively higher LOD and LOQ ranges which is potentially due to low observed recoveries ≤6 % and those compounds detected in negative ESI which generally has lower sensitivity when compared to positive ESI. Intra-day precision was expressed as the standard deviation of the recovery and varied at ≤1 – 31 %. The large variance of 31 % was associated with the compound triclocarban which suffered from carry over leading to lower precision. The mean absolute recoveries ranged from 4 to 89 %, with several compounds achieving a recovery >70 %. Compounds that showed lower recoveries were accepted if the standard deviation was <5 % as with the compound sulfamethazine (41 % recovery). Accuracy was assessed for only those compounds which had acceptable linearity (≥0.98) and method precision (≤20% RSD) by either by matrix matched calibration curves or internal standard (where available) quantification using a single calibrant (Table 2.6). Standard addition was not possible due to the variation in background levels of the contaminants between samples. Overall, the accuracy of the compounds was acceptable, however one compound (diazepam) displayed greater inaccuracy which is explained by larger variations of background concentrations present in the matrix as also shown by the SD. The accuracy assessment was limited by the background levels of contaminants present in the matrix and it was observed that due to the variation of these concentrations background correction was often not applicable. The performance of this method is similar to performance from other reported analytical methods for PPCP determination in aquatic invertebrates, fish, biosolids and other complex biological matrices [13-15, 33, 51]. Therefore,

from the method performance assessment it was deemed that 10 compounds displayed acceptable criteria for reliable and accurate quantification in line with guidelines from AstraZeneca. The remaining compounds were used for qualitative screening.

Table 2.6: Full method performance for compounds accepted for quantitative application.

Compound	t_R±SD[a] (min) n=6	SRM transitions	Mode	Range (ng g^{-1})	R^{2b} n≥5	LOD (ng g^{-1}) n=6	LOQ ± SD (ng g^{-1}) n=6	Intra-day accuracy ± SD (%) n ≥ 3	Abs. recovery & intra-day Precision (%) n=3	Ion sup. (%) n=6
Sulfamethazine	11.9±0.1	(279→186) (279→124)	(+)	25-10000	0.9987	4	15 ± 6[d]	95 ± 3[f]	41 ± 2	11 ± 2
Trimethoprim	16.8±0.1	(291→230) (291→123)	(+)	10-10000	0.9987	2	5 ± 4[c]	126 ± 31[g]	65 ± 1	13 ± 6
Metoprolol	19.7±0.1	(268→116) (268→159)	(+)	10-10000	0.9992	1	4 ± 1[d]	100 ± 6[f]	71 ± 5	11 ± 2
Propranolol	30.9±0.5	(260→116) (260→183)	(+)	50-10000	0.9952	13	61 ± 9[e]	81 ± 8[f]	52 ± 11	56 ± 4
Carbamazepine	31.3±0.1	(237→194)	(+)	25-10000	0.9983	2	6 ± 1[c]	124 ± 6[g]	69 ± 3	9 ± 2
Warfarin	22.7±0.1	(307→161) (307→250)	(-)	50-10000	0.9973	2	5 ± 1[c]	102 ± 9[g]	71 ± 3	28 ± 4
Temazepam	40.2±0.1	(301→255) (301→283)	(+)	10-10000	0.993	2	6 ± 1[c]	100 ± 3[g]	85 ± 1	11 ± 3
Diazepam	46.8±0.1	(285→153) (285→193)	(+)	10-10000	0.9991	2	5 ± 2[c]	176 ± 28[g]	89 ± 2	43 ± 3
Nimesulide	44.0±0.1	(307→229) (307→79)	(-)	25-10000	0.9945	3	13 ± 2[c]	97 ± 7[f]	87 ± 4	35 ± 3
Nifedipine	44.4±0.1	(347→315) (347→271)	(+)	10-10000	0.9985	1	4 ± 1[d]	104 ± 6[f]	70 ± 1	39 ± 4

[a]SD= standard deviation.
[b]n=5 concentration data points each performed in triplicate.
[c]Signal to noise ratio of 10:1 from 20 ng g^{-1} spiked matrix-matched sample.
[d]Signal to noise ratio of 10:1 from 75 ng g^{-1} spiked matrix-matched sample.
[e]Signal to noise ratio of 10:1 from 60 ng g^{-1} spiked matrix-matched sample.
[f]Using a 75 ng g^{-1} spiked sample (n= 3) and determined by matrix matched calibration (n= 3) in triplicate.
[g]Using a 20 ng g^{-1} spiked sample (n = 4) and determined by the relevant isotopically-labelled internal standard.

2.3.11 Method application

The optimised method was applied to determine the occurrence of the selected pharmaceuticals (carbamazepine, diazepam, temazepam, propranolol, metoprolol, nifedipine, nimesulide, sulfamethazine, trimethoprim and warfarin) from tributaries of the River Thames in the Greater London catchment area. Replicate grab samples of *G. pulex* and surface water were collected. The measurement of surface water concentrations were considered semi-quantitative as method performance was not assessed in water. In total, 6 compounds were quantified in *G. pulex* across all sites. Diclofenac was detected at every site however could not be quantified due to method performance limitations. To the authors' knowledge, there were no reported occurrence data in *G. pulex*. However, after the time of this study a paper by Inostroza et al., [52] developed an analytical method using *G. pulex* but applied it in the field to a similar animal, *Dikerogammarus spp*. The authors of this study reported concentrations of PPCPs reaching up to 2.83 ng g^{-1} ww and pesticides reaching up to 6.52 ng g^{-1} ww. Thus, occurrence data in other invertebrate species were used as a comparison for this study. Carbamazepine was the most frequently detected pharmaceutical across all the sites which may be expected due to the frequency of detection of this compound in different environmental compartments as reported by other authors [53, 54]. The maximum concentration of any pharmaceutical determined was 36 ng g^{-1} that corresponded to nimesulide. Both nimesulide and diazepam were detected across 4 sites at relatively higher concentrations when compared to the other pharmaceuticals that were detected. Nimesulide would be expected to have minimal input into the aquatic environment in the UK as it is not available for human consumption. However, the sources of input arise from veterinary purposes and it has also been detected in selected

nutritional supplements. The moderate hydrophobicity of this compound may explain the relatively higher concentrations and more frequent detection. Site 7 and 8 were the most contaminated.

Overall, the eight sites showed low contamination with many compounds detected below the LOQ or not detected at all. Diazepam and carbamazepine (among other PPCP residues) have been reported to reach up to 110 ng g^{-1} in fish liver tissues [51]. If hydrophobicity determines accumulation potential, it may explain the reason why these compounds are frequently detected across the sites as they have relatively high log*P* values for pharmaceuticals. However, carbamazepine and diazepam have been shown to have very low BCF in *G. pulex* of 7 and 38 respectively [31]. Temazepam and propranolol were not detected in any biota samples but were detected in surface water samples. However, both of these compounds are more hydrophobic than trimethoprim that was detected in *G. pulex*. This suggests that uptake of PPCPs in biota based on hydrophobicity models may not accurately reflect the accumulation potential of a compound in invertebrates and is the focus of later chapters. Other occurrence data has shown PPCP concentrations in fish reaching up to 22 ng mL^{-1} in plasma, 910 ng g^{-1} in brain tissue and 16 ng g^{-1} in liver tissue [55]. McEneff et al. [13], reported pharmaceutical concentrations of trimethoprim reaching up to 9 ng g^{-1} dw. Here, the maximum trimethoprim concentration reached 5 ng g^{-1} displaying comparable contamination. Klosterhaus et al. [14], also reported marine mollusc PPCP concentrations reaching up to 14 ng g^{-1} ww where carbamazepine was detected most frequently and reached up to 5 ng g^{-1} ww. Huerta et al., [56] determined the occurrence of pharmaceuticals in three freshwater invertebrates in which ibuprofen was determined reaching up to 183 ng g^{-1} dw and diclofenac reaching 12.4 ng g^{-1} dw. In addition endocrine disruptors were detected and

ranged between 7.7 ng g^{-1} dw (tris-(2-butoxyethyl)-phosphate) to 130 ng g^{-1} dw (nonylphenol).

Table 2.7: Occurrence of six pharmaceutical compounds detected in field collected G. pulex across eight sites. Concentrations are measured as ng g^{-1} dw.

Compounds	Site 1 (n=2)	Site 2 (n=3)	Site 3 (n=2)	Site 4 (n=3)	Site 5 (n=3)	Site 6 (n=2)	Site 7 (n=3)	Site 8 (n=2)
Carbamazepine	-	<LOQ	-	ND - <LOQ	<LOQ	-	ND - <LOQ	6
Diazepam	ND, 6	ND - 8	-	ND - 6	-	-	ND - 9	-
Temazepam	-	-	-	-	-	-	<LOQ	ND - <LOQ
Trimethoprim	-	-	-	-	-	-	ND - <LOQ	5
Warfarin	-	-	-	-	-	-	ND - 7	-
Nimesulide[a]	13, 36	ND - <LOQ	-	ND - <LOQ			ND - 16	

ND — not detected, all other compounds marked with '–'were also not detected.
[a] Quantified by three-point standard addition calibration.

These reported occurrence data are in agreement with the data reported here. Although the concentrations are low, potential adverse effects may be elicited through chronic exposure to these contaminants. Environmentally relevant levels of PPCPs have shown to lead to oxidative stress and tissue lesions in fish and molluscs [57]. An investigation into the behavioural effects, such as movement and feeding activity, of PPCP exposure have shown that the lowest observed effect concentration (LOEC) in *G. pulex* was 100 ng L^{-1} for fluoxetine and 10 ng L^{-1} for carbamazepine and ibuprofen [27]. When considering the measured surface water concentration of carbamazepine reached up to 344 ng L^{-1}, it leads to the possibility that these populations of animals may already be experiencing adverse effects. However, it should be considered that behaviour is a bespoke endpoint and as internal concentrations were not measured in the study by De Lange et al. [30] it is difficult to link cause and effect. Surface water data showed that carbamazepine and trimethoprim occurred at the highest concentrations of 344 ng L^{-1} and 289 ng L^{-1}, respectively. Across the eight sites,

Site 8 was observed to contain the highest concentrations of all pharmaceuticals with the exception of propranolol which reached up to 253 ng L^{-1} at Site 5. The higher concentrations of pharmaceuticals at Site 8 could be explained by the close proximity of this site to a WWTP effluent outfall pipe. This site is also reported to have a 'poor,' ecological status by the Environment Agency in 2012 [58]. However, these increased surface water concentrations did not correlate with higher concentrations in *G. pulex* (highest concentrations observed at Site 7). Site 5 also displayed relatively higher water concentrations of carbamazepine, trimethoprim and propranolol which also correlated poorly with the internal concentrations in *G. pulex* at the same site.

Table 2.8: Occurrence of pharmaceuticals (ng L^{-1}) detected in surface water samples (grab sampled) across eight sites of the Greater London catchment area.

Compounds	log*P* [56]	Site 1 (n=3)	Site 2 (n=3)	Site 3 (n=3)	Site 4 (n=3)	Site 5 (n=3)	Site 6 (n=3)	Site 7 (n=3)	Site 8 (n=3)
Carbamazepine	2.45	12 - 27	10 - 62	13 - 17	20 - 156	6 - 149	8 - 9	6 - 53	320 - 344
Diazepam	2.86	ND	ND - <LOQ	ND - 3	ND - <LOQ	ND - <LOQ	ND - <LOQ	<LOQ	4
Propranolol	3.48	ND - <LOQ	<LOQ - 59	8 - 22	<LOQ - 11	ND - 253	21 - 52	5 - 23	98 - 119
Temazepam	2.19	ND - <LOQ	<LOQ - 2	<LOQ	5 - 6	ND - <LOQ	ND	ND - LOQ	60 - 67
Trimethoprim	0.91	<LOQ - 8	ND - <LOQ	4 - 10	<LOQ - 48	ND - 41	6 - 16	<LOQ - 9	263 - 289
Warfarin	2.60	ND - <LOQ	ND - 53	<LOQ - 12	ND - <LOQ	ND - 9	11 - 14	ND - LOQ	15 - 29

ND – not detected

In comparison to several other monitoring studies of surface waters in the UK, carbamazepine has been detected frequently in the River Ely and the River Taff, reaching up to 684 ng L^{-1} [59]. Other studies have detected trimethoprim and propranolol reaching up to 40 ng L^{-1} and 215 ng L^{-1}, respectively [60, 61]. All six pharmaceuticals that were detected here have been reported across Europe and Asia in countries such as Spain, France and S. Korea [62-64]. Diazepam was the least detected compound with the highest concentration reaching 4 ng L^{-1}. In contrast, this was a frequently detected compound reaching relatively high concentrations in the biota samples which may suggest a potential to accumulate. However, occurrence data is limited in drawing conclusions about the potential of

accumulation. Furthermore, this ‘snapshot’ method of grab sampling would be expected to show poor correlation between water and biota concentrations. Alternative sampling methods such as composite and passive sampling would provide more detailed information about temporal flow. Temazepam and propranolol were not detected in any biota samples but were detected in surface water samples. Temporal fluctuations of water concentrations are not accounted for by grab sampling. Thus, internal concentrations will also be in constant state of flux that will lag behind changes in the external exposure concentration. This assumption is supported by the poor correlation between environmental compartments measured here. With this consideration it is potentially more useful to monitor contamination of biota than surface water alone when considering environmental risk of pharmaceuticals.

2.4 Conclusions

The occurrence of six pharmaceuticals were quantified in a freshwater aquatic invertebrate in several tributaries of the River Thames, with internal concentrations reaching up to 36 ng g^{-1} dw. An analytical method was developed and optimised which made use of ball-mill extraction, SPE and LC-MS/MS to reliably quantify 10 pharmaceutical compounds. Six pharmaceuticals were also quantified in surface water samples, where five compounds were also detected within the biota samples. The concentrations of pharmaceuticals were in agreement with other reported occurrence studies for both surface water and other aquatic species. It was found that surface water concentrations do not translate well into biota concentrations and therefore demonstrated the importance of measuring both when performing monitoring campaigns to assess environmental risk. Conclusions of field derived bioaccumulation is also limited

due to the poor correlation between the environmental compartments suggesting that further work into uptake and elimination kinetics is key to understanding the accumulation potential of compounds. The optimised method has provided useful information regarding an ecologically important freshwater invertebrate and can be used further to understand the kinetics of pharmaceutical accumulation.

2.5 References

1. Carson, R., *Silent spring*. 2002: Houghton Mifflin Harcourt.
2. Farrington, J.W., *Biogeochemical Processes Governing Exposure and Uptake of Organic Pollutant Compounds in Aquatic Organisms.* Environmental Health Perspectives, 1991. **90**(ArticleType: research-article / Full publication date: Jan., 1991 / Copyright © 1991 The National Institute of Environmental Health Sciences (NIEHS)): p. 75-84.
3. Brownawell, B.J. and J.W. Farrington, *Biogeochemistry of PCBs in interstitial waters of a coastal marine sediment.* Geochimica et Cosmochimica Acta, 1986. **50**(1): p. 157-169.
4. Pham, T.-T., et al., *Composition of PCBs and PAHs in the Montreal Urban Community Wastewater and in the Surface Water of the St. Lawrence River (Canada).* Water, Air, and Soil Pollution, 1999. **111**(1-4): p. 251-270.
5. Daughton, C.G. and T.A. Ternes, *Pharmaceuticals and personal care products in the environment: agents of subtle change?* Environmental Health Perspectives, 1999. **107**(Suppl 6): p. 907-938.
6. Ellis, J.B., *Pharmaceutical and personal care products (PPCPs) in urban receiving waters.* Environmental Pollution, 2006. **144**(1): p. 184-189.
7. Boyd, G.R., et al., *Pharmaceuticals and personal care products (PPCPs) in surface and treated waters of Louisiana, USA and Ontario, Canada.* Science of The Total Environment, 2003. **311**(1–3): p. 135-149.
8. Kim, J.-W., et al., *Occurrence of Pharmaceutical and Personal Care Products (PPCPs) in Surface Water from Mankyung River, South Korea.* Journal of Health Science, 2009. **55**(2): p. 249-258.

9. Barceló, D. and M. Petrovic, *Pharmaceuticals and personal care products (PPCPs) in the environment.* Analytical and Bioanalytical Chemistry, 2007. **387**(4): p. 1141-1142.

10. Hernandez-Ruiz, S., et al., *Quantifying PPCP interaction with dissolved organic matter in aqueous solution: combined use of fluorescence quenching and tandem mass spectrometry.* water research, 2012. **46**(4): p. 943-954.

11. Escher, B.I. and J.L. Hermens, *Peer reviewed: internal exposure: linking bioavailability to effects.* Environmental science & technology, 2004. **38**(23): p. 455A-462A.

12. Huerta, B., S. Rodríguez-Mozaz, and D. Barceló, *Pharmaceuticals in biota in the aquatic environment: analytical methods and environmental implications.* Analytical and Bioanalytical Chemistry, 2012. **404**(9): p. 2611-2624.

13. McEneff, G., et al., *A year-long study of the spatial occurrence and relative distribution of pharmaceutical residues in sewage effluent, receiving marine waters and marine bivalves.* Science of The Total Environment, 2014. **476–477**: p. 317-326.

14. Klosterhaus, S.L., et al., *Method validation and reconnaissance of pharmaceuticals, personal care products, and alkylphenols in surface waters, sediments, and mussels in an urban estuary.* Environment International, 2013. **54**: p. 92-99.

15. Dodder, N.G., et al., *Occurrence of contaminants of emerging concern in mussels (Mytilus spp.) along the California coast and the influence of land use, storm water discharge, and treated wastewater effluent.* Marine Pollution Bulletin, 2014. **81**(2): p. 340-346.

16. Martínez Bueno, M.J., et al., *Occurrence of venlafaxine residues and its metabolites in marine mussels at trace levels: development of analytical method and a monitoring program.* Analytical and Bioanalytical Chemistry, 2014. **406**(2): p. 601-610.

17. Bringolf, R.B., et al., *Environmental occurrence and reproductive effects of the pharmaceutical fluoxetine in native freshwater mussels.* Environmental Toxicology and Chemistry, 2010. **29**(6): p. 1311-1318.

18. Veith, G.D., D.L. DeFoe, and B.V. Bergstedt, *Measuring and Estimating the Bioconcentration Factor of Chemicals in Fish.* Journal of the Fisheries Research Board of Canada, 1979. **36**(9): p. 1040-1048.

19. Sijm, D.T.H.M. and A. van der Linde, *Size-Dependent Bioconcentration Kinetics of Hydrophobic Organic Chemicals in Fish Based on Diffusive Mass Transfer and Allometric Relationships.* Environmental Science & Technology, 1995. **29**(11): p. 2769-2777.

20. Gobas, F.A.P.C., *A model for predicting the bioaccumulation of hydrophobic organic chemicals in aquatic food-webs: application to Lake Ontario.* Ecological Modelling, 1993. **69**(1–2): p. 1-17.

21. Sugano, K., et al., *Coexistence of passive and carrier-mediated processes in drug transport.* Nat Rev Drug Discov, 2010. **9**(8): p. 597-614.

22. Dobson, P.D. and D.B. Kell, *Carrier-mediated cellular uptake of pharmaceutical drugs: an exception or the rule?* Nat Rev Drug Discov, 2008. **7**(3): p. 205-220.

23. Rand-Weaver, M., et al., *The Read-Across Hypothesis and Environmental Risk Assessment of Pharmaceuticals.* Environmental Science & Technology, 2013. **47**(20): p. 11384-11395.

24. Agatz, A., R. Ashauer, and C.D. Brown, *Imidacloprid perturbs feeding of Gammarus pulex at environmentally relevant concentrations.* Environmental Toxicology and Chemistry, 2014. **33**(3): p. 648-653.

25. Maltby, L., et al., *Evaluation of the Gammarus pulex in situ feeding assay as a biomonitor of water quality: Robustness, responsiveness, and relevance.* Environmental Toxicology and Chemistry, 2002. **21**(2): p. 361-368.

26. Friberg, N., et al., *The effect of brown trout (Salmo Trutta L.) on stream invertebrate drift, with special reference to Gammarus pulex L.* Hydrobiologia, 1994. **294**(2): p. 105-110.

27. De Lange, H.J., et al., *Behavioural responses of Gammarus pulex (Crustacea, Amphipoda) to low concentrations of pharmaceuticals.* Aquatic Toxicology, 2006. **78**(3): p. 209-216.

28. De Lange, H.J., E.T.H.M. Peeters, and M. Lürling, *Changes in Ventilation and Locomotion of Gammarus pulex (Crustacea, Amphipoda) in Response to Low Concentrations of Pharmaceuticals.* Human and Ecological Risk Assessment: An International Journal, 2009. **15**(1): p. 111-120.

29. Matthiessen, P., et al., *Use of a Gammarus pulex Bioassay to Measure the Effects of Transient Carbofuran Runoff from Farmland.* Ecotoxicology and Environmental Safety, 1995. **30**(2): p. 111-119.

30. De Lange, H.J., V. Sperber, and E.T.H.M. Peeters, *Avoidance of polycyclic aromatic hydrocarbon–contaminated sediments by the freshwater invertebrates Gammarus pulex and Asellus aquaticus.* Environmental Toxicology and Chemistry, 2006. **25**(2): p. 452-457.

31. Meredith-Williams, M., et al., *Uptake and depuration of pharmaceuticals in aquatic invertebrates.* Environmental Pollution, 2012. **165**: p. 250-258.

32. Barron, L., J. Tobin, and B. Paull, *Multi-residue determination of pharmaceuticals in sludge and sludge enriched soils using pressurized liquid extraction, solid phase extraction and liquid chromatography with tandem mass spectrometry.* J Environ Monit, 2008. **10**(3): p. 353-61.

33. Barron, L., J. Tobin, and B. Paull, *Multi-residue determination of pharmaceuticals in sludge and sludge enriched soils using pressurized liquid extraction, solid phase extraction and liquid chromatography with tandem mass spectrometry.* Journal of Environmental Monitoring, 2008. **10**(3): p. 353-361.

34. Lipinski, C.A., *Lead-and drug-like compounds: the rule-of-five revolution.* Drug Discovery Today: Technologies, 2004. **1**(4): p. 337-341.

35. Kamel, A., K. Colizza, and G. PGRD, *Collisionally-Induced Dissociation of Methimazole and Acetylsalicylic Acid: Proposed Mechanisms of Ion Formation using Hydrogen/Deuterium Exchange.*

36. Loftsson, T., et al., *Cyclodextrin Solubilization of the Antibacterial Agents Triclosan and Triclocarban: Effect of Ionization and Polymers.* Journal of inclusion phenomena and macrocyclic chemistry, 2005. **52**(1-2): p. 109-117.

37. Liang, B., et al., *Adsorption and degradation of triazophos, chlorpyrifos and their main hydrolytic metabolites in paddy soil from Chaohu Lake, China.* Journal of Environmental Management, 2011. **92**(9): p. 2229-2234.

38. Heard, C.M. and C. Screen, *Probing the permeation enhancement of mefenamic acid by ethanol across full-thickness skin, heat-separated*

epidermal membrane and heat-separated dermal membrane. International Journal of Pharmaceutics, 2008. **349**(1–2): p. 323-325.

39. Madikizela, L.M., S.F. Muthwa, and L. Chimuka, *Determination of Triclosan and Ketoprofen in river water and wastewater by solid phase extraction and high performance liquid chromatography.* South African Journal of Chemistry, 2014. **67**: p. 0-0.
40. Cras, J.J., et al., *Comparison of chemical cleaning methods of glass in preparation for silanization.* Biosensors and Bioelectronics, 1999. **14**(8–9): p. 683-688.
41. Straub, R. and R. Voyksner, *Negative ion formation in electrospray mass spectrometry.* Journal of the American Society for Mass Spectrometry, 1993. **4**(7): p. 578-587.
42. Chen, M., et al., *Determination of nine environmental phenols in urine by ultra-high-performance liquid chromatography–tandem mass spectrometry.* Journal of analytical toxicology, 2012. **36**(9): p. 608-615.
43. Furey, A., et al., *Ion suppression; A critical review on causes, evaluation, prevention and applications.* Talanta, 2013. **115**: p. 104-122.
44. Redshaw, C.H., V.G. Wootton, and S.J. Rowland, *Uptake of the pharmaceutical Fluoxetine Hydrochloride from growth medium by Brassicaceae.* Phytochemistry, 2008. **69**(13): p. 2510-2516.
45. Wu, X., J.L. Conkle, and J. Gan, *Multi-residue determination of pharmaceutical and personal care products in vegetables.* Journal of Chromatography A, 2012. **1254**: p. 78-86.
46. Annesley, T.M., *Ion Suppression in Mass Spectrometry.* Clinical Chemistry, 2003. **49**(7): p. 1041-1044.

47. McEneff, G., et al., *The determination of pharmaceutical residues in cooked and uncooked marine bivalves using pressurised liquid extraction, solid-phase extraction and liquid chromatography–tandem mass spectrometry.* Analytical and Bioanalytical Chemistry, 2013. **405**(29): p. 9509-9521.

48. Sakihama, Y. and H. Yamasaki, *Lipid Peroxidation Induced by Phenolics in Conjunction with Aluminum Ions.* Biologia Plantarum, 2002. **45**(2): p. 249-254.

49. Quarmby, R., et al., *Studies on the quaternary structure of the lobster exoskeleton carotenoprotein, crustacyanin.* Comparative Biochemistry and Physiology Part B: Comparative Biochemistry, 1977. **56**(1): p. 55-61.

50. LoBrutto, R., A. Jones, and Y.V. Kazakevich, *Effect of counter-anion concentration on retention in high-performance liquid chromatography of protonated basic analytes.* Journal of Chromatography A, 2001. **913**(1–2): p. 189-196.

51. Kwon, J.W., et al., *Determination of 17α-ethynylestradiol, carbamazepine, diazepam, simvastatin, and oxybenzone in fish livers.* Journal of AOAC International, 2009. **92**(1): p. 359-369.

52. Inostroza, P.A., et al., *Body burden of pesticides and wastewater-derived pollutants on freshwater invertebrates: Method development and application in the Danube River.* Environmental Pollution, 2016. **214**: p. 77-85.

53. Zhang, Y., S.-U. Geißen, and C. Gal, *Carbamazepine and diclofenac: Removal in wastewater treatment plants and occurrence in water bodies.* Chemosphere, 2008. **73**(8): p. 1151-1161.

54. Tixier, C., et al., *Occurrence and Fate of Carbamazepine, Clofibric Acid, Diclofenac, Ibuprofen, Ketoprofen, and Naproxen in Surface Waters.* Environmental Science & Technology, 2003. **37**(6): p. 1061-1068.

55. Tanoue, R., et al., *Simultaneous determination of polar pharmaceuticals and personal care products in biological organs and tissues.* Journal of Chromatography A, 2014. **1355**: p. 193-205.

56. Huerta, B., et al., *Development of an extraction and purification method for the determination of multi-class pharmaceuticals and endocrine disruptors in freshwater invertebrates.* Talanta, 2015. **132**: p. 373-381.

57. Mehinto, A.C., E.M. Hill, and C.R. Tyler, *Uptake and Biological Effects of Environmentally Relevant Concentrations of the Nonsteroidal Anti-inflammatory Pharmaceutical Diclofenac in Rainbow Trout (Oncorhynchus mykiss).* Environmental Science & Technology, 2010. **44**(6): p. 2176-2182.

58. Ehmann, P. *Beverley Brook Information Pack* 2013 [cited 2014 05/03]; Available from: http://webarchive.nationalarchives.gov.uk/20140328084622/http://www.environment-agency.gov.uk/static/documents/Research/Beverley_Brook.pdf.

59. Kasprzyk-Hordern, B., R.M. Dinsdale, and A.J. Guwy, *The occurrence of pharmaceuticals, personal care products, endocrine disruptors and illicit drugs in surface water in South Wales, UK.* Water Research, 2008. **42**(13): p. 3498-3518.

60. Ashton, D., M. Hilton, and K.V. Thomas, *Investigating the environmental transport of human pharmaceuticals to streams in the United Kingdom.* Science of The Total Environment, 2004. **333**(1–3): p. 167-184.

61. Roberts, P.H. and K.V. Thomas, *The occurrence of selected pharmaceuticals in wastewater effluent and surface waters of the lower Tyne catchment.* Science of The Total Environment, 2006. **356**(1–3): p. 143-153.

62. Feitosa-Felizzola, J. and S. Chiron, *Occurrence and distribution of selected antibiotics in a small Mediterranean stream (Arc River, Southern France).* Journal of Hydrology, 2009. **364**(1–2): p. 50-57.

63. Silva, B.F.d., et al., *Occurrence and distribution of pharmaceuticals in surface water, suspended solids and sediments of the Ebro river basin, Spain.* Chemosphere, 2011. **85**(8): p. 1331-1339.

64. Yoon, Y., et al., *Occurrence of endocrine disrupting compounds, pharmaceuticals, and personal care products in the Han River (Seoul, South Korea).* Science of The Total Environment, 2010. **408**(3): p. 636-643.

Chapter 3. The determination of uptake and elimination kinetics for selected pharmaceuticals using radiolabelled exposures in *Gammarus pulex*.

3.1 Introduction

As shown in the previous chapter, low level occurrence of several pharmaceuticals was determined in both surface waters and *G. pulex* collected in the Greater London catchment area. Other studies have also shown low level occurrence in biota such as mussels among other aquatic invertebrates [1-3]. The occurrence of these pharmaceuticals indicates that invertebrates have the potential to accumulate pharmaceuticals, which may lead to adverse effects throughout food chains. The effects of pharmaceuticals have previously been demonstrated in *G. pulex,* which led to significant changes in their behaviour including ventilation, feeding and locomotion when exposed to fluoxetine and ibuprofen between 10 – 100 ng L^{-1} [4, 5]. From reported occurrence data it can be assumed that acute effects such as mortality are unlikely to be observed in exposed organisms, as the concentrations are often several orders of magnitude below acute toxicity thresholds [6]. Therefore, measurement of sensitive sub-lethal effects such as behavioural changes, oxidative stress and alterations to organ function in fish and invertebrates could indicate early warning signs of stress [7-9].

Currently, environmental risk assessment of pharmaceuticals is required for licensing where standard acute toxicity tests (e.g. LC_{50}) are employed, unless the PEC:PNEC ratio is <1 where no further testing is required. However, as mentioned previously acute toxicity is less likely to be observed in the

environment therefore these types of standard toxicity tests do not yield much information for reliable risk assessment. Furthermore, there is a lack of focussed studies on the uptake and elimination kinetics of pharmaceuticals in biota leading to a lack of knowledge on whether pharmaceuticals do accumulate. Many of these studies to date, also only focus on vertebrate species such as fish for ecotoxicological testing, thus the potential for adverse effects in invertebrates is not well understood. Aquatic bioconcentration or bioaccumulation studies are used to identify whether a compound can accumulate through water or food exposure of the selected xenobiotic. The ratio between the concentration in the exposure route and the concentration inside the organism leads to a quantitative measure of the accumulation potential. Early models of accumulation were determined for compounds such as methylmercury in fish which considered variables such as the volume of water passing over the gills, the assimilation across the gills and the body mass of the organism [10]. Development of these toxicokinetic models have continued to focus on the assessment of other factors such as fish lipid content, lipid phase resistance, water phase resistance and compound hydrophobicity [11-14].

As mentioned, the BCF is a ratio between the concentrations in the water and in animals but it can also be determined using a kinetic estimation defined as the ratio between the uptake rate constant (k_1) and the elimination rate constant (k_2) [15]. The rate constants can be determined by using curve fitting algorithms in concentration-time plots of the toxicokinetic experiments. They can also be estimated simultaneously or sequentially, where the simultaneous method can be considered more biologically feasible, as uptake and elimination are not separate processes. REACH ANNEX XIII defines a compound to be accumulative when the ratio is ≥2,500 or very accumulative if the value is ≥5,000

[16]. Standard BCF tests such as the OECD 305 guideline [15] can be very time consuming (2-3 months), labour intensive studies that use a large number of fish and are considerably expensive. The combination of these factors with the sheer volume of pharmaceuticals to be tested leads to feasibility issues in risk assessment and is also counterproductive to policy aims such as the 3R's. Therefore, recent approaches have encompassed shorter exposure times and less time points to reduce the number of fish and increase the throughput of accumulation testing such as the 'minimised' OECD 305 test guideline [15]. Other authors have selected non-standard organisms (fish) such as *Gammarus*, utilising exposure periods of 4 – 7 days to assess the accumulation potential of xenobiotics [17-19]. Whilst these studies offer a potential alternative to the standard fish tests, the number of studies with invertebrates is limited and therefore the reliability of using these non-standard organisms for ecotoxicological testing should be assessed.

The aim of this work was to assess the accumulation potential of selected pharmaceuticals exposed at the upper range of environmental relevance in the non-standard organism *G. pulex*. Bioconcentration factors will be estimated using both sequential and simultaneous modelling as specified by the OECD 305 guidelines. Finally, the reliability of using these models on non-standard animals to estimate BCFs will be critically evaluated for the first time.

3.2 Materials & methods

3.2.1 Reagents, chemicals and consumables

Radio-labelled pharmaceuticals including ^{3}H-propranolol hydrochloride (29.0 Ci mmol^{-1},) was acquired from Amersham Biosciences. ^{3}H-metoprolol (29.7 Ci mmol^{-1}), ^{3}H-formoterol (18.5 Ci mmol^{-1}) and ^{3}H-terbutaline

(29.0 Ci mmol^{-1}) were obtained from Vitrax. ^{14}C-ibuprofen (2.03 Ci mmol^{-1}) was obtained from American Radiolabelled Chemicals Inc., (St Louis, US). ^{3}H-ranitidine (2.5 Ci mmol^{-1}) were obtained from Moravek Biochemicals, ^{14}C-diclofenac (0.063 Ci mmol^{-1}) and ^{3}H-imipramine hydrochloride (48.5 Ci mmol^{-1}) from Perkin-Elmer. All stock solutions were stored in ethanol. Hydrogen peroxide solution (30 % w/w) and analytical grade salts (>99 %) including sodium hydrogen carbonate, magnesium sulphate, calcium sulphate, potassium chloride were purchased from Sigma (Dorset, UK). Tissue solubiliser (Solvable^{TM}) and liquid scintillation cocktail (Hionic Fluor^{TM}) were purchased from Fischer Scientific Ltd (Loughborough, UK). Ultra-pure water was obtained from a Millipore Milli-Q water purification system with a specific resistance of 18.2 MΩ.cm or greater (Millipore, Bedford, MA, USA). 6-well culture plates were obtained from VWR (Leicestershire, UK).

3.2.2 Sample collection and culture maintenance

Gammarus pulex were collected by kick-sampling from the River Cray, South-East London, UK, 51°23'09.5"N 0°06'32.4"E. This site was previously shown (Chapter 2) to have low pharmaceutical contamination in both collected surface water and animal samples [20]. The populations were transported to the laboratory in 500 mL Nalgene^{TM} flasks filled with surface water from the sample collection site. Populations were rinsed with artificial freshwater (AFW) and then acclimatised to laboratory conditions (as specified below) for a minimum of 7 days before any exposure experiments were performed. AFW was prepared from 1.15 mM of $NaHCO_3$, 0.50 mM $MgSO_4$, 0.44 mM $CaSO_4$ and 0.05 mM of KCl dissolved in 20 L of ultra-pure water [21]. This water was subsequently aerated for several hours to remove dissolved carbonic acid and maximise the dissolved oxygen

concentrations. Each culture tank (n=8) was filled with 2.5 L of AFW and animals were fed with alder leaves that were previously collected from the collection site and conditioned by submersion in surface water for two days prior to use.

3.2.3 Toxicokinetic exposure and conditions

Toxicokinetic experiments were performed separately for each pharmaceutical for a total of 96h, which included a 48h uptake phase followed by a 48h depuration period. Individual adult organisms, both male and female (>5 mg wet weight) were placed in each well of 6-well culture plates. *G. pulex* were carefully transferred to well plates using blunt forceps to avoid any harm to the organisms before exposure. A single well contained one organism in 10 mL of exposure media (AFW and test compound) and only non-parasitised individuals were used (absence of *Pomphorhynchus laevis* indicated by the lack of an orange dot on the dorsal side of the animal). *G. pulex* were exposed to individual PhACs at a concentration of 1 µg L^{-1}, except for diclofenac and ibuprofen which were present at 10 µg L^{-1}. The higher exposure of these two compounds was due to the low activity of the radiolabel. The exposure concentrations were well below mortality thresholds (>1000-fold) for several of the compounds in *G. pulex* (diclofenac, propranolol, ibuprofen, metoprolol, ranitidine and imipramine) [22]. All exposure media contained <0.05 % of solvent (ethanol). A total of 33 organisms were used per exposure and were sampled (n=3/time-point) at 2, 5, 18, 24 and 48h in the uptake phase followed by the same time-points in the depuration phase.

Along with *G. pulex*, 50 µL of water was also sampled from each well for analysis of radioactivity and determination of test compound concentration in the media. Each sampled organism was washed in 10 mL of ultra-pure water for 10

seconds (n=6) and gently blotted dry to remove any excess exposure media and unbound compound to the cuticle of the animal. Organisms were weighed after sampling to determine body mass and then transferred to scintillation tubes for tissue solubilisation. Three individual organisms were also exposed to unspiked AFW in culture plates and sampled after 96h in a control experiment to account for any background radiation. Additionally, for each experiment, three wells without *G. pulex* were filled with exposure media to account for losses of the compound by sorption to the walls of culture plates. Culture plates were stored in sealed plastic containers with wet tissue to prevent evaporative losses during the static exposure. The light cycle followed 12:12h light:dark without a dusk/dawn transition period. All experiments were performed in a temperature controlled room at 15 °C (± 2 °C) and water *p*H was also monitored across each experiment and measured 8.2 ± 0.1 *p*H.

3.2.4 Sample preparation and liquid scintillation counting

Water samples (50 µL) collected from each exposure well were added to 2 mL of Hionic Fluor liquid scintillation cocktail and counted for radioactivity on a Beckman LS6500 instrument (Beckman Coulter, Inc.). Sampled *G. pulex* individuals were placed in a scintillation tube with 2 mL of tissue solubiliser and maintained at room temperature (approx. 20 °C) for 96h. Samples were shaken vigorously and then a 50 µL aliquot of the solubilised biotic extract was added to 2 mL of Hionic Fluor to be counted. To account for any difference in counts caused by colour quenching, hydrogen peroxide (200 µL) was added to a previously counted biotic extract and re-analysed (n=30). No difference in counts was observed with or without the presence of hydrogen peroxide. Therefore, all other biotic samples were counted without the addition of hydrogen peroxide. In

addition, chemiluminescence accounted for <0.01 % of the overall counts, and was therefore ignored.

3.2.5 Modelling bioconcentration factors

Parameter estimation of uptake rate constant (k_1) and depuration rate constant (k_2) was performed using a curve fitting algorithm via Minitab statistical software (Minitab Ltd., Coventry UK) and as outlined in the OECD 305 Fish Bioconcentration Guidelines [15]. The concentration of compound in the organism is assumed to follow first order kinetics and is expressed in Equation 3.1.

$$\frac{dC_{organism}}{dt} = k_1 \times [C_{water}] - k_2 \times [C_{organism}] \quad (3.1)$$

Where, $dC_{organism}/dt$ is the rate of change in the concentration of a compound within/on *G. pulex* (mg kg^{-1} day^{-1}), k_1 is the uptake rate constant (L kg^{-1} day^{-1}), k_2 is the elimination rate constant (day^{-1}), C_{water} is the concentration of test compound in the water (mg L^{-1}) and $C_{organism}$ is the concentration of test compound in the organism (mg kg^{-1}). Equation 3.1 was integrated into Equations 3.2 and 3.3 for fitting of curves to the uptake and depuration data. This method, known as the Levenberg–Marquardt algorithm, uses an iterative formula to minimise the residual errors between the observed and predicted data points and simultaneously estimates k_1 and k_2 values from the fitted curve i.e.

$$[C_{organism}] = [C_{water}] \times \frac{k_1}{k_2} \times (1 - e^{-k_2 t}), \text{ when } 0 < t < t_e \quad (3.2)$$

$$[C_{organism}] = [C_{water}] \times \frac{k_1}{k_2} \times (1 - e^{-k_2 (t - t_e)} - e^{-k_2 t}), \text{ when } t > t_e \quad (3.3)$$

Where, t is the time (days) and t_e is the end time of the uptake phase (days). At steady-state, the rate of uptake should be equal to the rate of

depuration and there should be no overall change in analyte concentration within *G. pulex*, as expressed by Equation 3.4.

$$k_1 \times [C_{water}] = k_2 \times [C_{organism}] \leftrightarrow \frac{k_1}{k_2} = \frac{[C_{fish}]}{[C_{water}]} = BCF \quad (3.4)$$

Where, BCF is the bioconcentration factor (L kg^{-1}). The BCF can also be estimated using a sequential method where a simple linear regression model is developed based on the depuration data only. With the assumption of first order kinetics, the model should fit a straight line and its slope represents the elimination rate constant as shown in Equation 3.5, i.e.

$$ln[C_{organism}] = -k_2 \times t + c \quad (3.5)$$

Where, ln[$C_{organism}$] is the natural log of the analyte concentration within *G. pulex* and *c* is the intercept, which here equals the natural log of the analyte concentration in the *G. pulex* (mg kg^{-1}) at the start of the depuration phase. The k_2 from Equation 3.5 can then be used as a parameter in the curve fitting algorithm to estimate k_1. The rearrangement of Equation 3.2 allows the value for k_1 to be calculated over the time interval specified, as shown in Equation 3.6 [23]. The assumptions of the equation are that the analyte water concentration and k_2 remain constant. The k_2 used in Equation 3.6 was directly estimated by using linear regression of the depuration data to obtain the slope (k_2). The value of k_1 should remain constant over the entire experiment.

$$k_1 = \frac{[C_{organism}] \times k_2}{[C_{water}] \times (1 - e^{-k_2 t})} \quad (3.6)$$

For this study, initial parameters for k_1 and k_2 were arbitrarily set at 0.1 in the software with C_{water} set in µg L^{-1}, *t* set at 48h and the maximum number of iterations was set at 200 upon which optimised k_1 and k_2 values were

subsequently derived. Confidence intervals (95 %) were plotted for curves and the overall model fits were assessed. The lack-of-fit test was calculated in the Minitab software and was used to assess the fit of the line by comparing the variation in response of the replicate data. Lack-of-fit was assessed at a significance level of 0.05. Correlation coefficients (R^2) were evaluated when the sequential method was used to estimate k_2. The distribution coefficient (Log$D_{8.2}$) was generated using ACD Labs Percepta software (Berks, UK), for the interpretation of estimated BCF values.

3.3 Results & discussion

3.3.1 Initial toxicokinetic experiments

Preliminary exposures were investigated to optimise experimental conditions to obtain the most reliable data. *G. pulex* individuals were placed into 6 and 12-well culture plates (10 mL and 5 mL volumes, respectively) and monitored over a 48h period. The 12-well culture plates showed increased mortality when compared to the 6-well (> 50% mortality). The higher mortality was possibly a result of low oxygen content in the smaller volume of water. The OECD 305 guidance document [15] states that mortality of exposures should be <20 %. Therefore, the 6-well culture plates were selected for all toxicokinetic experiments as the mortality of individuals in these plates remained <20 %.

The first toxicokinetic exposure was performed with propranolol which resulted in an unexpected uptake and elimination profile. As shown in Figure 3.1, there was initially a very rapid uptake of compound in the first 2h period of the exposure reaching a mean concentration of 660 ng g^{-1}. After this, the compound concentration in the animals was reduced significantly to a mean concentration of 127 ng g^{-1}, which indicated there was a rapid turnover (elimination proceeded

faster than uptake) of compound inside the animal. Reduction of the internal concentration by ~80 % would suggest that the clearance of propranolol became more rapid than the uptake. However, this only occurred after a lag period of the first two hours which may indicate there was a threshold concentration before detoxification enzymes began metabolism and elimination. After the first 24h, the remaining concentration of propranolol in *G. pulex* reached a plateau (some small scatter) which would indicate steady state has been achieved. In the final 48h of the experiment, individuals were placed into 'clean' water to allow depuration. In this time period the concentration of propranolol did not reduce any further which again was unexpected due to the observed rapid elimination of propranolol in the uptake phase. A possible explanation is that the radiolabelled carbon atoms have been metabolised and incorporated into the animals themselves leading to a residual background level of radioactivity.

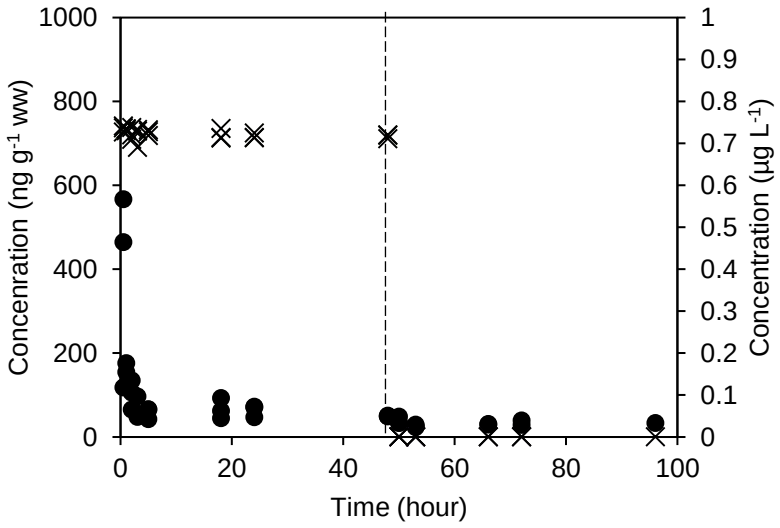

Figure 3.1: Toxicokinetic profile G. pulex exposed to propranolol at 1 µg L^{-1}

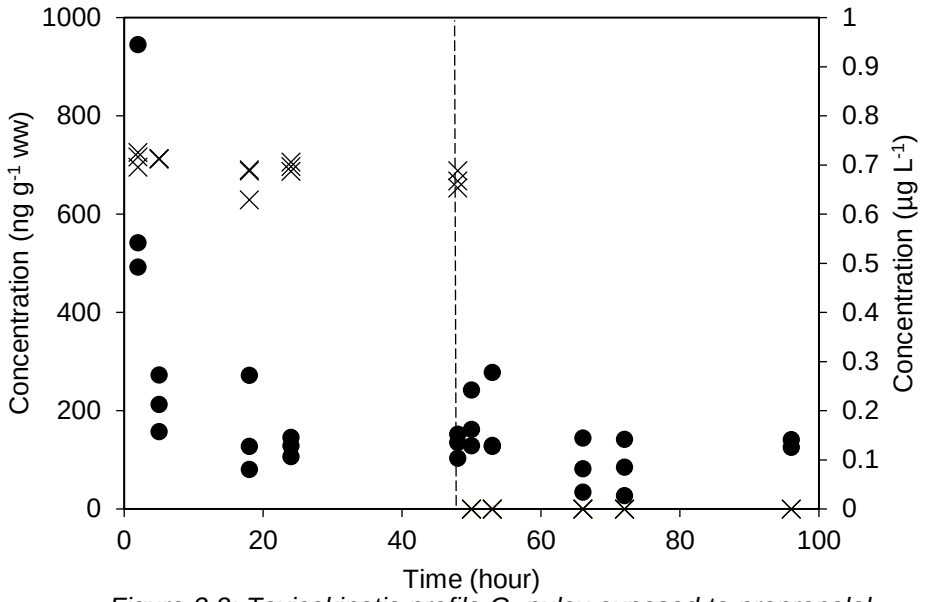

Figure 3.2: Toxicokinetic profile G. pulex exposed to propranolol at 1 µg L^{-1}.

Further investigation of this toxicokinetic profile was performed in the first instance to ensure repeatability. Additional time intervals were introduced for better characterisation of the initial uptake period. Early time intervals were selected at 0.5, 1, 2, 3 and 5h (Figure 3.2) and showed the same trend observed in the first exposure although the concentrations were lower in the earlier time intervals. The highest concentration was reached within 0.5h (mean = 379 ng g^{-1}), followed by significant decreases at 3h. A plateau was reached again in the uptake phase and when animals were removed to the depuration phase, the mean concentration remained at 32 n g^{-1}. As mentioned previously, the observed toxicokinetic profiles were unexpected and whilst biological interpretation of the data was plausible the unusual data could have also been a result of contamination leading to false counts.

A small experiment was performed which investigated two different tissue solubilisers (Soluene® 350 & Solvable™) and two scintillation cocktails (Ecolume™ & Hionic Fluor). When unexposed *G. pulex* organisms were solubilised with either Soluene® 350 or Solvable™ and then counted using

Ecolume™ unusually high radioactivity measured by disintegrations per minute (DPM) were observed (Table 3.1).

Table 3.1: Effect of tissue solubiliser and liquid scintillation cocktail on radiolabel activity.

Tissue Solubiliser	Scintillation Cocktail	*Gammarus* Sample?	Disintegrations Per Minute (DPM)
Solvable™	Hionic Fluor	No	13.85
Solvable™	Ecolume™	No	3938.58
Soluene® 350	Hionic Fluor	No	13.51
Soluene® 350	Hionic Fluor	Yes	14.45
Soluene® 350	Ecolume™	Yes	48759.94
Solvable™	Hionic Fluor	Yes	15.48
Solvable™	Ecolume™	Yes	2333.66

However, when Hionic Fluor was used the DPM were in line with background ^{14}C radiation levels. The high DPM counts observed with Ecolume™ were the result of false counts from chemiluminescence. In liquid scintillation counting instruments, the counts are the indirect measurement of radioactivity through the detection of photons. Thus, any reactions between the sample and liquid scintillation cocktail may produce photons (chemiluminescence). These photon emissions mimic the counts that would otherwise be produced from radioactivity. As both tissue solubilisers are highly alkaline solutions it is likely that the chemiluminescence resulted from this.

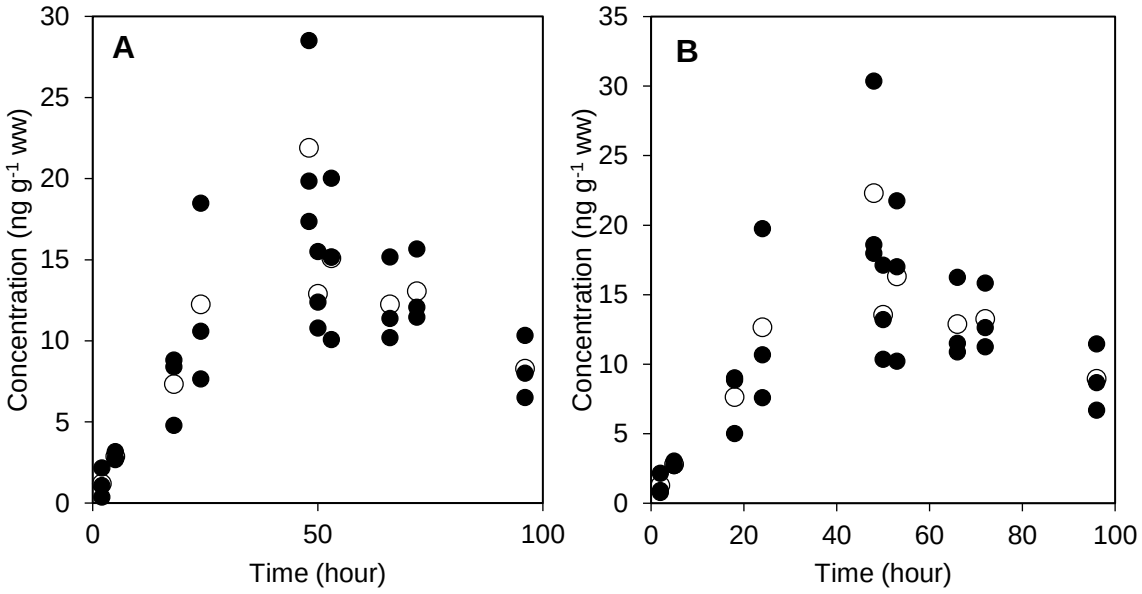

Figure 3.3: The effect of colour quenching on toxicokinetic profiles of G. pulex exposed to propranolol (1 µg L^{-1}). A – no hydrogen peroxide, B – addition of hydrogen peroxide. Open circles are mean concentration at each time point.

The exposure with propranolol was repeated using Hionic Fluor as a liquid scintillation cocktail to supress chemiluminescence. As shown in Figure 3.3, the profile observed was much more expected for a toxicokinetic plot. The uptake followed a steady increase reaching a mean concentration of 22 ng g^{-1} at 48 h, after removal to the depuration phase concentrations were reduced to a mean of 8 ng g^{-1}. The kinetic BCF was estimated to be 32, indicating that propranolol has a very low potential to accumulate in *G. pulex*. To ensure no colour quenching occurred during analysis, hydrogen peroxide (200 µL) was added to the samples and re-counted. The addition of hydrogen peroxide made no significant difference to measured DPM and therefore it was assumed that no colour quenching had occurred (Figure 3.3).

The OECD 305 model assumes that uptake and elimination follow first-order kinetics. However, when a line was plotted through the mean concentrations an R^2 of 0.991 was calculated indicating that over the plotted data the order of the reaction was zero-order, this was further supported by a natural logarithmic plot of concentration versus time which did not yield a straight line (Figure 3.4).

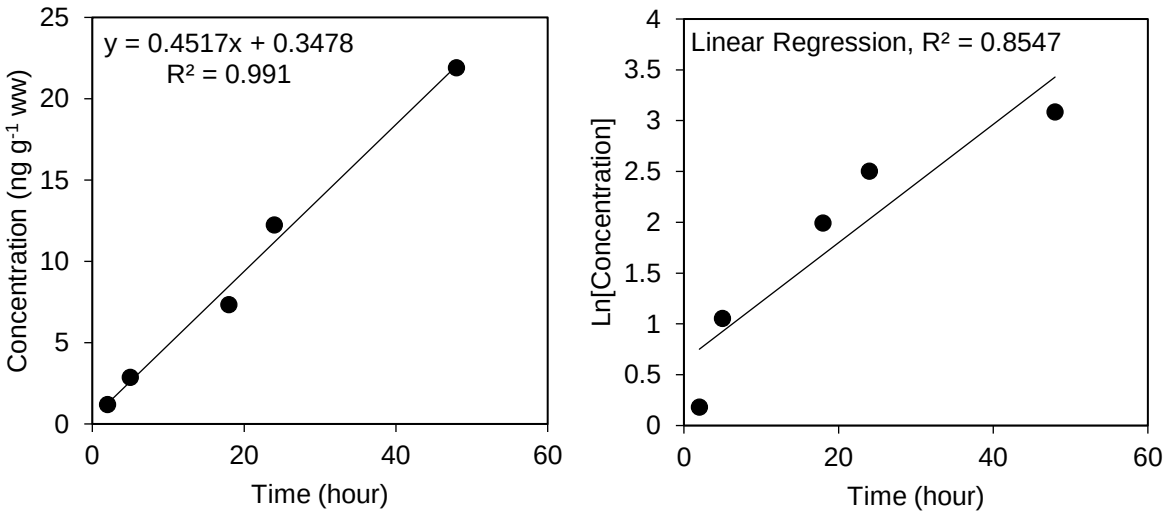

Figure 3.4: Concentration-time plots of propranolol in G. pulex.

Zero-order kinetics would suggest that propranolol is concentrated by carrier mediated uptake as the rate of uptake does not decrease over time. Thus, the uptake was independent of concentration and saturation of the carriers had occurred so that zero-order kinetics became predominant. This observation has potentially important implications as bioconcentration models often assume that uptake is by passive diffusion. Early models were developed using highly hydrophobic organic contaminants [11] and this could lead to unreliable uptake models for studies involving amphoteric compounds such as pharmaceuticals. Recently, several authors have stressed the importance of carrier mediated processes when modelling and considering uptake models [24, 25].

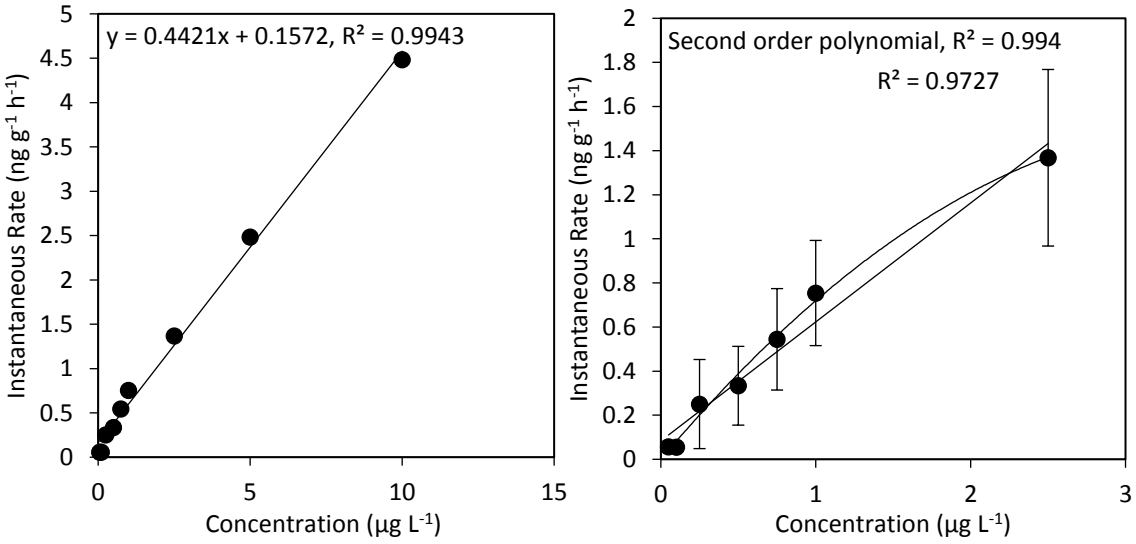

Figure 3.5: Initial uptake rates versus exposure concentration of propranolol in G. pulex (0.05 – 10 µg L^{-1})

To further investigate the order of kinetics and the type of uptake that occurred, a dose-response curve was plotted for varying concentrations of propranolol (50 ng L^{-1} to 10 µg L^{-1}). Figure 3.5 shows that at the lower concentrations from 0.05 to 2.5 µg L^{-1} there is slight curvature to the line indicating the instantaneous rate was slowing as the concentration of the exposure solution increased. The slowing of the uptake rate at a threshold concentration might

suggest a saturation event was occurring. At concentrations higher than 2.5 µg L^{-1} the line becomes linear (R^2 = 0.9993), indicating that the instantaneous uptake rate continued to increase with exposure concentrations, as would be expected of passive diffusion. The observed change in the instantaneous rates is evidence that both passive diffusion and carrier mediated uptake process are taking place simultaneously. This finding was observed in a separate study that studied the permeation of fish gill cell cultures to propranolol [26]. In addition, a previous study also demonstrated saturable uptake of propranolol at low concentrations in rats but when doses were increased passive diffusion became dominant [27]. However, as these processes occur simultaneously it becomes difficult to investigate further the contribution of each process to the uptake of a compound.

3.3.2 Population differences on the uptake and elimination of propranolol

Propranolol was taken for further investigation to see what effect, if any, different populations and acclimatisation periods had when they were used. The acclimatisation period of 1, 2 and 7 weeks were investigated to identify any differences in uptake or elimination. Individuals were collected from the same site but held in laboratory conditions for these time intervals. The internal concentrations in both the uptake and elimination phases were compared using a two factor ANOVA with replication. This allowed the statistical interpretation of variances between each acclimatisation group, the time interval in the exposure and the interaction between them.

The uptake data showed statistically significant differences between each group treatment and the time intervals when considered as separate factors. However, the interaction between these two factors showed no statistical significance (95 % confidence interval) which indicated that there was no

difference between acclimatisation on the uptake of propranolol in *G. pulex.* When comparing the elimination data, the same conclusion could be drawn as there was no statistical significance between the interaction between acclimatisation group and the time interval that samples were taken from. The ANOVA showed that overall there is no significant effect on the length of acclimatisation time on *G. pulex*. However, if samples are field collected a depuration period is still recommended of ≥ 1 week, so that any residual contamination is reduced or eliminated. Furthermore, unexposed organisms that have been depurated should also be screened for any residual contamination.

Populations from different sites may also show variability in their potential to bioconcentrate a compound. For example, a population from a polluted site may have upregulated expression of detoxification enzymes compared to animals that are collected from a pristine site. This has been observed in killifish (*Fundulus heteroclitus*) where pollution induced tolerance to metals and PAHs/PCBs have reduced the toxic sensitivity in pristine and contaminated sites [28, 29]. Alternatively, it is possible that polluted sites may lead to more stress on animals therefore their ability to eliminate xenobiotics may be reduced. An exposure experiment was performed on three groups of animals collected from different sites to assess any variability between different populations. Two groups were collected from urban areas (River Wandle, 51°25'25.4"N 0°11'01.9"W & River Cray, London) and the final collection site was located in a rural area (Ashes Hollow, Shropshire 52°31'59.7"N 2°50'20.1"W). ANOVA of the uptake and elimination from the three sites showed that there was no statistical significance between the uptake data. However, the elimination data between all three populations gave a *p*-value of 0.03, indicating there was a significant variance arising between the groups. To identify where the variance had arisen from,

groups were placed in a pair-wise manner and the ANOVA analysis repeated. There was no significant difference between the variance in elimination between the urban sites. However, one of the urban sites (River Wandle, Colliers Wood) when compared with the site in Shropshire showed a *p*-value of 0.03. Comparison of the internal concentrations during the elimination phase showed that after 48h the concentration of propranolol from the urban site had reduced below that of the Shropshire population (Figure 3.6).

Determination of BCFs resulted in 277 for the Shropshire population and 55 for the population from Colliers Wood, a difference of 5-fold. The difference in BCF values resulted from the lower k_2 value of the Shropshire population that was estimated at 0.002 d^{-1}, ~8.5-fold lower than in the population from Colliers Wood.

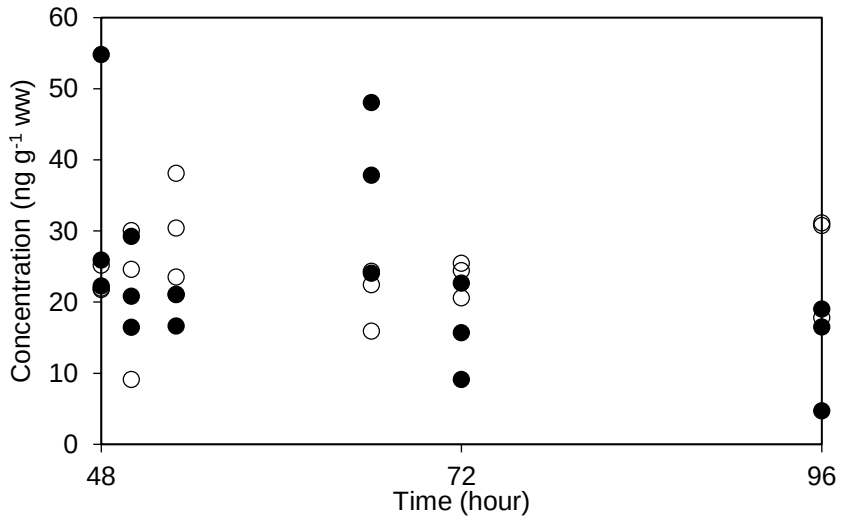

Figure 3.6: Elimination of propranolol from G. pulex, solid circles – River Wandle (urban site), open circles – Ashes Hollow (rural site). Measured propranolol concentration in water phase was 0.91 ± 0.046 µg L^{-1} (uptake) and 0.006 ± 0.004 µg L^{-1} (depuration).

This data potentially indicates that the animals from the Shropshire site had a lower turnover of propranolol due to reduced elimination. In comparison both urban populations had a much lower BCF for propranolol although only one site showed a statistically significant difference to the Shropshire population. Analysis of the water from each site showed that both the urban sites had contamination of several pharmaceuticals, reaching up to the mid ng L^{-1} range and

concentrations of propranolol were relatively high (>200 ng L^{-1}) [20, 30]. In contrast, the Shropshire site had very low level contamination (Table 3.2) with the highest concentrations reaching 28 ng L^{-1} (warfarin). The maximum propranolol concentration in the water was determined at 24 ng L^{-1}, approximately 10-fold lower than reported in the urban surface waters.

Table 3.2: Determined pharmaceutical concentrations in surface water and G. pulex from Ashes Hollow (Shropshire, rural site).

	Surface Water (ng L^{-1})			*G. pulex* (ng g^{-1} dw)		
Carbamazepine	5	6	5	N.D.	<LOQ	N.D.
Propranolol	10	24	<LOQ	<LOQ	160	N.D.
Diazepam	<LOQ	<LOQ	<LOQ	7	10	9
Trimethoprim	6	8	14	6	140	9
Temazepam	<LOQ	<LOQ	<LOQ	<LOQ	<LOQ	7
Warfarin	18	28	12	5	N.D.	N.D.

Overall, this data may indicate a potential adaptation/tolerance of populations from contaminated urban rivers to eliminate xenobiotics better than those populations from less contaminated sites. Previous works have shown adaptions of killifish to contaminated sediments and PCB pollution through alterations in CYP expression that were shown to be heritable traits (genetic and non-genetic mechanisms) [31-33]. Increased tolerance of biota has also been observed for heavy metals which demonstrates the possibility that pollution induced tolerance is an adaptation of biota to reduce body burdens of contaminants [34]. Whilst this work supports this, it should be considered that further work would be needed to substantiate this argument. In particular, more replicates, sites, different compounds and life history examination of the selected species would give further understanding to the induction of tolerance mechanisms.

3.3.4 The uptake and elimination of selected pharmaceuticals in *G. pulex*

Toxicokinetic experiments were performed for eight selected pharmaceuticals (Figure 3.7).

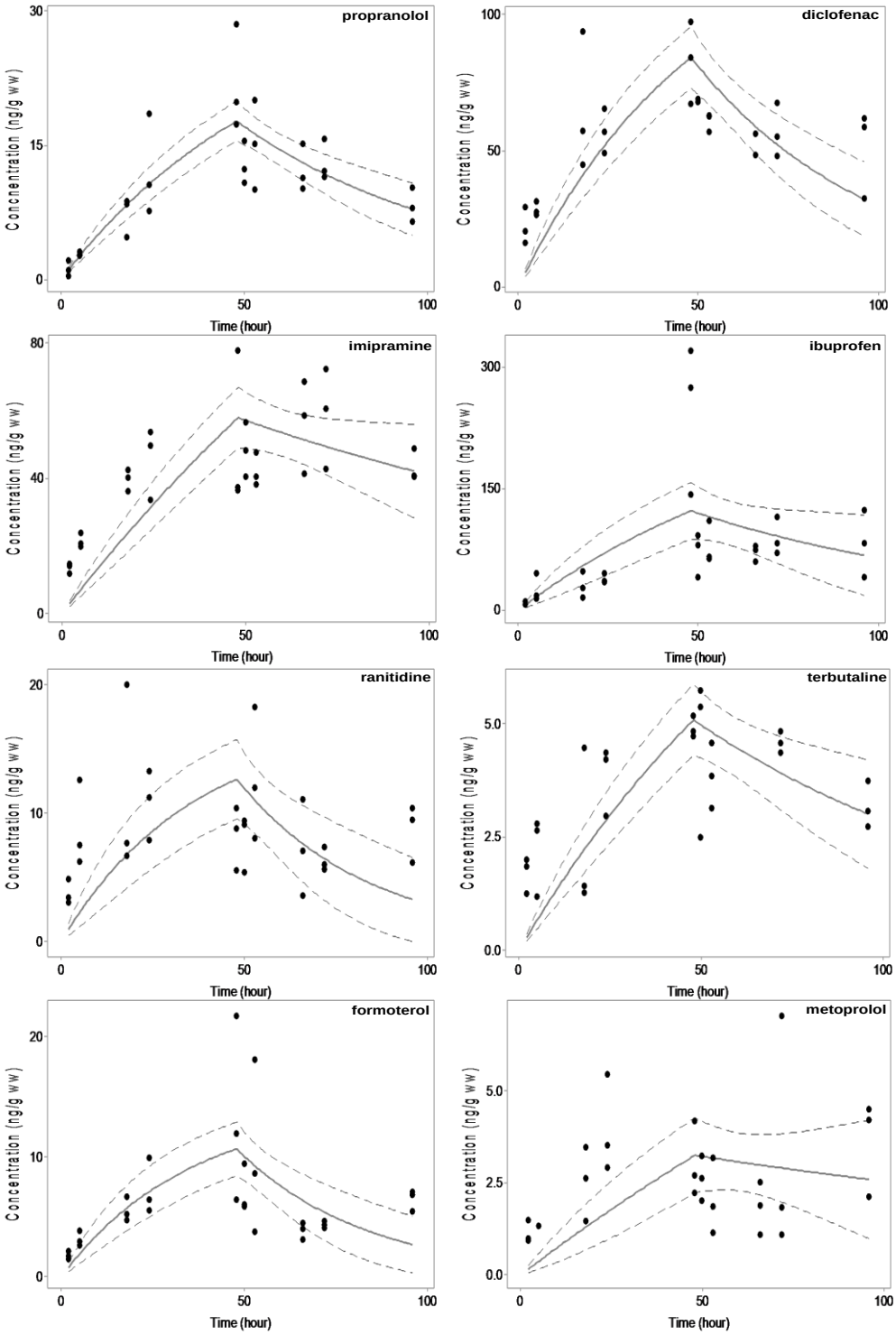

Figure 3.7: Uptake and elimination data for PPCPs in G. pulex. Dashed lines indicate 95 % confidence limits.

All exposures resulted in uptake from the earliest time point (2h), with the two compounds diclofenac and ibuprofen reaching the highest internal concentrations by 48h. The higher concentrations determined in the organisms here, resulted from these compounds being exposed at a higher concentration (10 µg L^{-1}) due to low activity of the radiolabel. The remaining six pharmaceuticals (1 µg $L^{-1)}$ showed maximal uptake phase concentrations of <80 ng g^{-1} ww. Analysis of water samples (Table 3.3) showed that the pharmaceuticals remained within 20 % of the nominal exposure concentrations with the exception of imipramine which showed a mean decrease of 52.2 %. The losses of analyte in the water phase could be due to several processes (separate from uptake into *G. pulex*) including photolysis, volatilisation, sorption and biotransformation by microorganisms. To account for these processes, control wells were set-up (no animals) to monitor for analyte loss. Analysis of water samples from the control wells resulted in RSDs of ≤5 % indicating that these processes involved with analyte loss were negligible. The variance observed could be explained by instrumental error. However, imipramine was again an exception to these observations (11% RSD) and showed a steady decrease in the control wells at each time interval measured. Imipramine had the highest log$D_{8.2}$ of 3.3 and thus the losses are likely to have resulted from sorption by *pi-pi* stacking or Van der Waals interactions to the plastic (polystyrene) culture plates.

After removal of the individuals to the depuration phase, animals showed varying elimination rates (Table 3.4). The lowest k_2 values were determined for imipramine (0.007 d^{-1}) and metoprolol (0.005 d^{-1}). However, the BCF of these two compounds differed greatly which resulted from the lowest observed uptake rate constant for metoprolol (0.076 L kg^{-1} d^{-1}) in contrast to imipramine which had the highest k_1 value (1.408 L kg^{-1} d^{-1}). With the exception of imipramine,

pharmaceuticals had relatively low uptake rates coupled with high elimination rates leading to low estimates of BCFs. All estimated BCFs remained ≤212 using the simultaneous method of estimation indicating that these selected pharmaceuticals were not accumulative. This is in line with regulatory guidelines which suggest that for a compound to be considered bioaccumulative a threshold value of 2,500 must be reached [16].

The low BCFs determined here could be explained by the relatively low hydrophobicity, as indicated by log*P* and log*D*. Hydrophobicity is generally considered the main factor governing bioaccumulation and many studies have shown the importance of this physicochemical property in relation to uptake of organic contaminants [11, 35]. However, pharmaceuticals are unique to these standard uptake models as they often have low hydrophobicity and can be ionised at multiple sites. Thus, these compounds could have the potential to concentrate in biota via different mechanisms such as carrier mediated transport. The BCFs reported in this study are in the range of BCFs observed in a separate study by Meredith-Williams et al., 2012 [17].

Table 3.3: Pharmaceutical water concentrations determined in the uptake and depuration exposure media.

Compound	Exposure Control (n=3) (ng mL^{-1})					Uptake Phase (ng mL^{-1})					Depuration Phase (ng mL^{-1})				
	2h	5h	18h	24h	48h	2h	5h	18h	24h	48h	2h	5h	18h	24h	48h
diclofenac	9.99	9.49	9.76	9.88	9.99	9.86	9.43	9.51	9.44	9.46	0.05	0.02	0.00	0.01	0.05
formoterol	1.08	1.01	1.00	1.07	0.96	0.92	0.96	0.90	0.96	0.85	0.02	0.03	0.03	0.01	0.04
ibuprofen	9.72	9.60	10.05	9.84	9.70	10.18	10.34	9.67	9.56	9.51	0.01	0.00	0.00	0.02	0.04
imipramine	0.79	0.73	0.64	0.63	0.61	0.57	0.55	0.54	0.60	0.48	0.01	0.01	0.03	0.04	0.04
metoprolol	1.04	1.02	1.05	1.02	1.02	0.98	0.95	0.94	0.98	1.05	0.02	0.01	0.02	0.02	0.02
ranitidine	1.05	1.03	1.04	1.02	0.98	0.99	0.96	0.88	0.99	0.94	0.01	0.01	0.03	0.01	0.02
terbutaline	1.04	0.97	1.01	0.98	0.97	0.96	0.90	0.94	0.92	0.92	0.07	0.07	0.08	0.08	0.14
propranolol	0.92	0.95	0.94	0.93	0.94	0.92	0.91	0.91	0.91	0.90	0.00	0.00	0.00	0.00	0.01

Table 3.4: Toxicokinetic parameters and bioconcentration factors for eight PPCPs.

Compound	Simultaneous BCF						Sequential BCF[a]							Sequential BCF[b]					
	k_1 (L kg^{-1} d^{-1})	SE	k_2 (d^{-1})	SE	*p*-value	BCF	k_1 (L kg^{-1} d^{-1})	SE	*p*-value	k_2 (d^{-1})	SE	*p*-value	BCF	k_1 (L kg^{-1} d^{-1})	SE	p-value	k_2 (d^{-1})	R^2	BCF
Propranolol	0.538	0.068	0.017	0.004	0.266	**32**	0.618	0.047	0.831	0.016	0.006	0.132	**39**	0.604	0.045	0.860	0.015	0.490	**42**
Formoterol	0.408	0.093	0.029	0.009	0.335	**14**	0.451	0.051	0.914	0.025	0.014	0.279	**18**	0.357	0.040	0.942	0.011	0.121	**33**
Imipramine	1.408	0.205	0.007	0.004	0.008	**212**	1.361	0.177	0.017	0.000	0.004	0.490	**3811**	1.360	0.177	0.017	0.000	0.001	**4533**
Metoprolol	0.076	0.022	0.005	0.008	0.073	**16**							N/A						
Terbutaline	0.136	0.020	0.011	0.004	0.026	**12**	0.135	0.016	0.027	0.006	0.003	0.381	**22**	0.117	0.016	0.027	0.006	0.200	**19**
Ranitidine	0.479	0.126	0.028	0.011	0.005	**17**	0.310	0.071	0.007	0.004	0.006	0.192	**81**	0.301	0.070	0.007	0.003	0.015	**112**
Diclofenac	0.273	0.037	0.020	0.005	0.002	**14**	0.253	0.025	0.017	0.009	0.003	0.156	**27**	0.269	0.026	0.023	0.013	0.243	**21**
Ibuprofen	0.338	0.094	0.012	0.008	0.000	**27**	0.582	0.097	0.013	0.022	0.014	0.004	**27**	0.488	0.073	0.029	0.010	0.093	**50**

[a]sequential using curve fitting method, [b]sequential using linear regression.
P-values were assessed via standard error (SE) and lack-of-fit tests.

The previous work reported BCFs of 6 pharmaceuticals in *G. pulex*, with 5 compounds remaining below a BCF of 270. One pharmaceutical (fluoxetine) had a measured BCF of 185,900 indicating that it was very bioaccumulative in *G. pulex.* However, this high BCF may be explained by the pharmacokinetics of fluoxetine where this compound inhibits its own metabolism resulting in an increasing half-life. Furthermore, this study only detected the radiolabel. Metabolites of fluoxetine such as norfluoxetine has a longer half-life than fluoxetine, which also increases over time (self-induced metabolic inhibition). Therefore, this high BCF is likely a result of the inhibited biotransformation and elimination.

The log$D_{8.2}$ of the eight pharmaceuticals was plotted against the measured log[BCF] values (Figure 3.8) and no obvious trend was observed. Generally, there was a slight increase in BCF from log*D* 1-3, but the data was limited and conclusions should be carefully considered. A study that investigated the uptake of pharmaceuticals in plants [36] showed plots of log*D* versus log[BCF] gave no observable trends for compounds which were ionisable. However, non-ionised compounds showed an increasing BCF when log*P* increased (i.e carbamazepine).

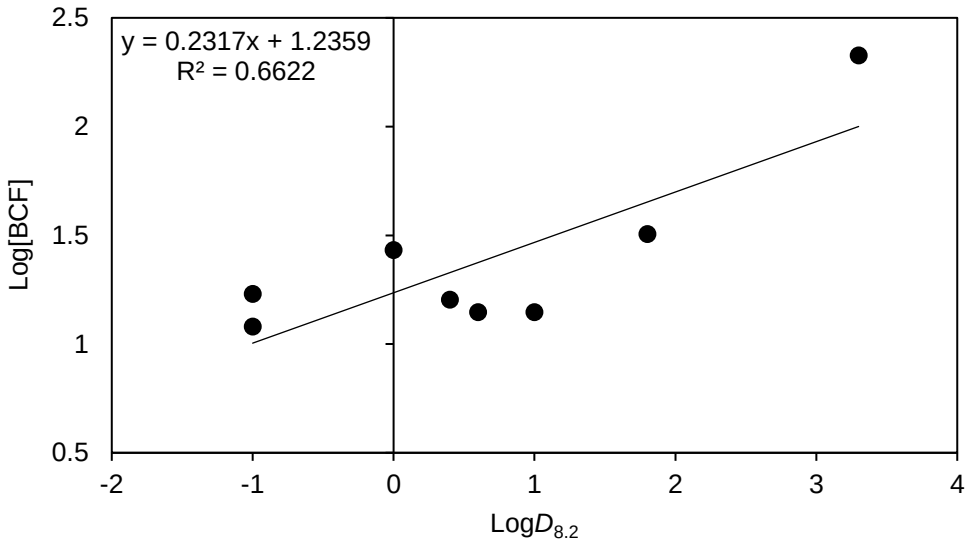

Figure 3.8: Log[BCF] versus log$D_{8.2}$ of the eight selected pharmaceuticals.

This suggests that bioaccumulation for non-ionisable pharmaceuticals may follow standard uptake models and assumptions with hydrophobicity as an important factor. However, for those compounds which are ionisable it is possible that hydrophobicity has less influence in determining the bioaccumulation potential of a compound. Other factors such as gill surface charge, pH of the gill boundary layer and carrier mediated transport (such as facilitated diffusion or active transport) may become more important in the uptake of these pharmaceutical compounds. The order of the uptake rate constants were imipramine > propranolol > formoterol and were also in agreement with the order of gill cell permeabilities (cm s^{-1}) reported by Stott et al., 2015 [26]. Finally, the low BCFs observed show the potential for pharmaceutical metabolism in non-target organisms. Metabolism suggests that there is conservation of cytochrome P450 enzymes within *G. pulex*, which has been shown in other aquatic invertebrates [37]. This is important for toxicokinetic modelling as bioaccumulation models do not often take into account metabolism of a xenobiotic and is a potential limitation for methods that use liquid scintillation counting for analysis.

3.3.5 Uptake rate constant assumptions and model reliability

OECD 305 guidelines specify that when estimating a kinetic BCF, two methods can be employed. The first is the simultaneous method where both k_1 and k_2 are calculated together versus the sequential method where k_2 is first estimated and the k_1 is derived from this estimate. In Figure 3.7, the toxicokinetic plots showed a lack-of-fit in several of the compound exposures. This was usually observed by an under-fitting of the curves in the uptake phase that is most apparent with the diclofenac, imipramine, ranitidine, terbutaline and metoprolol

experiments. When estimating the parameters k_1 and k_2, a p-value was generated for model lack-of-fits. When the parameters were estimated by the simultaneous method, 5 models showed a statistically significant lack-of-fit. If lack-of-fit is significant then it has important implications for BCF values as they could be over/underestimated leading to inaccurate risk assessment. Due to the poor fits observed, the parameters were re-estimated using the sequential method. In the sequential method, linear regression of the depuration data yields a direct estimate of k_2 that can be then input to calculate a k_1 value. Here, the R^2 value is an indication of the goodness-of-fit (Figure 3.9) and when the sequential method was used a higher estimated BCF when compared to those values generated by the simultaneous method (Table 3.4).

The over-estimation may result from poor estimates of the k_2, if deviation from linearity is observed indicating higher order kinetics. Whilst, there was scatter in the linear regression of the depuration phase overall, it was assumed that there were no significant non-linear plots. As a check, plots of $1/[C_{organism}]$ versus time showed that second order kinetics were not taking place (Figure 3.10). The k_2 estimates from the linear regression showed significantly reduced values when compared to the simultaneous k_2 estimates for the compounds imipramine (~7-fold), formoterol (~3-fold), terbutaline (~2-fold) and diclofenac (~1.5-fold). The reduced k_2 estimates would likely lead to larger BCF values as was most markedly observed with the BCF of imipramine and ranitidine. These BCFs differed by approximately 10-fold and 4-fold, respectively. Imipramine in particular would be classed as non-bioaccumulative (BCF <2500) when using the simultaneous method but bioaccumulative when using the sequential method. This further highlights the problems that would be associated with risk assessment associated with unreliable BCF estimates.

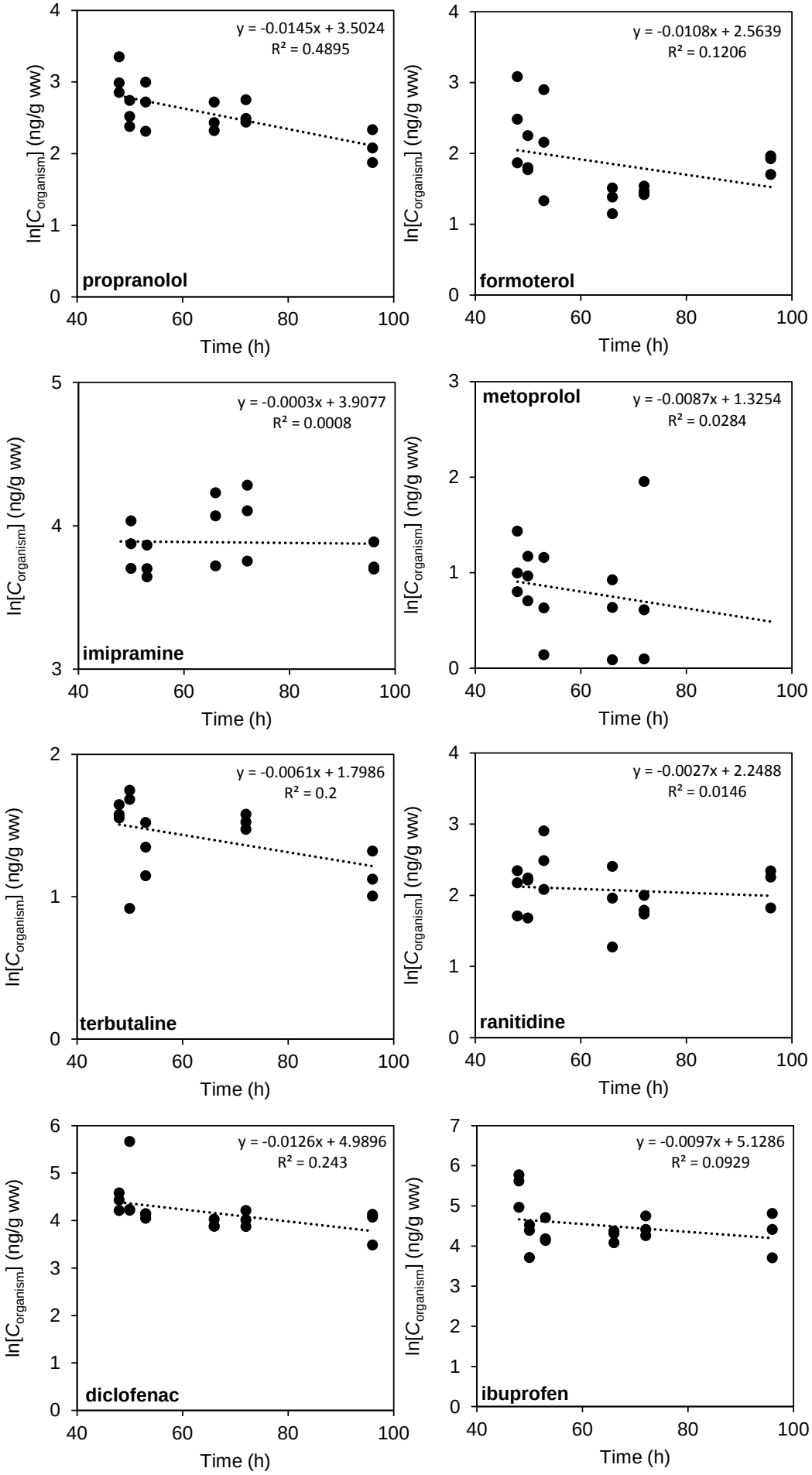

Figure 3.9: Linear regression curves to estimate k_2

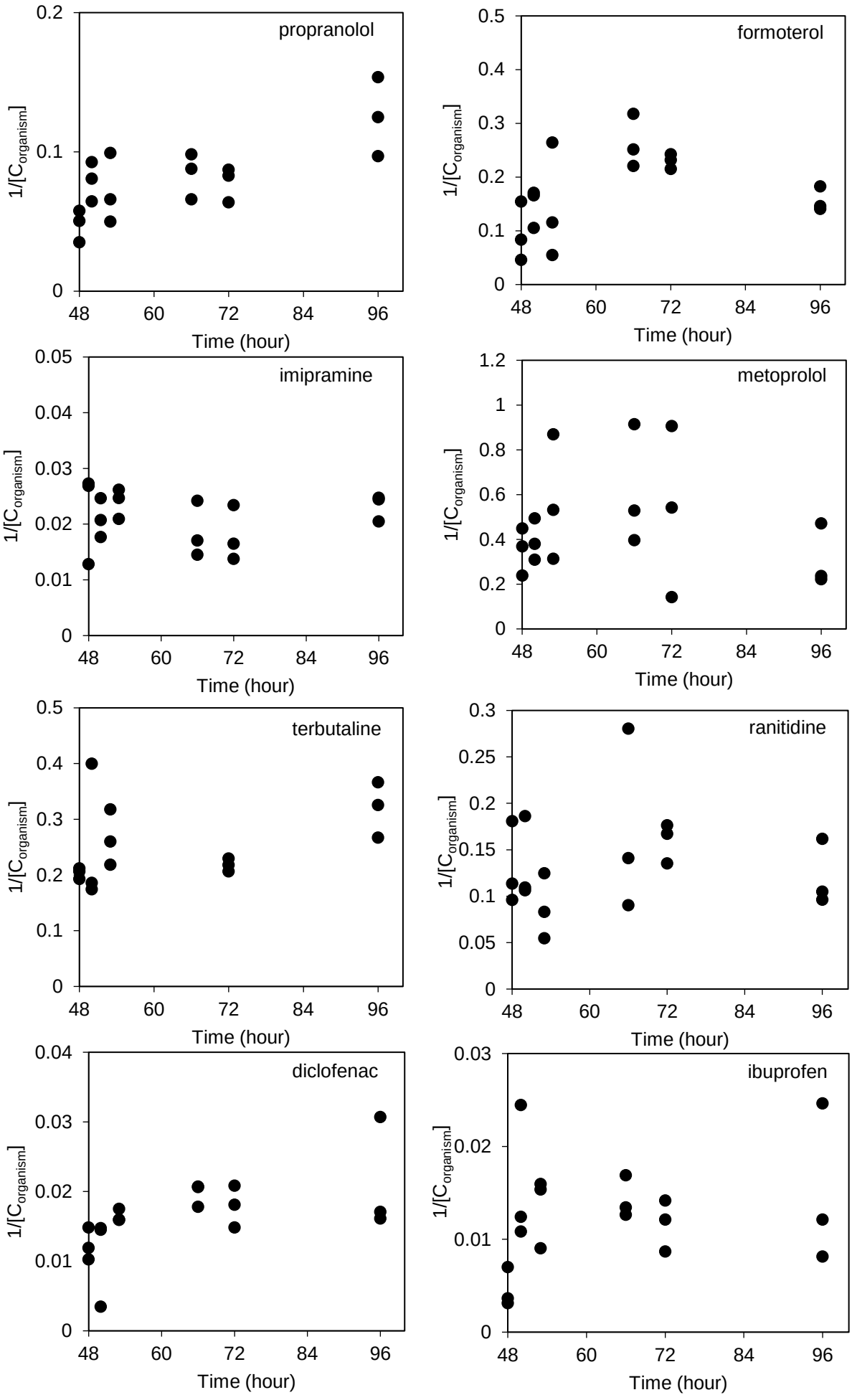

Figure 3.10:Plots of 1/[$C_{ogranism}$] for elimination phase data.

To further understand where the lack-of-fit arose from, the sequential method was repeated but a curve fitting algorithm (Levenberg-Marquardt) was used to estimate k_2 instead of linear regression. This algorithm iteratively adjusts parameters (k_1 and k_2) to minimise the sum of squares of the residuals between the independent and dependent variables. Thus, a lack-of-fit test was performed on both of the k_1 and k_2 curves, separately (Table 3.4). The *p*-values indicated that a statistically significant lack-of-fit resulted from the uptake phase data for five of the eight compounds (imipramine, ranitidine, terbutaline, diclofenac and ibuprofen). The lack-of-fit tests on the depuration data showed only one significant *p*-value for ibuprofen (0.004). This suggested that the simultaneous models showed a lack-of-fits shown due to poor fits in the uptake phase, which also agreed with the visual observation that curves were under-fitted in several cases. Metoprolol showed a zero to mildly increasing slope in the depuration data resulting from scatter, thus an estimate of k_2 could not be generated. The model uncertainties demonstrated, show that BCFs may potentially be limited from a regulatory perspective. As shown with imipramine, this compound triggered regulatory thresholds in one method of estimation but in a second estimation did not, which resulted from the model uncertainties in the uptake data.

The poor fit of the uptake curves indicated that the models used were not entirely reliable. Therefore, examination of the model assumptions was investigated to understand the reason for the lack-of-fit. The model assumes that C_w, k_1 and k_2 do not change over time. The first step was to investigate the k_1 assumption, which was performed as suggested by [38]. The k_1 rate constants for all eight compounds were estimated over each time interval and plotted in Figure 3.11. The plots showed a decreasing trend of the constant over time for the compounds diclofenac, imipramine, ranitidine, terbutaline, formoterol and

metoprolol. These decreases coincide with lack-of-fits for diclofenac, imipramine, ranitidine and terbutaline. Formoterol had no lack-of-fit in either uptake or elimination phase and metoprolol lack-of-fit could not be calculated for the sequential estimation. A potential limitation of this method was that the estimation of k_1 intervals required a k_2 value which could cause an apparent change in k_1, if it was in fact the k_2 that changed. In some cases a decrease was not observed in the k_1, for example the propranolol k_1 remained relatively constant throughout the exposure time period with a mean value of 0.58±0.23 L kg^{-1} d^{-1}. Good model fits in both the simultaneous and sequential methods for propranolol would suggest that a decrease in k_1 was the main reason for significant lack-of-fits in the other cases.

As mentioned previously, a changing k_2 could also lead to apparent changes in k_1. However, changes in k_2 would most likely manifest as decrease in the elimination rate constant over time. This assumption would hold true unless the compound induced its own metabolism or there was growth dilution. Therefore, a decreasing k_2 would result in increasing k_1 values. Furthermore, 6 of the elimination curves showed no statistically significant lack-of-fits and the linear regression of the elimination data showed no apparent trends (slope of the line). Changes in C_w would unlikely affect the rate constants as they should be independent of the pharmaceutical concentration in the water [39]. The measurement of pharmaceutical concentrations in the water phases also showed no significant losses except in the case of imipramine. Therefore, the lack-of-fits in the models are unlikely to be in response to either C_w or k_2 and are assumed to be the result of the decreases of k_1 over the exposure period.

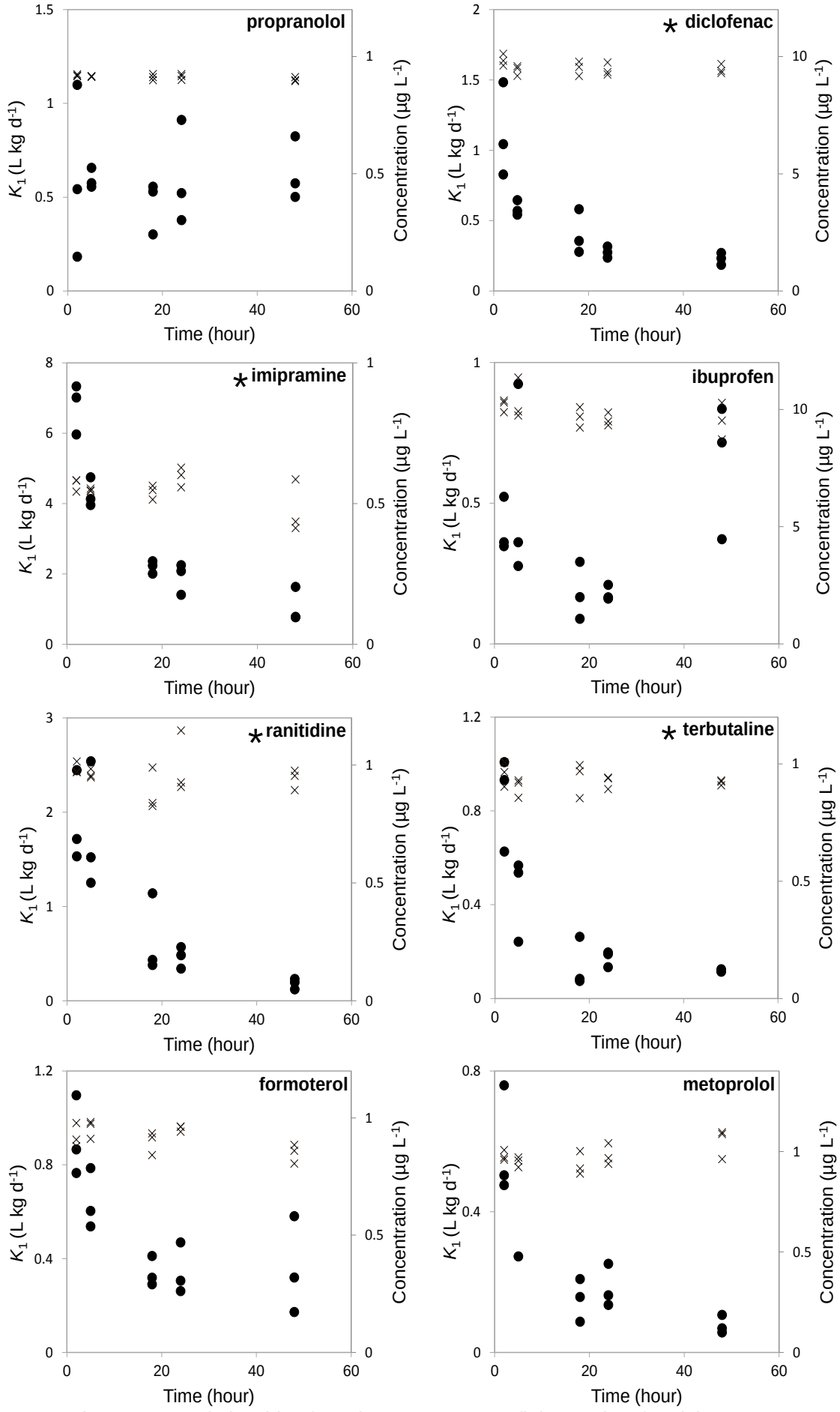

*Figure 3.11: Relationship of uptake rate constants (k_1) over time for eight PPCPs (black circles) and the respective concentrations in water (C_w) over time (crosses). * indicates significant lack-of-fit in the uptake phase*

3.3.6 Meta-analysis of micropollutant toxicokinetics in arthropod species to assess uptake rate constants

It should be taken into consideration that the study here was limited in drawing strong conclusions about model reliability as it was a relatively small study using one alternative animal model with pharmaceuticals that are relatively understudied in comparison to models that have been used for organic micro-pollutants [10, 12, 35] (e.g. PCBs, PAHs etc.) To identify whether this trend was observed with other classes of compounds and invertebrate species a meta-analysis of two studies from the literature was performed [18, 40]. Ashauer et al., [18] presented work on the accumulation of 14 organic micro-pollutants in *G. pulex* which showed variable BAFs ranging from 2 - 4466. The authors found that certain compounds showed a similar lack-of-fit. The raw data from this study was re-analysed using the modelling methods used here to identify any similar trends in k_1. The original study used bioaccumulation testing but showed that it accounted for a low proportion of the uptake. Therefore, it was assumed here in the re-analysis that uptake was via bioconcentration only. Similar to the finding presented in Table 3.4, models showed statistically significant lack-of-fits for several compounds in both simultaneous and sequential methods (Table 3.5). However, the sequential method again showed better model fits in the depuration data than in the uptake data again indicating that lack-of-fits were arising from the uptake phase. Although the models did not perform particularly well in several cases there was good agreement between the BAFs generated by Ashauer et al., [18] and the BCFs generated here. Interval values for k_1 were plotted against time for the 14 micro-pollutants to identify if the k_1 values were decreasing over time (Figure 3.12).

Table 3.5: Toxicokinetic parameters and standard errors (SE) for 14 organic micropollutants with bioconcentrations factors and lack-of-fit tests for each compound.

Compound		Simultaneous BCF						Sequential BCF						
	BAF[a]	k_1 (L kg^{-1} d^{-1})	SE	k_2 (d^{-1})	SE	*p*-value	BCF	k_1 (L kg^{-1} d^{-1})	SE	*p*-value	k_2 (d^{-1})	SE	*p*-value	BCF
4-nitrobenzyl chloride	**185**	666	665.740	4.540	4.540	0.000	**147**	259	28.324	0.00	1.212	0.149	0.230	**214**
2, 4-dichloroaniline	**56**	140	20.073	2.830	0.465	0.000	**50**	70	4.689	0.03	0.392	0.092	0.868	**179**
2, 4-dichlorophenol	**4466**	600	34.196	0.066	0.024	0.000	**9050**	750	48.646	0.00	0.010	0.018	0.400	**72728**
4, 6-dinitro-o-cresol	**37**	39	2.610	1.146	0.124	0.070	**34**	37	1.595	1.00	0.729	0.077	0.033	**51**
1, 2, 3-trichlorobenzene	**191**	1142	403.773	10.648	3.781	0.513	**107**	167	32.257	0.06	0.475	0.300	0.986	**351**
2, 4, 5-trichlorophenol	**2635**	941	79.280	0.252	0.064	0.001	**3729**	1091	109.906	0.21	0.131	0.039	0.001	**8327**
aldicarb	**2**	16	1.421	10.419	0.938	0.000	**2**	3	0.245	0.00	0.936	0.140	0.003	**3**
carbofuran	**65**	10	0.355	0.146	0.019	0.026	**68**	10	0.570	0.11	0.140	0.019	0.025	**72**
diazinon	**82**	276	24.271	3.569	0.3264	0.005	**77**	161	10.418	0.00	1.590	0.287	0.259	**101**
ethylacrylate	**87**	110	12.139	1.594	0.2446	0.000	**69**	67	5.122	0.00	0.204	0.033	0.000	**331**
hexachlorbenzene	**2915**	553	36.8714	0.221	0.046	0.000	**2505**	631	56.518	0.00	0.152	0.031	0.637	**4160**
imidacloprid	**7**	2	0.093	0.265	0.038	0.000	**7**	2	0.117	0.02	0.175	0.022	0.000	**13**
malathion	**114**	86	6.782	0.721	0.113	0.000	**120**	80	5.059	0.02	0.378	0.072	0.001	**212**
sea nine	**1732**	755	57.821	0.303	0.065	0.000	**2491**	950	69.141	0.05	0.123	0.020	0.084	**7696**

[a]Reported from Ashauer et al., 2010

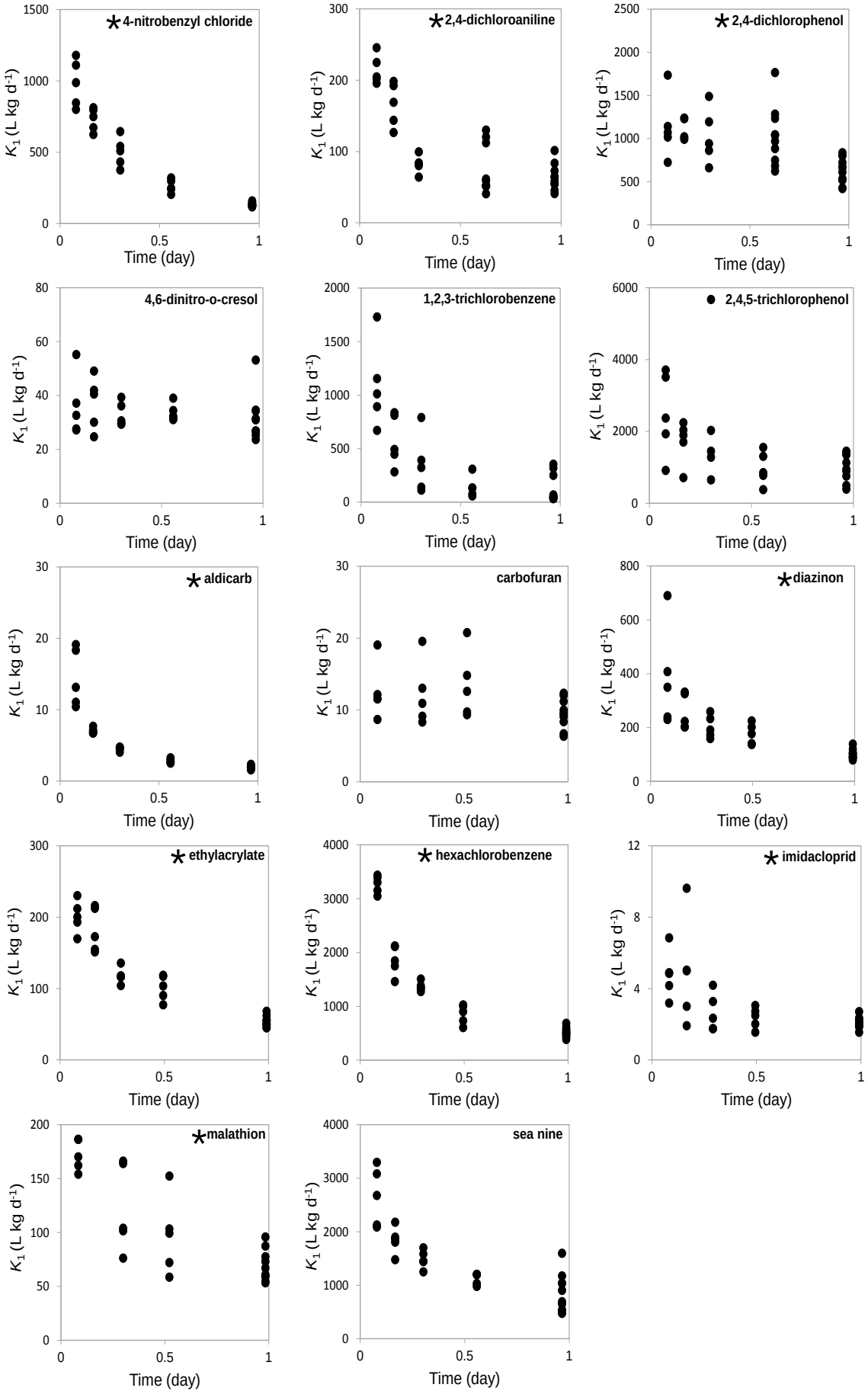

*Figure 3.12: Measurement of k_1 over time for 14 organic micro-pollutants. * indicates significant lack-of-fits in the uptake phase.*

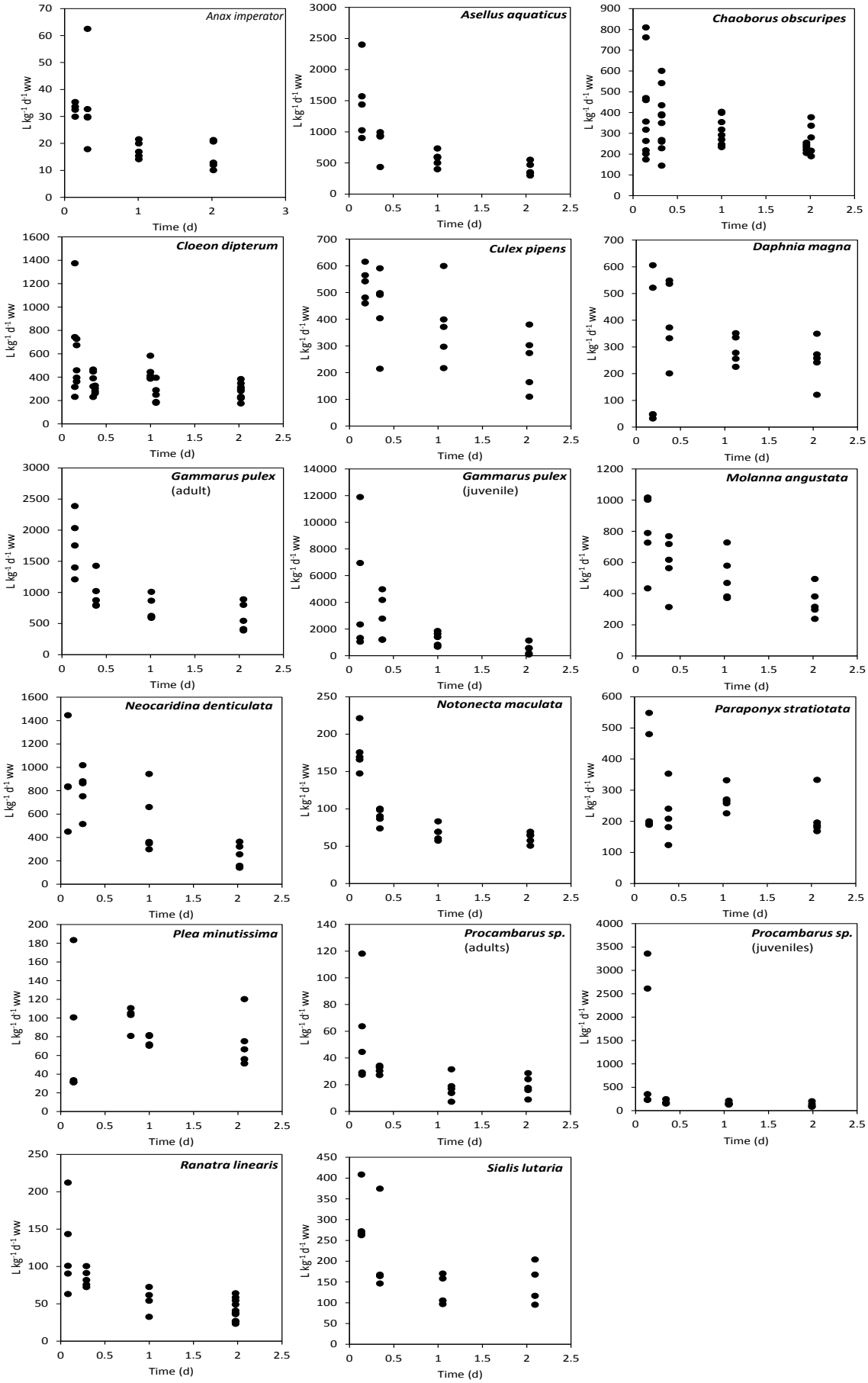

Figure 3.13: Measurement of k_1 over time for 15 different arthropod species exposed to chlorpyrifos. Raw data analysed from [39].

A systematic decrease of k_1 over the uptake phase was apparent for 9 of 14 compounds. The remaining 5 compounds showed less evident decreases in k_1, and four of these compounds showed no statistically significant lack-of-fit ($p > 0.05$). The compound 2,4-dichlorophenol showed no k_1 trends as reasoning for the observed lack-of-fit in the uptake phase. In addition to the analysis of different micro-pollutants, a meta-analysis of raw data from Rubach et al., [40] was also performed. This previous study focused on the uptake of chlorpyrifos in 15 different invertebrate species. When k_1 versus time was plotted (Figure 3.13) similar decreases in the k_1 value were observed. However, the trend was not as apparent as with previous examples and varied between the different species (Figure 3.11 & 3.12). This data would suggest that differences between the k_1 constancy may also result from specific species traits. However, trends in k_1 could also be compound specific, thus analysis of more compounds between species would be required to draw further conclusions. For example, if the k_1 constancy was solely dependent on a biological factor then all compounds would show a decrease in k_1. Thus, as this is only seen in certain compounds it could be related to physico-chemical properties or mode-of-actions of a compound.

If k_1 constancy did vary on a compound basis then toxicokinetic modelling is inherently inaccurate for environmental risk assessment. Therefore, the method used here [38] could be employed to assess the reliability of generated BCF values. The reasoning behind decreasing trends of k_1 over exposure time period could be explained by several mechanisms. The first of which is that a growth dilution effect may occur where the mass of the animals increases to give an increase in the elimination rate. This could cause an apparent decrease of k_1 in the uptake phase. However, the time scale used in these experiments [18, 40] were in the order of 4-6 days, thus growth would be assumed to be negligible but

further investigation would be required to show this. *G. pulex* has also been shown to alter respiration rates when fed on a poor diet [41]. As the animals were not fed here it is plausible that this may have affected uptake rates. However, the experiments by Ashauer et al., [18] were bioaccumulation experiments and so the animals were fed over the exposure period. Another possibility is that a toxicodynamic effect was occurring as a result of exposure of the compounds in non-target organisms. The work by Ashauer et al., [18] exposed organisms between 2-88 fold below the 24 h LC_{50} value which could be considered relatively high in some cases leading to toxic effects. In the pharmaceutical exposures presented here, the compounds were exposed ~1000 fold below LC_{50} toxicity values and thus toxic effects related to mortality were less likely [22]. Another consideration is that instantaneous sorption to the animals cuticle may have led to initially high k_1 values at the early time intervals. The relative percentage decrease of k_1 versus log*P* and log*D* is shown in Figure 3.14.

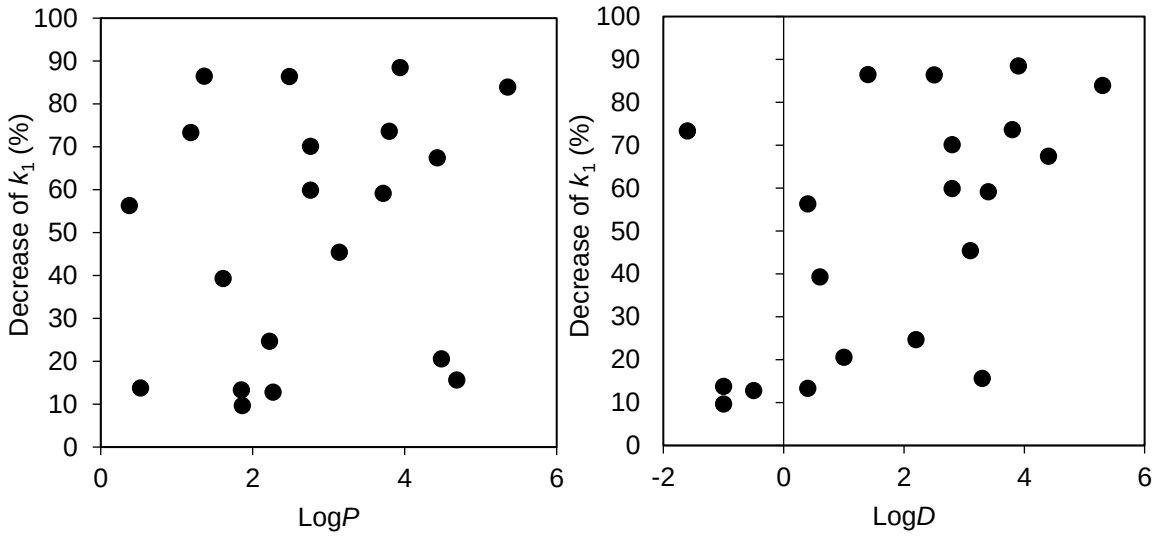

Figure.3.14: Relative decrease of k_1 against logP/D at respective exposure pH for pharmaceuticals (this study) and organic micropollutants (Ashauer et al., 2010). LogP/D estimated by ACD Labs Percepta.

The plots showed no correlation between k_1 decrease and hydrophobicity. However, sorption is governed by more than hydrophobicity and other factors

such as ionic states and polar topological surface area may have influence. Although it was not a part of the experimental design, animals that shed their exoskeleton during the pharmaceutical exposures were collected and analysed to determine the amount of compound bound to the cuticle. Table 3.6 shows the mass of pharmaceuticals that was determined from the exoskeleton and revealed that up to 24 % of the total compound mass determined from the animals was bound to the cuticle. However, it should be noted that the surface area of a shed exoskeleton is increased in comparison to a cuticle that is still attached to the animal. Thus, the relative mass of compound may be reduced. Furthermore, the data is limited and would need to be extended to more replicates and compounds to identify if this is the reason for a decreasing k_1 value. If the sorption does indeed explain the decrease of k_1 constants then it would suggest that physico-chemical properties rather than animal physiology determined the rate constant stability. Thus, k_1 constancy would vary on a compound by compound basis which is supported by the data shown here.

Table 3.6: Sorption of pharmaceuticals to G. pulex exoskeleton

Compound	Mean Compound Mass per Animal (n=3, pg)	Total Mass Compound on exoskeleton (pg)	Maximum concentration sorbed to exoskeleton (%)
Propranolol	336	44 (n=1)	13
Diclofenac	2070	368 (n=4)	18
Imipramine	1921	50 (n=2)	3
Ranitidine	238	58 (n=1)	24
Metoprolol	74	14 (n=2)	19

3.4 Conclusions

Preliminary data suggested that uptake of pharmaceuticals is likely to occur by both passive diffusion and carrier mediated transport. The data presented here shows that BCFs for the pharmaceuticals selected, showed a low

potential for accumulation. However, analysis of the model fits showed statistically significant lack-of-fits for several models that stemmed from the uptake phase data. When uptake data was analysed to determine k_1 values over specific time intervals, a decreasing trend was observed that explained the lack-of-fits in the uptake data. To determine if this was seen in previous studies using different compounds and invertebrates, a meta-analysis of the raw data was performed which revealed the same decreasing trends of the k_1 constants over time. The implications of these results are important as environmental risk assessment through BCF or BAF studies may potentially be somewhat inaccurate and lead to unexpected adverse effects in the aquatic environment. The mechanisms behind decreasing k_1 constants can be explained, in part, by the sorption of compounds to the cuticle of the animal suggesting that model reliability is determined on a compound specific basis. However, further investigation into the effect of sorption-desorption phenomena would be required to fully understand the effect. Furthermore, the role of metabolism on these standard uptake models should also be assessed.

3.5 References

1. McEneff, G., L. Barron, B. Kelleher, B. Paull, and B. Quinn, A year-long study of the spatial occurrence and relative distribution of pharmaceutical residues in sewage effluent, receiving marine waters and marine bivalves. *Science of the Total Environment*, 2014. **476**: p. 317-326.
2. Klosterhaus, S.L., R. Grace, M.C. Hamilton, and D. Yee, Method validation and reconnaissance of pharmaceuticals, personal care products, and alkylphenols in surface waters, sediments, and mussels in an urban estuary. *Environment international*, 2013. **54**: p. 92-99.
3. Rodríguez-Mozaz, S., B. Huerta, and D. Barceló, *Bioaccumulation of Emerging Contaminants in Aquatic Biota: Patterns of Pharmaceuticals in Mediterranean River Networks*, in *Emerging Contaminants in River Ecosystems: Occurrence and Effects Under Multiple Stress Conditions*, M. Petrovic, et al., Editors. 2016, Springer International Publishing: Cham. p. 121-141.
4. De Lange, H., W. Noordoven, A. Murk, M. Lürling, and E. Peeters, Behavioural responses of Gammarus pulex (Crustacea, Amphipoda) to low concentrations of pharmaceuticals. *Aquatic Toxicology*, 2006. **78**(3): p. 209-216.
5. De Lange, H., E.T. Peeters, and M. Lürling, Changes in ventilation and locomotion of Gammarus pulex (Crustacea, Amphipoda) in response to low concentrations of pharmaceuticals. *Human and Ecological Risk Assessment*, 2009. **15**(1): p. 111-120.
6. Quinn, B., F. Gagné, and C. Blaise, An investigation into the acute and chronic toxicity of eleven pharmaceuticals (and their solvents) found in

wastewater effluent on the cnidarian, Hydra attenuata. *Science of The Total Environment*, 2008. **389**(2–3): p. 306-314.

7. Martín-Díaz, M.L., F. Gagné, and C. Blaise, The use of biochemical responses to assess ecotoxicological effects of Pharmaceutical and Personal Care Products (PPCPs) after injection in the mussel Elliptio complanata. *Environmental Toxicology and Pharmacology*, 2009. **28**(2): p. 237-242.
8. Nassef, M., S. Matsumoto, M. Seki, F. Khalil, I.J. Kang, Y. Shimasaki, Y. Oshima, and T. Honjo, Acute effects of triclosan, diclofenac and carbamazepine on feeding performance of Japanese medaka fish (Oryzias latipes). *Chemosphere*, 2010. **80**(9): p. 1095-1100.
9. Galus, M., J. Jeyaranjaan, E. Smith, H. Li, C. Metcalfe, and J.Y. Wilson, Chronic effects of exposure to a pharmaceutical mixture and municipal wastewater in zebrafish. *Aquatic Toxicology*, 2013. **132–133**: p. 212-222.
10. Norstrom, R.J., A.E. McKinnon, and A.S.W. deFreitas, A Bioenergetics-Based Model for Pollutant Accumulation by Fish. Simulation of PCB and Methylmercury Residue Levels in Ottawa River Yellow Perch (Perca flavescens). *Journal of the Fisheries Research Board of Canada*, 1976. **33**(2): p. 248-267.
11. Gobas, F.A. and D. MacKay, Dynamics of hydrophobic organic chemical bioconcentration in fish. *Environmental Toxicology and Chemistry*, 1987. **6**(7): p. 495-504.
12. Veith, G.D., D.L. DeFoe, and B.V. Bergstedt, Measuring and estimating the bioconcentration factor of chemicals in fish. *Journal of the Fisheries Board of Canada*, 1979. **36**(9): p. 1040-1048.

13. Hendriks, A.J., A. van der Linde, G. Cornelissen, and D.T. Sijm, The power of size. 1. Rate constants and equilibrium ratios for accumulation of organic substances related to octanol-water partition ratio and species weight. *Environmental toxicology and chemistry*, 2001. **20**(7): p. 1399-1420.

14. Hendriks, A.J. and A. Heikens, The power of size. 2. Rate constants and equilibrium ratios for accumulation of inorganic substances related to species weight. *Environmental Toxicology and Chemistry*, 2001. **20**(7): p. 1421-1437.

15. OECD., *Test No. 305: Bioaccumulation in Fish: Aqueous and Dietary Exposure*. OECD Publishing.

16. Commission, E., *Regulation (EC) No 1907/2006 of the European Parliament and of the Council of 18 December 2006 concerning the Registration, Evaluation, Authorisation and Restriction of Chemicals (REACH), establishing a European Chemicals Agency, amending Directive 1999/45/EC and repealing Council Regulation (EEC) No 793/93 and Commission Regulation (EC) No 1488/94 as well as Council Directive 76/769/EEC and Commission Directives 91/155/EEC, 93/67/EEC, 93/105/EC and 2000/21/EC.* 2006: Official Journal of the European Union. p. 1 - 849.

17. Meredith-Williams, M., L.J. Carter, R. Fussell, D. Raffaelli, R. Ashauer, and A.B. Boxall, Uptake and depuration of pharmaceuticals in aquatic invertebrates. *Environmental pollution*, 2012. **165**: p. 250-258.

18. Ashauer, R., I. Caravatti, A. Hintermeister, and B.I. Escher, Bioaccumulation kinetics of organic xenobiotic pollutants in the freshwater

invertebrate Gammarus pulex modeled with prediction intervals. *Environmental Toxicology and Chemistry*, 2010. **29**(7): p. 1625-1636.

19. Ashauer, R., A. Hintermeister, I. O'Connor, M. Elumelu, J. Hollender, and B.I. Escher, Significance of xenobiotic metabolism for bioaccumulation kinetics of organic chemicals in Gammarus pulex. *Environmental science & technology*, 2012. **46**(6): p. 3498-3508.
20. Miller, T.H., G.L. McEneff, R.J. Brown, S.F. Owen, N.R. Bury, and L.P. Barron, Pharmaceuticals in the freshwater invertebrate, Gammarus pulex, determined using pulverised liquid extraction, solid phase extraction and liquid chromatography–tandem mass spectrometry. *Science of The Total Environment*, 2015. **511**(0): p. 153-160.
21. Agency, U.U.S.E.P., *Methods for measuring the acute toxicity of effluents and receiving waters to freshwater and marine organisms*, in *EPA-821-R-02-012*. 2002, USEPA.
22. Gómez-Canela, C., T.H. Miller, N.R. Bury, R. Tauler, and L.P. Barron, Targeted metabolomics of Gammarus pulex following controlled exposures to selected pharmaceuticals in water. *Science of The Total Environment*, 2016. **562**: p. 777-788.
23. Crookes, M.J. and D.N. Brooke, *Estimation of fish bioconcentration factor (BCF) from depuration data* 2011, Environment Agency: Bristol.
24. Zhan, X.-H., H.-L. Ma, L.-X. Zhou, J.-R. Liang, T.-H. Jiang, and G.-H. Xu, Accumulation of phenanthrene by roots of intact wheat (Triticum acstivnm L.) seedlings: passive or active uptake? *BMC Plant Biology*, 2010. **10**(1): p. 1-8.
25. Sugano, K., M. Kansy, P. Artursson, A. Avdeef, S. Bendels, L. Di, G.F. Ecker, B. Faller, H. Fischer, G. Gerebtzoff, H. Lennernaes, and F. Senner,

Coexistence of passive and carrier-mediated processes in drug transport. *Nat Rev Drug Discov*, 2010. **9**(8): p. 597-614.

26. Stott, L.C., S. Schnell, C. Hogstrand, S.F. Owen, and N.R. Bury, A primary fish gill cell culture model to assess pharmaceutical uptake and efflux: Evidence for passive and facilitated transport. *Aquatic Toxicology*, 2015. **159**: p. 127-137.
27. Kikuo, I., W. Jun, and S. Mariko, Age-dependence in capacity-limited uptake kinetics of propranolol by isolated rat hepatocytes. *Biochemical Pharmacology*, 1986. **35**(16): p. 2677-2681.
28. Weis, J.S., P. Weis, M. Heber, and S. Vaidya, Methylmercury tolerance of killifish (Fundulus heteroclitus) embryos from a polluted vs non-polluted environment. *Marine Biology*, 1981. **65**(3): p. 283-287.
29. Weis, J.S., Tolerance to Environmental Contaminants in the Mummichog, Fundulus heteroclitus. *Human and Ecological Risk Assessment: An International Journal*, 2002. **8**(5): p. 933-953.
30. Schnell, S., K. Bawa-Allah, A. Otitoloju, C. Hogstrand, T.H. Miller, L.P. Barron, and N.R. Bury, Environmental monitoring of urban streams using a primary fish gill cell culture system (FIGCS). *Ecotoxicology and Environmental Safety*, 2015. **120**: p. 279-285.
31. Reitzel, A.M., S.I. Karchner, D.G. Franks, B.R. Evans, D. Nacci, D. Champlin, V.M. Vieira, and M.E. Hahn, Genetic variation at aryl hydrocarbon receptor (AHR) loci in populations of Atlantic killifish (Fundulus heteroclitus) inhabiting polluted and reference habitats. *BMC Evolutionary Biology*, 2014. **14**(1): p. 1-18.

32. Meyer, J.N. and R.T. Di Giulio, Heritable adaptation and fitness costs in killifish (Fundulus heteroclitus) inhabiting a polluted estuary. *Ecological Applications*, 2003. **13**(2): p. 490-503.

33. Meyer, J.N., D.E. Nacci, and R.T. Di Giulio, Cytochrome P4501A (CYP1A) in Killifish (Fundulus heteroclitus): Heritability of Altered Expression and Relationship to Survival in Contaminated Sediments. *Toxicological Sciences*, 2002. **68**(1): p. 69-81.

34. Klerks, P.L. and J.S. Weis, Genetic adaptation to heavy metals in aquatic organisms: A review. *Environmental Pollution*, 1987. **45**(3): p. 173-205.

35. Gobas, F.A.P.C., A. Opperhuizen, and O. Hutzinger, Bioconcentration of hydrophobic chemicals in fish: Relationship with membrane permeation. *Environmental Toxicology and Chemistry*, 1986. **5**(7): p. 637-646.

36. Wu, X., F. Ernst, J.L. Conkle, and J. Gan, Comparative uptake and translocation of pharmaceutical and personal care products (PPCPs) by common vegetables. *Environment international*, 2013. **60**: p. 15-22.

37. Solé, M. and D.R. Livingstone, Components of the cytochrome P450-dependent monooxygenase system and 'NADPH-independent benzo [a] pyrene hydroxylase'activity in a wide range of marine invertebrate species. *Comparative Biochemistry and Physiology Part C: Toxicology & Pharmacology*, 2005. **141**(1): p. 20-31.

38. Crookes, M.J., & Brooke, D. N. *Estimation of fish bioconcentration factor (BCF) from depuration data*. 2011; Available from: http://publications.environment-agency.gov.uk.

39. van Leeuwen, C.J. and T.G. Vermeire, *Risk assessment of chemicals: an introduction*. 2007: Springer Science & Business Media.

40. Rubach, M.N., R. Ashauer, S.J. Maund, D.J. Baird, and P.J. Van den Brink, Toxicokinetic variation in 15 freshwater arthropod species exposed to the insecticide chlorpyrifos. *Environmental Toxicology and Chemistry*, 2010. **29**(10): p. 2225-2234.

41. Graça, M., L. Maltby, and P. Calow, Importance of fungi in the diet of Gammarus pulex and Asellus aquaticus. *Oecologia*, 1993. **96**(3): p. 304-309.

Chapter 4. The uptake, metabolism and elimination of selected pharmaceuticals in *G. pulex* using targeted LC-MS/MS.

4.1 Introduction

Extensive research into organic micropollutants has enabled the elucidation of the mechanisms for the uptake and accumulation of several environmental contaminants [1-3]. Due to the hydrophobic nature of these types of micropollutants, uptake was considered to be by passive diffusion across cellular membranes. Therefore, models for the uptake of organic micropollutants used physico-chemical properties such as log*P* to describe and predict the concentration of these compounds in biota [4-6]. However, pharmaceuticals are somewhat different in that they are often ionisable and amphoteric molecules. Thus, uptake models that use hydrophobicity to describe the accumulation of compounds in biota may not reliably predict the uptake of these classes of compounds.

Authors have shown that for compounds that remain neutral better correlations with hydrophobicity measurements (log*P/D*) are observed than for those compounds present in ionised states [7-9]. Other variables such as ion trapping, carrier mediated transport and partitioning to non-lipid components (protein binding) could influence the accumulation of pharmaceutical compounds [7, 8, 10]. Furthermore, much of the reported work has been performed in vertebrate species such as fish. Thus, the bioaccumulation of compounds in invertebrate species is not well understood. However, more recently several methods for the study of bioaccumulation of pharmaceuticals and other organic micropollutant compounds in several invertebrate species (bivalves and amphipods) have been developed using LC-MS [11-13].

A widely used method for estimating a bioconcentration factor or bioaccumulation factor in fish is described by the OECD 305 guidelines which has also been applied to invertebrates [14]. The BCF or BAF estimations using these guidelines can be determined using steady-state or kinetic measurements. The kinetic estimates utilise model equations for non-linear regression of the uptake and elimination data that generate the uptake rate constant (k_1) and elimination rate constant (k_2). These two parameters are used to estimate a BCF and the models assume that they do not change. However, recent investigation described in Chapter 3, showed that the OECD model led to significant lack-of-fits for measured data [15]. The lack-of-fits potentially resulted from a decreasing trend of k_1 over time. This finding was significant as model assumptions that do not hold true, could lead to under/over estimation of BCFs during risk assessment.

Possible causes for the decreases in k_1 could be related to several factors such as growth, metabolism and sorption processes. Metabolism in particular, is generally not considered in bioconcentration studies as analytical methods usually only monitor the total radioactivity of a compound by Liquid Scintillation Counting (LSC) [16] or the parent compound itself, if using LC- or GC-MS. Biotransformation could have a particularly strong effect on BCF estimates [17-19]. Xenobiotics can induce or inhibit their own metabolism or the metabolism of other compounds that will affect the clearance rate and hence the BCF [20]. For example, carbamazepine has been shown to induce the metabolism of clozapine [21]. Furthermore, the compounds fluoxetine and its main metabolite norfluoxetine have been shown to inhibit CYP450-2D6 activity which is the main enzyme that is involved with fluoxetine metabolism [22]. Predictive BCF models are either too simplistic (using only log*P* inputs) or do not accurately include

biotransformation rates, as accepted methods to measure metabolic products and the kinetics of biotransformation currently do not exist [23]. Several authors have applied *in vitro* intrinsic clearance rates to extrapolate to whole body biotransformation rates for predictive BCF modelling [24, 25]. However, these extrapolations measure only the loss of parent compound to predict whole body biotransformation. Thus, *in vitro* clearance rates may not reliably reflect whole body metabolic rates [26].

To the authors knowledge the only two studies have measured metabolites and their associated toxicokinetics. The authors used LC-HRMS or LC with a radioactivity detector to model the uptake and elimination profiles of organic micropollutants, fungicides and their metabolites in *G. pulex* [27, 28]. The Ashauer et al., study showed that the measurement of biotransformation improved the accuracy of BCF estimates when compared to estimates using total radioactivity counts. A further constraint to the study of xenometabolism is that *a priori* knowledge of biotransformation products in aquatic organisms is lacking leading to difficulty when developing targeted analytical methods [29]. Current methods have focussed on the determination of organic pollutants in fish, with little attention given to invertebrates or pharmaceutical biotransformation. Therefore, it is essential that methods are developed that can determine pharmaceutical metabolites to reliably assess the affect metabolism has on bioconcentration models.

The aim of this work was to further assess the bioconcentration potential of pharmaceuticals in *G. pulex* using targeted LC-MS/MS methods described in Chapter 2. BCFs will be estimated using the OECD 305 guidelines and kinetic parameters will be checked for constancy over time. Finally, the optimised LC-MS/MS method will be used for the determination of several Phase I and Phase

II biotransformation products of propranolol, carbamazepine and diazepam which have not been detected previously.

4.2 Materials & Methods

4.2.1 Reagents, chemicals and consumables

HPLC grade methanol, acetonitrile, acetone, ethyl acetate, dichloromethane and dimethyldichlorosiloxane were purchased from Fischer Scientific (Loughborough, UK). Analytical grade ammonium acetate was sourced from Sigma-Aldrich (Dorset, UK). Propranolol hydrochloride, ketoprofen, diclofenac sodium salt, bezafibrate, warfarin, flurbiprofen, indomethacin, ibuprofen sodium salt, meclofenamic acid sodium salt, gemfibrozil, atenolol, sulfamethoxazole, sulfamethazine sodium salt, furosemide, carbamazepine, nimesulide, (±)-metoprolol (+)-tartrate salt, triclocarban, cimetidine, ranitidine, antipyrin, temazepam, diazepam, fluoxetine, nifedipine, oxazepam, nordiazepam, carbamazepine-10, 11-epoxide, and mefenamic acid were all obtained from Sigma-Aldrich (Steinheim, Germany). Trimethoprim, caffeine, and naproxen were ordered from Fluka (Buchs, Switzerland). Stable isotope-labelled standards including carbamazepine-d_{10}, propranolol-d_7, temazepam-d_5 and diazepam-d_5 were ordered from Sigma-Aldrich. Sulfamethazine-d_4, nifedipine-d_4, metoprolol-d_7, trimethoprim-d_3 and warfarin-d_5 were ordered from QMX Laboratories (Essex, UK). The propranolol metabolites; 4-hydroxypropranolol, 4-hydroxypropranolol sulphate and 4-hydroxypropranolol glucuronide were sourced from Santa Cruz Biotechnology (Heidelberg, Germany). All pharmaceuticals were of a purity of ≥97 %. Analytical grade salts (>99 %) including sodium hydrogen carbonate, magnesium sulphate, calcium sulphate, potassium chloride were purchased from Sigma. Ultra-pure water was obtained

from a Millipore Milli-Q water purification system with a specific resistance of 18.2 MΩ.cm or greater (Millipore, Bedford, MA, USA).

4.2.2 Sample collection and culture maintenance

Gammarus pulex were collected by kick-sampling from the River Cray, South-East London, UK, 51°23'09.5"N 0°06'32.4"E. This site was previously shown to have low pharmaceutical contamination in both collected surface water and animal samples (Chapter 2) [30]. The populations were transported to the laboratory in 500 mL Nalgene™ flasks filled with surface water from the sample collection site. Populations were rinsed with artificial freshwater (AFW) and then acclimatised to laboratory conditions (as specified below) for a minimum of 7 days before any exposure experiments were performed. AFW was prepared from 1.15 mM of $NaHCO_3$, 0.50 mM $MgSO_4$, 0.44 mM $CaSO_4$ and 0.05 mM of KCl dissolved in 20 L of ultra-pure water. This water was subsequently aerated for several hours to remove dissolved carbonic acid and maximise the dissolved oxygen concentrations. Each culture tank (n=8) was filled with 2.5 L of AFW and animals were fed with either alder or hose chestnut leaves that were previously collected from the collection site and conditioned by submersion in surface water for two days prior to use.

4.2.3 Toxicokinetic exposure and conditions

Toxicokinetic experiments were performed separately for each pharmaceutical for a total of 96h which included a 48h uptake phase followed by a 48h depuration period. Individual adult organisms (n=25), both male and female (>5 mg wet weight) were placed in pyrex glass beakers. *G. pulex* were carefully transferred to beakers using blunt forceps to avoid any harm to the organisms

before exposure. Each beaker contained 25 organisms in 200 mL of exposure media (AFW and test compound). *G. pulex* were exposed to individual PPCPs at a concentration of 1 µg L^{-1}, except for propranolol and warfarin which were exposed at 10 µg L^{-1}. All exposure media contained <0.001 % of solvent (methanol). A total of 300 organisms were used per compound exposure and were sampled (n=3/time-point) at 6, 24, and 48h in the uptake phase followed by a single time point at 96h in the depuration phase. Control beakers were setup and sampled at the 96h time interval. These were subsequently analysed for any background contamination. The exposure media was replaced daily and water samples (n=3) were taken from working solutions and after 24h of exposure to ensure concentrations of the compounds remained constant in the AFW. Each animal sample was rinsed with ultra-pure water and then frozen at -20 ^{o}C. The light cycle followed 12:12h light:dark without a dusk/dawn transition period. All experiments were performed in a temperature controlled room at 15 °C (± 2 °C) and water *p*H was also monitored across each experiment and measured at an average of 8.19 ± 0.05 *p*H.

4.2.4 Sample preparation

Water samples collected from exposure experiments were filtered using Whatman filters (0.2 µM) and directly injected onto the LC-MS/MS for analysis. *G. pulex* samples were prepared as specified by in Chapter 2 [30]. Briefly, 50 mg of lyophilised *G. pulex* was ball-mill extracted in 5 mL of acetonitrile and diluted with 100 mL of ammonium acetate buffer for loading onto Waters HLB SPE cartridges (6 cc, 200 mg sorbent). After loading, samples were eluted using a mixture of ethyl acetate:acetone (50:50 v/v) which was subsequently evaporated

under nitrogen (99% purity) and reconstituted in starting LC mobile phase (90:10 v/v, 10 mM ammonium acetate buffer: acetonitrile).

4.2.5 Instrumental analysis

The determination of pharmaceuticals was previously outlined in Chapter 2 [30]. Briefly, samples were injected (20 µL) onto a Waters SunFire reversed-phase C_{18} column (150 mm x 2.1 mm, 2.5 µM particle size) and followed a gradient elution (total 75 min including 12.5 min re-equilibration time) using a mixture of acetonitrile and ultra-pure water with 10 mM ammonium acetate. Detection was performed using a Waters Quattro triple quadrupole mass analyser with an electrospray ionisation source operated in positive and negative polarity switching mode. Quantification of analytes was performed using 3-point internal standard calibration curves, where the ratio of non-labelled analyte area/concentration to a stable isotope labelled internal standard (SIL-IS) area/concentration form the graph axes. The exception to this was in the temazepam exposure where quantification was performed against a SIL-IS calibrant concentration. Compounds (hydroxypropranolol sulphate, carbamazepine epoxide, and imipramine) that were not quantified against internal standards due to availability issues, were quantified using 3-point external matrix matched calibration curves. Imipramine was included in the analysis due to the potential bioconcentration shown in Chapter 3.

4.2.6 Modelling bioconcentration factors

Parameter estimation of uptake rate constant (k_1) and depuration rate constant (k_2) was performed using a curve fitting algorithm via Minitab statistical

software (Minitab Ltd., Coventry UK) and as outlined in the OECD 305 Fish Bioconcentration Guidelines [14]. Detailed calculations were previously described in Chapter 3 and were used here to estimate the BCF for the minimised test designs.

4.3 Results & discussion

4.3.1 Method performance assessment

To perform each toxicokinetic experiment with *G. pulex*, each compound exposure would require approximately 750 animals. The requirement for this number of animals presents feasibility issues in terms of collecting animals, maintaining cultures and exposing organisms. Furthermore, the sheer volume of animals needed should require some ethical consideration for future best practices in invertebrate testing. Whilst, invertebrates are not a protected animal, policies that are aimed to reduce the number of animals in research (such as the 3Rs) should be extended to the invertebrate species. To reduce the number of animals that was required per exposure, the analytical method presented in Chapter 2, was adjusted to use a lower mass of lyophilised *G. pulex*. The mass was decreased by half, to 50 mg of lyophilised material. However, the reduction of material could affect the performance of the analytical method, mainly through sensitivity. To reduce any effects caused by a mass change, the reconstitution volume was also scaled down (250 µL) so that the ratio between the matrix components and analytes was kept constant. A recovery experiment was performed to characterise changes in the method performance that may have occurred through use of a lower mass and lower reconstitution volume.

Table 4.1 shows the comparison between analyte recovery when 100 or 50 mg of lyophilised material was extracted. Overall, the mean recovery of

analytes was greater when using the lower sample mass by an average of 19 % with the exception of sulfamethazine, cimetidine, flurbiprofen and nimesulide. However, when comparing the RSDs the higher sample mass showed much less deviation and therefore had greater precision. All cases showed better precision with the exception of caffeine and atenolol that displayed much lower deviation in the lower mass extraction.

Table 4.1: Comparison of method recovery and precision between different mass extractions of G. pulex. 50 mg extraction spiked at 200 ng g^{-1} (n=6). 100 mg extraction spiked at 1000 ng g^{-1} (n=3).

	100 mg			50 mg		
	Recovery (%)	SD	RSD (%)	Recovery (%)	SD	RSD (%)
Atenolol	4	1	22	6	0	5
Caffeine	8	7	87	19	2	13
Cimetidine	6	0	6	2	1	42
Sulfamethazine	41	2	5	37	7	20
Antipyrin	30	3	9	37	2	4
Trimethoprim	65	1	2	91	11	13
Furosemide	39	3	7	73	6	9
Metoprolol	71	5	7	99	14	15
Naproxen	44	1	2	66	13	20
Ketoprofen	41	2	5	69	28	40
Warfarin	71	3	4	86	4	5
Bezafibrate	39	4	10	42	6	14
Flurbiprofen	47	8	18	44	18	42
Propanolol	52	11	20	59	21	36
Carbamazepine	69	3	5	95	20	21
Indometacin	42	8	20	73	22	30
Temazepam	85	1	1	114	10	9
Nimesulide	87	4	5	64	5	8
Nifedipine	70	1	1	88	22	25
Diazepam	89	2	2	101	11	10
Gemfibrozil	79	21	27	100	54	54

ANOVA of the recovery means and their respective RSDs was performed to identify if there was statistical significance between the sample mass extraction. The *p*-value generated for the means was 0.138 and for the RSDs was 0.125, which was above the alpha level of 0.05 indicating that there was no statistically significant difference between the recovery and precision of the analytical method when using a lower sample mass. However, the analytical

method was validated for 10 pharmaceuticals (Table 4.2), thus a second ANOVA was performed for these 10 compounds. The *p*-values were 0.139 and 0.006 for the recovery mean and RSDs, respectively. This indicated that whilst the mean recoveries were not significantly different, the RSDs were. Comparison of the RSDs showed that extraction of a lower sample mass led to decreased precision. All 10 analytes had lower precision (mean difference of 12 ± 7 %) when compared to the extraction with 100 mg of *G. pulex*.

Table 4.2: Comparison of method recovery and precision for method validated compounds.

	100 mg		50 mg	
Compound	Recovery (%)	RSD (%)	Recovery (%)	RSD (%)
Sulfamethazine	41	5	37	20
Trimethoprim	65	2	91	13
Metoprolol	71	7	99	15
Warfarin	71	4	86	5
Propanolol	52	20	59	36
Carbamazepine	69	5	95	21
Temazepam	85	1	114	9
Nimesulide	87	5	64	8
Nifedipine	70	1	88	25
Diazepam	89	2	101	10

The lower precision could be due to two variables, the first of which was that the reconstitution volume was lower and therefore using smaller volumes led to lower precision due to less reliable volume measurement (i.e. pipetting errors). Secondly, whilst the ratio of matrix to analyte was kept constant, due to solid sample inhomogeneity there was the potential that inter-sample matrix varied more significantly than when compared to the use of a larger mass of *G. pulex* material. The variation in matrix between samples could lead to larger variation in extractions when using SPE cartridges and also greater variability in ionisation efficiency during MS analysis.

The quantification of matrix effects is presented in Table 4.3. Suppression was enhanced for 9 of the 10 compounds when compared to extraction of a larger mass. The average suppression effect was -51 ± 12 % for the 50 mg extraction whereas the suppression effect for the 100 mg extraction was -26 ± 3 %. The matrix effects were also more variable with the lower mass extraction. All compounds had higher variance with the exception of trimethoprim. ANOVA of the matrix effect and variance showed that the difference between the 100 mg and 50 mg extraction were significant (*p*-values were 0.006 and <0.001).

Table 4.3: Comparison of matrix effects between different mass extractions of G. pulex. 50 mg extraction spiked at 200 ng g^{-1} (n=6). 100 mg extraction spiked at 1000 ng g^{-1} (n=3).

	50 mg		100 mg	
Compound	Matrix Effect (%)	SD	Matrix Effect (%)	SD
Sulfamethazine	-26	8	-11	2
Trimethoprim	-60	5	-13	6
Metoprolol	-32	14	-11	2
Propranolol	-74	13	-56	4
Carbamazepine	-63	16	-9	2
Warfarin	-23	19	-28	4
Nimesulide	-67	9	-35	3
Temazepam	-38	9	-11	3
Diazepam	-73	6	-43	3
Nifedipine	-53	18	-39	4

A previous investigation into the effect soil sample mass on the precision of an analytical method for four heavy metals showed that between 1-5 g had no effect on the precision of three metals. However, the last heavy metal (lead) showed that the poorest RSDs were observed with the lowest mass of soil used in the method [31]. Whilst this method involved the analysis of heavy metals by flame atomic absorption spectroscopy (FAAS) which is different to the samples, analytes and instruments used here, it demonstrates the possibility that specific analytes can be affected by sample mass.

Whilst there was a statistical significance between the precision of the methods used, the lower mass still resulted in an acceptable method precision of ≤ 20 % RSD for 6 of the 10 compounds. The two compounds nifedipine and carbamazepine had RSDs of 25 % and 21 %, respectively. The final compound propranolol had an observed RSD of 36 %. This compound in the original method was also observed to have the lowest precision of the ten pharmaceuticals. The lower precision is likely to result, in addition to the variables mentioned above, from the variation in retention time reported in Chapter 2. The t_R will affect precision as the co-elution of matrix components will lead to greater variation in the MS signal response either through effects in droplet formation, transfer to gas phase ions or analyte charging [32]. Finally, whilst the precision may be lower for these compounds the recoveries and RSDs were determined without the addition of a stable isotope labelled internal standard (SIL-IS). The use of SIL-IS improved method precision for all compounds with RSDs ranging from 1 – 11 %. The compounds carbamazepine, nifedipine and propranolol showed significant improvement with RSDs of 2 %, 3 % and 11 %, respectively. It has been demonstrated that SIL-IS have improved precision during analytical method development [33].

4.3.2 Experimental design: reduction of time intervals

In addition to the reduction in the number of organisms, a reduction in the number of sampling time intervals was also required to ensure that these experiments remained feasible. Time points were selected at 6, 24, 48 and 96h so that the uptake phase had three time points and elimination phase contained two intervals. The additional time point in the uptake phase was selected so that any trends in k_1 could be identified. As discussed in the previous chapter, the lack-of-fits in the toxicokinetic modelling stemmed from the uptake phase data that was caused due to a decreasing trend of the k_1 rate constant. Whereas, the elimination data showed no obvious trends in relation to the lack-of-fits. The potential limitation when using a small number of time intervals is that the data may not reflect reliably the ability of a compound to concentrate as modelling is limited to a few data points. However, the OECD 305 guidelines contain a minimised test with just two time intervals in the uptake and elimination phase, respectively (e.g. day 14, 28, 35 & 42). This minimised test was proposed to reduce the number of animals used and reduce the cost of running a full study.

The minimised study design was evaluated in the literature and authors concluded that the test was valuable and offered reliable BCF estimation for regulatory purposes [34]. A second publication proposed that a minimised test design involving only two sampling time intervals in a 14d depuration period [35]. The authors of this work evaluated the previous published BCF studies and found that the use of this minimised test design was viable alternative to a full study design. Whilst support is for the use of minimised design, as our experiments here involved a non-standard species and much shorter uptake and depuration phases, re-evaluation of the uptake and elimination data from Chapter 3 was

performed to confirm whether a minimised test design here could also adequately estimate BCF values (Table 4.4).

A comparison was made between the BCFs generated by the full test design and a minimised test for both simultaneous and sequential methods of estimation. To determine if BCFs differed significantly an ANOVA was performed for each method of estimation and resulted in *p*-values of 0.95 for simultaneous BCFs, 0.43 for sequential BCFs and 0.45 for sequential BCFs determined using linear regression in the elimination phase data. These three *p*-values were >0.05 indicating that there were no statistically significant differences between the BCFs estimated using the full study design or the minimised design. Therefore, all non-radiolabelled exposures were performed using the minimised design.

Table 4.4: BCF estimation using a full study design and a minimised design using 4 time intervals (5, 24, 48 and 96h). SimBCF = simultaneous method, SeqBCF = sequential BCF as described in Chapter 3.

	Full Design			Minimised Design		
	SimBCF	SeqBCF	SeqBCF	SimBCF	SeqBCF	SeqBCF
Propranolol	32	39	42	36	34	34
Formoterol	14	18	33	26	26	29
Imipramine	212	3811	4533	177	420	685
Metoprolol	16	-		20	-	
Terbutaline	12	22	19	12	16	15
Ranitidine	17	81	112	30	-	9
Diclofenac	14	27	21	19	23	22
Ibuprofen	27	27	50	40	29	-

4.3.3 Exposure of *G. pulex* to non-radiolabelled pharmaceuticals

Non-radiolabelled toxicokinetic exposures were performed for a total of 11 compounds, the ten compounds previously validated plus the compound imipramine as this compound displayed increased bioconcentration relative to several other pharmaceuticals tested by LSC (Chapter 3). Quantifications of exposures were initially performed against a single SIL-IS calibrant fortified in each sample at 100 ng g^{-1} dw pre-extraction. The ratio between the non-labelled

standard and SIL-IS was used to quantify the amount of each pharmaceutical accumulated during the exposure period. Initial exposures were performed for carbamazepine, diazepam, temazepam and trimethoprim.

The toxicokinetic profiles for carbamazepine, diazepam and temazepam showed low level concentration of pharmaceuticals in the uptake phase reaching a maximum of 64 ng g^{-1} dw for the compound diazepam. The profiles showed that carbamazepine, diazepam and temazepam had reached or were very close to approaching apparent steady-state where the rate of uptake is equal to the rate of elimination and the system was in equilibrium. The short steady-state times indicated that these pharmaceuticals had a rapid turnover and were unlikely to accumulate significantly in these animals. Indeed, by the end of the 48h elimination phase, pharmaceutical response signals reached below the LOQ or LOD. Thus, supporting very rapid elimination of these pharmaceuticals. Figure 4.1 shows the concentration-time plots for these three pharmaceuticals modelled using the simultaneous method for BCF estimation. The BCFs were calculated as 21, 37 and 40 for carbamazepine, temazepam and diazepam. When considering factors that influence bioaccumulation, log*P* has been suggested to be a major factor when the value is <6 [36]. It would be expected that diazepam would have the highest BCF of these three pharmaceuticals as it has the greatest measure of hydrophobicity with a log*P* of 2.8 [37], in comparison to carbamazepine (2.45) and temazepam (2.2) [38, 39]. Therefore, it may be assumed that the BCFs should follow the order of diazepam > carbamazepine > temazepm. However, log*P* measurements can be considerably variable as reported in the literature. For example carbamazepine has reported log*P* values from 1.51 to 2.67 in which the lowest value may suggest that this compound should indeed have a lower BCF than that of diazepam or temazepam [40, 41].

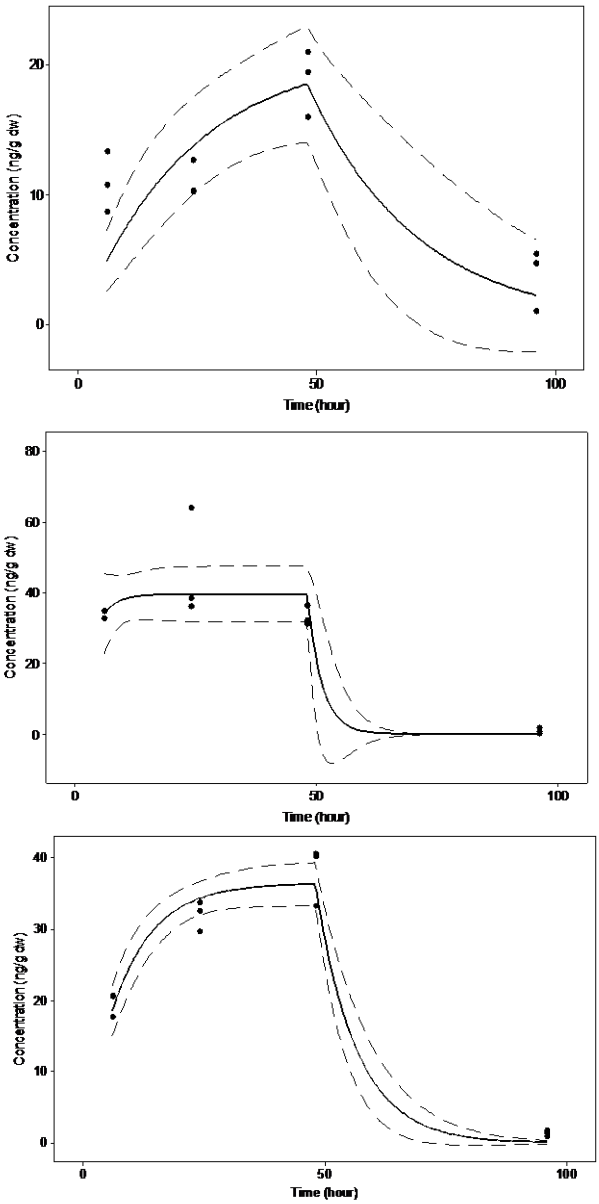

Figure 4.1: Toxicokinetic profiles of carbamazepine (top), diazepam (middle) and temazepam (bottom) in G. pulex exposed at 1 µg L^{-1}.

Further consideration of log*P* would also suggest there should be a significant difference between the BCFs of temazepam and diazepam as the difference in their log*P* values is considerable. Thus, suggesting log*P* as a sole predictor of bioconcentration may not be reliable.

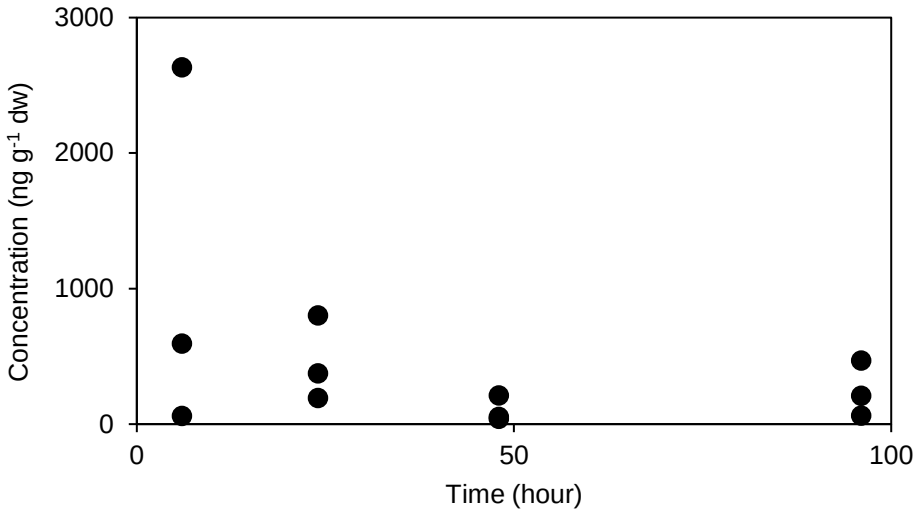

Figure 4.2: Toxicokinetic profile of trimethoprim in G. pulex exposed at 1 µg L^{-1}.

The last compound exposed using a single calibrant was trimethoprim. However, the quantification of this exposure was inconsistent as the scatter of internal concentrations was significant as shown in Figure 4.2. The concentrations in the uptake phase of the trimethoprim exposure ranged from 54-2635 ng g^{-1} dw and in the elimination phase ranged 63-470 ng g^{-1} dw. These high values could have potentially been caused by residual contamination from the environment where they were collected. However, concentrations in the µg g^{-1} range have not been previously reported and it is unlikely that these represented true measurements of uptake. A potential problem may have been the use of a single SIL-IS calibrant for quantification. Therefore, future toxicokinetic experiments were performed using a 3-point SIL-IS matrix matched calibration curve.

Using internal standard matrix matched calibration curves resulted in good linearity with R^2 ranged between 0.9897 – 1.000. This method was much superior for quantification than when compared to matrix matched calibration curves without the addition of SIL-ISs which had R^2 ranged from 0.8866 – 0.9972 (Figure 4.3). The compound imipramine had poor linearity (<0.95 R^2) and method performance (absolute recovery 156 % ± 25 % RSD) and was therefore excluded

from analysis. The trimethoprim exposure was repeated and gave improved results which showed much less variability and scatter in the data points. The maximum uptake concentration reached 22 ng g^{-1} dw and by the end of the elimination phase concentration reduced to below the LOD of 2 ng g^{-1}. Warfarin was exposed to animals at a concentration of 1 µg L^{-1}. However at this concentration no peaks were detected in any sample and the calibration curve gave a much lower response than was expected at the concentrations used (100 – 300 ng g^{-1} dw) when considering that the reported LOQ for this compound was 5 ng g^{-1} dw.

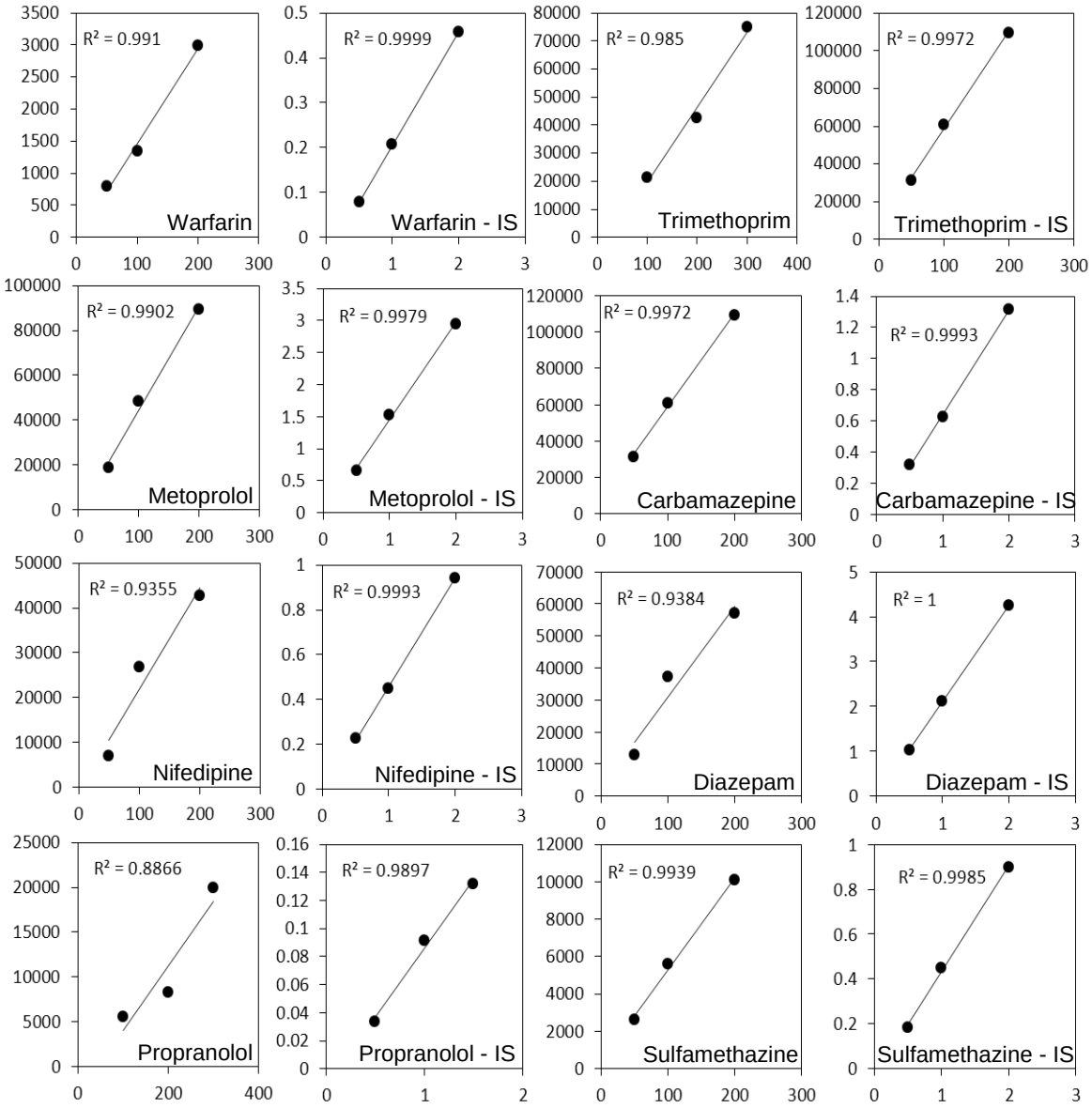

Figure 4.3: Comparison of matrix matched calibration curves with and without the addition of SIL-IS.

The exposure with warfarin was repeated at 10 µg L^{-1} and here peaks were detected but again the signal response for the analyte was approximately 10-fold lower than expected. A toxicokinetic exposure was also performed with nimesulide at 1 µg L^{-1} and similar to the initial warfarin exposure no peaks were detected in any sample that was analysed. The calibration series that was prepared was also not detected, even at the highest concentration of 200 ng g^{-1} dw. It was determined that the negative mode ESI on the mass analyser had a

severe loss of sensitivity. The nimesulide exposure was not replicated with a higher concentration because of the loss in sensitivity. Furthermore, water concentrations of nimesulide were only detectable at concentrations of 40 µg L^{-1} which were far above reported environmental levels of < 12 ng L^{-1} [42, 43]. Therefore, concentrations of this magnitude had lost environmental relevance in the exposure of this organism. The modelled toxicokinetic profiles for the remaining compounds are shown in Figure 4.4. The respective concentration of each pharmaceutical in the exposures is shown in Table 4.5. Water concentrations of the pharmaceuticals remained stable across the exposure period for carbamazepine, diazepam, temazepam, sulfamethazine, metoprolol and trimethoprim. Propranolol showed stable water concentrations over the first 24h however this declined by 28 % to an average of 6.41 µg L^{-1}. Nifedipine showed an average decrease of 39 % across both days of the uptake phase. It is possible that sorption was the cause in the reduction of nifedipine in the exposure media. However, an experiment was setup to monitor for sorption and it was found that nifedipine did not sorb to the glass beakers. Furthermore, no losses could be attributed to other processes such as volatilisation or degradation. This suggested the observed reduction of nifedipine in the water phase was attributed to the uptake by *G. pulex*. The final compound warfarin was unable to be quantified due to sensitivity issues with the MS whilst operated in the negative polarity mode. Maximal uptake concentrations in the animals were observed for the compound propranolol where this compound was exposed at a higher concentration of 10 µg L^{-1} due to a relatively high LOQ value. In this exposure, internal concentrations reached up to 519 ng g^{-1} with a mean value of 210 ng g^{-1} at the end of the uptake period. Warfarin also showed relatively higher

internal concentrations which again was explained by the higher exposure concentration.

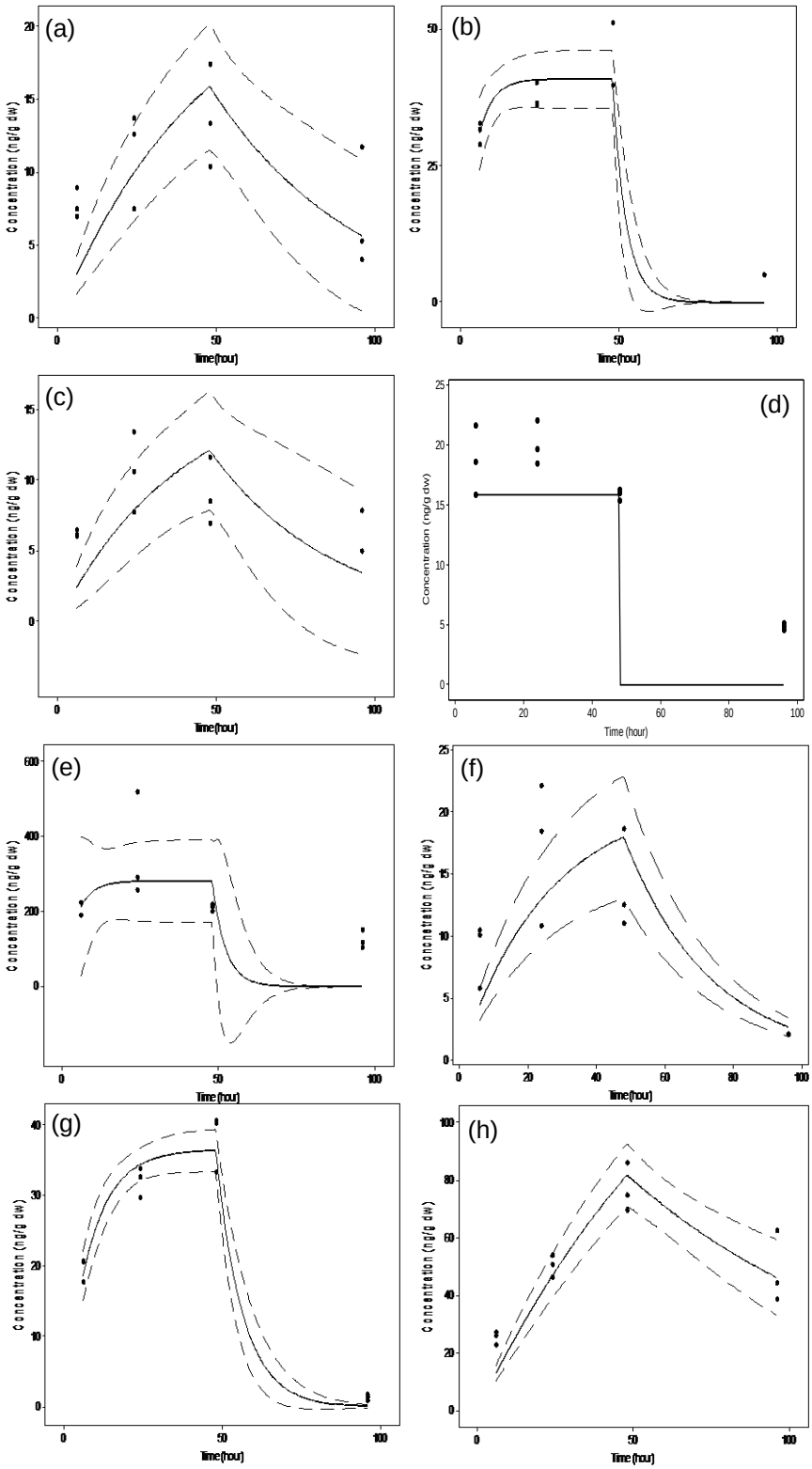

Figure 4.4: Toxicokinetic profiles of selected pharmaceuticals in G. pulex measured using LC-MS/MS. Solid line represents model fit, dashed lines represent 95 % confidence interval. (a) carbamazepine, (b) diazepam, (c) metoprolol, (d) nifedipine, (e) propranolol, (f) trimethoprim, (g) temazepam and (h) warfarin.

The data for this compound suggested that in contrast to other compounds this did not reach/approach steady state in the uptake period as no plateau was observed in the toxicokinetic profile. The remaining pharmaceuticals carbamazepine, diazepam, metoprolol, nifedipine, trimethoprim and temazepam exposed at 1 µg L^{-1} showed internal concentrations of ≤51 ng g^{-1} during the uptake phase. These internal concentrations showed rapid elimination and were reduced to ≤LOQ/LOD. The rapid turnover of all the pharmaceuticals suggests that bioaccumulation could be less relevant for these types of ionisable compounds.

Table 4.5: Water concentrations of pharmaceutical exposures. D1 and D2 represent initial pharmaceutical concentrations on day 1 and day 2, respectively. 24 h and 48 h represent the concentration after 24 h of exposure with either D1 or D2 solutions. All samples were taken in triplicate with the exception of D2 exposure media.

	Concentration (µg L^{-1})						
Compound	D1	SD	24 h	SD	D2	48 h	SD
Carbamazepine	1.12	0.03	1.01	0.05	1.08	1.07	0.02
Diazepam	1.02	0.03	0.86	0.05	1.04	0.89	0.11
Temazepam	0.96	0.03	0.85	0.03	1.17	1.03	0.00
Nifedipine	0.94	0.09	0.59	0.06	0.82	0.49	0.18
Sulfamethazine	1.06	0.07	0.99	0.17	0.89	0.71	0.15
Trimethoprim	1.09	0.04	1.01	0.11	0.99	0.97	0.04
Metoprolol	0.77	0.18	0.72	0.15	0.86	0.87	0.21
Propranolol	9.22	0.50	8.92	0.29	8.98	6.41	-

BCFs were generated using either simultaneous or sequential modelling as described previously in Chapter 3 (Table 4.6). The BCFs generated were in the order of trimethoprim and nifedipine < metoprolol < warfarin < carbamazepine < propranolol < temazepam < diazepam. The highest BCF generated by the simultaneous method was 41 for diazepam and the lowest estimation was 16 for both trimethoprim and nifedipine. These values remain significantly lower than any regulatory threshold to be considered bioaccumulative or very bioaccumulative [44]. The BCF values for propranolol and metoprolol were also compared with the BCFs generated by LSC in Chapter 3.

Table 4.6: Determination of BCFs using either simultaneous or sequential parametrisation of k_1 and k_2.

Compound	Simultaneous						Sequential						Sequential					
	k_1	SE	k_2	SE	*p*-value	BCF	k_1	SE	k_2	SE	*p*-value	BCF	k_1	SE	k_2	r^2	*p*-value	BCF
Carbamazepine	0.5307	0.115	0.0214	0.008	0.049	25	0.4418	0.054	0.014	0.007	0.07	32	0.4643	0.056	0.0158	0.534	0.08	29
Diazepam	9.5942	2.126	0.2349	0.058	0.028	41	2.6469	0.265	0.046	0.011	0	58	3.0917	0.280	0.0582	0.953	0.001	53
Temazepam	4.3326	0.556	0.1186	0.018	0.131	37	2.8514	0.116	0.0702	0.027	0.022	41	2.751	0.117	0.0669	0.9965	0.016	41
Trimethoprim	2.325	0.916	0.1488	0.066	0.376	16	0.8451	0.105	0.0402	0.017	0.066	21	0.837	0.105	0.0396	0.8468	0.064	21
Nifedipine	4677.31	n/a	295.66	n/a	n/a	16	0.7802	0.146	0.0248	0.001	0	31	0.7802	0.146	0.0248	0.9967	0	31
Warfarin*	0.2242	0.022	0.0119	0.003	0.043	19	0.2091	0.012	0.0096	0.003	0.066	22	0.2118	0.012	0.01	0.6989	0.072	21
Metoprolol	0.4413	0.135	0.0259	0.015	0.005	17	0.2788	0.046	0.0071	0.006	0.005	39	0.2855	0.047	0.0078	0.39	0.006	37
Propranolol*	6.596	5.797	0.2348	0.221	0.027	28	0.8059	0.181	0.0111	0.002	0.006	73	0.8116	0.182	0.0113	0.8543	0.006	72

SE = standard error

** 10 µg L^{-1} exposure*

Propranolol BCF was estimated to be 32 and metoprolol BCF was 16 (Chapter 3), which showed very good agreement with the values of 28 and 17 determined by LC-MS/MS here. The compound sulfamethazine was not detected in any sample and indicated that there was no accumulation of this compound in *G. pulex*. Sulfamethazine and metoprolol are relatively polar pharmaceuticals and it may be expected that these two compounds would not bioconcentrate. However, the compound nifedipine which is much more hydrophobic also shows a very low BCF. This further suggested that log*P* is not a reliable indicator for the bioconcentration of pharmaceuticals and the degree of ionisation may also play an important role in uptake and bioconcentration. Table 4.7 shows the log*P*, log*D* and predominant form of each pharmaceutical that was exposed in *G. pulex*.

Table 4.7: pH measurement of toxicokinetic experiments and the respective logP/D and ionisation states of each pharmaceutical.

Compound	pH (n=4)	SD	Log*P*	Log*D*	Predominant Form
Carbamazepine	8.09	0.03	2.28	2.3	Neutral
Diazepam	8.09	0.03	2.74	2.7	Neutral
Temazepam	8.50	0.12	2.12	2.1	Neutral
Trimethoprim	8.50	0.12	1.12	1.1	Neutral
Nimesulide	8.05	0.15	2.7	0.9	Anionic
Nifedipine	8.05	0.15	3.45	3.4	Neutral
Sulfamethazine	7.93	0.02	0.44	0.1	Neutral/Anionic*
Warfarin	8.20	0.08	3.11	-0.2	Anionic
Metoprolol	8.20	0.08	1.85	0.5	Cationic
Propranolol	8.27	0.11	3.26	2	Cationic

**approximately 1:1 of each state*
LogP/D estimated using ACD Labs

At the exposure media pH the pharmaceuticals carbamazepine, diazepam, temazepam, trimethoprim and nifedipine would have been in a predominantly neutral form. Nifedipine displayed the highest log*P* of 3.45 but had the same BCF estimated as trimethoprim a much more polar pharmaceutical with a log*P* value of 1.12. As mentioned previously, temazpam diazepam and carbamazepine all remain neutral however their respective BCFs do not follow any specific order when compared to their log*P*. Uptake models are usually based on neutral organic microcontaminants and is the reason that log*P* can be a good indicator of bioconcentration for these compounds when log*P* is <6. Therefore, neutral pharmaceuticals should be expected to show similar behaviour which is not observed in these experiments. However, the selection of pharmaceuticals is limited in size and therefore discernible trends may not be apparent. A plot of log*D/P* versus BCF showed that there were no identifiable trends (Figure 4.5) and supports that log*P* or log*D* measurements may not be reliable for risk assessments of pharmaceuticals.

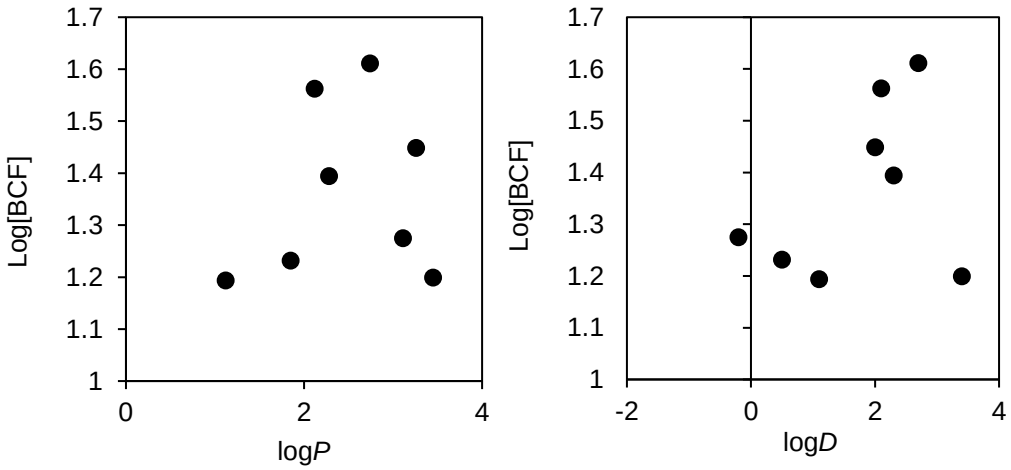

Figure 4.5: Comparison of log[BCF] and logP/D of the pharmaceuticals selected in the toxicokinetic experiments.

Consideration of the complexity of biological systems and the unique characteristics of pharmaceuticals it may be expected that uptake and bioconcentration is a much more complex process than can be predicted by

simple physicochemical properties. Many factors have been proposed and reported to influence the bioconcentration of pharmaceuticals including hydrophobicity, metabolism, bioavailability, environmental exposure scenarios, and carrier mediated uptake [45]. A particularly important factor is the environmental exposure as the complexity of environmental matrices on BCF may well increase or decrease predicted BCFs or BCF measured from *in vivo* laboratory exposures. Surface water temperature, pH, sediment layer and the composition of other components (pharmaceuticals, colloids, surfactants, organic chemicals etc.) can have an effect on the BCF [46].

Field-derived BAFs could be estimated for four compounds from the occurrence data presented in Chapter 2. These values were 4500, 1400, 556 and 19 for diazepam, warfarin, trimethoprim and carbamazepine, respectively. The only value that was in agreement with the BCFs estimated through the *in vivo* exposures was carbamazepine. The remaining three compounds showed field-derived BAFs that were significantly higher. Therefore, laboratory exposures my not present a reliable assessment for the accumulation potential of a compound in a 'real' exposure scenario. However, the main limitation of field derived BAFs is that surface water concentrations are subject to considerable temporal fluctuation and therefore it is difficult to understand what an individual has been exposed to over time leading to uncertainties in BAF measurement [47].

Comparison of the BCFs here with literature reported data showed good agreement for the two compounds carbamazepine and diazepam in *G. pulex* [11]. A second study also showed a BCF of 51 for diazepam in a marine mussel, *Mytilus galloprovincialis* [48]. In *Daphnia magna*, the BCF of propranolol varied from 18-83 which varied with exposure concentration [49]. However, few data or studies exist on the uptake of pharmaceuticals in invertebrates. Review of fish

data generally showed low level bioconcentration. For example, diazepam BCF in fish ranged from 2 - 146 depending on the tissue type [50], sulfamethazine BCF in sturgeons was shown to be 1 [51], carbamazepine BCF in two species of fish was < 7 depending on tissue [50] and propranolol was also estimated to have a BCF of < 1 [52]. These data further indicate that pharmaceuticals have a low potential of bioconcentration in biota and are in agreement with the values generated here for *G. pulex*.

The low accumulation of pharmaceuticals may be expected by relatively low hydrophobicity values. However, pharmaceuticals are innately designed to be metabolised and excreted from the body so that any adverse effects of drug accumulation are not experienced with the use of human and veterinary medicines [53]. Whilst, these organisms tested are not the target species, conservation of cytochrome enzymes among biota has widely been observed suggesting the ability of invertebrates to readily metabolise pharmaceuticals [54]. Therefore, accumulation of pharmaceuticals may not be as important as the determination of adverse effects such as sub-lethal endpoints for environmental risk assessment purposes.

4.3.4 Model fits and the estimation of uptake rate constants

As described previously in Chapter 3, the model fits of simultaneous and sequential BCF estimation showed a significant lack-of-fit for several pharmaceuticals. The lack-of-fit seemed to arise from the uptake phase data and therefore the rate constant was estimated over each time interval during the uptake period. This revealed that there was a decreasing trend in the k_1 rate constant which again violated one of the models assumptions. Lack-of-fits were observed from the simultaneous method of estimation for 5 compounds

(carbamazepine, propranolol, metoprolol, warfarin and diazepam) with 2 compounds showing no significant lack-of-fits (temazepam and trimethoprim). However, the *p*-value for carbamazepine and warfarin were 0.049 and 0.043 which indicated that the statistical significance was not as severe. Lack-of-fit for the final compound nifedipine was not possible to estimate due to the fit of the line as shown in Figure 4.4. The reason for this unusual fit is due to the large estimates of k_1 and k_2, which resulted from apparent steady state being reached ≤ 6 h. The sequential determination for BCF was performed to identify if better model fits were observed. As the elimination phase data contains only two time intervals, a lack-of-fit was not possible to calculate. Therefore, lack-of-fits were determined for the whole model. Using the sequential method led to the compounds warfarin and carbamazepine no longer having significant lack-of-fits (*p*-values > 0.05). However, temazepam showed a lack-of-fit in comparison to the simultaneous method. The BCFs generated by the sequential method showed higher estimates for all compounds studied. When linear regression was used to estimate k_2, the sequential estimation of k_1 showed very good agreement with the sequential curve fitting methods. The agreement resulted from only two time intervals in the elimination phase data which led to very similar estimates of k_2 as shown in Table 4.5.

As several significant lack-of-fits were observed, the k_1 rate constant was calculated over the time intervals for the uptake phase data (Figure 4.6). Similar to previous trends seen, k_1 was observed to decrease over time. These decreases again are potentially the cause of the lack-of-fits, as suggested in Chapter 3. However, in the cases of warfarin, carbamazepine, diazepam and temazepam an apparent plateau has been reached indicating that the k_1 is no longer decreasing with time. If k_1 has reached a constant value then it would be

possible to use this value to estimate a BCF using elimination phase k_2 value. For example, the average of the k_1 over the 48h time interval for these compounds resulted in BCFs of 20, 26, 40 and 48 for warfarin, carbamazepine, temazepam and diazepam.

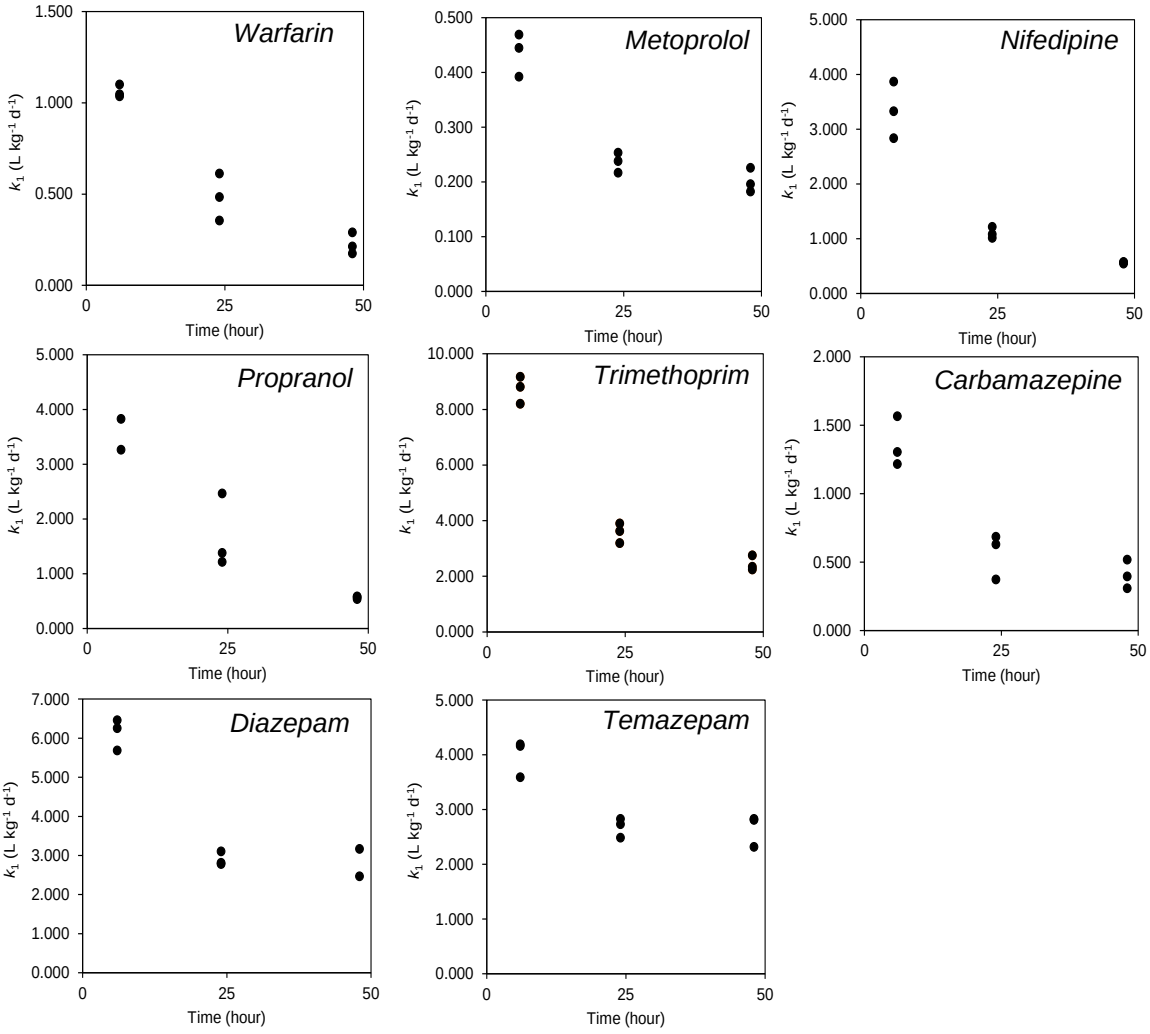

Figure 4.6: plots of k_1 over time for eight pharmaceuticals.

These values showed good agreement between the BCFs generated by the simultaneous method indicating this could provide an alternative method for BCF estimation when k_1 values are found to decrease over time. The initial decrease in k_1 between the 6 and 24h time points also showed a larger decrease than between the 24 to 48 h time interval. The larger decrease in the early time

point could be a result of sorption of the compound to the cuticle of the animal as discussed previously in Chapter 3. Whilst, several of the models showed lack-of-fits potentially arising from the decreasing value of k_1, due to the rapid turnover of these pharmaceuticals it is possible to calculate a BCF using steady state concentrations. The OECD 305 guideline suggests that it is appropriate to use BCF_{ss} if the concentrations have reached ≥95 % steady state [14]. A quick estimate of the time to reach 95 % steady state can be calculated using logP [14]. The maximum time for the compounds to reach 95 % steady state (based on log*P*) would be approximately 2.7 days. Therefore all compounds should have reached or approached apparent steady state in the uptake phase. Apparent steady state is recognised when the internal concentrations of three successive time intervals across 2 days are within ± 20 % of each other [14]. Table 4.8 shows the BCFs generated using steady state concentrations.

Table 4.8: Mean [pharmaceuticals] at each time interval in the toxicokinetic exposures, (n=3).

	Concentration (ng g^{-1} dw)							
	6h		24h		48h			
Compound	Mean	SD	Mean	SD	Mean	SD	Steady State?	BCF_{ss}
Warfarin	25	5	50	10	77	15	No	-
Metoprolol	6	1	11	2	9	2	Yes	9
Nifedipine	19	4	20	4	16	3	Yes	16
Propranolol	206	41	355	71	210	42	*	21
Trimethoprim	47	9	55	11	52	10	Yes	52
Carbamazepine	8	2	11	2	14	3	Yes	14
Diazepam	31	6	37	7	45	9	Yes	45
Temazepam	20	4	32	6	38	8	*	38

* *Approaching steady state*

Warfarin is the only compound observed to not approach steady state. Propranolol and temazepam are assumed to approach steady state as the concentrations are relatively constant and therefore a steady state BCF (BCF_{ss}) was also estimated for these two compounds. Comparison of BCF_{ss} and kinetic BCFs (BCF_k) showed that these values are all within good agreement of each

other. BCF_{ss} may be considered more reliable for BCF estimates as it does not rely on modelling assumptions to generate a value. The agreement of the values also suggests that whilst modelling approaches may show statistically significant lack-of-fits they are adequate enough to give a good estimate of the potential of a compound to bioconcentrate or bioaccumulate in an organism for regulatory purposes.

4.3.5 Metabolism of selected pharmaceuticals by *G. pulex*

It is important to consider metabolism of xenobiotics in non-target species. As data supports factors other than hydrophobicity can be important in accumulation, biotransformation could explain the variability of BCFs. Authors have demonstrated that *G. pulex* are able to metabolise a range of organic micropollutants, biocides and pharmaceuticals [27, 55]. Pharmaceuticals have been shown to undergo biotransformation through oxidative and conjugation reactions [56]. As the targeted LC-MS/MS method only determines the amount of parent compound, the BCFs presented above (Table 4.6) do not take into account the formation or accumulation of any metabolites. The metabolite half-lives in the body can be longer or shorter than the parent compound as they are modified by phase I or phase II metabolic processes leading to increased or decreased accumulation.

Selected pharmaceuticals (propranolol, carbamazepine and diazepam) were used in metabolism studies and several metabolites were targeted in the analytical method including 4-hydroxypropranolol (HP), 4-hydroxypropranolol sulphate (HP-SULPH), 4-hydroxypropranolol glucuronide (HP-GLU), carbamazepine-10,11-epoxide (CBZ-EPOX), oxazepam (OXAZ) and nordiazepam (NORDIAZ). The analytical method was previously optimised for the last diazepam metabolite, temazepam. A matrix effect and recovery

experiment was performed for these additional analytes before exposures were performed (Table 4.9).

Table 4.9: Matrix effect and recovery for the metabolites of selected pharmaceuticals (HLB sorbent). Samples spiked at 200 ng g^{-1} (n=6).

	Matrix Effect (%)	SD	Recovery (%)	SD	RSD (%)
CBZ-EPOX	8	4	103	14	13
HP-SULPH	-4	8	34	7	20
HP	-93	4	41	11	27
HP-GLU	-4	6	0	0	128
OXAZ	9	7	82	5	7
NORDIAZ	-31	9	92	7	8

The matrix effects or recovery for 4-hydroxypropranolol were unable to be determined due to poor stability in solution. 4-hydroxypropanolol has previously been reported to be particularly unstable [57] with samples that required additives to maintain stability. Overall, matrix effects were relatively similar between the metabolites ranging from 4 % suppression to 9 % enhancement. However an exception to this was nordiazepam which showed 31 % signal suppression. Metabolites showed good absolute recoveries ranging 82 – 103 % (≤13 % RSD) with the exception of the propranolol metabolites. 4-hydroxypropranolol sulphate had a lower recovery of 34 % with a 20 % RSD whilst 4-hydroxypropranolol glucuronide showed no recovery from the analytical method.

The lower recoveries and precision could arise from the fact that these two propranolol metabolites are transformed through phase II metabolism which involves conjugation to a moiety such as a glucuronide or sulphate. These conjugates therefore have very different physico-chemical properties to the parent compound and may lead to the lower recovery and precision by HLB sorbents. In particular sulphate and glucuronides are charged moieties and could potentially have better retention using ion exchange sorbents due to the

electrostatic interaction between the functional groups on the sorbent. The propranolol metabolites were extracted with three different cartridges, two of which were HyperSep™RetainCX and HyperSep™RetainAX cartridges containing ion exchange (electrostatic interaction) and non-polar sorption capacities through either sulfonic acid or quaternary amine functional groups on a modified polystyrene divinylbenzene polymer. The remaining sorbent was HyperSep™RetainPEP a polymeric cartridge containing polar and non-polar sorption capacities.

The recovery was performed without matrix (Table 4.10) and overall the ion exchange sorbents showed better recovery and precision of the metabolites in comparison to the PEP sorbent. Propranolol also showed the best recovery and precision on the RetainCX cartridge. The RetainAX showed a 356 % recovery which indicates that the propranolol metabolites may have been deconjugated by an acid/alkaline hydrolysis reaction during the loading or elution phase of the SPE cartridge.

Table 4.10: Comparison of SPE sorbents for the pre-concentration of propranolol and metabolites. Samples were spiked at 20 µg L^{-1} (n=6).

	CX		AX		PEP	
	Recovery		Recovery		Recovery	
Compound	(%)	SD	(%)	SD	(%)	SD
Propranolol	114	17	356	104	53	42
HP-GLU	44	5	52	5	21	14
HP-SULPH	88	10	40	4	50	12

Improved recoveries and precision were achieved using RetainCX cartridges, therefore these sorbents were used in a matrix effect and recovery experiment (Table 4.11) Matrix effects ranged from 12 % enhancement to 59 % suppression. Absolute recoveries were acceptable for propranolol and 4-hydroxypropranolol sulphate whereas the glucuronide metabolite showed very low recovery (3 %). Overall, the CX cartridges showed slightly better performance

than the HLB sorbent for the propranolol metabolites. However, as the recoveries and precision were not significant the propranolol metabolism experiment was performed in duplicate so quantification could be performed with both cartridges to achieve the best result.

Table 4.11: Matrix effect and recovery of propranolol and metabolites on a RetainCX cartridge. Samples were spiked at 200 ng g^{-1} (n=6).

Compound	Matrix Effect (%)	SD	Recovery (%)	SD	RSD (%)
HP-SULPH	12	8	45	6	13
HP-GLU	-33	5	3	1	33
PROP	-59	15	102	19	19

The exposure with carbamazepine, resulted in detectable peaks for carbamazepine-10,11-epoxide at 24h and 48h. The peak was confirmed by a single m/z transition and chromatographic retention time. The peaks were not quantifiable as they were below a signal to noise ratio of 10. The carbamazepine-10,11-epoxide peak was not detected at 96h suggesting that the metabolite had been eliminated from the organisms. The elimination would either be by excretion or further biotransformation as the epoxide is converted to carbamazepine-10,11–diol which is excreted as a free form or conjugate [58]. However, these metabolic pathways have been observed in human trials and therefore may vary in invertebrates. Limited data is available for biotransformation of xenobiotics in invertebrates. A previous study identified that carbamazepine was converted to its epoxide form and was the main metabolic pathway in the mussel, *Mytilus galloprovincialis*. Fish exposed to carbamazepine have also shown the presence of two carbamazepine metabolites, carbamazepine-10,11-epoxide and 2-hydroxycarbamazepine [59]. Quantification of the propranolol exposure made use of the data from the analytical method using the HLB SPE sorbent (Figure

4.7). Analysis of the RetainCX data gave a poor linearity (R^2 ≤0.95) in the calibration curves for propranolol and 4-hydroxypropranolol sulphate.

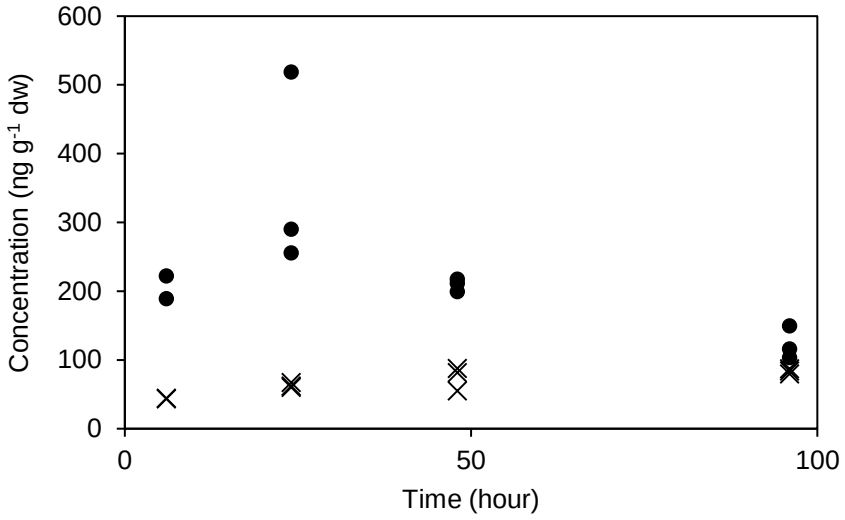

Figure 4.7: Concentration-time profile for propranolol (solid circles) and 4-hydroxypropranolol sulphate (crosses) in G. pulex.

The data showed that 4-hydroxypropranolol sulphate reached a mean concentration of 75 ng g^{-1} dw by the end of the uptake phase. The elimination phase showed no decreases in the concentration 4-hydroxypropranolol sulphate which showed a mean concentration of 84 ng g^{-1} dw at 96h. The increase in concentration of this metabolite could be attributed from the continued biotransformation of the parent compound. Determination of the parent compound propranolol showed a peak in the mean concentration at the 24h time interval which decreased by 48h. Decreases of internal concentrations during the uptake phase are indicative of active metabolic pathways. To the authors' knowledge, no propranolol metabolites have been identified in either fish or invertebrate. Human trials show that the major metabolites of propranolol were 4-hydroxypropranolol and napthoxylactic acid [60]. The relative importance of this sulphate conjugation pathway in *G. pulex* is not known as the napthoxylactic acid metabolite and glucuronide conjugate could not be determined. However, some

authors have suggested that sulphate and glucoside conjugation is the major metabolic process in invertebrates for the metabolism of aryl compounds [61, 62].

The final experiment was performed with diazepam and three metabolites were determined and quantified (Figure 4.8). Nordiazepam showed concentrations that reached a mean concentration of 60 ng g^{-1} dw in contrast to temazepam that reached a maximum mean concentration of 6 ng g^{-1} dw at 48h. The 10-fold difference in concentrations suggested that the biotransformation of diazepam to nordiazepam is the major metabolic pathway in contrast to the conversion of diazepam to temazepam.

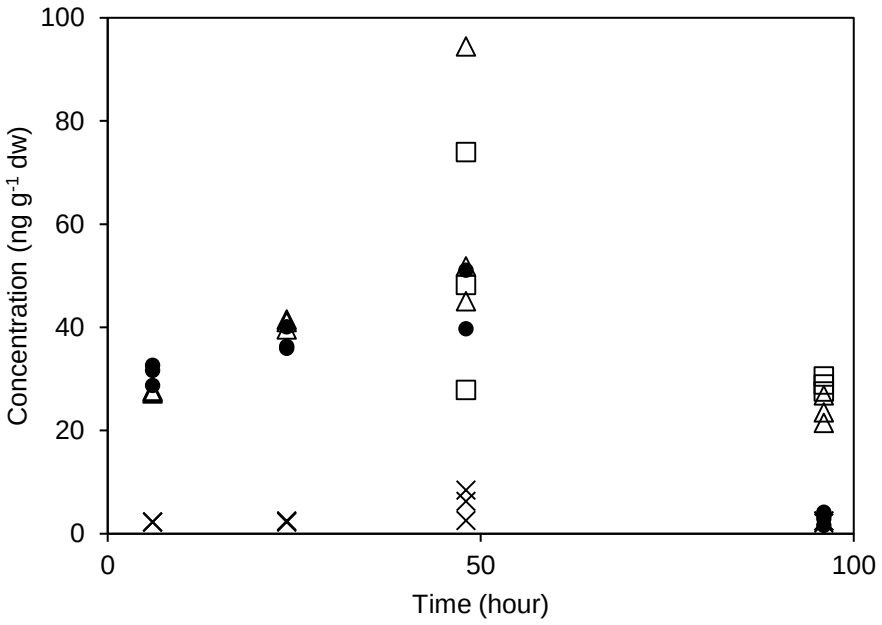

Figure 4.8: Concentration-time profile for diazepam (solid circles), nordiazepam (triangles), oxazepam (squares) and temazepam (crosses) in G. pulex

This agrees with mammalian data that shows the desmethylation of diazepam to nordiazepam is the primary metabolic pathway [63]. Temazepam was not detectable by the 96h time interval, suggesting this compound had been either excreted or further biotransformed to oxazepam. The elimination rate constant was determined at 0.0194 d^{-1} which is 3-fold lower than the elimination rate of diazepam. The estimated half-lives of diazepam and nordiazepam were

12h and 36h, respectively. The difference observed is also in agreement with the reported half-lives, as nordiazepam has a longer half-life (50-120h) than its parent compound diazepam (44h) [64]. The k_2 of temazepam was estimated at 0.016 d^{-1}, approximately 4-fold lower than the k_2 of temazepam when exposed to *G. pulex* as a parent compound. The lower k_2 may be explained by the apparent preferential metabolism of diazepam to nordiazepam. Thus, enzymes involved in the temazepam pathway may be less active. The final metabolite oxazepam was not detectable until 48h reaching a mean concentration of 50 ng g^{-1} dw. The biotransformation of diazepam to either nordiazepam or temazepam and further conversion to oxazepam would be rate liming steps leading to the apparent lag phase in the detection of oxazapem. The k_2 estimated for oxazepam was 0.009 d^{-1}, with mean internal concentrations reduced by 21 ng g^{-1} dw over the 48h depuration period. The half-life determined for oxazepam was 70h which is much greater than the reported single or multiple dose half-life in humans (9 – 11.6h) [65]. The difference in half-lives could be due to the continued conversion of nordiazpeam or temazepam to oxazepam after the uptake phase ended giving an apparent longer half-life. Furthermore, oxazepam is primarily excreted by conjugation with glucuronide moieties indicating that *G. pulex* may not readily metabolise oxazepam as well as in humans. The metabolite enrichment factors (MEFs) [27] for 4-hydroxypropranolol, nordiazpeam, temazpeam and oxazepam were determined to be 7.5, 64, 6 and 50, respectively. These MEFs can be compared to a ‘pseudo-BCF’ which would further indicate that these metabolites are not accumulative but the nordiazpeam and oxazepam bioconcentrate more than their parent compound diazepam. Furthermore, the summation of the parent BCFs and MEFs can give a BCF that would be comparable to those determined by total radioactivity counts [27]. For example the BCF of diazepam ranged from

41 – 58 whereas summation of the diazepam BCF and the MEFs would give a total BCF of 165. Thus, studies that only monitor the parent compound should be cautious when reporting BCFs if there is a high potential for biotransformation. Comparison of BCF_{total} (BCF_{parent} + MEF) to BCFs determined by LSC was not possible here. However, Ashauer et al., [27] reported that comparison BAF_{total} and BAF by LSC gave values that were within a single order of magnitude. However, the differentiation between metabolites and their parents gave better accuracy in parameter estimates (k_1/k_2) compared to radioactivity measurements [27]. The reason for this is that radioactivity measurements can over or underestimate elimination if biotransformation is not taken into account.

4.4 Conclusions

The data show that LC-MS/MS is a suitable technique for the measurement of uptake and elimination kinetics compared with more traditional approaches using liquid scintillation counting. The BCF estimates ranged from 16 – 41 for eight compounds (diazepam, temazepam, nifedipine, propranolol, metoprolol, carbamazepine, warfarin and trimethoprim) using the simultaneous method. Sequential parameterisation resulted in BCFs of 21 – 72 showing overestimates compared to the simultaneous method as also observed in Chapter 3. Similarly, models were shown to have significant lack-of-fits for six of the eight pharmaceuticals. The lack-of-fits also coincided with decreases in the uptake rate constant over time suggesting that poor model fits may have resulted from this trend. No trends were observed with BCF or log*D* or log*P* suggesting other factors other than compound hydrophobicity are important in bioconcentration. The role of metabolism was investigated for three selected pharmaceuticals (carbamazepine, propranolol and diazepam). *G. pulex* were

shown to metabolise all three pharmaceuticals into several different biotransformation products, indicating the conservation of cytochrome P450 enzymes in this species. The ability of *G. pulex* to readily metabolise these xenobiotics may explain, in part, the relatively low BCFs determined for pharmaceuticals in this work and the literature. Metabolic pathways and metabolites were found to be the same between vertebrate data. However, differences between half-lives were observed for the benzodiazepine compounds suggesting that rates of metabolism and elimination are different. Whilst, kinetics may differ the same metabolic pathways involved in elimination mean that human pharmacokinetic data is valuable for consideration of pharmaceuticals in environmental risk assessment. Analytical methods that only target and determine the parent compound in toxicokinetic studies may not reliably measure a 'true' BCF of the selected compound. It is advised that MS methods account for metabolites when estimating BCFs. Finally, the MEFs for the diazepam metabolites nordiazpeam and oxazepam showed that some metabolites had a higher potential to accumulate than the parent and remain in the body longer. These compounds may prove useful as biomarkers of exposure for field studies.

4.5 References

1. Mackay, D. and A. Fraser, Bioaccumulation of persistent organic chemicals: mechanisms and models. *Environmental Pollution*, 2000. **110**(3): p. 375-391.
2. Barber, M.C., L.A. Suárez, and R.R. Lassiter, Modelling Bioaccumulation of Organic Pollutants in Fish with an Application to PCBs in Lake Ontario Salmonids. *Canadian Journal of Fisheries and Aquatic Sciences*, 1991. **48**(2): p. 318-337.
3. Barber, M.C., L.A. Suérez, and R.R. Lassiter, Modeling bioconcentration of nonpolar organic pollutants by fish. *Environmental Toxicology and Chemistry*, 1988. **7**(7): p. 545-558.
4. Neely, W.B., D.R. Branson, and G.E. Blau, Partition coefficient to measure bioconcentration potential of organic chemicals in fish. *Environmental Science & Technology*, 1974. **8**(13): p. 1113-1115.
5. Veith, G.D., D.L. DeFoe, and B.V. Bergstedt, Measuring and Estimating the Bioconcentration Factor of Chemicals in Fish. *Journal of the Fisheries Research Board of Canada*, 1979. **36**(9): p. 1040-1048.
6. Kanazawa, J., Measurement of the bioconcentration factors of pesticides by freshwater fish and their correlation with physicochemical properties or acute toxicities. *Pesticide Science*, 1981. **12**(4): p. 417-424.
7. Fu, W., A. Franco, and S. Trapp, Methods for estimating the bioconcentration factor of ionizable organic chemicals. *Environmental Toxicology and Chemistry*, 2009. **28**(7): p. 1372-1379.
8. Klosterhaus, S.L., R. Grace, M.C. Hamilton, and D. Yee, Method validation and reconnaissance of pharmaceuticals, personal care products, and

alkylphenols in surface waters, sediments, and mussels in an urban estuary. *Environment International*, 2013. **54**: p. 92-99.

9. Wu, X., F. Ernst, J.L. Conkle, and J. Gan, Comparative uptake and translocation of pharmaceutical and personal care products (PPCPs) by common vegetables. *Environment International*, 2013. **60**: p. 15-22.
10. Stott, L.C., S. Schnell, C. Hogstrand, S.F. Owen, and N.R. Bury, A primary fish gill cell culture model to assess pharmaceutical uptake and efflux: Evidence for passive and facilitated transport. *Aquatic Toxicology*, 2015. **159**: p. 127-137.
11. Meredith-Williams, M., L.J. Carter, R. Fussell, D. Raffaelli, R. Ashauer, and A.B.A. Boxall, Uptake and depuration of pharmaceuticals in aquatic invertebrates. *Environmental Pollution*, 2012. **165**: p. 250-258.
12. Ashauer, R., I. Caravatti, A. Hintermeister, and B.I. Escher, Bioaccumulation kinetics of organic xenobiotic pollutants in the freshwater invertebrate *Gammarus pulex* modelled with prediction intervals. *Environmental Toxicology and Chemistry*, 2010. **29**(7): p. 1625-1636.
13. Ashauer, R., A. Boxall, and C. Brown, Uptake and Elimination of Chlorpyrifos and Pentachlorophenol into the Freshwater Amphipod *Gammarus pulex. Archives of Environmental Contamination and Toxicology*, 2006. **51**(4): p. 542-548.
14. OECD., *Test No. 305: Bioaccumulation in Fish: Aqueous and Dietary Exposure*. OECD Publishing.
15. Miller, T.H., G.L. McEneff, L.C. Stott, S.F. Owen, N.R. Bury, and L.P. Barron, Assessing the reliability of uptake and elimination kinetics modelling approaches for estimating bioconcentration factors in the

freshwater invertebrate, *Gammarus pulex. Science of The Total Environment*, 2016. **547**: p. 396-404.

16. Arnot, J.A. and F.A.P.C. Gobas, A review of bioconcentration factor (BCF) and bioaccumulation factor (BAF) assessments for organic chemicals in aquatic organisms*. Environmental Reviews*, 2006. **14**(4): p. 257-297.

17. de Wolf, W., J.H.M. de Bruijn, W. Seinen, and J.L.M. Hermens, Influence of Biotransformation on the Relationship between Bioconcentration Factors and Octanol-Water Partition Coefficients*. Environmental Science & Technology*, 1992. **26**(6): p. 1197-1201.

18. Oliver, B.G. and A.J. Niimi, Bioconcentration factors of some halogenated organics for rainbow trout: limitations in their use for prediction of environmental residues*. Environmental Science & Technology*, 1985. **19**(9): p. 842-849.

19. Opperhuizen, A. and D.T.H.M. Sijm, Bioaccumulation and biotransformation of polychlorinated dibenzo-p-dioxins and dibenzofurans in fish*. Environmental Toxicology and Chemistry*, 1990. **9**(2): p. 175-186.

20. Golan, D.E., A.H. Tashjian, and E.J. Armstrong, *Principles of pharmacology: the pathophysiologic basis of drug therapy*. 2011: Lippincott Williams & Wilkins.

21. Jerling, M., L. Lindström, U. Bondesson, and L. Bertilsson, Fluvoxamine Inhibition and Carbamazepine Induction of the Metabolism of Clozapine: Evidence from a Therapeutic Drug Monitoring Service*. Therapeutic Drug Monitoring*, 1994. **16**(4): p. 368-374.

22. Greenblatt, D.J., L.L. von Moltke, J. Schmider, J.S. Harmatz, and R.I. Shader, Inhibition of Human Cytochrome P450-3A Isoforms by Fluoxetine

and Norfluoxetine: *In Vitro* and *In Vivo* Studies*. The Journal of Clinical Pharmacology*, 1996. **36**(9): p. 792-798.

23. Cowan-Ellsberry, C.E., S.D. Dyer, S. Erhardt, M.J. Bernhard, A.L. Roe, M.E. Dowty, and A.V. Weisbrod, Approach for extrapolating in vitro metabolism data to refine bioconcentration factor estimates*. Chemosphere*, 2008. **70**(10): p. 1804-1817.

24. Arnot, J.A., D. Mackay, and M. Bonnell, Estimating metabolic biotransformation rates in fish from laboratory data*. Environmental Toxicology and Chemistry*, 2008. **27**(2): p. 341-351.

25. Nichols, J.W., D.B. Huggett, J.A. Arnot, P.N. Fitzsimmons, and C.E. Cowan-Ellsberry, Toward improved models for predicting bioconcentration of well-metabolized compounds by rainbow trout using measured rates of *in vitro* intrinsic clearance*. Environmental Toxicology and Chemistry*, 2013. **32**(7): p. 1611-1622.

26. Nichols, J.W., I.R. Schultz, and P.N. Fitzsimmons, In vitro–in vivo extrapolation of quantitative hepatic biotransformation data for fish: I. A review of methods, and strategies for incorporating intrinsic clearance estimates into chemical kinetic models*. Aquatic Toxicology*, 2006. **78**(1): p. 74-90.

27. Ashauer, R., A. Hintermeister, I. O'Connor, M. Elumelu, J. Hollender, and B.I. Escher, Significance of Xenobiotic Metabolism for Bioaccumulation Kinetics of Organic Chemicals in *Gammarus pulex. Environmental Science & Technology*, 2012. **46**(6): p. 3498-3508.

28. Rösch, A., S. Anliker, and J. Hollender, How Biotransformation influences Toxicokinetics of Azole Fungicides in the Aquatic Invertebrate *Gammarus pulex. Environmental science & technology*, 2016.

29. Celiz, M.D., J. Tso, and D.S. Aga, Pharmaceutical metabolites in the environment: Analytical challenges and ecological risks. *Environmental Toxicology and Chemistry*, 2009. **28**(12): p. 2473-2484.

30. Miller, T.H., G.L. McEneff, R.J. Brown, S.F. Owen, N.R. Bury, and L.P. Barron, Pharmaceuticals in the freshwater invertebrate, *Gammarus pulex*, determined using pulverised liquid extraction, solid phase extraction and liquid chromatography–tandem mass spectrometry. *Science of The Total Environment*, 2015. **511**: p. 153-160.

31. Davidson, M.C., S.P.C. Ferreira, and M.A. Ure, Some sources of variability in application of the three-stage sequential extraction procedure recommended by BCR to industrially-contaminated soil. *Fresenius' Journal of Analytical Chemistry*. **363**(5): p. 446-451.

32. Taylor, P.J., Matrix effects: the Achilles heel of quantitative high-performance liquid chromatography–electrospray–tandem mass spectrometry. *Clinical Biochemistry*, 2005. **38**(4): p. 328-334.

33. Stokvis, E., H. Rosing, and J.H. Beijnen, Stable isotopically labeled internal standards in quantitative bioanalysis using liquid chromatography/mass spectrometry: necessity or not? *Rapid Communications in Mass Spectrometry*, 2005. **19**(3): p. 401-407.

34. Carter, L.J., R. Ashauer, J.J. Ryan, and A.B.A. Boxall, Minimised Bioconcentration Tests: A Useful Tool for Assessing Chemical Uptake into Terrestrial and Aquatic Invertebrates? *Environmental Science & Technology*, 2014. **48**(22): p. 13497-13503.

35. Springer, T.A., P.D. Guiney, H.O. Krueger, and M.J. Jaber, Assessment of an approach to estimating aquatic bioconcentration factors using

reduced sampling. *Environmental Toxicology and Chemistry*, 2008. **27**(11): p. 2271-2280.

36. Dearden, J.C. and N.M. Shinnawei, Improved prediction of fish bioconcentration factor of Hydrophobic Chemicals. *SAR and QSAR in Environmental Research*, 2004. **15**(5-6): p. 449-455.

37. Kaur, P. and K. Kim, Pharmacokinetics and brain uptake of diazepam after intravenous and intranasal administration in rats and rabbits. *International journal of pharmaceutics*, 2008. **364**(1): p. 27-35.

38. Sethia, S. and E. Squillante, Solid dispersion of carbamazepine in PVP K30 by conventional solvent evaporation and supercritical methods. *International journal of pharmaceutics*, 2004. **272**(1): p. 1-10.

39. Mullett, W.M. and J. Pawliszyn, Direct LC analysis of five benzodiazepines in human urine and plasma using an ADS restricted access extraction column. *Journal of pharmaceutical and biomedical analysis*, 2001. **26**(5): p. 899-908.

40. Scheytt, T., P. Mersmann, R. Lindstädt, and T. Heberer, 1-Octanol/Water Partition Coefficients of 5 Pharmaceuticals from Human Medical Care: Carbamazepine, Clofibric Acid, Diclofenac, Ibuprofen, and Propyphenazone. *Water, Air, and Soil Pollution*. **165**(1): p. 3-11.

41. Regnery, J., J. Barringer, A.D. Wing, C. Hoppe-Jones, J. Teerlink, and J.E. Drewes, Start-up performance of a full-scale riverbank filtration site regarding removal of DOC, nutrients, and trace organic chemicals. *Chemosphere*, 2015. **127**: p. 136-142.

42. Caldas, S.S., C.M. Bolzan, J.R. Guilherme, M.A.K. Silveira, A.L.V. Escarrone, and E.G. Primel, Determination of pharmaceuticals, personal care products, and pesticides in surface and treated waters: method

development and survey. *Environmental Science and Pollution Research*, 2013. **20**(8): p. 5855-5863.

43. Sousa, M.A., C. Gonçalves, E. Cunha, J. Hajšlová, and M.F. Alpendurada, Cleanup strategies and advantages in the determination of several therapeutic classes of pharmaceuticals in wastewater samples by SPE–LC–MS/MS. *Analytical and Bioanalytical Chemistry*, 2010. **399**(2): p. 807-822.

44. Commission, E., *Regulation (EC) No 1907/2006 of the European Parliament and of the Council of 18 December 2006 concerning the Registration, Evaluation, Authorisation and Restriction of Chemicals (REACH), establishing a European Chemicals Agency, amending Directive 1999/45/EC and repealing Council Regulation (EEC) No 793/93 and Commission Regulation (EC) No 1488/94 as well as Council Directive 76/769/EEC and Commission Directives 91/155/EEC, 93/67/EEC, 93/105/EC and 2000/21/EC.* 2006: Official Journal of the European Union. p. 1 - 849.

45. Barron, M.G., Bioconcentration. Will water-borne organic chemicals accumulate in aquatic animals? *Environmental Science & Technology*, 1990. **24**(11): p. 1612-1618.

46. Brown, J.N., N. Paxéus, L. Förlin, and D.G.J. Larsson, Variations in bioconcentration of human pharmaceuticals from sewage effluents into fish blood plasma. *Environmental Toxicology and Pharmacology*, 2007. **24**(3): p. 267-274.

47. Burkhard, L.P., Factors influencing the design of bioaccumulation factor and biota-sediment accumulation factor field studies. *Environmental Toxicology and Chemistry*, 2003. **22**(2): p. 351-360.

48. Gomez, E., M. Bachelot, C. Boillot, D. Munaron, S. Chiron, C. Casellas, and H. Fenet, Bioconcentration of two pharmaceuticals (benzodiazepines) and two personal care products (UV filters) in marine mussels (*Mytilus galloprovincialis*) under controlled laboratory conditions*. Environmental Science and Pollution Research*, 2012. **19**(7): p. 2561-2569.

49. Ding, J., G. Lu, J. Liu, H. Yang, and Y. Li, Uptake, depuration, and bioconcentration of two pharmaceuticals, roxithromycin and propranolol, in *Daphnia magna. Ecotoxicology and Environmental Safety*, 2016. **126**: p. 85-93.

50. Garcia, S.N., M. Foster, L.A. Constantine, and D.B. Huggett, Field and laboratory fish tissue accumulation of the anti-convulsant drug carbamazepine*. Ecotoxicology and Environmental Safety*, 2012. **84**: p. 207-211.

51. Hou, X., J. Shen, S. Zhang, H. Jiang, and J.R. Coats, Bioconcentration and Elimination of Sulfamethazine and Its Main Metabolite in Sturgeon (*Acipenser schrenkii*)*. Journal of Agricultural and Food Chemistry*, 2003. **51**(26): p. 7725-7729.

52. Gomez, C.F., L. Constantine, and D.B. Huggett, The influence of gill and liver metabolism on the predicted bioconcentration of three pharmaceuticals in fish*. Chemosphere*, 2010. **81**(10): p. 1189-1195.

53. Kumar, G.N. and S. Surapaneni, Role of drug metabolism in drug discovery and development*. Medicinal Research Reviews*, 2001. **21**(5): p. 397-411.

54. Snyder, M.J., Cytochrome P450 enzymes in aquatic invertebrates: recent advances and future directions*. Aquatic Toxicology*, 2000. **48**(4): p. 529-547.

55. Bletsou, A.A., J. Jeon, J. Hollender, E. Archontaki, and N.S. Thomaidis, Targeted and non-targeted liquid chromatography-mass spectrometric workflows for identification of transformation products of emerging pollutants in the aquatic environment. *TrAC Trends in Analytical Chemistry*, 2015. **66**: p. 32-44.

56. Jeon, J., D. Kurth, and J. Hollender, Biotransformation Pathways of Biocides and Pharmaceuticals in Freshwater Crustaceans Based on Structure Elucidation of Metabolites Using High Resolution Mass Spectrometry. *Chemical Research in Toxicology*, 2013. **26**(3): p. 313-324.

57. Pritchard, J.F., D.W. Schneck, and A.H. Hayes, Determination of propranolol and six metabolites in human urine by high-pressure liquid chromatography. *Journal of Chromatography B: Biomedical Sciences and Applications*, 1979. **162**(1): p. 47-58.

58. Kudriakova, T.B., L.A. Sirota, G.I. Rozova, and V.A. Gorkov, Autoinduction and steady-state pharmacokinetics of carbamazepine and its major metabolites. *British Journal of Clinical Pharmacology*, 1992. **33**(6): p. 611-615.

59. Boillot, C., M.J. Martinez Bueno, D. Munaron, M. Le Dreau, O. Mathieu, A. David, H. Fenet, C. Casellas, and E. Gomez, *In vivo* exposure of marine mussels to carbamazepine and 10-hydroxy-10,11-dihydro-carbamazepine: Bioconcentration and metabolization. *Science of The Total Environment*, 2015. **532**: p. 564-570.

60. WALLE, T. and T.E. GAFFNEY, Propranolol metabolism in man and dog: mass spectrometric identification of six new metabolites. *Journal of Pharmacology and Experimental Therapeutics*, 1972. **182**(1): p. 83-92.

61. Ikenaka, Y., M. Ishizaka, H. Eun, and Y. Miyabara, Glucose–sulfate conjugates as a new phase II metabolite formed by aquatic crustaceans. *Biochemical and Biophysical Research Communications*, 2007. **360**(2): p. 490-495.

62. Livingstone, D.R., The fate of organic xenobiotics in aquatic ecosystems: quantitative and qualitative differences in biotransformation by invertebrates and fish. *Comparative Biochemistry and Physiology Part A: Molecular & Integrative Physiology*, 1998. **120**(1): p. 43-49.

63. Umezawa, H., X.-P. Lee, Y. Arima, C. Hasegawa, A. Marumo, T. Kumazawa, and K. Sato, Determination of diazepam and its metabolites in human urine by liquid chromatography/tandem mass spectrometry using a hydrophilic polymer column. *Rapid Communications in Mass Spectrometry*, 2008. **22**(15): p. 2333-2341.

64. Reinach, B., G. de Sousa, P. Dostert, R. Ings, J. Gugenheim, and R. Rahmani, Comparative effects of rifabutin and rifampicin on cytochromes P450 and UDP-glucuronosyl-transferases expression in fresh and cryopreserved human hepatocytes. *Chemico-Biological Interactions*, 1999. **121**(1): p. 37-48.

65. Greenblatt, D.J., Clinical pharmacokinetics of oxazepam and lorazepam. *Clinical pharmacokinetics*, 1981. **6**(2): p. 89-105.

Chapter 5. The application of artificial neural networks to model sampling rates onto polar organic chemical integrative samplers.

5.1 Introduction

The contamination of the aquatic environment with various organic contaminants have been the focus on environmental monitoring campaigns, especially where chemical regulation has been introduced by the Water Framework Directive (WFD) and the EU Registration, Evaluation, Authorisation and Restriction of Chemicals (REACH) [1, 2]. Monitoring of the aquatic environments can often involve high frequency sampling using either grab or composite samples. Both, grab and composite sampling have limitations that they do not represent the temporal variation of contaminant concentrations. These types of sampling are also labour and resource intensive leading to difficulties in practical application of long term monitoring campaigns. In an alternative approach, passive sampling devices (PSDs) are being increasingly employed in the monitoring of aquatic environments. PSDs offer the capability to determine a time-integrated average of contaminant concentrations in surface and wastewaters over extended periods [3]. These sampling devices minimise sample preparation and allow *in situ* pre-concentration of analytes that increase sensitivities of analytical methods when compared with point-sampling [4].

Similar to the bioconcentration work, much of the early investigations focused on non-ionisable organic micropollutants. PSDs such as semi-permeable membrane devices (SPMDs) have been used for the determination of compounds such as organochlorines and other hydrophobic organic contaminants over the last three decades [5-8]. However, an emerging type of PSD is the polar organic chemical integrative sampler (POCIS) that can be used

to determine a range of chemically diverse compounds (polar and nonpolar), including pharmaceuticals [9-15]. Whilst these POCIS devices have several advantages, they also suffer from limitations when performing quantitative studies. The accuracy and reliability of experimental measurements in the estimation of sampling rates including the limited amount of reported R_s and the variability of R_s between experimental determinations are the main limitations of POCIS devices [9, 16, 17]. Furthermore, calibration of POCIS devices are also resource intensive leading to the possibility that *in silico* modelling approaches could overcome these limitations by predicting R_s without the need for experimental determinations.

A previous investigation by Stephen et al., [18] used Sherwood's correlation to the estimate the kinetic parameter, aqueous boundary layer mass transfer coefficient (k_f). This empirical approach led to errors ranging from +40 % to -20 % for a limited number of compounds. Alternative to empirical approaches, quantitative structure-property relationships (QSPR) methods for the parameterisation of desired output functions are becoming more frequently used in ecotoxicological fields [19-21]. The reason for the increased use is that the experimental determination of variables such as occurrence, fate and effects of contaminants is unfeasible due to the sheer volume of compounds available and with regulatory directives in place such as REACH [22]. QSPR models used a set of predictor variables to model a desired output function, where predictors are often molecular descriptors describing the topology, geometry or physico-chemical properties of a molecule [23]. These models can vary from simple regressions, or can be more complex involving non-linear functions such as those used by machine learning methods. One type of machine learning algorithm is an

artificial neural network (ANN) that have been used to predict log*P*, biosolid and soil sorption coefficients (K_D) and chromatographic t_R [24-30].

ANNs are comprised of several layers including an input layer (descriptors), hidden layer (nodes) and output layer (response). The molecular descriptors are related to the output layer by non-linear functions in the hidden layer, which can contain several interconnected layers and nodes. The residual errors are monitored and reduced iteratively by adjusting statistical weights attached to each descriptor and node in the hidden layer(s). ANN testing is split into a training subset where the model learns, a verification subset for supervised learning where the model knows the output but does not use them to learn and a test set where the output is hidden from the network. The predictive ability of the network is evaluated by the verification and test subsets. In addition, ANN can be used for mechanistic interpretation of important descriptors to the response variable leading to knowledge discovery of underlying processes. Therefore, the application of ANN to POCIS could greatly increase the applicability of PSDs in environmental monitoring studies through bypassing the need for laboratory or *in situ* calibrations.

The aim of this work was to investigate the applicability of ANNs to model and predict R_S for POCIS devices for a range of compounds including pharmaceuticals, herbicides, pesticides and steroid hormones. Successful application could suggest the applicability of ANNs to model more complex uptake processes such as bioconcentration. Objectives were to identify suitable molecular descriptors to build, train and test ANN models and then finally to externally validate the ANN model using new R_S data determined by laboratory calibrations.

5.2 Materials & methods

5.2.1 Reagents

All chemical reagents were of analytical grade purity (>98 %). Alprazolam, clonazepam, diazepam, flunitrazepam, lorazepam, midazolam, nitrazepam, and oxazepam were obtained from Nerliens Meszansky (Oslo, Norway). All reagents were prepared as stock solutions in methanol (MeOH) at a concentration of 100 µg mL^{-1} and stored at –20 ^{o}C. Standard mixtures were prepared for spiking in POCIS exposures, at 1 µg mL^{-1} and stored in MeOH at -20 ^{o}C. Diazepam-d_5 and oxazepam-d_5 were purchased at 100 ng mL^{-1} in MeOH (Nerliens Meszansky) and stored at -20 ^{o}C. Ultrapure water was obtained by the purification of demineralised water in an Elga Maxima Ultrapure Water purification system to a resistivity of ≥18 MΩ cm (Elga, Lane End, UK). Ammonium formate (≥99 %), HPLC grade formic acid, water, MeOH and MeCN were purchased from Sigma-Aldrich (Oslo, Norway). Sodium hydrogen carbonate was acquired from Merck (Oslo, Norway). Oasis HLB bulk sorbent was purchased from Waters (Oslo, Norway) and polyethersulfone (PES) membranes were acquired from VWR (Oslo, Norway)

5.2.2 POCIS assembly

POCIS were assembled in-house as detailed in previous investigations [31]. Briefly, 220 mg of Oasis HLB bulk sorbent was sandwiched between two PES membranes. The PES membranes were then placed between two stainless steel rings, with exposure area of 46 cm^2 which were then tightened together with nuts and bolts to physically compress and seal the sorbent inside the device. Once devices were assembled they were stored in air tight aluminium foil lined bags until required for exposure in the calibration experiment.

5.2.3 Laboratory calibration of sampling rates to test ANN generalisability

Sampling rates (L d^{-1}) were determined using a static renewal method over a 14-day exposure period and in a similar manner to those data generated in the literature which was used for ANN modelling in the present study [32]. Briefly, 3 L high-density polyethylene vessels were filled with ultra-pure water, pH adjusted to 7.6 with 20 mg L^{-1} $NaHCO_3$ and spiked with the mixture of respective compounds to expose the POCIS. Each vessel contained three POCIS devices for exposure to an aqueous-based standard mixture of 200 ng L^{-1} of each target compound (solvent <0.001 %). This standard solution was prepared and replaced daily in 3 L volumetric flasks to maintain the nominal concentration. Following this, all three POCIS were removed from each vessel at day 4, 7 and 14, rinsed with ultrapure water and frozen at -20^{o}C. A control vessel containing only fortified exposure medium (no POCIS) was also set up to monitor losses due to transformation, volatilisation and sorption. Exposure media in all vessels was agitated using a magnetic stirrer at 200 rpm during this time. Vessels were stored in the dark and Parafilm (VWR International, Oslo, Norway) was used as a seal to prevent evaporative losses. Water samples (1 mL) were taken from each beaker on day 4, 7 and 14 for analysis. Control POCIS devices (n=3) were also exposed in parallel (no analytes present) and extracted at the end of the experiment on day 14. All elements of the calibration experiment were performed in a temperature controlled room at 20^{o}C.

5.2.4 POCIS extraction

Frozen POCIS discs were carefully disassembled and the HLB sorbent material rinsed with ultra-pure water into an empty SPE cartridge housing

containing a single frit (20 µm pore size). Once all sorbent material was in the cartridge, the top frit was added and the sorbent bed washed with 5 mL of ultra-pure water. SPE tubes were dried under low vacuum for 30 min. Elution was carried out with 5 mL of MeOH in two stages and the eluate dried down under nitrogen (purity >99 %) at 35^{o}C for 40 min. The dried residue was then reconstituted in 0.5 mL of starting mobile phase.

5.2.5 Analytical and instrumental conditions

The analysis of the 8 benzodiazepines was performed on an Acquity UPLC System coupled to a Xevo™ G2-S QTof mass spectrometer (Waters, Milford, MA, USA) with an on-line two-dimensional method for both sample extraction and analyte separation. The pre-column used for the sample extraction was an Oasis HLB Direct Connect HP loading column (2.1 x 30 mm, 20 µm, Waters Corp). Mobile phase (isocratic 0.5 mL min^{-1}) for the loading pump (i.e. sample extraction) was 0.2 % (v/v) ammonium hydroxide and 10 % (v/v) methanol in water. Washing of the loading column was performed with 0.1 % formic acid in methanol (isocratic 1.5 mL min^{-1}) in between each injection. Analyte separation was performed on an Acquity UPLC BEH C_{18} column (1.7 µm, 50 x 2.1 mm) from Waters (Milford, MA, USA) at 50 °C. Gradient elution (0.6 mL min^{-1}) for analyte separation was with 0.1% (v/v) formic acid in water (phase A) and 0.1 % formic acid in methanol (phase B). Sample volumes of 200 µL were injected onto the loading column. After 1.5 minutes the flow direction was reversed and the analyte was back-flushed onto the chromatographic column for elution and separation. The chromatographic separation gradient was as follows: Initial conditions of 1% Phase A then a ramp to 98% Phase A over 3 minutes. Hold and wash at 98% Phase A for 1 minute before returning to initial conditions. MS data was acquired

in MS^E-mode where exact mass of precursor and fragment ions were collected over the range 50 – 600 *m/z*. The MS^E acquisition mode provides two traces; one with low energy (LE) for molecular ions; and one with high energy (HE) for generating fragment ions. Quantification was performed on the accurate molecular ion (see Table 5.1). Confirmation was via the identification of at least two-fragment ions using HE within an accuracy of 5 ppm and a retention time window within 2.5% error.

Table 5.1: LC-HRMS parameters for determination of benozdiazepines.

Compound	t_R (min)	Internal Standard	Precursor Ion (measured m/z)	Main Product Ion (m/z)
Oxazepam	3.26	Oxazepam-d5	287.05817	241.0528
Nitrazepam	3.26	Oxazepam-d5	282.08731	236.0945
Clonazepam	3.29	Oxazepam-d5	316.04833	270.0555
Lorazepam	3.29	Oxazepam-d5	321.0192	275.0138
Alprazolam	3.31	Oxazepam-d5	309.09014	281.0715
Midazolam	3.31	Diazepam-d5	326.08547	291.1167
Flunitrazepam	3.37	Diazepam-d5	314.09353	268.1007
Diazepam	3.58	Diazepam-d5	285.07891	193.0886

5.2.6 Estimation of R_s from laboratory calibrations

Determination of time-weighted average concentrations of compounds in the bulk phase require calibration of POCIS devices by estimating the R_s [33]. A first order single compartment model can be used to represent the uptake and elimination of a compound on the PSD shown by Equation 5.1.

$$C_s(t) = C_w \frac{k_1}{k_2} (1 - e^{-k_2 t}) \quad (5.1)$$

Where, $C_s(t)$ is the concentration of compound (ng g^{-1}) on the receiving phase (sorbent) at time, *t*. C_w is the concentration of compound in the water phase (ng L^{-1}), k_1 is the uptake rate constant of the compound onto the sorbent (L g^{-1} d^{-1}), k_2 is the elimination rate constant of the compound from the sorbent (d^{-1}) and t is the time (d). However, calibration requires that POCIS devices are operated

in the kinetic regime where the sorbent acts as a 'sink,' and thus k_2 is negligible, reducing the expression to Equation 5.2.

$$C_s(t) = C_w k_1 t \quad (5.2)$$

Equation 5.2 can be re-expressed to link the concentration in the sorbent to the concentration in the water phase using the sampling rate shown in Equation 5.3.

$$C_s = \frac{C_w R_s t}{M_s} \quad (5.3)$$

Where, R_s is the sampling rate (L d^{-1}) and M_s is the mass of sorbent used in the PSD (g). Thus, Equation 5.3 can be rearranged to determine the R_s when the C_s and C_w are measured.

5.2.7 Selection of datasets, molecular descriptors and ANN architecture

POCIS R_s data were compiled into a database from reported publications from 2007 to present. Of these, the sub-selection of R_s for ANN modelling was from two articles by Fauvelle et al. [32] and Morin et al. [34], which were generated using similar experimental conditions and gave the largest suitable dataset overall (Table 5.2). In total, n=73 compounds were used covering herbicides, pesticides, endocrine disrupting compounds and pharmaceuticals. Where duplicate compound R_s data existed, both values were removed entirely from the dataset. Simplified molecular input line entry system (SMILES) strings were generated from Chemspider (Royal Society of Chemistry, UK). From these strings n=185 molecular descriptors were generated from Parameter Client freeware (Virtual Computational Chemistry Laboratory, Munich, Germany) and an additional n=16 descriptors were from ACD labs Percepta software (Advanced Chemistry Development Laboratories, ON, Canada).

Table 5.2: Dataset used for modelling R_s with ANN

Case #	Compound	R_s (L d^{-1})	Case #	Compound	R_s (L d^{-1})
1	2,4 dichlorphenol	0.068	38	ketoprofen	0.118
2	2,4-D	0.045	39	lorazepam	0.205
3	3,4-dichloroaniline	0.241	40	MCPA	0.037
4	4-methylbenzylidene camphor	0.215	41	mecoprop	0.053
5	acebutolol	0.166	42	megesterol Acetate	0.265
6	acetochlor ESA	0.201	43	mesotrione	0.078
7	acetochlor OA	0.14	44	metazachlor	0.148
8	atenolol	0.025	45	methomyl	0.146
9	azoxystrobine	0.202	46	metolachlor	0.305
10	bentazon	0.16	47	metolachlor ESA	0.17
11	betaxolol	0.217	48	metolachlor OA	0.124
12	bezafibrate	0.146	49	metoprolol	0.195
13	bisphenol A	0.245	50	metoxuron	0.245
14	bisprolol	0.161	51	metsulfuron-Me	0.127
15	carbamazepine	0.188	52	nadolol	0.114
16	chlorfenvinphos	0.279	53	naproxen	0.084
17	chlorsulfuron	0.13	54	nicosulfuron	0.09
18	chlortoluron	0.264	55	oxazepam	0.226
19	DEA	0.286	56	oxprenolol	0.185
20	DET	0.421	57	prochloraz	0.208
21	DIA	0.323	58	progesterone	0.346
22	dichlorprop	0.053	59	propranolol	0.165
23	diclofenac	0.225	60	pyrimicarb	0.259
24	diclofop	0.085	61	simazine	0.216
25	dimetomorph	0.261	62	sotalol	0.036
26	estriol	0.185	63	sulcotrione	0.09
27	estrone	0.23	64	sulfamethoxazole	0.03
28	ethinylestradiol	0.26	65	t-butylphenol	0.398
29	fenoprop	0.113	66	terbuthylazine	0.321
30	furosemide	0.129	67	testosterone	0.28
31	ibuprofen	0.118	68	thiodicarb	0.21
32	iodosulfuron	0.187	69	timolol	0.21
33	ioxynil	0.343	70	t-Octylphenol	0.065
34	IPPMU	0.234	71	trimethoprim	0.162
35	IPPU	0.232	72	α-Estradiol	0.239
36	irgarol	0.287	73	β-Estradiol	0.221
37	isoproturon	0.207			

2,4-D – 2,4-dichlorophenoxyacetic acid, ESA - ethanesulfonic acid, OA – oxanilic acid, DEA – deethylatrazine, DET – diethyltryptamine, desisopropylatrazine, IPPMU – monodesmethyl-isoproturon, IPPU – didesmethyl-isoproturon, MCPA - 2-methyl-4-chlorophenoxyacetic acid, Me – methyl.

For optimisation of ANN models, two sub-selections from all 201 descriptors were investigated for comparative performance. The first was made by applying genetic selection algorithms which short-listed 24 molecular

descriptors for subsequent ANN modelling (see Table 5.3 for shortlisted descriptors). The second sub-set of molecular descriptors was chosen based on previous work for prediction of chromatographic retention time (16 molecular descriptors in total). For both datasets, several network types were tested for predictive ability using Trajan 6.0 neural network software (Trajan Software Ltd., Lincolnshire, UK), these included radial basis function (RBF), generalised regression neural networks (GRNNs) and multi-layer perceptrons (MLPs). The optimised network architecture was a four-layer MLP using two types of training algorithms, the first was back propagation (BP) and the second being conjugate gradient descent (GCD). The first and fourth layers were the inputs (using the set of descriptors previously used for chromatographic retention modelling) and outputs (R_S), respectively, and the second and third layers (hidden layers) contained 14 and 9 nodes, respectively. The subsets of cases presented to the retention time descriptor model (RTD) were split so that 51 compounds were used for training, 11 compounds for verification and 11 compounds for testing the networks (optimised). The genetic algorithm feature selected model (GSD) was split as 45:14:14 for the training, verification and test subsets, respectively (optimised).

Table 5.3: Molecular descriptors used to develop ANN models for R_s prediction

Descriptor	Definition
Ss	sum of Kier-Hall electrotopological states
Ms	mean electrotopologcial state
nAT	number of atoms
nBO	number of non-H bonds
ZM2	second Zagreb index
ICR	radial centric information index
ZM1V	first Zagreb index by valence vertex degrees
MAXDN	maximal electopological negative variation
SCBO	sum of conventional bond orders (H-depleted)
RBF	rotatable bond fraction
Snar	Narumi simple topological index (log function)
Xt	total structure connectivity index
Dz	Pogliani index
Pol	polarity number
MSD	mean square distance index (Balaban)
Har	Harary H index
RHyDP	reciprocal hyper-distance-path index
ww	hyper detour index
S0K	Kier symmetry index
SE1G	absolute eigenvalue sum on geometry matrix
Har2	square reciprocal distance sum index
ALogP	Ghose-Crippen octanol-water partition coefficient
AlogP2	squared Ghose-Crippen octanol-water partition coefficient
LogD	distribution coefficient
nTB	number of triple bonds
nC	number of carbon atoms
nO	number of oxygen atoms
nR04	number for 4-membered rings
nR05	number for 5-membered rings
nR06	number for 6-membered rings
nR07	number for7-membered rings
nR08	number for 8-membered rings
nR09	number for 9-membered rings
Ui	Unsaturation index
Hy	Hydrophilic factor
nBnz	number of benzene-like rings
MLOGP	Moriguchi octanol-water partition coefficient

5.3 Results & discussion

5.3.1 The application of ANNs to model R_S on POCIS

The selection of the molecular descriptors yielded two optimised models for the prediction of R_S onto POCIS. Feature selection using a genetic algorithm which shortlisted 24 descriptors for modelling the selected dataset, whereas 16 descriptors were selected from a previous investigation that used ANNs to predict t_R on a C_{18} reversed-phase chromatographic column [27, 28]. The genetic algorithm, similar to neural networks, was created to mimic a biological function (evolution). The algorithm converts the molecular descriptors into a binary string and maps them against an output function (R_S). These binary strings are used to produce 'progeny' strings that reduce the error associated with the output function. After feature selection, the descriptors were used for modelling where an optimised multilayer perceptron (MLP) was produced with a 24:17:14:1 architecture (GSD-model).

Regression analysis of the training, verification and test subsets showed an R^2 of 0.8800, 0.8694 and 0.8050, respectively for the GSD-model (Figure 5.1). The residual error for each subset was 0.084, 0.062 and 0.116, respectively. Overall, the model showed good predictive accuracy for 16 compounds with predicted R_S values within 20 % of the measured value. Larger inaccuracies were observed for two compounds, 2,4-dichlorophenoxyacetic acid (59 %) and timolol (31 %), in the verification subset. The test subset showed greater errors for compounds such as sotalol (80 %), acetochlor ethaneslufonic acid (40 %), diclofenac (39%) and suclotrione (38 %). The reason for this could be related to poor learning on the training set. For example, mesotrione has a large inaccuracy (59 %) which is a structurally similar compound to sulcotrione.

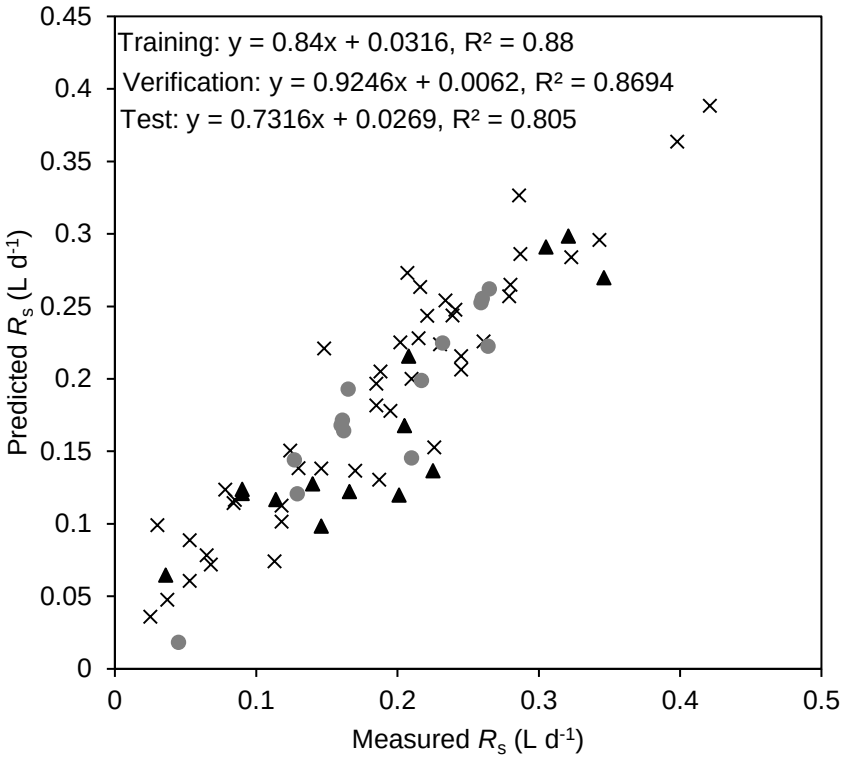

Figure 5.1: Regression analysis of the GSD model. Crosses represent training data, circles verification data and triangle test data.

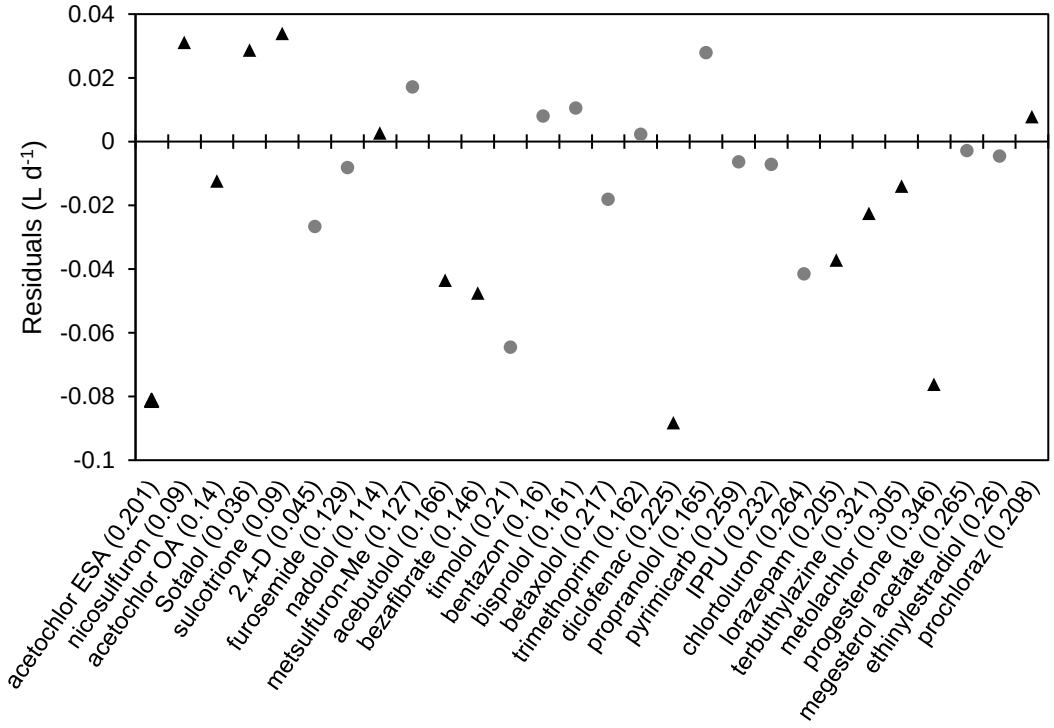

Figure 5.2: Raw residuals for the verification and test case predictions by the GSD-model. Circles represent verification data and triangles test data.

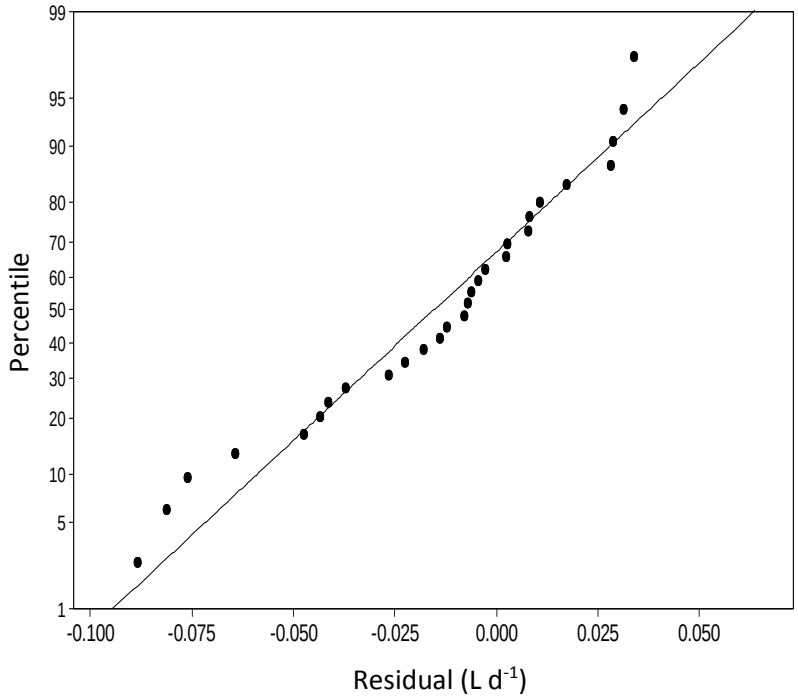

Figure 5.3: Normal probability plot of residuals in the GSD-model MLP. P-value = 0.205, alpha = 0.05.

The larger inaccuracies may also relate to sulfonated compounds where training was not optimal for these functional groups. The average predicted R_S values for both verification and test subset were within 19 % of the experimental value. The average absolute error for both subsets was 0.028 ± 0.025 L d^{-1} indicating that the model showed good predictive accuracy. The plot of residuals for model (Figure 5.2) indicated that there may have been some bias in the predictions as the data points were skewed towards the negative *y*-axis. A normal probability plot of the residuals (Figure 5.3) showed that they followed a normal distribution which suggested the data were not biased and the model was appropriated for predictive application.

In an alternative approach, descriptors used for retention time modelling were applied here to predict R_S [27, 28]. The POCIS sorbent material was Oasis HLB, a copolymer of divinylbenzene and N-vinylpyrrolidone that allows interaction with both polar and non-polar compounds. Previous authors have

demonstrated that sorption to HLB polymers is achieved predominantly through Van der Waals interaction attributed to the non-polar surface area of the sorbent (London dispersion forces) [35]. As retention on reversed-phase columns is also mainly attributable to dispersion forces. The use of previously validated descriptors for retention time modelling could offer a suitable approach R_S [36]. Figure 5.4 shows the correlation between predicted and measured R_S for the RTD-model.

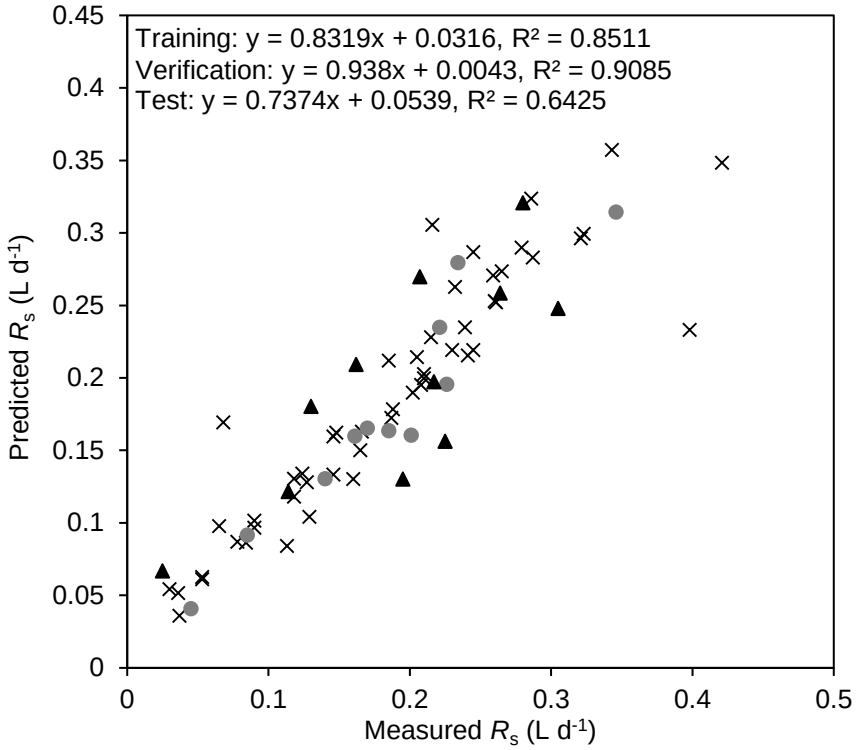

Figure 5.4: Regression analysis of the RTD-model. Crosses represent training data, circles verification data and triangle test data.

The model architecture was a four-layered MLP with a 16:15:9:1 structure. Overall the R^2 was 0.8511, 0.9085 and 0.6425 for the training, verification and test subsets respectively. The correlation coefficients showed slightly better fits for the verification subset in the RTD-model whereas the R^2 was better for the test subset in the GSD-model. However, it should be noted that the cases in each subsets were not identical as they were selected at random. The GSD-model also

contained a larger number of predictors that could lead to overfitting and reduce the generalisability of the model.

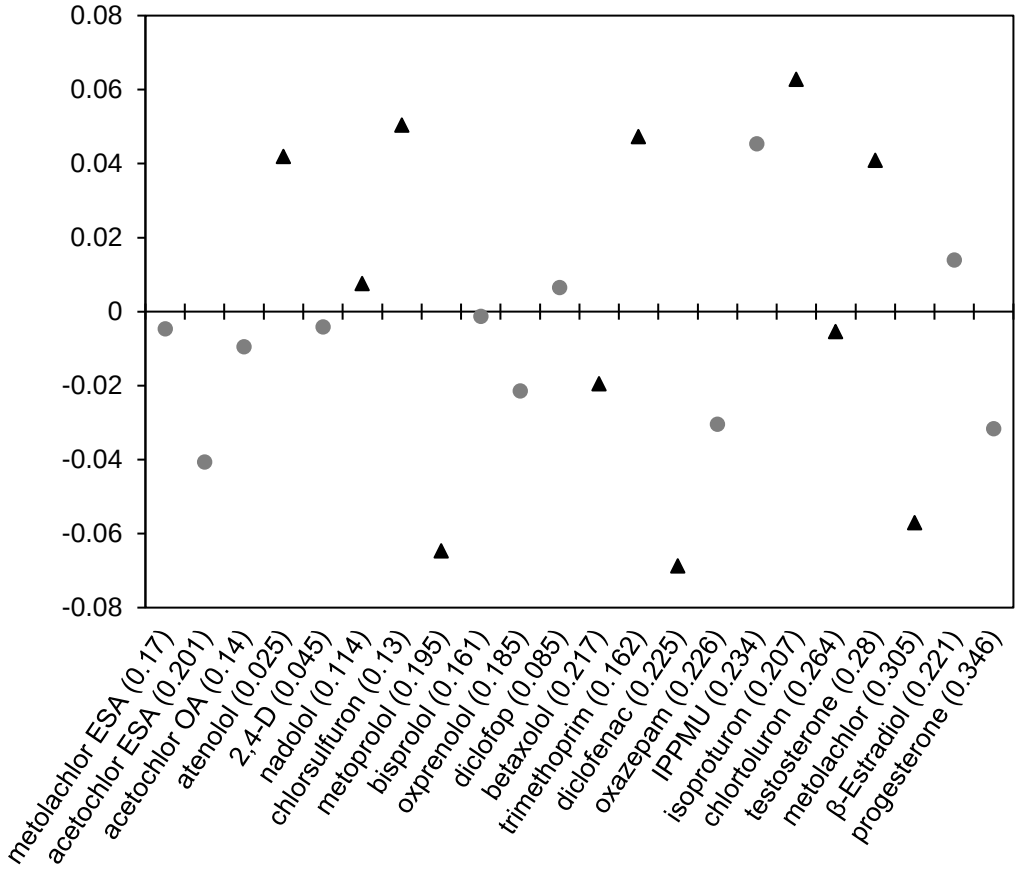

Figure 5.5: Raw residuals of the verification and test cases predicted by the RTD-model. Circles represent verification data and triangles test data.

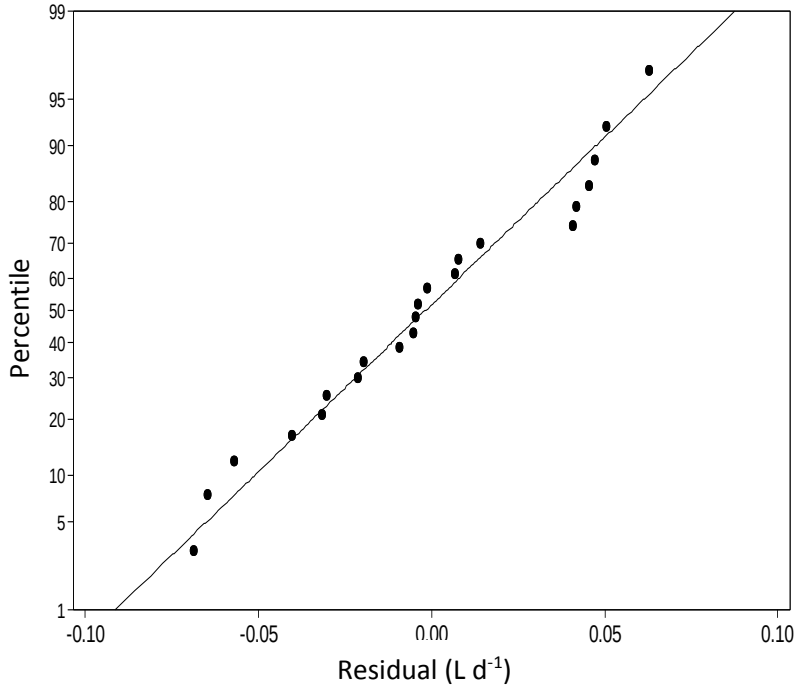

Figure 5.6: Normal probability plot of the raw residuals from the RTD-model. P-value = 0.492, alpha = 0.05.

The residual error was for the training, verification and test subsets were 0.092, 0.062 and 0.121, respectively. Similar to the previous model, the RTD-model showed good predictive accuracy with R_S values predicted within an average of 22 % of the measured value for both verification and test subsets. The plot of residuals showed that all data points were randomly distributed and a normal probability plot also showed the distribution was normal which indicated the molecular descriptors had appropriate explanatory power for the output function (Figure 5.5 & 5.6). The average predicted error was 0.031 ± 0.021 L d^{-1} showing that the average prediction was slightly worse for the RTD-model, whilst the variance was slightly better compared to the GSD-model. The verification subset showed no large errors with all predictions ≤ 20 % of the measured R_S value. The test subset showed two large errors which corresponded to the compound atenolol (168 %) and chlorsulfuron (39 %).

The lowest measured R_S was atenolol (0.025 L d^{-1}) in the RTD-model test subset which gave a relatively poor prediction of 0.067 L d^{-1}. A possible explanation was that the high polarity (log*P* = 0.34) of this molecule resulted in a poor prediction. However, in both residual plots (Figure 5.2 & 5.5) when compounds were ordered by log*D* no trend was observed with the predictive accuracy of the ANNs. The removal of atenolol, resulted in an average prediction error of 15 % for both the verification and test subsets. Whilst no trend was observed between log*D* and predictive accuracy, the HLB copolymer does not retain very polar compounds well (See Chapter 2, Section 2.3.3). Thus, experimentally determined R_S values may suffer from inaccurate estimations which could translate into poor predictive accuracy for modelling approaches. This highlights the importance of accurate and reliably measured data when used as an output function. Furthermore, the dataset used was from two separate

investigations that whilst had relatively similar experimental designs, inconsistencies between the laboratory estimations may also contribute to modelling inaccuracies. Overall, considering the potential inaccuracies of measured R_S data both models presented here, showed good predictive accuracy for application in passive sampling fields [9].

5.3.2 Interpretation of molecular descriptors used to model R_s data

A sensitivity analysis was performed to identify which molecular descriptors in either model were important to the prediction of R_S. Figure 5.7 shows the relative importance of each descriptor to the RTD- model. The top five descriptors were Log*D*, Mlog*P*, Alog*P* and n*Bnz* and n*C* which agreed with Bäuerlein et al., [35] that showed hydrophobicity and *pi-pi* bonds were dominant in sorption of compounds to HLB copolymers. Furthermore, these authors showed that hydrophilic surface area did show contribution to chemical sorption. Interestingly, the molecular descriptors *Hy*, n*O* were also relatively important to the network with error ratios of 1.108 and 1.2034, respectively. The descriptor *Hy* relates to the number of hydrophilic groups (such as hydroxyl and thiol) and n*O* is the number of oxygen atoms which due the electronegativity in organic compounds will contribute to dipole or induced dipole interactions. Other important descriptors were shown to be the n*TB* (1.2165), n*R05* (1.2041) and n*R09* (1.4544). The importance of the *n*-membered ring descriptors could be attributed to molecular size and thus could affect the diffusivity of molecules through the water boundary layer and PES membrane [37] or could lead to steric effects between the sorbent and sorbate. A previous investigation showed that size descriptors were important for predicting soil sorption coefficients in non-ionic organic pesticides [38].

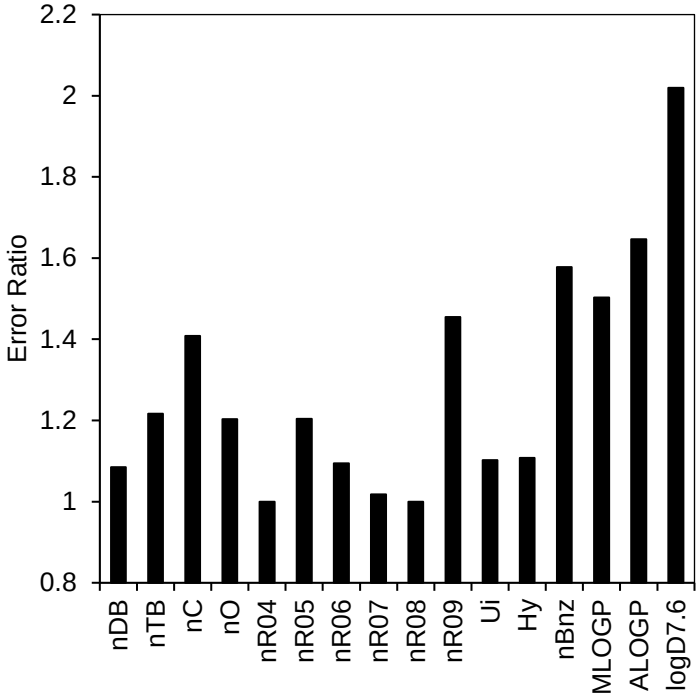

Figure 5.7: Sensitivity analysis of descriptors used in the chromatographic RTD-model. Error ratios > 1 indicate relative importance to the model where < 1 hinders the model accuracy.

The n*R04* descriptors and n*R08* descriptors showed an err

or ratio of 1, which indicated that they had no effect on the predictive accuracy of the model. The reason for this was that no cases in the dataset had 4- or 8-membered rings, thus, these were ignored by the ANN model. Log*D* was identified as the most important descriptor to the model. A plot of log*D* versus measured R_S revealed a weak correlation of R^2 = 0.3191 (Figure 5.8). The weak correlation suggested that log*D* does influence sampling rates but it is likely affected by several other factors related to either the molecule itself or experimental conditions such as temperature, pH and flow velocity.

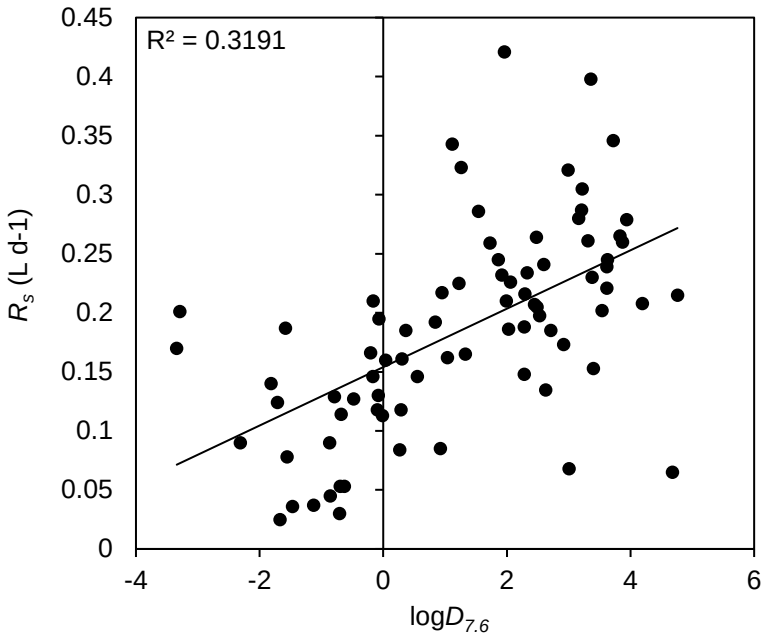

Figure 5.8: Correlation between logD descriptor (ACD labs) and sampling rate (R_s)

Furthermore, sorption of the compounds to the PES membrane can affect R_s, such that more hydrophobic compounds cross the membrane at a slower rate leading to an observed lag phase in the accumulation on the HLB sorbent [39]. A separate study showed a plot of log*D* versus R_s gave a correlation coefficient of R^2=0.37 (n=322 cases) [40]. The authors suggested that ionised species have lower R_s values than when compared to neutral forms [40, 41]. In addition to the sorption of the compounds to the passive sampler, diffusion is also an important mechanism in PSD uptake. Authors have suggested that diffusion is the sole factor governing sampling rates for PSDs [42]. The descriptors mentioned above whilst are involved with the HLB sorbent interactions, may also relate to diffusion processes due to the number of factors to affect diffusion such as dipole moments, polarizability, molecular size and electrostatic charge. Furthermore, diffusion-only uptake rates were determine using partition samplers such as silicone rubbers [42] whereas POCIS are an adsorption sampler and therefore suggests that sorption in addition to diffusion may affect sampling rates. This is demonstrated by the performance reference compound method where it has limited applicability to POCIS as the deuterated analogue is not released from the

sample due to adsorption on the copolymer [43-45]. However, the contribution from diffusion and adsorption processes which govern the sampling rate in adsorption samplers remains unclear. Thus, more studies are required to understand the mechanisms of diffusion across the water boundary layer/PES membrane and the sorption to the PES membrane/HLB sorbent.

Prediction of sampling rate may also be improved by including alternative descriptors such as diffusion coefficients. However, including descriptors such as these could lead to greater uncertainty as estimated of diffusion coefficients can be based off several different methods [46]. Furthermore, diffusion will be affected by several different environmental factors including hydrodynamic conditions that could not be accounted for in modelling approaches. Finally, including large numbers of descriptors to account for the number different mechanisms that govern sampling rates could be disadvantageous as it would limit the generalisability of the model to new data. A collinearity assessment of the descriptors was performed so that interpretations of individual predictors in the ANN were appropriate. Table 5.4 shows the correlation coefficients of each individual descriptor.

Table 5.4: Collinearity assessment using Pearson's correlation between molecular descriptors used in the RTD-model.

	nDB	nTB	nC	nO	nR04	nR05	nR06	nR07	nR08	nR09	Ui	Hy	nBnz	MLOGP	ALOGP	logD
nTB	-0.108															
nC	0.23	0.144														
nO	0.705	0.001	0.405													
nR04	*	*	*	*												
nR05	0.014	0.061	0.41	-0.094	*											
nR06	0.184	0.221	0.723	0.212	*	0.42										
nR07	0.082	-0.043	0.079	-0.127	*	-0.097	0.131									
nR08	*	*	*	*	*	*	*	*								
nR09	-0.012	0.148	0.509	-0.061	*	0.638	0.682	-0.073	*							
Ui	0.321	0.113	0.209	0.439	*	-0.175	0.254	0.269	*	-0.383						
Hy	-0.279	-0.11	-0.318	-0.116	*	-0.145	-0.169	0.039	*	-0.157	0.047					
nBnz	-0.018	0.125	0.332	0.204	*	-0.189	0.303	0.357	*	-0.205	0.671	-0.136				
MLOGP	-0.273	0.2	0.36	-0.361	*	0.308	0.477	0.129	*	0.43	-0.014	-0.455	0.296			
ALOGP	-0.276	0.218	0.387	-0.266	*	0.329	0.366	0.081	*	0.35	0.04	-0.53	0.371	0.898		
logD	-0.368	0.172	0.187	-0.607	*	0.384	0.306	0.113	*	0.405	-0.245	-0.275	-0.03	0.677	0.615	
Rs	-0.253	0.191	0.021	-0.487	*	0.134	0.114	0.046	*	0.263	-0.309	-0.051	-0.295	0.35	0.199	0.59

** Could not be calculated as molecules were absent of 4- and 8-membered rings.*

A threshold value for high collinearity has been given in the literature of R>0.7 [47]. In total, three descriptor pairs showed high collinearity that were n*DB*:n*O* (0.705), n*C*:n*R06* (0.723) and Mlog*P*:Alog*P* (0.898). These collinearities may be expected as the Ghose-Crippen log*P* and Moriguchi log*P* are measures of the octanol-water partition coefficient estimated by regression equations. Similarly, the number of double bonds would be correlated with the number of oxygen atoms, as oxygen atoms will often form double bonds in organic molecules (carbonyl groups). The consequence of collinearity is that the relative importance of the paired descriptors cannot be determined and therefore the sensitivity analysis can be limited. Whilst, collinearity may lead to descriptor redundancy it does not, however, affect predictive ability [48]. Thus, whilst it is more difficult to interpret, understanding of the underlying process will reduce the limitations associated with collinearity [47]. Furthermore, the focus of machine learning is primarily concerned with prediction rather than interpretation. As collinearity does not affect predictive accuracy, it is not of concern for the sole purpose of predicting R_S [48]. A sensitivity analysis was also performed for the GSD model. However, assessment of collinearity was very high for multiple molecular descriptors (Table 5.5) and thus interpretation of this model was not appropriate.

Table 5.5: Collinearity assessment of the GSD-model using Pearson's correlation.

	Ss	Ms	nAT	nBO	ZM2	ICR	ZM1V	MAXDN	SCBO	RBF	Snar	Xt	Dz	Pol	MSD	Har	RHyDp	ww	S0K	Seig	Har2	ALOGP	ALOGP2	LogD
Ms	0.402																							
nAT	0.57	-0.446																						
nBO	0.845	-0.115	0.845																					
ZM2	0.742	-0.174	0.798	0.958																				
ICR	0.613	-0.151	0.759	0.717	0.588																			
ZM1V	0.973	0.376	0.528	0.823	0.708	0.582																		
MAXDN	0.682	0.735	0.049	0.309	0.245	0.15	0.641																	
SCBO	0.913	0.079	0.695	0.961	0.9	0.637	0.907	0.448																
RBF	0.332	0.259	0.2	0.101	-0.142	0.465	0.329	0.305	0.112															
Snar	0.791	-0.181	0.829	0.991	0.956	0.704	0.776	0.235	0.948	0.049														
Xt	-0.773	0.191	-0.837	-0.96	-0.916	-0.726	-0.742	-0.274	-0.913	-0.118	-0.962													
Dz	0.933	0.059	0.801	0.966	0.868	0.745	0.917	0.454	0.956	0.299	0.933	-0.912												
Pol	0.735	-0.126	0.755	0.927	0.984	0.512	0.7	0.262	0.879	-0.187	0.921	-0.876	0.84											
MSD	-0.476	0.039	-0.387	-0.612	-0.742	0.026	-0.448	-0.262	-0.617	0.444	-0.61	0.608	-0.507	-0.795										
Har	0.843	-0.098	0.831	0.995	0.975	0.666	0.817	0.324	0.957	0.042	0.982	-0.945	0.954	0.956	-0.67									
RHyDp	0.845	-0.09	0.827	0.993	0.974	0.657	0.82	0.33	0.957	0.04	0.979	-0.941	0.953	0.958	-0.677	1								
ww	0.527	-0.283	0.699	0.813	0.891	0.49	0.514	0.02	0.724	-0.264	0.834	-0.718	0.688	0.891	-0.606	0.838	0.839							
S0K	0.885	-0.01	0.819	0.976	0.909	0.719	0.862	0.38	0.945	0.206	0.955	-0.909	0.977	0.885	-0.55	0.97	0.97	0.78						
Seig	0.606	-0.416	0.997	0.875	0.835	0.751	0.561	0.079	0.732	0.178	0.859	-0.861	0.828	0.796	-0.438	0.865	0.862	0.732	0.848					
Har2	0.869	-0.058	0.823	0.992	0.956	0.667	0.848	0.35	0.963	0.09	0.974	-0.927	0.968	0.94	-0.645	0.996	0.997	0.823	0.98	0.857				
ALOGP	-0.128	-0.393	0.097	0.146	0.236	0.002	-0.191	-0.402	0.1	-0.294	0.193	-0.185	-0.008	0.24	-0.298	0.153	0.15	0.257	0.075	0.125	0.12			
ALOGP2	-0.059	-0.355	0.128	0.196	0.282	0.056	-0.128	-0.347	0.155	-0.265	0.238	-0.223	0.051	0.276	-0.294	0.203	0.199	0.283	0.125	0.157	0.171	0.975		
LogD	-0.394	-0.664	0.035	-0.015	0.112	-0.135	-0.369	-0.675	-0.102	-0.525	0.046	0.022	-0.192	0.11	-0.168	0	-0.002	0.261	-0.122	0.043	-0.031	0.615	0.588	
Rs	-0.297	-0.511	0.051	-0.05	0.027	-0.242	-0.255	-0.446	-0.135	-0.337	-0.024	0.073	-0.145	0.041	-0.161	-0.031	-0.029	0.142	-0.097	0.052	-0.039	0.199	0.142	0.59

5.3.3 Comparison of measured with predicted R_S variance

As mentioned previously, the input data to the model has a strong influence on the accuracy of a models predictive ability. Measured R_S data can vary considerably when calibration studies are performed in the laboratory or field. Figure 5.9 showed the variance of experimental R_S and predicted R_S (across triplicate networks). The largest observed variance in the used dataset corresponded to the compound diclofop that had an RSD of (60 %, n=15 measurements) [32]. Furthermore, R_S can often vary by more than two-fold depending on the experimental design used for estimation [33]. Thus, measured R_S data are not true values and so the predictive ability of the ANN could be hindered.

The main difference between the two studies in the dataset, is that one method used static renewal whereas the second study used a flow-through system for R_S measurement [32, 34]. Whilst the experimental conditions were similar (pH, temperature) the difference between flow through and static renewal could result in significant difference between the R_S estimates. For example, 6 compounds that were included in both studies had variable R_S values where the absolute variance for all 6 compounds was 0.088 ±0.072 L day^{-1} between measurements. The average RSD of the measured R_S data was 11 % with a mean standard deviation of ± 0.017 L d^{-1}. The average variance across triplicate networks (RTD-based) for verification and test subsets was ± 0.023 L d^{-1} indicating that the variance across predictions was similar to that of experimentally determined data. In 45 % of all cases the standard deviation was lower through predictive estimation of R_S than compared with experimental estimation of R_S.

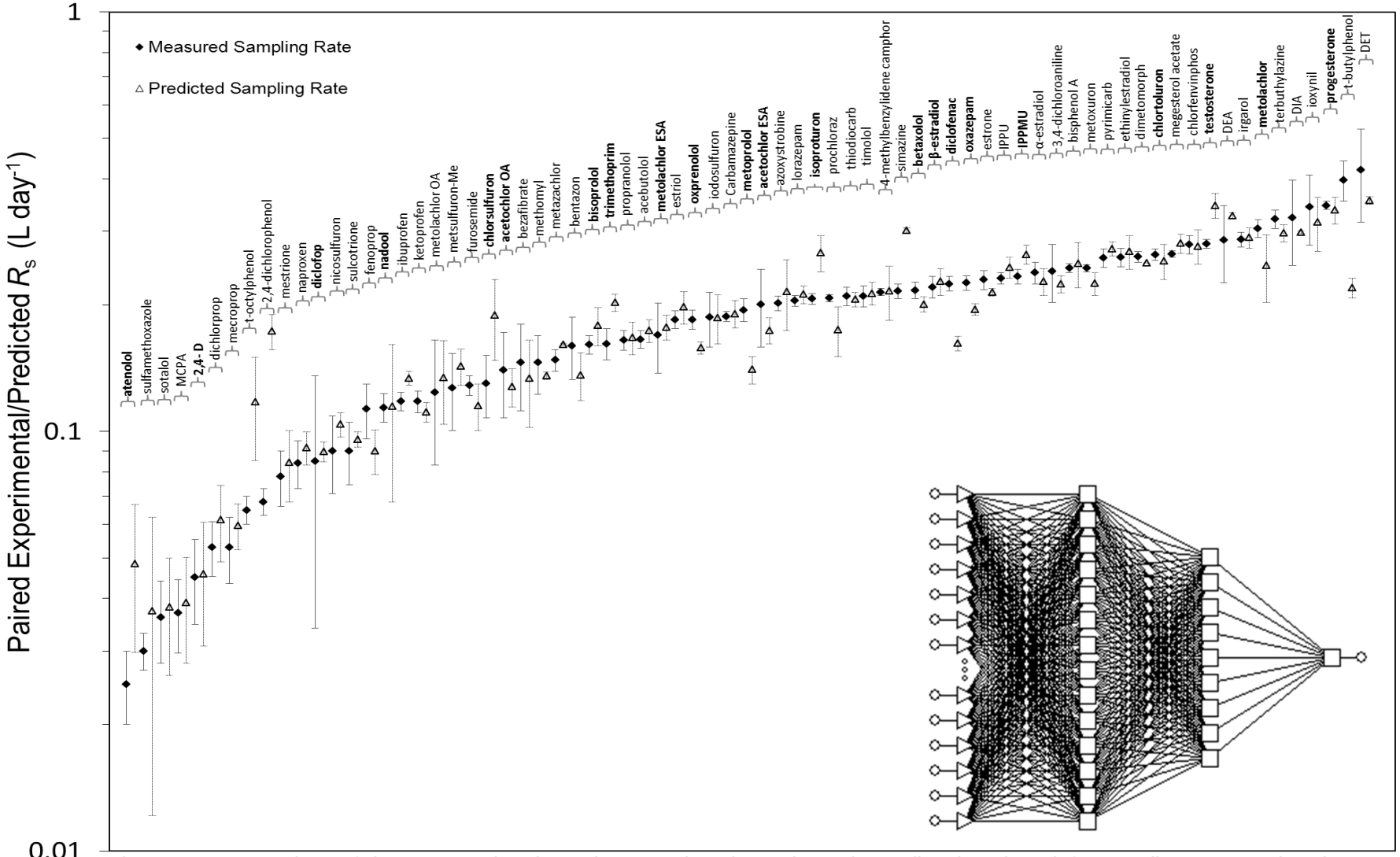

Figure 5.9: Comparison of the measured variance in R_s against the variance in predicted R_s (n=73) from replicate RPLC-descriptor networks (n=3). Inset: Optimised 16-14-9-1 ANN model built using RPLC-derived molecular descriptors.

In particular cases, the experimental deviation was large for compounds such as diclofop, DET, DIA and ioxynil. The larger variations in measured values could potentially be caused by several factors such as flow rate, temperature and pH. Consideration of ANN predictions where experimental variation is large is important for evaluating the model performance. For example, acetochlor ESA had a poor predictive accuracy however the variance of the predicted values (across triplicate networks) overlapped with the reported experimental variation. A review by Harman et al., suggests that due to the influence of several factors and the error associated with measurements, reported R_s data should be considered as an approximation [49].

A limitation in the passive sampling field for POCIS is that no standardised methods or guidelines for R_s determination exist. Therefore, comparison of literature values is difficult and the number of R_s data available for modelling applications is also limited. In the absence of these guidelines, the models shown herein offers similar accuracy and precision without the drawbacks of experimental determinations. Calibration experiments can take up to several weeks to several months that require large masses of reference material for flow-through or static renewals. Furthermore, *in situ* experiments require high frequency sampling to determine water concentration leading to high costs in analysis. Overall, experimental determination is resource and labour intensive in comparison to modelling approaches that avoid these factors.

5.3.4 Laboratory calibration of R_s and external validation of the ANN models

In addition to the 73 compound dataset, the R_s was determined for several benzodiazepines to be used as an external test set to validate the models. Eight compounds including nitrazepam, clonazepam, lorazepam, oxazepam,

alprazolam, flunitrazepam, diazepam and midazolam were exposed to POCIS devices in a static renewal method at the same temperature and pH used in the original dataset. The selection of structurally similar compounds for the external test set was deliberate to ensure that the model could accurately predict R_S for compounds with similar molecular descriptors. Pharmaceuticals in the bulk and receiving phase were determined by a 5-point standard calibration curve fortified with SIL-IS (Figure 5.10).

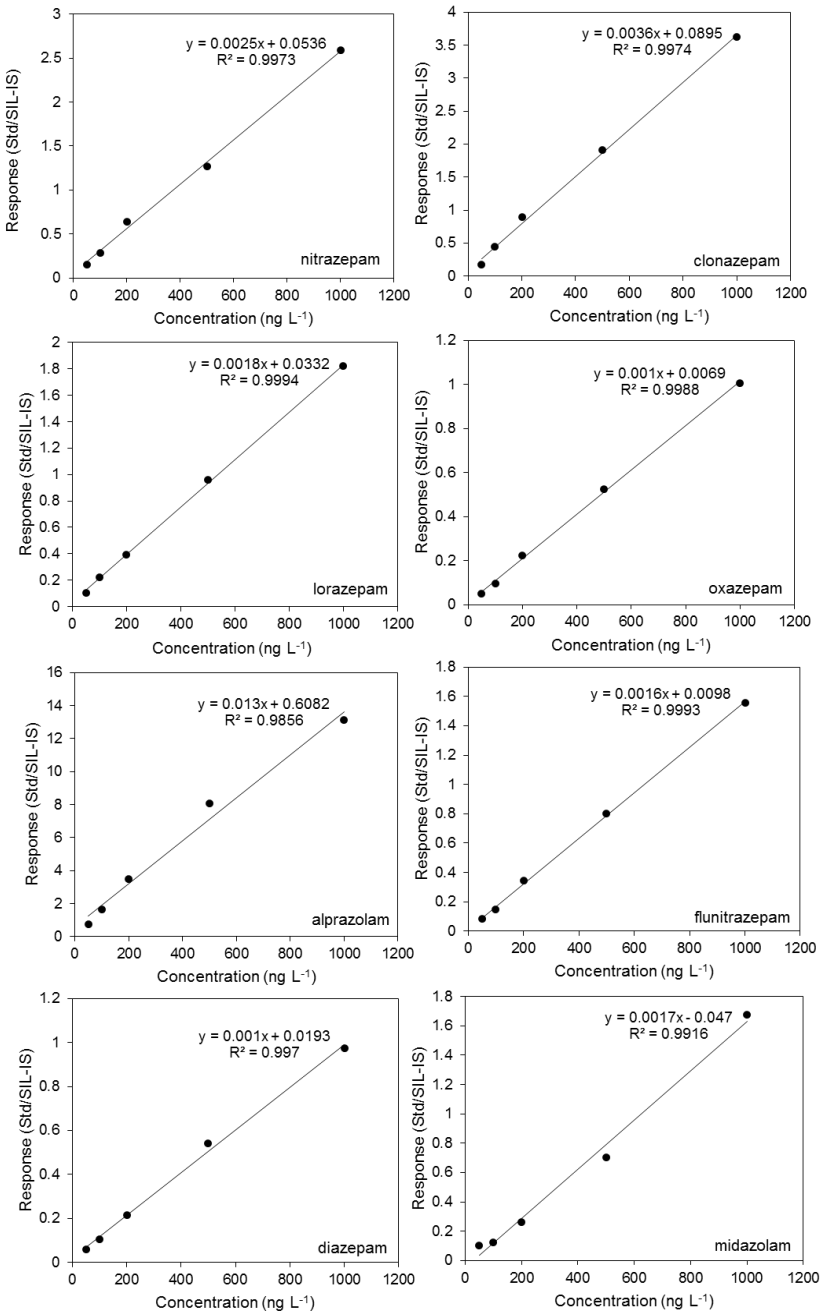

Figure 5.10: SIL-IS 5-point calibration curve (50- 1000 ng L^{-1}) for the eight benzodiazepine compounds. SIL-IS spiked at 1000 ng L^{-1}.

The linearity of the calibration curves for all compounds ranged from R^2=0.9856 – 0.9994 and was acceptable for quantification purposes. The pharmaceutical concentrations in the water phase were determined and are given in Table 5.6.

Table 5.6: Benzodiazepine concentration determined in the exposure media. Initial concentration was determined in triplicate (nominal concentration was 200 ng L^{-1}).

	ng L^{-1}				
Compound	Initial Concentration	SD	Day 4	Day 7	Day 14
Nitrazepam	193	4	137	142	138
Clonazepam	197	7	135	137	140
Lorazepam	195	8	136	137	134
Oxazepam	195	5	136	137	134
Alprazolam	190	4	138	128	133
Flunitrazepam	185	6	129	135	129
Diazepam	226	12	144	143	145
Midazolam	350	25	257	259	283

SD – standard deviation

The initial concentrations of the pharmaceuticals were all close to the nominal value of 200 ng L^{-1} with the exception of midazolam that was determined at an average of 350 ng L^{-1}. The concentrations of all pharmaceuticals declined by an average of 66 ng L^{-1} for samples that were taken at each time interval. The loss of compounds is attributed solely to the sorption of compound onto the receiving phase. A small degradation study (beaker with no POCIS devices) revealed that concentrations of compounds did not decrease over the two week period which indicated that degradation, volatilisation or sorption (to the beaker) were not significant. The total mass of pharmaceuticals accumulated by the POCIS devices were plotted over time in Figure 5.11.

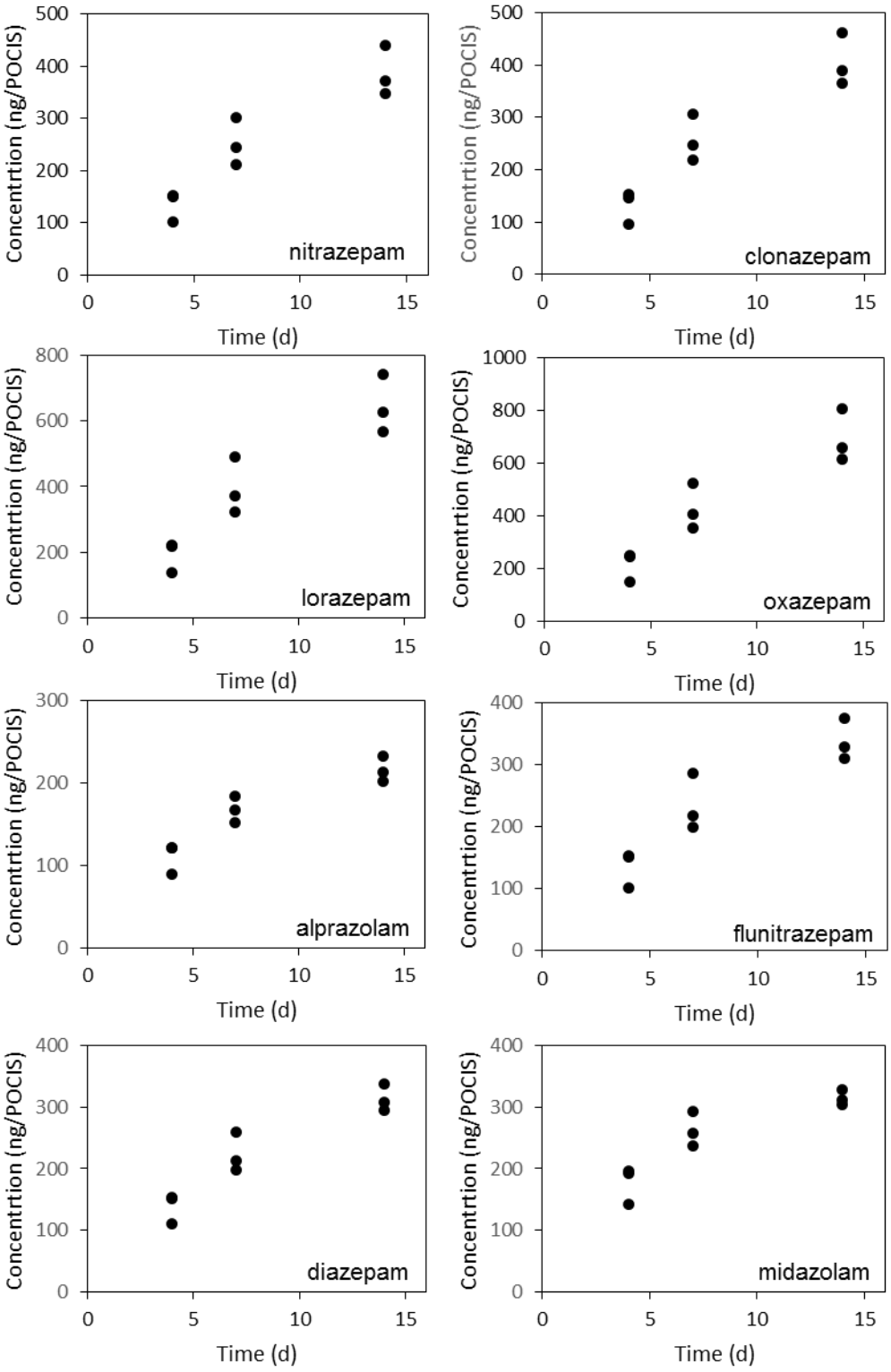

Figure 5.11: Accumulation of respective benzodiazepine compounds per POCIS device determined in triplicate across the two week exposure period.

The compounds alprazolam accumulated the least onto the HLB sorbent with an average total mass of 215 ng on day 14. Oxazepam accumulated the most with an average mass of 692 ng by the end of the exposure period. The deviation from linearity in the plots of sampler concentration versus time indicates that at 14 days these compounds are approaching the pseudo-linear phase where they are no longer suitable for calibration of R_S. Table 5.7 shows the estimated R_S for the eight benzodiazepines and the respective standard deviations.

Table 5.7: Estimated R_s values (n=9) determined by LC-HRMS for the benzodiazepine compounds

Compound	R_s (L d^{-1})	SD (L d^{-1})	RSD (%)
Nitrazepam	0.192	0.025	13
Clonazepam	0.198	0.025	13
Lorazepam	0.302	0.033	11
Oxazepam	0.327	0.038	12
Alprazolam	0.135	0.040	29
Flunitrazepam	0.186	0.036	19
Diazepam	0.173	0.039	23
Midazolam	0.153	0.053	35

The two compounds lorazepam and oxazepam were originally included the 73 compound dataset but were determined here to characterise the difference between the method of estimation used here and the method of Morin et al., [34]. The R_S determined by Morin et al., were lower by approximately 0.1 L d^{-1} for both compounds, indicating that the difference between static renewal and flow-through estimates can be considerable. The standard deviations for the six compounds varied from ±0.024 to ±0.055 L d^{-1}. The average RSD for all compounds was 20 ±6 % (flunitrazepam: 19 %; clonazepam: 13 %; nitrazepam: 13 %; midazolam: 23%; diazepam: 23 %; and alprazolam: 29 %). The R_S for these six benzodiazepines were predicted by both optimised ANNs (RTD- and GSD-models) and are shown in Figure 5.12.

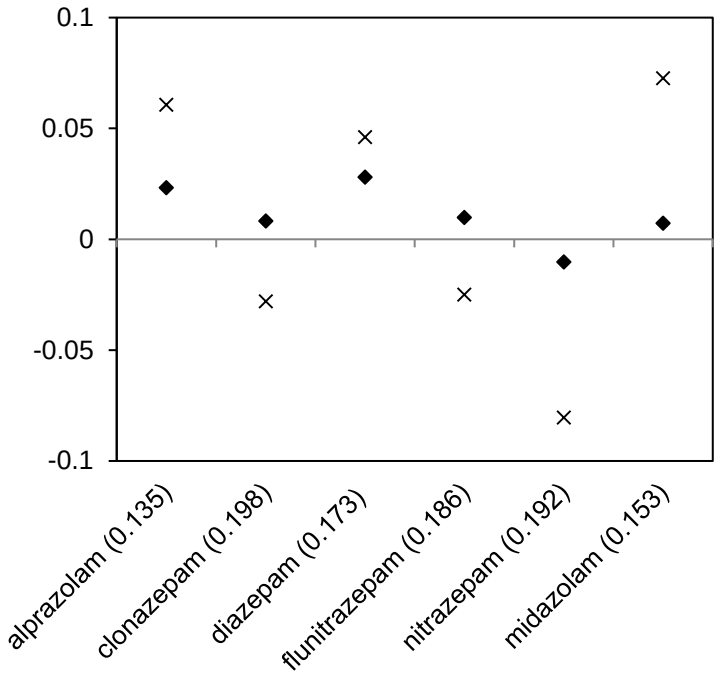

Figure 5.12: Raw residuals of predicted R_S for the benzodiazepine test set by both the GSD-model and RTD-model. Parentheses show measured R_S value.

Each model had only one benzodiazepine present in the training subset, which for the RTD-model was lorazepam and for the GSD-model was oxazepam. The RTD-model showed very good predictive accuracy for the external test set with all compounds predicted within 20 % of thee measured value. The two largest errors were predicted for diazepam and alprazolam with a 16 % and 17 % inaccuracy, respectively. However, these two compounds also had the largest RSDs which indicated the variance could affect the predictive ability of the ANN. The remaining four benzodiazepines were ≤ 5 % inaccurate. The average absolute error for all compounds was 0.0145 L d^{-1}. In comparison, the GSD-model performed more poorly. The average absolute prediction error was ~3 fold higher at 0.0437 L d^{-1}. The two largest errors corresponded to nitrazepam and midazolam that were 37 % and 43 % inaccurate, respectively.

The poorer predictive accuracy of the GSD-model might have been related to the higher number of descriptors used by this model. As model complexity increases, either by the number of predictors or the number of nodes in the

hidden layer, the potential for overfitting and a reduction in the generalisability of the model becomes greater. These predictions show that ANN modelling approaches are accurate enough for practical use in passive sampling works. Furthermore, future applications could be used for *in situ* calibrations where laboratory R_S estimates do not translate well into field R_S due to matrix effects and cases where R_S cannot be determined in the field [40]. *In silico* approaches offer a viable alternative to overcome these limitations. PSDs also have the potential to be used as a surrogate for biota in the determination of BCFs. Previous studies have demonstrated that concentrations in PSD devices are correlated with concentrations accumulated in benthic polychaetes and terrestrial *Eisenia fetidia* [50, 51]. However, in contrast to estimating R_S data, the PSDs are allowed to reach equilibrium where the elimination rate from the device is no longer negligible.

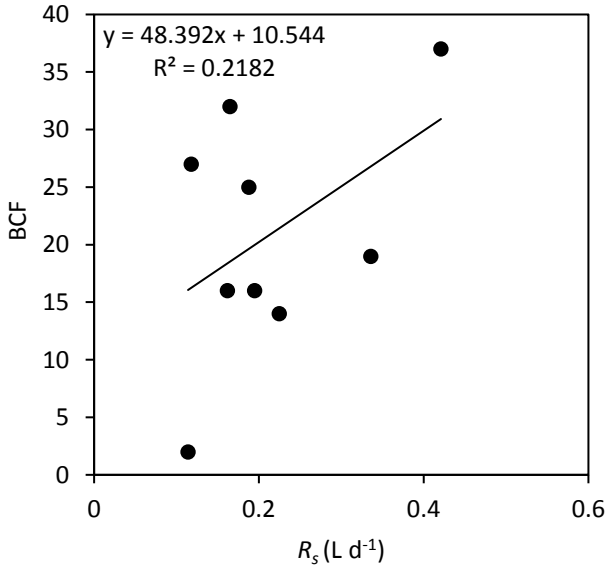

Figure 5.13: Correlation of R_S and BCF for selected pharmaceutical compounds including; propranolol, metoprolol, warfarin, diclofenac, trimethoprim, ibuprofen, sulfamethazine, temazepam and carbamazepine. BCFs determined in Chapter 3 & 4, R_S data taken from [14, 15, 34].

R_S is very weakly correlated with BCF in biota (Figure 5.13). The reason for the poor correlation is that R_S is estimated when the device acts as a 'sink,' thus elimination is negligible. The equilibrated concentrations could be used to predict bioaccumulation potentials. However, whilst PSDs would take into account environmental influence (pH, flow, temperature etc.) and physico-chemical properties of the compounds, they would fail to take into account biotic factors (i.e. metabolism, growth, respiration etc.). Thus, effects of elimination and uptake where carrier mediated uptake is also involved, will likely mean that bioaccumulation would be overestimated. The biomimetic properties of PSDs to be used as surrogates for BCF estimations is understudied and further works would be need to fully evaluate the potential of this application. Nevertheless, *in silico* modelling could offer a powerful approach in this type of application.

5.3.5 The limitations of ANNs to modelling selected outputs

As mentioned previously, model complexity can affect the performance of the models predictive ability. Complexity in the form of number of descriptors, hidden layers or hidden nodes all lead to an overfitting phenomenon. Overfitting occurs where models have learned the data they are given and have lost generalisability to make new predictions. However, increased model complexity, in some cases, is required to adequately model a desired response. With these cases, it essential to have a larger number of observations than inputs, otherwise models can lack any degrees of freedom thus losing statistical power to reject or accept a model. An initial ANN model was developed for the estimation of R_S (previous to the two models presented above). The model was feature selected using a forward selection algorithm, which down-selected 55 descriptors. Figure 5.14 shows the 55:20:11:1 MLP, with R^2 of 0.7168, 0.9721 and 0.9303 for the

training, verification and test subset, respectively. The verification and test subset showed excellent predictive accuracy whilst the training subset showed relatively lower accuracy. The training of the network can be halted early, when the verification error is low and the training error can remain relatively high. This is a form of regularisation known as early stopping which is used to prevent overfitting of ANNs [52].

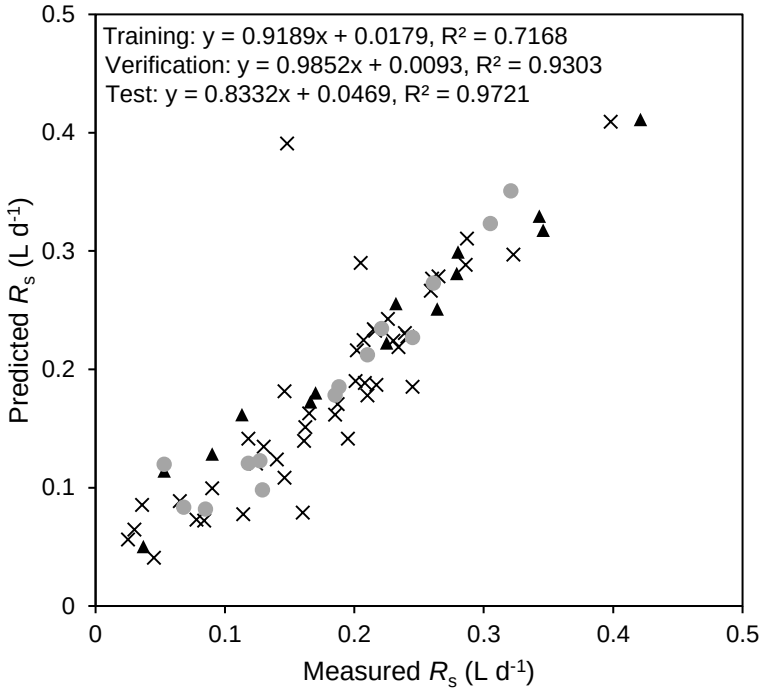

Figure 5.14: Regression analysis of predicted versus measured R_s data by a forward selected, 55:20:11:1 MLP. Crosses represent training data, circles varication data and triangles test data.

However, the model shown in Figure 5.14 was applied to the external test set of benzodiazepines which resulted in extremely poor predictions of ≥ 0.6 L d^{-1}, ~3-fold larger than the measured R_s values. The poor predictive accuracy suggested that the model was over-fitted to the data and had lost generalisability. Even with the use of regularisation, overfitting can remain problematic with the use of ANNs and likely resulted from the combination of a high number of input descriptors and small dataset used (n=73 cases). To overcome potential

problems caused by overfitting it is essential that developed models are well tested with large datasets to ensure machine learning approaches are reliable when it comes to ‘real world’ application.

5.4 Conclusions

Two ANN models were developed to predict R_s from POCIS samplers for a range of chemically diverse compounds covering pharmaceutical, pesticides, herbicides and endocrine disruptors. A feature selection algorithm known as a genetic algorithm was used to down-select descriptors relevant to prediction of R_s. This model showed good predictive accuracy for the verification and test subsets with an average absolute error of 0.028 ± 0.025 L d^{-1}. An alternative approach used previously selected descriptors for chromatographic retention time prediction. This model again showed similar predictive ability with an average absolute error of 0.031 ± 0.021 L d^{-1}. The interpretation of the models showed that descriptors related to hydrophobicity and Van der Waals interactions were dominant which agreed with previous mechanistic studies on sorption to POCIS sorbents. However, mechanistic interpretation of ANNs should be treated cautiously where collinearity or multicollinearity exists between input descriptors. Both optimised models were externally validated using laboratory calibrated R_s for several benzodiazepines. The calibrations showed that due to the decrease in water concentrations of static renewals, the use of flow-through calibrations allow more reliable and accurate determination of R_s. The model using retention descriptors showed better predictive performance in comparison to the model selected using the genetic algorithm. ANNs gave comparable reliability in predictions to experimental determinations of R_s showing that they have a good potential to be used for this application. However, the number of cases was

relatively small and so future works would need to be performed with a larger datasets to fully assess the applicability of ANNs in R_S prediction. Although, without established standardised guidelines and methods of R_S measurement the application of modelling approaches are likely to be hindered. Finally, critical evaluation of ANNs is of key importance as models can be prone to overfitting available data leading to poor predictive ability. With this in mind the performance of ANNs discussed in this Chapter suggest that ANNs could be used to model more complex uptake processes such as the accumulation potential of contaminants in biota.

5.5 References

1. *Commission, E., Regulation (EC) No 1907/2006 of the European Parliament and of the Council of 18 December 2006 concerning the Registration, Evaluation, Authorisation and Restriction of Chemicals (REACH), establishing a European Chemicals Agency, amending Directive 1999/45/EC and repealing Council Regulation (EEC) No 793/93 and Commission Regulation (EC) No 1488/94 as well as Council Directive 76/769/EEC and Commission Directives 91/155/EEC, 93/67/EEC, 93/105/EC and 2000/21/EC. Official Journal of the European Union, 2006.* ***L396****: p. 1 - 849.*
2. *Commission, E., Directive 2000/60/EC of the European Parliament and of the Council of 23 October 2000 establishing a framework for Community action in the field of water policy Official Journal of the European Union, 2000.* ***L327****: p. 1 - 73.*
3. *Vrana, B., I.J. Allan, R. Greenwood, G.A. Mills, E. Dominiak, K. Svensson, J. Knutsson, and G. Morrison, Passive sampling techniques for monitoring pollutants in water. TrAC Trends in Analytical Chemistry, 2005.* ***24****(10): p. 845-868.*
4. *Miège, C., H. Budzinski, R. Jacquet, C. Soulier, T. Pelte, and M. Coquery, Polar organic chemical integrative sampler (POCIS): application for monitoring organic micropollutants in wastewater effluent and surface water. Journal of Environmental Monitoring, 2012.* ***14****(2): p. 626-635.*
5. *Prest, H.F., B.J. Richardson, L.A. Jacobson, J. Vedder, and M. Martin, Monitoring organochlorines with semi-permeable membrane devices (SPMDs) and mussels (Mytilus edulis) in Corio Bay, Victoria, Australia. Marine Pollution Bulletin, 1995.* ***30****(8): p. 543-554.*

6. *Gale, R.W., Three-Compartment Model for Contaminant Accumulation by Semipermeable Membrane Devices. Environmental Science & Technology, 1998.* ***32****(15): p. 2292-2300.*

7. *Huckins, J.N., J.D. Petty, C.E. Orazio, J.A. Lebo, R.C. Clark, V.L. Gibson, W.R. Gala, and K.R. Echols, Determination of Uptake Kinetics (Sampling Rates) by Lipid-Containing Semipermeable Membrane Devices (SPMDs) for Polycyclic Aromatic Hydrocarbons (PAHs) in Water. Environmental Science & Technology, 1999.* ***33****(21): p. 3918-3923.*

8. *Bartkow, M.E., K. Booij, K.E. Kennedy, J.F. Müller, and D.W. Hawker, Passive air sampling theory for semivolatile organic compounds. Chemosphere, 2005.* ***60****(2): p. 170-176.*

9. *Harman, C., M. Reid, and K.V. Thomas, In Situ Calibration of a Passive Sampling Device for Selected Illicit Drugs and Their Metabolites in Wastewater, And Subsequent Year-Long Assessment of Community Drug Usage. Environmental Science & Technology, 2011.* ***45****(13): p. 5676-5682.*

10. *Bailly, E., Y. Levi, and S. Karolak, Calibration and field evaluation of polar organic chemical integrative sampler (POCIS) for monitoring pharmaceuticals in hospital wastewater. Environmental Pollution, 2013.* ***174****: p. 100-105.*

11. *Fedorova, G., T. Randak, O. Golovko, V. Kodes, K. Grabicova, and R. Grabic, A passive sampling method for detecting analgesics, psycholeptics, antidepressants and illicit drugs in aquatic environments in the Czech Republic. Science of The Total Environment, 2014.* ***487****: p. 681-687.*

12. *Martínez Bueno, M.J., S. Herrera, D. Munaron, C. Boillot, H. Fenet, S. Chiron, and E. Gómez, POCIS passive samplers as a monitoring tool for pharmaceutical residues and their transformation products in marine environment. Environmental Science and Pollution Research, 2014: p. 1-11.*

13. *Baz-Lomba, J.A., M.J. Reid, and K.V. Thomas, Target and suspect screening of psychoactive substances in sewage-based samples by UHPLC-QTOF. Analytica Chimica Acta, 2016.* ***914****: p. 81-90.*

14. *Bayen, S., H. Zhang, M.M. Desai, S.K. Ooi, and B.C. Kelly, Occurrence and distribution of pharmaceutically active and endocrine disrupting compounds in Singapore's marine environment: influence of hydrodynamics and physical–chemical properties. Environmental pollution, 2013.* ***182****: p. 1-8.*

15. *MacLeod, S.L., E.L. McClure, and C.S. Wong, Laboratory calibration and field deployment of the polar organic chemical integrative sampler for pharmaceuticals and personal care products in wastewater and surface water. Environmental Toxicology and Chemistry, 2007.* ***26****(12): p. 2517-2529.*

16. *Mazzella, N., S. Lissalde, S. Moreira, F. Delmas, P. Mazellier, and J.N. Huckins, Evaluation of the Use of Performance Reference Compounds in an Oasis-HLB Adsorbent Based Passive Sampler for Improving Water Concentration Estimates of Polar Herbicides in Freshwater. Environmental Science & Technology, 2010.* ***44****(5): p. 1713-1719.*

17. *Harman, C., I.J. Allan, and P.S. Bäuerlein, The Challenge of Exposure Correction for Polar Passive Samplers ・ The PRC and the POCIS. Environmental Science & Technology, 2011.* ***45****(21): p. 9120-9121.*

18. *Stephens, B.S., A. Kapernick, G. Eaglesham, and J. Mueller, Aquatic Passive Sampling of Herbicides on Naked Particle Loaded Membranes: Accelerated Measurement and Empirical Estimation of Kinetic Parameters. Environmental Science & Technology, 2005.* ***39****(22): p. 8891-8897.*

19. *Niu, J., L. Wang, and Z. Yang, QSPRs on photodegradation half-lives of atmospheric chlorinated polycyclic aromatic hydrocarbons associated with particulates. Ecotoxicology and Environmental Safety, 2007.* ***66****(2): p. 272-277.*

20. *Samghani, K. and M. HosseinFatemi, Developing a support vector machine based QSPR model for prediction of half-life of some herbicides. Ecotoxicology and Environmental Safety, 2016.* ***129****: p. 10-15.*

21. *Xu, H.-Y., J.-W. Zou, J.-Q. Min, and W. Wang, A quantitative structure–property relationship analysis of soot–water partition coefficients for persistent organic pollutants. Ecotoxicology and Environmental Safety, 2012.* ***80****: p. 1-5.*

22. *Sahlin, U., Uncertainty in QSAR predictions. Altern Lab Anim, 2013.* ***41****(1): p. 111-25.*

23. *Katritzky, A.R., V.S. Lobanov, and M. Karelson, QSPR: the correlation and quantitative prediction of chemical and physical properties from structure. Chem. Soc. Rev., 1995.* ***24****(4): p. 279-287.*

24. *Bade, R., L. Bijlsma, J.V. Sancho, and F. Hernández, Critical evaluation of a simple retention time predictor based on LogKow as a complementary tool in the identification of emerging contaminants in water. Talanta, 2015.* ***139****: p. 143-149.*

25. *Barron, L. and G. McEneff, Gradient liquid chromatographic retention time prediction for suspect screening applications: A critical assessment of a generalised artificial neural network-based approach across ten multi-residue reversed-phase analytical methods Talanta, 2015.* ***In Press****.*

26. *Luan, F., C. Xue, R. Zhang, C. Zhao, M. Liu, Z. Hu, and B. Fan, Prediction of retention time of a variety of volatile organic compounds based on the heuristic method and support vector machine. Analytica Chimica Acta, 2005.* ***537****(1–2): p. 101-110.*

27. *Miller, T.H., A. Musenga, D.A. Cowan, and L.P. Barron, Prediction of Chromatographic Retention Time in High-Resolution Anti-Doping Screening Data Using Artificial Neural Networks. Analytical Chemistry, 2013.* ***85****(21): p. 10330-10337.*

28. *Munro, K., T.H. Miller, C.P.B. Martins, A.M. Edge, D.A. Cowan, and L.P. Barron, Artificial neural network modelling of pharmaceutical residue retention times in wastewater extracts using gradient liquid chromatography-high resolution mass spectrometry data. Journal of Chromatography A, 2015.* ***1396****: p. 34-44.*

29. *Padmanabhan, J., R. Parthasarathi, V. Subramanian, and P.K. Chattaraj, QSPR models for polychlorinated biphenyls: n-Octanol/water partition coefficient. Bioorganic & Medicinal Chemistry, 2006.* ***14****(4): p. 1021-1028.*

30. *Barron, L., J. Havel, M. Purcell, M. Szpak, B. Kelleher, and B. Paull, Predicting sorption of pharmaceuticals and personal care products onto soil and digested sludge using artificial neural networks. Analyst, 2009.* ***134****(4): p. 663-670.*

31. *Alvarez, D.A., J.D. Petty, J.N. Huckins, T.L. Jones-Lepp, D.T. Getting, J.P. Goddard, and S.E. Manahan, Development of a passive, in situ,*

integrative sampler for hydrophilic organic contaminants in aquatic environments. Environmental Toxicology and Chemistry, 2004. ***23****(7): p. 1640-1648.*

32. *Fauvelle, V., N. Mazzella, F. Delmas, K. Madarassou, M. Eon, and H. Budzinski, Use of Mixed-Mode Ion Exchange Sorbent for the Passive Sampling of Organic Acids by Polar Organic Chemical Integrative Sampler (POCIS). Environmental Science & Technology, 2012.* ***46****(24): p. 13344-13353.*
33. *Morin, N., C. Miège, M. Coquery, and J. Randon, Chemical calibration, performance, validation and applications of the polar organic chemical integrative sampler (POCIS) in aquatic environments. TrAC Trends in Analytical Chemistry, 2012.* ***36****: p. 144-175.*
34. *Morin, N., J. Camilleri, C. Cren-Olivé, M. Coquery, and C. Miège, Determination of uptake kinetics and sampling rates for 56 organic micropollutants using "pharmaceutical" POCIS. Talanta, 2013.* ***109****: p. 61-73.*
35. *Bäuerlein, P.S., J.E. Mansell, T.L. ter Laak, and P. de Voogt, Sorption Behavior of Charged and Neutral Polar Organic Compounds on Solid Phase Extraction Materials: Which Functional Group Governs Sorption? Environmental Science & Technology, 2012.* ***46****(2): p. 954-961.*
36. *Dorsey, J.G. and K.A. Dill, The molecular mechanism of retention in reversed-phase liquid chromatography. Chemical Reviews, 1989.* ***89****(2): p. 331-346.*
37. *Vrana, B., G.A. Mills, M. Kotterman, P. Leonards, K. Booij, and R. Greenwood, Modelling and field application of the Chemcatcher passive*

sampler calibration data for the monitoring of hydrophobic organic pollutants in water. Environmental Pollution, 2007. ***145****(3): p. 895-904.*

38. *Gramatica, P., M. Corradi, and V. Consonni, Modelling and prediction of soil sorption coefficients of non-ionic organic pesticides by molecular descriptors. Chemosphere, 2000.* ***41****(5): p. 763-777.*
39. *Vermeirssen, E.L.M., C. Dietschweiler, B.I. Escher, J. van der Voet, and J. Hollender, Transfer Kinetics of Polar Organic Compounds over Polyethersulfone Membranes in the Passive Samplers Pocis and Chemcatcher. Environmental Science & Technology, 2012.* ***46****(12): p. 6759-6766.*
40. *Moschet, C., E.L.M. Vermeirssen, H. Singer, C. Stamm, and J. Hollender, Evaluation of in-situ calibration of Chemcatcher passive samplers for 322 micropollutants in agricultural and urban affected rivers. Water Research, 2015.* ***71****: p. 306-317.*
41. *Li, H., P.A. Helm, G. Paterson, and C.D. Metcalfe, The effects of dissolved organic matter and pH on sampling rates for polar organic chemical integrative samplers (POCIS). Chemosphere, 2011.* ***83****(3): p. 271-280.*
42. *Rusina, T.P., F. Smedes, M. Koblizkova, and J. Klanova, Calibration of silicone rubber passive samplers: experimental and modeled relations between sampling rate and compound properties. Environmental science & technology, 2009.* ***44****(1): p. 362-367.*
43. *Alvarez, D.A., J.D. Petty, J.N. Huckins, T.L. Jones‐Lepp, D.T. Getting, J.P. Goddard, and S.E. Manahan, Development of a passive, in situ, integrative sampler for hydrophilic organic contaminants in aquatic environments. Environmental Toxicology and Chemistry, 2004.* ***23****(7): p. 1640-1648.*

44. *La-Scalea, M.A., C.M.S. Menezes, and E.I. Ferreira, Molecular volume calculation using AM1 semi-empirical method toward diffusion coefficients and electrophoretic mobility estimates in aqueous solution. Journal of Molecular Structure: THEOCHEM, 2005.* ***730****(1): p. 111-120.*

45. *Gharagheizi, F., Determination of diffusion coefficient of organic compounds in water using a simple molecular-based method. Industrial & Engineering Chemistry Research, 2012.* ***51****(6): p. 2797-2803.*

46. *Schramke, J.A., S.F. Murphy, W.J. Doucette, and W.D. Hintze, Prediction of aqueous diffusion coefficients for organic compounds at 25 C. Chemosphere, 1999.* ***38****(10): p. 2381-2406.*

47. *Dormann, C.F., J. Elith, S. Bacher, C. Buchmann, G. Carl, G. Carré, J.R.G. Marquéz, B. Gruber, B. Lafourcade, P.J. Leitão, T. Münkemüller, C. McClean, P.E. Osborne, B. Reineking, B. Schröder, A.K. Skidmore, D. Zurell, and S. Lautenbach, Collinearity: a review of methods to deal with it and a simulation study evaluating their performance. Ecography, 2013.* ***36****(1): p. 27-46.*

48. *Mason, C.H. and W.D. Perreault Jr, Collinearity, power, and interpretation of multiple regression analysis. Journal of marketing research, 1991: p. 268-280.*

49. *Harman, C., I.J. Allan, and E.L.M. Vermeirssen, Calibration and use of the polar organic chemical integrative sampler—a critical review. Environmental Toxicology and Chemistry, 2012.* ***31****(12): p. 2724-2738.*

50. *Vinturella, A.E., R.M. Burgess, B.A. Coull, K.M. Thompson, and J.P. Shine, Use of Passive Samplers To Mimic Uptake of Polycyclic Aromatic Hydrocarbons by Benthic Polychaetes. Environmental Science & Technology, 2004.* ***38****(4): p. 1154-1160.*

51. *Gomez-Eyles, J.L., M.T.O. Jonker, M.E. Hodson, and C.D. Collins, Passive Samplers Provide a Better Prediction of PAH Bioaccumulation in Earthworms and Plant Roots than Exhaustive, Mild Solvent, and Cyclodextrin Extractions. Environmental Science & Technology, 2012.* ***46****(2): p. 962-969.*

52. *Almeida, J.S., Predictive non-linear modeling of complex data by artificial neural networks. Current opinion in biotechnology, 2002.* ***13****(1): p. 72-76.*

Chapter 6. The application of artificial neural networks to predict bioconcentration factors in fish and invertebrates.

6.1 Introduction

Under REACH [1], guidelines are provided for industries to ensure that their products do not cause adverse harm to human health and the environment. The document states that any chemical manufactured in quantities exceeding 10 tonnes per annum must submit a chemical safety assessment (CSA).

For environmental risk assessment, one important part of the CSA is the persistent, bioaccumulative and toxicity (PBT) assessment that evaluates the potential of environmental harm using a weight-of-evidence approach. This approach involves the use of all available data to assess a chemical substance. The bioaccumulation potential is important to characterise the risk posed to biota and this part of the assessment uses all available screening and assessment information to identify whether a chemical will reach the thresholds of bioaccumulative (B) or very bioacccumlative (vB). Screening information comprises relatively simple data such as physico-chemical properties including molecular size, log*P*, octanol solubility, biomimetic properties of passive sampling devices and read-across information [2].

Part of the read-across information is the use of quantitative structure activity relationships (QSAR) which use a set of molecular descriptors to predict an output such as a BCF. Read-across can either have a biological or chemical basis [3], where chemical read-across uses similarity of chemical classes to predict endpoints. In the biological read-across the conservation of molecular targets and receptors across different taxonomic groups are used to predict endpoints. QSARs are becoming increasingly popular within ecotoxicological

fields as they represent, perhaps, the only realistically feasible scenario to assess the environmental risk of the several thousand chemicals that are available on the market [4]. In addition, QSAR models can be used to reduce or replace animal testing as suggested by the replacement, reduction and refinement (3Rs) framework which is an important ethical consideration [5].

QSARs can be relatively simple using linear regression methods or can become increasingly complex where *in silico* approaches are used such as artificial neural networks (ANNs) or support vector machines (SVMs). Many early models were linear regressions that were trained on a relatively small number of hydrophobic organic contaminants [6-8]. As hydrophobicity has been demonstrated to be a predominant factor in bioaccumulation these models often used log*P* as an input descriptor which fails to take into account the ionisation state of a compound [9]. Other input descriptors used have covered molecular size, topological and geometrical descriptors among others [10-12]. More recently, authors have used more complex QSARs involving artificial neural networks and support vector machines to model BCFs [13-15]. However, the ANN modelling used in only one investigation showed predictions for only 9 test compounds. Therefore, the reliability of the model for BCF estimation is low. The use of complex models has been demonstrated to offer better predictive accuracy than simpler models [16]. In addition to the use of QSARs for PBT assessments, modelling approaches can allow mechanistic interpretation of descriptors to identify factors that influence the bioaccumulation potential. QSAR models have only been applied to modelling fish BCF data (e.g. *Cyprinus carpio*, *Pimephales promelas* and *Onchorhynchus mykiss*) due to the availability of relatively large datasets [9]. However, the potential for bioaccumulation in other taxa such as the invertebrates is not well characterised. At present, invertebrate models do not

exist as there is a lack of available data. The development of QSAR models for the invertebrate phyla would begin to address the knowledge gap relate to the bioaccumulation potential in these animals.

The aim of this work was to evaluate the use of ANNs to model BCFs in both fish and invertebrates. A large fish dataset would be used to develop ANN models to improve the accuracy and reliability in comparison to the single ANN study reported in the literature. The developed model would be applied to invertebrate BCF data reported from the literature and in previous chapters to assess the potential for cross-species prediction. In addition, separate modelling was applied to the available invertebrate data. Finally, the developed models would be used to interpret the importance of molecular descriptors to the ability of a chemical to accumulate in biota. The presented work aims to improve on currently available QSAR models for environmental risk assessment.

6.2 Materials & methods

6.2.1 Descriptor generation

Bioconcentration factors were collated from the Cefic LRI project EC07 in collaboration with EURAS which established the BCF gold standard database across multiple fish species and is freely available at http://ambit.sourceforge.net/euras/. BCFs were down-selected to reduce variability between different species and experimental conditions. The BCFs were selected from the fish species *Cyprinus carpio* reported from the Chemicals Inspection and Testing Institute (now the Chemicals Evaluation and Research Institute, CERI). Using the single reference source resulted in the largest sample (*n*=353) of BCFs for modelling purposes. The reported BCFs covered compounds including pigments, pesticides, fungicides, herbicides, insecticides, polyaromatic

hydrocarbons (PAHs) and polychlorinated biphenyls (PCBs). Other compounds within the dataset included organochlorines, nitroaromatics, alkylphenols, aromatic hydrocarbons, organosulfurs and organotins which generally serve as precursors to compounds such as pesticides, plastic polymers, detergents, dyes etc., during industrial synthesis. The invertebrate BCF dataset (*n=34*) was collated from literature reported data [17-20] and from data presented in Chapters 3 & 4 for the species *G. pulex*. The dataset was comprised of only pharmaceuticals and pesticides. Simplified molecular input line entry system (SMILES) strings were generated from Chemspider (Royal Society of Chemistry, UK). Molecular descriptors as inputs for BCF prediction were generated from SMILES strings using Parameter Client (Virtual Computational Chemistry Laboratory, Munich, Germany), and ACD Labs Percepta (Advanced Chemistry Development Laboratories, ON, Canada). A total of 180 descriptors were generated which covered constitutional, topological, geometrical and physico-chemical properties.

6.2.2 Descriptor selection for ANN modelling

Descriptors were down-selected using three different algorithms, the first of which was a genetic algorithm (GA). The GA converts descriptors into binary strings which are then used in a generalised neural network (GRNN) to assess accuracy. The GA parameters were set to population = 500, generations = 250, mutation rate = 0.1 and cross-over rate = 1. The remaining two selection methods were part of stepwise regression which included a forwards selection algorithm (FA) and backwards selection algorithm (BA). The FA is initialised by including only 1 descriptor to model the desired output, then a second descriptor is included and a new model is assessed for performance. This process is repeated until

model performance does not improve. In BA the opposite occurs, initially all descriptors are included and then single descriptors are sequentially removed until model performance no longer increases. The feature selection algorithms used a GRNN to monitor the error associated with the selected descriptors, where descriptor sets were optimised when the error showed no improvement. The use of GRNN for descriptor selection is that they are very fast and require minimal processing power.

6.2.3 Model design and optimisation

Several neural network types were tested Trajan 6.0 neural network software (Trajan Software Ltd., Lincolnshire, UK) which included generalised regression neural networks (GRNN), radial basis function networks (RBF) and multilayer perceptrons (MLP). From the down-selection of input descriptors the optimised model was a four layer MLP which used two training algorithms referred to as back propagation (BP) and conjugate gradient descent (CGD). The first and fourth layers were the inputs (molecular descriptors) and outputs (log*BCF*), respectively. The second and third layers (hidden layers) contained 10 and 8 nodes, respectively. Regularisation was performed with the use of early stopping to prevent over-training of the dataset. The subsets of cases presented to the neural networks were split so that 242 compounds were used for training (70 %), 55 compounds for verification (15 %) and 55 compounds for testing the networks (15 %).

6.3 Results & discussion

6.3.1 Feature selection of descriptors to predict bioconcentration factors

The reduction in the number of descriptors is desirable so that inputs which are not associated to the selected output are removed. The decrease in the number of inputs can also prevent over-fitting of the model, allowing better generalisablity. In particular, for applications when the sample size is relatively low. The first stepwise algorithm was FA that was used in two successions. The descriptor sets that were down-selected were then used to model logBCF (Figure 6.1). These models showed the lowest errors across the verification and test subsets and gave overall R^2 of 0.7448 and 0.7629 between the successive rounds of forwards selection.

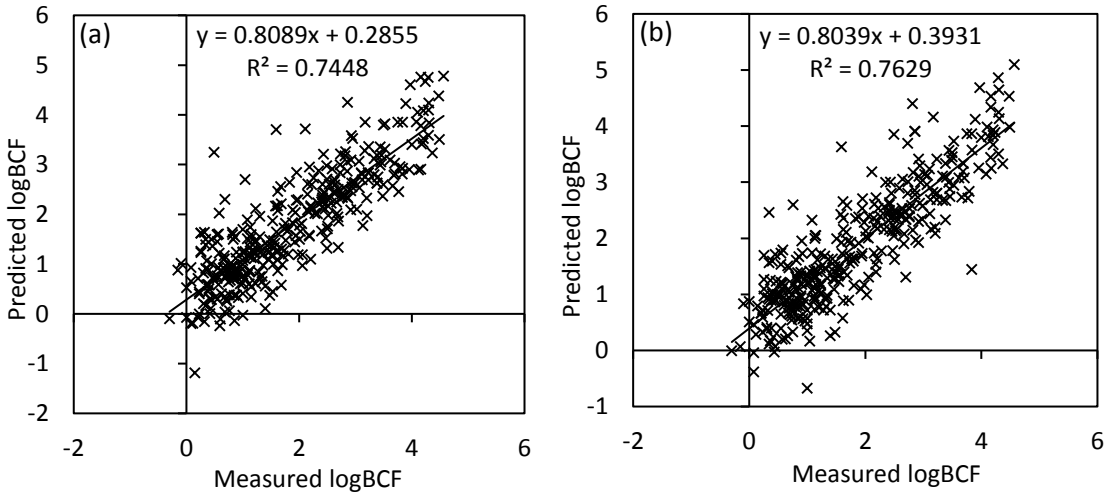

Figure 6.1: Regression analysis of the forwards selected MLPs. (a) first round of forwards selection, (b) second round of forwards selection.

In a second approach, BA was used in two successive rounds of feature selection. Training of the BA selected descriptor sets also produced identical models to those shown in Figure 6.1, indicating that either FA or BA selection did not differ during feature selection and selected the same descriptors. Training length of the descriptor set was increased to observe any possible improvement

in the performance of the models. The training resulted in an improved model shown in Figure 6.2, which had an overall R^2 of 0.7825 which showed a slight improvement to the models presented in Figure 6.1. The individual subsets had an R^2 of 0.8377 for the training set, 0.738 for the verification set and 0.6025 for the test set. As an alternative to stepwise feature selection, a GA was used to down select the number of independent variables. The again successive rounds of the GA was used to reduce the number of descriptors to a total of 66 from 180. Further rounds of the GA did not reduce the number of descriptors below this.

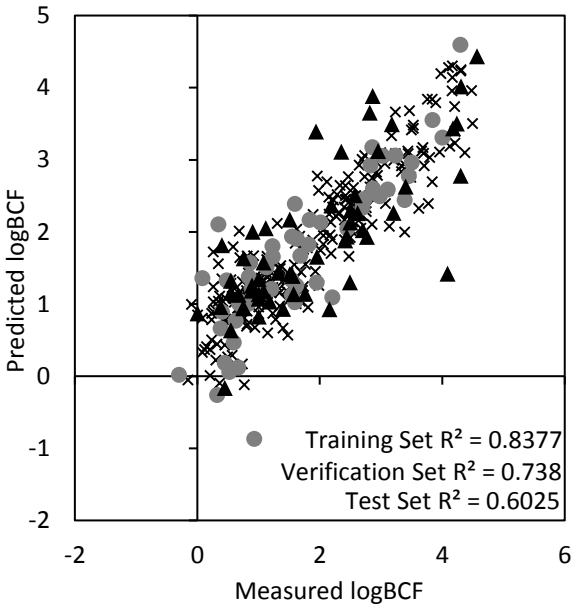

Figure 6.2: Regression analysis of the backwards selected MLP. Crosses represent the training set, circles represent the verification subset and triangles represent the test set.

Training of MLPs using the GA-descriptors resulted in a model (Figure 6.3) that showed similar performance to the BA-model previously shown. The individual R^2 for the training, verification and test subsets were 0.8765, 0.7734 and 0.5967, respectively. The root mean square error (RMSE) of the verification and test set was 0.55 and 0.70, respectively. The model showed good improvement in the training set whereas the verification and test subset were

slightly worse than when compared to the BA-model. Whilst the performance of the models were relatively good the number of descriptors remained high and further optimisation of the models was required. The descriptor set selected by the GA was used in further modelling attempts. The reason for the selection of the GA descriptor set over the stepwise algorithms is that GA finds a solution from multiple points in the population of the descriptors whereas stepwise will find a solution from a single starting point and therefore can get stuck in local minima.

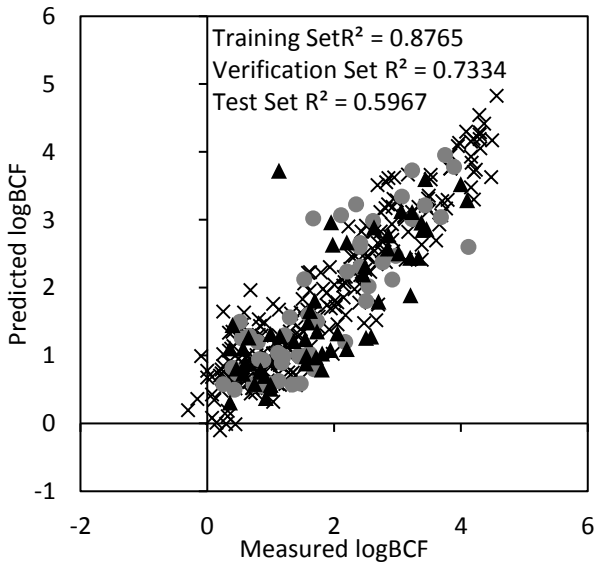

Figure 6.3: Regression analysis of the GA MLP. Crosses represent the training set, circles represent the verification subset and triangles represent the test set.

The 66 descriptors from the GA-model were reduced in number by arbitrarily selecting the 22 most important descriptors to the model shown in Table 6.1. In addition to these descriptors, an additional two were included that were log*D* and the number of hydrogen acceptor groups (*Hacc*) as these descriptors might be important when predicting BCFs of pharmaceuticals. Previous investigations have shown varying relationships between log*D* and bioconcentration. Furthermore, the majority of pharmaceuticals contain amine groups which act as weak bases. The final descriptor list is shown in Table 6.1 and was used to optimise ANNs further.

Table 6.1: Top 22 descriptors selected from the GA-MLP based on ranking determined by their respective error ratio.

Descriptor	Error Ratio	Rank
MAXDP	1.4036	1
TPSA(Tot)	1.3564	2
SPI	1.154	3
STN	1.1336	4
MAXDN	1.0947	5
MW	1.0932	6
ICR	1.0911	7
ASP	1.088	8
nN	1.0772	9
Ms	1.0757	10
nR06	1.075	11
nH	1.074	12
Ram	1.074	13
nCL	1.073	14
Hdon	1.071	15
nX	1.068	16
Dz	1.067	17
nCIC	1.064	18
Me	1.062	19
Hnar	1.06	20
nO	1.055	21
nC	1.055	22

Initially, all descriptors were included and used to train MLPs until the lowest error across the verification and test subset was observed. A four-layer MLP was selected (Figure 6.4) which demonstrated RMSE across the verification and test subset of 0.53 and 0.68, respectively. The model showed an R^2 of 0.8153 for the training subset, 0.813 for the verification subset and 0.6469 for the test subset. Overall, the model showed slightly better performance compared to previous models using larger numbers of descriptors. Whilst the number of descriptors was decreased substantially from the original dataset there is the

potential that 24 descriptors was still too many and could be limiting the performance of the network and the generalisability to new data.

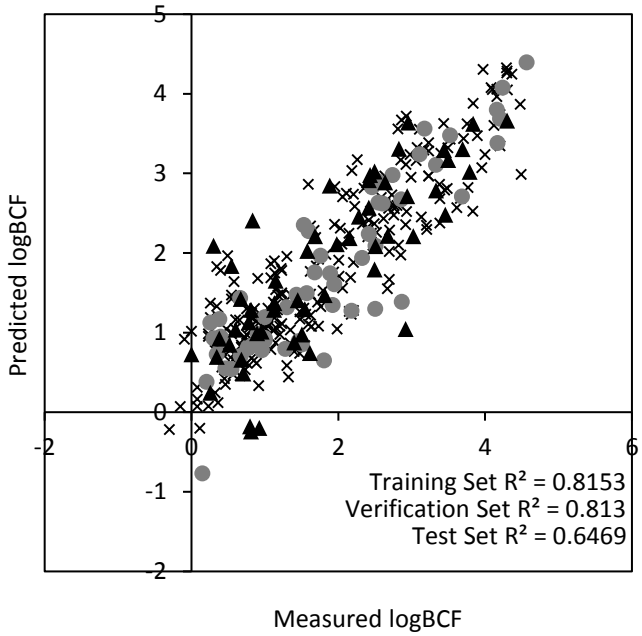

Figure 6.4: Regression of the 24 descriptor MLP. Crosses represent the training set, circles represent the verification set and triangles represent the test set.

An ideal model should maintain simplicity whilst still being able to map the output function. Therefore, a subset of the 24 descriptors was selected at random by the software based on improved model accuracy. The subset contained 14 descriptors and was used to develop an optimised model with a 14:14-10:1 architecture. The model showed improvement in all data subsets when compared to the previous model with 24 input descriptors. The R^2 of the 14 descriptor model was 0.8874 for the training set, 0.8191 for the verification set and 0.7021 for the test set (Figure 6.5). Analysis of the raw residuals for both the verification and test subsets showed that 64 % of the cases were predicted to within ±0.5 logBCF units (Figure 6.6). The average absolute error (± SD) of the verification subset was 0.38 ±0.36 logBCF units and 0.53 ±0.36 logBCF units for the test subset. These errors when transformed correspond to average absolute errors of 2037 L kg^{-1} for the verification and 1092 L kg^{-1} for the test set.

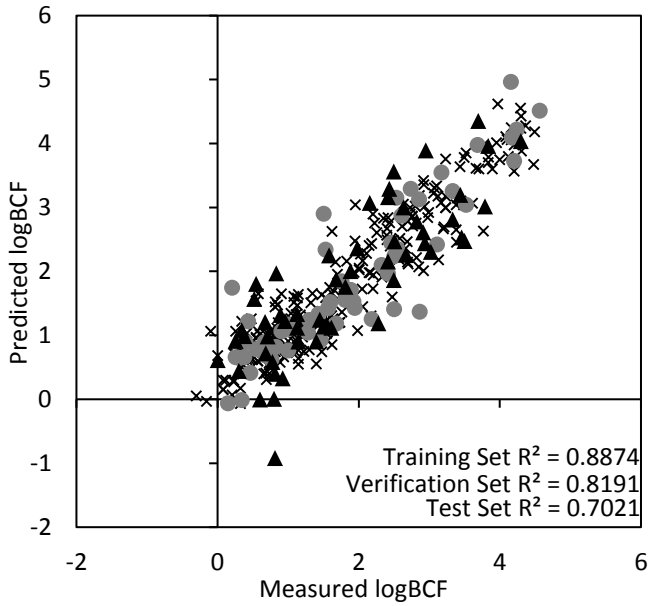

Figure 6.5: Regression of the 14 descriptor MLP. Crosses represent the training set, circles represent the verification set and triangles represent the test set.

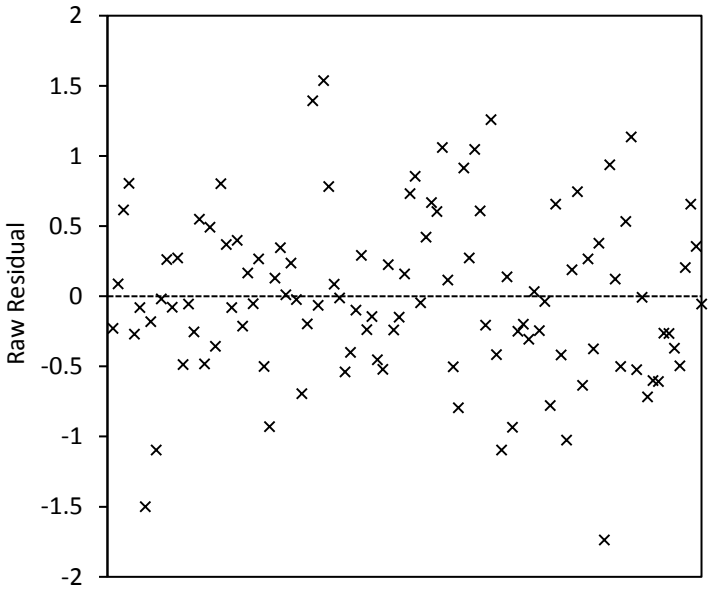

Figure 6.6: Raw residuals of the verification and test subsets in the 14 descriptor MLP.

Previous investigations have used linear regressions in QSARs to predict BCFs with some success [8, 9]. Dearden and Shinnawei used a QSAR approach to predict BCFs for 135 chemicals with an R^2 of 0.637 and a standard error of the estimate of 0.661 logBCF units, in comparison to the 14 descriptor MLP

presented herein with an average standard error 0.58 logBCF units [11]. Another QSAR model by Sahu and Singh [21] used multiple linear regression to predict BCFs for 131 organic compounds with a standard error of estimate of 0.556 log units. However, this model was not applied to a test dataset, thus the reliability of the model is unknown. A majority of QSAR approaches use log*P* as a descriptor and therefore were limited for those compounds with log*P* >6 due to poor diffusion through cellular membranes [22] or those which are ionisable such as pharmaceuticals. In alternative approaches to linear QSAR models, ANNs have been applied to BCF prediction similar to this work. A MLP predicted BCFs for 9 test compounds with an average absolute error of 0.33 ±0.22 log units [15]. Whilst, the error is relatively low, the assessment of the MLP performance and generalisability is extremely limited due to the low number of compounds used for testing. In a second attempt to use machine learning, Zhao et al., used support vector machines to predict BCFs [14]. The model showed an R^2 of 0.6917 for an external test set with a standard deviation in error of prediction of 0.69 logBCF units for 119 compounds.

Comparison of literature data with the model presented above demonstrated that the performance of the MLP herein showed improvement to the predictive models currently available. Whilst the 14 descriptor MLP showed relatively good predictive accuracy, there were particular cases within the verification and test subsets showed large relative percentage errors of their measured value. The percentage error was plotted against the measured BCF value which indicated that below a threshold the BCF prediction error increased (Figure 6.7). For cases that had a logBCF <1 the percentage error increased which suggested the MLP performed more poorly for compounds that do not bioconcentrate.

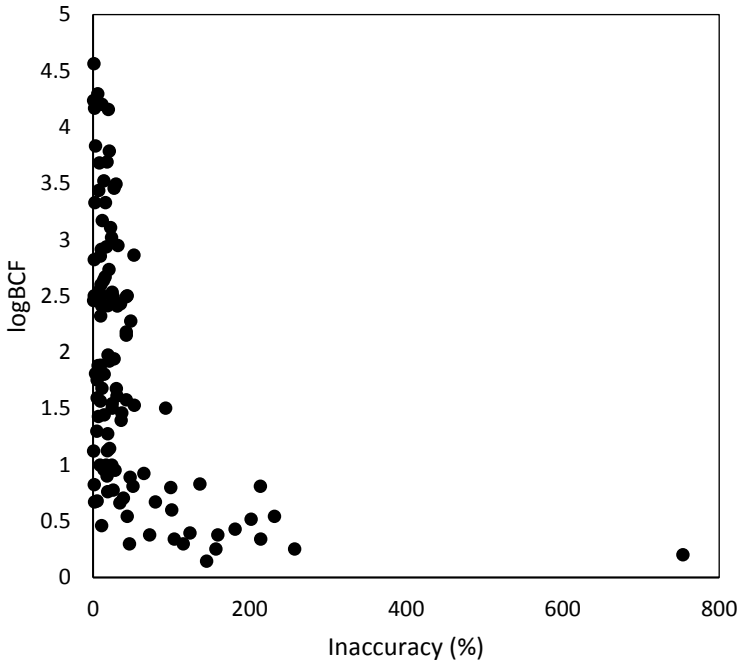

Figure 6.7: The percentage inaccuracy of the verification and test subsets from the 14 descriptor MLP relative to the measure logBCF. Structure inset is azoic coupling component 5 and corresponded to the largest relative error.

The largest error corresponded to a dye referred to as azoic coupling component 5 which is a moderately hydrophobic compound (logD_7 = 3.41) that is insoluble in water which may potentially explain its low logBCF of 0.2. Several other large errors (>50 %) corresponded to range of chemically diverse compounds which were absent of structural similarity. The lower errors for these compounds may be explained by analogous training cases. Azoic coupling component 2 was present in the training set and showed poor predictive accuracy (77 % inaccuracy) which could potentially explain the poor prediction of azoic coupling component 5. In a second example, two benzoic acid analogues that showed poor performance in the verification/test subset also corresponded to benzoic acid in the training data that was 78 % inaccurate. In another case, two compounds which contained phosphate (triallylphosphate and triethylphosphate) showed poor training accuracy which also paralleled two inaccurate compounds with phosphate groups in the verification/test subsets (tris(1,3-dichloroisopropyl) phosphate and trimethyl phosphate). However, it should be considered that poor

predictive accuracy may not always be explained by the training data. Two phosphate containing compounds in the training subset showed relatively good predictive accuracy, tris(2-ethylhexyl) phosphate (23 % error) and tris(2-butoxyethyl) phosphate (34 % error).

BCFs should only be considered an estimate as they are subject to experimental error and variance in their determination. Therefore, the precision and absolute error of predictions might not be considered as important as in other modelling applications. What is of crucial value for modelling BCFs is whether models can correctly classify molecules as bioaccumulative (B) or very bioaccumulative (vB) during PBT testing under REACH guidelines. The threshold values of B is a BCF of 2000 and for vB is a BCF of 5000, regardless of the exact value if these thresholds are exceeded regulation around the chemical will be enforced. The use of the 14 descriptor MLP as a categorical classifier was evaluated by assessing the number of correctly classified cases in the verification and test subsets (Figure 6.8). The model demonstrated good performance as a classifier with 98 compounds correctly classified as either non-bioaccumulative, B or vB. However, the model incorrectly classified a total of 12 cases with 5 identified as false positives and 7 as false negatives. Within the false negative category two cases, 2,2',3,3'-tetrachloro-4,4'-diaminodiphenylmethan and 1,2,4,5-tetrachlorobenzene, were identified as vB instead of B and the remaining compounds were predicted as non-bioaccumulative instead of B/vB. The false negatives classed as non-bioaccumulative would pose the most risk to the environment whereas false positives would likely lead to economic losses for the producers of the chemical. With this in mind it should still be considered that this model could aid in prioritisation efforts. Furthermore, to avoid a situation of over/under regulation a threshold tolerance could be applied to the predicted

values so that if the BCF was within a certain percentage of the REACH threshold for B or vB experimental testing could be pursued.

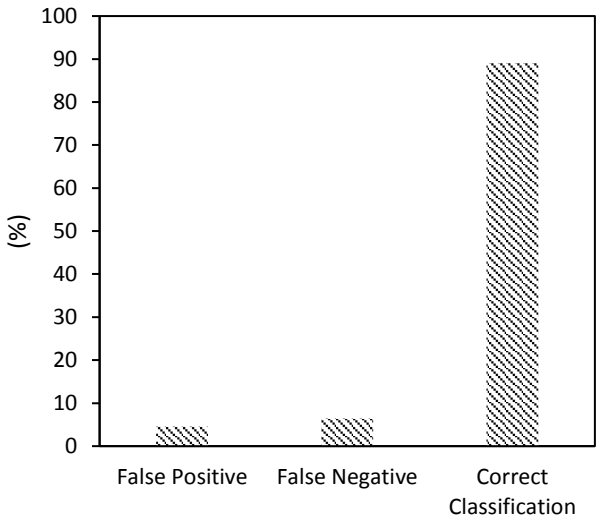

Figure 6.8: The percentage of compounds in the verification and test subsets (n =110) correctly classified or predicted as a false positive or negative relative to PBT testing thresholds.

Zhao et al., also showed a similar misclassification rate of 10 % for all compounds tested [14]. However, a bias was applied to the data which reduced to the misclassification to 0 %. Whilst the MLP showed acceptable predictive accuracy for the tested data, the model will only perform as well as the data it is trained on. It has been shown that estimation of BCFs can suffer from many sources of error and variation including instrumental performance (analysis), kinetic modelling approaches (Chapter 3), biological variability (age, health, lipid content etc.) and experimental conditions (pH, temperature, dissolved oxygen etc.) [23-26]. Due to these numerous sources of error and variation, reported BCFs have differed by 1-2 orders of magnitude [27] even within the same species. Furthermore, experimental conditions may not be recorded or reported. For example, the BCF gold standard dataset used herein did not report individual pH values for the BCF experiments. Instead the dataset described only the range of pH which varied from 6.0 to 8.5. BCFs have been previously demonstrated to change as a result of pH [26]. Therefore, predictive accuracy of the model may

be limited by descriptors that require pH data, such as log*D* unless it is measured during experiments. For simplicity here, the log*D* descriptor was calculated at a pH of 7 but this value could differ significantly if the exposure pH was different, thus leading to limitations in the current modelling approach. Furthermore, predicted physicochemical properties such as those used here (i.e. log*D* from ACD labs) could also limit the predictive ability of the model. As these estimated properties will contain some uncertainty it is possible that departure from the true value may hinder the model from learning the trends in the data. Furthermore, as the majority of chemical descriptors (with the exception of constitutional descriptors) are estimated the full extent to which this will affect the predictive ability of machine learning approaches is beyond the scope of this work. Thus, where available experimentally determined data is recommended over the use of predicted input descriptors (even with the errors associated with experimental measurement) as suggested by [28].

In addition to the reliability of BCF estimates, it is also possible that BCF prediction will be limited by biotic factors. The descriptors used in the model are abiotic and only cover the physico-chemical properties of the compounds studied. Biotic factors such as ventilation rates, age, and metabolic rates could affect BCF estimates and thus the model would not account for these variables [29]. Thus, QSAR approaches, whether linear or non-linear, omit the biology which would likely explain the variation in the data not described by the chemistry of the molecules. However, even with the limitations discussed, the *in silico* approach presented could potentially offer a much needed alternative to the experimental determination of BCFs that are costly and both time and labour intensive. At the very least the use of ANNs could direct prioritisation efforts for compounds that may lead to the greatest environmental risk.

6.3.2 Cross-species prediction of bioconcentration factors in invertebrates

Bioconcentration studies at present have focussed on fish species with little attention towards the invertebrate phyla. This phyla is the largest and most diverse animal group. Thus, determining the behaviour of contaminants across the invertebrates will be crucial to assessing environmental risk. The primary site of bioconcentration in aquatic animals is across the gills [30] with the exception of sediment-dwelling organisms that is likely to be through dermal contact. There is a potential for significant difference of BCFs between the vertebrate and invertebrate phyla. The difference between the phyla will manifest through biological and physiological variables including size, enzyme specification, lipid content, and respiration strategy among others [31]. Even within the same taxa considerable differences between BCFs have been observed [32].

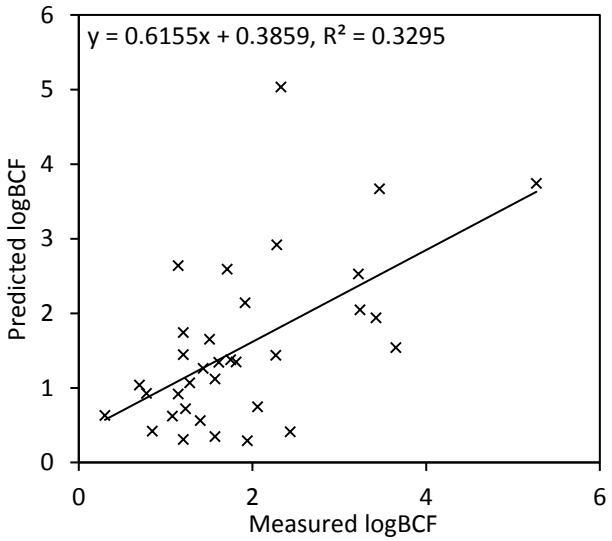

Figure 6.9: Cross species prediction using the 14 descriptor MLP to predict the measured G. pulex BCFs.

Whilst models exist for the prediction of BCF in fish currently there are no models available for invertebrates. The lack of available BCF data is the main limitation for modelling approaches to predict the bioconcentration potential in

invertebrates. However, as the model above demonstrated acceptable predictive accuracy for prediction of BCFs in a fish species it had the potential to be used in cross species prediction. BCFs generated in Chapters 3 & 4 along with literature reported data were used to determine whether the previously described model would adequately predict bioconcentration in the arthropod, *G. pulex*. The regression between predicted BCFs using the fish-based model and the measured BCFs in *G. pulex* showed a weak correlation of R^2 0.3295 suggesting that the generalisation between the species was relatively poor (Figure 6.9). The average absolute error was 0.80 ±0.65 log units which corresponded to 45 % inaccuracy, indicating lower predictive accuracy and greater variance compared with the BCF predictions for fish. The largest absolute error corresponded to the compound imipramine which was over estimated by 2.7 logBCF units (Figure 6.10).

The over-estimation was interesting as this compound was previously shown in Chapter 3 to have a variable BCF (212 – 4533) depending on the method of estimation (simultaneous versus sequential). The variability stemmed from statistically significant lacks-of-fit of the kinetic models which further indicates that the reliability of BCFs may limit the predictive ability of modelling approaches. The low accuracy of the cross-species prediction may also be in relation to the factors mentioned above where biological and physiological traits are considerably variable between fish and invertebrates. A previous investigation found that there is a significant difference in BCFs between trophic levels with higher trophic levels having increased BCFs [32]. This trend would suggest that the BCF predictions of the invertebrates might be overestimated but the opposite was observed with approximately 62% of cases underestimated. In addition to the biological complexity between species, another confounding factor

to affect the predictive accuracy is the compound class encountered by the model.

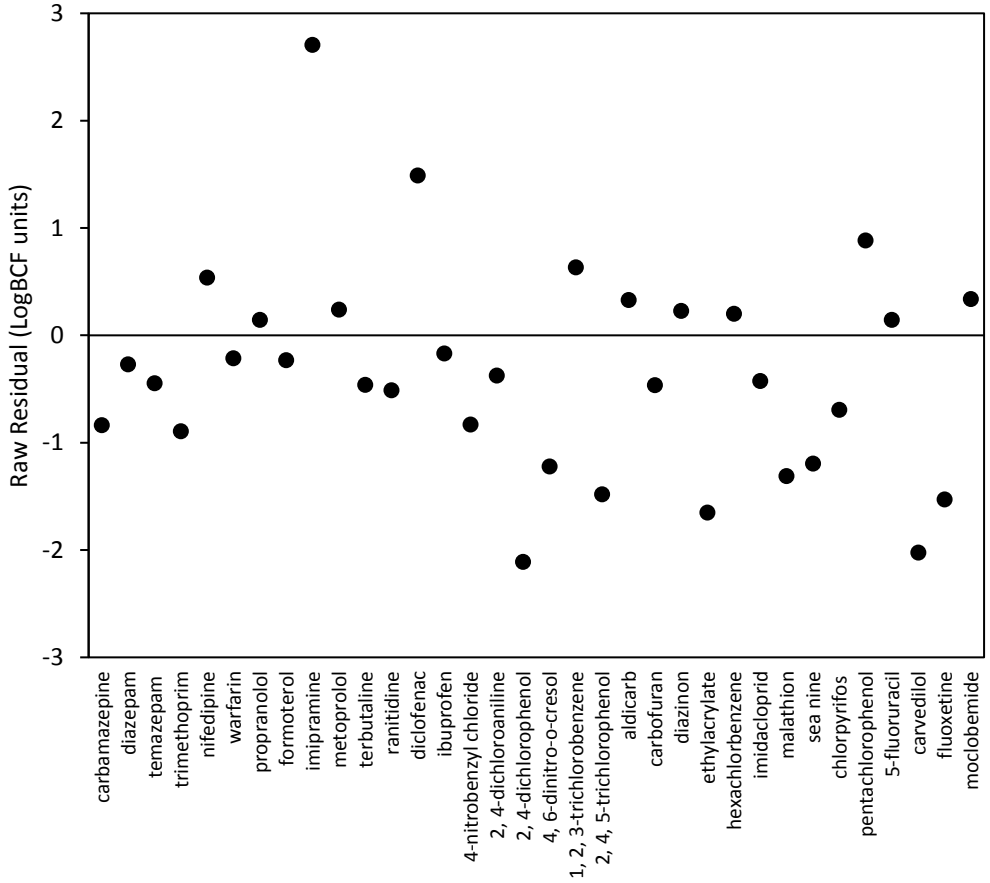

Figure 6.10: Raw residuals for the G. pulex BCF predictions using the 14 descriptor MLP.

The fish-based modelling included no pharmaceutical compounds within the dataset whereas the invertebrate BCFs contained 18 compounds that were classed as pharmaceuticals. This class of compounds is uniquely placed relative to the other classes of compounds present in the dataset. Pharmaceuticals are amphoteric molecules with multiples sites of ionisation. Thus, their bioconcentration potential may not follow similar relationships with neutral hydrophobic organic contaminants such as PCBs and PAHs. As the model has not encountered pharmaceuticals previously, it is possible that the generalisability for these types of compounds is limited. The model was

reinitialised and trained *ab initio* using the invertebrate BCF data with the same 14 input descriptors used by the fish-based model.

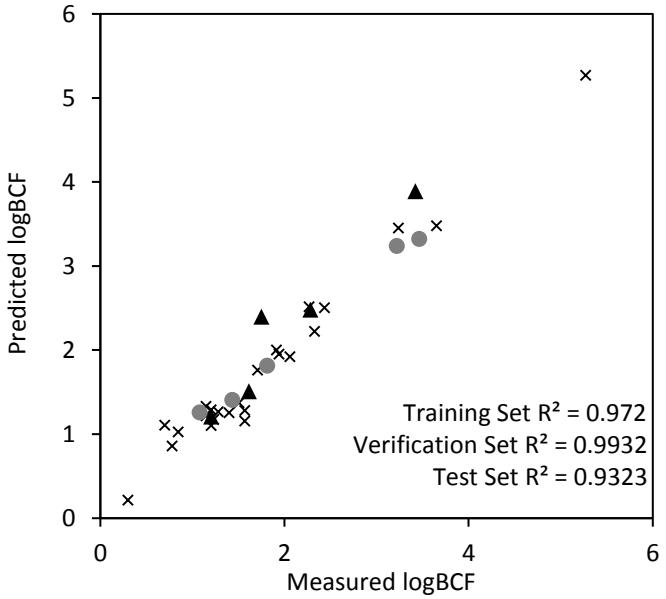

Figure 6.11: Regression of the 14 descriptor MLP retrained using the invertebrate dataset. Crosses are training data, circles are verification data and triangles are test data.

A 4-layer MLP with a 14:14-10:1 architecture demonstrated good predictive accuracy for this limited dataset (Figure 6.11). The regression of the data subsets gave an overall R^2 of 0.9605 with 0.972 for the training set, 0.9932 for the verification set and 0.9323 for the test set. The successful retraining of the model to invertebrate data suggests that cross species prediction might be difficult due to the biological variation between different taxa. Overall, the model demonstrated good accuracy across the verification and test subset with an average absolute error of 0.07 ±0.08 logBCF units for the verification set and 0.29 ±0.27 logBCF units for the test set. Whilst the predictive accuracy of the retrained model is relatively good it is also limited due to the number of cases used in the verification and test subsets. A much larger dataset would be needed to fully

validate the models performance but nevertheless the model demonstrates a very good potential for the prediction of BCF data for an invertebrate species.

6.3.4 Importance of descriptors related to species and compound class

The importance of the 14 descriptors to the MLP for the fish-based and invertebrate-based models was assessed. The sensitivity of the network to the input descriptors for the fish-based model is shown in Figure 6.12. The most important descriptor determined was the topological polar surface area (TPSA) with an error ratio of 2.08 which indicated that the model error increased the most upon removal of this descriptor. Previous investigations have demonstrated that descriptors related to polarizability, hydrophobicity and hydrogen bonding of the molecule is important to modelling BCFs [11, 14, 33]. TPSA is defined as the surface area occupied by nitrogen and oxygen atoms including connected hydrogen atoms [34].

This descriptor is related to both polarity of the molecule and the hydrogen

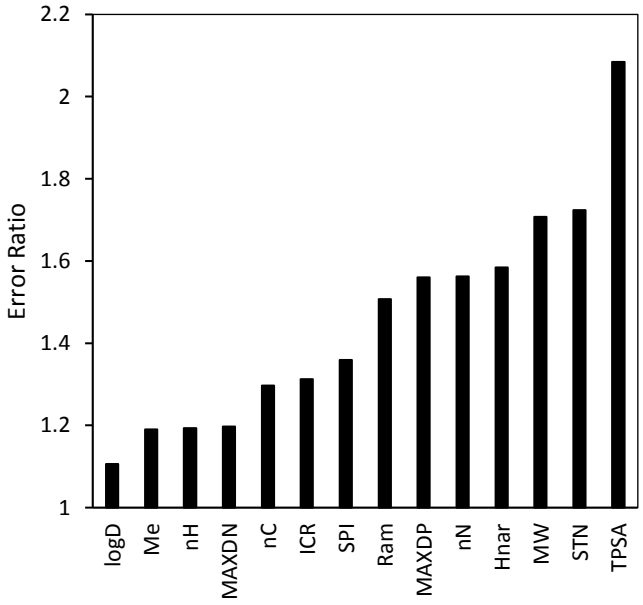

Figure 6.12: Sensitivity analysis of the 14 descriptors in the fish-based MLP.

bonding capacity and thus will reflect the ability of the molecule to permeate membrane barriers. In medicinal applications, a lower TPSA is more successful at permeating cellular membranes [34]. This observation is in agreement with the

collinearity assessment, where there was an observed negative Pearson's correlation of -0.403 between logBCF and TPSA (Table 6.2). The negative sign also agrees with an investigation by Papa et al., which identified the same trend between TPSA and bioconcentration [35]. The relationship between bioconcentration and TPSA may be as a result of several factors. First, the increased permeation of molecules with lower TPSA through membranes may be explained by the hydrophobic lipid bilayer as it would retard diffusion of increasingly polar molecules. Secondly, it is also possible that the polar groups may bind to membrane surfaces instead of diffusing across the epithelium. The final consideration of TPSA is that it will also relate to the hydration shell around a molecule and thus a compounds solubility in water [36, 37].

Table 6.2: Collinearity assessment of the 14 descriptors used in the fish-based MLP using Pearsons' correlation.

	MW	Me	nH	nC	nN	ICR	MAXDN	MAXDP	Hnar	STN	TPSA	logD	Ram	SPI
Me	0.135													
nH	0.401	-0.55												
nC	0.619	-0.448	0.774											
nN	0.097	0.003	0.035	0.139										
ICR	0.581	-0.273	0.603	0.768	0.258									
MAXDN	0.385	0.61	-0.052	0.001	0.11	0.192								
MAXDP	0.466	0.181	0.243	0.396	0.203	0.452	0.653							
Hnar	0.023	-0.549	0.216	0.506	0.13	0.309	-0.362	-0.06						
STN	0.275	-0.241	0.02	0.56	0.177	0.306	-0.132	0.19	0.748					
TPSA	0.274	0.095	0.124	0.183	0.589	0.391	0.505	0.589	-0.016	0.095				
logD	0.453	-0.092	0.358	0.475	-0.213	0.347	0.002	0.029	0.179	0.211	-0.221			
Ram	0.696	0.231	0.107	0.497	0.156	0.361	0.443	0.526	0.015	0.522	0.305	0.259		
SPI	0.794	0.169	0.437	0.558	0.21	0.566	0.557	0.634	-0.227	0.074	0.442	0.28	0.787	
logBCF	0.295	-0.147	0.137	0.341	-0.295	0.104	-0.228	-0.197	0.248	0.368	-0.403	0.455	0.309	0.121

Another important descriptor was molecular weight (*MW*) which may be expected as the size of a molecule will affect permeation and diffusion through membranes as demonstrated by Lipinski's rule of 5 in pharmaceutical development [38]. These rules are used to ensure that pharmaceuticals will be bioavailable during oral dose administration. It has been demonstrated that dye pigments did not show bioaccumulation in fish as a result of their molecular size [39]. In another study, it suggested that there was a threshold diameter value of 1.5 nm which governed bioconcentration in addition to hydrophobicity [40]. As molecular weight is a function of molecular size it is no surprise that *MW* was important to the model.

The descriptors *STN*, *Hnar*, *Ram*, *SPI* and *ICR* are topological descriptors that relate to chemical graph theory. Chemical graph theory is used to represent a molecules structure where vertices correspond to atoms, edges correspond to chemical bonds and vertex degrees are the number of bonds associated with an atom [41]. The indices can be useful for differentiating between structural isomers (with the exception of optical isomerism) and have been used in many fields to determine and interpret relationships between different processes and activities. The descriptors *STN* (spanning tree number), *Hnar* (Narumi harmonic topoligcal index) and *Ram* (ramification index) were important to the model by varying degrees (error ratio 1.35 – 1.72). These descriptors are indices that are related to molecular branching (in acyclic and polycyclic graphs). The importance of these descriptors to the model could be explained by their reflection of molecular size, which is supported by the moderate collinearity of *Ram* and *SPI* with *MW*. *ICR* the radial centric information index is related to the molecular shape and thus could influence bioconcentration through steric effects including hindrance to diffusion and permeation through cellular membranes [42].

MAXDN and *MAXDP* are electrotopological descriptors that relate to the partial charges on atoms relative to their topological position in the molecule. Therefore the descriptors *MAXDN* and *MAXDP* relate to the nucleophilicity and electrophilicity of the molecule, respectively [43]. As mentioned previously, polarity of the molecule is important in accumulation due to the interaction with cellular membranes. In addition, it is also possible that these descriptors may also relate to accumulation through metabolism as metabolic processes of xenobiotics is often through nucleophilic attack of the substrate.

Whilst assessing the importance of descriptors to developed models it is critical to evaluate any collinearity or multicollinearity. The collinearity of the descriptors showed that molecular weight was collinear with *SPI* (*R*=0.794) and *Ram* (*R*=0.696). The descriptor Ram was also collinear with *SPI* (R=0.787) and another topological index *STN* was collinear with *HNar* (*R*=0.748). The relation between these topological descriptors and molecular weight is that they all describe molecular size (shape, volume, weight) to some extent. Number of carbons was also collinear with the number of hydrogens which would be expected as these are organic compounds. As a small number of descriptors showed collinearity the rank importance of the descriptors should be approached with caution. Whilst the error ratio is higher for certain descriptors that are collinear, their removal from the network model may not correctly determine the ratio value as the remaining collinear descriptor will carry some redundant information.

The invertebrate-based MLP used the same descriptors but the network was retrained. The new model generated was assessed for both descriptor sensitivity and collinearity (Figure 6.13 and Table 6.3).

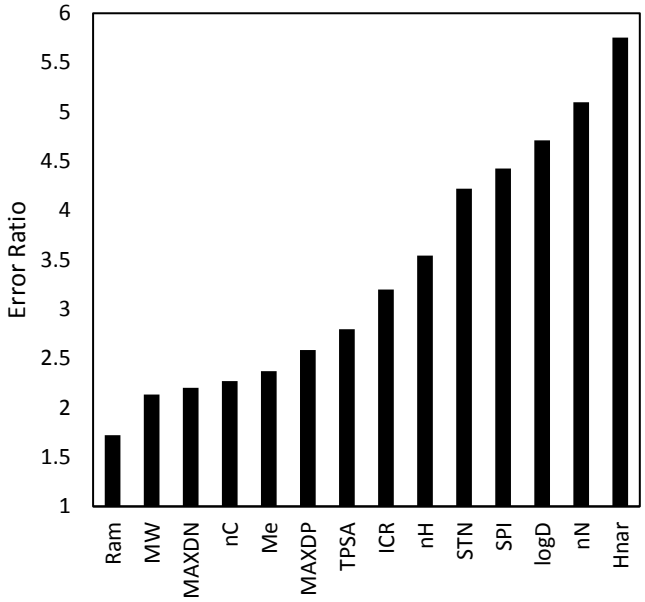

Figure 6.13: Sensitivity analysis of the 14 descriptors in the invertebrate-based MLP

As expected the relative importance of the descriptors have changed from the fish-based model. The most important descriptor was *HNar* (error ratio = 5.75) followed by *nN* (error ratio = 5.09) and log*D* (error ratio = 4.71). The increased importance of the number of nitrogen atoms will reflect the number of pharmaceutical compounds in the dataset which are often amine or amide containing molecules. In addition, log*D* has moved from the least important descriptor in the fish-based model to the top three descriptors in the invertebrate model. The increased sensitivity of the model to log*D* will also relate to the training of the model with pharmaceuticals. As this class of compounds contain multiple ionisation sites it would be expected that fraction of ionised and neutral species would affect bioconcentration. The lesser importance of log*D* in the fish-based model is that the dataset contained a majority of neutral compounds. Thus, stresses the importance of the inclusion of ionisation for current BCF models as a key consideration.

Table 6.3: Collinearity assessment of the 14 descriptors in the invertebrate-based MLP using Pearsons' correlation.

	MW	Me	nH	nC	nN	ICR	MAXDN	MAXDP	Hnar	Ram	SPI	STN	TPSA	logD
Me	-0.287													
nH	0.619	-0.825												
nC	0.734	-0.681	0.819											
nN	0.266	-0.239	0.339	0.271										
ICR	0.609	-0.736	0.888	0.741	0.471									
MAXDN	0.216	0.026	0.087	0.023	0.008	0.176								
MAXDP	0.304	-0.254	0.301	0.431	0.042	0.411	0.34							
Hnar	0.498	-0.537	0.524	0.795	0.425	0.582	-0.161	0.328						
Ram	0.772	-0.169	0.417	0.715	0.251	0.326	0.139	0.371	0.462					
SPI	0.799	-0.34	0.673	0.596	0.296	0.608	0.388	0.359	0.171	0.733				
STN	0.504	-0.352	0.361	0.788	0.315	0.364	-0.171	0.31	0.904	0.67	0.173			
TPSA	0.387	-0.204	0.424	0.187	0.503	0.468	0.369	0.325	-0.042	0.344	0.679	-0.105		
logD	0.368	0.077	-0.072	0.066	-0.245	-0.147	-0.062	-0.247	0.115	0.169	0.032	0.148	-0.31	
logBCF	0.088	0.227	-0.201	-0.088	-0.432	-0.199	0.298	-0.231	-0.099	-0.07	-0.113	-0.049	-0.423	0.627

The difference of log*D* between the fish-based and invertebrate-based model can also be observed through regression of log*D* and logBCF (Figure 6.14). The regressions demonstrated that log*D* in the *G. pulex* dataset had a higher R^2 of 0.3927 compared with an R^2 of 0.2069 for the fish dataset.

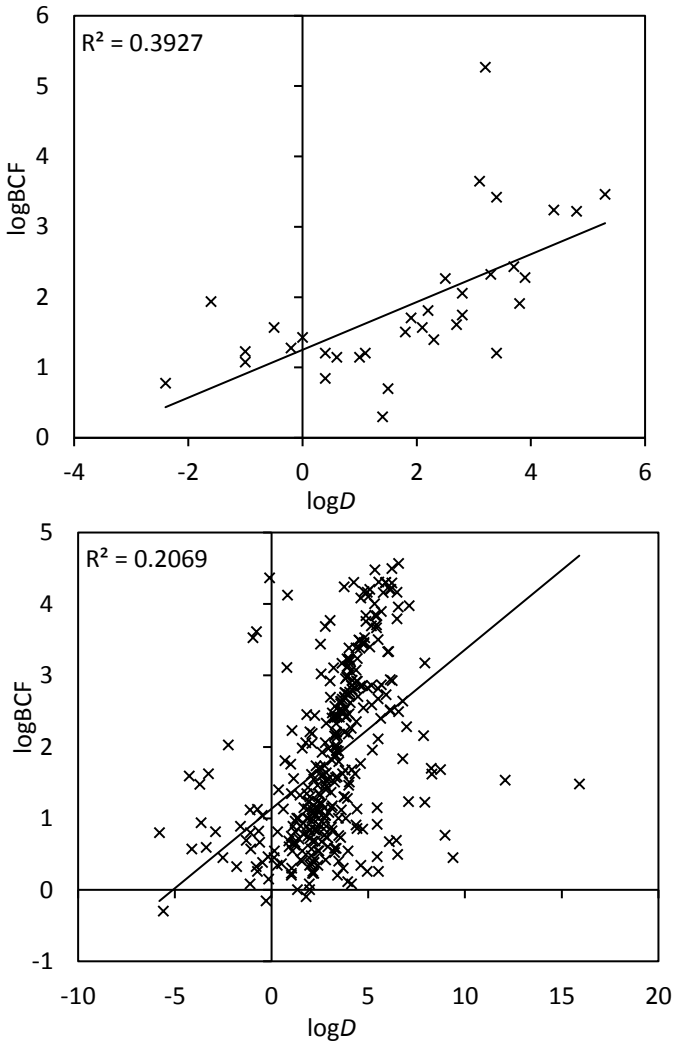

Figure 6.14: Relationship between logD and measured logBCF for the invertebrate dataset (top) and the fish dataset (bottom).

From the observed fish-based plot a general increase in logBCF as log*D* increases. However, compounds exceeding a log*D* of 6 the logBCF no longer increases. This observation has been demonstrated in previous investigations concerned with hydrophobic organic contaminants [27]. The threshold value reflects that highly hydrophobic compounds cannot diffuse across cellular membranes thus bioconcentration is reduced. In addition, these hydrophobic

compound have reduced bioavailability due to adsorption onto particulate and dissolved organic matter [44] Whilst hydrophobicity is the principal component attributed to bioconcentration prediction, it is possible that carrier-mediated transport may also play an important role. Both models presented demonstrated that other variables also strongly influence BCF prediction. Thus, QSAR models that rely solely on log*P* or log*D* are limited in their application. As a final point, it is important to consider that descriptors not used in this work may also have a potential for BCF modelling. For example, pigment solubility was suggested to influence BCF and therefore log*S* may be a useful descriptor. Furthermore, as the major mechanism of transport across epithelia tissue is passive diffusion it is also possible that diffusion coefficients may also be an important descriptor for consideration.

6.4 Conclusions

The application of ANNs to predict BCFs showed a good potential with >70 % of the variance in measured values described by the developed models. The models presented showed an improvement or similar accuracy to currently available QSAR models. Prediction accuracy may potentially be improved by the use of more reliable experimental data and larger datasets to represent the diversity of xenobiotics which are found as environmental contaminants. However, the improvement to prediction accuracy may also be limited by varying biological, physiological and environmental factors. Cross-species prediction of BCF between fish and invertebrates was also limited in application. The model did not perform well for predicting BCFs in *G. pulex* which may also be explained by differing biological and physiological traits. A new ANN model was developed and represents the first model to successfully predict invertebrate BCFs.

However, the type of model tested here is only single class of machine learning models. The applicability of other in silico methods such as support vector machines and tree-based learning should be investigated. A comparative study could reveal the most useful models for predicting accumulation in the environment. The model showed good accuracy in BCF prediction but a larger dataset would be required to fully assess the generalisability of the model to new compounds. Mechanistic interpretation of the models showed that in addition to hydrophobicity, molecular size, polarity, and ionisation of a compounds were important factors related to bioconcentration. Overall, the application of non-linear modelling methods to predict BCF holds promise and can be used to screen or prioritise compounds for environmental risk assessment such as PBT testing under REACH.

6.5 References

1. Commission, E., *Regulation (EC) No 1907/2006 of the European Parliament and of the Council of 18 December 2006 concerning the Registration, Evaluation, Authorisation and Restriction of Chemicals (REACH), establishing a European Chemicals Agency, amending Directive 1999/45/EC and repealing Council Regulation (EEC) No 793/93 and Commission Regulation (EC) No 1488/94 as well as Council Directive 76/769/EEC and Commission Directives 91/155/EEC, 93/67/EEC, 93/105/EC and 2000/21/EC.* 2006: Official Journal of the European Union. p. 1 - 849.
2. Agency, E.C., Guidance on Information Requirements and Chemical Safety Assessment Chapter R.11: PBT/vPvB Assessment*.* 2014.
3. Rand-Weaver, M., L. Margiotta-Casaluci, A. Patel, G.H. Panter, S.F. Owen, and J.P. Sumpter, The read-across hypothesis and environmental risk assessment of pharmaceuticals*. Environmental science & technology*, 2013. **47**(20): p. 11384-11395.
4. Gissi, A., O. Nicolotti, A. Carotti, D. Gadaleta, A. Lombardo, and E. Benfenati, Integration of QSAR models for bioconcentration suitable for REACH*. Science of The Total Environment*, 2013. **456–457**: p. 325-332.
5. de Wolf, W., M. Comber, P. Douben, S. Gimeno, M. Holt, M. Léonard, A. Lillicrap, D. Sijm, R. van Egmond, A. Weisbrod, and G. Whale, Animal use replacement, reduction, and refinement: Development of an integrated testing strategy for bioconcentration of chemicals in fish*. Integrated Environmental Assessment and Management*, 2007. **3**(1): p. 3-17.

6. Isnard, P. and S. Lambert, Estimating bioconcentration factors from octanol-water partition coefficient and aqueous solubility. *Chemosphere*, 1988. **17**(1): p. 21-34.

7. Schüürmann, G. and W. Klein, Advances in Environmental Hazard and Risk Assessment 1987 Advances in bioconcentration prediction. *Chemosphere*, 1988. **17**(8): p. 1551-1574.

8. Veith, G.D., D.L. DeFoe, and B.V. Bergstedt, Measuring and Estimating the Bioconcentration Factor of Chemicals in Fish. *Journal of the Fisheries Research Board of Canada*, 1979. **36**(9): p. 1040-1048.

9. Devillers, J., S. Bintein, and D. Domine, Comparison of BCF models based on log P. *Chemosphere*, 1996. **33**(6): p. 1047-1065.

10. Sabljić, A. and M. Protić, Molecular connectivity: A novel method for prediction of bioconcentration factor of hazardous chemicals. *Chemico-Biological Interactions*, 1982. **42**(3): p. 301-310.

11. Dearden, J.C. and N.M. Shinnawei, Improved prediction of fish bioconcentration factor of Hydrophobic Chemicals. *SAR and QSAR in Environmental Research*, 2004. **15**(5-6): p. 449-455.

12. Tao, S., H. Hu, X. Lu, R.W. Dawson, and F. Xu, Fragment constant method for prediction of fish bioconcentration factors of non-polar chemicals. *Chemosphere*, 2000. **41**(10): p. 1563-1568.

13. Lombardo, A., A. Roncaglioni, E. Boriani, C. Milan, and E. Benfenati, Assessment and validation of the CAESAR predictive model for bioconcentration factor (BCF) in fish. *Chemistry Central Journal*, 2010. **4**(1): p. 1.

14. Zhao, C., E. Boriani, A. Chana, A. Roncaglioni, and E. Benfenati, A new hybrid system of QSAR models for predicting bioconcentration factors (BCF). *Chemosphere*, 2008. **73**(11): p. 1701-1707.

15. Fatemi, M.H., M. Jalali-Heravi, and E. Konuze, Prediction of bioconcentration factor using genetic algorithm and artificial neural network. *Analytica Chimica Acta*, 2003. **486**(1): p. 101-108.

16. Grisoni, F., V. Consonni, S. Villa, M. Vighi, and R. Todeschini, QSAR models for bioconcentration: Is the increase in the complexity justified by more accurate predictions? *Chemosphere*, 2015. **127**: p. 171-179.

17. Ashauer, R., I. Caravatti, A. Hintermeister, and B.I. Escher, Bioaccumulation kinetics of organic xenobiotic pollutants in the freshwater invertebrate Gammarus pulex modeled with prediction intervals. *Environmental Toxicology and Chemistry*, 2010. **29**(7): p. 1625-1636.

18. Meredith-Williams, M., L.J. Carter, R. Fussell, D. Raffaelli, R. Ashauer, and A.B.A. Boxall, Uptake and depuration of pharmaceuticals in aquatic invertebrates. *Environmental Pollution*, 2012. **165**: p. 250-258.

19. Ashauer, R., A. Boxall, and C. Brown, Uptake and Elimination of Chlorpyrifos and Pentachlorophenol into the Freshwater Amphipod Gammarus pulex. *Archives of Environmental Contamination and Toxicology*, 2006. **51**(4): p. 542-548.

20. Miller, T.H., G.L. McEneff, L.C. Stott, S.F. Owen, N.R. Bury, and L.P. Barron, Assessing the reliability of uptake and elimination kinetics modelling approaches for estimating bioconcentration factors in the freshwater invertebrate, Gammarus pulex. *Science of The Total Environment*, 2016. **547**: p. 396-404.

21. Sahu, V.K. and R.K. Singh, Prediction of the Bioconcentration Factor of Organic Compounds in Fish. *CLEAN – Soil, Air, Water*, 2009. **37**(11): p. 850-857.

22. Devillers, J., D. Domine, S. Bintein, and W. Karcher, FISH BIOCONCENTRATION MODELING WITH LOG P. *Toxicology Methods*, 1998. **8**(1): p. 1-10.

23. Arnot, J.A. and F.A.P.C. Gobas, A review of bioconcentration factor (BCF) and bioaccumulation factor (BAF) assessments for organic chemicals in aquatic organisms. *Environmental Reviews*, 2006. **14**(4): p. 257-297.

24. van der Heijden, S.A. and M.T.O. Jonker, Intra- and Interspecies Variation in Bioconcentration Potential of Polychlorinated Biphenyls: Are All Lipids Equal? *Environmental Science & Technology*, 2011. **45**(24): p. 10408-10414.

25. Brown, J.N., N. Paxéus, L. Förlin, and D.G.J. Larsson, Variations in bioconcentration of human pharmaceuticals from sewage effluents into fish blood plasma. *Environmental Toxicology and Pharmacology*, 2007. **24**(3): p. 267-274.

26. Nakamura, Y., H. Yamamoto, J. Sekizawa, T. Kondo, N. Hirai, and N. Tatarazako, The effects of pH on fluoxetine in Japanese medaka (Oryzias latipes): Acute toxicity in fish larvae and bioaccumulation in juvenile fish. *Chemosphere*, 2008. **70**(5): p. 865-873.

27. Wang, Y., Y. Wen, J.J. Li, J. He, W.C. Qin, L.M. Su, and Y.H. Zhao, Investigation on the relationship between bioconcentration factor and distribution coefficient based on class-based compounds: The factors that affect bioconcentration. *Environmental Toxicology and Pharmacology*, 2014. **38**(2): p. 388-396.

28. Miller, T.H., A. Musenga, D.A. Cowan, and L.P. Barron, Prediction of Chromatographic Retention Time in High-Resolution Anti-Doping Screening Data Using Artificial Neural Networks. *Analytical Chemistry*, 2013. **85**(21): p. 10330-10337.

29. Mackay, D. and A. Fraser, Bioaccumulation of persistent organic chemicals: mechanisms and models. *Environmental Pollution*, 2000. **110**(3): p. 375-391.

30. Hayton, W.L. and M.G. Barron, Rate-limiting barriers to xenobiotic uptake by the gill. *Environmental Toxicology and Chemistry*, 1990. **9**(2): p. 151-157.

31. LeBlanc, G.A., Trophic-Level Differences in the Bioconcentration of Chemicals: Implications in Assessing Environmental Biomagnification. *Environmental Science & Technology*, 1995. **29**(1): p. 154-160.

32. Rubach, M.N., R. Ashauer, S.J. Maund, D.J. Baird, and P.J. Van den Brink, Toxicokinetic variation in 15 freshwater arthropod species exposed to the insecticide chlorpyrifos. *Environmental Toxicology and Chemistry*, 2010. **29**(10): p. 2225-2234.

33. Gramatica, P. and E. Papa, QSAR Modeling of Bioconcentration Factor by theoretical molecular descriptors. *QSAR & Combinatorial Science*, 2003. **22**(3): p. 374-385.

34. Pajouhesh, H. and G.R. Lenz, Medicinal Chemical Properties of Successful Central Nervous System Drugs. *NeuroRX*, 2005. **2**(4): p. 541-553.

35. Papa, E., J.C. Dearden, and P. Gramatica, Linear QSAR regression models for the prediction of bioconcentration factors by physicochemical

properties and structural theoretical molecular descriptors. *Chemosphere*, 2007. **67**(2): p. 351-358.

36. Barron, M.G., Bioconcentration. Will water-borne organic chemicals accumulate in aquatic animals? *Environmental Science & Technology*, 1990. **24**(11): p. 1612-1618.

37. Skyner, R., J. McDonagh, C. Groom, T. van Mourik, and J. Mitchell, A review of methods for the calculation of solution free energies and the modelling of systems in solution. *Physical Chemistry Chemical Physics*, 2015. **17**(9): p. 6174-6191.

38. Tice, C.M., Selecting the right compounds for screening: does Lipinski's Rule of 5 for pharmaceuticals apply to agrochemicals? *Pest Management Science*, 2001. **57**(1): p. 3-16.

39. Anliker, R., P. Moser, and D. Poppinger, Advances in Environmental Hazard and Risk Assessment 1987 Bioaccumulation of dyestuffs and organic pigments in fish. Relationships to hydrophobicity and steric factors. *Chemosphere*, 1988. **17**(8): p. 1631-1644.

40. Dimitrov, S.D., N.C. Dimitrova, J.D. Walker, G.D. Veith, and O.G. Mekenyan, *Predicting bioconcentration factors of highly hydrophobic chemicals. Effects of molecular size*, in *Pure and Applied Chemistry*. 2002. p. 1823.

41. García-Domenech, R., J. Gálvez, J.V. de Julián-Ortiz, and L. Pogliani, Some New Trends in Chemical Graph Theory. *Chemical Reviews*, 2008. **108**(3): p. 1127-1169.

42. Liang, G., Y. Liu, B. Shi, J. Zhao, and J. Zheng, An Index for Characterization of Natural and Non-Natural Amino Acids for Peptidomimetics. *PLoS ONE*, 2013. **8**(7): p. e67844.

43. Gramatica, P., M. Corradi, and V. Consonni, Modelling and prediction of soil sorption coefficients of non-ionic organic pesticides by molecular descriptors. *Chemosphere*, 2000. **41**(5): p. 763-777.

44. Haitzer, M., S. Höss, W. Traunspurger, and C. Steinberg, Effects of dissolved organic matter (DOM) on the bioconcentration of organic chemicals in aquatic organisms — a review —. *Chemosphere*, 1998. **37**(7): p. 1335-1362.

Chapter 7. Concluding Remarks

7.1 Conclusions

In summary, the work presented has included; (a) an analytical method using LC-MS/MS was developed to determine pharmaceuticals in *G. pulex*, (b) the assessment of the validity of BCF models for pharmaceutical uptake in invertebrates was critically assessed, (c) ANNs were successfully used to predict uptake onto POCIS devices, (d) Phase I and Phase II pharmaceutical metabolites were determined in *G. pulex* and (e) ANNs were successfully used to predict BCFs in fish and invertebrates (*G. pulex*).

Bioconcentration factors in *G. pulex,* have successfully been modelled using ANNs which has not been previously achieved. The occurrence of several selected pharmaceuticals around the Greater London catchment area in *G. pulex* determined by LC-MS/MS was low. The method developed was relatively simple and overcame the analytical challenges associated with complex biological samples. However, the method was suitable for only 10 compounds that was extended to include several other metabolites. This is a relatively small space occupied when compared to the total number of pharmaceuticals available and their associated physico-chemical properties. Further testing of different sample preparation steps such as pressurised liquid extraction and different SPE sorbents may have improved the method diversity for a larger suite of PhACs.

From the spatial study across London, pharmaceuticals most frequently detected and those reaching higher concentrations were collected from a site that was situated in close proximity to a WWTP. Thus, wild populations of animals most likely at risk are those areas which receive and are close to effluent outfalls from WWTPs. In addition, the study revealed that concentrations of

pharmaceuticals in surface waters did not translate well into animal body burden concentrations, due to factors such as temporal and spatial fluctuations in surface water contaminant levels. Therefore, to characterise risk it is proposed that monitoring campaigns should focus on the occurrence in biota, in addition to surface water. To avoid temporal flow limitations, passive sampling can be used to give a time-weighted average which may be more useful in monitoring campaigns. Furthermore, the available data for occurrence of pharmaceuticals in invertebrates is lacking and internalised concentrations are key to understanding the potential for risk in the environment. Thus future research efforts should focus on the use of biomonitoring for environmental risk assessment. To the authors knowledge the data presented herein was the first monitoring study for PhACs in invertebrates or fish in the UK (with the exception of endocrine disrupting compounds which have had much greater focus).

G. pulex were exposed *in vivo* to determine the toxicokinetics and further understand the potential of pharmaceuticals to bioconcentrate in invertebrates. The radiolabelled exposure of selected pharmaceuticals revealed that this group of compounds demonstrated a low potential to bioconcentrate and did not trigger any regulatory thresholds (BCF ≥ 2000). BCFs ranged from 12, for the β2 adrenergic receptor agonist terbutaline, to 212 for the tricyclic antidepressant imipramine. However, the models were further examined and it was observed that assumptions of the first order kinetic model concerning the constancy of the k_1 rate constant did not hold true for several of the compounds that were exposed. The deviation from constancy was further examined through meta-analysis of literature available data for organic micropollutants and further supported that selected compounds did not have a stable k_1 rate constant during the uptake phase. The deviations in the k_1 rate constant were potentially a compound

specific phenomenon that could be related to some specific physio-chemical property such as the sorption potential of the compound to the cuticle of the animals. As the model assumptions were demonstrated to be incorrect in particular cases it indicates that the currently used first order one compartment model may not be suitable to characterise the uptake and elimination of pharmaceuticals. Modification to the models, such as incorporating ionised and neutral speciation rate constants, could further improve the modelling approaches for estimation of accumulation. Alternatively, multi-compartment models may also give more reliable toxicokinetic data, thus future work should aim to develop kinetic models that can be used for pharmaceuticals in fish and invertebrates. However, the authors recommend that at present toxicokinetic data should be checked for lack-of-fit and to determine whether the uptake rate constant is consistent.

Further toxicokinetic exposures were performed using the developed LC-MS method presented in Chapter 2. The use of LC-MS was cross-validated with two compounds which demonstrated that the method can be used to determine uptake and elimination kinetics. In addition the analytical method was also used to study the biotransformation products of some of the selected pharmaceuticals including propranolol, carbamazepine and diazepam. The LC-MS determination revealed that *G. pulex* are capable of Phase I and Phase II metabolism of pharmaceuticals. The first pharmaceutical sulphate conjugate to be detected in *G. pulex* was presented in Chapter 4, indicating that propranolol was extensively biotransformed to hydroxypropranolol sulphate. Thus, may explain the reason that the selected pharmaceuticals were demonstrated to show low bioconcentration potentials. Metabolism is relatively understudied within environmental toxicology and could be important for determining

bioconcentration and the fate of PhACs once they are internalised within an organism. The advantage for pharmaceuticals here is that pre-clinical and clinical data could be used to inform studies about possible biotransformation products and whether they are pharmacologically active. With the advent of high mass accuracy instruments (i.e. Orbitrap) it is also possible that even without available reference materials tentative identification could be based on measured m/z and also retention time modelling. The ANNs used to model bioconcentration in this work have also been used to model retention time for unknowns in surface waters and wastewaters. Finally, the identification of biotransformed products would also be useful in assessing exposure-effect relationships. In addition, the use of LC-MS methodologies offer more accurate estimations of individual parameters (k_1/k_2) for parent and biotransformed compounds. However, the limitation of this approach was that LC-MS methods that do not determine metabolites may underestimate the total body burden of a compound (precursor + metabolite).

Modelling approaches were investigated for both uptake on passive sampling devices and in biota. Models were developed using ANNs and demonstrated reliable prediction of uptake onto POCIS devices. As PSDs can determine a time weighted average concentration, demonstrating that modelling uptake onto POCIS devices is valuable in the field for biomonitoring studies. The work presented in Chapter 5, showed a strong potential to reduce the need for labour and resource intensive experimental measurements. Furthermore, PSDs could have biomimetic properties that would be useful for bioconcentration tests. The correlation of R_s with BCFs showed a poor linear correlation. As PSDs do not actively metabolise and eliminate chemicals it may explain the weak correlation.

The ANN modelling was extended to a fish (*Cyprinus carpio*) database of bioconcentration factors as invertebrate datasets do not exist. Overall, the modelling approach showed relatively good predictive accuracy in fish and was related to molecular descriptors that would be expected to influence uptake and elimination. The developed fish model was applied to the invertebrate BCFs determined in Chapters 3 and 4. However, the model was not applicable to the invertebrate data. Thus, this indicated that either cross-species prediction, the prediction of pharmaceutical compounds or a combination of both hindered the predictive ability of the model. Therefore, a new model was developed for the invertebrate pharmaceutical BCF data. This model again showed good predictive accuracy using the same molecular descriptors in the fish model but with a different order of importance. Thus, it suggested that pharmaceutical predictions may not be applicable from models developed with more traditional contaminant substances such as PAHs, PCBs, organochlorines, etc. The limitation to this is that the modelling approaches were limited in the number of training and test cases. Thus, to fully validate the developed models, more data points were required. Nonetheless, the models demonstrated that the potential for ANNs in prediction of bioconcentration is suitable and holds promise from a regulatory perspective for risk assessment of the environment. As a final consideration, and whilst this work assessed the use of ANNs for predictive ability, there are many different types of machine learning methods that are available. Thus, the use of alternative *in silico* approaches such as deep neural networks, support vector machines and tree-based learning could potentially improve predictive ability and generalisability.

7.2 Future perspectives and challenges

Ecotoxicology remains an ever expanding field where future research needs have been highlighted in the current work presented. Perhaps the most essential focus should be on the use of invertebrates for environmental risk assessments. This phylum is of critical importance to ecosystem functioning and environmental services that are invaluable to anthropogenic activities. Thus, increased monitoring and vigilance concerning this group of organisms is required to further understand the risk of chemical pollutants in the environment. The extent of metabolism of chemical contaminants is also poorly understood as many studies overlook the role of biotransformation in occurrence, toxicokinetics and effect-based studies. Even with the predominance of fish studies, metabolism is still poorly characterised within this group of animals.

A further challenge within the field is to delineate the variance associated from laboratory based studies to those data acquired in the field. The differences are likely to stem from the complex interactions between biotic and abiotic factors in the field. Without understanding the relevance of laboratory based studies to a realistic exposure scenario our risk assessments can be considered as relatively low quality. In addition, the challenge of also delineating the effect of complex chemical mixtures is a very challenging prospect. However, due to the complexity it is likely that machine learning algorithms may offer a viable solution to these challenges. Thus, the inclusion of intelligent computing is essential within the field. Whilst the ANN modelling here showed a good potential for predictive ecotoxicology it requires further work and there are several other types of algorithms including those used in deep learning which is becoming more popular. Predictive ecotoxicology is also perhaps the only feasible solution to

assess the sheer volume of chemicals that are manufactured and that will eventually enter either terrestrial or aquatic environments.

The data presented demonstrated that pharmaceuticals are likely to have a relatively low bioconcentration or bioaccumulation potential with the exception of specific cases. Thus, whilst further work is required to fully conclude this statement, future efforts should also focus on whether pharmaceuticals have the potential to cause adverse effects at their innately low level concentrations. However, studies often fail to fully link cause to effects. Thus, it is essential that cause and effect relationships are understood (e.g. adverse outcome pathway framework) where emerging fields such as environmental metabolomics will be key to this knowledge discovery, so that risk characterisation and assessment is reliable.

Appendix

September 20, 2016
Volume 50
Number 18
pubs.acs.org/est

Environmental Science & Technology

In silico passive sampling prediction

CELEBRATING 50 YEARS

ACS Publications
Most Trusted. Most Cited. Most Read.

www.acs.org

analytical chemistry

Article

pubs.acs.org/ac

Prediction of Chromatographic Retention Time in High-Resolution Anti-Doping Screening Data Using Artificial Neural Networks

Thomas H. Miller, Alessandro Musenga, David A. Cowan, and Leon P. Barron*

Analytical & Environmental Sciences Division, School of Biomedical Sciences, King's College London, 150 Stamford Street, London SE1 9NH, United Kingdom

Supporting Information

ABSTRACT: The computational generation of gradient retention time data for retrospective detection of suspected sports doping species in postanalysis human urine sample data is presented herein. Retention data for a selection of 86 compounds included in the London 2012 Olympic and Paralympic Games drug testing schedule were used to train, verify, and test a range of computational models for this purpose. Spiked urine samples were analyzed using solid phase extraction followed by ultrahigh-pressure gradient liquid chromatography coupled to electrospray ionization high-resolution mass spectrometry. Most analyte retention times varied ≤0.2 min over the relatively short runtime of 10 min. Predicted retention times were within 0.5 min of experimental values for 12 out of 15 blind test compounds (largest error: 0.97 min). Minimizing the variance in predictive ability across replicate networks of identical architecture is presented for the first time along with a quantitative discussion of the contribution of each selected molecular descriptor toward the overall predicted value. The performance of neural computing predictions for isobaric compound retention time is also discussed. This work presents the application of neural networks to the prediction of gradient retention time in archived high-resolution urine analysis sample data for the first time in the field of anti-doping.

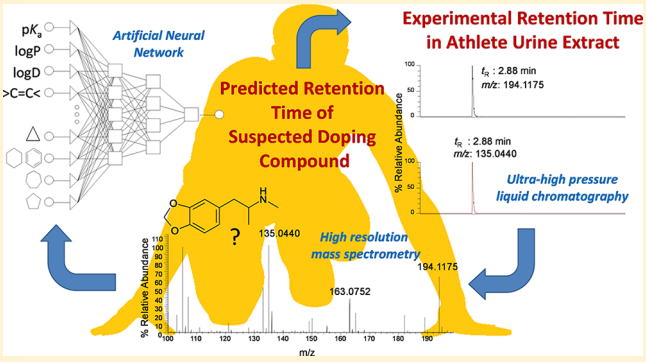

Drug testing in sport is becoming more and more challenging because cheats rapidly switch to new or designer drugs to avoid being caught by anti-doping tests. Because of this, in 2011 the World Anti-Doping Agency introduced a new section in the Prohibited List to specify that any substance not approved for human therapeutic use is prohibited.[1] Unfortunately however, there is normally a delay between new substances being used by cheats and the screening methods being implemented to detect them.

New technologies in analytical chemistry now exist which offer a much more flexible and universal approach compared to targeted-type screening analyses. In particular, liquid chromatography with full data capture high-resolution mass spectrometry (LC-HRMS) is becoming very popular for drug screening because it generally permits the addition of new analytes to a screening method with little/no modification to the method. One of the most promising features is the possibility for retrospective analysis of postacquisition data sets.[2,3] The flexibility of the HRMS approach was exploited in our laboratory during the London 2012 Olympic and Paralympic Games, where an LC-HRMS screen was employed for the detection of nearly 200 analytes within a single assay.[4] When permitted, in accordance with the International Standard for Laboratories,[5] all sample data acquired by this technique could be reprocessed and re-evaluated (for example, where intelligence becomes available about the potential use of new substances). However, several challenges still exist for retrospective detection of drug species in both new and archived samples. Analytical reference standards are not always available, especially for new or analogous compounds which may be synthesized relatively easily and with sufficient efficacy for practical use by athletes. Moreover, the exact operating conditions of analytical equipment may not be reproducible at a later date when a repeat analysis is required. For example, chromatograms generated from separate analyses even using the same columns may differ due to phase aging and loss of performance. Therefore, more effort is required to interpret the original data.

Predictive computing techniques, such as artificial neural networks (ANNs), can interpret underlying trends in complex data sets by learning from case examples. There are several types of ANN, but the feed-forward multilayer type is commonly the most used across a range of scientific applications such as analytical chemistry, environmental science, and molecular biology.[6−10] By interconnecting a set of input data with a series of hidden layer neurons, statistical weights and biases between them are systematically optimized toward producing a minimized error overall output. In the training phase, the ANN requires a known true value as a comparator and once an acceptable number of training cycles (or epochs) is determined,

Received: July 18, 2013
Accepted: September 22, 2013
Published: September 23, 2013

   dx.doi.org/10.1021/ac4024878 | Anal. Chem. 2013, 85, 10330−10337

the optimized ANN can be used to predict the same output where experimentally derived data is unavailable (i.e., a blind test). In this case, information about a set of analytes or chromatographic system (as inputs) and the experimentally derived retention data for standards within spiked, matrix-matched samples (as an output) could provide a useful body of information for an ANN to predict retention time retrospectively under the conditions observed at the time.

Research to characterize retention behavior has used linear solvation energy relationships (LSERs). These use solute descriptors and linear regression modeling to predict a retention parameter for a particular set of compounds. Both algorithm-based and predictive ANN approaches have incorporated the use of LSERs as inputs to estimate retention (usually as retention factor, k) across a number of chromatographic modes,[11−14] column formats,[15−17] for method optimization purposes,[18−22] to predict retention behavior across column formats, or to estimate the retention of unknowns.[23−25] Each LSER solute descriptor must be calculated, and each coefficient is usually obtained via measured retention data for a set of representative compounds. Thus, the time to produce an accurate LSER model can be significant (as well as especially challenging for ionizable compounds in particular[15,18]). As LSER coefficients for retention modeling also depend on observed retention on a stationary phase, factors such as the age of the phase may lead to observable differences and lower accuracy over time. Furthermore, the exact composition of a changing mobile phase under gradient conditions is very difficult to characterize and requires the inclusion of extra variables such as purity and individual system dwell time, for example. While the investigation of LSERs in retention modeling advances, ANN-based predictive approaches using alternative descriptors may therefore hold promise for more immediate application.

The aim of this work was to investigate the use of ANNs for the prediction of retention time in archived urine analysis data from the London 2012 Olympic and Paralympic Games using a method employing ultrahigh-pressure liquid chromatography coupled to HRMS. In particular, the selection of alternative molecular descriptor data to those used in LSERs is presented, along with a study of the ANN dependency on these descriptors and the variance across replicated ANNs. Lastly, this work aimed to assess whether ANNs could be used to discriminate structurally similar and/or isobaric species.

EXPERIMENTAL SECTION

Reagents. For a detailed account of all reagents used in the experimental please see the accompanying Supporting Information,[26] Table S2. For those compounds where no certificate of analysis was available, a solution of each compound was infused separately into the HRMS, and full scan data were acquired without any applied collisionally induced dissociation. The internal calibrator was caffeine. Identity was considered confirmed where m/z values within 2 ppm of the theoretical value were achieved along with a consistent fragmentation pattern.

Urine Sample Preparation. Drug-free urine samples were collected from 15 healthy volunteers, anonymized, divided into 1 mL aliquots, and stored at −10 °C until analysis. Each aliquot was then spiked with all reference compounds. Following addition of internal standards and glucuronide hydrolysis reagents (see SI, S 2.0), formic acid was added to the samples. This solution was then extracted on Bond-Elut Plexa PCX (60 mg, 3 mL barrel) solid phase extraction (SPE) cartridges (Agilent Technologies, Lake Forest, CA). Cartridges were preconditioned with 0.5 mL of methanol and 0.5 mL of 2% v/v formic acid. After loading, cartridges were washed with 1 mL each of 2% formic acid, water, and 20:80 v/v methanol/water. Elution was performed in 3 mL of 3% (v/v) ammonium hydroxide in methanol/acetonitrile (50:50, v/v). Extracts were dried under nitrogen at 60 °C and then reconstituted to 100 μL of 0.3% v/v formic acid in 95:5 v/v water/acetonitrile.

Instrumental Conditions. For all separations, a Waters Acquity UPLC ultrahigh-pressure liquid chromatographic system was used (Waters, Milford, MA, USA). Separations were performed on a Waters Acquity BEH-C_{18} column (2.1 × 50 mm, 1.7 μm). Gradient elution was performed as follows: 95:5 water/acetonitrile (both in 0.3% formic acid) for 0.5 min; then to 80:20 for 3.0 min; a linear ramp to 75:25 for 2.0 min; to 43:57 for 1.5 min; finally, to 10:90 for 1 min. Total time for the gradient elution was 8 min, followed by 2 min for re-equilibration. Separations were performed at 0.3 mL/min and at 30 °C throughout. The injection volume was 10 μL. The syringe and injector were washed sequentially with 0.2% formic acid in acetonitrile/water (30:70, v/v) and methanol/acetonitrile (90:10, v/v) up to 5 times each before every run to avoid carryover.

Detection was performed using fast polarity switching high-resolution mass spectrometry on an Exactive instrument (Thermo Fisher Scientific, San Jose, CA) equipped with a heated electrospray ionization (HESI-II) source. Enhanced-resolution mode was employed at 25 000 fwhm resolution. Three events occurred during each acquisition cycle by performing a full scan both in positive and negative ionization mode (both with disabled CID) followed by a full scan in positive ionization mode only with CID (HCD collision energy 30 eV). For a full description of other HRMS conditions, see the SI.

Molecular Descriptors, Neural Network Prediction Models and Architectures. Eighteen molecular descriptors were generated for each compound in the optimized network. Of these, 15 descriptors were computed using Parameter Client freeware (Virtual Computational Chemistry Laboratory, Munich, Germany) using canonical simplified molecular-input line entry system strings (SMILES, Table S1). Descriptors including pK_a, Ghose−Crippen and Moriguchi log P (AlogP or MlogP), number of double bonds (nDB), number of four- to nine-membered rings (nR04-nR09), and number of carbon or oxygen atoms (nC or nO) were used for network optimization. A full list of other descriptors is detailed in Table S1 and Figure 3. To investigate the use of predicted pK_a values, Percepta PhysChem Profiler (ACD Laboratories, ON, Canada) software was used. All predicted retention times (t_r^P) were performed using licensed ANN software (Trajan Software Ltd., Lincolnshire, U.K.) and compared with experimentally determined retention time (t_r^E). A selection of ANN types and architectures were investigated including linear, radial basis function (RBF), probabilistic neural networks (PNN), and multilayer perceptrons (MLPs).

RESULTS AND DISCUSSION

Experimentally Determined Chromatographic Retention Time and Reproducibility. This screening method was used during the 2012 Olympic Games for the detection of nearly 200 compounds in our ISO 17025 accredited laboratory. All of these species were detectable at concentrations corresponding to 50% of the WADA minimum required performance level[27] in force at that time in spiked, drug-free urine. On average, peak widths at baseline were of the order of ∼0.15 min with some

dx.doi.org/10.1021/ac4024878 | Anal. Chem. 2013, 85, 10330−10337

notable exceptions. For example, peak widths for morphine and etilefrine were 0.3 and 0.4 min, respectively, with some variability between urine samples. In order to examine the potential usefulness of computational tools for the retrospective generation of retention times in archived data, the reliability of generated chromatographic retention data was first evaluated. An in-depth evaluation of other method validation experiments including selectivity, sensitivity, and limits of detection is given elsewhere.[4] The evaluation of retention time reproducibility was performed using 15 different urine samples analyzed in groups of five with groups being analyzed on different days. Rather than expressing the reproducibility as a relative standard deviation, the maximum variation in retention time was preferred, since the aim was to establish a suitable detection window. The maximum within-day t_r^E variability was 0.22, 0.23, and 0.32 min for the three groups of five urine samples, respectively. Considering all 15 urine samples together (three groups, three different days), the maximum retention time variability was 0.35 min (i.e., ±0.175 min). Data analyses during screening were normally performed by reviewing extracted ion chromatograms with an m/z window of ±5 ppm and a retention time window of ±0.5 min. Athlete urine samples were always run using a "bracketed" approach to take into account phase aging and to ensure system performance throughout the entire batch acquisition.

Selection of Molecular Descriptors, Network Type and Architecture. By generating SMILES strings for each compound, an initial set of >200 diverse molecular descriptors were generated. While the instrumental screening method incorporated a larger number of compounds in practice, the number studied here was limited to those compounds with literature reported, experimentally derived pK_a values (as this descriptor was not initially available within the Parameter Client software). Given that the majority of these compounds were fully/partly ionized in the mobile phase, this descriptor was considered important for the potential prediction of retention times. Multiple network types and architectures were examined. On the whole, it was observed that use of a larger number of inputs did not offer advantages in terms of prediction accuracy, and a much smaller set was ultimately more practical and yielded better correlations. As a result, some descriptors were not included in the model which might have otherwise been expected under reversed-phase chromatography conditions such as analyte topological surface area, number of atoms containing lone pairs of electrons (e.g., oxygen or nitrogen atoms), or molecular weight.

Whether using a large or small input descriptor set, a linear-type network offered no detectable correlation (R^2 and slope both <0.1 in all cases) between t_r^E and t_r^P and irrespective of whether inputs were used for training, verification, or blind testing. As such, this network type was removed from consideration. Alternative network types, on the other hand, offered better performance and the best correlation coefficients achieved for each type ranged from R^2 = 0.86 (RBF) to 0.98 (4-layer MLP) with the slope (m) ranging from 0.97 (3-layer MLP) to 1.03 (PNN), again for all 86 compounds. The best network shown in Figure 1a was a feed-forward, back-propagation-type MLP with two hidden layers of five and four nodes, respectively. This 18:5:4:1 MLP architecture was trained using 18 molecular descriptors using 61 compounds. Verification was performed with 10 compounds, and training of the network was ceased when a minimum for residual error was observed (2000 epochs here). The network was "blind" tested using 15 additional compounds displaying structural variance and a spread of input

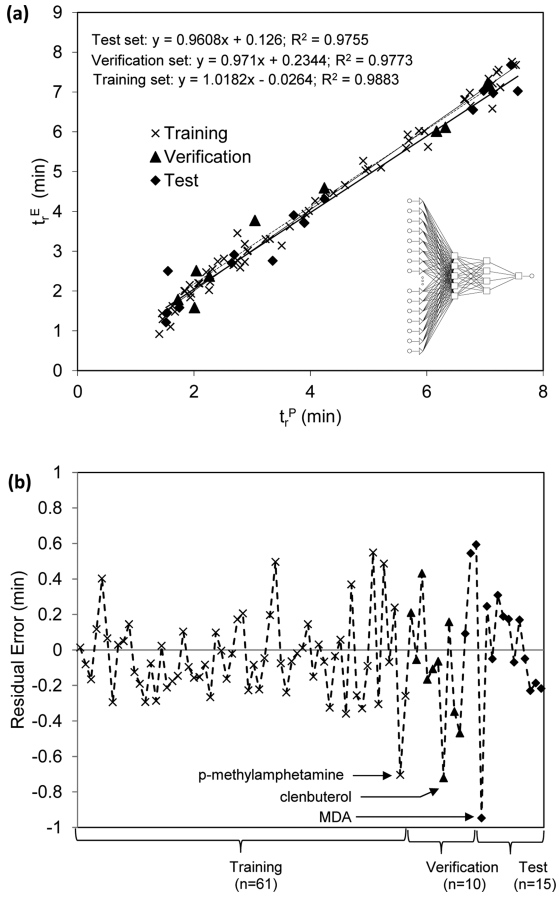

Figure 1. (a) Correlation between experimentally derived (t_r^E) and predicted (t_r^P) retention times using the optimized 18:5:4:1 multilayer perceptron (inset) trained for 2000 epochs; (b) residual errors in t_r^P using the optimized network for all analytes (n = 86). All raw data represented in Table S2 in the SI.

data and t_r^E data across the 10 min runtime. Data for t_r^E was not used by the ANN for test compounds (see Table S2), and performance was observed after training and verification. When the data set was divided into training, verification, and blind testing data, their respective m and R^2 values remained satisfactory and were also better than the corresponding plots for PNN, RBF, and 3-layer MLP networks. By examining the residual errors in the entire data set (Figure 1b), it was observed that retention time could be predicted within 0.5 min of t_r^E for 80 out of 86 compounds (~93%). This window was initially selected to cover the window employed during the experimental screening outlined above. In particular, t_r^P for 97%, 90%, and 80% of the training, verification, and test compounds, respectively, lay within this window. In fact, for the test set alone, this level of accuracy was maintained even to ±0.3 min of t_r^E. Therefore, these results show that this type of network offered promising predictive ability for most compounds in a relatively rapid gradient separation. The largest residual errors were observed for MDA, clenbuterol, and p-methylamphetamine at −0.947 min (used within the test set), −0.721 min (in verification set), and −0.704 min (in training set), respectively. Therefore, all species could be predicted within 1 min of t_r^E. However, it should be noted that this ANN was specifically tailored for this chromatographic system and method. If applied to other separation systems and modes, it is likely that similar descriptor and ANN optimization experiments would be

dx.doi.org/10.1021/ac4024878 | Anal. Chem. 2013, 85, 10330−10337

necessary. It is also important to note that the number of cases used here is relatively small in comparison to some work using several hundred training compounds for ANN modeling in both GC and LC.[28−30] Therefore, predicted retention times for unknowns with partial overlap to the training structural feature set may be limited. For example, larger molecules with markedly different logP or multiple pK_a values may make prediction problematic. Increasing the number of training cases may solve this in the future and perhaps more immediately through incorporation of non-WADA regulated compounds to expand the training set further.

Consistency in t_r^P Using Replicate Networks of Identical Type and Architecture. One of the main issues with ANNs is that training follows a random process toward minimizing the overall error. However, at larger numbers of training epochs, networks may become overtrained, and while training set errors may be minimized, the verification set error can increase (as it is not used by the software itself during the training process). The user often manually defines where training ceases by observing where the combined verification set residual error is at its lowest. In some cases, this verification error is lowest at lower numbers of training epochs but where training errors may remain high. Therefore, the variability in network connection weightings may be very different from network to network (even with identical architectures), and a balance is required potentially toward achieving some consistency. In this case, replicate networks (n = 10) using the optimized architecture were built to examine consistency and the range of t_r^P values for the verification, and test sets were plotted as Figure 2. Also, shown alongside each t_r^P entry in Figure 2 is the t_r^E variance of the analytical method for comparison purposes. By stopping training between 2000 and 3900 epochs in each case (where verification and training error combined were lowest), it was found that relatively consistent input weightings were achieved, and t_r^P performance could be maintained. To our knowledge, this has not been shown previously in predictive chromatographic retention studies. However, and despite their accuracies and consistencies, t_r^E data for 6/15 blind test set compounds still lay outside the range of t_r^P values generated by all 10 networks. Of these, and of particular interest, were three structurally related species: dimethylamphetamine, MDA, and phentermine. As synthetic compounds of this general type often only have slight variations in their molecular structure, this approach could be very useful to predict retention time for an array of related species where a reference standard is unavailable. The average t_r^P errors across all 10 networks for these three compounds were +0.97, −0.62, and −0.24 min (t_r^E = 2.76, 2.50, and 2.91 min), respectively. The lowest respective errors in t_r^P achieved by any one network were +0.59, −0.57, and −0.07 min. By comparison, and upon inspection of the average t_r^P error for other related species within the training set, compounds such as MDMA, benzphetamine, fenfluramine, and methamphetamine all performed reasonably well (average absolute error of 0.08−0.18 min from t_r^E for all 10 networks). However, and as noted earlier, average t_r^P error for *p*-methylamphetamine was the worst case in the training set at an average of −0.44 min across all networks. In the verification set, only one related compound, amphetamine, yielded 0.13 min error in t_r^P (t_r^E = 2.37 min). Therefore, these figures suggest that dimethylamphetamine and MDA may be unusual cases and that ANN predictive ability for unknowns may not, on average, be poorer for these types of compound. With regard to the general test set, all verification and test compound retention times could be predicted within 1 min

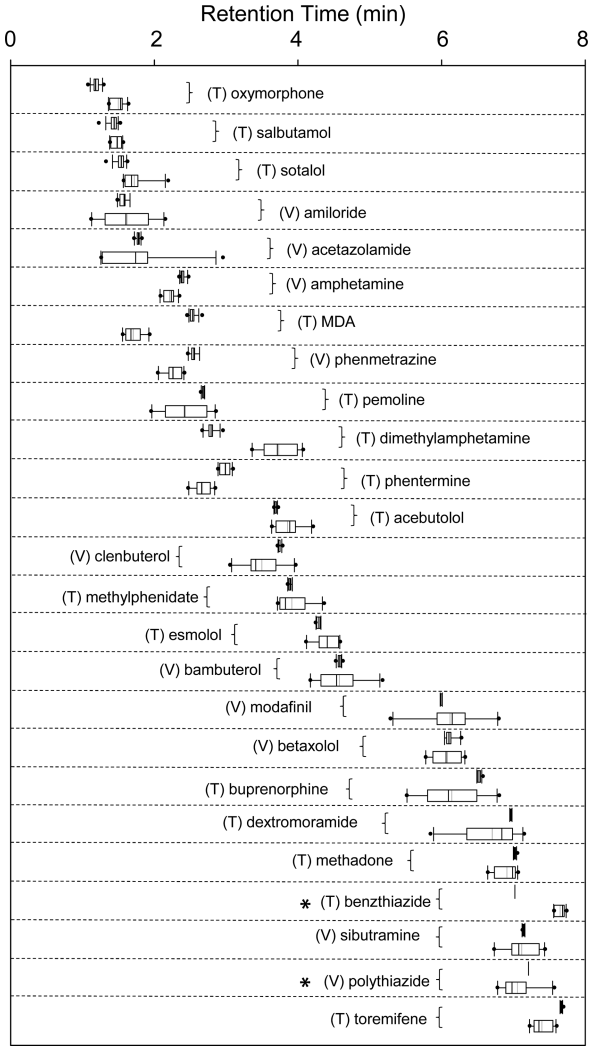

Figure 2. Paired comparisons of measured t_r^E variability (left-hand box) from n = 15 volunteer urine data versus t_r^P variability for n = 10 replicate 18:5:4:1 MLP networks (right-hand box). Data is presented for the verification (marked V) and blind-test compounds (marked T) only. Boxes represent 25−75th percentile, whiskers represent 10−90th percentile, and dots are outliers. Thin lines represent the median, and thick lines represent the mean. *Experimental variance was not determined for benthiazide and polythiazide, and reported values represent a single measurement. For all raw data (including for the training set), please refer to Tables S3 and S4 in the SI.

of t_r^E (with average ± standard deviation of t_r^P error for all 25 compounds = 0.3 ± 0.2 min for all 10 networks). In comparison to the maximum measured experimental variance above (0.35 min), the potential for using multiple networks to predict retention time shows promise. Therefore, the window for ANN accuracy could be set at ±0.5 min in total (again, also comparable to the experimental retention time window used in practice during the Olympic and Paralympic Games). Each network required a few minutes to build, train, verify, and test. Therefore, this in silico approach could represent a significant saving in terms of time, effort, and cost when used in combination with a semitargeted post-data-acquisition analysis of an athlete urine sample. Samples from the Olympic Games are stored for a total of 8 years in case reanalysis is required at a later date. However, this is not the case for most other sporting events where negative urine samples are discarded after 3 months unless probable cause

dx.doi.org/10.1021/ac4024878 | Anal. Chem. 2013, 85, 10330−10337

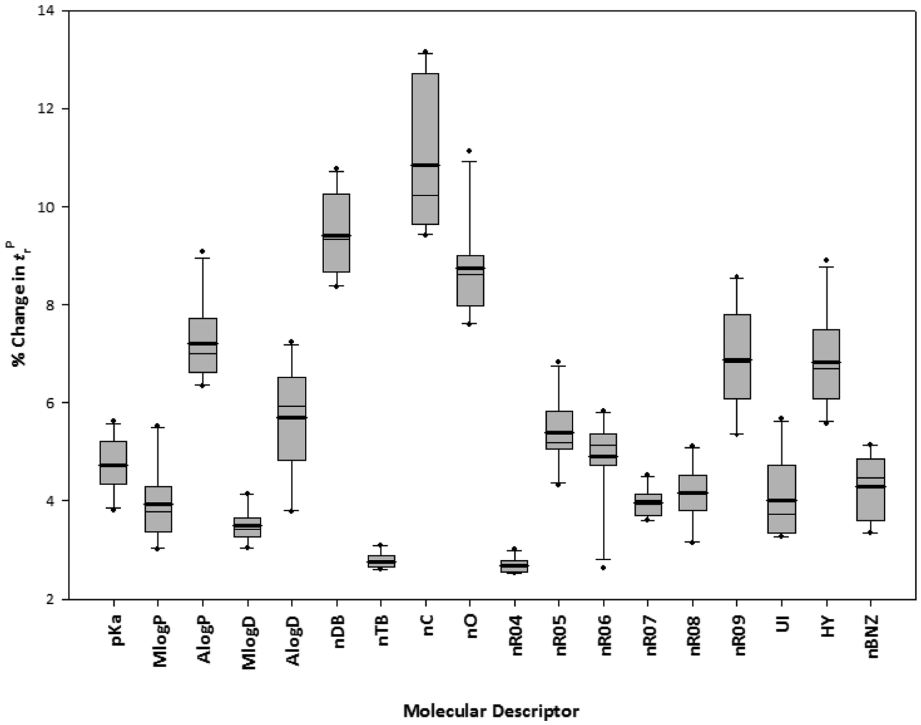

Figure 3. Percentage change in t_r^P relative to t_r^E upon systematic removal of each molecular descriptor from 10 replicate 15:5:4:1 MLP networks. Boxes include data from the 25th−75th percentile, the median (thin line), and the mean (thick line). Error bars include the 5th and 95th percentile, and dots represent outliers. For all molecular descriptor definitions, please see the Experimental Section or Table S1 in the SI.

for prolonged storage is justified. As several isobaric compounds can exist, HRMS data alone may be considered insufficient for this purpose. Therefore, the benefits of ANN predictions could aid in the investigation of doping before analysis, before the reporting stage, and after the reporting stage. When used in combination with HRMS, this gives added value, especially in directing which analytical reference materials are to be synthesized.

Molecular Descriptor Contribution toward t_r^P and Variance across Replicate Networks. Using the optimized MLP network, the contribution of each descriptor toward the generation of t_r^P was calculated for a single compound, A, by determining the absolute deviation, D_A, arising from sequential removal of one descriptor, i, at a time.[31] Data were inputted into eq 1 below to calculate the overall variance, V_A, arising for that compound. Values for V_A for each compound (denoted A = 1−61) were then used to determine the overall percentage change in accuracy of predicted retention time for all compounds, $\Delta t_r^P(\%)$, for the removal of that descriptor according to eq 2.

$$V_A = \frac{(D_A)_i}{\sum_{i=1-18}(D_A)_i} \quad (1)$$

$$\Delta t_r^P(\%) = \frac{100.V_A}{\sum_{A=1-61} V_A} \quad (2)$$

The contribution of each descriptor toward t_r^P was different. Using the optimized network, the top five contributing molecular descriptors (in decreasing order) to t_r^P for all compounds using the best network were nC (17.5% change in t_r^P when removed), nR09 (10.0% change), nO (9.9% change), nDB (8.8% change), and ALogP (8.2% change). Overall, some of these Δt_r^P values were unsurprising given that silica-C_{18} was used as a stationary phase. For experimentally derived descriptors, however, removal of pK_a only resulted in a change of 3.8%, but subsequent removal of AlogD and MlogD resulted in Δt_r^P of ≤3% each. As expected, descriptors such as the number nR04 having little or no incidence resulted in small Δt_r^P when removed. Examination of the data relative to t_r^E revealed that predictions were on the whole worse with the removal of selected descriptors.

To further understand the variability across replicate networks, this experiment was repeated for nine additional replicate networks. The contribution and variance of each descriptor is shown as Figure 3. Taking the mean values, the top five contributing molecular descriptors were the same as reported above, albeit in a slightly different order (from highest to lowest: nC, nDB, nO, AlogP, and nR09). This indicated that ANNs could be replicated with acceptable consistency in their operation. Interestingly, the largest measured variance in t_r^P across replicate ANNs for removal of a single descriptor was also observed as the most highly contributing descriptor, nC, at ∼11%. Removal of descriptors which resulted in the lowest % t_r^P variance were also those which were used least by ANNs during prediction. However, for the rest of the descriptor set, no trend was apparent to conclude that a more heavily used input would result in a higher variance when omitted from replicate networks. Furthermore, it was observed again that AlogP was repeatedly used in preference to MlogP in t_r predictions. MlogP has been shown previously to be a less accurate descriptor in comparison to other available computational models and in respect to experimentally derived logP.[32] Here, it was observed that MlogP data offered poorer discrimination between some species and especially those of isobaric mass. It was also apparent that this had a consequential effect on the use of AlogD over MlogD as a preferred input descriptor of the two. However, as a null % change was not observed by removing MlogP from the data set in any network, it was still used to some degree by ANNs.

dx.doi.org/10.1021/ac4024878 | Anal. Chem. 2013, 85, 10330−10337

Table 1. Performance of ANNs for Predictions of t_r for Isobaric and Isomeric Compounds

Compound	Monoisotopic Mass (Da) (Calculated *m/z* for $[M+H]^+$ ion)	Molecular Formula	Structure	AlogP (MlogP)	pK_a [ref.]	t_r^E (min)	t_r^P (min)
Metipranolol	309.1940 (310.2013)	$C_{17}H_{27}NO_4$	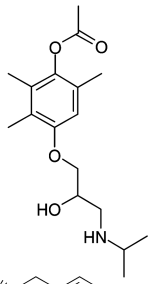	2.86 (2.35)	9.18[34]	5.62	6.02
Nadolol	309.1940 (310.2013)	$C_{17}H_{27}NO_4$	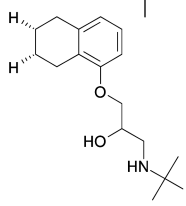	1.15 (1.36)	9.67[35]	2.81	2.52
Phentermine	149.1205 (150.1277)	$C_{10}H_{15}N$	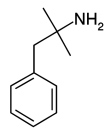	1.84 (2.55)	10.1[36]	2.91	2.69
Methamphetamine	149.1205 (150.1277)	$C_{10}H_{15}N$	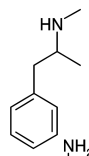	2.07 (2.55)	9.87[37]	2.59	2.80
p-methylamphetamine	149.1205 (150.1277)	$C_{10}H_{15}N$	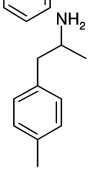	2.12 (2.55)	10.0[38]	3.45	2.75
Ephedrine SMILE: O[C@H](c1ccccc1)[C@@H](NC)C	165.1154 (166.1226)	$C_{10}H_{15}NO$	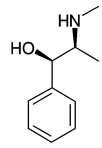	1.24 (1.66)	9.60[39]	2.00	1.84
Pseudoephedrine SMILE: O[C@@H](c1ccccc1)[C@@H](NC)C	165.1154 (166.1226)	$C_{10}H_{15}NO$	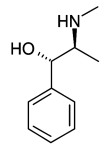	1.24 (1.66)	9.80[40]	2.00	1.85

Substitution of Experimentally Derived pK_a with Predicted pK_a. In practice, retention on reversed-phase media is likely to be heavily dependent on analyte logP and pK_a (and subsequently logD). The molecular description software used here could generate predicted analyte logP but not pK_a. The initial use of experimentally derived pK_a data from the literature overcame this problem and resulted in satisfactory t_r^P accuracy, as shown earlier. However, the availability of (or indeed the ability to generate) experimental pK_a significantly limits the usefulness of this ANN approach if it is to be used in postacquisition data mining. The use of a separate pK_a prediction software package was therefore investigated as a possible alternative. In an initial

dx.doi.org/10.1021/ac4024878 | *Anal. Chem.* 2013, 85, 10330−10337

experiment, experimentally derived pK_a data were removed from the input data set and replaced directly with predicted values into the pretrained ANN. With this substitution, a very slight reduction in t_r^P accuracy was observed, but it still remained acceptable (not shown). The network in Figure 1a generated an overall t_r^P/t_r^E correlation with a slope of 1.00 (R^2 = 0.98) compared with 0.95 (R^2 = 0.98), in this case across all 86 analytes. This obviously indicated some minor discrepancies between numerical values in these data sets. To further understand the importance of predicted versus experimentally derived pK_a as ANN inputs, a new network of identical architecture was retrained using computationally derived pK_a values to observe whether prediction accuracy could be restored. From this, it was seen that t_r^P accuracy was marginally worse using computed pK_a (Figure S3), but it still remained acceptable overall (overall slope = 0.94; R^2 = 0.95). In previous work, Livingstone also showed that predicted pK_a data can display inaccuracies up to 1.5 log units (using a larger compound set than here).[32] Thus, in ANN predictions of test compound retention time, experimentally derived data should be used where possible, but predicted values could potentially be substituted with awareness that accuracy may be slightly affected. The apparent pH of gradient LC eluent composition and its effect on analyte ionization (and hence AlogD or MlogD) is another consideration when using pK_a data derived experimentally from, or predicted in, aqueous media alone. The apparent pH of buffered aqueous−organic solutions has been shown to increase in up to 60% acetonitrile content. Similarly, a range of analyte pK_a values have also been shown to change in organic media.[33] Despite this, the use of aqueous-derived pK_a and experimental t_r data for training here resulted in no discernible loss in predictive ability across the gradient.

Performance of ANNs for Isobaric and Isomeric Compounds. If the ANN approach is to work in any realistic scenario with HRMS detection, then t_r^P accuracy should be high for compounds which are both isobaric and which display high degrees of structural similarity. From the list of compounds used in this study, several such cases existed (Table 1). Nadolol and metipranolol, both nonselective beta-blockers, display an identical mass and molecular formula, but differ slightly in their molecular structure and logP. Experimentally, this translated to a 2-fold difference in their retention times on this C_{18} phase. In this case, the optimized ANN performed well by predicting retention within 0.4 min for both compounds despite their high structural and pK_a similarity. Differences in logP could have accounted for this performance, as it was used here in the calculation of logD. The hydrophilic factor was calculated on the basis of the number of atoms in a molecule, the number of carbon atoms, and the number of hydrophilic groups (such as −OH or −NH for example). Unsaturation indices are calculated on the basis of the number of atoms containing proton deficiencies (e.g., aromatic rings or multiple bonds). Therefore, these latter two descriptors could be considered loosely correlated with logP on a fundamental level. Therefore, it might be somewhat unsurprising that this resulted in higher accuracy in this case given the nature of the separation mode.

In a second similar case involving the isobaric compounds, phentermine and methamphetamine t_r^P accuracy remained high (±0.22 min from t_r^E), but the order of elution was incorrectly predicted. Furthermore, t_r^P for a third isobaric compound, *p*-methylamphetamine was predicted as similar to that of phentermine and methamphetamine but was less accurate to its t_r^E at −0.7 min. All three of these compounds had identical MlogP data but only slightly differing AlogP and pK_a values. For the majority of the other 13 compounds eluting between methamphetamine and *p*-methylamphetamine and where descriptor diversity was more pronounced, this was less of a problem and t_r^P inaccuracy remained <0.5 min.

As a third case example, a set of diastereoisomers were chosen: ephedrine and pseudoephedrine. With identical mass, molecular formula, atomic connections, AlogP, and MlogP, it was somewhat unsurprising that they remained experimentally unresolved on this stationary phase. While their pK_a values were 0.3 units apart, and therefore a little further apart than of those species in the previous example, this had little effect on t_r^P (within 0.15 min of t_r^E for both species). While further work on the use of ANN using resolved diastereoisomers is required, it should be noted that the SMILES strings used here employ a string of characters that specified the structure of a selected molecule including its spatial arrangements. Optical isomerism in SMILES strings is designated by the '@' symbol. Where a single '@' is used, this represents the substituent groups giving rise to the chirality being positioned anticlockwise around the chiral atom, whereas two symbols ('@@') indicate clockwise orientation of the groups around the chiral atom. Therefore, as this may lead to a difference in molecular description, then this could be used by the ANN to differentiate such species. Naturally, this would also depend on the importance of the molecular descriptor itself to the generation of t_r^P (similar to Figure 3).

CONCLUSION

This work showed that ANNs could be used to predict chromatographic retention times for 93% of all selected doping-related compounds to within 0.5 min of their true value and to within 1 min for all other compounds. All compounds were detected in a urine extract matrix and were separated under gradient elution conditions. When applied to the prediction of unknowns alone, the same level of accuracy was maintained. Variance across replicate networks of identical architecture revealed that descriptors were used to similar degrees toward prediction of retention time. This approach could be used with quantitative structure−activity relationships alone, but it is recommended that analyte pK_a should be experimentally derived for ANN training. Ultimately, prediction of retention times in archived screening data would simplify and aid data reprocessing as a complementary tool to retrospective analysis both in the identification of unknowns and where reference materials were not originally included in the analytical screen. Therefore, the combination of full data capture HRMS and in silico predictive approaches could improve the capability for semitargeted urine sample screening before, during, and after major sporting events.

ASSOCIATED CONTENT

Supporting Information

Tables containing the raw data relating to experimental and predicted retention times for all compounds and experiments herein; molecular descriptors and associated ANN input data; all ANN models and architectures. This material is available free of charge via the Internet at http://pubs.acs.org.

AUTHOR INFORMATION

Corresponding Author

*E-mail: leon.barron@kcl.ac.uk. Fax: +44 20 7848 4980. Tel.: +44 20 7848 3842.

Notes

The authors declare no competing financial interest.

■ ACKNOWLEDGMENTS

The authors would like to thank Drs David Barlow and Mark Parkin for constructive discussion on earlier drafts of this manuscript.

■ REFERENCES

(1) World Anti-Doping Agency. The World Anti-Doping Code: The 2011 Prohibited List. Montreal, Canada, 2012.
(2) Thevis, M.; Thomas, A.; Schaenzer, W. *Anal. Bioanal. Chem.* **2011**, *401*, 405.
(3) Ojanpera, I.; Kolmonen, M.; Pelander, A. *Anal. Bioanal. Chem.* **2012**, *403*, 1203.
(4) Musenga, A.; Cowan, D. A. *J. Chromatogr., A* **2013**, *1288*, 82.
(5) World Anti-Doping Agency. International Standard for Laboratories, Version 7.0. Montreal, Canada, 2013.
(6) Alvarez-Guerra, M.; Ballabio, D.; Amigo, J. M.; Bro, R.; Viguri, J. R. *Environ. Pollut.* **2010**, *158*, 607.
(7) Zaqoot, H. A.; Baloch, A.; Ansari, A. K.; Unar, M. A. *Appl. Artif. Intell.* **2010**, *24*, 667.
(8) Nikolos, I. K.; Stergiadi, M.; Papadopoulou, M. P.; Karatzas, G. P. *Hydrol. Processes* **2008**, *22*, 3337.
(9) Shoji, R. *Curr. Comput.-Aided Drug Des.* **2005**, *1*, 65.
(10) Wang, X.K.; Liu, T.H.; Cao, S.Y. Predictions of Water and Sediment Processes Using Artificial Neural Networks in Small Watershed. In *Proceedings of the Ninth International Symposium on River Sedimentation, Vols. 1-4*, Yichang, China, October 18-21; Hu, C., Tan, Y., Zhou, Z., Shao, X., Liu, C., Eds.; 2004, pp 2312−2317.
(11) Morgan, P. E.; Barlow, D. J.; Hanna-Brown, M.; Flanagan, R. J. *Chromatographia* **2012**, *75*, 693.
(12) Madden, J. E.; Avdalovic, N.; Haddad, P. R.; Havel, J. *J. Chromatogr., A* **2001**, *910*, 173.
(13) Quiming, N. S.; Denola, N. L.; Bin Samsuri, S. R.; Saito, Y.; Jinno, K. *J. Sep. Sci.* **2008**, *31*, 1537.
(14) Gupta, V. K.; Khani, H.; Ahmadi-Roudi, B.; Mirakhorli, S.; Fereyduni, E.; Agarwal, S. *Talanta* **2011**, *83*, 1014.
(15) D'Archivio, A. A.; Giannitto, A.; Maggi, M. A.; Ruggieri, F. *Anal. Chim. Acta* **2012**, *717*, 52.
(16) D'Archivio, A. A.; Incani, A.; Ruggieri, F. *J. Chromatogr., A* **2011**, *1218*, 8679.
(17) D'Archivio, A. A.; Maggi, M. A.; Ruggieri, F. *J. Sep. Sci.* **2010**, *33*, 155.
(18) D'Archivio, A. A.; Maggi, M. A.; Ruggieri, F. *Anal. Chim. Acta* **2011**, *690*, 35.
(19) D'Archivio, A. A.; Ruggieri, F.; Mazzeo, P.; Tettamanti, E. *Anal. Chim. Acta* **2007**, *593*, 140.
(20) Berges, R.; Sanz-Nebot, V.; Barbosa, J. *J. Chromatogr., A* **2000**, *869*, 27.
(21) Pompe, M.; Razinger, M.; Novic, M.; Veber, M. *Anal. Chim. Acta* **1997**, *348*, 215.
(22) Quiming, N. S.; Denola, N. L.; Ueta, I.; Saito, Y.; Tatematsu, S.; Jinno, K. *Anal. Chim. Acta* **2007**, *598*, 41.
(23) Shinoda, K.; Sugimoto, M.; Yachie, N.; Sugiyama, N.; Masuda, T.; Robert, M.; Soga, T.; Tomita, M. *J. Proteome Res.* **2006**, *5*, 3312.
(24) Petritis, K.; Kangas, L. J.; Yan, B.; Monroe, M. E.; Strittmatter, E. F.; Qjan, W.-J.; Adkins, J. N.; Moore, R. J.; Xu, Y.; Lipton, M. S.; Ii, D. G. C.; Smith, R. D. *Anal. Chem.* **2006**, *78*, 5026.
(25) Malenovic, A.; Jancic-Stojanovic, B.; Kostic, N.; Ivanovic, D.; Medenica, M. *Chromatographia* **2011**, *73*, 993.
(26) Abraham, M. H.; Ibrahim, A.; A.M., Z. *J. Chromatogr., A* **2004**, 29.
(27) World Anti-Doping Agency. Technical Document TD2010MRPL. Montreal, Canada, 2010.
(28) Kaliszan, R. *Chem. Rev.* **2007**, *107*, 3212.
(29) Héberger, K. *J. Chromatogr., A* **2007**, *1158*, 273.
(30) Albaugh, D. R.; Hall, L. M.; Hill, D. W.; Kertesz, T. M.; Parham, M.; Hall, L. H.; Grant, D. F. *J. Chem. Inf. Model.* **2009**, *49*, 788.
(31) Barron, L.; Havel, J.; Purcell, M.; Szpak, M.; Kelleher, B.; Paull, B. *Analyst* **2009**, *134*, 663.
(32) Livingstone, D. J.. Theoretical Property Predictions. In *Frontiers in Medicinal Chemistry*; Atta-ur-Rahman, Reitz, A. B.; Bentham Science Publishers, Ltd.: The Netherlands, 2004, p 545.
(33) Subirats, X.; Roses, M.; Bosch, E. *Sep. Purif. Rev.* **2007**, *36*, 231.
(34) Schappler, J.; Guillarme, D.; Rudaz, S.; Veuthey, J.-L. *Electrophoresis* **2008**, *29*, 11.
(35) Devlin, R. G.; Duchin, K. L.; Fleiss, P. M. *Br. J. Clin. Pharmacol.* **1981**, *12*, 393.
(36) Katsu, T.; Ido, K.; Kataoka, K. *Anal. Sci.* **2001**, *17*, 745.
(37) Fan, Y.; Feng, Y.-Q.; Zhang, J.-T.; Da, S.-L.; Zhang, M. *J. Chromatogr., A* **2005**, *1074*, 9.
(38) Twitchett, P. J.; Gorvin, A. E. P.; Moffat, A. C. *J. Chromatogr.* **1976**, *120*, 359.
(39) Liu, X.; Pohl, C.; Woodruff, A.; Chen, J. *J. Chromatogr., A* **2011**, *1218*, 3407.
(40) Jones, R.; Marnham, G. *J. Pharm. Pharmacol.* **1980**, *32*, 820.

■ NOTE ADDED AFTER ASAP PUBLICATION

This paper was published on the Web on October 4, 2013. Table 1 was corrected, and a revision to the text was added. The corrected version was reposted on October 8, 2013.

Science of the Total Environment 511 (2015) 153–160

Contents lists available at ScienceDirect

Science of the Total Environment

journal homepage: www.elsevier.com/locate/scitotenv

Pharmaceuticals in the freshwater invertebrate, *Gammarus pulex*, determined using pulverised liquid extraction, solid phase extraction and liquid chromatography–tandem mass spectrometry

Thomas H. Miller [a], Gillian L. McEneff [a], Rebecca J. Brown [b,1], Stewart F. Owen [b], Nicolas R. Bury [a], Leon P. Barron [a,*]

[a] Analytical & Environmental Sciences Division, Faculty of Life Sciences and Medicine, King's College London, 150 Stamford Street, London SE1 9NH, UK
[b] AstraZeneca, Global Environment, Alderley Park, Macclesfield, Cheshire SK10 4TF, UK

HIGHLIGHTS

- Analytical method considerations for small invertebrates are presented.
- Application of method to screening of *G. pulex* for 29 pharmaceuticals
- Method validated for quantitation of 10 pharmaceuticals in *G. pulex*
- Six pharmaceutical residues were determined up to 36 ng g^{-1} in *G. pulex*.
- Five identified compounds in *G. pulex* are present in river water up to 344 ng/L.

GRAPHICAL ABSTRACT

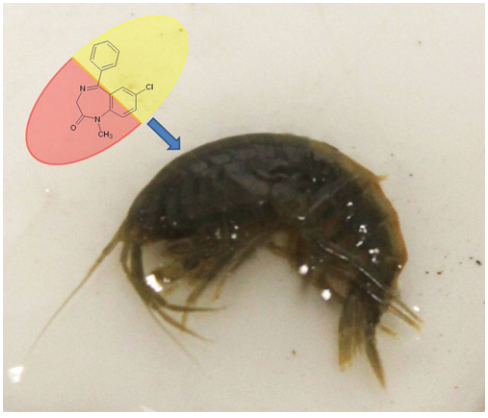

ARTICLE INFO

Article history:
Received 17 November 2014
Received in revised form 12 December 2014
Accepted 13 December 2014
Available online 23 December 2014

Editor: D. Barcelo

Keywords:
Gammarus pulex
Environmental analysis
Emerging contaminants
Occurrence

ABSTRACT

The development, characterisation and application of a new analytical method for multi-residue PPCP determination in the freshwater amphipod, *Gammarus pulex* are presented. Analysis was performed using pulverised liquid extraction (PuLE), solid phase extraction (SPE) and liquid chromatography–tandem mass spectrometry (LC–MS/MS). Qualitative method performance offered excellent limits of detection at <20 ng g^{-1} for 18 out of 29 compounds. For quantitative application, linearity and precision were considered acceptable for 10 compounds across the ng-μg g^{-1} range ($R^2 \geq 0.99$; ≤20% relative standard deviation respectively). The method was applied to the analysis of *G. pulex* and river water sourced from six tributaries of the River Thames. Carbamazepine, diazepam, nimesulide, trimethoprim and warfarin were determined in *G. pulex* samples at low ng g^{-1} (dry weight) concentrations across these sites. Temazepam and diclofenac were also detected, but were not quantifiable. Six pharmaceuticals were quantified in surface waters across the eight sites at concentrations ranging from 3 to 344 ng L^{-1}. The possibility for confirmatory detection and subsequent quantification of pharmaceutical residues in benthic organisms such as *G. pulex* will enable further understanding on the susceptibility and ecological effects of PPCPs in the aquatic environment.

* Corresponding author.
E-mail address: leon.barron@kcl.ac.uk (L.P. Barron).
[1] Current Address: WCA, Brunel House, Volunteer Way, Faringdon, Oxfordshire, SN7 7YR.

http://dx.doi.org/10.1016/j.scitotenv.2014.12.034
0048-9697/

1. Introduction

The continuous influx of pharmaceuticals and personal care products (PPCPs) into the aquatic environment via wastewater treatment plant (WWTP) effluent is driving research into the field of ecotoxicology due to a rising concern for the health of biota residing in contaminated waters. Numerous monitoring studies have been carried out to assess the extent of PPCP contamination in wastewater effluent and impacted surface waters such as rivers, lakes and seawater with PPCP residues detected up to μg L^{-1} concentrations (Ashton et al., 2004; Behera et al., 2011; Brown et al., 2006; Carmona et al., 2014; Kosma et al., 2010; McEneff et al., 2014; Roberts and Thomas, 2006; Thomas and Hilton, 2004; Vazquez-Roig et al., 2013). The release of pharmaceuticals at low μg L^{-1} concentrations has been shown to impact on the quality of the surrounding aquatic environment in Europe and America (Corcoran et al., 2010; Huerta et al., 2012). However the paradigm of transient exposure to temporal flow makes the environmental risk assessment complex. Internal concentrations are clearly the key to better understanding (and therefore prediction) of risk (Rand-Weaver et al., 2013). The exposure of wild-caught and caged biota to contaminated surface waters over extended periods of time have revealed the potential for PPCP uptake and subsequent adverse chronic effects (Dodder et al., 2014; Gatidou et al., 2010; Huerta et al., 2013; Subedi et al., 2012). It is widely believed that bioaccumulation of contaminants occurs through passive diffusion where the hydrophobicity of the compound (log*P*) largely describes their permeability through membranes (Hamelink and Spacie, 1977; McKim et al., 1985). However, due to their ability to ionise and undergo various transformation processes, there is mounting evidence to support carrier mediated transport of PPCPs through facilitated diffusion and active transport (Dobson and Kell, 2008; Schultz et al., 2010). PPCP occurrence data in aquatic biota is of particular importance as results may highlight highly bioaccumulative compounds that may direct the attention of future risk assessment and management strategies for PPCPs. Furthermore, and given that several thousand pharmaceutical compounds currently exist on the market, this represents a significant challenge. It is of interest to enable discovery of PPCPs in the environment, which might not otherwise be predicted using simple log*P*-based approaches and analytical methods to detect these are urgently required to aid in prioritisation efforts.

Aside from localised monitoring programmes, the only international body in the EU to recognise PPCPs as an emerging environmental concern was, until recently, the Oslo–Paris Convention for the Protection of the Marine Environment of the North-East Atlantic (OSPAR) Commission. Pharmaceuticals remained outside the scope for regulation and formal monitoring under the European Water Framework Directive (WFD). However, following the results of numerous European monitoring studies at a national level, the list of priority pollutants has recently been revised with the addition of a 'watch list' of new compounds. This list includes the anti-inflammatory, diclofenac and the hormones, 17α-ethinylestradiol and 17β-estradiol, which are not subject to regulation, but are instead closely monitored in EU surface waters for possible future addition to the priority list (Commission, 2012).

Gammarus pulex has many attributes for use in biomonitoring studies. It is a freshwater benthic dwelling detritivore which has an important role in freshwater food chains as a food source for other invertebrates, fish and birds (Friberg et al., 1994; Maltby et al., 2002). *G. pulex* is widely distributed in freshwater rivers and tributaries across Europe and can be collected in large numbers using simple kick sampling techniques. More importantly *G. pulex* has already been used as a model organism for assessing both the adverse effects (De Lange et al., 2006, 2009) and uptake potential of PPCPs (Meredith-Williams et al., 2012) as well as other common pollutants (Ashauer et al., 2012; Nyman et al., 2012). The main disadvantage of using *G. pulex* in biomonitoring is their small size which poses a significant analytical challenge for multi-residue screening. A trade-off exists between achieving suitable method sensitivity and using the minimum number of specimens to make a single measurement. Very few methods exist for PPCP residue analysis of such small species in the aquatic environment. It is generally accepted that liquid or gas chromatography coupled to mass spectrometry offers the sensitivity and selectivity required. It has been successfully applied to the analysis of other smaller invertebrate species such as *Chironomus tentans* and *Hyallela azteca* (Dussault et al., 2009; Klosterhaus et al., 2013). However, robust analytical methods to determine PPCP residue occurrence in *G. pulex* are still lacking.

This paper presents, for the first time, the occurrence and relative distribution of PPCPs in surface waters and *G. pulex* collected from several tributaries located in the greater London catchment area. The aim of this study was to evaluate the extent of contamination in surface waters flowing into the River Thames and to investigate the potential for the crustacean, *G. pulex*, to be utilised in future monitoring studies as an indicator for PPCP pollution.

2. Materials and methods

2.1. Reagents, chemicals and consumables

HPLC grade methanol, acetonitrile, acetone, ethyl acetate, dichloromethane and dimethyldichlorosiloxane were purchased from Fischer Scientific (Loughborough, UK). Analytical grade ammonium acetate was sourced from Sigma-Aldrich (Dorset, UK). Propranolol hydrochloride, ketoprofen, diclofenac sodium salt, bezafibrate, warfarin, flurbiprofen, indomethacin, ibuprofen sodium salt, meclofenamic acid sodium salt, gemfibrozil, atenolol, sulfamethoxazole, sulfamethazine sodium salt, furosemide, carbamazepine, nimesulide, (±)-metoprolol (+)-tartrate salt, triclocarban, cimetidine, ranitidine, antipyrin, temazepam, diazepam, fluoxetine, nifedipine and mefenamic acid were all obtained from Sigma-Aldrich (Steinheim, Germany). Trimethoprim, caffeine, and naproxen were ordered from Fluka (Buchs, Switzerland). Stable isotope-labelled standards including carbamazepine-d_{10}, propranolol-d_7, temazepam-d_5 and diazepam-d_5 were ordered from Sigma-Aldrich. Trimethoprim-d_3 and warfarin-d_5 were ordered from QMX Laboratories (Essex, UK). All pharmaceuticals were of a purity of ≥97%. Ultra-pure water was obtained from a Millipore Milli-Q water purification system with a specific resistance of 18.3 M Ω cm or greater (Millipore, Bedford, MA, USA). Stock solutions (1 mg mL^{-1}) were prepared in methanol and stored in silanised amber vials (40 mL). Working solutions were prepared daily in ultra-pure water, as required. All solutions were stored at 4 °C and in the dark for optimum stability.

2.2. Sample collection and preparation

G. pulex and surface waters were sourced from eight tributaries of the River Thames, UK. These were spread across the greater London catchment area and included the River Wandle (Sites 1 and 2), the River Quaggy (Site 3), the River Ravenstone (Site 4), the River Cray (Sites 5 and 6), the River Darent (Site 7) and Beverley Brook (Site 8). The specific locations of the selected sites are shown in Fig. 1. Adult specimens were collected in September 2012 via the kick sampling netting method and weighed >5 mg (wet weight). Samples were transported back to the laboratory in Nalgene™ flasks containing 500 mL of freshwater obtained from each corresponding sampling site. A bulk sample of *G. pulex* from Site 1 was used in all analytical method optimisation experiments and was taken 6 months prior to samples from the same site used for analyte reporting. *G. pulex* were wiped free of debris, rinsed immediately with ultra-pure water (n = 3) and gently blotted dry before freezing at −20 °C. A separate 1 L grab sample of surface water at each site was also collected and transported back to the laboratory in 500 mL Nalgene™ flasks. Water samples were also frozen at −20 °C until analysis. All glassware was washed in HPLC-grade solvents prior to use and on a monthly basis silanised by washing each vessel with 10% (*v*/*v*) dichlorodimethylsilane

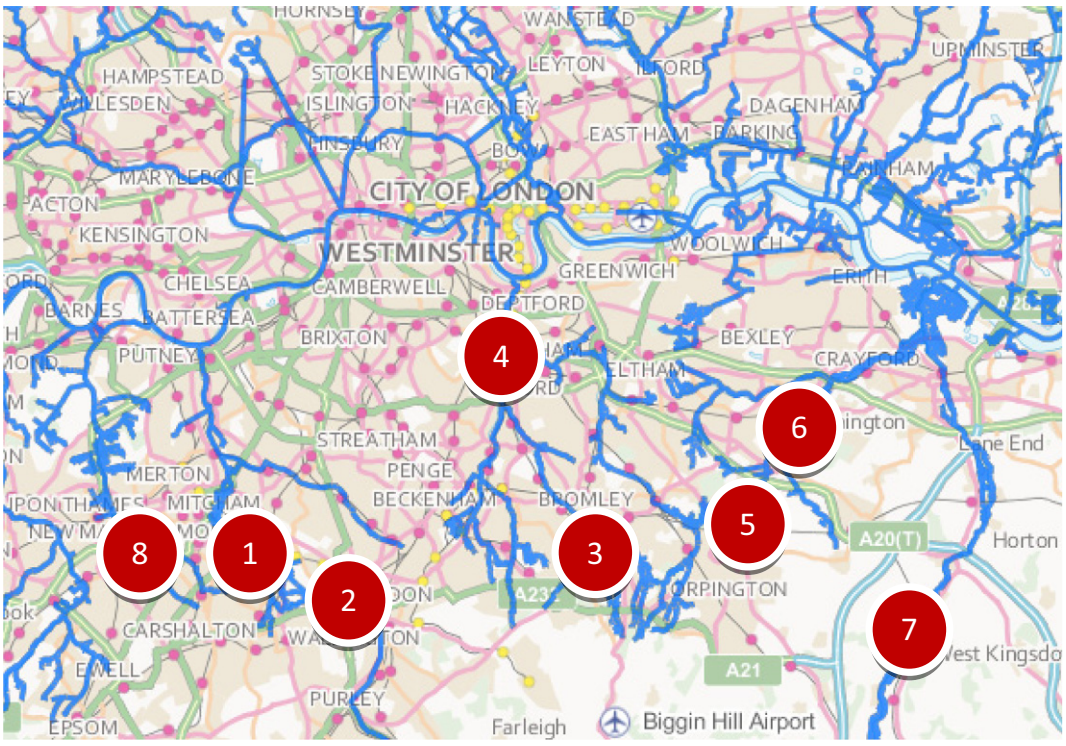

Fig. 1. Locations from which samples of *G. pulex* and surface waters were collected. Sites 1 and 2 — River Wandle, Site 3 — River Quaggy, Site 4 — River Ravensbourne, Sites 5 and 6 — River Cray, Site 7 — River Darent, and Site 8 — Beverley Brook. Map used with permission and contains Environment Agency information (© Environment Agency and database right).

solution in dichloromethane (n = 3) and followed by a sequence of triplicate rinses with each of dichloromethane, methanol and ultrapure water respectively.

2.3. Sample extraction and clean-up

Prior to extraction, frozen *G. pulex* samples were freeze-dried at −50 °C under vacuum for 24 h and ground into a coarse material using a clean pestle and mortar. Pulverised liquid extraction (PuLE) was performed on an Ultra-Turrax® tube driver (IKA, Staufen, Germany). The tube driver was used with an extraction vessel for sample homogenisation and extraction. The contents of the extraction tube were agitated and pulverised at a set rate by means of a rotor and glass beads located inside the tube. For each analysis, freeze-dried composite sample material from each sampling site (0.1 g) was transferred to a 20 mL extraction tube (IKA) with any necessary spiking carried out directly onto the solid matrix using a 100 μL volume of an appropriate working solution followed by 5 mL of acetonitrile. Two glass beads (diameter = 5 mm) were then added to the extraction tube to enable further pulverisation of the sample and the tube agitated at 2500 rotations per minute (rpm) for 5 min (optimised). Following extraction and settling, an aliquot of the supernatant (4.5 mL) was diluted to 100 mL with 10 mM ammonium acetate in ultra-pure water (pH 6.5). Solid phase extraction (SPE) was then carried out as in previously published work on a similar selection of compounds (Barron et al., 2008) on the diluted sample using Oasis HLB cartridges (6 mL, 200 mg, Waters Corp., Hertfordshire, UK). Before loading of the sample, SPE cartridges were first conditioned with 6 mL of methanol and 6 mL of ultra-pure water. After sample extraction, cartridges were then washed with 1 mL ultra-pure water and dried for ~30 min under a vacuum. Sample extracts were eluted with 10 mL of 50:50 (*v*/*v*) ethyl acetate:acetone and dried under pure nitrogen (1.0 bar) and heated at 30 °C using a TurboVap (Biotage, Uppsala, Sweden). Extract residues were reconstituted in 0.5 mL 90:10 (*v*/*v*) 10 mM ammonium acetate in water:acetonitrile. Surface water samples (100 mL) were adjusted to pH 6.5 with ammonium acetate (1 mL of a 1 M solution). Water samples then underwent SPE and reconstitution as described above. Any necessary spiking or liquid volume measurements were carried out using positive displacement pipettes (Gilson Microman, Villiers-le-Bel, France).

2.4. Instrumental conditions

A previously published chromatographic method for the analysis of PPCPs in soil and sludge was adapted and applied to a biological matrix (*G. pulex*) (Barron et al., 2008). Briefly, liquid chromatography (LC) was performed on an Agilent 1100 series LC system (Agilent Technologies, Cheshire, UK) using a Waters SunFire C_{18} column (3.5 μm, 2.1 mm × 150 mm, Waters Corp., Milford, MA, USA) with a KrudKatcher™ Ultra guard column (0.1 mm ID, 0.5 μm filter, Phenomenex, Macclesfield, UK) at a flow rate of 0.2 mL min^{-1} and an injection volume of 20 μL. Mobile phases were 90:10 (*v*/*v*) 10 mM ammonium acetate in water:acetonitrile (A) and 20:80 (*v*/*v*) 10 mM ammonium acetate in water:acetonitrile (B). The profile followed a linear ramp of mobile phase B which increased to 10% at 5 min, 35% at 28 min, 40% at 35 min, 50% at 40 min and 100% at 55 min and was held for a further 7.5 min before returning to initial conditions. Re-equilibration time was 12.5 min resulting in an overall run time of 75 min. Detection and quantification was carried out with a Waters Quattro triple quadrupole mass spectrometer (Waters Corp., Milford, MA, USA) equipped with an atmospheric pressure interface–electrospray ionisation (API–ESI) source. Mass spectrometric (MS) analysis was carried out in selected reaction monitoring (SRM) mode using positive–negative ionisation polarity switching. A scan rate of 0.03 min was utilised with a minimum of 15 points per peak measuring ±0.5 mass units for all transitions monitored. Confirmation of the selected compounds was achieved using both retention time and two transitions (MSn^2 fragment ions where possible) with the most intense fragment ion selected for analyte quantification (Table 1). MS conditions as well as all SRM transitions are summarised in Tables S1 and S2 of the supplementary information and were determined by

direct infusion using a syringe pump which delivered 300 mL h^{-1} of analyte solution.

2.5. Method performance characteristics and quality control

For this study, method performance characteristics are presented for *G. pulex* only. Matrix-matched calibration curves were generated for biota to assess method performance. Linearity was determined by measuring the peak area at concentrations from 0.01 to 10 μg g^{-1} for the *G. pulex* ($n \geq 5$ for each compound). Limits of detection (LODs) were determined as the lowest concentration of analyte which produced a signal-to-noise (S/N) ratio of 3:1. Limits of quantification (LOQs) were determined as that analyte concentration to give an S/N ratio of 10:1. Both LOD and LOQ were calculated using the S/N ratios of low concentration spiked samples and precision checked at this level for $n = 6$ replicates to ensure satisfactory performance. Instrumental retention time and method precision (intra-day) experiments were performed for $n = 6$ replicate injections of a biotic sample spiked at 1 μg g^{-1}. Method accuracy (intra-day) was determined using a biotic sample spiked at 20 ng g^{-1} for all compounds except for sulfamethazine, metoprolol, propranolol, nimesulide and nifedipine, where the biotic sample was spiked at 75 ng g^{-1} ($n \geq 3$). Recovery was determined by comparing spiked samples at 1 μg g^{-1} in *G. pulex* ($n = 6$ and which was also used to assess mid-range method precision) to sample extracts spiked post-extraction ($n = 3$) at the expected final concentration. Control samples were also analysed for background correction purposes, where necessary. The measurement of ion suppression or enhancement in ESI–MS involved the comparison of sample extracts spiked post-extraction to a 100 ng g^{-1} working solution mixture ($n = 3$). The target analytes in both surface waters and biota were quantified based on their peak areas relative to that of an isotopically-labelled internal standard or, where unavailable, by external matrix-matched calibration. Relative recovery in *G. pulex* was measured following the analysis of spiked biotic samples (analytes and the internal standard at 100 ng g^{-1} each) by comparing the analyte peak areas to that of the internal standard ($n = 12$).

Mobile phase A was injected between samples from each site as well as between matrix-matched standards and controls to minimise the possibility of carry over. Direct infusion of a propranolol standard (1 μg mL^{-1}) was carried out before each batch analysis to ensure that the MS was operating satisfactorily. None of the targeted analytes were detected in any solvents, reagents or ultra-pure water used in this study.

3. Results and discussion

3.1. Optimisation of analytical methods for G. pulex

The presence of pharmaceuticals in aquatic organisms, particularly molluscs, has been previously investigated using extraction techniques such as pressurised liquid extraction (PLE) or ultrasound-assisted solvent extraction which involve the use of high temperatures, pressures and/or relatively large volumes of organic solvent (Cueva-Mestanza et al., 2008; McEneff et al., 2013). Other studies have utilised PuLE as a simple and fast extraction method for the quantification of pharmaceuticals in solid dosage forms (Kok and Debets, 2001). Due to the complexity of biological tissues (and especially here where keratinous material was present), PuLE was used here to simultaneously blend and extract all material before SPE. For this purpose, a specially designed extraction vial was used and was equipped with a rotor for agitation of the sample, liquid and two glass beads. The beads were required for satisfactory agitation and pulverisation of the *G. pulex* material, but also were considered valuable to potentially confer flexibility in the future for extraction of whole tissues/specimens where necessary. Sorption to glass beads was briefly investigated here by performing the extraction procedure on a mixed 1 μg mL^{-1} standard solution of all analytes prepared in the extraction solvent. The use of silanised glass beads did not yield higher analyte recoveries than those

Table 1
Method performance characteristics for *G. pulex* analysis.

Compound	$t_R \pm$ SD[a] (min) $n = 6$	SRM transitions	ESI Mode	Range (ng g^{-1})	R^{2b} $n \geq 5$	LOD (ng g^{-1}) $n = 6$	LOQ ± SD (ng g^{-1}) $n = 6$	Intra-day accuracy ± SD (%) $n \geq 3$	Absolute recovery & intra-day precision (%) $n = 6$	Ion suppression (%) $n = 6$
Sulfamethazine	11.9 ± 0.1	(279 → 186) (279 → 124)	(+)	25–10,000	0.9987	4	15 ± 6[d]	95 ± 3[f]	41 ± 2	11 ± 2
Trimethoprim	16.8 ± 0.1	(291 → 230) (291 → 123)	(+)	10–10,000	0.9987	2	5 ± 4[c]	126 ± 31[g]	65 ± 1	13 ± 6
Metoprolol	19.7 ± 0.1	(268 → 116) (268 → 159)	(+)	10–10,000	0.9992	1	4 ± 1[d]	100 ± 6[f]	71 ± 5	11 ± 2
Propranolol	30.9 ± 0.5	(260 → 116) (260 → 183)	(+)	50–10,000	0.9952	13	61 ± 9[e]	81 ± 8[f]	52 ± 11	56 ± 4
Carbamazepine	31.3 ± 0.1	(237 → 194)	(+)	25–10,000	0.9983	2	6 ± 1[c]	124 ± 6[g]	69 ± 3	9 ± 2
Warfarin	22.7 ± 0.1	(307 → 161) (307 → 250)	(−)	50–10,000	0.9973	2	5 ± 1[c]	102 ± 9[g]	71 ± 3	28 ± 4
Temazepam	40.2 ± 0.1	(301 → 255) (301 → 283)	(+)	10–10,000	0.993	2	6 ± 1[c]	100 ± 3[g]	85 ± 1	11 ± 3
Diazepam	46.8 ± 0.1	(285 → 153) (285 → 193)	(+)	10–10,000	0.9991	2	5 ± 2[c]	176 ± 28[g]	89 ± 2	43 ± 3
Nimesulide	44.0 ± 0.1	(307 → 229) (307 → 79)	(−)	25–10,000	0.9945	3	13 ± 2[c]	97 ± 7[f]	87 ± 4	35 ± 3
Nifedipine	44.4 ± 0.1	(347 → 315) (347 → 271)	(+)	10–10,000	0.9985	1	4 ± 1[d]	104 ± 6[f]	70 ± 1	39 ± 4

[a] SD = standard deviation.
[b] $n > 5$ concentration data points each performed in triplicate.
[c] Signal to noise ratio of 10:1 from 20 ng g^{-1} spiked matrix-matched sample.
[d] Signal to noise ratio of 10:1 from 75 ng g^{-1} spiked matrix-matched sample.
[e] Signal to noise ratio of 10:1 from 60 ng g^{-1} spiked matrix-matched sample.
[f] Using a 75 ng g^{-1} spiked sample ($n = 3$) and determined by matrix matched calibration ($n = 3$) in triplicate.
[g] Using a 20 ng g^{-1} spiked sample ($n = 4$) and determined by the relevant isotopically-labelled internal standard.

achieved using unsilanised glass beads. Therefore, glass bead silanisation was not required (see Table S2).

The extraction of pharmaceuticals from aqueous samples is generally performed by SPE and HLB-type SPE cartridges enable the extraction of both polar and non-polar compounds from both water and biological extracts (Baker and Kasprzyk-Hordern, 2011a; Barron et al., 2008; Gomez et al., 2006; Weigel et al., 2004). The effect of the sample pH prior to SPE was investigated at pH 2, 7 and 10 (n = 3). A sample pH of 7 yielded the highest recoveries and lowest variability for the selected analytes. Sample reconstitution volumes of 0.1 mL and 0.5 mL were also investigated. As shown in Table S4, analyte recovery using a reconstitution volume of 0.5 mL was higher overall than that of 0.1 mL. In particular, compounds such as diazepam, gemfibrozil, triclocarban, ibuprofen, diclofenac and nimesulide showed moderately higher recoveries when reconstituted to 0.5 mL. Solubility of a dried matrix residue may have been a limiting factor at the reduced reconstitution solvent volume. Furthermore, matrix suppression effects in ESI–MS are likely to increase with a more concentrated sample extract (as was observed here). Although a thorough sample clean-up method was developed, final extracts of the *G. pulex* contained an immiscible red-pigmented liquid. A likely identity for this contaminant is astaxanthin, a relatively non-polar carotenoid pigment found in crustaceans (Johnson and An, 1991), but further analysis would be required to confirm this. Attempts to remove this substance from the ground *G. pulex* sample via liquid–liquid extraction (using a 50:50 (*v*/*v*) solution of acetonitrile with hydrochloric acid at pH 2 and hexane) did not prove successful. Additional approaches such as centrifugation and neutral alumina addition were also investigated (the latter of which is often used to remove pigments), but the substance remained in the sample extract and analyte recoveries did not improve (data not shown). Therefore, a 0.5 mL reconstitution volume in 90:10 (*v*/*v*) 10 mM ammonium acetate in water:acetonitrile was considered optimised.

In line with many other studies, LC–MS/MS was the chosen analytical technique for the confirmatory detection and subsequent determination of PPCPs in surface waters and *G. pulex*. A 10 mM ammonium acetate solution in a mixture of acetonitrile and water was selected again as a suitable mobile phase for reversed-phase separations in line with previously published work (Barron et al., 2008). The mobile phase gradients and column temperature (20, 30, 40 and 45 °C) were further optimised to allow better separation of more PPCPs. A column oven temperature of 45 °C offered the best separation of all compounds. For mass spectrometry, direct infusion was carried out initially in full scan mode to determine the most abundant precursor ion for each analyte and to optimise MS parameters for the best signal response. Compounds yielded $[M + H]^+$, $[M - H]^-$ or $[M\text{-}COOH]^-$ precursor ions in positive or negative polarity ESI–MS mode. Furthermore, SRM performed under positive–negative switching mode yielded MS/MS data for 29 analytes (Table S2). Secondary fragment ion transitions were observed for 21 of these compounds.

3.2. Method performance characteristics

Few validated multi-residue methods exist for PPCP determination in biota due to their complexity, variability, and potential to cause analytical matrix effects. Therefore, a larger number of compounds were included in the method development process originally as it was expected that some would not meet acceptable method performance criteria for quantitative analysis of small biotic samples. Those considered acceptable are presented in Table 1 (data from the full method performance experiment are shown in Tables S4 and S5). Method performance in surface waters is not presented here, but the method was deemed suitable for semi-quantitative purposes as it was based on previously published work (Lacey et al., 2012; Lacey et al., 2008). Instrumental retention time precision in *G. pulex* matrix was <0.5% for all analytes except for propranolol which was 1.7% (n = 6). For method linearity, correlation coefficients of $R^2 > 0.98$ (n ≥ 5 data points) were achieved for triplicate experiments, again in *G. pulex* matrix, over the calibration range for 18 compounds. Twelve compounds achieved unacceptable correlation coefficients and were included for qualitative purposes only (Table S5). Following the assessment of linearity, limits of quantitation (LOQs) of the method were determined for 23 analytes and lay between 4 and 687 ng g^{-1}. Intra-day method reproducibility was <30% for 20 analytes at 1 μg/g. Mean absolute recoveries of 28 analytes ranged from 4 to 89% (n = 6) with eight compounds displaying absolute recoveries >70%. Overall, it was observed that compounds

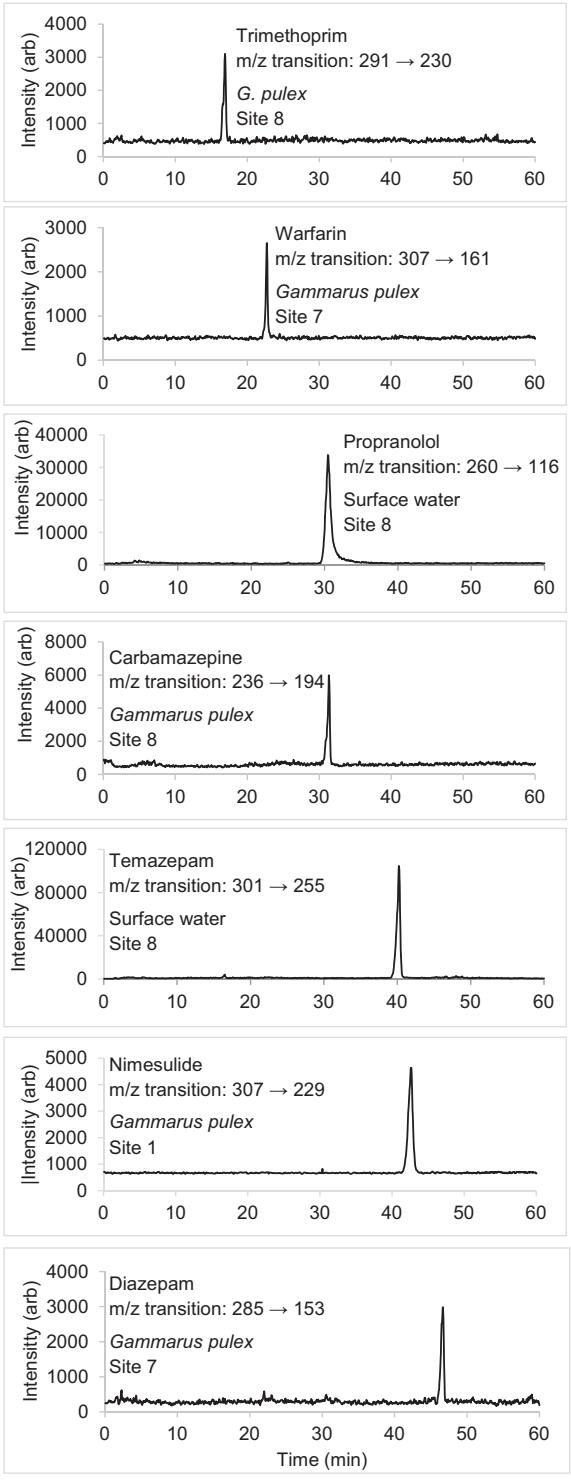

Fig. 2. Example extracted ion chromatograms of PPCPs detected in surface waters and *G. pulex* sampled from each of the eight selected sites.

determined in negative ESI–MS mode demonstrated lower recoveries than compounds detected in positive ESI–MS mode. Significant signal suppression was observed in *G. pulex* matrix as per Table S4 and signals for 6 of 29 compounds were suppressed greater than 50% in comparison to a standard mixture. The precision and recovery of this method in *G. pulex* correlates to data reported by Klosterhaus et al. (2013) for the analysis of PPCPs in mussels from San Francisco Bay. Other similar studies carried out on mussel and fish tissues, and other complex matrices such as biosolids and sludge, have shown similar method performance for PPCPs (Dodder et al., 2014; McEneff et al., 2013). Overall, and of the 29 PPCPs initially included in method development and performance characterisation, 10 compounds (carbamazepine, trimethoprim, warfarin, diazepam, temazepam, propranolol, nifedipine, nimesulide, sulfamethazine and metoprolol) showed acceptable method performance for quantification purposes. Precision was also maintained for these compounds when measured near the LOQ across n = 6 replicates.

3.3. Application to G. pulex and surface waters in tributaries of the River Thames, UK

The developed methods were applied to the identification of pharmaceutical residues in water and biotic samples. Surface water samples (500 mL) and *G. pulex* (n ≈ 60–100 specimens) were used for replicate analysis across the selected sites. As the surface water and biotic samples were collected by grab sampling, the results presented represent pharmaceutical concentrations present at that point in time. Example extracted ion chromatograms for compounds quantified in surface waters and *G. pulex*, are shown in Fig. 2.

Of the 29 compounds included in the analytical method for qualitative screening of invertebrate tissues, a total of 6 compounds were quantified in *G. pulex* (Table 2). Diclofenac was also detected at all sites but was not quantifiable due to method performance limitations (Table S5). Due to the lack of information regarding pharmaceutical uptake in *G. pulex*, similar occurrence studies on other species were used for comparison. Five compounds were quantified across the eight sites at concentrations ≤36 ng g^{-1} dry weight (Table 2). Carbamazepine was the most frequently detected compound, which is perhaps unsurprising as this compound has been reported in several solid and biological matrices (Barron et al., 2008; Huerta et al., 2013). Site 7 was the most contaminated of all sites. Diazepam was quantifiable across four sites at concentrations ≤9 ng g^{-1} dry weight. Kwon and co-workers detected several PPCP residues including carbamazepine and diazepam in fish livers and the latter was determined at concentrations up to 110 ng g^{-1} wet weight (Kwon et al., 2009). If hydrophobicity is to be considered a reliable quantity for bioaccumulation of PPCPs, then this may be explained given their moderate hydrophobicity relative to other PPCPs (log*P* = 2.45 and 2.86, respectively) (Barron et al., 2009). However, Meredith-Williams et al. recently studied bioconcentration of diazepam and carbamazepine in *G. pulex*, both of which were found to be minimal with BCF values of 38 and 7, respectively. As these compounds have relatively higher log*P* values in comparison to most other pharmaceuticals, it suggests that uptake models based on hydrophobicity may not accurately represent the potential for a compound to bioconcentrate in invertebrates. Tanoue et al. recently presented an analytical method for the determination of 17 intermediate-polarity PPCPs (log*P* = 1.40–5.74) and its application to biological tissue from Japanese fish and birds (Tanoue et al., 2014). Up to 13 PPCPs were determined across fish plasma (0.03–22 ng mL^{-1}), the brain and liver tissue (1–910 and 0.11–16 ng g^{-1} wet weight respectively) and all 17 were detected in the surrounding aquatic environment (at 3–871 ng L^{-1}). McEneff et al. investigated pharmaceutical concentrations in marine bivalves residing in effluent-contaminated seawater. The antibiotic, trimethoprim, measured highest at concentrations up to 9 ng g^{-1} dry weight and carbamazepine was also detected, but below its LOQ (McEneff et al., 2014). Here, trimethoprim was only quantifiable at Site 8 at 5 ng g^{-1} dry weight. Nimesulide was quantified at slightly higher concentrations on average. This coincides with the results from surface water analysis where nimesulide was detected in samples from Sites 1 to 4 and 7. Nimesulide was banned in the Republic of Ireland in 2007 due to risks associated with hepatic failure and it is not available on the UK market as a pharmaceutical for human consumption. However, sources of input into the environment still exist via veterinary routes and in addition this compound has also been found in selected food supplements (Lacey et al., 2012; MHRA, 2014).

Adverse effects such as increased oxidative stress and tissue lesions have been observed following the exposure of species such as fish and molluscs to environmentally relevant PPCP concentrations. A study carried out by De Lange et al. (2006) investigated the behavioural responses of *G. pulex* when exposed to environmentally relevant concentrations (from 0.1 ng L^{-1} up to 1 mg L^{-1}) of the pharmaceuticals carbamazepine, fluoxetine and ibuprofen (De Lange et al., 2006). The lowest observed effect concentration (LOEC) for fluoxetine was reported as 100 ng L^{-1} and the LOEC for ibuprofen and carbamazepine was measured at even lower concentrations at 10 ng L^{-1}. However, it was noted that the reduced activity observed in *G. pulex* exposed to carbamazepine (≥10 ng L^{-1}) was not significantly different to the control exposure. Carbamazepine was measured at concentrations up to 344 ng L^{-1} in the surface waters from Site 8. Further work is still required to establish reliable LOEC levels for pharmaceuticals both in isolation and when present as a mixture (Arnold et al., 2014; Brooks, 2014). Indeed, with ongoing extensive debate in the literature questioning the validity and reproducibility of experiments revealing effects on bespoke endpoints (Sumpter et al., 2014), it is clearly essential to have the tools available to measure both the exposure concentrations (water) and internal concentrations in order to attribute cause and effect.

With respect to surface waters, six PPCPs were detected at quantifiable levels across all sites at concentrations ranging from 3 to 344 ng L^{-1} (Table 3). Carbamazepine and trimethoprim measured highest at concentrations of 344 ng L^{-1} and 289 ng L^{-1}, respectively. From the eight sites, all of the selected analytes measured at their highest concentration at Site 8, with the exception of propranolol which measured at concentrations >250 ng L^{-1} at Site 5. An effluent outfall pipe lay in close proximity to Site 8, and potentially higher concentrations of pharmaceutical contamination in river water were

Table 2
Pharmaceutical residues (ng g^{-1}) detected in *Gammarus pulex* material sampled from eight sites located on the tributaries of the River Thames, UK. Note: diclofenac was detected at all sites but was not quantifiable based on method performance limitations.

Compounds	Site 1 n = 2	Site 2 n = 3	Site 3 n = 2	Site 4 n = 3	Site 5 n = 3	Site 6 n = 2	Site 7 n = 3	Site 8 n = 2
Carbamazepine	–	<LOQ	–	ND–< LOQ	<LOQ	–	ND– < LOQ	6
Diazepam	ND, 6	ND–8	–	ND–6	–	–	ND–9	–
Temazepam	–	–	–	–	–	–	<LOQ	ND– < LOQ
Trimethoprim	–	–	–	–	–	–	ND– < LOQ	5
Warfarin	–	–	–	–	–	–	ND–7	–
Nimesulide[a]	13, 36	ND– < LOQ	–	ND– < LOQ			ND–16	

ND — not detected, all other compounds marked with '–'were also not detected.
[a] Quantified by three-point standard addition calibration.

Table 3
Pharmaceutical residues (ng L^{-1}) detected in surface water sampled from eight sites located on the tributaries of the River Thames, UK.

Compounds	log*P* (Barron et al., 2009)	Site 1 n = 3	Site 2 n = 3	Site 3 n = 3	Site 4 n = 3	Site 5 n = 3	Site 6 n = 3	Site 7 n = 3	Site 8 n = 3
Carbamazepine	2.45	12–27	10–62	13–17	20–156	6–149	8–9	6–53	320–344
Diazepam	2.86	ND	ND–<LOQ	ND–3	ND–<LOQ	ND–<LOQ	ND–<LOQ	<LOQ	4
Propranolol	3.48	ND–<LOQ	<LOQ–59	8–22	<LOQ–11	ND–253	21–52	5–23	98–119
Temazepam	2.19	ND–<LOQ	<LOQ–2	<LOQ	5–6	ND–<LOQ	ND	ND–LOQ	60–67
Trimethoprim	0.91	<LOQ–8	ND–<LOQ	4–10	<LOQ–48	ND–41	6–16	<LOQ–9	263–289
Warfarin	2.60	ND–<LOQ	ND–53	<LOQ–12	ND–<LOQ	ND–9	11–14	ND–LOQ	15–29

ND — not detected.

measured as a result. However, this did not translate across to elevated concentrations measured in *G. pulex* (highest internal concentrations measured at Site 7). The Beverley Brook tributary was previously classed as having 'poor ecological status' by the Environment Agency in 2012 for failures in surrounding ecology, water chemistry and morphology standards (Ehmann, 2013). River water samples from Site 5 were also found to contain relatively high concentrations of carbamazepine, propranolol and trimethoprim. Besides direct input from WWTPs, other sources of pharmaceutical contamination include sewage from the numerous combined sewer overflows serving this river catchment area which overflow during periods of heavy rainfall and interestingly, have been shown to intermittently discharge sewage into surface waters even without precipitation (Buerge et al., 2006). The Environment Agency (England) has reported poor status for two groundwater bodies which predominantly supply the river flow through Sites 5, 6 and 7 (Gorman, 2013). Although most of the PPCPs were detected at all three of these sites, surface water samples from the River Cray (Sites 6 and 7) were found to contain relatively low residue concentrations overall. Diazepam was the least detected compound in water and measured concentrations were 3 and 4 ng L^{-1} at Sites 3 and 8, respectively.

As expected from this 'snapshot' collection method, there was poor correlation between water and *G. pulex* measured concentrations (compare Tables 2 and 3). Temazepam and propranolol were both measured in water (propranolol in 7 of the 8 sites), but neither were detected within any *G. pulex* despite having higher Log*P* values than trimethoprim which was measured in these organisms. This would further support the hypothesis that for invertebrates, uptake is driven by more than hydrophobicity alone. Intuitively one would predict a constant state of flux in the uptake and depuration of compounds as the flow of water and external exposure changes, and the poor correlation could support that. Therefore, measuring concentrations within the organism is likely to be more relevant (and important) for understanding risk than external water alone.

Several monitoring studies have been carried out in freshwater throughout the UK. A study carried out on the River Taff and the River Ely in Wales consistently detected the presence of carbamazepine at concentrations up to 684 ng L^{-1}. Several recent monitoring studies have detected the presence of propranolol and trimethoprim in surface waters across the UK at concentrations up to 40 ng L^{-1} and 215 ng L^{-1}, respectively (Ashton et al., 2004; Baker and Kasprzyk-Hordern, 2011b; Roberts and Thomas, 2006). The benzodiazepines, temazepam and diazepam have also been reported in river water measuring at concentrations of 53 ng L^{-1} and 1 ng L^{-1}, respectively (Baker and Kasprzyk-Hordern, 2011a). All six selected pharmaceuticals detected here have also been determined in river waters around Europe and Asia at concentrations measuring up to 1 μg L^{-1} in countries such as South Korea, Spain and France (Feitosa-Felizzola and Chiron, 2009; Silva et al., 2011; Yoon et al., 2010).

4. Conclusions

For the first time, the occurrence of six pharmaceuticals was reported from measured internal concentrations in the river shrimp, *G. pulex*, and its surrounding waters. An analytical method involving PuLE, SPE and LC–MS/MS was optimised and applied to surface waters and *G. pulex* samples collected from eight sites along several tributaries of the River Thames. Five pharmaceuticals detected in the freshwater samples were also found to occur in exposed *G. pulex* at concentrations up to 36 ng g^{-1} dry weight, although direct correlation with water concentrations at individual sites was not possible. Carbamazepine and trimethoprim measured highest in river water at concentrations up to 344 ng L^{-1} and 289 ng L^{-1}, respectively. These findings provide new knowledge on the occurrence of pharmaceutical residues in a key aquatic invertebrate, and tools to further investigate their potential effects via internal concentration measurement.

Acknowledgements

This work was conducted with funding from the Biotechnology and Biological Sciences Research Council (BBSRC) CASE industrial scholarship scheme (Reference BB/K501177/1) and AstraZeneca Global SHE research programme. AstraZeneca is a biopharmaceutical company specialising in the discovery, development, manufacturing and marketing of prescription medicines, including some products measured here. Funding bodies played no role in the design of the study or decision to publish. The authors declare no financial conflict of interest.

Appendix A. Supplementary data

Supplementary data to this article can be found online at http://dx.doi.org/10.1016/j.scitotenv.2014.12.034.

References

Arnold, K.E., Brown, A.R., Ankley, G.T., Sumpter, J.P., 2014. Medicating the environment: assessing risks of pharmaceuticals to wildlife and ecosystems. Philos. Trans. R. Soc. B Biol. Sci. 369.

Ashauer, R., Hintermeister, A., O'Connor, I., Elumelu, M., Hollender, J., Escher, B.I., 2012. Significance of xenobiotic metabolism for bioaccumulation kinetics of organic chemicals in *Gammarus pulex*. Environ. Sci. Technol. 46, 3498–3508.

Ashton, D., Hilton, M., Thomas, K.V., 2004. Investigating the environmental transport of human pharmaceuticals to streams in the United Kingdom. Sci. Total Environ. 333, 167–184.

Baker, D.R., Kasprzyk-Hordern, B., 2011a. Multi-residue analysis of drugs of abuse in wastewater and surface water by solid-phase extraction and liquid chromatography–positive electrospray ionisation tandem mass spectrometry. J. Chromatogr. A 1218, 1620–1631.

Baker, D.R., Kasprzyk-Hordern, B., 2011b. Multi-residue determination of the sorption of illicit drugs and pharmaceuticals to wastewater suspended particulate matter using pressurised liquid extraction, solid phase extraction and liquid chromatography coupled with tandem mass spectrometry. J. Chromatogr. A 1218, 7901–7913.

Barron, L., Tobin, J., Paull, B., 2008. Multi-residue determination of pharmaceuticals in sludge and sludge enriched soils using pressurized liquid extraction, solid phase extraction and liquid chromatography with tandem mass spectrometry. J. Environ. Monit. 10, 353–361.

Barron, L., Havel, J., Purcell, M., Szpak, M., Kelleher, B., Paull, B., 2009. Predicting sorption of pharmaceuticals and personal care products onto soil and digested sludge using artificial neural networks. Analyst 134, 663–670.

Behera, S.K., Kim, H.W., Oh, J.E., Park, H.S., 2011. Occurrence and removal of antibiotics, hormones and several other pharmaceuticals in wastewater treatment plants of the largest industrial city of Korea. Sci. Total Environ. 409, 4351–4360.

Brooks, B.W., 2014. Fish on Prozac (and Zoloft): ten years later. Aquat. Toxicol. 151, 61–67.

Brown, K.D., Kulis, J., Thomson, B., Chapman, T.H., Mawhinney, D.B., 2006. Occurrence of antibiotics in hospital, residential, and dairy effluent, municipal wastewater, and the Rio Grande in New Mexico. Sci. Total Environ. 366, 772–783.

Buerge, I.J., Poiger, T., Müller, M.D., Buser, H.-R., 2006. Combined sewer overflows to surface waters detected by the anthropogenic marker caffeine. Environ. Sci. Technol. 40, 4096–4102.
Carmona, E., Andreu, V., Pico, Y., 2014. Occurrence of acidic pharmaceuticals and personal care products in Tuna River Basin: from waste to drinking water. Sci. Total Environ. 484, 53–63.
Commission E, 2012. Commission Proposal on Priority Substances (COM(2011)876). p. 2014.
Corcoran, J., Winter, M.J., Tyler, C.R., 2010. Pharmaceuticals in the aquatic environment: a critical review of the evidence for health effects in fish. Crit. Rev. Toxicol. 40, 287–304.
Cueva-Mestanza, R., Torres-Padrón, M., Sosa-Ferrera, Z., Santana-Rodríguez, J., 2008. Microwave-assisted micellar extraction coupled with solid-phase extraction for preconcentration of pharmaceuticals in molluscs prior to determination by HPLC. Biomed. Chromatogr. 22, 1115–1122.
De Lange, H.J., Noordoven, W., Murk, A.J., Lürling, M., Peeters, E.T.H.M., 2006. Behavioural responses of *Gammarus pulex* (Crustacea, Amphipoda) to low concentrations of pharmaceuticals. Aquat. Toxicol. 78, 209–216.
De Lange, H.J., Peeters, E.T.H.M., Lürling, M., 2009. Changes in ventilation and locomotion of Gammarus pulex (Crustacea, Amphipoda) in response to low concentrations of pharmaceuticals. Human and Ecological Risk Assessment 15 (1), 111–120.
Dobson, P.D., Kell, D.B., 2008. Carrier-mediated cellular uptake of pharmaceutical drugs: an exception or the rule? Nat. Rev. Drug Discov. 7, 205–220.
Dodder, N.G., Maruya, K.A., Lee Ferguson, P., Grace, R., Klosterhaus, S., La Guardia, M.J., et al., 2014. Occurrence of contaminants of emerging concern in mussels (Mytilus spp.) along the California coast and the influence of land use, storm water discharge, and treated wastewater effluent. Mar. Pollut. Bull. 81, 340–346.
Dussault, È.B., Balakrishnan, V.K., Solomon, K.R., Sibley, P.K., 2009. Matrix effects on mass spectrometric determinations of four pharmaceuticals and personal care products in water, sediments, and biota. Can. J. Chem. 87, 662–672.
Ehmann, P., 2013. Beverley Brook Information Pack 2014. Environment Agency.
Feitosa-Felizzola, J., Chiron, S., 2009. Occurrence and distribution of selected antibiotics in a small Mediterranean stream (Arc River, Southern France). J. Hydrol. 364, 50–57.
Friberg, N., Andersen, T.H., Hansen, H.O., Iversen, T.M., Jacobsen, D., Krøjgaard, L., et al., 1994. The effect of brown trout (*Salmo Trutta* L.) on stream invertebrate drift, with special reference to *Gammarus pulex* L. Hydrobiologia 294, 105–110.
Gatidou, G., Vassalou, E., Thomaidis, N.S., 2010. Bioconcentration of selected endocrine disrupting compounds in the Mediterranean mussel, *Mytilus galloprovincialis*. Mar. Pollut. Bull. 60, 2111–2116.
Gomez, M.J., Petrovic, M., Fernandez-Alba, A.R., Barcelo, D., 2006. Determination of pharmaceuticals of various therapeutic classes by solid-phase extraction and liquid chromatography-tandem mass spectrometry analysis in hospital effluent wastewaters. J. Chromatogr. A 1114, 224–233.
Gorman, A., 2013. Water Body Action Plan 2014. Environment Agency.
Hamelink, J.L., Spacie, A., 1977. Fish and chemicals: the process of accumulation. Annu. Rev. Pharmacol. Toxicol. 17, 167–177.
Huerta, B., Rodriguez-Mozaz, S., Barcelo, D., 2012. Pharmaceuticals in biota in the aquatic environment: analytical methods and environmental implications. Anal. Bioanal. Chem. 404, 2611–2624.
Huerta, B., Jakimska, A., Gros, M., Rodriguez-Mozaz, S., Barcelo, D., 2013. Analysis of multi-class pharmaceuticals in fish tissues by ultra-high-performance liquid chromatography tandem mass spectrometry. J. Chromatogr. A 1288, 63–72.
Johnson, E.A., An, G.-H., 1991. Astaxanthin from microbial sources. Crit. Rev. Biotechnol. 11, 297–326.
Klosterhaus, S.L., Grace, R., Hamilton, M.C., Yee, D., 2013. Method validation and reconnaissance of pharmaceuticals, personal care products, and alkylphenols in surface waters, sediments, and mussels in an urban estuary. Environ. Int. 54, 92–99.
Kok, S.J., Debets, A.J.J., 2001. Fast sample preparation for analysis of tablets and capsules: the ball-mill extraction method. J. Pharm. Biomed. Anal. 26, 599–604.
Kosma, C.I., Lambropoulou, D.A., Albanis, T.A., 2010. Occurrence and removal of PPCPs in municipal and hospital wastewaters in Greece. J. Hazard. Mater. 179, 804–817.
Kwon, J.-W., Armbrust, K.L., Vidal-Dorsch, D., Bay, S.M., Xia, K., 2009. Determination of 17 alpha-ethynylestradiol, carbamazepine, diazepam, simvastatin, and oxybenzone in fish livers. J. AOAC Int. 92, 359–369.
Lacey, C., McMahon, G., Bones, J., Barron, L., Morrissey, A., Tobin, J.M., 2008. An LC–MS method for the determination of pharmaceutical compounds in wastewater treatment plant influent and effluent samples. Talanta 75, 1089–1097.
Lacey, C., Basha, S., Morrissey, A., Tobin, J., 2012. Occurrence of pharmaceutical compounds in wastewater process streams in Dublin, Ireland. Environ. Monit. Assess. 184, 1049–1062.
Maltby, L., Clayton, S.A., Wood, R.M., McLoughlin, N., 2002. Evaluation of the *Gammarus pulex* in situ feeding assay as a biomonitor of water quality: robustness, responsiveness, and relevance. Environ. Toxicol. Chem. 21, 361–368.
McEneff, G., Barron, L., Kelleher, B., Paull, B., Quinn, B., 2013. The determination of pharmaceutical residues in cooked and uncooked marine bivalves using pressurised liquid extraction, solid-phase extraction and liquid chromatography–tandem mass spectrometry. Anal. Bioanal. Chem. 405, 9509–9521.
McEneff, G., Barron, L., Kelleher, B., Paull, B., Quinn, B., 2014. A year-long study of the spatial occurrence and relative distribution of pharmaceutical residues in sewage effluent, receiving marine waters and marine bivalves. Sci. Total Environ. 476–477, 317–326.
McKim, J., Schmieder, P., Veith, G., 1985. Absorption dynamics of organic chemical transport across trout gills as related to octanol–water partition coefficient. Toxicol. Appl. Pharmacol. 77, 1–10.
Meredith-Williams, M., Carter, L.J., Fussell, R., Raffaelli, D., Ashauer, R., Boxall, A.B.A., 2012. Uptake and depuration of pharmaceuticals in aquatic invertebrates. Environ. Pollut. 165, 250–258.
MHRA, 2014. Medicines and Healthcare Products Regulatory Agency. p. 2014.
Nyman, A.-M., Schirmer, K., Ashauer, R., 2012. Toxicokinetic–toxicodynamic modelling of survival of *Gammarus pulex* in multiple pulse exposures to propiconazole: model assumptions, calibration data requirements and predictive power. Ecotoxicology 21, 1828–1840.
Rand-Weaver, M., Margiotta-Casaluci, L., Patel, A., Panter, G.H., Owen, S.F., Sumpter, J.P., 2013. The read-across hypothesis and environmental risk assessment of pharmaceuticals. Environ. Sci. Technol. 47, 11384–11395.
Roberts, P.H., Thomas, K.V., 2006. The occurrence of selected pharmaceuticals in wastewater effluent and surface waters of the lower Tyne catchment. Sci. Total Environ. 356, 143–153.
Schultz, M.M., Furlong, E.T., Kolpin, D.W., Werner, S.L., Schoenfuss, H.L., Barber, L.B., et al., 2010. Antidepressant pharmaceuticals in two U.S. effluent-impacted streams: occurrence and fate in water and sediment, and selective uptake in fish neural tissue. Environ. Sci. Technol. 44, 1918–1925.
Silva, B.F.d, Jelic, A., López-Serna, R., Mozeto, A.A., Petrovic, M., Barceló, D., 2011. Occurrence and distribution of pharmaceuticals in surface water, suspended solids and sediments of the Ebro river basin, Spain. Chemosphere 85, 1331–1339.
Subedi, B., Du, B., Chambliss, C.K., Koschorreck, J., Rudel, H., Quack, M., et al., 2012. Occurrence of pharmaceuticals and personal care products in German fish tissue: a national study. Environ. Sci. Technol. 46, 9047–9054.
Sumpter, J.P., Donnachie, R.L., Johnson, A.C., 2014. The apparently very variable potency of the anti-depressant fluoxetine. Aquat. Toxicol. 151, 57–60.
Tanoue, R., Nomiyama, K., Nakamura, H., Hayashi, T., Kim, J.-W., Isobe, T., et al., 2014. Simultaneous determination of polar pharmaceuticals and personal care products in biological organs and tissues. J. Chromatogr. A 1355, 193–205.
Thomas, K.V., Hilton, M.J., 2004. The occurrence of selected human pharmaceutical compounds in UK estuaries. Mar. Pollut. Bull. 49, 436–444.
Vazquez-Roig, P., Blasco, C., Pico, Y., 2013. Advances in the analysis of legal and illegal drugs in the aquatic environment. Trac-Trends Anal. Chem. 50, 65–77.
Weigel, S., Kallenborn, R., Hühnerfuss, H., 2004. Simultaneous solid-phase extraction of acidic, neutral and basic pharmaceuticals from aqueous samples at ambient (neutral) pH and their determination by gas chromatography–mass spectrometry. J. Chromatogr. A 1023, 183–195.
Yoon, Y., Ryu, J., Oh, J., Choi, B.-G., Snyder, S.A., 2010. Occurrence of endocrine disrupting compounds, pharmaceuticals, and personal care products in the Han River (Seoul, South Korea). Sci. Total Environ. 408, 636–643.

Journal of Chromatography A, 1396 (2015) 34–44

Contents lists available at ScienceDirect

Journal of Chromatography A

journal homepage: www.elsevier.com/locate/chroma

Artificial neural network modelling of pharmaceutical residue retention times in wastewater extracts using gradient liquid chromatography-high resolution mass spectrometry data

Kelly Munro[a], Thomas H. Miller[a], Claudia P.B. Martins[b], Anthony M. Edge[c], David A. Cowan[a], Leon P. Barron[a,*]

[a] Analytical & Environmental Sciences Division, King's College London, 150 Stamford Street, SE1 9NH London, United Kingdom
[b] Thermo Fisher Scientific, 355 River Oaks Parkway, San Jose, CA 95134, USA
[c] Thermo Fisher Scientific, Tudor Road, Runcorn, United Kingdom

ARTICLE INFO

Article history:
Received 10 November 2014
Received in revised form 27 February 2015
Accepted 23 March 2015
Available online 30 March 2015

Keywords:
Artificial neural networks
Retention time prediction
Semi-targeted detection
Reversed-phase liquid chromatography
High resolution mass spectrometry

ABSTRACT

The modelling and prediction of reversed-phase chromatographic retention time (t_R) under gradient elution conditions for 166 pharmaceuticals in wastewater extracts is presented using artificial neural networks for the first time. Radial basis function, multilayer perceptron and generalised regression neural networks were investigated and a comparison of their predictive ability for model solutions discussed. For real world application, the effect of matrix complexity on t_R measurements is presented. Measured t_R for some compounds in influent wastewater varied by >1 min in comparison to t_R in model solutions. Similarly, matrix impact on artificial neural network predictive ability was addressed towards developing a more robust approach for routine screening applications. Overall, the best neural network had a predictive accuracy of <1.3 min at the 75th percentile of all measured t_R data in wastewater samples (<10% of the total runtime). Coefficients of determination for 30 blind test compounds in wastewater matrices lay at or above $R^2 = 0.92$. Finally, the model was evaluated for application to the semi-targeted identification of pharmaceutical residues during a weeklong wastewater sampling campaign. The model successfully identified native compounds at a rate of 83 ± 4% and 73 ± 5% in influent and effluent extracts, respectively. The use of an HRMS database and the optimised ANN model was also applied to shortlisting of 37 additional compounds in wastewater. Ultimately, this research will potentially enable faster identification of emerging contaminants in the environment through more efficient post-acquisition data mining.

1. Introduction

Characterising the breadth of occurrence of pharmaceuticals and personal care products (PPCPs) in the aquatic environment has been on-going for the past two decades [1]. In most developed countries, wastewater treatment plant effluents often act as identifiable sources, and, given that they often serve large communities, the potential exists for larger numbers of PPCPs to enter receiving waters via effluent as a result. Several multi-residue analytical methods have been applied to PPCP determination in environmental matrices [2–5] and mostly employ a targeted approach where compounds are pre-selected. Recent methods for larger numbers of PPCPs have used online [6] or offline [7,8] solid phase extraction (SPE) [9] for clean-up and concentration of wastewater samples followed by analysis with gas chromatography (GC) [10,11] or liquid chromatography (LC) coupled to various modes of mass spectrometry (MS) [8,12–15]. However, as >3000 licensed PPCPs exist, targeted approaches only allow characterisation of a small portion of PPCP occurrence. Methods for such large numbers of compounds are often limited by unfeasibly long cycle times for tandem MS experiments or full m/z range scanning using lower resolution instruments.

Relatively recent efforts have focused on hyphenation to high resolution mass spectrometry (HRMS) for multi-residue screening [16–19]. The combination of full-scan m/z data acquisition at or below ppm m/z accuracy and at high resolution has enabled datasets to be interpreted in a non-targeted or semi-targeted manner post-analysis [20–22]. By using full-scan HRMS instruments for

* Corresponding author. Tel.: +44 20 7848 3842; fax: +44 20 7848 4980.
E-mail address: leon.barron@kcl.ac.uk (L.P. Barron).

http://dx.doi.org/10.1016/j.chroma.2015.03.063
0021-9673/

detection, larger numbers of compounds can be screened in a single run and such methods have been applied to >400 compounds in wastewater [23]. Full scan and tandem MS/all-ion fragmentation experiments may also yield useful information to identify new compounds, but a number of chromatographic peaks and/or potential candidates with matching m/z may still exist before confirmation becomes feasible. For this reason, there still exists a requirement to confirm compound identity using analyte retention time from the chromatographic separation. Confirmation efforts are further limited by the availability of PPCP reference materials, but also their metabolites and transformation products. Importantly, this may also require consideration of other isomeric and/or isobaric compounds.

The use of *in silico* retention time modelling tools may prove useful in post-data acquisition analysis, at the very least, to help direct synthesis/acquisition of analytical reference materials for more rapid compound confirmation. Linear solvation-energy relationships (LSERs) have been used for modelling solute retention behaviour in chromatography for some time [24–26]. As a more flexible and practical alternative, researchers have also used artificial neural networks (ANNs) to model retention in several chromatographic modes [27–29] and formats [30–32]; for method optimisation purposes [33–37]; or to estimate unknown compound retention [38–40]. Fragkaki and colleagues recently compared the use of linear regression, partial least squares and ANNs for the prediction of relative retention time of 64 derivatised steroid compounds in gradient GC-MS [41]. Recently, we developed and applied ANNs for the generation of sports doping compound retention time in urine extracts, which were collected by LC-HRMS during the London 2012 Olympic Games [42]. Using a short 8-min reversed-phase gradient for 86 compounds, all predicted retention times (t_R^P) were within 1.0 min of measured retention time (t_R^M) and 12/15 blind test compounds were predicted to within 0.5 min of the true value. However, the number of compounds used may be limited for use as the basis for broad-scope application to *in silico* wastewater analysis given that a potentially larger diversity and number of compounds are likely to exist simultaneously in samples of such high complexity.

The aim of this work was therefore to evaluate and confirm ANN modelling as a useful tool for semi-targeted screening of residues in influent and effluent wastewater extracts. In particular, the objectives were to model a larger number of compound retention times than included previously; to assess the effect of matrix on the reliability of t_R^M data for ANN training; to assess ANN t_R^P performance and to apply ANNs to the identification of trace PPCPs in real samples during a week-long wastewater sampling campaign. This represents the first study of its kind to use ANN modelling tools with LC-HRMS datasets for semi-targeted PPCP screening purposes.

2. Experimental

2.1. Reagents

All reagents were of analytical grade unless otherwise specified. HPLC grade methanol, acetonitrile, dichloromethane and dimethyldichlorosiloxane were purchased from Fisher Scientific (Loughborough, UK). Ammonium acetate and 37% (w/v) hydrochloric acid solution were sourced from Sigma-Aldrich (Gillingham, Dorset, UK). Ultrapure water was obtained from a Millipore Synergy-UV water purification system with a resistivity of 18.2 MΩ cm (Millipore, Bedford, USA). Analytical grade reference compounds were purchased from several different manufacturers or donated by other laboratories. Stock standards were prepared at concentrations of 1 mg/mL in methanol and stored in silanised amber vials at 4 °C in the dark when not in use. All 166 reference compounds used for retention time modelling are listed in the supplementary information (SI).

2.2. Analytical instrumentation and conditions

Unless otherwise stated, all instrumentation, equipment and associated software was procured from Thermo Fisher Scientific (San Jose, CA, USA). An Accela ultra high performance liquid chromatography system was used for all work presented herein. Sample injection was performed using a HTS-A5 autosampler with sample storage compartment temperature control set at 10 °C. Separations were performed on a 150 × 2.1 mm, 2.6 μm solid-core particle Accucore C_{18} analytical column which was configured with a matching 10 × 2.1 mm, 2.6 μm particle size Accucore C_{18} guard. Temperature was maintained at 24 °C. The flow rate of mobile phase was 0.4 mL/min and the injection volume was 20 μL in order to achieve acceptable sensitivity in wastewater extracts. A binary gradient elution profile of 90:10 to 20:80 10 mM ammonium acetate in water:acetonitrile (mobile phase A and B, respectively; apparent pH = 5.2) was used over 27.5 min as follows: 0% B for 2.5 min; a linear ramp to 30% B from 2.5 to 7.5 min; an isocratic stage of 30% B from 7.5 to 12.5 min; a linear ramp to 40% B from 12.5 to 15 min; a linear ramp to 100% B from 15.0 to 20.0 min; and then maintained at 100% B from 20.0 to 27.5 min. Re-equilibration time was 7.5 min.

Detection was performed using an Exactive HRMS instrument fitted with a heated electrospray ionisation source (HESI-II). Separate chromatographic runs of all samples and model solutions were performed in either positive or negative ionisation mode. Nitrogen was used within the HESI-II source and the collision cell. Enhanced resolution mode was employed at 50,000 FWHM. Two MS experiments occurred during each acquisition cycle by performing a full scan without higher energy collisional dissociation (HCD) followed by a full scan with HCD enabled (collision energy: 20 eV). The cycle time was approximately 2 s, resulting in 1.2 scans per second due to the switching between full scan and HCD fragmentation experiments. The automatic gain control target was set to balanced, meaning that ~10^6 ions were collected in the C-trap before being sent to the Orbitrap for acquisition. The sheath gas, auxiliary gas and sweep gas flow rate settings were 50, 10 and 0 arbitrary units, respectively. The capillary temperature was 350 °C; the heater temperature was 300 °C; and the positive/negative spray voltages were +4.50 kV and −3.00 kV. The scan range was m/z 100–1000 for all MS experiments. All acquisition data was processed using Xcalibur v 2.0 software. The HRMS instrument was calibrated prior to use by infusion of a mixture of caffeine, MRFA (met-arg-phe-ala) and UltraMark 1621® (a mixture of fluorinated phosphazines) prepared in a solvent of acetonitrile/methanol/acetic acid for positive mode ESI-HRMS. For negative ESI-HRMS mode calibration infusion of a solution containing sodium dodecyl sulfate (SDS), sodium taurocholate and Ultramark 1621® was performed in the same solvent.

2.3. Sample preparation procedures

Samples of wastewater influent (taken immediately after the fine screen) and effluent were obtained from a major sewage treatment works in London (population equivalent = 3.4 million). Wastewater was collected as seven consecutive, separate 24-h composite samples across a 1-week period from 11 to 17 March 2014 (using a set 60-min sampling interval). Samples were refrigerated and transported to the laboratory in Nalgene bottles and adjusted to pH 2 using 37% (w/v) hydrochloric acid solution and stored frozen at −20 °C until analysis. Glassware was silanised to reduce analyte adsorption to glass surfaces. This included a rinse with 50:50 (v/v) methanol:water before triplicate rinses with dichloromethane. A 10:90 (v/v) dimethyldichlorosilane/dichloromethane

solution was then used to silanise the container, followed by triplicate sets of rinses with each of dichloromethane and 50:50 methanol:water. Before extraction, samples were thawed and filtered under vacuum using Whatman GF/F 0.7 μm glass microfibre filters. For quantification of mephedrone in influents, a pooled wastewater sample was used to generate a background-subtracted matrix-matched calibration curve over 5–2500 ng/L. In addition to this, $n = 3$ quality control 250 ng/L matrix-matched standards were determined to ensure method inaccuracy remained below 20%. HyperSep Retain Polar Enhanced Polymer (PEP) SPE cartridges (200 mg, 6 mL barrel) were used for extraction of influent and effluent wastewater samples. Cartridges were conditioned with 4 mL methanol followed by 4 mL ultrapure water. A 100 mL sample was loaded onto the cartridge followed by a wash step of 4 mL 5:95 (v/v) methanol:water and dried under vacuum for 10 min. Bound solutes were subsequently eluted with 4 mL methanol into a pre-silanised tapered glass tube. Eluted extracts were evaporated to dryness under N_2 at 35 °C and reconstituted in 100 μL of mobile phase A. For retention modelling purposes only, and to generate matrix-matched standards, dried extracts were reconstituted in 100 μL of a 250 μg/L standard of all compounds prepared in mobile phase A. The reconstituted samples were sonicated for 10 min before being transferred to pre-silanised and crimped septum-capped amber glass vials. Extracts were stored at 4 °C and in the dark and analysed within 24 h.

2.4. Molecular description, ANN models and architectures

In line with previously published works [42,43], canonical simplified molecular line entry system strings (SMILES) were created for all 166 compounds using ChemSpider freeware (Royal Society of Chemistry, UK). Using Parameter Client freeware (Virtual Computational Chemistry Laboratory, Munich, Germany), fifteen molecular descriptors were generated as inputs to ANN models which included the number of double and triple bonds (nDB or nTB), the number of carbon and oxygen atoms (nC or nO), the number of 4–9 membered rings (nR04–nR09), unsaturation index (UI), hydrophilic factor [2], number of benzene rings (nBnz), and Moriguchi and Ghose-Crippen log *P* (Mlog*P* and Alog*P*, respectively). Data for two additional molecular descriptors (log *D* and pK_a) were generated using Percepta PhysChem Profiler (ACD Laboratories, ON, Canada).

Prediction of retention times was performed using the Trajan 6.0 neural network simulator (Trajan Software Ltd., Lincolnshire, UK) and compared with measured retention time in matrix matched standards. Optimisation of each ANN type and architecture was performed in a number of stages. Firstly, all 17 input variables listed were included in the design phase followed by a second stage which enabled subset selections to assess any improved correlation or performance-limiting input variables. In these first two steps, case input variable data were randomised across training, verification and blind test experiments. When a suitable architecture was identified, a third stage of optimisation involved randomising all but the blind test cases to identify the best model. For application, all case datasets were subsequently fixed. Networks were set to balance their verification set errors against network diversity to cover as many architectures as possible across all model types. For multilayer perceptrons (MLPs) in particular, and for each set of design parameters, ANN architectures were tested over 30 min intervals and following this, the best 50 networks were selected based on correlation and output error. Three- and four-layer MLPs were included and within each hidden layer the number of nodes tested was ≤14 (software suggested value). For radial basis functions (RBFs), probabilistic neural networks (PNNs) and generalised regression neural networks (GRNNs), 10^8 architectures were investigated in each optimisation step. Fifty of the best RBF/GRNN networks were again ranked by correlation and output error. The maximum number of nodes tested in RBF hidden layers was 42 (software suggested value). Pruning was only applied to GRNNs and fan-out weight thresholds for input variables and hidden layer units were set to ≤0.05.

2.5. Post-acquisition data mining and peak selection

Post-acquisition automated peak selection was performed for influent and effluent sample data using TraceFinder™ version 3.1 software (Thermo); a separate peak selection process was performed for both the positive and negative ionisation mode runs for each sample. Acquired HRMS data only was screened against the commercially available ThermoFisher spectral library which contained data for 1492 compounds comprising pesticides, herbicides, fungicides, pharmaceuticals, metabolites and illicit drugs (and inclusive of all 166 compounds selected for retention modelling herein). Neither empirical retention time nor peak width were used for database searching to simulate a semi-targeted approach. Identification criteria were applied within the software for automatic peak selection. With the exception of precursor ion peak area, the same identification criteria were applied in both the positive and negative ESI-HRMS screening methods. A mass tolerance of 5 ppm was applied (i.e. precursors, fragments and isotope ions). Where confirmation was required, and in addition to the accurate mass of the precursor ion, the most abundant matching fragment ion (with the HCD cell enabled) was used. Initial intensity thresholds for automated screening of precursor ions were set at 50:1 signal-noise ratio (S/N) and peak area ≥50,000 AU/peak for positively ionised precursor ions and ≥10,000 AU/peak for negatively ionised. Lastly, an 80% fit threshold to theoretical isotope profile was set, with an acceptable intensity threshold deviation for each isotope ion set at 25% of the theoretical value. The isotopic fit threshold represents the deviation allowed between the measured and theoretical isotopic patterns, based on the performed pattern matching. The allowed intensity deviation considers the intensity of the isotope ion relative to the monoisotopic ion. Following the automated screen of wastewater data, manual inspection of all shortlisted peaks was performed to identify viable chromatographic peaks (see Section 3.4) for subsequent t_R matching with ANN and then confirmation with its reference standard t_R^M in the relevant matrix. Further criteria for acceptance included peak profile and definition (Gaussian-like profile with $n \geq 10$ datapoints/peak). A second manual check of the S/N ratio (≥3:1) was then applied to exclude erroneous peak identifications in the first automated screen.

3. Results and discussion

3.1. Modelling retention time in standard solutions using ANNs

Initial assessment of the comparative performance of ANN t_R predictions was performed without including the influence of matrix. The choice of molecular descriptors was based on our previous work which showed that these input variables contributed significantly to retention time modelling under reversed-phase conditions. It was found that, for all ANN types, a 120:16:30 split of cases across training, verification and blind test experiments yielded the best results for consistent comparison purposes. A comparison between three network types and architectures is shown in Fig. 1. A MLP network consists of a number of nodes housed within discrete layers. Input nodes are fully interconnected to these layers via non-linear activation functions. Inputs are mapped onto a set of required output values (t_R^M) and supervised learning is iterative and based on back-propagation. RBFs employ real-value functions which depend only on proximity from the origin or a single discrete

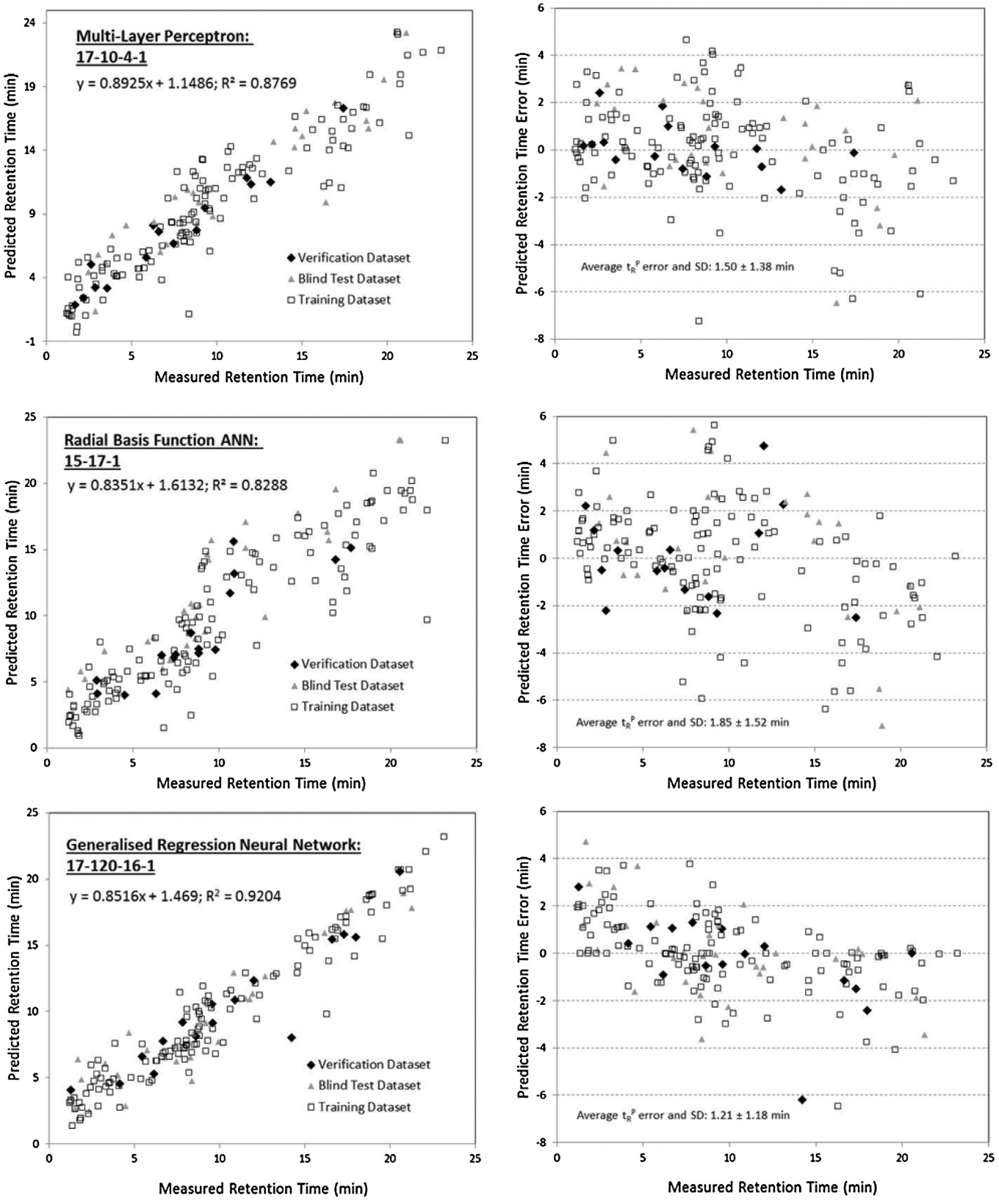

Fig. 1. The best correlation of predicted versus measured retention times achieved for MLPs, RBFs and GRNNs (left) and associated predicted retention time errors for each (on the right).

point. Lastly, GRNN-type ANNs combine an RBF layer with a linear activation function layer [9]. This network yielded the best performance overall (Fig. 1) and, along with RBFs, required a fraction of the time to optimise, train, verify and test (<10 s for 10^8 models) in comparison to MLPs. GRNNs also displayed excellent consistency across different architectures and case allocations. The optimised GRNN displayed correlation data of $y = 0.8684x + 1.3313$ ($R^2 = 0.9327$) for the training set; $y = 0.7907x + 1.8897$ ($R^2 = 0.8738$) for the verification set; and $y = 0.8075x + 1.8936$ ($R^2 = 0.8858$) for blind test cases. In particular, the average absolute t_R^P error and standard deviation for the blind test dataset was 1.39 ± 1.29 min. It was clear that ANN t_R accuracy thresholds were required by considering a portion of the case data which lay within a reasonable percentile of t_R^P error and accepting that some false negatives would be encountered as a result. Moreover, as the GRNN-type network offered markedly better results than either the RBF or MLP-type networks at this stage in the process, it was not likely, and indeed found, that this would change with inclusion of a matrix effect.

3.2. Effect of wastewater matrix on measured retention time

Most retention modelling works have similarly focussed on data derived from standards prepared in purified solvents [30,44]. Certainly for targeted methods, it is reasonable to expect that an optimised extraction procedure would eliminate or suitably minimise matrix effects. However, the value of semi-targeted data screening lies in characterisation of extra matrix components, which may later become analytes. Therefore, co-extraction of a matrix component could be considered advantageous in some respects. The SPE sorbent used here consisted of a hydrophilic–lipophilic balanced (HLB) type chemistry which has been widely adopted along with a similar protocol for this application [45,46]. However, a disparity exists in SPE concentration factors across the literature, which range from 100 to 2500-fold to achieve acceptable sensitivity and mostly for target analytes [47–53]. Several studies also used rapid gradient separations prior to mass spectrometry and reported significant MS signal suppression (often >50%) showing that matrix exists at high enough concentrations, even after application of SPE clean-up, to interfere with validated analytical methods [47,48,50]. Matrix effects on measured retention time are rarely reported, but can be overcome by using matrix-matched standards instead. Herein, an intermediate concentration factor of 1000-fold followed by a moderately long separation of 27.5 min was used in an attempt to balance this matrix effect with adequate sensitivity for broad, semi-targeted qualitative screening at the ng/L concentration level.

Seven individual 24-h composite samples of both influent and effluent wastewaters across a week were used to prepare matrix-matched standards in order to compile average t_R^M data in each matrix type separately. This was preferred over replicate data from a single composite sample of any one wastewater type (or combination thereof) to show how daily composition may affect t_R^M. As can be observed in Fig. 2(a), a mean t_R^M shift for all compounds in wastewater extracts was evident in comparison to model solutions. As a result, several important considerations for t_R predictions became apparent. Firstly, under these conditions, the majority of compounds displayed an overall increase in t_R^M irrespective of sample type meaning that use of non-matrix matched standards was generally considered inappropriate for comparison with wastewater data for confirmation purposes. Secondly, compounds eluting in the first 7 min of the gradient separation suffered the largest change in t_R^M in comparison to model solutions. More pronounced matrix effects over this window were observed for compounds in influent wastewater in particular with examples of the worst retention shifts being +0.99, +1.00 and +1.03 min for pindolol, phenmetrazine and MDMA, respectively, which all eluted

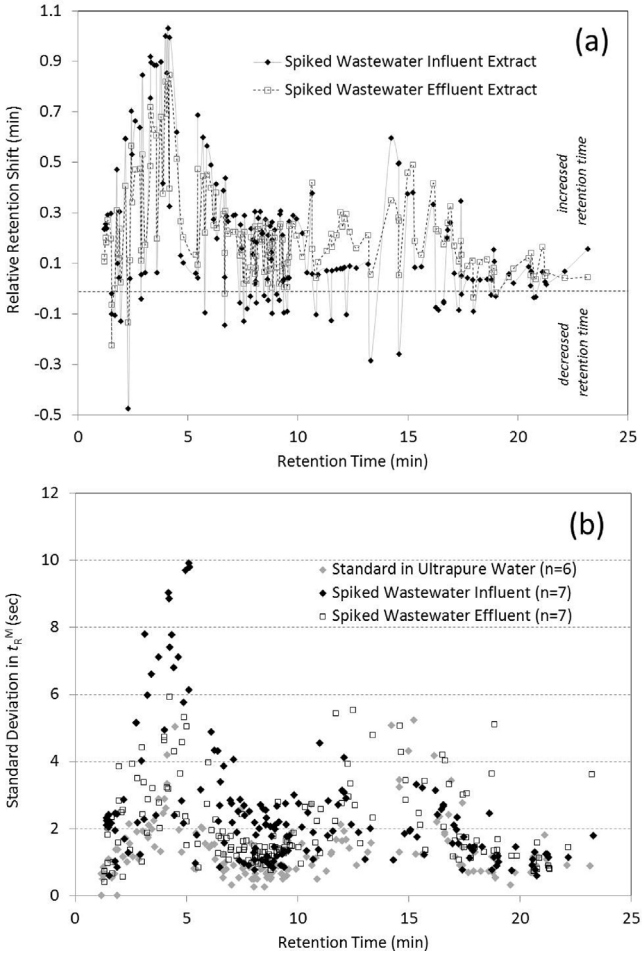

Fig. 2. The effect of matrix on (a) relative retention time in wastewater to a standard in ultra-pure water and (b) t_R^M standard deviation for standard solutions and spiked wastewater samples taken across a 1-week period.

consecutively. Past this initial 7-min elution window, the differences between influent and effluent matrix effects on t_R^M were less obvious. Thirdly, it was observed that inter-day t_R^M measurement variance on the whole was again largest for influent, followed by treated effluent and then model solutions over the same 7-min elution window (Fig. 2(b)). However, this variance was still well within acceptable method reproducibility limits (average $t_R^M \pm 15$ s [54]). Examination of total ion chromatograms revealed a broad matrix elution profile over this timeframe (maximum intensity = 4×10^8), which may have accounted for retention shifts and inter-sample variance. Even after SPE, influent and effluent wastewater extracts were coloured showing that such a matrix effect with such a widely adopted methodology was still possible. Most t_R^M variance after this initial 7-min window for all sample types was <1% relative standard deviation (RSD). The largest standard deviation of mean retention time was 10 s for MDMA in influent wastewater ($t_R^M = 5.12$ min). The mean of the measured t_R^M standard deviations for all compounds was 2.5 ± 1.9 s and 2.1 ± 1.2 s for influent and effluent, respectively. The range of peak widths (at baseline) measured for all compounds lay within the range of ~0.2–0.5 min.

3.3. Performance of GRNNs for spiked wastewater extracts

Direct replacement of t_R^M data in the GRNN for those measured in either matrix resulted in a poorer correlation overall. In an attempt to understand the robustness of GRNN networks, $n = 6$ identical model architectures were created for each sample type and trained

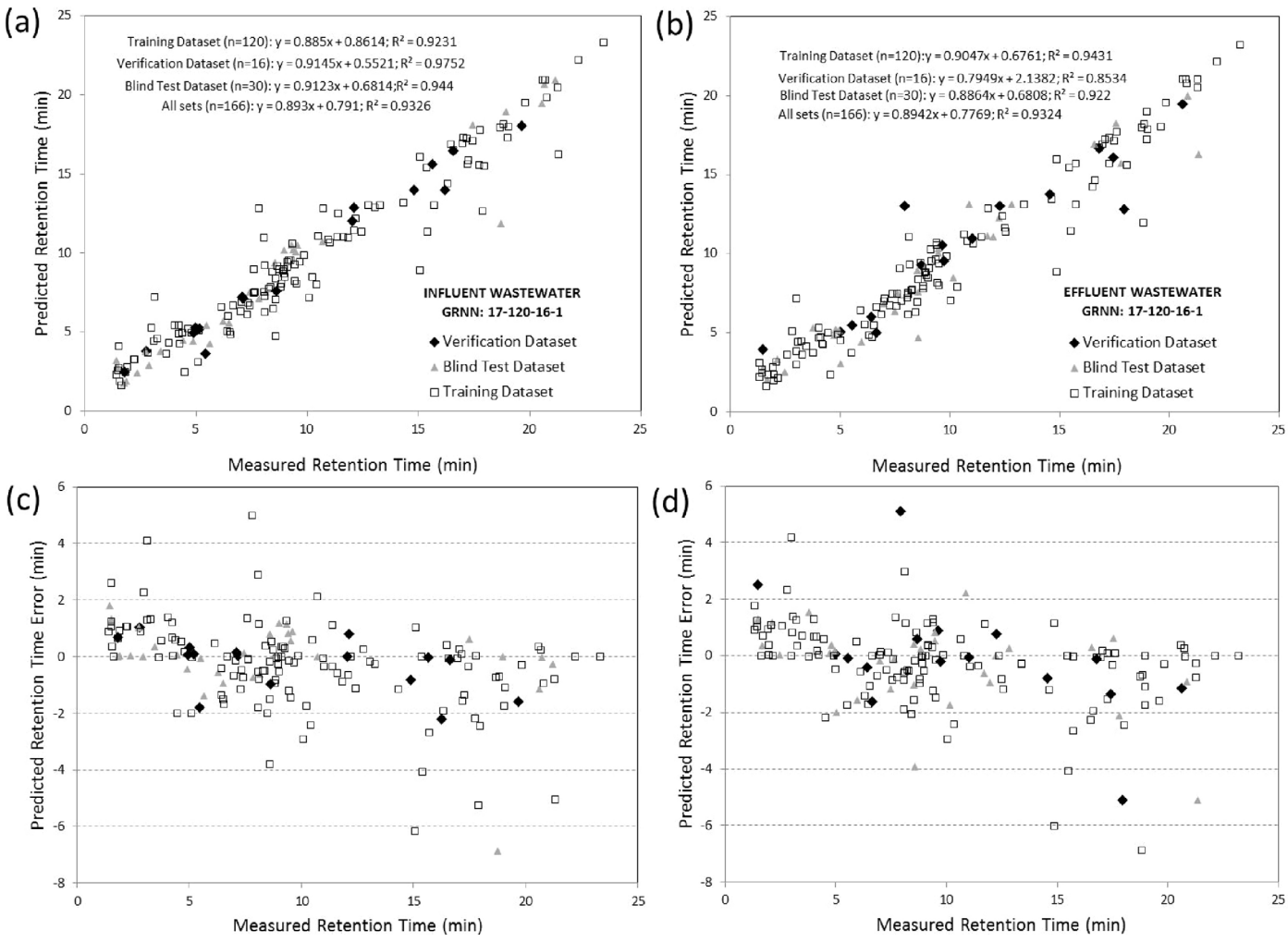

Fig. 3. Predicted versus measured retention times in (a) influent and (b) effluent wastewaters using the optimised 17-120-16-30 GRNN. The predicted retention time error for each compound across the gradient run-time is shown as (c) for influent and as (d) for effluent.

ab initio using the mean of t_R^M for each compound in each matrix. The predictive ability of the GRNN model recovered and correlation coefficients even slightly improved. For the best network applied to influent wastewater (Fig. 3(a) and (c)), the average and standard deviation of absolute t_R^P error for the entire 166 cases and the 30 blind test cases in isolation were 0.98 ± 1.16 min and 0.79 ± 1.26 min, respectively. All but one of the absolute blind test case t_R^P errors lay within a window of 1.81 min. Mean and standard deviation of t_R^P errors for the full dataset and blind test cases for effluent (Fig. 3(b) and (d)) were 0.99 ± 1.17 min and 1.06 ± 1.15 min, respectively and three of the absolute blind test case t_R^P errors lay outside 1.81 min by comparison.

Examination of replicate GRNN models showed that each input variable was used to similar degrees across matrices (Fig. 4). Error ratios >1 represented a worsening of network performance with removal of that descriptor. The top five molecular descriptors for t_R prediction in both wastewater matrix types were nDB, logD, nO, pK_a and nBnz in descending order. The consistency of input variable dependency across all 18 networks tested showed that this GRNN model could potentially be used robustly in bracketed-type analyses where matrix-matched standards could be analysed before and after each batch of wastewater samples (a) for relative comparison purposes to rule out within-batch column fouling events and (b) for better application to retention modelling by accounting for the operational conditions at the time of analysis.

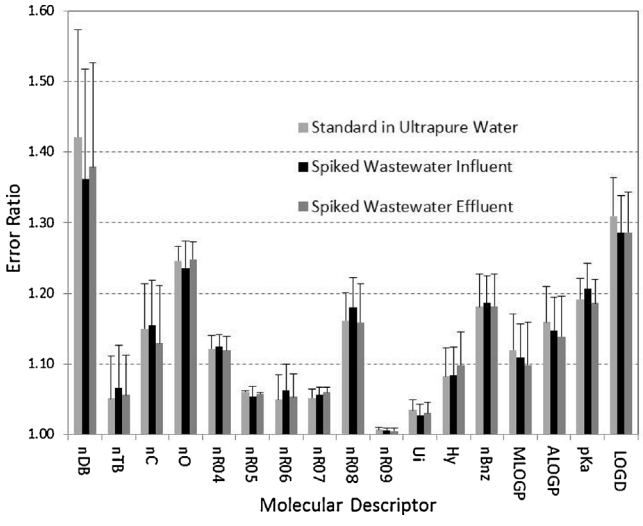

Fig. 4. Replicate network sensitivity to removal of individual molecular descriptor input variables. The error ratio represents the additional error in t_R^P where that variable was omitted from the network to that of t_R^P error where all network variables were included. Error bars represent standard deviation of the results from $n = 6$ replicate networks for each of standards in ultrapure water and spiked wastewater extracts.

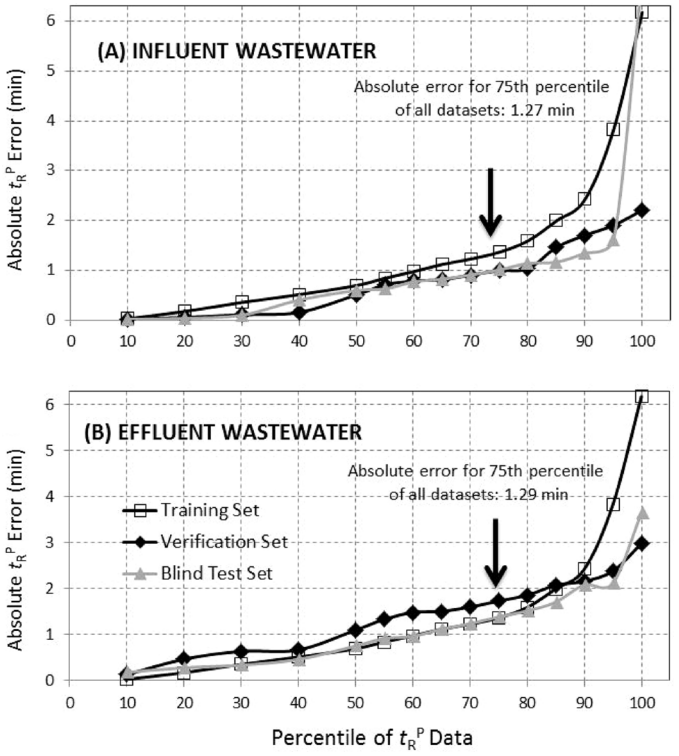

Fig. 5. Plots of absolute t_R^P error versus percentile of each training, verification and blind test dataset for (a) influent wastewater and (b) effluent wastewater.

As can be seen in Fig. 5, plots of absolute t_R^P error in either matrix relative to the percentile of data from each of the training, verification and blind test datasets revealed a moderate increase in error up to ~75–85% of the data population where it subsequently increased markedly due to the contribution of outliers. Therefore, taking the 75th percentile of all datasets across both sample types, this corresponded to a t_R^P error of 1.30 min (i.e. an elution window of 2.60 min in total and <10% of total runtime). Whilst this threshold represented a potential 25% false negative rate, extension or reduction of this threshold resulted in either an impractically wide or narrow retention window relative to peak width for this chromatographic system. As discussed later, the false negative rate was shown to be sample dependent in practice. Therefore, this limit enabled practical and rapid shortlisting of larger numbers of viable suspect compounds in a poorly understood sample. Obviously, thresholds may be adjusted to extend the scope of the semi-targeted approach in the future if needed by including more compounds during ANN training or by using a different set of chromatographic conditions. The application of ANNs to semi-targeted screening, however, is not intended for confirmatory identification and should only be used to reduce the time required to source appropriate standard reference materials for this purpose.

3.4. Trace screening of wastewater samples and evaluation of GRNN retention time predictions

Unspiked aliquots of the same 24-h composite samples of wastewater were analysed to characterise target PPCP occurrence across the week. Peak selection was performed using a much larger database than the 166 target compounds used to simulate a more realistic data mining exercise. In several cases, matching m/z data existed within this wider database along with target compound data. Automated peak selection yielded between 2500 and 3000 peaks for influent and between 1200 and 1900 peaks in effluent samples depending on the day (irrespective of the ESI mode). Despite the application of filters (as in Section 2.5), some shortlisted peaks were not deemed satisfactory and were easily excluded (e.g. they were not discrete/obvious chromatographic peaks, or were integrated regions of noise). Manual inspection reduced this number to ~700 viable peaks in both influent and effluent positive ionisation data, with a lower number observed for negative ionisation (~500 influent/~300 effluent). As multiple peaks often existed for each suspect compound, this correlated to ~350 positively ionised compounds in both influent and effluent, again with a lower number observed for negative ionisation (~250 influent/~200 effluent).

In the first instance, data for the 166 target compounds were extracted for confirmation and ANN t_R^P evaluation. Retention time confirmation was based on US EPA Method 1694 guidelines for PPCP identification whereby chromatographic peaks must elute within ±15 s of the matrix-matched standard t_R^M [54]. Here, this was taken as the average of all seven spiked influent or effluent retention times recorded across the week (inter-day t_R^M). For ANN t_R^P matching, the window was set as before at ±1.30 min. Out of the full 166 compounds used in this work, post-acquisition LC-HRMS data-mining yielded matching m/z and isotope profiles for between 70 and 82 compounds per day in wastewater (positive mode ESI-HRMS), with a lower number (19–67) observed using negative mode ESI-HRMS (Table 1 and SI). Individual compound occurrence across all samples, as well as comparison of ANN suspect shortlisting and matrix-matched standard confirmation are shown in the SI. On average, similar numbers of positively ionised compounds were confirmed using a matrix-matched standard in influent and effluent wastewaters (30–36 compounds/day). When comparing to t_R^P data, this corresponded to an overall mean % ANN success rate of 83 ± 4% and 73 ± 5% for PPCPs at trace concentrations in influent and effluent samples, respectively ($p = 0.007$). The ANN correctly excluded the presence of between 32 and 44% of TraceFinder-shortlisted compounds in wastewater each day.

Mephedrone represented an interesting example of an illicit compound which occurred in both influent and effluent wastewater on all days. Taking influent on its own, it also represented a blind test compound which could be used to reliably evaluate the semi-targeted approach using LC-HRMS data and ANN together. As can be observed from Fig. 6(a), an excellent retention time prediction match was achieved with the optimised GRNN at realistic concentration levels. Retention time was then confirmed using a matrix-matched standard along with matching isotopic m/z profiles (Fig. 6(b)). Following this, the concentration of this compound was estimated in influent wastewater across the week at concentrations ranging between 42 and 160 ng/L with the highest concentration measured on a Saturday ($R^2 = 0.9980$; method performance given in the SI).

For the majority of ions with m/z within the ±5 ppm match window, more than one viable chromatographic peak was detected (two to four viable peaks were often identified across the runtime). These mostly constituted a number of well separated peaks (e.g. codeine, betaxolol, efaproxiral, cathinone, mephedrone and bunolol) or, in some cases, a number of closely eluting/unresolved peaks (e.g. isometheptene and metipranolol). In a few cases, larger numbers of viable peaks were detected even when using such a narrow m/z match window. Table 2 shows that up to 15 viable chromatographic peaks were identified for suspected tramadol occurrence (included as a blind test case) in wastewater. Preliminary identification of this compound without a reference standard would be very challenging due to the presence of other isobaric species. Application of the ANN reduced this number to three suspect peaks in both influent and effluent data on all days. Examination of CID data yielded no identifiable ion signatures within this m/z scan range, making this an especially difficult case for occurrence confirmation. For this application using this type of

Table 1
Application of LC-HRMS and ANN prediction models to determine the occurrence of 166 selected PPCPs in unspiked influent and effluent wastewaters over a week long sampling campaign at a London-based WWTP (11th–17th March, 2014). See SI for individual compound occurrence and matching t_R^M data.

	Influent wastewater							Effluent wastewater						
Sampling Day	1	2	3	4	5	6	7	1	2	3	4	5	6	7
Number of targeted compounds shortlisted by TraceFinder software	130	134	89	134	137	140	137	116	120	121	119	121	122	112
Number of shortlisted compounds excluded	59	61	42	69	67	62	64	49	53	60	56	58	56	53
Number of confirmed compounds using ANN + matrix-matched standard	39	37	28	36	41	36	38	28	29	31	29	35	34	31
Number of extra confirmed compounds using a matrix-matched standard only (i.e. ANN false negative)	6	10	6	6	7	11	7	13	17	9	12	11	10	10
Number of extra suspected compounds using ANN only (i.e. ANN false positive)	26	26	13	24	22	31	28	26	21	21	22	17	21	18
Total number compounds confirmed (with standard only)	45	47	34	42	48	47	45	41	46	40	41	46	44	41
Success rate for ANN (%)	*87*	*79*	*82*	*86*	*85*	*77*	*84*	68	63	78	71	76	77	76
Mean % ANN success rate ± standard deviation (n = 7)				**83 ± 4**							**73 ± 5**			

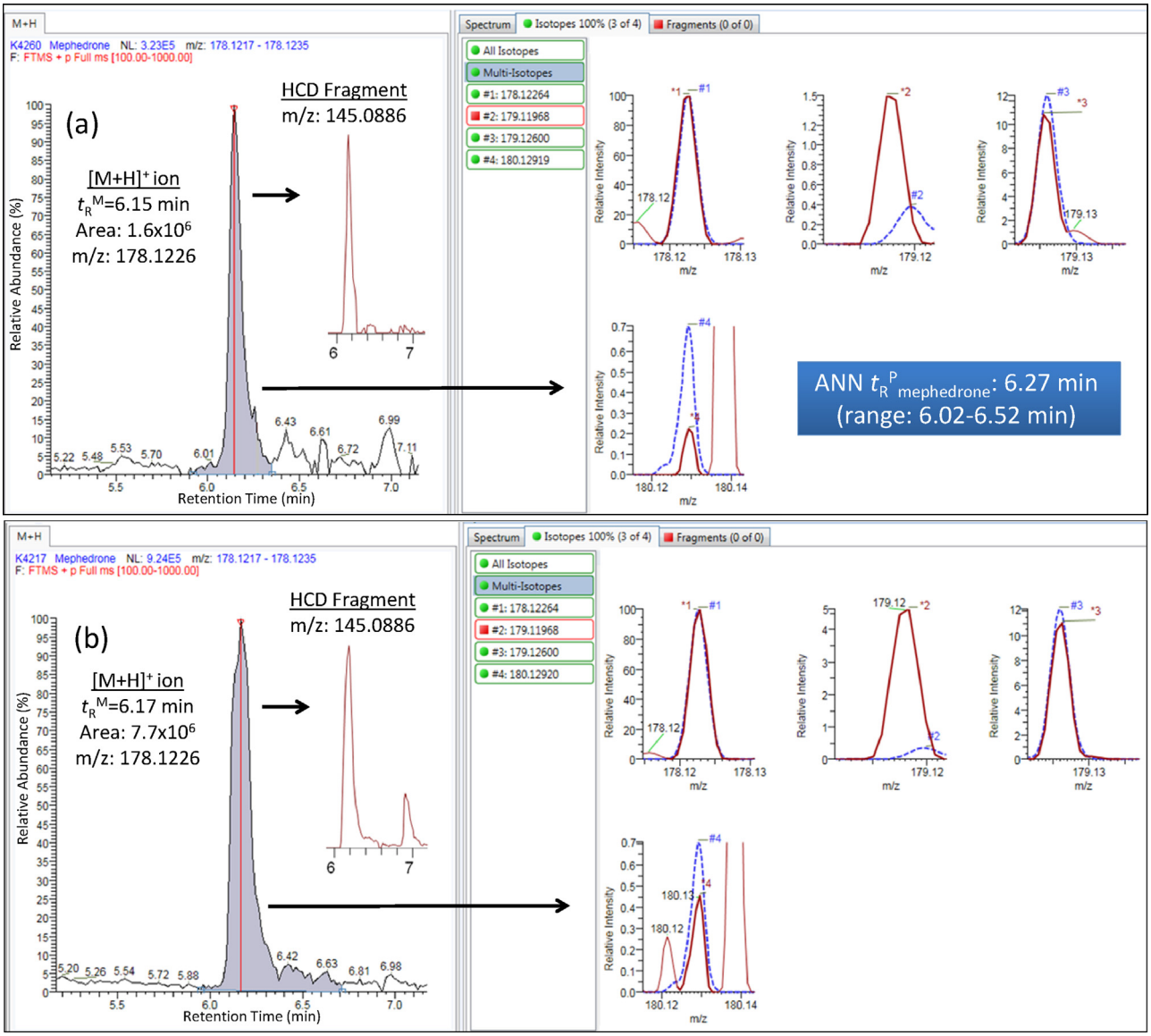

Fig. 6. Extracted ion chromatograms confirming the presence of mephedrone in (a) an unspiked influent wastewater sample and (b) a 250 μg/L matrix matched standard. The left panel in (a) and (b) both show the $[M+H]^+$ ion of mephedrone (acquired in full scan mode) and its corresponding product ion (m/z 145.0886). Values listed for the $[M+H]^+$ and product ion represent the calculated m/z. The right panel shows the isotopic profile comparison between the measured $[M+H]^+$ ion in wastewater relevant to a software-generated theoretical isotopic profile.

Table 2
Shortlist of viable chromatographic peak retention times recorded using LC-HRMS for suspected tramadol occurrence in unspiked influent and effluent wastewaters. Retention times given in bold italics shading represent confirmatory identification of tramadol using HRMS data as well as ANN and from a matrix-matched standard. Retention data given in italics shading represent only those additional peaks suspected to be tramadol using HRMS and ANN data alone.

Calculated tramadol $[M+H]^+$ *m/z*: 264.1958

Influent wastewater

Analyte in influent:	7.44 min	(Range: 7.19–7.69 min)[a]
Analyte ANN in influent:	7.56 min	(Range: 6.26–8.86 min)[b]

							Viable peak (min)							
Sampling day	t_R1	t_R2	t_R3	t_R4	t_R5	t_R6	t_R7	t_R8	t_R9	t_R10	t_R11	t_R12	t_R13	t_R14	t_R15
Day 1	2.57	5.78	*6.54*	***7.41***	*8.53*				11.74		16.30				
Day 2	2.58	5.75	*6.55*	***7.42***	*8.53*				11.76		16.31				
Day 3	2.57	5.73	*6.52*	***7.39***	*8.52*				11.77		16.30				
Day 4	2.45	5.75	*6.50*	***7.39***	*8.54*		9.31	10.04		15.95		16.71	18.43	19.05	19.92
Day 5	2.46	5.73	*6.48*	***7.35***	*8.49*	9.20			11.74	15.93	16.28				
Day 6	2.56	5.77	*6.57*	***7.47***	*8.58*						16.33				
Day 7	2.59	5.76	*6.56*	***7.43***	*8.54*						16.30				

Effluent wastewater

Analyte in effluent:	7.38 min	(Range: 7.13–7.63 min)[a]
Analyte ANN in effluent:	7.49 min	(Range: 6.19–8.79 min)[b]

							Viable peak (min)						
Sampling day	t_R1	t_R2	t_R3	t_R4	t_R5	t_R6	t_R7	t_R8	t_R9	t_R10	t_R11	t_R12	t_R13	t_R14
Day 1	2.27	4.33	5.66	*6.39*	***7.31***	*8.45*	8.83		11.73	15.91	16.24	18.39	19.03	19.88
Day 2	2.28	4.36	5.69	*6.41*	***7.31***	*8.46*	8.83		11.74	15.94	16.27	18.39	19.03	19.88
Day 3	2.29	4.37	5.70	*6.44*	***7.35***	*8.50*	8.85		11.75	15.95	16.30	18.43	19.05	19.92
Day 4	2.29	4.40	5.70	*6.44*	***7.35***	*8.48*	8.86	9.31	11.79	15.98	16.32	18.42	19.05	19.92
Day 5	2.29	4.42	5.72	*6.44*	***7.35***	*8.48*			11.75	16.28		18.41	19.89	
Day 6	2.30	4.42	5.71	*6.44*	***7.34***	*8.48*	8.83		11.78	15.96	16.28	18.42	19.04	19.89
Day 7	2.33	4.45	5.74	*6.45*	***7.34***	*8.48*	8.83	9.27	11.79	15.98	18.42	19.05	19.90	

[a] Range for confirmation of tramadol occurrence defined as ±15 s of in a spiked sample extract.
[b] Range defined as ±1.30 min.

LC-HRMS instrumentation, it reinforces the requirement for good chromatographic separation of compounds during screening. After comparison with a matrix-matched standard, tramadol was identified chromatographically as one of the ANN-shortlisted peaks in all samples across the week. Pethidine, as another example, was identified in much the same manner (Table 3). Influent samples yielded multiple chromatographic peaks with matching m/z. However, whilst perhaps more regular occurrence was observed for other peaks, one peak at ~8.90 min was found to be a match with ANN (which was subsequently confirmed with a matrix-matched standard at 8.80 min). In contrast, effluent samples yielded significantly more viable peaks with matching m/z. Some of these peaks

Table 3
Shortlist of viable chromatographic peak retention times recorded using LC-HRMS for suspected pethidine occurrence in unspiked influent and effluent wastewaters. Retention data given in bold italics shading represent confirmatory identification of pethidine using HRMS data as well as ANN and from a matrix-matched standard. Retention data given in italics shading represent only those additional peaks suspected to be pethidine using HRMS and ANN data alone.

Calculated pethidine td:paraenter $[M+H]^+$ *m/z:* 248.1645

Influent wastewater

Analyte in influent:	8.80 min	(Range: 8.55–9.05 min)[a]
Analyte ANN in influent:	7.86 min	(Range: 6.56-9.16 min)[b]

					Viable peak (min)	
Sampling day	t_R1	t_R2	t_R3	t_R4	t_R5	t_R6
Day 1	–	2.29	–	3.40	–	–
Day 2	–	2.28	–	3.36	–	–
Day 3	–	2.28	–	–	–	–
Day 4	2.18		3.17	–	***8.90***	–
Day 5	2.18		3.13	–	***8.89***	–
Day 6	–	2.28	–	–	–	–
Day 7	–	2.32	–	–	–	14.22

Effluent wastewater

Analyte in effluent:	8.78 min	(Range: 8.53-9.03 min)[a]
Analyte ANN in effluent:	7.79 min	(Range: 6.49-9.09 min)[b]

					Viable peak (min)					
Sampling day	t_R1	t_R2	t_R3	t_R4	t_R5	t_R6	t_R7	t_R8	t_R9	t_R10
Day 1	–	2.90	–	–	6.48	–	***8.87***	17.82	–	–
Day 2	1.43	2.95	3.93	–	*6.53*	*8.55*	***8.88***	17.44	17.82	–
Day 3	1.45	2.98	–	–	–	*8.57*	***8.90***	17.84	–	–
Day 4	–	2.96	–	–	*6.54*	–	***8.91***	17.48	17.86	18.28
Day 5	1.44	2.98	–	6.30	*6.52*	–	***8.89***	17.84	–	–
Day 6	1.44	3.02	–	–	*6.53*	–	***8.90***	17.48	17.83	18.25
Day 7	1.46	3.06	–	–	*6.50*	*8.56*	***8.90***		–	–

[a] Range for confirmation of pethidine occurrence defined as ±15 s of in a spiked sample extract.
[b] Range defined as ±1.30 min.

occurred on most/all days. The ANN narrowed a total of ten viable peaks to three in this case and confirmation was then achieved with the matrix-matched standard. Obviously, and where the information exists, HCD fragments may be used to eliminate more of these peaks, but these would not necessarily be known in a semi-targeted application however.

Lastly, this semi-targeted approach was applied to additional pharmaceutical residue matches occurring in an influent wastewater sample. Following HRMS data screening, 95 compounds were shortlisted, again with many showing multiple chromatographic peaks at isobaric m/z. Molecular descriptors were generated and following the GRNN prediction, 37 compounds were found to match measured sample retention times. All shortlisted compounds, along with their HRMS and t_R^M data are detailed in the SI. Interestingly, whilst none of these compounds were used in the development of ANN models, many have been previously detected in wastewater systems. Such examples included clozapine, fenoprofen, ibuprofen, naproxen, sertraline and salbutamol [55–57]. It is important to note however, such SPE methods may not recover all compound types and coupled with a relatively small database in comparison to the number of pharmaceuticals available, in reality this is still likely to represent an under-estimation of total PPCP occurrence. Moreover, it must be re-stated here that, despite application of ANNs and an HRMS database, confirmatory identification of these compounds is still required using a reference standard, and preferably one prepared in matrix.

4. Conclusion

Modelling of PPCP retention times from gradient reversed-phase chromatography of influent and effluent wastewater extracts has been successfully demonstrated for the first time. By selecting a range of molecular descriptors, predictions at the 75th percentile of all compound data were within 1.30 min of t_R^M. Discrimination of structurally similar/isobaric compounds was also possible in most cases and demonstrated acceptable t_R^P accuracy. Application to real wastewater from a week-long sampling campaign showed that ANNs could be used successfully for trace detection with similar performance. Furthermore, the application of ANNs for retention time prediction markedly reduced the number of viable chromatographic peaks for each compound and also accurately excluded compounds from wastewater data. Ultimately, this approach will allow more rapid characterisation of PPCP occurrence in wastewaters by directing the synthesis of likely candidate reference materials.

Acknowledgments

The authors gratefully acknowledge primary funding for this work from the Environmental Sustainability Knowledge Transfer Network, Engineering and Physical Sciences Research Council (EPSRC) and Thermo Fisher Scientific to support a CASE industrial scholarship for K. Munro (Reference: EP/J502029/1). Thanks are also extended to the Biotechnology and Biological Sciences Research Council (BBSRC) and AstraZeneca (under the Global SHE research programme) for award of a CASE industrial scholarship for T. Miller who collaborated on this project (Reference: BB/K501177/1). Funding bodies played no role in the design of the study or decision to publish. The authors declare no financial conflict of interest. Thanks are also extended to Alessandro Musenga for his assistance with reference standards and to the staff within the Centre of Excellence in Mass Spectrometry at KCL for technical support.

Appendix A. Supplementary data

Supplementary data associated with this article can be found, in the online version, at http://dx.doi.org/10.1016/j.chroma.2015.03.063

References

[1] C.G. Daughton, T.A. Ternes, Pharmaceuticals and personal care products in the environment: agents of subtle change? Environ. Health Persp. 107 (1999) 907.
[2] J.-W. Kim, B.R. Ramaswamy, K.-H. Chang, T. Isobe, S. Tanabe, Multiresidue analytical method for the determination of antimicrobials, preservatives, benzotriazole UV stabilizers, flame retardants and plasticizers in fish using ultra high performance liquid chromatography coupled with tandem mass spectrometry, J. Chromatogr. A 1218 (2011) 3511.
[3] J. Nurmi, J. Pellinen, Multiresidue method for the analysis of emerging contaminants in wastewater by ultra performance liquid chromatography-time-of-flight mass spectrometry, J. Chromatogr. A 1218 (2011) 6712.
[4] E. Perez-Carrera, M. Hansen, V.M. Leon, E. Bjorklund, K.A. Krogh, B. Halling-Sorensen, E. Gonzalez-Mazo, Multiresidue method for the determination of 32 human and veterinary pharmaceuticals in soil and sediment by pressurized-liquid extraction and LC-MS/MS, Anal. Bioanal. Chem. 398 (2010) 1173.
[5] D.R. Baker, L. Barron, B. Kasprzyk-Hordern, Illicit and pharmaceutical drug consumption estimated via wastewater analysis. Part A: chemical analysis and drug use estimates, Sci. Tot. Environ. 487 (2014) 629.
[6] S. Idder, L. Ley, P. Mazellier, H. Budzinski, Quantitative on-line preconcentration-liquid chromatography coupled with tandem mass spectrometry method for the determination of pharmaceutical compounds in water, Anal. Chim. Acta 805 (2013) 107.
[7] M. Laven, T. Alsberg, Y. Yu, M. Adolfsson-Erici, H. Sun, Serial mixed-mode cation- and anion-exchange solid-phase extraction for separation of basic, neutral and acidic pharmaceuticals in wastewater and analysis by high-performance liquid chromatography-quadrupole time-of-flight mass spectrometry, J. Chromatogr. A 1216 (2009) 49.
[8] M.J. Martinez Bueno, A. Agueera, M. Dolores Hernando, M. Jose Gomez, Evaluation of various liquid chromatography-quadrupole-linear ion trap-mass spectrometry operation modes applied to the analysis of organic pollutants in wastewaters, J. Chromatogr. A 1216 (2009) 5995.
[9] D.F. Specht, A general regression neural network, Neural Networks IEEE Trans. 2 (1991) 568.
[10] O.A.H. Jones, N. Voulvoulis, J.N. Lester, Analytical method development for the simultaneous determination of five human pharmaceuticals in water and wastewater samples by gas chromatography-mass spectrometry, Chromatographia 58 (2003) 471.
[11] N. Migowska, M. Caban, P. Stepnowski, J. Kumirska, Simultaneous analysis of non-steroidal anti-inflammatory drugs and estrogenic hormones in water and wastewater samples using gas chromatography-mass spectrometry and gas chromatography with electron capture detection, Sci. Tot. Environ. 441 (2012) 77.
[12] R. Grabic, J. Fick, R.H. Lindberg, G. Fedorova, M. Tysklind, Multi-residue method for trace level determination of pharmaceuticals in environmental samples using liquid chromatography coupled to triple quadrupole mass spectrometry, Talanta 100 (2012) 183.
[13] R. Loos, S. Tavazzi, B. Paracchini, E. Canuti, C. Weissteiner, Analysis of polar organic contaminants in surface water of the northern Adriatic Sea by solid-phase extraction followed by ultrahigh-pressure liquid chromatography-QTRAP(A (R)) MS using a hybrid triple-quadrupole linear ion trap instrument, Anal. Bioanal. Chem. 405 (2013) 5875.
[14] M. Petrovic, B. Skrbic, J. Zivancev, L. Ferrando-Climent, D. Barcelo, Determination of 81 pharmaceutical drugs by high performance liquid chromatography coupled to mass spectrometry with hybrid triple quadrupole-linear ion trap in different types of water in Serbia, Sci. Tot. Environ. 468 (2014) 415.
[15] W. Peysson, E. Vulliet, Determination of 136 pharmaceuticals and hormones in sewage sludge using quick, easy, cheap, effective, rugged and safe extraction followed by analysis with liquid chromatography-time-of-flight-mass spectrometry, J. Chromatogr. A 1290 (2013) 46.
[16] C.L. Chitescu, E. Oosterink, J. de Jong, A.A.M. Stolker, Ultrasonic or accelerated solvent extraction followed by U-HPLC-high mass accuracy MS for screening of pharmaceuticals and fungicides in soil and plant samples, Talanta 88 (2012) 653.
[17] F. Wode, C. Reilich, P. van Baar, U. Duennbier, M. Jekel, T. Reemtsma, Multiresidue analytical method for the simultaneous determination of 72 micropollutants in aqueous samples with ultra high performance liquid chromatography-high resolution mass spectrometry, J. Chromatogr. A 1270 (2012) 118.
[18] L. Vergeynst, H. Van Langenhove, P. Joos, K. Demeestere, Suspect screening and target quantification of multi-class pharmaceuticals in surface water based on large-volume injection liquid chromatography and time-of-flight mass spectrometry, Anal. Bioanal. Chem. 406 (2014) 2533.
[19] L. Bijlsma, E. Emke, F. Hernandez, P. de Voogt, Investigation of drugs of abuse and relevant metabolites in Dutch sewage water by liquid chromatography coupled to high resolution mass spectrometry, Chemosphere 89 (2012) 1399.
[20] M. Schriks, J.A. van Leerdam, S.C. van der Linden, B. van der Burg, A.P. van Wezel, P. de Voogt, High-resolution mass spectrometric identification and

quantification of glucocorticoid compounds in various wastewaters in The Netherlands, Environ. Sci. Tech. 44 (2010) 4766.
[21] F. Hernandez, M. Ibanez, E. Gracia-Lor, J.V. Sancho, Retrospective LC-QTOF-MS analysis searching for pharmaceutical metabolites in urban wastewater, J. Sep. Sci. 34 (2011) 3517.
[22] M. Ibanez, C. Guerrero, J.V. Sancho, F. Hernandez, Screening of antibiotics in surface and wastewater samples by ultra-high-pressure liquid chromatography coupled to hybrid quadrupole time-of-flight mass spectrometry, J. Chromatogr. A 1216 (2009) 2529.
[23] J. Robles-Molina, F.J. Lara-Ortega, B. Gilbert-Lopez, J.F. Garcia-Reyes, A. Molina-Diaz, Multi-residue method for the determination of over 400 priority and emerging pollutants in water and wastewater by solid-phase extraction and liquid chromatography-time-of-flight mass spectrometry, J. Chromatogr. A 1350 (2014) 30.
[24] J.W. Li, Prediction of internal standards in reversed-phase liquid chromatography IV. Correlation and prediction of retention in reversed-phase ion-pair chromatography based on linear solvation energy relationships, Anal. Chim. Acta 522 (2004) 113.
[25] M. Tian, K.H. Row, Study of retention in micellar liquid chromatography on a C(18) column on the basis of linear solvation energy relationships, B. Korean Chem. Soc. 29 (2008) 979.
[26] M. Vitha, P.W. Carr, The chemical interpretation and practice of linear solvation energy relationships in chromatography, J. Chromatogr. A 1126 (2006) 143.
[27] J.E. Madden, N. Avdalovic, P.R. Haddad, J. Havel, Prediction of retention times for anions in linear gradient elution ion chromatography with hydroxide eluents using artificial neural networks, J. Chromatogr. A 910 (2001) 173.
[28] N.S. Quiming, N.L. Denola, S.R. Bin Samsuri, Y. Saito, K. Jinno, Development of retention prediction models for adrenoreceptor agonists and antagonists on a polyvinyl alcohol-bonded stationary phase in hydrophilic interaction chromatography, J. Sep. Sci. 31 (2008) 1537.
[29] V.K. Gupta, H. Khani, B. Ahmadi-Roudi, S. Mirakhorli, E. Fereyduni, S. Agarwal, Prediction of capillary gas chromatographic retention times of fatty acid methyl esters in human blood using MLR, PLS and back-propagation artificial neural networks, Talanta 83 (2011) 1014.
[30] A.A. D'Archivio, A. Giannitto, M.A. Maggi, F. Ruggieri, Cross-column retention prediction in reversed-phase high-performance liquid chromatography by artificial neural network modelling, Anal. Chim. Acta 717 (2012) 52.
[31] A.A. D'Archivio, A. Incani, F. Ruggieri, Cross-column prediction of gas-chromatographic retention of polychlorinated biphenyls by artificial neural networks, J. Chromatogr. A 1218 (2011) 8679.
[32] A.A. D'Archivio, M.A. Maggi, F. Ruggieri, Multiple-column RP-HPLC retention modelling based on solvatochromic or theoretical solute descriptors, J. Sep. Sci. 33 (2010) 155.
[33] A.A. D'Archivio, M.A. Maggi, F. Ruggieri, Multi-variable retention modelling in reversed-phase high-performance liquid chromatography based on the solvation method: a comparison between curvilinear and artificial neural network regression, Anal. Chim. Acta 690 (2011) 35.
[34] A.A. D'Archivio, F. Ruggieri, P. Mazzeo, E. Tettamanti, Modelling of retention of pesticides in reversed-phase high-performance liquid chromatography: quantitative structure-retention relationships based on solute quantum-chemical descriptors and experimental (solvatochromic and spin-probe) mobile phase descriptors, Anal. Chim. Acta 593 (2007) 140.
[35] R. Berges, V. Sanz-Nebot, J. Barbosa, Modelling retention in liquid chromatography as a function of solvent composition and pH of the mobile phase, J. Chromatogr. A 869 (2000) 27.
[36] M. Pompe, M. Razinger, M. Novic, M. Veber, Modelling of gas chromatographic retention indices using counterpropagation neural networks, Anal. Chim. Acta 348 (1997) 215.
[37] N.S. Quiming, N.L. Denola, I. Ueta, Y. Saito, S. Tatematsu, K. Jinno, Retention prediction of adrenoreceptor agonists and antagonists on a diol column in hydrophilic interaction chromatography, Anal. Chim. Acta 598 (2007) 41.
[38] K. Shinoda, M. Sugimoto, N. Yachie, N. Sugiyama, T. Masuda, M. Robert, T. Soga, M. Tomita, Prediction of liquid chromatographic retention times of peptides generated by protease digestion of the Escherichia coli proteome using artificial neural networks, J. Proteome Res. 5 (2006) 3312.
[39] K. Petritis, L.J. Kangas, B. Yan, M.E. Monroe, E.F. Strittmatter, W.-J. Qian, J.N. Adkins, R.J. Moore, Y. Xu, M.S. Lipton, D.G.C. li, R.D. Smith, Improved peptide elution time prediction for reversed-phase liquid chromatography-MS by incorporating peptide sequence information, Anal. Chem. 78 (2006) 5026.
[40] A. Malenovic, B. Jancic-Stojanovic, N. Kostic, D. Ivanovic, M. Medenica, Optimization of artificial neural networks for modeling of atorvastatin and its impurities retention in micellar liquid chromatography, Chromatographia 73 (2011) 993.
[41] A.G. Fragkaki, E. Farmaki, N. Thomaidis, A. Tsantili-Kakoulidou, Y.S. Angelis, M. Koupparis, C. Georgakopoulos, Comparison of multiple linear regression, partial least squares and artificial neural networks for prediction of gas chromatographic relative retention times of trimethylsilylated anabolic androgenic steroids, J. Chromatogr. A 1256 (2012) 232.
[42] T.H. Miller, A. Musenga, D.A. Cowan, L.P. Barron, Prediction of chromatographic retention time in high-resolution anti-doping screening data using artificial neural networks, Anal. Chem. 85 (2013) 10330.
[43] L. Barron, J. Havel, M. Purcell, M. Szpak, B. Kelleher, B. Paull, Predicting sorption of pharmaceuticals and personal care products onto soil and digested sludge using artificial neural networks, Analyst 134 (2009) 663.
[44] D.R. Albaugh, L.M. Hall, D.W. Hill, T.M. Kertesz, M. Parham, L.H. Hall, D.F. Grant, Prediction of HPLC retention index using artificial neural networks and IGroup E-state indices, J. Chem. Inf. Model. 49 (2009) 788.
[45] N.V. Heuett, C.E. Ramirez, A. Fernandez, P.R. Gardinali, Analysis of drugs of abuse by online SPE-LC high resolution mass spectrometry: communal assessment of consumption, Sci. Tot. Environ. 511 (2015) 319.
[46] M. Petrovic, M. Farré, M.L. de Alda, S. Perez, C. Postigo, M. Köck, J. Radjenovic, M. Gros, D. Barcelo, Recent trends in the liquid chromatography–mass spectrometry analysis of organic contaminants in environmental samples, J. Chromatogr. A 1217 (2010) 4004.
[47] M. Petrovic, M. Gros, D. Barcelo, Multi-residue analysis of pharmaceuticals in wastewater by ultra-performance liquid chromatography–quadrupole–time-of-flight mass spectrometry, J. Chromatogr. A 1124 (2006) 68.
[48] E. Gracia-Lor, J.V. Sancho, F. Hernández, Simultaneous determination of acidic, neutral and basic pharmaceuticals in urban wastewater by ultra high-pressure liquid chromatography-tandem mass spectrometry, J. Chromatogr. A 1217 (2010) 622.
[49] K.H. Langford, K.V. Thomas, Determination of pharmaceutical compounds in hospital effluents and their contribution to wastewater treatment works, Environ. Int. 35 (2009) 766.
[50] A.L. Batt, M.S. Kostich, J.M. Lazorchak, Analysis of ecologically relevant pharmaceuticals in wastewater and surface water using selective solid-phase extraction and UPLC-MS/MS, Anal. Chem. 80 (2008) 5021.
[51] A.L.N. van Nuijs, B. Pecceu, L. Theunis, N. Dubois, C. Charlier, P.G. Jorens, L. Bervoets, R. Blust, H. Neels, A. Covaci, Cocaine and metabolites in waste and surface water across Belgium, Environ. Pollut. 157 (2009) 123.
[52] B. Shao, D. Chen, J. Zhang, Y. Wu, C. Sun, Determination of 76 pharmaceutical drugs by liquid chromatography–tandem mass spectrometry in slaughterhouse wastewater, J. Chromatogr. A 1216 (2009) 8312.
[53] B. Kasprzyk-Hordern, R.M. Dinsdale, A.J. Guwy, The effect of signal suppression and mobile phase composition on the simultaneous analysis of multiple classes of acidic/neutral pharmaceuticals and personal care products in surface water by solid-phase extraction and ultra performance liquid chromatography-negative electrospray tandem mass spectrometry, Talanta 74 (2008) 1299.
[54] USEPA, Method 1694: Pharmaceuticals and Personal Care Products in Water, Soil, Sediment, and Biosolids by HPLC/MS/MS (2007).
[55] S. Yuan, X. Jiang, X. Xia, H. Zhang, S. Zheng, Detection, occurrence and fate of 22 psychiatric pharmaceuticals in psychiatric hospital and municipal wastewater treatment plants in Beijing, China, Chemosphere 90 (2013) 2520.
[56] L. Lishman, S.A. Smyth, K. Sarafin, S. Kleywegt, J. Toito, T. Peart, B. Lee, M. Servos, M. Beland, P. Seto, Occurrence and reductions of pharmaceuticals and personal care products and estrogens by municipal wastewater treatment plants in Ontario, Canada, Sci. Tot. Environ. 367 (2006) 544.
[57] A. Lajeunesse, S.A. Smyth, K. Barclay, S. Sauvé, C. Gagnon, Distribution of antidepressant residues in wastewater and biosolids following different treatment processes by municipal wastewater treatment plants in Canada, Water Res. 46 (2012) 5600.

Ecotoxicology and Environmental Safety 120 (2015) 279–285

Contents lists available at ScienceDirect

Ecotoxicology and Environmental Safety

journal homepage: www.elsevier.com/locate/ecoenv

Environmental monitoring of urban streams using a primary fish gill cell culture system (FIGCS)

Sabine Schnell [a], Kafilat Bawa-Allah [b], Adebayo Otitoloju [b], Christer Hogstrand [a], Thomas H. Miller [c], Leon P. Barron [c], Nic R. Bury [a,*]

[a] Division of Diabetes and Nutritional Sciences, Faculty of Life Sciences and Medicine, King's College London, Franklin Wilkins Building, 150 Stamford Street, London SE1 9NH, United Kingdom
[b] Ecotoxicology Laboratory, Department of Zoology, Faculty of Science, University of Lagos, Akoka, 101017 Lagos, Nigeria
[c] Analytical and Environmental Sciences Division, Faculty of Life Sciences and Medicine, King's College London, Franklin Wilkins Building, 150 Stamford Street, London SE1 9NH, United Kingdom

ARTICLE INFO

Article history:
Received 30 April 2015
Received in revised form
6 June 2015
Accepted 8 June 2015
Available online 17 June 2015

Keywords:
cyp1a1
cyp3
Metallothionein
Fish
Environmental monitoring
Cell culture
3Rs

ABSTRACT

The primary fish gill cell culture system (FIGCS) is an *in vitro* technique which has the potential to replace animals in whole effluent toxicity tests. In the current study FIGCS were transported into the field and exposed to filtered (0.2 μm) river water for 24 h from 4 sites, on 2 different sampling dates. Sites 1 and 2 are situated in an urban catchment (River Wandle, London, UK) with site 1 downstream of a sewage treatment work; site 3 is located in a suburban park (River Cray, Kent, UK), and site 4 is more rural (River Darent, Kent, UK). The change in transepithelial electrical resistance (TER), the expression of the metal responsive genes metallothionein A (*mta*) and B (*mtb*), cytochrome P450 1A1 (*cyp1a1*) and 3A27 (*cyp3a27*), involved in phase 1 metabolism, were assessed following exposure to sample water for 24 h. TER was comparable between FIGCS exposed to 0.2 μm filtered river water and those exposed to synthetic moderately soft water for 24 h. During the first sampling time, there was an increase in *mta*, *cyp1a1* and *cyp3a27* gene expression in epithelium exposed to water from sites 1 and 2, and during the second sampling period an increase in *cyp3a27* gene expression at sites 1 and 4. Urban river water is a complex mixture of contaminants (e.g., metals, pesticides, pharmaceuticals and polyaromatic hydrocarbons) and the increase in the expression of genes encoding *mta*, *cyp1a1* and *cyp3a27* in FIGCS is indicative of the presence of biologically active pollutants.

1. Introduction

A large number of fish are used each year for waste effluent toxicity testing, with an estimated 3 million being used in the US alone see Tanneberger et al. (2013). There is a desire worldwide to reduce the number of fish used in toxicity testing and thus reliable alternatives are being investigated. A number of studies have assessed fish cell lines as alternative methodologies with success (Davoren et al., 2005; Dayeh et al., 2009; Kinani et al., 2010; Schnell et al., 2013). However, a drawback to using cell lines for waterborne toxicity is that they are often unable to tolerate hypoosomotic water. To overcome this, water has to be modified by the addition of osmolytes to ensure osmotic tonicity between the external medium and the intracellular compartment. An alternative approach is the use of a primary FIsh Gill Cell culture System (FIGCS; Walker et al., 2008; Minghetti et al., 2014, Bury et al., 2014). This method uses a double seeding technique and ensures that the epithelium contains the different cell types characteristic of an intact gill (Fletcher et al., 2000; Walker et al., 2007). When grown on permeable supports, the membrane forms a polarised tight epithelium with transepithelial electrical resistance (TER) measurements exceeding 10 KΩ. At this stage the epithelium is able to tolerate the application of water on the apical surface for up to 48 h. The property of tolerating freshwater has led to the use of the system for physiological studies see Wood et al. (2002), the assessment of pharmaceutical uptake (Stott et al., 2015) and toxicity of pollutants within the aquatic environment (Sandbacka et al., 1999, Bury et al., 2014).

A recent study also explored the potential for FIGCS to be used for environmental monitoring of natural waters (Minghetti et al., 2014). In this study the cells were transported 1000 km in a temperature controlled container and were exposed in the field to metal-contaminated river water under non-sterile conditions. The

* Corresponding author.
E-mail address: nic.bury@kcl.ac.uk (N.R. Bury).

http://dx.doi.org/10.1016/j.ecoenv.2015.06.012
0147-6513/

membrane maintained integrity, showing comparable changes in TER after 24 h between those exposed to river water and those exposed to reconstituted sterile water. The cells also showed no signs of cell mortality, as measured by the Methylthiazol Tetrazolium (MTT) assay, but they did show an increase in expression of the genes encoding for the metal binding proteins metallothionein A and B (Minghetti et al., 2014), demonstrating the presence of bioreactive metals.

The previous study (Minghetti et al., 2014) specifically targeted rivers in Cornwall, South West England as they are known to have elevated metals with very little other pollutant load and in the laboratory the primary gill cells are known to respond to metals with increased expression of *mta* and *mtb* genes (Walker et al., 2007). The FIGCS output (gene expression) is an integrative response that takes into account the over lying water chemistry, which determines metal speciation, and the ability of the metal to enter the cell and bind to intracellular receptors in sufficient quantities to cause an effect. If this system is to be used more widely to detect the presence of compounds that may elicit a biological effect, it is necessary to evaluate the response of the cells to more complex aquatic matrices. Thus, the aims of the current study are to expose the primary gill cell culture to a further 3 sites on urban rivers in London, UK, and one site on a more rural river in Kent, UK, that potentially have a far complex mixture of pollutants than the metal contaminated rivers in Cornwall (Minghetti et al., 2014) and to measure the expression of genes encoding for *mta* and *mtb*, as well as *cyp1a1* and *cyp3a27*, enzymes which are involved in phase 1 organic compound metabolism (Uno et al., 2012), as well as TER following 24 h of exposure to the river water. An increased transcription of *mta* and *mtb* indicate transactivation through metal-responsive transcription factor-1 (Mtf1) (Olsson et al., 1995; Samson and Gedamu, 1995), whilst increased levels of mRNA for *cyp1a1* and *cyp3a27* are indicative of increased activity of the aryl hydrocarbon receptor (Ahr) and the pregnane-X-receptor /retinoic acid-X-receptor (Pxr/Rxr) heteroduplex, respectively (Uno et al., 2012).

2. Materials and methods

2.1. Study sites and water chemistry

The 4 study sites were on the River Wandle at Colliers Wood (site 1, latitude 51.420368; longitude −0.181487) and Beddington (site 2, 51.370284; −0.125072), the river Cray at Sidcup (site 3, 51.428425; 0.132730), all in South East London, and the River Darent at Lullingstone (site 4, 51.362372, 0.196315) in Kent, UK. Site 1 on the River Wandle is highly urbanised and is approximately 4.5 km downstream of Beddington Sewage Treatment Works (STW) which receives wastewater from approximately 360,000 people. Site 2 is above the input from Beddington STW, but is still within a heavily urbanised catchment, receiving drainage from the Borough of Croydon. Site 3 is within a suburban park, whilst Site 4 is within a rural setting; however the River Darent flows through suburban area of Sevenoaks, Kent. The first sampling date was 2.12.2013 and the second sampling on 11.12.2013.

Water pH, conductivity, temperature and suspended solids were measured using a Hanna Hi991300 probe. For chemical analysis water samples were collected in the field in low density polyethylene bottles and immediately frozen and stored at −20 °C on returning to the laboratory. Total and Mg hardness and alkalinity were measured colourimetrically, and for Cu and Zn analysis water samples were filtered (0.2 μm filters) and acidified prior to measurement via inductively coupled plasma mass spectrometer (Aglient 7700x ICP-MS). For analysis of pharmaceuticals, sample clean-up and pre-concentration was achieved by solid phase extraction (SPE) on Waters Oasis mixed-mode hydrophilic lipophilic balanced (HLB) cartridges, 6 cc, 200 mg sorbent (Waters Corporation, Milford, MA, USA), similarly to our previous works (Lacey et al., 2008; Barron, et al., 2008, 2009; Miller et al., 2015). Briefly, 100 mL aliquots of surface water samples were adjusted to pH 6.5 with ammonium acetate (1 mL of a 1 M solution). SPE cartridges were conditioned with 6 mL of MeOH and ultra-pure water followed by sample loading. Cartridges were then washed with 1 mL ultra-pure water and dried for ~30 min under a vacuum. Cartridges were eluted in 10 mL of 50:50 ethyl acetate: acetone and dried under N_2 and at 30 °C using a TurboVap (Biotage, Uppsala, Sweden). The dried extract residues were reconstituted in 0.5 mL of 90:10 (v/v) 10 mM ammonium acetate in water:acetonitrile and transferred to a septum capped vial. Analysis was performed on an Agilent 1100 high pressure liquid chromatography system interfaced to Waters Quattro triple quadrupole mass spectrometer according to the conditions listed in Miller et al. (2015). Separations were performed on a C_{18} reversed-phase column (Waters Sunfire $C_{18,}$ 2.1 × 150 mm, 2.5 μm). Multiple reaction monitoring was used to detect characteristic transitions of all targeted pharmaceutical compounds. Concentrations of all pharmaceuticals are expressed as single-shot quantitation measurements based on comparison to a single matrix matched calibrant at 200 ng L^{-1} spiking level (in triplicate). Therefore concentrations should be considered as semi-quantitiative. These were extracted alongside unspiked samples ($n=3$) for background correction purposes.

2.2. Cell culture and field exposures

Primary gill cell culture techniques and exposure methods followed the methods described in Minghetti et al. (2014). Rainbow trout (*Oncorhynchus mykiss*) were obtained from a local trout farm. Primary gill cell cultures were prepared from fish of 80–100 g. All fish were housed at King's College London where they were maintained in fibreglass tanks (1000 L) with flowing and aerated de-chlorinated City of London tap water ($[Na^+]$= 0.53 mM; $[Ca^{2+}]$=0.92 mM; $[Mg^{2+}]$=0.14 mM; $[K^+]$=0.066 mM; $[NH_4^+]$=0.027 mM), which was passed through activated carbon, mechanical and biological filters. Water temperature was maintained at 14 °C, while photoperiod was held constant (12 h light, 12 h dark). Fish were fed daily a one-percent (w/w) ration of trout pellets. The primary gill cells were isolated and cultured as described in Fletcher et al. (2000) and prepared using the double seeding technique as described in Kelly et al. (2000) and Walker et al. (2007). Sterile techniques were used throughout all cell culture procedures. Briefly, for each seeding, 2 fish were sacrificed (following local UK Home Office schedule 1), the gills were dissected out and the gill filaments were subject to cleaning and tryptic digestion (0.05% Trypsin-EDTA; Invitrogen). Isolated rainbow trout gill cells were seeded onto cyclopore polyethylene terephthalate membrane (cell, surface area 0.9 cm^2, pore size 0.4 μm, Falcon) at a cell density of 1.2×10^6 per insert, in Leibovitz (L-15) medium (Invitrogen) supplemented with antibiotics (5% foetal bovine serum (FBS); Sigma, 2% penicillin and streptomycin (PEST); Invitrogen and 2% gentamicin; GIBCO v/v). After 24 h incubation at 18 °C in an air atmosphere cool incubator (Sanyo Mir-253), the cells were washed twice in phosphate-buffered saline (PBS) to remove debris and another seeding of primary gill cells was added at the same density per insert, and cultured in supplemented L-15 medium. After a further 24 h incubation another PBS wash followed and supplemented L-15 was replaced at a volume of 1.5 mL in the apical chamber of the insert and 2.0 mL in the basolateral chamber. Cultures were grown at 18 °C. After 96 h the gill cell system was cultured using L-15 medium +5% FBS, but without antibiotics with complete medium changes every 48 h. The

development of an intact gill epithelium was monitored daily through 'blank'-corrected measurements of transepithelial electrical resistance (TER) using a custom-modified epithelial tissue voltohmeter (EVOMX; World Precision Instruments) fitted with chopstick electrodes (STX-2). Inserts with a TER > 10 KΩ (range 10–32.2 KΩ) were used for the study.

To avoid any potential alterations in water chemistry when transporting samples from the field to the laboratory for toxicity testing we chose to transport the primary gill cell cultures to the field in a Labcold portable medical refrigerator (Model RPDF0012D) at 18 °C and expose to water directly taken from the sites, before being transported back to the laboratory. Two field trips were conducted in early December 2013 and inserts used in each trip had been derived from 4 biological replicates. Prior to travelling into the field the TER was measured for each insert. In the field, media was removed and the cells washed with PBS. To the basolateral compartment fresh L15 media was added and to the apical compartment either unfiltered or filtered (0.2 μm filters) river water or filtered medium-soft water (MSW: $[Na^+]$=0.770 mM; $[Cl^-]$=0.757; $[Ca^{2+}]$=0.340 mM; $[Mg^{2+}]$=0.152 mM; $[K^+]$=0.077 mM; $[HCO_3]$=0.771; $[SO_4]$=0.152). The inserts were transferred back to the lab and remained in the Labcold portable medical refrigerator at 18 °C for 24 h.

2.3. QPCR

Total RNA was extracted from cells using TRIzol® Reagent (Ambion, UK) and phase separation performed using Phase Lock heavy tubes (5prime, USA). The purified total RNA was DNase treated (TURBO DNase kit, Ambion, UK) and cDNA synthesis was performed following the manufacturer's instruction (Advantage RT for PCR kit, Clontech) from 0.5 μg of total RNA. Primers for qPCR of target genes metallothionein A (*mta*) and B (*mtb*) and cytochrome P450 1A1 (*cyp1a1*) and 3A27 (*cyp3a27*), as well as the reference gene elongation factor 1 beta (*eef1b*) were designed using Primer-BLAST (http://www.ncbi.nlm.nih.gov/tools/primer-blast/), see Table 1 for details. Only 1 reference gene (*eef1b*) was tested because the invariability of its expression has previously been established in the gill cell culture (Minghetti et al., 2014). All amplified cDNA had been previously sequence verified (Minghetti et al., 2014; Schnell et al. unpublished data). For each sample, qPCR was run in triplicate on an ABI-prism 7900 HT qPCR thermocycler using SYBR-green Premix Taq II (Takara, RR820A). QPCR conditions followed those suggested by Takara, except for *mta* and *mtb*, where a 3 step programme was applied, 95 °C for 5 s, 55 °C for 30 s and 72 °C for 30 s. After 40 cycles, specificity of reactions was checked by inspecting melting curve profiles. Gene expression of target genes were normalised to *eef1B* and expressed as fold change relative to those in the control MSW controls.

2.4. Statistics

All data are presented as means+SEM. TER data (expressed as a % of pre-exposed conditions) and gene expression, expressed as a ratio of the expression measured in MSW controls. Differences ($p < 0.05$) between the gene expression levels at each site and the water controls was assessed via a Student's *t*-test (SigmaPlot v 12.0) on log transformed data.

3. Results

Site 1 is downstream of Beddington STW discharge and receives input from a catchment that has a greater proportion of impervious cover compared to the other sites. At this site the highest measured pH, conductivity, total dissolved solids (TDS), hardness alkalinity, metal content and pharmaceutical concentrations were recorded (Tables 2 and 3), with the pH reaching 8.77, conductivity 801 μS/cm, total hardness 233 mg $CaCO_3$ L^{-1} and alkalinity 170 mg $CaCO_3$ L^{-1}. Dissolved copper levels exceeded the United Kingdom Environmental Quality Standards (EQS) for waters with a hardness of between 200–250 mg $CaCO_3$ L^{-1} [dissolved Cu EQS 10 μg L^{-1}] at both sample points with concentrations of 26 and 14.1 μg L^{-1}, the EQSs were not exceed at the other sites. Dissolved zinc concentrations were also highest at site 1, but these did not exceed the EQS (Table 2 – for waters of 200–250 mg $CaCO_3$ L^{-1} Zn EQS 300 μg L^{-1}). Pharmaceuticals were detected at each site on both of the sampling times with the highest concentrations determined at site 1. The highest of these was carbamazepine at 552 and 298 ng L^{-1}, followed by ranitidine at 359 and 179 ng L^{-1}, propranolol at 207 and 212 ng L^{-1}, and trimethroprim at 156 and 162 ng L^{-1}. Of the other compounds, atentolol, cimetidine and bezafibrate were also detected at site 1 at both sampling points. At sites 2, 3 and 4 caffeine was also present along with carbamazepine and propranolol. Of the other drugs measured at sites 2, 3 and 4 atenolol, ranitidine, metoprolol, temazepam and diazepam were occasionally detected (see Table 3 for full details). The pharmaceutical concentrations were generally lower at the second sampling point (Table 3).

On both sampling days the TER of FIGCS exposed to filtered (0.2 μm) river water following 24 h exposures were comparable to the TER of FIGCS exposed to MSW (Fig. 1). FIGCS exposed to unfiltered urban river water showed a drop in TER of between 75% and 90% (data not shown).

Gene expression levels were only performed on those cell cultures exposed to the filtered river water, because the large drop in TER on exposure to unfiltered water was presumed to be due to a loss of membrane integrity and potentially cell death. The gene expression levels of *mta* were significantly elevated at site 1 and 2 on the first sampling date. At all other sites and on the second sampling date *mta* was not induced compared to the controls. *mtb* did not differ from the MSW treatment during either of the two field trips (Fig. 2a and b). Expression of *cyp1a1* was also elevated at sites 1 and 2 on the first sampling, but not at the other sites and not on the second sampling date. *Cyp3a27* expression was elevated also at sites 1 and 2 during the first trip and during the second exposure at sites 1 and site 4 during the second trip. Expression of *cyp3a27* was unaffected at the other sites at the other sampling time (Fig. 2).

Table 1
Primer details and GenBank (http://www.ncbi.nim.nih.gov/) accession number.

Gene name	Forward primer 5′ – 3′	Reverse primer 5′-3′	GenBank accession number
mta	ACACCCAGACAAACTACTAC	GGTACAAAAGCTATGCTCAA	M18103
mtb	GCTCTAAAACTGGCTCTTGC	GTCTAGGCTCAAGATGGTAC	M18104
cyp1a1	TGACCCGGAGCTGTGGAAGGAG	CAGCCTTTGGAGCAGGATGGCC	U62796
cyp3a27	ACATGGAGACGGATCCGCAGTG	AAGCTGTGCTGGTGACCACGTC	U96077
eef1b	TTGGCGGCATAGGCTGCGATTC	TGGGCCAGTATGGTCCTTCCGG	FP321654

Table 2
Water chemistry and metal concentrations at the 4 study sites.

	Site 1		Site 2		Site 3		Site 4	
	2/12/13	11/12/13	2/12/13	11/12/13	2/12/13	11/12/13	2/12/13	11/12/13
pH	8.77	8.49	7.33	7.26	7.6	7.92	7.63	7.61
Conductivity (μS/cm)	790	801	709	609	626	645	555	556
TDS (ppm)	403	403	308	310	316	325	284	286
Total hardness	203	233	162	166	149	141	152	158
Calcium hardness	195	206	145	141	139	121	138	135
Alkalinity	170.2	165.2	130.1	115.1	120.1	120.1	110.1	95.1
Cu ($\mu g\ L^{-1}$)	26	14.1	2.45	1.55	1.11	3.71	2.3	1.74
Zn ($\mu g\ L^{-1}$)	36.3	15.5	6.38	4.81	0.6	3.25	1.51	2.61

Hardness and alkalinity expressed as (mg $CaCO_3\ L^{-1}$)

4. Discussion

The present study showed that the primary fish gill cell culture system (FIGCS) can be transported to the field to sample urban rivers, withstands filtered urban river water for 24 h and exhibits altered expression of genes encoding the metal binding protein metallothionein A and two phase 1 enzymes cytochrome P4501A1 and 3A27. Previous work had demonstrated the ability of the primary gill cells to be transported to the field for environmental monitoring of rivers contaminated with metals in the South-West of England (Minghetti et al., 2014). The current work corroborates the findings that these cells show increased *mta* expression when exposed to natural waters with elevated Cu and also extends this observation to show that the cells can also detect chemicals capable of inducing *cyp1a1* and *cyp3a27* expression. This supports the use of the primary gill cells as a potential tool for detecting biologically active chemicals in natural waters.

The transepithelial electrical resistance (TER) is a measure of membrane integrity and the gill cultures form exceedingly tight epithelia with TERs $>10\ K\Omega$ (Fletcher et al., 2000; Bury et al., 2014). In the laboratory the application of water to inserts where the TER is still rising causes a further rapid rise in the TER before dropping to around or below the starting TER (Schnell personal observation): this can be maintained for 24–48 h (Walker et al., 2007; Stott et al., 2015). Previously, the application of natural water from metal contaminated rivers in the field, whether unfiltered or filtered (0.2 μm filter), had no significant effect on the TER after 24 h if compared to inserts that received synthetic water or media change in the field (Minghetti et al., 2014). Similarly, FIGCS transported into the field and exposed to (0.2 μm) filtered urban river waters for 24 h show a comparable TER to FIGCS exposed to MSW under the same conditions (Fig. 1). However, exposure of the cells to unfiltered urban river water caused a rapid decline in TER (data not shown). Urban streams receive a considerable amount of particulate matter, including bacteria from faecal contamination and the assumption is that this is toxic to the cells.

The most prominent molecular response measured in the cultured cells was an induction of *cypa3a27* at sites 1 and 2 during the first sampling trip (Fig. 2). The rainbow trout *cyp3a27* belongs to the CYP3A subfamily of cytochrome p450 monooxygenases involved in xenobiotic phase 1 metabolism (Uno et al., 2012); the trout sequence is similar to the human CYP3A4 (Lee et al., 1998). Cyp3a27 is associated with steroid and other xenobiotic metabolism in hepatocytes (Buhler et al., 2000), but it is also highly expressed, >2 fold higher than the liver, in the pyloric caeca and anterior intestine of rainbow trout, suggesting an important role in first phase metabolism of xenobiotics present in the diet (Lee et al., 2001). Cyp3A27 is also expressed in rainbow trout gills and increases during a salinity challenge and facilitates the metabolism of the pesticide fenthion (Lavado et al., 2009).

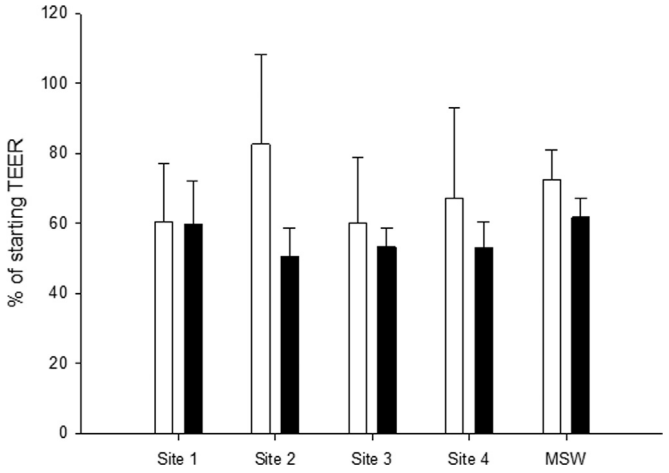

Fig. 1. Transepithelial electrical resistance (TER) of inserts exposed to filtered (0.2 μm) river water from the 4 sites from the first (white bars, 2.12.13) and second (black bars, 11.12.13) sampling period and medium soft water (MSW). Values represent an average of 4–6 inserts ± SEM and are expressed as a % of the starting TER prior to changing the media for water after 24 h exposure.

It is estimated that the *hCYP3A4* gene is induced by an estimated 50% of all therapeutic drugs, primarily via the pregnane-X-receptor signalling, and potentially other pathways (Luo et al., 2002; Luo et al., 2004). Consequently, the study chose to analyse for the presence of pharmaceuticals using previously established methods (Lacey et al., 2008; Barron, et al., 2008, 2009; Miller et al., 2015). Of the pharmaceuticals measured in the river, carbamazepine was the highest at Site 1 on both sampling times (Table 3) and this drug is known to induce *CYP3A* gene expression in humans (Oscarson et al., 2006) and rats (Tateishi et al., 1999). However, the concentrations of carbamazepine often used in the mammalian studies (e.g. Usui et al., 2003; Kamiguchi et al., 2010) are around the known clinical plasma concentrations of 25.39 $\mu mol\ L^{-1}$ (reported in Usui et al., 2003) which is equivalent to 5992 μg/L, a value in excess of an order of magnitude higher than that measured at site during the first sampling time point ([carbamazepine]=552 ng/L). It is difficult to associate an elevation in *cyp3a27* expression solely with carbamazepine, as the expression of this gene was also seen at site 2 (first sampling period) and site 4 (second sampling period), where there were significantly lower pharmaceutical concentrations (Table 3). In addition, within the mixture of pharmaceuticals measured at site 1 there are compounds such as cimetidine and ranitidine (Table 3), which are inhibitors of *CYP3A4* gene expression (Martínez et al., 1999). The CYP3 family of enzymes are known for their oxidative transformation of xenobiotics including, in addition to pharmaceuticals, pesticides (Lavado et al., 2009) and polyaromatic hydrocarbons (Zanette et al., 2013). For example, in the bivalve *Mytilus edulis*, *cyp3-like 1* and *cyp3-like 2* genes were induced by beta-

naphthalene and PCB126, respectively (Zanette et al., 2013). The current results would suggest that, besides pharmaceuticals, there are other compounds present in these urban rivers that are inducers of *cyp3a27* gene expression in the primary gill cell cultures.

The induction of *CYP1A1* gene occurs via the arhyl-hydrocarbon receptor (AHR) and is associated with the detoxification of poly-aromatic hydrocarbons (Billard et al., 2006). The catchment of the river Wandle (sites 1 and 2) is heavily urbanised and the induction *cyp1a1* in the primary gill cell at sites 1 and 2 during the first sampling period may reflect the presence of PAHs (Fig. 2), which,

Table 3
Semi-quantitative results for pharmaceutical concentrations measured in surface waters across 4 study sites.

	Site 1		Site 2		Site 3		Site 4	
	2/12/13	11/12/13	2/12/13	11/12/13	2/12/13	11/12/13	2/12/13	11/12/13
Atenolol	143 (6)	81 (71)	ND	ND	ND	2.6 (0.5)	ND	ND
Caffeine	251 (47)	111 (22)	247(100)	321 (70)	463(119)	127 (23)	89 (36)	87 (9)
Cimetidine	103 (12)	44 (13)	ND	ND	ND	ND	ND	ND
Rantidine	359 (51)	179 (152)	ND	ND	16.7 (29)	ND	ND	16 (23)
Sulfamehtazine	1.6 (2.8)	6.3 (10.9)	ND	ND	ND	ND	ND	ND
Antipyrin	ND	21 (35)	ND	ND	ND	ND	ND	ND
Trimethoprim	156 (3)	162 (6)	ND	ND	ND	ND	ND	ND
Metoprolol	22 (0.6)	9.7 (5)	0.7 (1.2)	ND	5.3 (0.7)	1.4 (1.2)	ND	ND
Ketaprofen	27 (5)	43 (35)	ND	ND	ND	ND	ND	ND
Bezafibrate	108 (32)	102 (7)	ND	ND	ND	ND	ND	ND
Propranolol	207 (40)	212 (54)	71 (35)	181 (108)	105 (29)	72 (14)	63 (46)	105 (10)
Carbamazepine	552 (22)	298 (136)	7.9 (3)	8.3 (0.2)	4.8 (0.1)	9.1 (5.1)	3.7 (3)	2.7 (0.2)
Indometacin	50 (12)	ND	ND	ND	ND	ND	ND	ND
Naproxen	561 (9)	339 (144)	ND	ND	ND	ND	ND	ND
Warfarin	9.1 (16)	59 (63)	ND	ND	ND	ND	ND	ND
Gemfibrozil	ND	ND	ND	ND	ND	ND	ND	ND
Nimesulide	ND	ND	ND	ND	ND	ND	ND	ND
Temazepan	69 (5)	55 (3.6)	2 (0.3)	ND	ND	ND	ND	ND
Diazepam	3.9 (4.5)	ND	28 (19)	ND	9.4 (12)	7.4 (7.1)	ND	ND
Nifedipine	ND	ND	ND	ND	ND	ND	ND	ND

Values in ng/L. Values represent average+SD in parentheses of triplicate measurement from a single water sample. NB The same water was used for the exposure. ND: not detected.

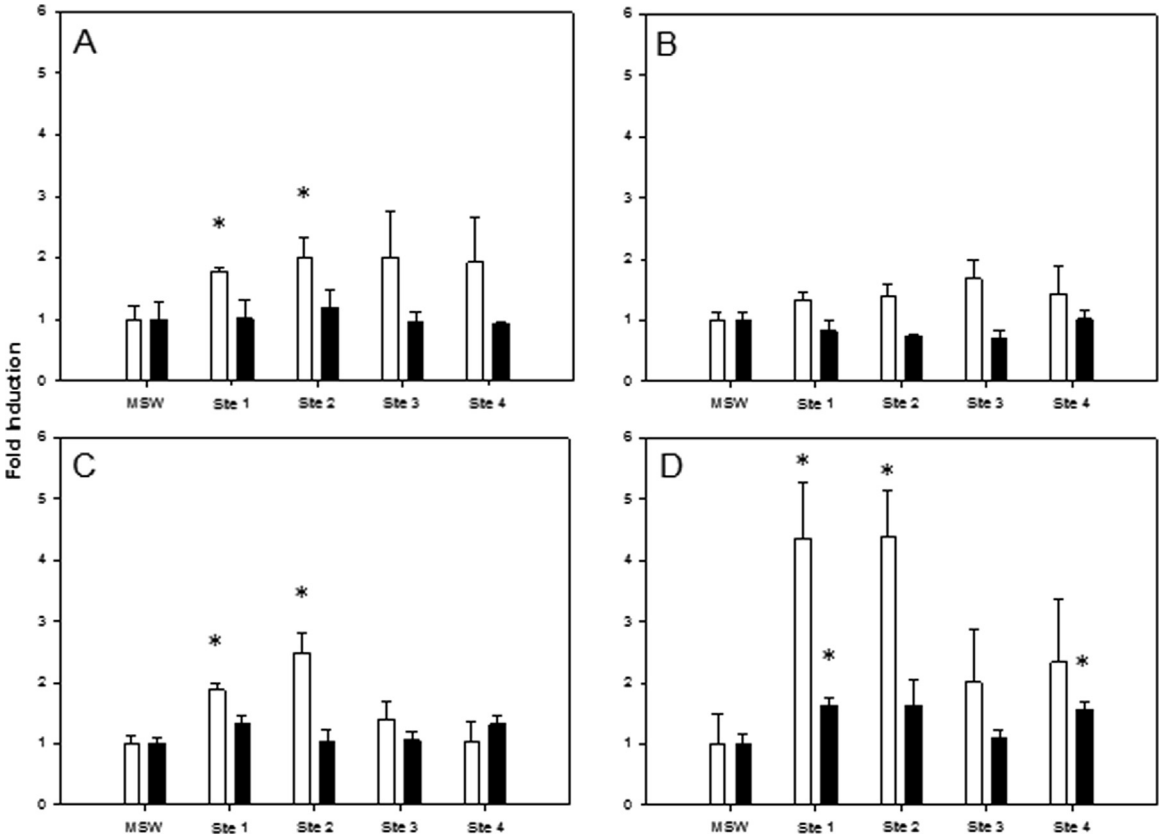

Fig. 2. Fold induction of primary gill cell culture (A) metallothioenin a and (B) b, as well as (C) cytochrome p4501a1 and (D) 3a27 genes exposed to filtered (0.2 μm) river water from the 4 sites from the first (white bars, 2.12.13) and second (black bars, 11.12.13) sampling period. Values are expressed as fold induction of expression in cells exposed to moderately soft water (MSW). Values represent an average of 4–5 inserts ± SEM and asterisks indicates significance difference to MSW (Student's *t*-test, $P < 0.05$).

also may influence *cyp3a* expression levels (Zanette et al., 2013). However, again the situation may be more complicated because caged rainbow trout exposed to a complex mixture of compounds from STW effluent, including pharmaceuticals, in Uppsala, Sweden show a large increase in the expression of various isoforms of *cyp1* (*cyp1c3, 1c2, 1c1, 1a3 1a1*) (Jonsson et al., 2010), and in the gills of stickleback exposed to pharmaceutical production waste effluent also show an increase in *cyp1a1* expression (Beijer et al., 2013). In contrast, carbamazepine has been shown to inhibit Cyp1a1 enzyme activity in fish hepatocytes (Laville et al., 2004). Thus, this increase in *cyp1a1* and *cyp3a27* expression is better described as the detection of CYP1a and CYP3a-active pollutants, than specific classes of compounds.

The induction of *mta* was only observed at sites 1 and 2 during the first sample period (Fig. 2). The lack of induction of *mtb* may reflect the fewer number of metal response elements (MREs) present in the promoter region of this gene (Olsson et al., 1995; Samson and Gedamu, 1995). At site 1 at this time there is elevated Cu concentrations above the EQS and high Zn, although this does not exceed the EQS (Table 2). The concentrations of Cu are similar to those measured at Relubbus (30.5 μg/L) and St Erth (20.2 μg/L) on the river Hayle that induced *mta* expression in FIGCS (Minghetti et al., 2014). However, at site 2 the Cu and Zn levels are less than at site 1 and are similar to those at the other two sites, and the concentrations of Cu (2.45 μg/L) and Zn (6.38 μg/L) are not expected to induce *mta* expression in the primary gill cells, based on previous work with natural waters and addition of metals to synthetic waters in the laboratory (Walker et al., 2007; Minghetti et al., 2014). Consequently, either other metals that have not been measured or other inducers of *mta* gene expression are present in these water samples. MT may also act as a free radical scavenger (Kling and Olsson, 2000). Some pharmaceuticals and personal care products have been shown to affect reactive oxygen species(ROS) production in rainbow trout gonad cell line (RTG-2) (Ferandez et al., 2013) and PAHs are known to induce free radical production (e.g. Wells and Winn, 1996; Zhu et al., 2014). The distal region of the rainbow trout *mta* promoter possess both activator protein 1 (AP1) and a nuclear factor interleukin-6 (NF-IL6) elements that have been shown to play a direct role in *mta* induction in response to paraquat, an herbicide that induces ROS (Kling et al., 2013). In addition, FIGCS treated with H_2O_2, that produces ROS, show an increase in *mta* and *b* gene expression, as well as other antioxidant genes (Chung et al., 2005). The antioxidant gene expression is attenuated by the zinc chelator *N,N,N′,N′*-tetrakis(2-pyridylmethyl) ethylenediamine (TPEN), suggesting that the response to ROS in FIGCS is in part mediated by an increase in intracellular zinc concentrations (Chung et al., 2005).

The study further demonstrates the potential for the primary fish gill cell culture system (FIGCS) to be used for environmental monitoring and shows that that genes associated with metal exposure and biotransformation of organic compounds are present in FIGCS and are induced on exposure to filtered (0.2 μm) urban river water. Natural waters contain a mixture of pollutants, for example at site 1 elevations in dissolved Cu and Zn, along with the identification of the presence of 16 pharmaceuticals were made (Tables 2 and 3), but, this is only likely to be a fraction of the chemicals present with urban rivers likely to possess PAHs from road run-off as well as pesticides and herbicides. The primary gill cell *mta*, *cyp1a1* and *3a27* gene expression is thus an integrated measure of the bioactive compounds, whether they are inducers or inhibitors of gene expression, present in a complex natural river matrix.

Acknowledgements

SS was supported by a National Centre for the Replacement, Refinement and Reduction of Animals in Research (NC3Rs reference G10000081) awarded to NB and CH. TM was supported by a Biotechnology and Biological Sciences Research Council (BBSRC) (BB/K501177/1). We would also like to thank Brian Smith from the Natural History Museum, London, for the water metal analysis.

References

Barron, L., Tobin, J., Paull, B., 2008. Multi-residue determination of pharmaceuticals in sludge and sludge enriched soils using pressurized liquid extraction, solid phase extraction and liquid chromatography with tandem mass spectrometry. J. Environ. Monit. 10, 353–361.

Barron, L., Havel, J., Purcell, M., Szpak, M., Kelleher, B., Paull, B., 2009. Predicting sorption of pharmaceuticals and personal care products onto soil and digested sludge using artificial neural networks. Analyst 134, 663–670.

Beijer, K., Gao, K., Jönsson, M.E., Larsson, D.G., Brunström, B., Brandt, I., 2013. Effluent from drug manufacturing affects cytochrome P450 1 regulation and function in fish. Chemosphere 90, 1149–1157.

Billard, S.M., Timme_Laragy, A.R., Wassenberg, D.M., Cockman, C., Di Giullo, R.T., 2006. The role of the aryl hydrocarbon receptor pathway in mediating synergistic developmental toxicity of polycyclic aromatic hydrocarbons to zebrafish. Toxicol. Sci. 92, 526–536.

Buhler, D.R., Miranda, C.L., Henderson, M.C., Yang, Y.H., Lee, S.J., Wang-Buhler, J.L., 2000. Effects of 17β estr5adiol and testosterone on hepatic mRNA/protein levels and catalytic activities of CYP2M1, CYP2K1 and CYP3A27 in rainbow trout (*Oncorhynchus mykiss*). Toxicol. Appl. Pharmacol. 168, 91–101.

Bury, N.R., Schnell, S., Hogstrand, C., 2014. Gill cell culture systems as models for aquatic environmental monitoring. J. Exp. Biol. 217, 639–650.

Chung, M.-J., Walker, P.A., Brown, R.W., Hogstrand, C., 2005. ZINC-mediated gene expression offers protection against H_2O_2-induced cytotoxicity. Toxicol. Appl. Pharmacol. 205, 225–236.

Davoren, M., Ni Shuilleabhain, S., Hartl, M.G.J., Sheehan, D., O'Brien, N.M., O'Halloran, J., Van Belt, F.N.A.M., Mothersill, C., 2005. Assessing the potential of fish cell lines as tools for the cytotoxicity testing of estuarine sediment aqueous elutriates. Toxicol. In Vitr. 19, 421–431.

Dayeh, V.R., Schirmer, K., Bols, N.C., 2009. Ammonia-containing industrial effluents, lethal to Rainbow Trout, induce vacuolisation and Neutral Red uptake in the Rainbow Trout gill cell line, RTgill-W1. ATLA 37, 77–87.

Ferandez, C., Carbonell, G., Babin, M., 2013. Effects of individual and a mixture of pharmaceuticals and personal-care products on cytotoxicity, EROD activity and ROS production in a rainbow trout gonadal cell line (RTG-2). J. Appl. Toxicol. 33, 1203–1212.

Fletcher, M., Kelly, S.P., Pärt, P., O'Donnell, M.J., Wood, C.M., 2000. Transport properties of cultured branchial epithelia from freshwater rainbow trout: A novel preparation with mitochondria-rich cells. J. Exp. Biol. 203, 1523–1537.

Jonsson, M.E., Gao, K., Olsson, J.A., Goldstone, J.V., Brandt, I., 2010. Induction patterns of new CYP1 genes in environmental exposed rainbow trout. Aquat. Toxicol. 98, 311–321.

Kamiguchi, N., Aoyama, E., Okuda, T., Moriwaki, T., 2010. A 96-well plate assay for CYP4503A induction using cyropreserved human hepatocytes. Drug Metab. Dispos. 38, 1912–1916.

Kelly, S.P., Fletcher, M., Pärt, P., Wood, C.M., 2000. Procedures for the preparation and culture of 'reconstructed' rainbow trout branchial epithelia. Methods Cell Sci. 22, 153–163.

Kinani, S., Bouchonnet, S., Creusot, N., Bourcier, S., Balaguer, P., Porcher, J.-M., Ait-Aissa, S., 2010. Bioanalytical characterisation of multiple endocrine- and dioxin-like activities in sediments from reference and impacted small rivers. Environ. Pollut. 158, 74–83.

Kling, P.G., Olsson, P., 2000. Involvement of differential metallothionein expression in free radical sensitivity of RTG-2 and CHSE-214 cells. Free Radic. Biol. Med. 28, 1628–1637.

Kling, P., Modig, C., Mujahed, H., Khalaf, H., von Hofsten, J., Olsson, P.-E., 2013. Differential regulation of the rainbow trout (*Oncorhynchus mykiss*) MT-A gene by nuclear factor interleukin-6 and activator protein-1. BMC Mol. Biol. 14, 28.

Lacey, C., McMahon, G., Bones, J., Barron, L., Morrissey, A., Tobin, J., 2008. An LC-MS method for the determination of pharmaceutical compounds in wastewater treatment plant influent and effluent samples. Talanta 75, 1089–1097.

Lavado, R., Rimoldi, J.M., Schlenk, D., 2009. Mechanism of fenthion activation in rainbow trout (*Oncorhynchus mykiss*) acclimated to hypersaline environments. Toxicol. Appl. Pharmacol. 235, 143–152.

Laville, N., Ait-Aissa, S., Gomez, E., Casellas, C., Porcher, J.M., 2004. Effects of human pharmaceuticals on cytotoxicity, EROD activity and ROS production in fish hepatocytes. Toxicology 196, 41–55.

Lee, S.-J., Wang-Butler, J.L., Cok, I., Yu, T.S., Yang, Y.H., Miranda, C.L., Lech, J., Buhler, D.R., 1998. Cloning, sequencing and tissue expression of CY3A27, a new member of the CYP3A subfamily from embryonic and adult rainbow trout livers. Arch. Biochem. Biophys. 360, 53–61.

Lee, S.-J., Hedstrom, O.R., Fischer, K., Wang-Buhler, J.-L., Sen, A., Cok, I., Buhler, D.R.,

2001. Immunohistochemical localisation and differential expression of cytochrome P450 2 A27 in the gastrointestinal tract of rainbow trout. Toxicol. Appl. Pharmacol. 177, 94–102.
Luo, G., Cunningham, M., Lim, S., Burn, T., Lin, J., Sinz, M., Hamilton, G., Rizzo, C., Jolley, S., Gilbert, D., Downey, A., Mudra, D., Graham, R., Carroll, K., Xie, J., Madan, A., Parkinson, A., Christ, D., Selling, B., Lecluyse, E., Gan, L.-S., 2002. CYP3A4 induction by drugs: correlation between a pregnane x receptor reporter gene assay and CYP3A4 expression in human hepatocytes. Drug Metab. Dispos. 30, 795–804.
Luo, G., Guenthner, T., Gan, L.S., Humphreys, W.G., 2004. CYP3A4 induction by xenobiotics: biochemistry, experimental methods and impact on drug discovery and development. Drug Metab. 5, 483–505.
Miller, T.H., McEneff, G.L., Brown, R.J., Owen, S.F., Bury, N.R., Baron, L.P., 2015. Pharmaceuticals in the freshwater invertebrate, *Gammarus pulex*, determined using pulverised liquid extraction, solid phase extraction and liquid chromatography–tandem mass spectrometry. Sci. Total Environ. 511, 153–160.
Martínez, C., Albet, C., Agúndez, J.A., Herrero, E., Carrillo, J.A., Márquez, M., Benítez, J., Ortiz, J.A. l, 1999. Comparative in vitro and in vivo inhibition of cytochrome P450 CYP1A2, CYP2D6, and CYP3A by H2-receptor antagonists. Clin. Pharmacol. Ther. 65, 369–376.
Minghetti, M., Schnell, S., Chadwick, M.A., Hogstrand, C., Bury, N.R., 2014. A primary Fish Gill Cell System (FIGCS) for environmental monitoring of river waters. Aquat. Toxicol. 154, 184–192.
Oscarson, M., Zanger, U.M., Rifki, O.F., Klein, K., Eichelbaum, M., Meyer, U.A., 2006. Transcriptional profiling of genes induced in the livers of patients treated with carbamaepine. Clin. Pharmacol. Ther. 80, 440–456.
Olsson, P.E., Kling, P., Erkell, L.J., Kille, P., 1995. Structural and functional analysis of the rainbow trout (*Oncorhynchus mykiss*) metallothionein-A gene. Eur. J Biochem. 230, 34924–34928.
Samson, S.L., Gedamu, L., 1995. Metal-responsive elements of the rainbow trout metallothionein-B gene function for basal and metal-induced activity. J. Biol. Chem. 270, 6864–6871.
Sandbacka, M., Pärt, P., Isomaa, B., 1999. Gill epithelial cells as tools for toxicity screening—comparison between primary cultures, cells in suspension and epithelia on filters. Aquat. Toxicol. 46, 23–32.
Schnell, S., Olivares, A., Piña, B., Echarvarri-Erasun, B., Lacorte, S., Porte, C., 2013. The combined use of the PLHC-1 cell line and the recombinant yeast assay to assess the environmental quality of estuarine and coastal sediments. Mar. Pollut. Bull. 77, 282–289.
Stott, L.C., Schnell, S., Hogstrand, C., Owen, S.F., Bury, N.R., 2015. A primary fish gill cell culture model to assess pharmaceutical uptake and efflux: evidence for passive and facilaitated transport. Aquat. Toxicol. 159, 127–137.
Tanneberger, K., Knöbel, M., Busser, F.J., Sinnige, T.L., Hermens, J.L., Schirmer, K., 2013. Predicting fish acute toxicity using a fish gill cell line-based toxicity assay. Environ. Sci. Technol. 47, 1110–1119.
Tateishi, T., Asoh, M., Nakura, H., Watanabe, M., Tanaka, M., Kumai, T., Kobayashi, S., 1999. Carbamazepine induces multiple cytochrome P450 subfamilies in rats. Chem. Biol. Interact. 117, 257–268.
Uno, T., Ishizuka, M., Itakura, T., 2012. Cytochrome P450 (CYP) in fish. Environ. Toxicol. Pharmacol. 34, 1–13.
Usui, T., Saitoh, Y., Komada, F., 2003. Induciton of CYP3As in HepG2 cells by several drugs – Association between induction of CYP3A4 and expression of glucocorticoid receptor. Biol. Pharm. Bull. 24, 510–517.
Walker, P.A., Bury, N.R., Hogstrand, C., 2007. Influence of culture conditions on metal-induced responses in a cultured rainbow trout gill epithelium. Environ. Sci. Technol. 41, 6505–6513.
Walker, P.A., Kille, P., Scott, A., Bury., N.R., Hogstrand, C., 2008. An *in vitro* method to assess toxicity of waterborne metals to fish. Toxicol. Appl. Pharmacol. 30, 67–77.
Wells, P.G., Winn, L.M., 1996. Biochemical toxicology of chemical teratogenesis. Crit. Rev. Biochem. Mol. Biol. 31, 1–40.
Wood, C.M., Kelly, S.P., Zhou, B., Fletcher, M., O'Donnell, M., Eletti, B., Pärt, P., 2002. Cultured gill epithelia as models for the freshwater fish gill. Biochim. Biophys. Acta 1566, 72–83.
Zanette, J., Jenny, M.J., Goldstone, J.V., Parente, T., Woodin, B.R., Bainy, A.C.D., Stegeman, J.J., 2013. Identification and expression of multiple CYP-1like and CYP-3 like genes in the bivalve mollusc *Mytilus edulis*. Aquat. Toxicol. 128, 101–112.
Zhu, W., Cromie, M.M., Cai, Q., Lv, T., Singh, K., Gao, W., 2014. Curcumin and vitamin E protect against adverse effects of benzo[a]pyrene in lung epithelial cells. PLoS One 9 (3), e92992.

Science of the Total Environment 538 (2015) 934–941

Contents lists available at ScienceDirect

Science of the Total Environment

journal homepage: www.elsevier.com/locate/scitotenv

Suspect screening of large numbers of emerging contaminants in environmental waters using artificial neural networks for chromatographic retention time prediction and high resolution mass spectrometry data analysis

Richard Bade [a], Lubertus Bijlsma [a], Thomas H. Miller [b], Leon P. Barron [b], Juan Vicente Sancho [a], Felix Hernández [a,*]

[a] Research Institute for Pesticides and Water, University Jaume I, Avda. Sos Baynat, E-12071 Castellón, Spain
[b] Analytical & Environmental Sciences Division, Faculty of Life Sciences and Medicine, King's College London, 150 Stamford Street, London SE1 9NH, United Kingdom

HIGHLIGHTS

- A retention time predictor based on artificial neural networks is presented.
- Using 550 compounds, 90% could be predicted within 2 min.
- A notable number of peaks (false positives) could be discarded for further research.
- Useful in the tentative identification of metabolites and transformation products
- This approach highly facilitates wide-scope screening of organic contaminants.

GRAPHICAL ABSTRACT

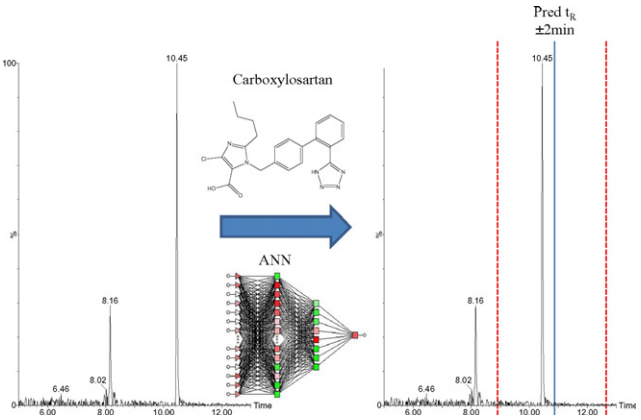

ARTICLE INFO

Article history:
Received 6 July 2015
Received in revised form 14 August 2015
Accepted 14 August 2015
Available online 28 September 2015

Editor: D. Barcelo

Keywords:
Retention time prediction
Artificial neural networks
Time-of-flight high resolution mass spectrometry
Screening of emerging contaminants

ABSTRACT

The recent development of broad-scope high resolution mass spectrometry (HRMS) screening methods has resulted in a much improved capability for new compound identification in environmental samples. However, positive identifications at the ng/L concentration level rely on analytical reference standards for chromatographic retention time (t_R) and mass spectral comparisons. Chromatographic t_R prediction can play a role in increasing confidence in suspect screening efforts for new compounds in the environment, especially when standards are not available, but reliable methods are lacking. The current work focuses on the development of artificial neural networks (ANNs) for t_R prediction in gradient reversed-phase liquid chromatography and applied along with HRMS data to suspect screening of wastewater and environmental surface water samples. Based on a compound t_R dataset of >500 compounds, an optimized 4-layer back-propagation multi-layer perceptron model enabled predictions for 85% of all compounds to within 2 min of their measured t_R for training (n = 344) and verification (n = 100) datasets. To evaluate the ANN ability for generalization to new data, the model was further tested using 100 randomly selected compounds and revealed 95% prediction accuracy within the 2-minute elution interval. Given the increasing concern on the presence of drug metabolites and other transformation products (TPs) in the aquatic environment, the model was applied along with HRMS data for preliminary identification of

* Corresponding author.
E-mail address: felix.hernandez@uji.es (F. Hernández).

http://dx.doi.org/10.1016/j.scitotenv.2015.08.078

pharmaceutically-related compounds in real samples. Examples of compounds where reference standards were subsequently acquired and later confirmed are also presented. To our knowledge, this work presents for the first time, the successful application of an accurate retention time predictor and HRMS data-mining using the largest number of compounds to preliminarily identify new or emerging contaminants in wastewater and surface waters.

1. Introduction

The number of emerging contaminants in the aquatic environment is increasing, due to urbanization and subsequent societal and industrial needs (Pal et al., 2014). The development of liquid chromatography–high resolution mass spectrometry (LC–HRMS) technologies has revolutionized the analysis of emerging contaminants in environmental waters, and especially for screening of large numbers of compounds (Agüera et al., 2013; Gómez et al., 2010; Hernández et al., 2011; Hogenboom et al., 2009). HRMS instruments allow the recording of full-scan spectra with high mass accuracy and resolution, thus making it possible to search for any given compound based on its exact mass.

There has been much interest in improving the confidence in the identification of small molecules with HRMS; from potential positives through to detection and finally confirmation (Hernández et al., 2015a; Schymanski et al., 2014). The main distinguishing factor between these levels is the (non-) availability of reference standards. Suspect screening refers to compounds tentatively identified based solely on HRMS data and comparable spectral libraries. Confirmation requires reference standards. An additional tool to increase the confidence in the tentative identification of compounds for which standards are unavailable is reliable and accurate t_R prediction. This is of particular relevance in the case of degradation/transformation products (TPs), which can reach the aquatic environment in high concentrations, but commonly for which reference standards are less accessible. Chemical risk assessment is therefore significantly challenging for such compounds.

Prediction of t_R plays an important role in the qualitative identification of emerging contaminants. Many different approaches to t_R prediction exist and range from the simple (Kern et al., 2009; Nurmi et al., 2012) to the complex (Goryński et al., 2013; Ji et al., 2009; Kaliszan et al., 2003; Ukić et al., 2014a). For example, logK_{ow} models can be derived using freely accessible data from chemical databases such as ChemSpider and PubChem, as well as freeware prediction sources such as VCCLABS. Its use in t_R prediction is extremely simple to implement. It is frequently used in environmental studies for the description of the fate of various pollutants and as a simple t_R predictor for TPs (Kern et al., 2009) and emerging contaminants (Bade et al., 2015; Nurmi et al., 2012). Alongside simple algorithms, other and more complex in silico approaches now exist which are based on quantitative structure–retention relationship (QSRR) modeling, including artificial neural networks, support vector machines and random forests (Giaginis and Tsantili-Kakoulidou, 2012; Héberger, 2007). The principal aim of QSRR is to predict retention data from the molecular structure and its physicochemical properties, using a range of input descriptors and measured t_R data. One QSRR method gaining recent attention for broad screening using high resolution techniques is the use of artificial neural networks (ANNs), a predictive computing technique that has shown itself as a promising t_R predictor with potentially higher accuracy than classical models (Miller et al., 2013; Ukić et al., 2014b). The design of ANNs were inspired by the human brain and differ from classical computer programs in that they generally employ non-linear learning techniques using a set of case examples (i.e. a training dataset) (Kaliszan et al., 2003). In the training phase, the ANN requires a range of suitable molecular descriptors as well as the true output value (in this case, measured t_R) to use for comparison with predicted values. At the same time, a second dataset of case examples is often used for verification and to assess overall ANN predictive error. The true output values in the verification set are generally not employed for learning, but the number of training cycles can be stopped by the user or the software when the overall measured error across all cases is at its minimum. Therefore, ANN learning is generally an iterative process and once an acceptable number of training cycles is reached, the optimized ANN can be applied to predict the output where experimentally derived data are unavailable (Miller et al., 2013). In some cases, a third dataset can be used after the model has been finalized to 'blind test' the predictive power of the network. Its use is even more pertinent for analyses where large number of new analytes are expected to occur and with potentially high variance from sample to sample, such as in environmental and municipal water samples. Therefore, since information from the sample includes chromatographic t_R as well as HRMS data, it makes this interpretation of suspect occurrence more accessible in the first instance.

The aim of this work was to develop and evaluate ANN for predictions of unknown chromatographic t_R in suspect screening of environmental waters. To the best of our knowledge, this method includes the largest range of physicochemically diverse compounds for this purpose ($n = 544$ in total) and includes both neutral and charged compounds eluted under gradient reversed-phase LC conditions. Lastly, this work aimed to improve upon a recent logK_{ow}-based t_R prediction approach (Bade et al., 2015) using the ANNs as an alternative. This work, for the first time, presents the use of ANN for identification of additional suspect compounds (including metabolites and TPs) in wastewater and surface water samples both with and without reference standards.

2. Experimental

2.1. Reagents and chemicals

A total of 544 analytical grade reference materials were used for preparation of model solutions at 25 μg/L or 50 μg/L (diluted from mixed standard solutions in methanol or acetonitrile with water) for ANN modeling of t_R. These included pesticides, drugs of abuse, human/veterinary pharmaceuticals and mycotoxins (See Supplementary Information (SI) Table S1 for all compounds used in this study). These covered a large range of molecular hydrophobicity (logK_{ow} −3 to 9). Information relating to 595 standards was available (Bade et al., 2015), however after transforming the compounds using SMILES codes, some errors were observed, leading to incomplete data, and a further 42 were removed from the initial ANN method development (Section 3.1) to use in a subsequent blind test (Section 3.2). Further details relating to these compounds can be found elsewhere (Bade et al., 2015; Hernández et al., 2015b).

2.2. Water samples for suspect identification

A total of 44 composite (24-h) influent and effluent wastewater (IWW and EWW) samples and grab surface water (SW) samples were used to demonstrate the application of the developed ANN model. All these samples were previously used in different studies performed at our lab using the same analytical instrumentation for analysis (Hernández et al., 2015a). All measured t_R data herein were generated using ultra-high pressure liquid chromatography coupled to quadrupole-time of flight mass spectrometry (UHPLC–QTOF-MS).

2.3. UHPLC-QTOF MS

A Waters Acquity UPLC system (Waters, Milford, MA, USA) was interfaced to a hybrid quadrupole-orthogonal acceleration-TOF mass

spectrometer (XEVO G2 QTOF, Waters Micromass, Manchester, UK), using a electrospray ionization (ESI) Z-Spray interface operating in positive mode. The chromatographic separation was performed using an Acquity UPLC BEH C_{18} 100 × 2.1 mm, 1.7 μm particle size column (Waters) at a flow rate of 300 μl/min. Gradient elution was performed using mobile phases of A = H_2O and B = MeOH, both containing 0.01% HCOOH. The initial percentage of B was 10%, which was linearly increased to 90% in 14 min, followed by a 2 min isocratic period and, then, returned to initial conditions during 2 min. The total run time was 18 min. Nitrogen was used as the drying gas and nebulizing gas.

MS data were acquired over an m/z range of 50–1000. A capillary voltage of 0.7 kV and cone voltage of 20 V were used. Collision gas was argon 99.995% (Praxair, Valencia, Spain). The desolvation temperature was set to 600 °C, and the source temperature to 135 °C. The column temperature was set to 40 °C. MS data was acquired in MS^E mode, selecting a collision energy of 4 eV for low energy (LE) and a ramp of 15–40 eV for high energy (HE). The LE and HE functions settings were for both a scan time of 0.4 s (Hernández et al., 2011; Ibáñez et al., 2013).

Processing of MS data was made using ChromaLynx XS application manager (within MassLynx v 4.1; Waters Corporation). The following parameters were used: mass window 0.020 Da (for positive ID ≤ 0.010 Da), peak width at 5% height: 6 s, peak-to-peak baseline noise: 1000 and threshold absolute area 500. When manually searching the data for all peaks in an eXtracted Ion Chromatogram (XIC), a chromatographic peak was thought viable when above an intensity threshold of 3000 counts.

2.4. Molecular description and neural network optimization procedures

Compound log*D* data (for a mobile phase of pH = 3.2) were generated using Percepta PhysChem Profiler (ACD Laboratories, ON, Canada) and for all other descriptors, Parameter Client freeware was used (Virtual Computational Chemistry Laboratory, Munich, Germany). Canonical simplified molecular line entry system strings (SMILES) were created using ChemSpider freeware (Royal Society of Chemistry, UK) for 544 compounds and from these 16 molecular descriptors (as ANN inputs) were generated including the number of double and triple bonds (nDB or nTB), the number of carbon and oxygen atoms (nC or nO), the number of 4–9 membered rings (nR04-nR09), unsaturation index (UI), hydrophilic factor (Hy), Moriguchi and Ghose–Crippen logP (MlogP and AlogP respectively) as well as with software predicted logK_{ow} data (Tetko et al., 2005). Prediction of t_R (as the designated single output) via neural networks was performed using Trajan version 6.0 neural network simulator (Trajan Software Ltd., Lincolnshire, U.K.) and compared with experimentally determined t_R via correlation graphs as well as assessment of residual errors. Table S1 has all compounds and their respective predicted and experimental t_R and ANN subset.

3. Results and discussion

In a previous study, we developed a simple t_R prediction model based on logK_{ow} of nearly 600 compounds, predicted using freeware (Bade et al., 2015). This resulted in approximately 70% of all compounds being predicted within 2 min of the measured t_R, and 95% within 4 min. This technique was simple to implement and facilitated the removal of several false positives. However, when investigating unknowns and compounds for which reference standards were unavailable, it was concluded that a more robust, accurate and precise methodology was still needed. In this vein, ANNs were considered as an alternative. Recent work successfully used ANN for a similar purpose, albeit using a much smaller set of compounds of 86 and 166 compounds in either study and focused only on pharmaceuticals (Miller et al., 2013; Munro et al., 2015). It is unlikely that this fully represents the breadth of alternative compound classes and chemistries potentially occurring simultaneously in environmental waters. However, these models successfully predicted t_R for a range of blind test drug compounds in wastewater and urine to warrant further investigation here using a much larger case dataset.

3.1. Prediction of t_R using Artificial Neural Networks (ANNs)

The molecular descriptors chosen were based on the previous work wherein more than 200 descriptors were evaluated (Miller et al., 2013). As the same type of reversed-phase column and LC system were used in both studies, the same descriptors were hoped to provide similar results. These descriptors were used again to also assess the possibility for transferring the model to another laboratory and to extend the prediction to a much larger set of chemically diverse compounds. Collinearity data for all molecular descriptors and retention time are given in the SI. Higher Pearson correlations were observed for hydrophobicity-based descriptors with retention time as was perhaps expected (maximum R = 0.823 with logK_{ow}). Similarly, these descriptors also showed some collinearity with each other (R ≤ 0.889) which prevented strong conclusions to be drawn regarding their relative importance to an ANN model. As molecular descriptors selected were from previous investigations, there is also the possibility that additional descriptors may have had more importance to retention prediction on this system. For example, retention on reversed-phase media is not only dependent on hydrophobic interactions, but also steric and shape effects. Large molecules may not interact with the stationary phase well and thus show reduced retention (Wilson et al., 2002). A simple Pearson correlation was examined for a selection of potentially relevant additional descriptors covering charge states, geometrical, topological and physicochemical properties. Overall, most of these descriptors showed weak relationships <0.5 except for the descriptor BTLA96 which showed a negative Pearson coefficient of −0.649.

Over 100,000 network architectures for each model type were initially investigated for their predictive ability across five different ANN model types including 3- and 4-layer multi-layer perceptrons (MLPs), generalized regression neural networks (GRNNs), radial basis functions (RBFs), linear neural networks and probabilistic neural networks (PNN). For training, 344 cases were used along with 100 cases for both verification and blind testing of network performance. Cases were randomly assigned at the beginning of each network test to prevent any bias from pre-selection. Upon selection of the 'best' model statistics (minimum/maximum values, interquartile ranges, standard deviations, medians and means) were generated to ensure that a fair representation of cases and descriptors were present in each dataset subset (see SI). The diversity of ANN types and architectures tested was balanced against the error generated. For network design and testing the omission of input descriptors was included as an option. One hundred of the best networks (software selected) were retained for further investigation which mainly comprised of MLPs, GRNNs and RBFs. Overall for this separation system, the best correlations of predicted versus experimentally measured t_R were observed using MLPs in comparison to all other types and these correlations were in agreement with previous works despite different compounds being used for training, verification and blind testing (Barron et al., 2009; Miller et al., 2013; Munro et al., 2015). The finalized network was found to be a 4-layer 16-19-9-1 MLP using all 16 molecular descriptors as inputs (Fig. 1). The source code (in C) for this ANN has been attached in the SI. Reducing the number of descriptors further worsened predictive accuracy of the blind test set in general. This ANN type and architecture was chosen based on the lowest absolute errors (i.e. predicted t_R-measured t_R) in the training, verification and blind test sets across all networks. Therefore, ANN architecture was based on performance and the software designer tool was used to optimize the number and composition of hidden layers. The coefficients of determination (R^2) were between 0.86 and 0.90 between the three sets, which was already a marked improvement on that obtained from our previous study at $R^2 = 0.67$. Furthermore, the root-mean-squared error (RMSE) of the blind set of compounds (1.03 min) is less than half that of our previous work (2.19 min) (Bade et al., 2015).

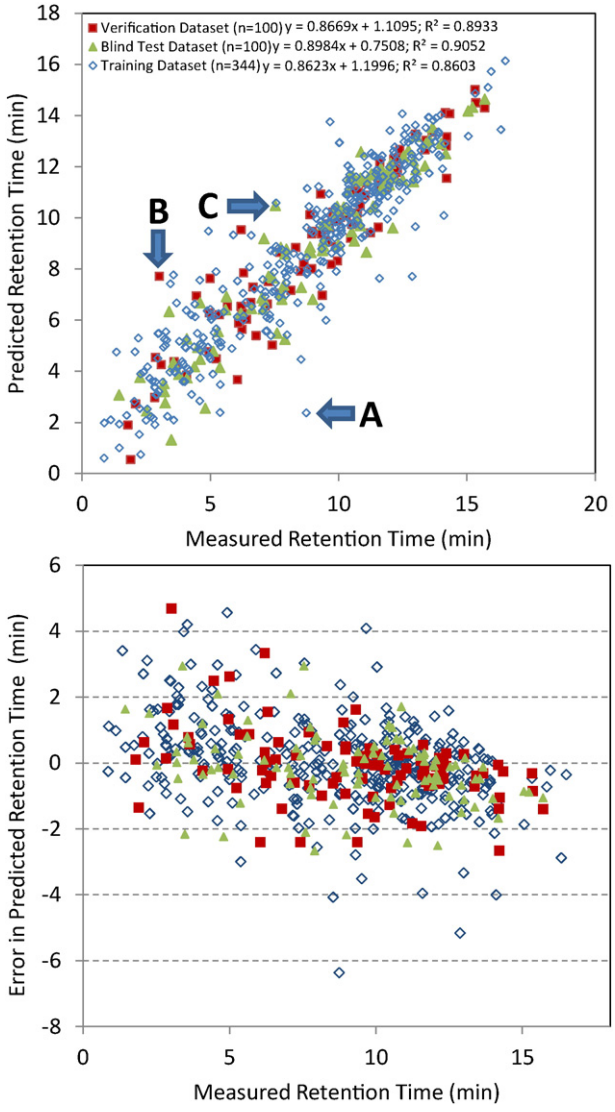

Fig. 1. TOP: Correlation of measured and predicted t_R for all compounds. The worst outliers in each set are also shown: A = atenolol (training set, error of −6.21 min); B = levamisole (verification set, +5.19 min); C = metosulam (blind set, +3.56 min). BOTTOM: Residual errors for all compounds in each dataset. For training, verification and blind test sets, n = 344, 100 and 100 compounds respectively.

The maximum measured t_R on this chromatographic system was 16.50 min (narasin; an antibiotic) and the lowest was 0.86 min (methamidophos; an organophosphate insecticide). For all compounds within this retention window of 15.64 min, the mean error in t_R prediction was <6% using this ANN approach for all compounds. Overall, the mean absolute errors and standard deviations were recorded as 0.97 ± 0.95 min (training set); 0.79 ± 0.85 min (verification set); 0.79 ± 0.69 min (blind test set); and 0.91 ± 0.89 min (all sets combined). When focussing specifically on the blind test set which was used to simulate a true application of the approach, 95% of compounds had predicted t_R values within 2.00 min of the measured value and the maximum error was 3.56 min for metosulam (Fig. 2). However, across the other datasets some larger errors were recorded in isolated cases. Table 1 shows that for all datasets, 90% of all 544 compounds could be predicted to within 2.00 min of the measured t_r value. Upon sub-division of the datasets, 85% of the compounds in the training and verification sets and 95% of compounds in the blind test set were predicted to within two minutes of the measured value. The maximum error recorded within the training set was +6.25 min (for the beta blocker atenolol; measured t_r = 2.49 min); within the verification set was +5.19 min (for the anti-helminthic drug levamisole; measured t_r = 3.02 min) and within the blind test set was +3.56 min (for the pesticide, metosulam; measured t_r = 7.54 min).

Prediction errors for all cases were investigated again with respect to any apparent trends and it was found that a very slight over-estimation existed for poorly retained compounds, as well as the converse for strongly retained compounds. Recent work focussing on modeling a smaller number of compounds in wastewater also revealed a similarly slight bias, but used a different network type (a GRNN) (Munro et al., 2015). When examining those compounds with absolute errors >2.00 min (54 compounds in total across all sets), these were spread across the entire compound retention range (mean measured t_R = 7.81 ± 3.93). However, a slight over-estimation was again apparent for 29 compounds with t_R from 1.34–5.38 min (mean measured t_R = 2.97 min). Reduced under-estimation was observed for the remaining 25 compounds eluting between 5.38–16.30 min (mean measured t_R = 10.67 min for these compounds). Seventeen compounds eluting <5.38 min were over-estimated and t_R for eleven were under-estimated when eluting >10.00 min.

The contribution of each descriptor towards the final prediction output was investigated using the ANN software sensitivity analysis tool. In this test, each molecular descriptor is removed and treated as missing by the ANN. A new predicted t_R is generated and a ratio calculated between the network error with a given input omitted to the error of the network with a complete input dataset. Ratios >1 indicated higher importance in the prediction. Perhaps not surprisingly for a reversed-phase chromatography system, the most important molecular descriptors and their measured error ratios were: logD (1.443), logK_{ow} (1.182), AlogP (1.114), nO (1.096), UI (1.006) MlogP (1.023), Hy (1.017), nDB (1.012), nR04-nR09 (all 1.000–1.063), nTB (1.004) and nC (1.002) Hydrophobicity-based descriptors are likely to show importance as retention on reversed-phase media is primarily by van der Waals interactions. Again, while these descriptors together show their combined importance to the network, moderate collinearity between them means relative error ratios should be treated with caution for these descriptors (Table SI). However, such collinearity should not adversely affect predictive ability of the model. The lowest ratio was observed for nR04 with a ratio of 1.000 meaning no change in network performance was measured for its removal. Within the dataset, only 14 compounds had 4-membered rings (amoxicillin, ampicillin, cefaclor, cefadroxil, cefalexin, cefotaxime, cefquinome, cefuroxime, cloxacillin, dicloxacillin, heptenophos, oxacillin, oxasulfuron, and penicillin G). Inclusion of nR04 still resulted in better performance in comparison to any other type or architecture investigated during the network optimization stage and so was retained as a descriptor in the final ANN model. Error ratios discussed above represent that of the entire dataset (training, verification and blind test). Sensitivity analysis (see SI) of each set separately revealed excellent consistency across all sets, showing that predictive accuracy was likely to be the dominant contributors to error ratios rather than over-fitting of the training set alone.

3.2. Use of ANN as a t_R predictor in environmental water samples

In wide-scope screening methods, where thousands of compounds are searched, it is of great importance to have secondary techniques for aid in the identification process. While reference standards can unequivocally confirm the identification of a compound, purchasing and maintaining standards for all compounds is prohibitively expensive. Data acquired from MS fragmentation of suspect compounds may also direct investigations. Furthermore, for many TPs, reference standards are not available and therefore alternate means for confidence in detection/identification are necessary. Although it is not comparatively informative as mass spectra, t_R prediction models can be very helpful in gaining more confidence in the obtained data and reducing time-consuming data processing. Most importantly, the application of t_R prediction is not to replace the use of reference standards, but to help

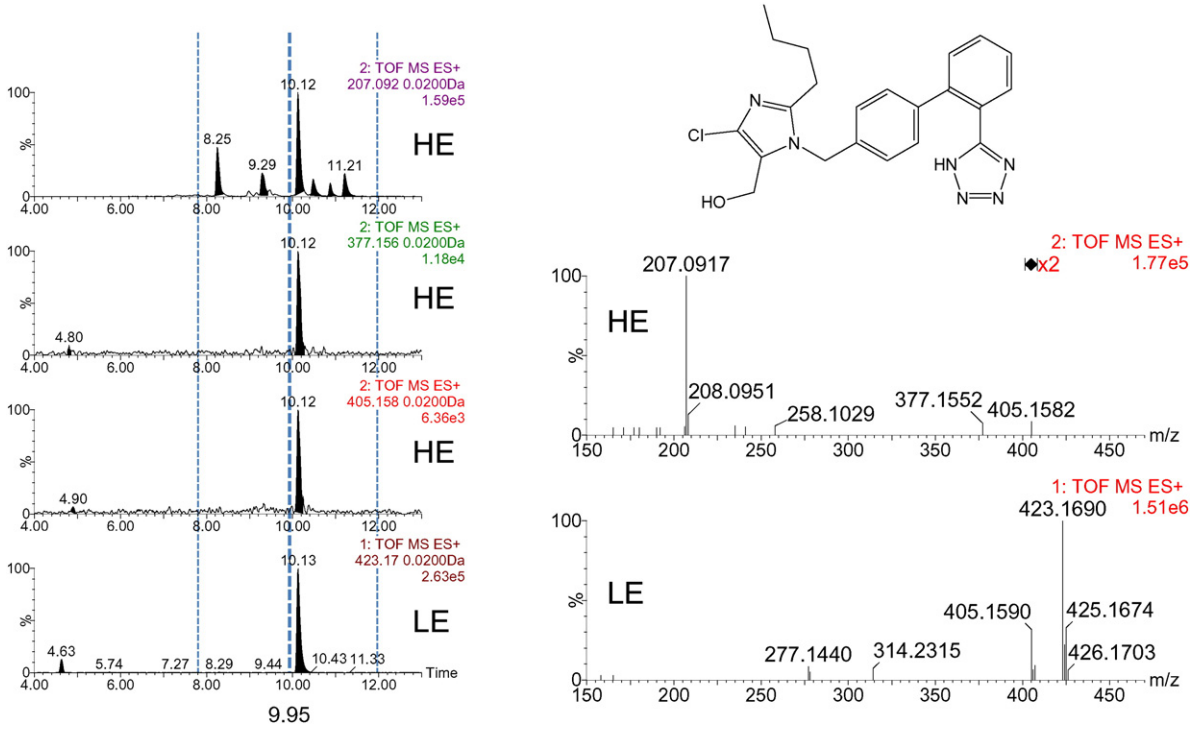

Fig. 2. LEFT: eXtracted Ion Chromatograms (XICs) of losartan in an EWW sample, together with ANN t_R prediction (9.95 min) and associated ±2 minute window (dotted lines; center dashed line is the ANN-predicted value). RIGHT: Mass spectra from LE (bottom) and HE (top), showing fragment ions (423.158, 377.156, 207.092).

(along with MS/MS data) to direct synthesis efforts for confirmation in the usual manner. Prediction of t_R is best used at the beginning of this process and is especially useful when at a certain exact mass (i.e. (de)protonated molecule of a suspect compound), more than one chromatographic peak appears in the corresponding XIC.

Along these lines, and to test the "blind" skills of the ANN in a real environmental application, the 100 blind compounds as well as an additional set of compounds from our previous study not initially used into the ANN method (a total of 142 compounds), including primarily metabolites and TPs were searched. None of these compounds were in the training or verification sets used for ANN development. From this list of 142 compounds, 46 were finally selected and searched in 44 water samples (EWW, IWW and SW) using ChromaLynx and the ANN predicted t_R, based on their possible occurrence in the environment (Table S2) (Gracia-Lor et al., 2010, 2011; Hernández et al., 2015a; Zuccato et al., 2006). For further confidence, and to see how many false positive chromatographic peaks (above the intensity threshold) could be disregarded, fragment ions were also included in the detection process (Table S3). When a compound was identified on the basis of the accurate mass of the (de)protonated molecule and at least one fragment ion in at least one sample it was included in this test, leaving 26 compounds of various chemical classes and including nine metabolites, for only some of which standards were available in our laboratory (Table 2). A t_R window of 2 min was used in this section, as 95% of all compounds in the ANN blind set were within this window, thereby giving high confidence that almost all compounds should be found. The only compound found to have a t_R outside that of the ANN predicted 2 minute window was codeine. The incorporation of the ANN predicted t_R allowed almost half (49%) of all chromatographic peaks to be ignored, and even after removing codeine from the calculation, 48% could be disregarded. Furthermore, all but three compounds had a reduction in the median number of potential positive peaks, while 11 compounds had a median value of only one chromatographic peak remaining after the introduction of the ANN predicted window.

In this section, examples are shown in the identification of losartan (originally tentatively identified with t_R prediction before a reference standard was purchased) and the tentative identification of the metabolites 10,11-dihydroxy carbamazepine and O-desmethyl venlafaxine (no reference standard available).

3.2.1. Assignment with reference standards

Losartan is a pharmaceutical used to treat hypertension that has been both predicted (Howard and Muir, 2013; Oosterhuis et al., 2013) and detected in environmental waters (Hernández et al., 2015a; Matsuo et al., 2011). Its presence in a suspect list is thus warranted, and its exact mass was incorporated into our HRMS database. When screening WW and SW samples, XICs at the exact mass of losartan (*m/z* 423.1700) resulted in two chromatographic peaks (4.63 and 10.13 min) (Fig. 2, bottom left). The ANN t_R predictor was used and calculated a t_R of 9.95 min. This is almost exactly the t_R of one of the peaks, but it is worth noting than even after incorporating a ±2 minute window only one peak warranted further investigation. Nevertheless, both peaks could have conceivably corresponded to losartan, therefore further research was conducted.

Table 1
Summary of predicted t_R errors for all ANN test sets. Numbers given in italics are those which fall below the proposed 2-min window limit.

Percentile of compounds	50	55	60	65	70	75	80	85	90	95
Predicted t_R error/min										
All sets (n = 544)	*0.66*	*0.75*	*0.85*	*0.97*	*1.05*	*1.19*	*1.39*	*1.56*	*1.96*	2.80
Training set (n = 344)	*0.70*	*0.81*	*0.89*	*1.02*	*1.13*	*1.24*	*1.45*	*1.70*	2.21	2.87
Verification set (n = 100)	*0.51*	*0.59*	*0.64*	*0.76*	*0.89*	*0.99*	*1.35*	*1.44*	*1.60*	2.43
Blind test set (n = 100)	*0.70*	*0.78*	*0.84*	*0.89*	*1.01*	*1.08*	*1.16*	*1.34*	*1.63*	*1.99*

Table 2
All compounds used for testing ANN predicted t_R, together with the number of samples each compound was detected, average number of peaks in the XIC and the ±2 minute window and the predicted and sample t_R.

Compound	Detection rate out of 44 samples	Median peaks per XIC (range)	Median peaks inside ± 2 min t_R window (range)	Predicted t_R (min)	Sample t_R (min)	Inaccuracy in predicted t_R (min)
10,11-Dihydroxy carbamazepine[a]	30	2 (1–4)	1 (1–3)	6.29	6.66	0.37
2-Hydroxy-terbuthylazine[b]	6	6 (4–8)	2 (1–3)	4.24	5.50	1.26
4-Desmethoxy omeprazole[a]	33	1 (1–2)	1 (1–2)	8.15	6.29	−1.86
4-Formylamino-antipyrine[b,c]	37	2 (1–8)	2 (1–4)	3.53	3.70	0.17
a-Hydroxy metoprolol[a]	17	5 (2–10)	3 (2–4)	2.73	3.30	0.57
Benzoylecgonine[b]	40	3 (1–6)	2 (1–5)	4.11	4.65	0.54
Bezafibrate[b]	2	6 (4–7)	1 (1–1)	10.80	10.78	−0.02
Caffeine[a]	40	3 (1–6)	1 (1–3)	3.17	3.83	0.66
Carbamazepine[b]	40	3 (1–10)	3 (1–5)	7.73	8.82	1.09
Carboxy losartan[a]	35	2 (1–3)	1 (1–1)	10.75	10.44	−0.31
Codeine[b]	25	5 (1–7)	1 (0–3)	4.85	2.46	−2.39
Cotinine[a]	32	10 (4–14)	5 (3–7)	2.00	1.81	−0.19
Diazinon[b,c]	4	3 (2–5)	2 (1–2)	11.64	12.50	0.86
Diclofenac[b]	13	1 (1–2)	1 (1–1)	11.71	12.17	0.46
Gemfibrozil[b]	13	4 (3–7)	2 (1–4)	12.29	13.34	1.05
Lidocaine[a]	40	5 (1–11)	2 (1–4)	5.21	4.24	−0.97
Lincomycin[b,c]	14	4 (2–8)	2 (1–4)	4.28	3.73	−0.55
Losartan[b]	42	2 (1–4)	2 (1–3)	9.95	10.13	−0.18
Metoprolol[a]	24	3 (1–9)	1 (1–3)	4.07	5.44	1.37
Naproxen[b]	32	7 (4–11)	2 (1–4)	10.06	10.54	0.48
O-desmethylvenlafaxine[a]	29	3 (2–5)	3 (1–5)	5.76	4.68	−1.08
Paraxanthine[a]	39	7 (2–12)	3 (2–4)	2.03	2.97	0.94
Ranitidine[a]	23	4 (2–6)	1 (1–1)	3.03	2.10	−0.93
Terbuthylazine[b,c]	4	1 (1–3)	1 (1–2)	9.60	10.78	1.18
Trimethoprim[b]	32	7 (2–10)	4 (1–6)	3.11	3.52	0.41
Valsartan[b]	39	2 (1–7)	1 (1–3)	10.90	11.24	0.34

[a] Standard not available in laboratory Sample t_R was based on HRMS data and the incorporation of fragment ions.
[b] Standard available in laboratory.
[c] Compound in blind set of ANN.

The LE and HE mass spectrum of the peak at 10.13 min was investigated for fragment ions: m/z 207.0917 ($C_{14}H_{11}N_2$, −2.4 ppm), 377.1552 ($C_{22}H_{22}N_4Cl$, +5 ppm) and 405.1590 ($C_{22}H_{22}N_4Cl$, −2.3 ppm) (Fig. 2, right). Literature (Hernández et al., 2015a) and the mass spectral database MassBank (Horai et al., 2010) were also searched to aid in the confidence of these fragment ions. It was found that these three fragment ions did indeed correspond to losartan. As seen in the figure, all associated fragments corresponded to the peak at 10.13 min, following the assertion of the t_R predictor. Furthermore, it is clearly seen that none of the fragment ions correspond with that of the other peak in the LE (4.63 min). A standard was later purchased and injected, unequivocally confirming that the peak at 10.13 min did correspond to losartan.

3.2.2. Tentative identification of metabolites without standard reference materials

The elimination of false positives in suspect analysis is challenging, especially the environmental matrices investigated herein (SW and WW) as thousands of compounds may be present. Suspect screening, by definition, does not rely on reference standards (Krauss et al., 2010). While the exact mass capability of HRMS has gone some way to avoid false positives, even at narrow mass window chromatograms, matrix inferences can be present, thereby hindering confident identification (Bade et al., 2015; Croley et al., 2012). A precise t_R predictor can therefore be a great additional means of identification.

Most research of emerging contaminants in the environment has focused on parent compounds, however many compounds can be at least partially metabolized or degraded in natural conditions (Jakimska et al., 2014). In this respect, the tentative identification of two major metabolites of carbamazepine and venlafaxine were explored: 10,11-dihydroxy carbamazepine and O-desmethyl venlafaxine (Fig. 3a). More than one chromatographic peak was observed at the exact mass of each protonated molecule. The ANN t_R predictor was then used to try to help minimize the number of peaks to be analyzed, with the predicted t_R calculated to be 6.29 and 5.76 min for 10,11-dihydroxy carbamazepine and O-desmethyl venlafaxine, respectively.

Two large (~4.00 and 6.66 min) and one small (~4.90 min) peaks are seen in the LE XIC of 10,11-dihydroxy carbamazepine (m/z = 271.1080). The predicted t_R was calculated to be 6.29 min and by including a ±2 minute window as in Section 3.2.1, the large peak at ~4.00 min could be disregarded, leaving the peaks at 6.66 and ~4.90 min. The ability to focus on fewer peaks is the primary aim and benefit of t_R prediction in environmental screening applications for unknowns. While having only one (correct) peak remaining is ideal, being able to disregard some peaks gives credence to the use of t_R prediction in the identification process. To aid in the differentiation of these peaks, fragment ions were sought in literature, whereby one group performed an MS/MS experiment with a QTOF instrument to find the fragment ions of 10,11-dihydroxy carbamazepine (271.1080, 236.0706, 210.0913 and 180.0808) (Ferrer and Thurman, 2012). As the XICs in the figure show, all fragment ions have the peak at 6.65 min in common. This provides great confidence that this peak is indeed from 10,11-dihydroxy carbamazepine, however for unequivocal identification, a standard would still have to be purchased.

The example of O-desmethyl venlafaxine represented the worst case scenario, where no peaks could be removed after application of the ±2 minute limit window. However, it must be noted that this was a rare case and only occurred for three of 26 compounds. In the LE XIC, two large (4.69 and 5.00 min) and two small peaks (~4.20 and 6.50 min) are seen. Even after incorporating the ANN predicted t_R and associated window (5.76 ± 2 min), all four peaks are still of interest. With the peaks being so close together, even using a ±1.3 minute window (corresponding to ~80% of compounds being successfully inside this window) would result in the correct elimination of only one small peak. In this situation, fragment ions have to be used to gain further information on the identity. Fragment ions were thus searched in literature (Herrera-Lopez et al., 2014) and investigated in the HE. Fig. 3b shows all ions corresponding to the peak at 4.69 min. While the ANN predicted t_R and associated window did include O-desmethyl venlafaxine, all other peaks in the LE XIC were also inside, meaning that no further confidence could be gained by t_R prediction, rather through the investigation of fragment ions.

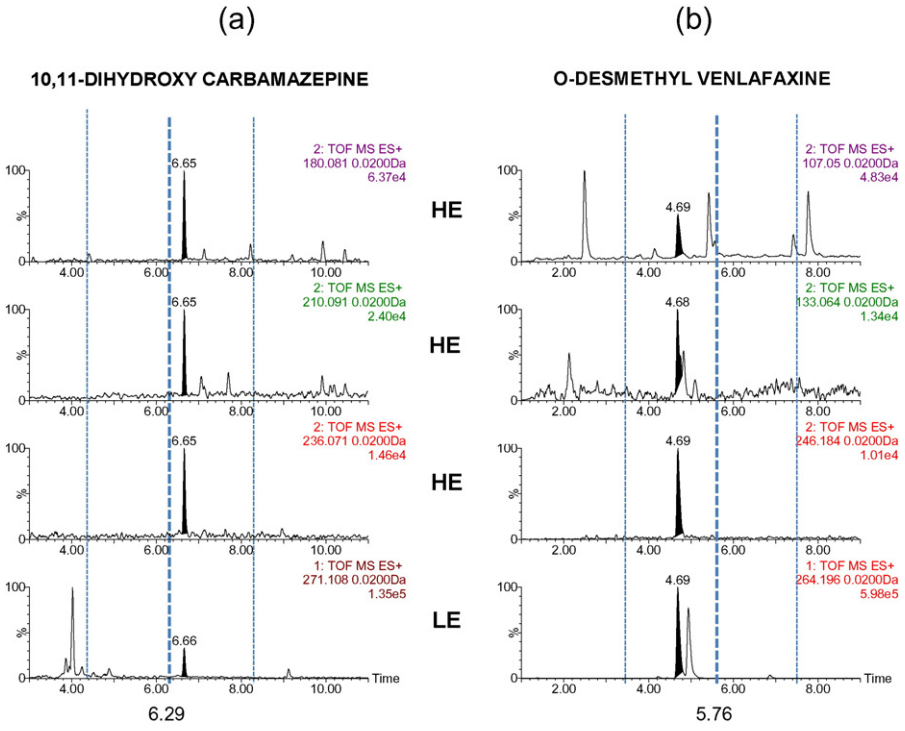

Fig. 3. Tentative identification of 10,11-dihydroxy carbamazepine (a) and O-desmethyl venlafaxine (b) in an IWW and EWW sample respectively, together with ANN prediction and ±2 minute window.

Nevertheless, the combination of ANN predicted t_R and fragment ions led to the tentative identification of this compound.

While the examples explained here show the successful assignment of chromatographic peaks, it is impossible to have total confidence with t_R prediction. In cases where there is more than one peak in the XIC, and the predicted peak is found to be incorrect, the peaks slightly outside the prediction window will also have to be investigated. Nevertheless, with data processing nowadays being the most time consuming part of environmental screening methods, the time saved by incorporating t_R prediction outweighs the possibility of false negatives (and positives).

These examples clearly show the utility of ANN as a t_R predictor, not just for its ability to disregard some false positive peaks, but also for its accuracy and subsequent confidence for tentatively identified compounds. It is therefore recommended when performing large scope (e.g. >1000 compounds) screening of environmental samples to include accurate t_R prediction in the strategy used for identification. This is particularly useful in the investigation of metabolites and TPs, for which standards can be very costly or unavailable.

4. Conclusions

This work showed the development and use of a t_R predictor based on artificial neural networks. In particular, a four layer multilayer perceptron successfully modeled retention of 544 compounds under these separation conditions. Overall, 90% of all compounds eluted within 2.00 min of the predicted value and for 100 blind test compounds, 95% were predicted within this window. The network was applied to additional suspect compound occurrence in wide-scope screening based on the use of LC-HRMS, demonstrating that it can reduce the number of false negatives or positives. This saves time and effort in the tentative identification of the compounds detected, as only those chromatographic peaks that fit the predicted t_R need to be focused on. Several representative examples are given to illustrate the usefulness of the complementary use of precise t_R prediction in large suspect screening of emerging contaminants. It is recommended to include this prediction for the identification of suspect compounds, particularly in the investigation of metabolites and TPs of organic contaminants, for which reference standards are commonly less accessible.

Acknowledgments

Richard Bade acknowledges the European Union for his Early Stage Researcher (ESR) contract as part of the EU-International Training Network SEWPROF (Marie Curie — PEOPLE Grant #317205).

The financial support from the Spanish Ministry of Economy and Competitiveness (Ref CTQ2012-36189), and Generalitat Valenciana, Spain (research group of excellence PROMETEO II/2014/023; ISIC 2012/016) is also acknowledged.

Thanks are also extended to the Biotechnology and Biological Sciences Research Council (BBSRC) and AstraZeneca (under the Global SHE research program) for award of a CASE industrial scholarship for T. Miller who collaborated on this project (Reference: BB/K501177/1).

Appendix A. Supplementary data

Supplementary data to this article can be found online at http://dx.doi.org/10.1016/j.scitotenv.2015.08.078.

References

Agüera, A., Martínez Bueno, M.J., Fernández-Alba, A.R., 2013. New trends in the analytical determination of emerging contaminants and their transformation products in environmental waters. Environ. Sci. Pollut. Res. Int. 20, 3496–3515. http://dx.doi.org/10.1007/s11356-013-1586-0.

Bade, R., Bijlsma, L., Sancho, J.V., Hernández, F., 2015. Critical evaluation of a simple retention time predictor based on LogKow as a complementary tool in the identification of emerging contaminants in water. Talanta 139, 143–149. http://dx.doi.org/10.1016/j.talanta.2015.02.055.

Barron, L., Havel, J., Purcell, M., Szpak, M., Kelleher, B., Paull, B., 2009. Predicting sorption of pharmaceuticals and personal care products onto soil and digested sludge using artificial neural networks. Analyst 134, 663–670. http://dx.doi.org/10.1039/b817822d.

Croley, T.R., White, K.D., Callahan, J.H., Musser, S.M., 2012. The chromatographic role in high resolution mass spectrometry for non-targeted analysis. J. Am. Soc. Mass Spectrom. 23, 1569–1578. http://dx.doi.org/10.1007/s13361-012-0392-0.

Ferrer, I., Thurman, E.M., 2012. Analysis of 100 pharmaceuticals and their degradates in water samples by liquid chromatography/quadrupole time-of-flight mass spectrometry. J. Chromatogr. A 1259, 148–157. http://dx.doi.org/10.1016/j.chroma.2012.03.059.
Giaginis, C., Tsantili-Kakoulidou, A., 2012. Quantitative structure–retention relationships as useful tool to characterize chromatographic systems and their potential to simulate biological processes. Chromatographia 76, 211–226. http://dx.doi.org/10.1007/s10337-012-2374-6.
Gómez, M.J., Gómez-Ramos, M.M., Malato, O., Mezcua, M., Férnandez-Alba, A.R., 2010. Rapid automated screening, identification and quantification of organic micro-contaminants and their main transformation products in wastewater and river waters using liquid chromatography–quadrupole-time-of-flight mass spectrometry with an accurate-mass. J. Chromatogr. A 1217, 7038–7054. http://dx.doi.org/10.1016/j.chroma.2010.08.070.
Goryński, K., Bojko, B., Nowaczyk, A., Buciński, A., Pawliszyn, J., Kaliszan, R., 2013. Quantitative structure–retention relationships models for prediction of high performance liquid chromatography retention time of small molecules: endogenous metabolites and banned compounds. Anal. Chim. Acta 797, 13–19. http://dx.doi.org/10.1016/j.aca.2013.08.025.
Gracia-Lor, E., Sancho, J.V., Hernandez, F., 2010. Simultaneous determination of acidic, neutral and basic pharmaceuticals in urban wastewater by ultra high-pressure liquid chromatography–tandem mass spectrometry. J. Chromatogr. a 1217, 622–632. http://dx.doi.org/10.1016/j.chroma.2009.11.090.
Gracia-Lor, E., Sancho, J.V., Hernandez, F., 2011. Multi-class determination of around 50 pharmaceuticals, including 26 antibiotics, in environmental and wastewater samples by ultra-high performance liquid chromatography–tandem mass spectrometry. J. Chromatogr. A 1218, 2264–2275. http://dx.doi.org/10.1016/j.chroma.2011.02.026.
Héberger, K., 2007. Quantitative structure–(chromatographic) retention relationships. J. Chromatogr. A 1158, 273–305. http://dx.doi.org/10.1016/j.chroma.2007.03.108.
Hernández, F., Bijlsma, L., Sancho, J.V., Díaz, R., Ibáñez, M., 2011. Rapid wide-scope screening of drugs of abuse, prescription drugs with potential for abuse and their metabolites in influent and effluent urban wastewater by ultrahigh pressure liquid chromatography–quadrupole-time-of-flight-mass spectrometry. Anal. Chim. Acta 684, 87–97. http://dx.doi.org/10.1016/j.aca.2010.10.043.
Hernández, F., Ibáñez, M., Botero-Coy, A.-M., Bade, R., Bustos-López, M.C., Rincón, J., Moncayo, A., Bijlsma, L., 2015a. LC-QTOF MS screening of more than 1,000 licit and illicit drugs and their metabolites in wastewater and surface waters from the area of Bogotá. Colombia. Anal. Bioanal. Chem. 407, 6405–6416. http://dx.doi.org/10.1007/s00216-015-8796-x.
Hernández, F., Ibáñez, M., Portolés, T., Cervera, M.I., Sancho, J.V., López, F.J., 2015b. Advancing towards universal screening for organic pollutants in waters. J. Hazard. Mater. 282, 86–95. http://dx.doi.org/10.1016/j.jhazmat.2014.08.006.
Herrera-Lopez, S., Hernando, M.D., García-Calvo, E., Fernández-Alba, A.R., Ulaszewska, M.M., 2014. Simultaneous screening of targeted and non-targeted contaminants using an LC–QTOF-MS system and automated MS/MS library searching. J. Mass Spectrom. 49, 878–893. http://dx.doi.org/10.1002/jms.3428.
Hogenboom, A.C., van Leerdam, J.A., de Voogt, P., 2009. Accurate mass screening and identification of emerging contaminants in environmental samples by liquid chromatography-hybrid linear ion trap Orbitrap mass spectrometry. J. Chromatogr. A 1216, 510–519. http://dx.doi.org/10.1016/j.chroma.2008.08.053.
Horai, H., Arita, M., Kanaya, S., Nihei, Y., Ikeda, T., Suwa, K., Ojima, Y., Tanaka, K., Tanaka, S., Aoshima, K., Oda, Y., Kakazu, Y., Kusano, M., Tohge, T., Matsuda, F., Sawada, Y., Hirai, M.Y., Nakanishi, H., Ikeda, K., Akimoto, N., Maoka, T., Takahashi, H., Ara, T., Sakurai, N., Suzuki, H., Shibata, D., Neumann, S., Iida, T., Tanaka, K., Funatsu, K., Matsuura, F., Soga, T., Taguchi, R., Saito, K., Nishioka, T., 2010. MassBank: a public repository for sharing mass spectral data for life sciences. J. Mass Spectrom. 45, 703–714. http://dx.doi.org/10.1002/jms.1777.
Howard, P.H., Muir, D.C.G., 2013. Identifying new persistent and bioaccumulative organics among chemicals in commerce. III: byproducts, impurities, and transformation products. Environ. Sci. Technol. 47, 5259–5266. http://dx.doi.org/10.1021/es4004075.
Ibáñez, M., Bijlsma, L., van Nuijs, A.L.N., Sancho, J.V., Haro, G., Covaci, A., Hernández, F., 2013. Quadrupole-time-of-flight mass spectrometry screening for synthetic cannabinoids in herbal blends. J. Mass Spectrom. 48, 685–694. http://dx.doi.org/10.1002/jms.3217.
Jakimska, A., Kot-Wasik, A., Namieśnik, J., 2014. The current state-of-the-art in the determination of pharmaceutical residues in environmental matrices using hyphenated techniques. Crit. Rev. Anal. Chem. 44, 277–298. http://dx.doi.org/10.1080/10408347.2013.835244.
Ji, C., Li, Y., Su, L., Zhang, X., Chen, X., 2009. Quantitative structure–retention relationships for mycotoxins and fungal metabolites in LC–MS/MS. J. Sep. Sci. 32, 3967–3979. http://dx.doi.org/10.1002/jssc.200900441.
Kaliszan, R., Baczek, T., Bucinknski, A., Buszewski, B., Sztupecka, M., 2003. Prediction of gradient retention from the linear solvent strength (LSS) model, quantitative structure–retention relationships (QSRR), and artificial neural networks (ANN). J. Sep. Sci. 26, 271–282. http://dx.doi.org/10.1002/jssc.200390033.
Kern, S., Fenner, K., Singer, H.P., Schwarzenbach, R.P., Hollender, J., 2009. Identification of transformation products of organic contaminants in natural waters by computer-aided prediction and high-resolution mass spectrometry. Environ. Sci. Technol. 43, 7039–7046. http://dx.doi.org/10.1021/es901979h.
Krauss, M., Singer, H., Hollender, J., 2010. LC-high resolution MS in environmental analysis: from target screening to the identification of unknowns. Anal. Bioanal. Chem. 397, 943–951. http://dx.doi.org/10.1007/s00216-010-3608-9.
Matsuo, H., Sakamoto, H., Arizono, K., Shinohara, R., 2011. Behavior of pharmaceuticals in waste water treatment plant in Japan. Bull. Environ. Contam. Toxicol. 87, 31–35. http://dx.doi.org/10.1007/s00128-011-0299-7.
Miller, T.H., Musenga, A., Cowan, D.A., Barron, L.P., 2013. Prediction of chromatographic retention time in high-resolution anti-doping screening data using artificial neural networks. Anal. Chem. 85, 10330–10337. http://dx.doi.org/10.1021/ac4024878.
Munro, K., Miller, T.H., Martins, C.P.B., Edge, A.M., Cowan, D. a, Barron, L.P., 2015. Artificial neural network modelling of pharmaceutical residue retention times in wastewater extracts using gradient liquid chromatography–high resolution mass spectrometry data. J. Chromatogr. A 1396, 33–44. http://dx.doi.org/10.1016/j.chroma.2015.03.063.
Nurmi, J., Pellinen, J., Rantalainen, A.-L., 2012. Critical evaluation of screening techniques for emerging environmental contaminants based on accurate mass measurements with time-of-flight mass spectrometry. J. Mass Spectrom. 47, 303–312. http://dx.doi.org/10.1002/jms.2964.
Oosterhuis, M., Sacher, F., ter Laak, T.L., 2013. Prediction of concentration levels of metformin and other high consumption pharmaceuticals in wastewater and regional surface water based on sales data. Sci. Total Environ. 442, 380–388. http://dx.doi.org/10.1016/j.scitotenv.2012.10.046.
Pal, A., He, Y., Jekel, M., Reinhard, M., Gin, K.Y.H., 2014. Emerging contaminants of public health significance as water quality indicator compounds in the urban water cycle. Environ. Int. 71, 46–62. http://dx.doi.org/10.1016/j.envint.2014.05.025.
Schymanski, E.L., Jeon, J., Gulde, R., Fenner, K., Ruff, M., Singer, H.P., Hollender, J., 2014. Identifying small molecules via high resolution mass spectrometry: communicating confidence. Environ. Sci. Technol. http://dx.doi.org/10.1021/es5002105.
Tetko, I.V., Gasteiger, J., Todeschini, R., Mauri, A., Livingstone, D., Ertl, P., Palyulin, V., Radchenko, E., Zefirov, N.S., Makarenko, A.S., Tanchuk, V.Y., Prokopenko, V.V., 2005. Virtual computational chemistry laboratory — design and description. J. Comput. Aided Mol. Des. 19, 453–463. http://dx.doi.org/10.1007/s10822-005-8694-y.
Ukić, Š., Novak, M., Žuvela, P., Avdalović, N., Liu, Y., Buszewski, B., Bolanča, T., 2014a. Development of gradient retention model in ion chromatography. Part I: conventional QSRR approach. Chromatographia 77, 985–996. http://dx.doi.org/10.1007/s10337-014-2653-5.
Ukić, Š., Novak, M., Žuvela, P., Avdalović, N., Liu, Y., Buszewski, B., Bolanča, T., 2014b. Development of gradient retention model in ion chromatography. Part II: artificial intelligence QSRR approach. Chromatographia 77, 997–1007. http://dx.doi.org/10.1007/s10337-014-2653-5.
Wilson, N.S., Dolan, J.W., Snyder, L.R., Carr, P.W., Sander, L.C., 2002. Column selectivity in reversed-phase liquid chromatography: III. The physico-chemical basis of selectivity. J. Chromatogr. A 961, 217–236. http://dx.doi.org/10.1016/S0021-9673(02)00658-1.
Zuccato, E., Castiglioni, S., Fanelli, R., Reitano, G., Bagnati, R., Chiabrando, C., Pomati, F., Rossetti, C., Calamari, D., 2006. Pharmaceuticals in the environment in Italy: causes, occurrence, effects and control. Environ. Sci. Pollut. Res. Int. 13, 15–21. http://dx.doi.org/10.1065/espr2006.01.004.

Science of the Total Environment 547 (2016) 396–404

Contents lists available at ScienceDirect

Science of the Total Environment

journal homepage: www.elsevier.com/locate/scitotenv

Assessing the reliability of uptake and elimination kinetics modelling approaches for estimating bioconcentration factors in the freshwater invertebrate, *Gammarus pulex*

Thomas H. Miller [a,b], Gillian L. McEneff [a], Lucy C. Stott [c], Stewart F. Owen [b], Nicolas R. Bury [c,1], Leon P. Barron [a,*,1]

[a] Analytical & Environmental Sciences Division, Faculty of Life Sciences and Medicine, King's College London, 150 Stamford Street, London SE1 9NH, United Kingdom
[b] AstraZeneca, Global Environment, Alderley Park, Macclesfield, Cheshire SK10 4TF, United Kingdom
[c] Division of Diabetes and Nutritional Sciences, Faculty of Life Sciences and Medicine, King's College London, Franklin Wilkins Building, 150 Stamford Street, London SE1 9NH, United Kingdom

HIGHLIGHTS

- Toxicokinetics for eight pharmaceuticals are presented in *Gammarus pulex*.
- Bioconcentration factors ranged from 12 to 4533 and depended on the method used.
- Decreasing trends in the uptake (k_1) rate constants were observed.
- Recognised models and their assumptions may lead to BCF estimation inaccuracies.
- Meta-analysis of previous toxicokinetic work revealed similar trends in k_1.

GRAPHICAL ABSTRACT

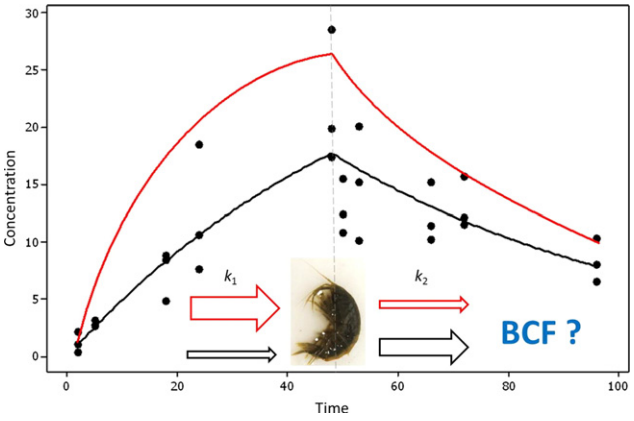

ARTICLE INFO

Article history:
Received 13 October 2015
Received in revised form 18 December 2015
Accepted 29 December 2015
Available online 12 January 2016

Editor: Kevin V. Thomas

Keywords:
Pharmaceuticals
Pesticides
Toxicokinetics
Bioconcentration
Invertebrates

ABSTRACT

This study considers whether the current standard toxicokinetic methods are an accurate and applicable assessment of xenobiotic exposure in an aquatic freshwater invertebrate. An *in vivo* exposure examined the uptake and elimination kinetics for eight pharmaceutical compounds in the amphipod crustacean, *Gammarus pulex* by measuring their concentrations in both biological material and in the exposure medium over a 96 h period. Selected pharmaceuticals included two anti-inflammatories (diclofenac and ibuprofen), two beta-blockers (propranolol and metoprolol), an anti-depressant (imipramine), an anti-histamine (ranitidine) and two beta-agonists (formoterol and terbutaline). Kinetic bioconcentration factors (BCFs) for the selected pharmaceuticals were derived from a first-order one-compartment model using either the simultaneous or sequential modelling methods. Using the simultaneous method for parameter estimation, BCF values ranged from 12 to 212. In contrast, the sequential method for parameter estimation resulted in bioconcentration factors ranging from 19 to 4533. Observed toxicokinetic plots showed statistically significant lack-of-fits and further interrogation of the models revealed a decreasing trend in the uptake rate constant over time for rantidine, diclofenac, imipramine, metoprolol, formoterol and terbutaline. Previous published toxicokinetic data for 14 organic micro-pollutants

* Corresponding author.
E-mail address: leon.barron@kcl.ac.uk (L.P. Barron).
[1] Both of these authors co-led this work.

http://dx.doi.org/10.1016/j.scitotenv.2015.12.145

were also assessed and similar trends were identified to those observed in this study. The decreasing trend of the uptake rate constant over time highlights the need to interpret modelled data more comprehensively to ensure uncertainties associated with uptake and elimination parameters for determining bioconcentration factors are minimised.

1. Introduction

The pseudo-persistent nature of pharmaceuticals and personal care products (PPCPs) has been highlighted in recent years as an environmental concern and has led to the introduction of a watch list under the EU Water Framework Directive which includes an anti-inflammatory, diclofenac, and two hormones, the synthetic ethinyl-estradiol (EE2) and natural estradiol (2013/39/EU, 2013). Several thousand PPCPs are currently available worldwide and whilst measured environmental concentrations typically range from low ng L^{-1} to high μg L^{-1}, their potential to effect an ecotoxicological response and/or bioaccumulate in a range of biota still remains understudied (De Lange et al., 2006; Contardo-Jara et al., 2011).

Ecotoxicological studies have shown that measured PPCP concentrations in surface waters would be highly unlikely to cause acute effects on exposed organisms (Crane et al., 2006). However, chronic exposure has been linked to behavioural activity changes, increased oxidative stress and alterations to the function of several vital organs in fish and invertebrates (Heckmann et al., 2007; Fernández et al., 2013). Aquatic invertebrates such as molluscs and smaller crustacean species have been previously utilised for monitoring PPCPs in the natural aquatic environment. Most recently, the freshwater amphipod, *Gammarus pulex*, was found to contain residues of carbamazepine, diazepam, nimesulide, trimethoprim and warfarin measuring at low ng g^{-1} concentrations in UK streams (Miller et al., 2015). PPCP uptake has also been previously observed at low ng g^{-1} concentrations in wild and caged mussel species collected from the coast of Ireland, the Bohai Sea in China, the Mediterranean Sea and San Francisco Bay, highlighting the extent of PPCP contamination worldwide (McEneff et al., 2014; Li et al., 2012; Bueno et al., 2013; Klosterhaus et al., 2013). EU Directive 93/39/EEC requires an environmental risk assessment to be carried out prior to drug licencing in order to determine any significant toxicological risks associated with a xenobiotic (Straub, 2002). Under the regulatory guidelines, environmental toxicity testing of pharmaceuticals requires standard acute toxicity tests, such as LC_{50} testing, to be carried out unless the predicted environmental concentration (PEC)/predicted no effect concentration (PNEC) ratio is <1, whereby no further toxicity testing is required. Standardised toxicity tests on aquatic organisms are generally limited to algae (*Desmodesmus subspicatus* or *Pseudokirchneriella subcapitata*), *Daphnia magna* and/or fish (e.g. *Danio rerio*) considered as good model species from freshwater environments. Furthermore, a lack of published research generally exists on the uptake and depuration kinetics of PPCPs both in target and non-target aquatic species to help elucidate potential acute versus chronic effects.

Toxicokinetic studies identify whether a compound will accumulate to potentially toxic levels in/on the organism itself over time or potentially act as a source of toxicity in higher trophic organisms (Ashauer & Escher, 2010). In aquatic species, this can involve the study of either accumulation of compounds via water exposure only (i.e. bioconcentration), or via exposure through both water and diet (i.e. bioaccumulation or biomagnification) (Oliver & Niimi, 1983; Meador et al., 1995). Fish exposure studies often allow a time period for the compound of interest to reach steady-state within the organism, where the rate of uptake is equal to the rate of depuration. However, this time can vary considerably and has led to the application of kinetic modelling where uptake and elimination rates are estimated and used to derive a bioconcentration factor (BCF) (Veith et al., 1979). This factor can be determined in two ways: (a) as a ratio of either the compound concentrations in the organism and the water phase at steady-state, or (b) as the ratio of the uptake (k_1) and elimination (k_2) rate constants (Kenaga, 1972). This approach has been widely evaluated in the literature. Earlier models, such as those for methylmercury in fish (Norstrom et al., 1976) considered several variables including volume of water passing the gills, assimilation across the gills and body weight of the organism. More recent models have been developed to also account for water-phase and lipid-phase resistance, fish lipid content and compound logK_{ow} (Veith et al., 1979; Gobas & MacKay, 1987; Hendriks & Heikens, 2001). A widely known and accepted model used to calculate the bioaccumulation of a compound in fish via aqueous and dietary exposure is outlined in the Organisation for Economic Co-Operation and Development (OECD) 305 guidelines (OECD, Test No. 305). These guidelines present two methods for estimation of k_1 and k_2. The sequential method can be performed in one of two ways, a k_2 value can be estimated by linear regression and then curve fitting methods are applied to find k_1. Alternatively, curve fitting methods can be used to estimate k_2 first which is then used to estimate k_1. The simultaneous model calculates both k_1 and k_2 together and is considered a potentially more reliable and realistic model for concurrent uptake and elimination processes occurring in biological systems. Considering the number of PPCPs available on the market that may require testing under EU REACH legislation (European Commission, 2006), the time scales (2 week acclimatisation followed by 28 days for the uptake phase alone unless steady-state is achieved sooner) and number of organisms required for each test (n = 4 per time-point for each exposure) the testing regime to apply to all chemicals under REACH would appear unfeasible. Furthermore, current policy aims to reduce the number of fish used for scientific research, thus current methods proposed such as the OECD guidelines should account for this more ethical approach (Carter et al., 2014; Browne, 2013). Several recent studies assessing BCF have utilised shorter exposure times with experiments lasting only 4–7 days using aquatic invertebrates as a means to assess the potential for substance to bioaccumulate in aquatic organisms (Ashauer et al., 2006; Meredith-Williams et al., 2012). These ecotoxicological studies are important to direct future risk assessment and essential when considering contaminant monitoring in water, sediment and biota.

In the present study, an *in vivo* experiment was carried out to determine the uptake and depuration kinetics of environmentally relevant (low μg·L^{-1}) concentrations of several selected PPCPs in the common freshwater invertebrate, *G. pulex*, using radioactive labels and liquid scintillation analysis. Lastly, the OECD 305 guidelines currently used for modelling of uptake and elimination kinetics in aquatic species are critically evaluated for the first time based on the results obtained both in this study and other published works on micropollutants.

2. Materials and methods

2.1. Reagents, chemicals and consumables

Radio-labelled pharmaceuticals including ^{3}H-propranolol hydrochloride (29.0 Ci $mmol^{-1}$) were acquired from Amersham Biosciences. ^{3}H-metoprolol (29.7 Ci $mmol^{-1}$), ^{3}H-formoterol (18.5 Ci $mmol^{-1}$) and ^{3}H-terbutaline (29.0 Ci $mmol^{-1}$) were obtained from Vitrax. ^{14}C-ibuprofen (2.03 Ci $mmol^{-1}$) was obtained from American Radiolabelled Chemicals Inc. (St Louis, US). ^{3}H-ranitidine (2.5 Ci $mmol^{-1}$) was obtained from Moravek Biochemicals, ^{14}C-diclofenac (0.063 Ci $mmol^{-1}$) and ^{3}H-imipramine hydrochloride (48.5 Ci $mmol^{-1}$) from Perkin-Elmer. All stock solutions were stored in ethanol. Hydrogen peroxide solution

(30% w/w) and analytical grade salts (>99%) including sodium hydrogen carbonate, magnesium sulphate, calcium sulphate, potassium chloride were purchased from Sigma (Dorset, UK). Tissue solubiliser (Solvable™) and liquid scintillation cocktail (Hionic Fluor™) were purchased from Fischer Scientific Ltd. (Loughborough, UK). Ultra-pure water was obtained from a Millipore Milli-Q water purification system with a specific resistance of 18.2 MΩ·cm or greater (Millipore, Bedford, MA, USA). 6-Well culture plates were obtained from VWR (Leicestershire, UK).

2.2. Sample collection and culture maintenance

G. pulex were collected by kick-sampling from the River Cray, South-East London, UK, 51°23′09.5″N 0°06′32.4″E. This site was previously shown to have low pharmaceutical contamination in both collected surface water and animal samples (Miller et al., 2015). The populations were transported to the laboratory in 500 mL Nalgene™ flasks filled with surface water from the sample collection site. Populations were rinsed with artificial freshwater (AFW) and then acclimatised to laboratory conditions (as specified below) for a minimum of 7 days before any exposure experiments were performed. AFW was prepared from 1.15 mM of $NaHCO_3$, 0.50 mM $MgSO_4$, 0.44 mM $CaSO_4$ and 0.05 mM of KCl dissolved in 20 L of ultra-pure water. This water was subsequently aerated for several hours to remove dissolved carbonic acid and maximise the dissolved oxygen concentrations. Each culture tank (n = 8) was filled with 2.5 L of AFW and animals were fed with alder leaves that were previously collected from the sampling site and conditioned by submersion in surface water for two days prior to use.

2.3. Toxicokinetic exposure and conditions

Toxicokinetic experiments were performed separately for each pharmaceutical for a total of 96 h which included a 48 h uptake phase followed by a 48 h depuration period. Individual adult organisms, both male and female and each >5 mg wet weight, were placed in each well of 6-well culture plates. *G. pulex* were carefully transferred to well plates using blunt forceps to avoid any harm to the organisms before exposure. A single well contained one organism in 10 mL of exposure media (AFW and test compound) and only non-parasitised individuals were used (absence of *Pomphorhynchus laevis* indicated by the lack of an orange dot on the dorsal side of the animal). *G. pulex* were exposed to individual PPCPs at a concentration of 1 μg·L^{-1}, except for diclofenac and ibuprofen which were present at 10 μg·L^{-1}. The higher exposure of these two compounds was due to the low activity of the radiolabel. All exposure media contained <0.05% of solvent (ethanol). A total of 33 organisms were used per exposure and were sampled (n = 3/time-point) at 2, 5, 18, 24 and 48 h in the uptake phase followed by the same time-points in the depuration phase. Along with *G. pulex*, 50 μL water was also sampled from each well for analysis of radioactivity. Each sampled organism was washed in 10 mL of ultra-pure water for 10 s (n = 6) and gently blotted dry to remove any excess exposure media and unbound compound to the cuticle of the animal. Organisms were weighed after sampling to determine body mass and then transferred to scintillation tubes for tissue solubilisation. Three individual organisms were also exposed to unspiked AFW in culture plates and sampled after 96 h in a control experiment to account for any background radiation. Additionally, for each experiment, three wells without *G. pulex* were filled with exposure media to account for losses of the compound by sorption to the walls of culture plates. Culture plates were stored in sealed plastic containers with wet tissue to prevent evaporative losses during the static exposure. The light cycle followed 12:12 h light:dark without a dusk/dawn transition period. All experiments were performed in a temperature controlled room at 15 °C (±2 °C) and water pH was also measured across each experiment at 8.2 ± 0.1.

2.4. Sample preparation and liquid scintillation counting

Water samples (50 μL) collected from each exposure well were added to 2 mL of Hionic Fluor liquid scintillation cocktail and counted for radioactivity on a Beckman LS6500 instrument (Beckman Coulter, Inc.). Sampled *G. pulex* individuals were placed in a scintillation tube with 2 mL of tissue solubiliser and maintained at room temperature (approx. 20 °C) for 96 h. Samples were shaken vigorously and then a 50 μL aliquot of the solubilised biotic extract was added to 2 mL of Hionic Fluor to be counted. To account for any difference in counts caused by colour quenching, hydrogen peroxide (200 μL) was added to a previously counted biotic extract and re-analysed. No difference in counts was observed with or without the presence of hydrogen peroxide, therefore, all other biotic samples were counted without the addition of hydrogen peroxide. In addition, chemiluminescence accounted for <0.01% of the overall counts, and was therefore ignored.

2.5. Modelling bioconcentration factors

Parameter estimation of uptake rate constant (k_1) and depuration rate constant (k_2) was performed using a curve fitting algorithm via Minitab statistical software (Minitab Ltd., Coventry, UK) and as outlined in the OECD 305 Fish Bioconcentration Guidelines (OECD, Test No. 305). The concentration of compound in the organism is assumed to follow first order kinetics and is expressed in Eq. (1),

$$\frac{dC_{organism}}{dt} = k_1 \times [C_{water}] - k_2 \times [C_{organism}] \quad (1)$$

where, $dC_{organism}/dt$ is the rate of change in the concentration of a compound within/on *G. pulex* (mg kg^{-1} day^{-1}), k_1 is the uptake rate constant (L kg^{-1} day^{-1}), k_2 is the elimination rate constant (day^{-1}), C_{water} is the concentration in the water (mg L^{-1}) and $C_{organism}$ is the concentration in the organism (mg kg^{-1}). Eq. (1) was integrated into Eqs. (2) and (3) for fitting of curves to the uptake and depuration data. This method, known as the Levenberg–Marquardt algorithm, uses an iterative formula to minimise the residual errors between the observed and predicted data points and simultaneously estimates k_1 and k_2 values from the fitted curve i.e.

$$[C_{organism}] = [C_{water}] \times \frac{k_1}{k_2} \times \left(1 - e^{-k_2 t}\right), \quad \text{when } 0 < t < t_e \quad (2)$$

$$[C_{organism}] = [C_{water}] \times \frac{k_1}{k_2} \times \left(1 - e^{-k_2 (t - t_e)} - e^{-k_2 t}\right), \quad \text{when } t > t_e \quad (3)$$

where, t is the time (days) and t_e is the end time of the uptake phase (days). At steady-state, the rate of uptake should be equal to the rate of depuration and there should be no overall change in analyte concentration within *G. pulex*, as expressed by Eq. (4),

$$k_1 \times [C_{water}] = k_2 \times [C_{organism}] \leftrightarrow \frac{k_1}{k_2} = \frac{[C_{fish}]}{[C_{water}]} = BCF \quad (4)$$

where, BCF is the bioconcentration factor (L kg^{-1}). BCF can also be estimated using a sequential method where a simple linear regression model is developed based on the depuration data only. With the assumption of first order kinetics, the model should fit a straight line and its slope represents the elimination rate constant as shown in Eq. (5), i.e.

$$\ln [C_{organism}] = -k_2 \times t + c \quad (5)$$

where, $\ln[C_{organism}]$ is the natural log of the analyte concentration within *G. pulex* and c is the intercept, which here equals the natural log of the analyte concentration in the *G. pulex* at the start of the depuration phase. The k_2 from Eq. (5) can then be used as a parameter in the

curve fitting algorithm to estimate k_1. The rearrangement of Eq. (2) allows the value for k_1 to be calculated over the time interval specified, as shown in Eq. (6) (Crookes & Brooke, 2011). The assumptions of the equation are that analyte concentration in the water and k_2 remain constant. The k_2 used in Eq. (6) was directly estimated by using linear regression of the depuration data to obtain the slope (k_2). The value of k_1 should remain constant over the entire experiment.

$$k_1 = \frac{[C_{organism}] \times k_2}{[C_{water}] \times (1 - e^{-k_2 \times t})} \quad (6)$$

For this study, initial parameters for k_1 and k_2 were arbitrarily set at 0.1 in the software with C_{water} set in μg L^{-1}, t set at 48 h and the maximum number of iterations was set at 200 upon which optimised k_1 and k_2 values were subsequently derived. Confidence intervals (95%) were plotted for curves and the overall model fits were assessed. The lack-of-fit test was calculated in the Minitab software and was used to assess the fit of the line by comparing the variation in response of the replicate data. Lack-of-fit was assessed at a significance level of 0.05. Correlation coefficients (r^2) were evaluated when the sequential method was used to estimate k_2. The distribution coefficient (log$D$) was generated using ACD Labs Percepta software for the interpretation of estimated BCF values. All compound information is displayed in Table S2 of the SI.

3. Results and discussion

3.1. Uptake and elimination kinetics for selected PPCPs within G. pulex

The exposure concentration of each PPCP was selected to approximate the higher ranges of trace pharmaceutical occurrence in the aquatic environment to maintain practically quantifiable limits for reliable analysis (Miller et al., 2015; Hilton & Thomas, 2003; Thomas & Hilton, 2004). Considering that natural uptake and depuration are not separate processes, the BCF values for the selected compounds were determined using the simultaneous model described above (Table 1). Uptake of each pharmaceutical was observed in *G. pulex* as early as 2 h from the point of exposure. The highest residue concentrations measured in *G. pulex* at the 48 h timepoint were ibuprofen and diclofenac, potentially corresponding to the elevated exposure concentrations of 10 μg L^{-1}. All other compounds exposed at 1 μg L^{-1} measured <80 ng g^{-1} ww after 48 h uptake (Fig. 1). The rate of PPCP uptake measured in the exposed *G. pulex* corresponds to the decreases in PPCP concentration measured in the spiked AFW. The largest decrease in PPCP concentration was observed for imipramine, where analyte concentrations in the water decreased to an average of 0.478 μg L^{-1} corresponding to a 52.2% loss. After 48 h, formoterol concentration also decreased in water by 15% to an average of 0.85 μg L^{-1}. The exposure concentrations of the remaining compounds did not decrease by ≥10% (Fig. 2 and Table S1). Additional sources of potential PPCP loss in the aqueous phase should be mentioned and include photolysis, volatilisation, metabolism by microorganisms and sorption to the walls of the exposure well. Of these processes sorption was accounted for by control wells with exposure media only and was shown to account for negligible losses in water concentration except in the case of imipramine (Table S1). Within 2 h, there was a 27% loss of imipramine and within 48 h the loss increased to 39%. As quantification was performed by LSC, any degradation products resulting from transformation or photolysis would contribute towards the total radioactivity and counted as the precursor compound. However, it should be considered that these formed products may potentially have different accumulation potentials and hence latent uptake and elimination kinetics.

Following removal from the contaminated source, relatively high elimination rates were measured for most of the selected compounds. However, imipramine showed increased uptake (k_1 = 1.408 L kg^{-1} day^{-1}), but lower elimination (k_2 = 0.007 day^{-1}), resulting in the highest BCF value measured at 212. Diclofenac has the

Table 1
Toxicokinetic parameters and bioconcentration factors for eight PPCPs.

Compound	Simultaneous BCF					Sequential BCF[a]					Sequential BCF[b]				
	k_1 (L kg^{-1} day^{-1})	SE	k_2 (day^{-1})	SE	*p*-Value	BCF	k_1 (L kg^{-1} day^{-1})	SE	*p*-Value	k_2 (day^{-1})	SE	*p*-Value	BCF	k_1 (L kg^{-1} day^{-1})	SE	*p*-Value	k_2 (day^{-1})	r^2	BCF
Propranolol	0.538	0.068	0.017	0.004	0.266	32	0.618	0.047	0.831	0.016	0.006	0.132	39	0.604	0.045	0.860	0.015	0.490	42
Formoterol	0.408	0.093	0.029	0.009	0.335	14	0.451	0.051	0.914	0.025	0.014	0.279	18	0.357	0.040	0.942	0.011	0.121	33
Imipramine	1.408	0.205	0.007	0.004	0.008	212	1.361	0.177	0.017	0.000	0.004	0.490	3811	1.360	0.177	0.017	0.000	0.001	4533
Metoprolol	0.076	0.022	0.005	0.008	0.073	16	N/A												
Terbutaline	0.136	0.020	0.011	0.004	0.026	12	0.135	0.016	0.027	0.006	0.003	0.381	22	0.117	0.016	0.027	0.006	0.200	19
Ranitidine	0.479	0.126	0.028	0.011	0.005	17	0.310	0.071	0.007	0.004	0.006	0.192	81	0.301	0.070	0.007	0.003	0.015	112
Diclofenac	0.273	0.037	0.020	0.005	0.002	14	0.253	0.025	0.017	0.009	0.003	0.156	27	0.269	0.026	0.023	0.013	0.243	21
Ibuprofen	0.338	0.094	0.012	0.008	0.000	27	0.582	0.097	0.013	0.022	0.014	0.004	27	0.488	0.073	0.029	0.010	0.093	50

p-Values were assessed via standard error (SE) and lack-of-fit tests.
[a] Sequential using curve fitting method.
[b] Sequential using linear regression.

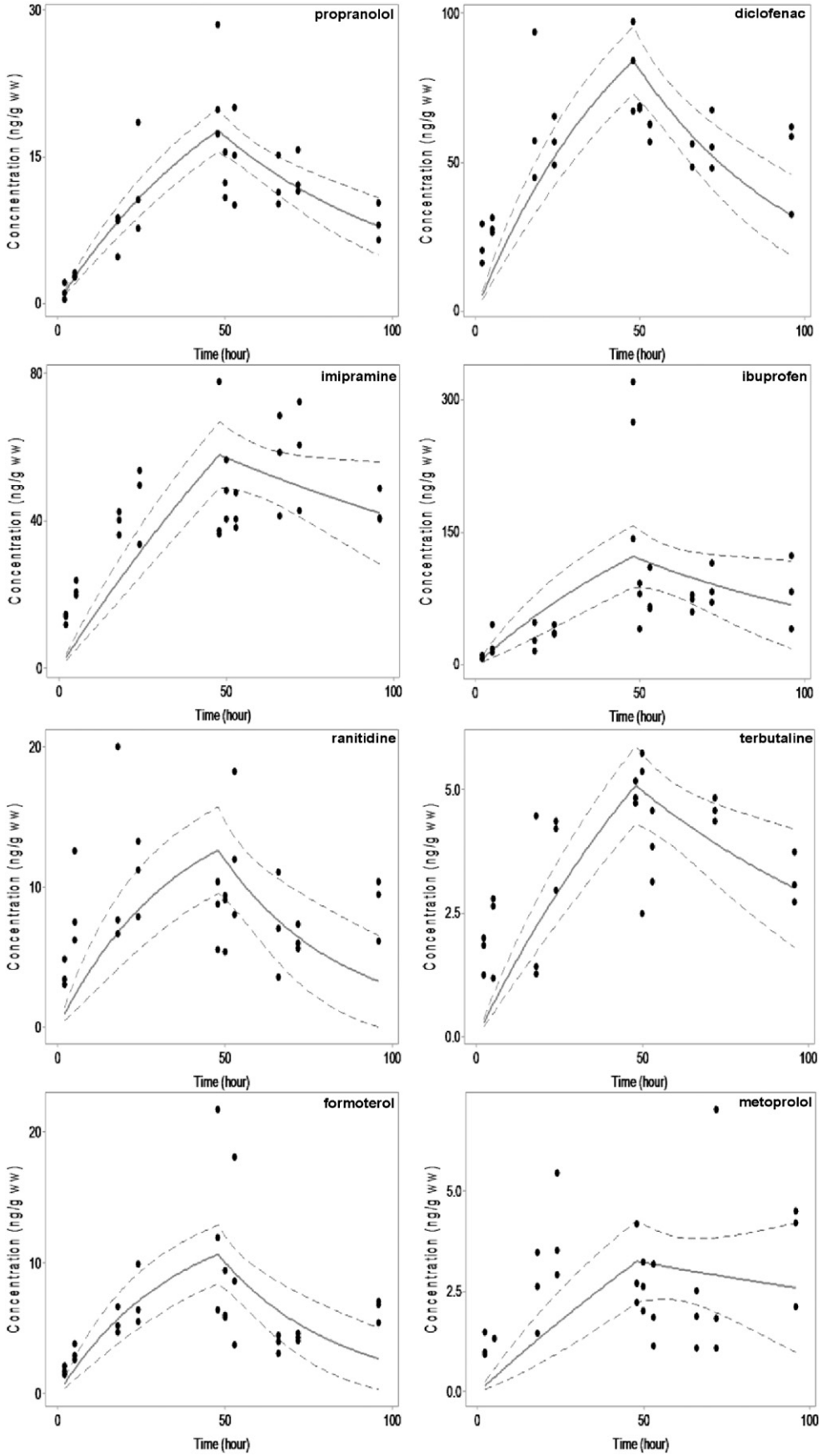

Fig. 1. Uptake and elimination data for PPCPs in *G. pulex*. Dashed lines indicate 95% confidence limits.

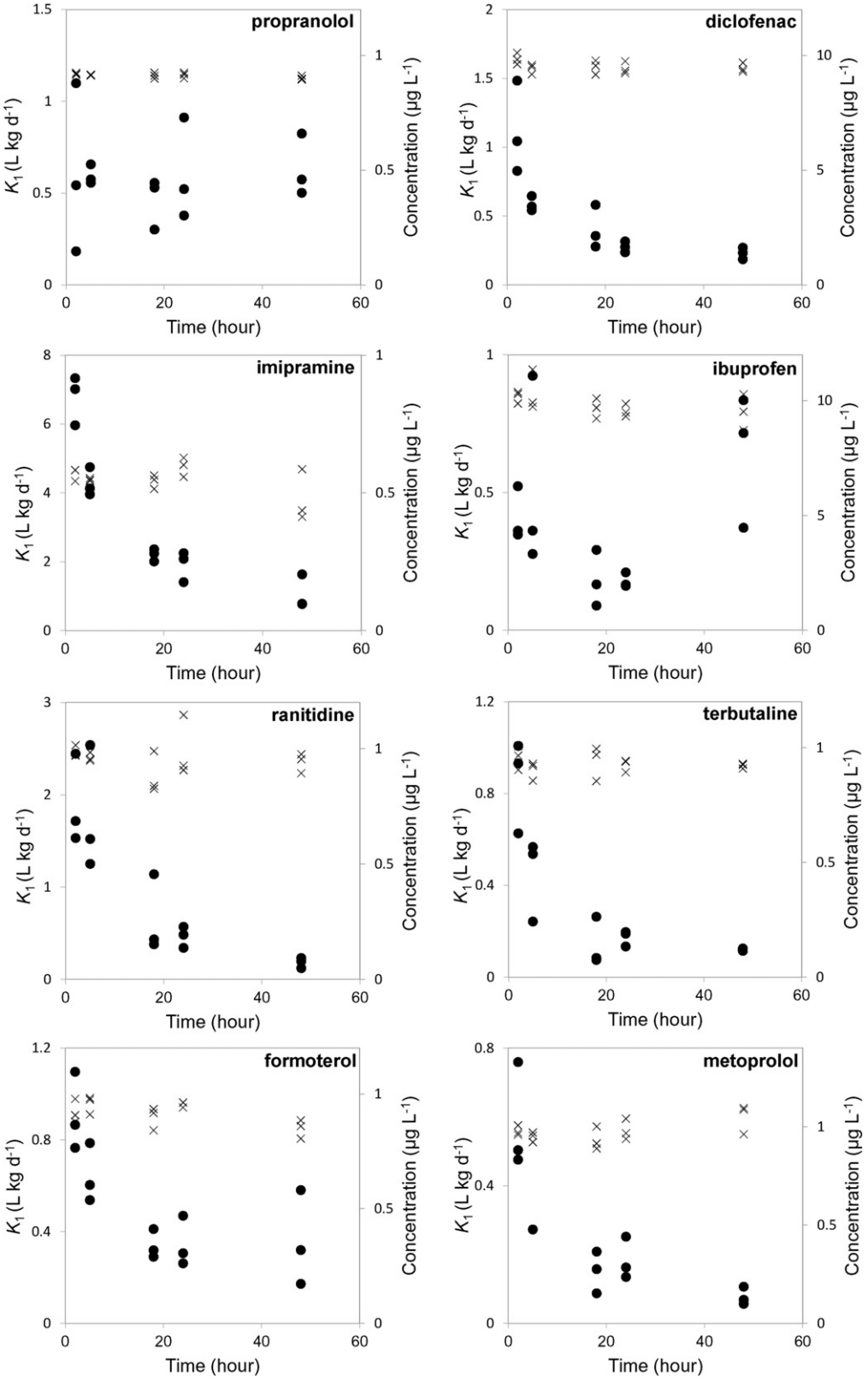

Fig. 2. Relationship of uptake rate constants (k_1) over time for eight PPCPs (black circles) and the respective water concentrations (C_w) over time (crosses).

same log*P* value as imipramine at 4.4 ($\log D_{8.2} = -1.1$) but attained a significantly lower BCF value of 14 due to its high rate of elimination. Ibuprofen, another acidic drug with a log*P* of 3.5 (calculated $\log D_{8.2} = -0.1$), also had a low BCF value determined at 27. The BCF values for the four compounds with log*P* < 2. (i.e. metoprolol, ranitidine, terbutaline and formoterol) were determined between 12 and 17. Hydrophobicity is generally considered a major factor when determining the bioaccumulation potential of a compound. However, uptake studies related to pharmaceuticals in several species of plants, for example, showed poor correlations between $\log D_{ow}$ and logBCF and especially

so for ionised molecules (Wu et al., 2013). Low bioconcentration of the selected PPCPs was in agreement with a study by Meredith-Williams et al., in which toxicokinetic data for six pharmaceuticals within *G. pulex* was shown with the exception of fluoxetine, a selective serotonin reuptake inhibitor (BCF = 185,900) (Meredith-Williams et al., 2012). In the cases of diclofenac, ibuprofen, imipramine and propranolol, log*P* is similar (3.3–4.7). Therefore, using an uptake model based on hydrophobicity, it would be logical to assume similar uptake rates. A potential reason for their difference could be physicochemical in nature, e.g. due to their anionic or cationic nature as well as the degree of ionisation and logD_{ow} value (Erickson et al., 2006). It could also be due to biological factors such as gill surface charge or the boundary layer between the bulk water and the gill surface (Tao et al., 2001). Uptake across the gill may also occur by more than simple passive diffusion for these ionic compounds and thus carrier mediated transport may also have influence on the different ionic species (Sugano et al., 2010; Kell & Oliver, 2014). The increased uptake constants of imipramine, propranolol and formoterol are in agreement with reported gill cell permeabilities to these compounds in the same order of imipramine > propranolol > formoterol (Stott et al., 2015). The low concentrations of PPCP residues measured in the *G. pulex* and unspiked AFW post-exposure highlights the ability for *G. pulex* to readily metabolise and eliminate xenobiotics, as previously shown by Nyman et al. (2014) and Ashauer et al. (2012). This evidence suggests there is conservation of cytochrome P450 enzymes, similarly observed in other aquatic invertebrate species (Solé & Livingstone, 2005).

3.2. Comparison of simultaneous versus sequential uptake and depuration process models

Methods used for the calculation of BCF values in *G. pulex* are summarised in Table 1 and also include uptake and elimination constants (±standard error). Many of the toxicokinetic plots in Fig. 1 are shown to have some lack-of-fit. The *p*-value generated from a lack-of-fit test shows that in the simultaneous method there are 5 models that have a statistically significant lack-of-fit indicating potentially inaccurate and unreliable BCF values. It is possible that several large outliers could influence the lack-of-fit test, thus resulting in a statistical significance when potentially none exists. When using the simultaneous method, if a poor fit exists, then the sequential method should be investigated as a potential alternative. The linear regression of the depuration phase data points gives a direct estimate of k_2. The goodness-of-fit is interpreted by visual inspection of the linearity and the r^2 (Fig. S1). Consideration of the sequential method showed an over-estimation of BCF values when compared to the simultaneous model. Deviations from linearity can indicate higher order kinetics. Simple plots of $1/[C_{organism}]$ here did not indicate second order kinetics and therefore k_2 values from plots of $\ln[C_{organism}]$ were accepted. Low r^2 values for some compounds were likely due to the scatter in measured internal concentrations. Comparison of derived k_2 values showed that imipramine, formoterol, ranitidine, diclofenac and terbutaline had significantly lower elimination constants in comparison to the simultaneous model approach (Table 1). Markedly reduced estimations in k_2 for imipramine and ranitidine corresponded to a large increase in BCF for ranitidine, increasing 4-fold, and imipramine, increasing >10-fold to ~4200 on average between curve fitting and linear regression approaches. Given the inherent non-standard method we have applied, further work would be necessary to better understand this apparently high BCF and we would caution reliance on this value from such a limited study. When using a curve fitting method to calculate an elimination constant in the sequential method there was good agreement between the linear regression estimates of k_2, indicating the estimate of k_2 was correct. The p-values for the curve fits indicated that there was only one statistical lack-of-fit for the k_2 value generated for ibuprofen. Uptake curves displayed a poor fit (as shown for imipramine concentration in *G. pulex*, which was consistently under-estimated). In addition, uptake constants in Table 1 specifically showed significant lack-of-fit for all compounds except propranolol and formoterol (p-value > 0.05). In fitting the depuration data using the sequential approach, a zero to mildly increasing slope was observed overall for metoprolol due to a wider scatter of data. A k_2 value could not therefore be calculated for metoprolol. The potential for model uncertainty highlighted in this study is significant from a regulatory perspective, especially for compounds such as imipramine that was determined to be accumulative using the sequential method and non-accumulative using the simultaneous method (European Commission, 2006).

3.3. Assessment of k_1, k_2 and C_w constancy

The OECD 305 model makes several assumptions that C_w, k_1 and k_2 do not change over time. To assess the potential validity of the k_1 constancy assumption in the first instance, k_1 was derived at each time point accordingly (Crookes & Brooke, 2011). It should be noted that a potential limitation to this approach was that the equation to calculate k_1 uses the k_2 estimate from the depuration phase, but this was deemed sufficient to identify any trends in any variation observed. As the lack-of-fit tests of the simultaneous method showed significant lacks-of-fit a direct estimation of k_2 from linear regression is used in Eq. (6) for simplicity and increased reliability. When plotted against time (Fig. 2), a clear reduction in k_1 over the exposure period was observed (especially for imipramine and diclofenac). Some random variance was also observed, such as for propranolol, which resulted in a relatively constant

Table 2
Toxicokinetic parameters and standard errors (SE) for 14 organic micropollutants with bioconcentrations factors and lack-of-fit tests for each compound.

Compound	BAF[a]	Simultaneous BCF						Sequential BCF						
		k_1 (L kg^{-1} day^{-1})	SE	k_2 (day^{-1})	SE	p-Value	BCF	k_1 (L kg^{-1} day^{-1})	SE	p-Value	k_2 (day^{-1})	SE	p-Value	BCF
4-Nitrobenzyl chloride	185	666	665.740	4.540	4.540	0.000	147	259	28.324	0.00	1.212	0.149	0.230	214
2,4-Dichloroaniline	56	140	20.073	2.830	0.465	0.000	50	70	4.689	0.03	0.392	0.092	0.868	179
2,4-Dichlorophenol	4466	600	34.196	0.066	0.024	0.000	9050	750	48.646	0.00	0.010	0.018	0.400	72,728
4,6-Dinitro-o-cresol	37	39	2.610	1.146	0.124	0.070	34	37	1.595	1.00	0.729	0.077	0.033	51
1,2,3-Trichlorobenzene	191	1142	403.773	10.648	3.781	0.513	107	167	32.257	0.06	0.475	0.300	0.986	351
2,4,5-Trichlorophenol	2635	941	79.280	0.252	0.064	0.001	3729	1091	109.906	0.21	0.131	0.039	0.001	8327
Aldicarb	2	16	1.421	10.419	0.938	0.000	2	3	0.245	0.00	0.936	0.140	0.003	3
Carbofuran	65	10	0.355	0.146	0.019	0.026	68	10	0.570	0.11	0.140	0.019	0.025	72
Diazinon	82	276	24.271	3.569	0.3264	0.005	77	161	10.418	0.00	1.590	0.287	0.259	101
Ethylacrylate	87	110	12.139	1.594	0.2446	0.000	69	67	5.122	0.00	0.204	0.033	0.000	331
Hexachlorobenzene	2915	553	36.8714	0.221	0.046	0.000	2505	631	56.518	0.00	0.152	0.031	0.637	4160
Imidacloprid	7	2	0.093	0.265	0.038	0.000	7	2	0.117	0.02	0.175	0.022	0.000	13
Malathion	114	86	6.782	0.721	0.113	0.000	120	80	5.059	0.02	0.378	0.072	0.001	212
Sea nine	1732	755	57.821	0.303	0.065	0.000	2491	950	69.141	0.05	0.123	0.020	0.084	7696

[a] Reported from Ashauer et al. (2010).

average k_1 value of 0.58 (±0.23), as would be expected. The simultaneous and sequential models estimated its k_1 value to be 0.54 and 0.62 L kg^{-1} day^{-1}, respectively and therefore showed reasonable agreement. This observation is significant as propranolol showed no lack-of-fit in the uptake curve; therefore, the agreement indicates that a lack-of-fit arises from variable k_1 values over time.

This suggests that a decreasing k_1 trend is the cause of the poor model fits although it is possible that this may also be caused by a changing k_2 value (giving an apparent decrease in k_1) or variable exposure concentrations in the water. However, water was monitored during the course of the experiments to account for any losses (Fig. 2 & Table S1) and the only compound that showed any significant loss was imipramine (>20% nominal concentration). The k_1 and k_2 values should also be independent of pharmaceutical concentrations in the aqueous phase thus the trend observed is not in response to this variable (van Leeuwen & Vermeire, 2007). A change in k_2 is likely to be represented as a decrease over time (unless the compound induces its own metabolism) assuming growth has a negligible effect and therefore would not account for decreases in k_1. The elimination curves also showed no lack-of-fit for 6 compounds and the linear regression showed no trends of changing k_2 values. The trend observed therefore is not in response to the parameters C_w or k_2 and we therefore suggest the variability in uptake (decreasing k_1) trend is the cause of the poor model fit.

3.4. Performance of OECD models using other micro-pollutant studies in *G. pulex*

G. pulex has been shown to metabolise organic compounds with low bioaccumulation factors previously observed (<1500) (Ashauer et al., 2012). As defined by Annex XIII of the REACH criteria, for a compound to be considered bioaccumulative the BCF/BAF should be >2000 (European Commission, 2006). Other work by Ashauer et al. investigated the toxicokinetics of 14 micro-pollutants in *G. pulex* and presented higher BCFs for three polychlorophenols in particular (Ashauer et al., 2010). As discussed by the authors, correlations showed an observable lack-of-fit in some cases. A slightly different model to the OECD 305 model was used in this work, where changes in C_w were accounted for as well as inclusion of an extra statistical algorithm to select the best parameter combinations of k_1 and k_2. However, when applying the OECD 305 models to BAF prediction, it is important to understand whether this is likely to be inaccurate and, amongst other reasons, potentially due to variation in k_1, k_2 or C_w. To determine if any similar trends could be identified in other published *G. pulex* toxicokinetics studies, raw data from Ashauer et al., was re-examined using the OECD 305 modelling approach and presented in Table 2 (Ashauer et al., 2010). Although the authors' experiments were originally designed for determination of bioaccumulation, the report showed this to account for a small percentage of accumulation. Therefore, feeding was not included in any calculations. Similar to our findings for pharmaceuticals, both models displayed a statistically significant lack-of-fit for these organic micro-pollutant compounds. When the sequential method was applied, better fits were obtained for the depuration phase in comparison to the uptake phase. However, despite models used herein not performing as well overall, there was good agreement between the predicted BCF values and those generated by Ashauer et al. The data was then used to plot k_1 versus time (Fig. S2), and again an obvious systematic decrease was observed for 9 out of 14 compounds. Statistical lack-of-fits ($p < 0.05$) were observed in the sequential uptake model especially for 4-nitrobenzylchloride, ethylacrylate, diazinon, aldicarb and hexachlorobenzene ($p < 0.001$). The latter two compounds were notable cases where the spread of replicate k_1 data at each time-point was especially narrow and so the trend in k_1 reduction over time was apparent. Of the remaining five compounds, trends in k_1 were less evident and were coupled with $p > 0.05$ for lack-of-fit for four compounds using the sequential uptake model. The remaining compound, 2,4-dichlorophenol, showed no obvious trends in k_1 variance as the major reason for the observed lack-of-fit in the uptake phase. In summary, k_1 data could be considered reliable for only 5 of 14 compounds using the OECD 305 sequential model. In addition to the data of these 14 different organic pollutants, we also reassessed data from an exposure study of chlorpyrifos across 15 different invertebrate species to assess the issue more broadly (Rubach et al., 2010). Decreases in k_1 were observed in several species and the trend was somewhat similar, albeit with larger scatter of the data (Fig. S3). This also identifies a further limitation that metabolism is likely to affect k_1 and k_2 values thus the differences in k_1 constancy between organisms may be as a result of biotransformation. The study showed considerable differences between species in uptake and elimination rates showing that species type may affect the constancy of k_1 in particular and further studies are required using more compounds between different species to fully assess this possibility. If the assumption of k_1 constancy varies on a compound-by-compound basis, curve fitting methods to predict BCF are likely to be inherently inaccurate for environmental risk assessment purposes for *G. pulex*. Therefore, it is suggested that the approach taken herein (Crookes & Brooke, 2011) could be used to check the reliability of BCF data where a statistical lack-of-fit exists for this species.

Decreasing k_1 could be explained by several possible mechanisms. The first is that growth dilution could cause an apparent decrease in k_1 due to the mass of the organism increasing while the concentration of substance remains the same. However, this situation is unlikely given the short timescales of this work and that of Ashauer et al. (Ashauer et al., 2010). Therefore, growth of *G. pulex* is assumed to be negligible, particularly as this is regulated in line with their moulting cycle. However, further investigation would be required to fully support this. A second possibility is that *G. pulex* have been shown to alter respiration rates in the presence of a poor diet (Graça et al., 1993). As the animals were not fed during these experiments, it is possible that this slowed uptake. However, the toxicokinetic experiments by Ashauer et al. involved feeding organisms over their uptake period suggesting the uptake trend is not in response to diet induced factors (Ashauer et al., 2010). As these compounds are exposed to non-target animals, it is also possible that toxicodynamic effects could affect uptake, which is more easily interpreted using the dataset by Ashauer et al., where the exposure concentration was between 2 and 88 fold below the 24 h LC_{50} value. However for our dataset, mortality was not significantly higher than in controls for pharmaceuticals at the exposure concentrations used. Another consideration is that instantaneous sorption to the animal cuticle could account for the initially high k_1 constants. However, an examination of the decrease in uptake rate against log*D* and log*P* revealed no correlation and compounds displayed independent k_1 decreases (Fig. S4). However, log*D* only governs sorption to a certain extent and other physicochemical properties including polar/topological surface area, ionic state, amongst others, could influence sorption onto the exoskeleton. Where animals shed their exoskeleton during the exposure period, these were collected, weighed wet and radioactivity measured in a brief experiment. It was found that the maximum concentration of five of the eight pharmaceuticals on the exoskeleton material recovered did not exceed 24% of total compound mass in the animal in these cases (Table S3). Therefore, reduction in k_1 via this mechanism is indeed plausible, but extended measurements across more compounds, conditions and replicates are recommended for full characterisation of this process. The potential for sorption as the reason for changes in k_1 is not based on physiology, but rather on the physicochemical properties of the xenobiotic itself, suggesting that rate constant stability may be compound specific.

4. Conclusions

This work demonstrates the importance of data interpretation using multiple modelling methods to estimate BCFs. Specifically, the comparative assessment of model lack-of-fits for both simultaneous and

sequential models (where k_2 remains constant) is recommended to reliably estimate and to ensure the accuracy of xenobiotic risk assessments. A decreasing trend in the uptake rate constant over time was apparent which disrupted the validity of the standard model assumptions tested, and suggests that more complex models are needed to describe accumulation of xenobiotics in invertebrates, more particularly in *G. pulex*. Kinetic BCF/BAF are an estimate of steady-state values, but it is possible that these models are adequate enough to indicate whether a compound may have a potential to accumulate or not. It is now important to identify whether such trends are also observed more generally across different species as well as a fuller investigation into the roles sorption and metabolism have in these standard models.

Acknowledgements

This work was conducted under funding from the Biotechnology and Biological Sciences Research Council (BBSRC) CASE industrial scholarship scheme (Reference BB/K501177/1) and AstraZeneca Global SHE research programme. AstraZeneca is a biopharmaceutical company specialising in the discovery, development, manufacturing and marketing of prescription medicines, including some products measured here. Funding bodies played no role in the design of the study or decision to publish. The authors declare no financial conflict of interest.

Appendix A. Supplementary data

Supplementary data to this article can be found online at http://dx.doi.org/10.1016/j.scitotenv.2015.12.145.

References

European Union water framework directive, Official Journal of the European Communities, OJL226.
Ashauer, R., Escher, B.I., 2010. Advantages of toxicokinetic and toxicodynamic modelling in aquatic ecotoxicology and risk assessment. J. Environ. Monit. 12 (11), 2056–2061.
Ashauer, R., Boxall, A., Brown, C., 2006. Uptake and elimination of chlorpyrifos and pentachlorophenol into the freshwater amphipod *Gammarus pulex*. Arch. Environ. Contam. Toxicol. 51 (4), 542–548.
Ashauer, R., et al., 2010. Bioaccumulation kinetics of organic xenobiotic pollutants in the freshwater invertebrate *Gammarus pulex* modeled with prediction intervals. Environ. Toxicol. Chem. 29 (7), 1625–1636.
Ashauer, R., et al., 2012. Significance of xenobiotic metabolism for bioaccumulation kinetics of organic chemicals in *Gammarus pulex*. Environ. Sci. Technol. 46 (6), 3498–3508.
Browne, J., 2013. 2010 to 2015 Government Policy: Animal Research and Testing. Home Office.
Bueno, M.J.M., et al., 2013. Fast and easy extraction combined with high resolution-mass spectrometry for residue analysis of two anticonvulsants and their transformation products in marine mussels. J. Chromatogr. A 1305, 27–34.
Carter, L.J., et al., 2014. Minimised bioconcentration tests: a useful tool for assessing chemical uptake into terrestrial and aquatic invertebrates? Environ. Sci. Technol. 48 (22), 13497–13503.
Contardo-Jara, V., et al., 2011. Exposure to human pharmaceuticals Carbamazepine, Ibuprofen and Bezafibrate causes molecular effects in *Dreissena polymorpha*. Aquat. Toxicol. 105 (3–4), 428–437.
Crane, M., Watts, C., Boucard, T., 2006. Chronic aquatic environmental risks from exposure to human pharmaceuticals. Sci. Total Environ. 367 (1), 23–41.
Crookes, M.J., Brooke, D.N., 2011. Estimation of Fish Bioconcentration Factor (BCF) From Depuration Data. Environment Agency, Bristol.
De Lange, H.J., et al., 2006. Behavioural responses of *Gammarus pulex* (Crustacea, Amphipoda) to low concentrations of pharmaceuticals. Aquat. Toxicol. 78 (3), 209–216.
Erickson, R.J., et al., 2006. Uptake and elimination of ionizable organic chemicals at fish gills: II. Observed and predicted effects of pH, alkalinity, and chemical properties. Environ. Toxicol. Chem. 25 (6), 1522–1532.
European Commission, 2006. Regulation (EC) No 1907/2006 of the European Parliament and of the Council of 18 December 2006 concerning the Registration, Evaluation, Authorisation and Restriction of Chemicals (REACH), establishing a European Chemicals Agency, amending Directive 1999/45/EC and repealing Council Regulation (EEC) No 793/93 and Commission Regulation (EC) No 1488/94 as well as Council Directive 76/769/EEC and Commission Directives 91/155/EEC, 93/67/EEC, 93/105/EC and 2000/21/EC. Off. J. Eur. Union L396, 1–849.
Fernández, C., Carbonell, G., Babín, M., 2013. Effects of individual and a mixture of pharmaceuticals and personal-care products on cytotoxicity, EROD activity and ROS production in a rainbow trout gonadal cell line (RTG-2). J. Appl. Toxicol. 33 (11), 1203–1212.
Gobas, F.A.P.C., MacKay, D., 1987. Dynamics of hydrophobic organic chemical bioconcentration in fish. Environ. Toxicol. Chem. 6 (7), 495–504.
Graça, M.A.S., Maltby, L., Calow, P., 1993. Importance of fungi in the diet of *Gammarus pulex* and *Asellus aquaticus*. Oecologia 96 (3), 304–309.
Heckmann, L.-H., et al., 2007. Chronic toxicity of ibuprofen to *Daphnia magna*: effects on life history traits and population dynamics. Toxicol. Lett. 172 (3), 137–145.
Hendriks, A.J., Heikens, A., 2001. The power of size. 2. Rate constants and equilibrium ratios for accumulation of inorganic substances related to species weight. Environ. Toxicol. Chem. 20 (7), 1421–1437.
Hilton, M.J., Thomas, K.V., 2003. Determination of selected human pharmaceutical compounds in effluent and surface water samples by high-performance liquid chromatography–electrospray tandem mass spectrometry. J. Chromatogr. A 1015 (1–2), 129–141.
Kell, D.B., Oliver, S.G., 2014. How drugs get into cells: tested and testable predictions to help discriminate between transporter-mediated uptake and lipoidal bilayer diffusion. Front. Pharmacol. 5, 231.
Kenaga, E., 1972. Guidelines for environmental study of pesticides: determination of bioconcentration potential. In: Gunther, F., Gunther, J. (Eds.), Residue Reviews. Springer, New York, pp. 73–113.
Klosterhaus, S.L., et al., 2013. Method validation and reconnaissance of pharmaceuticals, personal care products, and alkylphenols in surface waters, sediments, and mussels in an urban estuary. Environ. Int. 54, 92–99.
Li, W.H., et al., 2012. Investigation of antibiotics in mollusks from coastal waters in the Bohai Sea of China. Environ. Pollut. 162, 56–62.
McEneff, G., et al., 2014. A year-long study of the spatial occurrence and relative distribution of pharmaceutical residues in sewage effluent, receiving marine waters and marine bivalves. Sci. Total Environ. 476, 317–326.
Meador, J.P., et al., 1995. Bioaccumulation of polycyclic aromatic hydrocarbons by marine organisms. In: Ware, G. (Ed.), Reviews of Environmental Contamination and Toxicology. Springer, New York, pp. 79–165.
Meredith-Williams, M., et al., 2012. Uptake and depuration of pharmaceuticals in aquatic invertebrates. Environ. Pollut. 165 (0), 250–258.
Miller, T.H., et al., 2015. Pharmaceuticals in the freshwater invertebrate, *Gammarus pulex*, determined using pulverised liquid extraction, solid phase extraction and liquid chromatography–tandem mass spectrometry. Sci. Total Environ. 511 (0), 153–160.
Norstrom, R.J., McKinnon, A.E., deFreitas, A.S.W., 1976. A bioenergetics-based model for pollutant accumulation by fish. Simulation of PCB and methylmercury residue levels in Ottawa River yellow perch (*Perca flavescens*). J. Fish. Res. Board Can. 33 (2), 248–267.
Nyman, A.-M., Schirmer, K., Ashauer, R., 2014. Importance of toxicokinetics for interspecies variation in sensitivity to chemicals. Environ. Sci. Technol. 48 (10), 5946–5954.
OECD, Test No. 305. Bioaccumulation in Fish: Aqueous and Dietary Exposure: OECD Publishing.
Oliver, B.G., Niimi, A.J., 1983. Bioconcentration of chlorobenzenes from water by rainbow trout: correlations with partition coefficients and environmental residues. Environ. Sci. Technol. 17 (5), 287–291.
Rubach, M.N., et al., 2010. Toxicokinetic variation in 15 freshwater arthropod species exposed to the insecticide chlorpyrifos. Environ. Toxicol. Chem. 29 (10), 2225–2234.
Solé, M., Livingstone, D.R., 2005. Components of the cytochrome P450-dependent monooxygenase system and 'NADPH-independent benzo[a]pyrene hydroxylase' activity in a wide range of marine invertebrate species. Comp. Biochem. Physiol. C Toxicol. Pharmacol. 141 (1), 20–31.
Stott, L.C., et al., 2015. A primary fish gill cell culture model to assess pharmaceutical uptake and efflux: evidence for passive and facilitated transport. Aquat. Toxicol. 159 (0), 127–137.
Straub, J.O., 2002. Environmental risk assessment for new human pharmaceuticals in the European Union according to the draft guideline/discussion paper of January 2001. Toxicol. Lett. 131 (1–2), 137–143.
Sugano, K., et al., 2010. Coexistence of passive and carrier-mediated processes in drug transport. Nat. Rev. Drug Discov. 9 (8), 597–614.
Tao, S., et al., 2001. Simulation of acid–base condition and copper speciation in the fish gill microenvironment. Comput. Chem. 25 (3), 215–222.
Thomas, K.V., Hilton, M.J., 2004. The occurrence of selected human pharmaceutical compounds in UK estuaries. Mar. Pollut. Bull. 49 (5–6), 436–444.
van Leeuwen, C.J., Vermeire, T., 2007. Risk Assessment of Chemicals: An Introduction. Springer Science & Business Media, New York.
Veith, G.D., DeFoe, D.L., Bergstedt, B.V., 1979. Measuring and estimating the bioconcentration factor of chemicals in fish. J. Fish. Res. Board Can. 36 (9), 1040–1048.
Wu, X., et al., 2013. Comparative uptake and translocation of pharmaceutical and personal care products (PPCPs) by common vegetables. Environ. Int. 60 (0), 15–22.

Science of the Total Environment 562 (2016) 777–788

Contents lists available at ScienceDirect

Science of the Total Environment

journal homepage: www.elsevier.com/locate/scitotenv

Targeted metabolomics of *Gammarus pulex* following controlled exposures to selected pharmaceuticals in water

Cristian Gómez-Canela [a,b,*], Thomas H. Miller [b], Nicolas R. Bury [c], Romà Tauler [a], Leon P. Barron [b]

[a] Department of Environmental Chemistry, IDAEA-CSIC, Jordi Girona 18-26, 08034 Barcelona, Catalonia, Spain
[b] Analytical & Environmental Sciences Division, Faculty of Life Sciences and Medicine, King's College London, 150 Stamford Street, London SE1 9NH, UK
[c] Diabetes and Nutritional Sciences, Faculty of Life Sciences and Medicine, King's College London, 150 Stamford Street, London SE1 9NH, UK

HIGHLIGHTS

- Metabolites of *Gammarus pulex* were determined following liquid chromatography coupled high resolution mass spectrometry.
- The toxicity study of 26 pharmaceuticals in *Gammarus pulex* show values between 0.57 mg L^{-1} to >250 mg L^{-1}.
- Variations in the metabolite concentrations were detected in the pharmaceuticals exposed samples respect to control samples.
- Pathway alterations related to protein synthesis, oxidative stress and signaling cascades were observed in exposed samples.

GRAPHICAL ABSTRACT

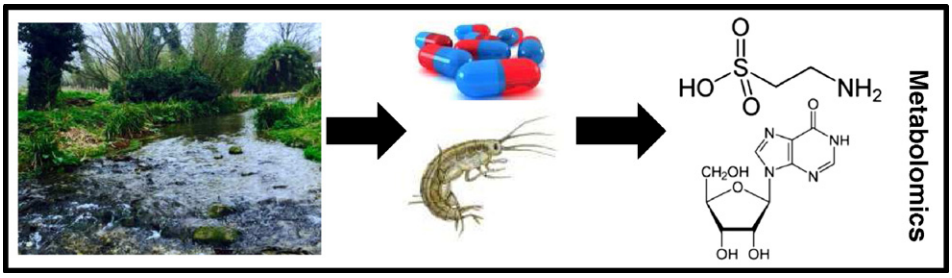

ARTICLE INFO

Article history:
Received 30 October 2015
Received in revised form 24 March 2016
Accepted 24 March 2016
Available online 22 April 2016

Editor: D. Barcelo

Keywords:
Pharmaceuticals
LC-HRMS
Gammarus pulex
Aquatic toxicology
Metabolomics

ABSTRACT

The effects of pharmaceuticals and personal care products (PPCPs) on aquatic organisms represent a significant current concern. Herein, a targeted metabolomics approach using liquid chromatography-high resolution mass spectrometry (LC-HRMS) is presented to characterise concentration changes in 29 selected metabolites following exposures of aquatic invertebrates, *Gammarus pulex*, to pharmaceuticals. Method performance revealed excellent linearity ($R^2 > 0.99$), precision (0.1–19%) and lower instrumental limits of detection (0.002–0.20 ng) for all metabolites studied. Three pharmaceuticals were selected representing the low, middle and high range of measured acute measured toxicities (of a total of 26 compounds). Gammarids were exposed to both the no-observed-adverse-effect-level (NOAEL) and the lowest-observed-adverse-effect-level (LOAEL) of triclosan (0.1 and 0.3 mg L^{-1}), nimesulide (0.5 and 1.4 mg L^{-1}) and propranolol (100 and 153 mg L^{-1}) over 24 h. Quantitative metabolite profiling was then performed. Significant changes in metabolite concentrations relative to controls are presented and display distinct clustered trends for each pharmaceutical. Approximately 37% (triclosan), 33% (nimesulide) and 46% (propranolol) of metabolites showed statistically significant time-related effects. Observed changes are also discussed with respect to internal concentrations of the three pharmaceuticals measured using a method based on pulverised liquid extraction, solid phase extraction and LC-MS/MS. Potential metabolic pathways that may be affected by such exposures are also discussed. This represents the first study focussing on quantitative, targeted metabolomics of this lower trophic level benthic invertebrate that may elucidate biomarkers for future risk assessment.

* Corresponding author at: Department of Environmental Chemistry, IDAEA-CSIC, Jordi Girona 18-26, 08034 Barcelona, Catalonia, Spain.
E-mail address: cristian.gomez@cid.csic.es (C. Gómez-Canela).

http://dx.doi.org/10.1016/j.scitotenv.2016.03.181

1. Introduction

In the last decade, pharmaceuticals have been recognised as an emerging class of environmental contaminants and their fate, occurrence and physicochemical behaviour in the aquatic environment have been extensively studied and reviewed (Daughton and Ternes, 1999; Evgenidou et al., 2015; Monteiro and Boxall, 2010). The ecotoxicological consequences of incomplete removal of pharmaceuticals or their metabolites in wastewater or drinking water treatment plants (WWTP/DWTP) are a matter of current environmental concern which still requires further research (Gómez-Canela et al., 2013). Furthermore, pharmaceuticals designed for hospital use are suspected to have more adverse effects than other pharmaceuticals regarding their effect on the aquatic environment (Gómez-Canela et al., 2014; Franquet-Griell et al., 2015). As such, in the last decade, much research has focused on understanding the occurrence and effects (Heberer, 2002) of these contaminants in exposed organisms. Recently, we developed a multi-residue analytical method and determined occurrence of pharmaceuticals in tributaries of the River Thames and in *Gammarus pulex* (*G. pulex*) at ng L^{-1} and ng g^{-1} concentrations respectively across eight sites (Miller et al., 2015). *G. pulex* is a small, low trophic level species of amphipod crustacean found in freshwaters across Europe and is very common throughout the United Kingdom (UK). *G. pulex* has many attributes for use in biomonitoring studies including its important role in freshwater food chains where they serve as a food source for other invertebrates, fish and birds (Maltby et al., 2002). This organism has also been extensively used in contaminant monitoring including toxicity assays for various pollutants such as metals, pharmaceuticals, PAHs/PCBs and natural stressors which has shown the importance of this species in environmental risk assessment (Bourgeault et al., 2013; Coulaud et al., 2011; De Lange et al., 2006, 2009; Lebrun et al., 2012; Maltby et al., 2002; Pellet et al., 2014; Schaller et al., 2011; Vellinger et al., 2012).

Studies of the effects of pharmaceuticals on low trophic level invertebrate organisms such as *G. pulex* using high resolution confirmatory chemical analysis techniques are lacking. In particular, metabolomics may reduce this knowledge gap by directing effect-based studies that reveal alternative markers or end-points to assess potential toxicity of contaminants. Advances in mass spectrometry (MS) over the last decade have enabled better characterization of the links between the metabolome and phenotype (Dettmer et al., 2007; Villas-Bôas et al., 2005). Targeted liquid chromatography coupled to mass spectrometry (LC-MS) is the technique of choice for the reliable quantitation of known, pre-selected metabolites. It is an approach that will increasingly be used to apply knowledge discovered by non-targeted metabolomics; i.e. the eventual targeted measurement of a metabolic biomarker signature that can predict exposure to a specific environmental stress (Viant, 2008; Viant and Sommer, 2013). Metabolomics studies have made use of high resolution, confirmatory analytical techniques such as nuclear magnetic resonance (NMR) or hyphenated MS technologies to characterise large numbers of compounds for metabolic profiling (targeted) (Zhang et al., 2012). With the development of high resolution mass spectrometry (HRMS), non-targeted screening of several thousand compounds has become possible for studying larger portions of the metabolome in contrast to NMR, which is often limited by low sensitivity (Dunn et al., 2005; Zhang et al., 2012). Early investigations focused on human, plant and microbial metabolomes (Frisvad and Filtenborg, 1983; Horning and Horning, 1971; Taylor et al., 2002; Tweeddale et al., 1998). Other studies have identified changes in metabolomic profiles in mussels resulting from hypoxic conditions; biomarkers associated with withering syndrome in abalone sea snails; and responses to ethinylestradiol (EE2) by rainbow trout (Hines et al., 2007; Samuelsson et al., 2006; Viant et al., 2003). Approaches to characterise the metabolome can involve non-targeted or targeted strategies where for quantitative purposes, targeted analysis offers greater accuracy and precision (Griffiths et al., 2010; Lei et al., 2011).

The aim of the present study was to develop a targeted multi-residue method for the determination of 29 metabolites pertaining to different biochemical classes (amino acids, organic acids, nucleosides, nucleotides, and sugars) using LC-HRMS. As a full scan method also suitable for non-target analysis, the analytical performance of the method was evaluated quantitatively in terms of comprehensive mass spectral characterization, selectivity, sensitivity, intra- and inter-day precision, range and linearity. Acute toxicity of 26 pharmaceuticals in *G. pulex* was also assessed as an initial screen for compound selection for metabolomics. Three pharmaceuticals showing low, median and high measured LC_{50} values were then selected for exposures at no-observed-adverse-effect-level (NOAEL) and lowest-observed-adverse-effect-level (LOAEL) concentrations to evaluate alterations in the metabolite profile at 2, 6 and 24 h. This represents the first environmental metabolomics-based investigation of *G. pulex* by determining changes in endogenous metabolites in response to pharmaceutical residue exposure.

2. Materials and methods

2.1. Reagents, chemicals and consumables

All pharmaceuticals were purchased from Sigma-Aldrich (Steinheim, Germany) and Fluka (Buchs, Switzerland) with a purity of ≥97%. HPLC grade acetone, dimethylsulfoxide (DMSO), ethanol (EtOH) and methanol (MeOH) were purchased from Fischer Scientific (Loughborough, UK). Ultra-pure water was sourced from a Millipore Milli-Q water purification system with a specific resistance of 18.2 MΩ cm or greater (Millipore, Bedford, MA, USA). Stock solutions (40 mg mL^{-1}) were prepared in ultrapure water, acetone, MeOH, EtOH or DMSO, respectively. All stock solutions were stored in silanised amber vials (40 mL) and at −20 °C in the dark for optimum stability. Organic solvent concentration (acetone, MeOH, EtOH and DMSO) in aqueous solutions used for toxicity testing was negligible. Metabolite standards (organic acids, nucleosides, nucleotides, sugars and amino acids) were supplied by Sigma Aldrich (Steinheim, Germany) and Fluka (Buchs, Switzerland). In addition, the isotopically-labelled algal amino acid mixture (98 atom% as ^{13}C, 98 atom% as ^{15}N) was provided from Sigma Aldrich. The targeted metabolome studied was comprised of 15 amino acids (AAs), 4 nucleosides, 2 nucleotides, 1 sugar, 3 organic acids and 4 compounds related to other families. Full details of the target metabolites and the labelled compounds are shown in Table 1. Finally, the 26 pharmaceutical compounds belonging to 12 different therapeutic classes are listed in Table S1.

2.2. Sample collection and preparation

Adult *G. pulex* were collected several times between September 2014 and April 2015 from the River Cray, UK, a tributary of the River Darent that feeds into the River Thames (51°23′10.5″N 0°06′34.8″E). Adult specimens were collected via the kick sampling netting method. Samples were transported back to the laboratory in Nalgene™ flasks containing a 500 mL grab sample of freshwater obtained from the River Cray. This site has previously been demonstrated to have low pharmaceutical contamination (<LOQ) (Miller et al., 2015). After collection, *G. pulex* were stored in different artificial freshwater tanks and acclimatized for a minimum of 2–3 days at 15 ± 2 °C under a 12 h:12 h light:dark cycle to allow depuration of any residual contamination. The freshwater crustaceans were fed ad libitum with a minimum of three horse-chestnut leaf discs (Ashauer et al., 2011). Artificial freshwater (AFW) was prepared following United States Environmental Protection Agency (USEPA) regulation (USEPA, 2002). Briefly, 1.20 g $MgSO_4$, 1.92 g $NaHCO_3$ and 0.080 g KCl were added to 19 L of ultra-pure water that was aerated overnight. In parallel, 1.20 g of $CaSO_4 \cdot 2H_2O$ was added to 1 L of Milli-Q water and mixed with the previous salt solution

Table 1
Target analytes for metabolic profiling. Kegg number, molecular formula, molecular weight (Mw) and mass spectral characterization (ordered by metabolic group) by LC-HRMS. Instrumental method performance. F: slope; R^2: regression coefficient; IDL: instrumental detection limit; RSD: relative standard deviation; MDL: method detection limit.

Target compounds	KEGG number	Formula	Mw	Exact mass	$[M-H]^-$	Linearity (ng μL^{-1})	Calibration type	F	R^2	IDL (ng)	Intra-day precision (5 ng μL^{-1})	Inter-day precision (5 ng μL^{-1})	% Recovery ± RSD, $n = 3$	MDL (ng g^{-1})
L-2-Amino-*n*-butyric acid (AABA)	C00334	$C_4H_9NO_2$	103.06	103.0633	102.0560	0.05–15	External	1e6	0.993	0.06	9	2	107 ± 14	13.9
L-Alanine	C00041	$C_3H_7NO_2$	89.05	89.0477	88.0404	0.05–15	External	1e6	0.998	0.03	8	8	92 ± 9	0.99
L-Aspartic acid	C00049	$C_4H_7NO_4$	133.04	133.0375	132.0302	0.05–15	External	4e5	0.995	0.20	4	14	87 ± 11	22.7
L-Citrulline	C00327	$C_6H_{13}N_3O_3$	175.09	175.0957	174.0884	0.1–15	External	1e6	0.999	0.15	2	6	87 ± 1	23.9
L-Isoleucine	C00407	$C_6H_{13}NO_2$	131.09	131.0946	130.0873	0.1–15	Internal	4.5	0.998	0.03	12	6	42 ± 8	0.28
L-Leucine	C00123	$C_6H_{13}NO_2$	131.09	131.0946	130.0873	0.1–15	Internal	1.6	0.994	0.02	13	9	99 ± 1	0.47
L-Methionine	C00073	$C_5H_{11}NO_2S$	149.05	149.0510	148.0437	0.05–15	Internal	21	0.997	0.02	5	6	67 ± 14	2.66
L-Ornithine hydrochloride	C00077	$C_5H_{12}N_2O_2$	132.10	132.0899	131.0826	0.05–15	Internal	0.83	0.994	0.01	4	8	109 ± 6	3.51
L-Phenylalanine	C00079	$C_9H_{11}NO_2$	165.08	165.0790	164.0717	0.1–15	Internal	1.6	0.996	0.02	14	14	97 ± 4	0.42
L-(−)-Proline	C00148	$C_5H_9NO_2$	115.06	115.0633	114.0560	0.05–15	Internal	1.2	0.997	0.01	5	11	87 ± 8	1.13
L-Serine	C00065	$C_3H_7NO_3$	105.04	105.0426	104.0353	0.05–15	Internal	1.1	0.996	0.01	13	13	88 ± 14	9.50
L-Threonine	C00188	$C_4H_9NO_3$	119.05	119.0582	118.0509	0.1–15	Internal	2.0	0.999	0.2	13	7	103 ± 11	3.59
L-Tryptophan	C00078	$C_{11}H_{12}N_2O_2$	204.09	204.0899	203.0826	0.1–15	External	7e6	0.998	0.02	8	6	102 ± 5	1.35
L-Tyrosine	C00082	$C_9H_{11}NO_3$	181.07	181.0739	180.0666	0.1–15	External	2.1	0.996	0.03	7	12	80 ± 8	0.35
L-Valine	C00183	$C_5H_{11}NO_2$	117.08	117.0790	116.0717	0.05–15	Internal	1.3	0.991	0.05	12	13	91 ± 6	0.80
Cytidine	C00475	$C_9H_{13}N_3O_5$	243.08	243.0855	242.0777	0.05–15	External	3e6	0.999	0.01	8	1	110 ± 9	1.94
Inosine	C00294	$C_{10}H_{12}N_4O_5$	268.09	268.0808	267.0734	0.01–15	Internal	1.01	0.995	0.002	1	14	108 ± 8	0.04
Thymidine	C00214	$C_{10}H_{14}N_2O_5$	242.20	242.0903	241.0829	0.05–15	Internal	0.7	0.991	0.01	7	5	99 ± 7	0.50
Uridine	C00299	$C_9H_{12}N_2O_6$	244.07	244.0695	243.0622	0.05–15	External	2e6	0.997	0.03	7	5	138 ± 2	0.33
ADP	C00008	$C_{10}H_{15}N_5O_{10}P_2$	427.03	427.0294	426.0221	3–15	External	7e5	0.993	0.15	9	11	25 ± 11	162
NADH	C00004	$C_{21}H_{27}N_7O_{14}P_2$	663.07	663.1091	662.1018	0.1–15	External	1e6	0.990	0.06	2	19	162 ± 10	7.80
Trehalose	C01083	$C_{12}H_{22}O_{11}$	342.12	342.1162	341.1089	0.05–15	External	2e6	0.996	0.01	10	0.2	81 ± 7	1.03
Creatine	C00300	$C_4H_9N_3O_2$	131.07	131.0695	130.0622	0.1–15	External	3e5	0.991	0.11	3	0.5	107 ± 2	37.3
Phthalic acid	C01606	$C_8H_6O_4$	166.14	166.0266	165.0193	0.1–15	External	1e6	0.997	0.01	6	7	102 ± 2	13.6
Taurine	C00245	$C_2H_7NO_3S$	125.01	125.0147	124.0073	0.05–15	Internal	2.03	0.992	0.03	8	14	92 ± 20	0.23
1,7-Dimethylxanthine	C13747	$C_7H_8N_4O_2$	180.20	180.0647	179.0574	0.05–15	Internal	1.19	0.997	0.01	10	13	72 ± 4	2.33
Hypoxanthine	C00262	$C_5H_4N_4O$	136.04	136.0385	135.0312	0.01–15	External	8e6	0.991	0.004	4	9	102 ± 7	0.47
Pyridoxine	C00314	$C_8H_{11}NO_3$	169.20	169.0739	168.0666	0.05–15	External	3e6	0.94	0.07	6	0.1	105 ± 10	21.6
(−)-Riboflavin	C00255	$C_{17}H_{20}N_4O_6$	376.37	376.1383	375.1310	0.1–15	Internal	0.9	0.996	0.04	12	9	89 ± 7	6.50
$^{13}C,^{15}N$-Isoleucine[a]	–	$C_6H_{13}NO_2$	138.12	138.1115	137.1041	–	–	–	–	–	–	–	–	–
$^{13}C,^{15}N$-Leucine[a]	–	$C_6H_{13}NO_2$	138.12	138.1115	137.1041	–	–	–	–	–	–	–	–	–
$^{13}C,^{15}N$-Methionine[a]	–	$C_5H_{11}NO_2S$	155.17	155.0646	154.0573	–	–	–	–	–	–	–	–	–
$^{13}C,^{15}N$-Phenylalanine[a]	–	$C_9H_{11}NO_2$	175.12	175.1057	174.0984	–	–	–	–	–	–	–	–	–
$^{13}C,^{15}N$-Proline[a]	–	$C_5H_9NO_2$	121.09	121.0769	120.0695	–	–	–	–	–	–	–	–	–
$^{13}C,^{15}N$-Serine[a]	–	$C_3H_7NO_3$	109.08	109.0495	108.0422	–	–	–	–	–	–	–	–	–
$^{13}C,^{15}N$-Threonine[a]	–	$C_4H_9NO_3$	124.08	124.0685	123.0611	–	–	–	–	–	–	–	–	–
$^{13}C,^{15}N$-Valine[a]	–	$C_5H_{11}NO_2$	123.10	123.0925	122.0852	–	–	–	–	–	–	–	–	–

[a] Internal standards used to quantify (Algal AA mixture).

to make a total 20 L of AFW (USEPA, United States Environmental Protection Agency USEPA, 2002).

2.3. Pharmaceutical exposures

To select specific pharmaceuticals, the concentrations for exposures and subsequent metabolite profiling, a series of acute toxicity tests to 26 pharmaceuticals were initially performed following the Organization for Economic Co-operation and Development (OECD) 1488/94 guideline (European Communities Commission, 1996). Lethal median concentration effects and its 95% confidence interval (CI), were estimated by fitting immobility concentration responses to the Hill regression model (Eq. 1).

$$I(C_i) = \frac{1}{1 + \left(\frac{C_i}{LC_{50}}\right)^{-Hill}} \quad (1)$$

Where, $I(C_i)$ is the proportion of immobile animals at concentration C_i; C_i is the concentration of the respective compound (i); LC_{50} is the median lethal concentration to the 50% of population and *Hill* is the shape constant, which depends on the parameters adjusted in the regression model. From these toxicity profiles the NOAEL and the LOAEL were determined. Exposure experiments were performed in Pyrex® beakers, each containing 200 mL of AFW at 15 °C and ten adult animals (>5 mg wet weight, ww). Live/dead animals were counted after 24 h by gently prodding and observing movement of appendages. The pharmaceutical concentrations tested were in the range of 0.01 to 250 mg L^{-1}. Control (AFW only) and solvent controls showed no measurable toxicity. Concentrations where 100, 50 and 0% of the animals died were repeated in duplicate or triplicate.

From the initial toxicity tests on 26 pharmaceuticals, 3 were chosen for metabolomics studies representing the high (triclosan), medium (nimesulide) and low (propranolol) range of measured acute toxicity. Each exposure consisted of *G. pulex* exposed at the NOAEL (C_1) and a second higher concentration at the LOAEL (C_2) as follows: triclosan, C_1 = 0.1 mg L^{-1}/C_2 = 0.3 mg L^{-1}; nimesulide, C_1 = 0.5 mg L^{-1}/C_2 = 1.4 mg L^{-1}; and propranolol, C_1 = 100 mg L^{-1}/C_2 = 153 mg L^{-1}. Approximately 100 specimens were introduced in a tank containing 1 L of AFW (control), 1 L of AFW spiked with C_1 and 1 L of AFW with C_2. At three different times (2, 6 and 24 h), 4 replicates of live *G. pulex* (a pool of 6–7 animals for each replicate) were collected, frozen on dry ice and then stored at −80 °C before metabolite profiling was performed. A preliminary extraction protocol with 1, 3, 6 and 10 animals showed that a pool of 6–7 *G. pulex* provided the best method recoveries.

Quantification of pharmaceutical concentrations in *G. pulex* at the 24 h exposure interval was performed. Separate exposures were set up in triplicate in beakers containing 200 mL of exposure solution (AFW spiked with the respective C_1 pharmaceutical dose) and 20 organisms. At 24 h, animals were immediately rinsed with ultra-pure water and then frozen at −20 °C for 24 h. Full analytical method details are described in Miller et al., 2015. Prior to extraction, frozen *G. pulex* samples were lyophilised at −50 °C under vacuum for 48 h and milled in an agate mortar to a fine powder. For each analysis, 20 mg of a lyophilised composite sample were transferred to 2 mL polypropylene tubes (Eppendorf®, Hamburg, Germany), for solid-liquid extraction (SLE). After the addition of 80 μL of stable isotope-labelled internal standards at concentrations between 3.29 and 43.11 ng μL^{-1} (final concentration dependent on the AA concentration in the stock reference material mixture), 800 μL of MeOH:HPLC water (90:10) mixture was added and the samples were thoroughly mixed using a Vortex mixer. Then, samples were shaken for 25 min on a vibration plate (IKA® KS 260 basic) and centrifuged at 14,000 rpm for 25 min at 0 °C. Finally, the supernatant was transferred to a chromatographic vial by using a 0.20 μM syringe filter (Whatman, GE Healthcare Life Sciences, Buckinghamshire, UK). All samples were stored at −80 °C until LC-HRMS analysis.

2.4. Internal pharmaceutical residue determination and metabolite profiling

Internal concentrations of pharmaceuticals in *G. pulex* were determined using a previously described method (Miller et al., 2015). Briefly, 50 mg of lyophilised *G. pulex* were extracted in 5 mL of acetonitrile and pre-concentrated on Oasis HLB SPE cartridges (6 mL, 200 mg sorbent). The extract was eluted, dried-down and reconstituted in starting LC mobile phase. The chromatographic separation followed a 75 min gradient (including 12.5 min re-equilibration) using water and acetonitrile with 10 mM ammonium acetate salt. Separation was achieved using a Waters Sunfire C_{18} reversed-phase column (2.1 × 150 mm, 2.5 μM particle size) and detection was performed by a Waters Quattro triple quadrupole mass analyser using positive and negative electrospray ionization polarity switching (Waters Corporation, Milford, MA, USA). Organic acids, nucleosides, nucleotides, sugars and AAs were measured using LC–HRMS. An Exactive™ mass spectrometer equipped with heated electrospray ionization (H-ESI) source was used (Thermo Fisher Scientific, Bremen, Germany). The system was equipped with a HTC PAL autosampler and a Surveyor MS Plus pump. A TSK Gel-Amide 80 column (2 × 250 mm, 5 μm) for analyte separation was purchased from Sigma Aldrich. Mobile phases were binary mixtures of acetonitrile (A) and 5 mM ammonium acetate (pH 5) in HPLC-grade water (B). Gradient elution started at 75% A and 25% B, which was increased linearly to 30% B in 8 min, increased linearly to 60% B to 12 min and then held for a further 5 min. Initial conditions were returned in 3 min and the system was stabilized after a total equilibration time of 10 min (total run time = 30 min). The flow rate was set at 150 μL min^{-1} and the injection volume was 5 μL. Metabolites were analysed under positive/negative ESI mode, but better resolution was obtained in negative ionization mode and so this was used for all experiments. Full scan acquisition over a mass range of 80–800 Da was performed at 70,000 full width at half maximum (FWHM) and spray voltage at 3.00 kV, capillary voltage at 30 V, skimmer voltage at 28 V and tube lens voltage at 130 V were used. A sheath gas flow rate of 45 arbitrary units (au), an auxiliary gas flow rate of 10 au and a capillary temperature at 300 °C were selected.

2.5. Method performance and quantification

Method performance for internal pharmaceutical residue concentrations in *G. pulex* are described elsewhere (Miller et al., 2015). Here, pharmaceutical residue quantification in exposed *G. pulex* was performed by a 3-point matrix-matched calibration curve. For nimesulide, spiking concentrations were 2.5, 5 and 10 μg g^{-1}; for triclosan, these were 1, 2.5 and 5 μg g^{-1}; and for propranolol these were 1, 2.5 and 5 mg g^{-1}. The calibration range for endogenous metabolites was from 0.01 to 15 ng μL^{-1}, using 9 calibration points. The algal amino acid mixture-^{13}C,^{15}N (see Table 1) was used as internal standard (IS) for extraction and analytical control. L-ornithine hydrochloride, inosine, thymidine, taurine, 1.7-dimethylxanthine and (−)-riboflavin were quantified using either ^{13}C,^{15}N-proline or ^{13}C,^{15}N-tyrosine as the internal standard. The remaining 15 compounds were quantified using external calibration and the target compound itself was used as external standard. The instrumental detection limit (IDL) was initially calculated as that concentration giving a signal intensity of 1×10^3, and afterwards measured experimentally by injecting a standard concentration that gave this signal intensity. The method detection limit (MDL) was calculated following the same procedure, using spiked lyophilised *G. pulex* samples at a concentration of 1 μg g^{-1}. Intra-assay variation was assessed using five consecutive injections of 5 ng μL^{-1} standard solution, and inter-assay variation was determined by measuring the same standard solution on four different days. Solvent blanks did not contain

any of the investigated analytes, indicating no carry-over between LC-HRMS runs. Recovery studies were performed in triplicate, using lyophilised *G. pulex* samples spiked at 1 μg g^{-1} with the metabolites mixture and the algal amino acid mixture-^{13}C, ^{15}N. Five replicates of a pool with 6–7 *G. pulex* were analysed first and the traces of target compounds were subtracted.

2.6. Statistical analysis

Two-way ANOVA considering significant *p* values ≤ 0.05 was used as a first step to select metabolites with significant changes and to further explore their concentration and time trends. Thus, *p* values were derived and examined to determine any differences between exposed and control specimens, and to evaluate the effect of the exposure time. All data satisfied the assumptions of normality and homoscedasticity. In addition, all calculations were performed in MATLAB software version R2013b.

3. Results and discussion

3.1. Analytical method performance

Good correlation coefficients ($R^2 \geq 0.99$) were obtained for 29 metabolites (Table 1). Responses for fifteen metabolites were linear from 0.05 to 15 ng μL^{-1}; and for 11 other metabolites, linearity ranged from 0.1 to 15 ng μL^{-1}. Signals for inosine and hypoxanthine were linear over the range of 0.01 to 15 ng μL^{-1}; and ADP in the range 3 to 15 ng μL^{-1}. Therefore, given that this represents a lower concentration range of 10 to 1500 ng g^{-1}, these were considered fit for purpose for this study. IDL ranged from 0.002 to 0.20 ng, and intra and inter-day precision ranges were from 1 to 14% and from 0.1 to 19%, respectively at the 5 ng μL^{-1} concentration level. Twenty seven compounds showed recoveries within the range of 42 ± 8% to 138 ± 2% (Table 1). Overall, recoveries were acceptable and showed excellent precision. However, the two nucleotides ADP and NADH displayed poorer recoveries of 25 ± 11% and 162 ± 10%, respectively. Finally, the MDL ranged from 0.04 (inosine) to 37.3 ng g^{-1} (creatine), with the exception of ADP, for which sensitivity was low as would be expected due to the lower recovery observed (MDL: 162 ng g^{-1}). The extracted ion chromatograms of a target metabolite mixed solution at 5 ng μL^{-1} using the TSK Gel-Amide 80 HILIC column is shown in Fig. 1. In summary, the method performance of this analytical method indicated that reliable quantitative measurements could be made for most metabolites and with minimal variance contribution from the matrix. Moreover, as this method incorporated HRMS in full-scan mode, *post hoc* untargeted data analysis of the metabolome remains possible if required.

3.2. Acute toxicity, 24-h pharmaceutical exposures and observed changes in target metabolite concentrations

Acute toxicity tests revealed LC_{50} at the mg L^{-1} level for most of the 26 tested pharmaceuticals. Similar values have been obtained in other freshwater crustaceans (see Table S3). Kim et al. (2009) studied the acute toxicity of pharmaceuticals and personal care products in the freshwater crustacean, *Thamnocephalus platyurus (T. platyurus)*. They reported a similar LC_{50} value to the present study for triclosan (0.57 mg L^{-1}), but not for propranolol which lay at 10.31 mg L^{-1} (Kim et al., 2009). These values provide a means of ranking the toxic risk, but such values are not environmentally relevant as pharmaceuticals are generally found at concentrations approximately one to two orders of magnitude less (Miller et al., 2015). Therefore, it is unlikely that the majority of these compounds will display any significant acute toxicity. Nonetheless, as a starting point and based on these data, exposures were performed at NOAEL and LOAEL concentrations for triclosan, nimesulide and propranolol to represent compounds at the high, median and low range of measured LC_{50} (Figs. S1–S3).

3.2.1. Triclosan

Triclosan, the most toxic of the selected pharmaceuticals (LC_{50} 0.57 mg L^{-1}) measured here, caused changes in the metabolite concentrations in *G. pulex* at 0.1 mg L^{-1} (C_1) and 0.3 mg L^{-1} (C_2), and was dose responsive. Exposure to triclosan produced significant changes (Two-way ANOVA, $p < 0.05$) in 19 metabolites: 13 amino acids (L-alanine, cytidine, L-citrulline, L-isoleucine, L-leucine, L-methionine, L-phenylalanine, L-proline, taurine, L-threonine, L-tryptophan, L-tyrosine and L-valine), inosine and uridine (nucleosides) and others like trehalose, hypoxanthine, riboflavin and thymidine (Table 2 and Figure S4). However, only the concentration of 37% of metabolites changed significantly (up or down) across the exposure time. L-isoleucine, L-phenylalanine, L-(−)-proline, taurine, L-threonine, L-tyrosine, L-valine, inosine and thymidine concentrations varied significantly ($p < 0.05$) with exposure duration (Table 2). A 2-way ANOVA was used to evaluate the interaction between dose and time factors. Cytidine, L-methionine, L-phenylalanine and L-(−)-proline were the only metabolites that had significant interactions (Table 2). As shown in Figure S4, all metabolites except L-citrulline changed in their mean concentrations at C_1 relative to the controls. Some metabolites increased more than two to three-fold in comparison to controls such as L-tryptophan, hypoxanthine, L-alanine, L-isoleucine, L-threonine, L-valine and L-thymidine. In other cases, measured concentrations between the exposed and control samples decreased over time (ADP and L-proline). Similar trends occurred at C_2 where the 75% of the metabolites increased in their concentration, with the remaining metabolites showing no significant changes (also see Table S1). Table S2 shows the metabolite concentrations determined from all conditions studied. To more conveniently highlight trends, Fig. 2 represents the fold change values at each exposure concentration with respect to controls and plotted in a heat map and hierarchical analysis revealed two distinct clusters (A & B). In general, and for each metabolite in Cluster A of Fig. 2, the fold changes in gammarid metabolites exposed at C_1 decreased across the 24-h period. On the contrary, Cluster B generally showed the opposite trend where concentrations of metabolites mostly increased. In the case of samples exposed at C_2, eight metabolites of Cluster A (L-aspartic acid, L-leucine, L-valine, L-methionine, inosine, taurine, L-tyrosine and thymidine) had a fold increase and the remainder showed a slight decrease in concentration. The metabolites of Cluster B also showed fold decreases along the 24-h period and the opposite effect to those exposed at C_1.

3.2.2. Nimesulide

Exposure to nimesulide produced significant changes (Two-way ANOVA, $P < 0.05$) for 83% of the metabolites analysed, including most amino acids (except L-alanine), such as inosine, uridine and other metabolites including hypoxanthine, riboflavin and thymidine (Table 2 and Fig. S5). L-2-amino-*n*-butyric (AABA), L-alanine, L-aspartic acid, cytidine, L-citrulline, L-leucine, L-(−)-proline, L-serine, trehalose and thymidine showed a time-related effect (Table 2), affecting 42% of the metabolites studied. On the other hand, considering the interaction between time and dose factor, significant differences ($p < 0.05$) in all metabolites except for L-tyrosine and NADH were detected (Table 2). Nimesulide exposures induced changes in the metabolome of *G. pulex* in comparison to controls (Fig. S5). A heat map of nimesulide was prepared as before and hierarchical analysis again revealed two clusters (Fig. 3). In this case, at C_1, all the metabolites except trehalose had fold increases along the 24-h period (Cluster A, Fig. 3). Specifically, L-alanine, (−)-riboflavin, cytidine, hypoxanthine, L-tryptophan, inosine, taurine, L-tyrosine and NADH suffered the more important changes (garnet colour). On the other hand, trehalose (Cluster B, Fig. 3) showed the opposite trend and, at 24-h exposure time, the fold change had decreased (blue). In the samples exposed at C_2, the metabolites in Cluster A began with positive fold changes (red/orange) at 2-h exposure time and decreased (blue) at 24-h exposure time, with the exception of NADH, ADP and trehalose (Cluster B, Fig. 3).

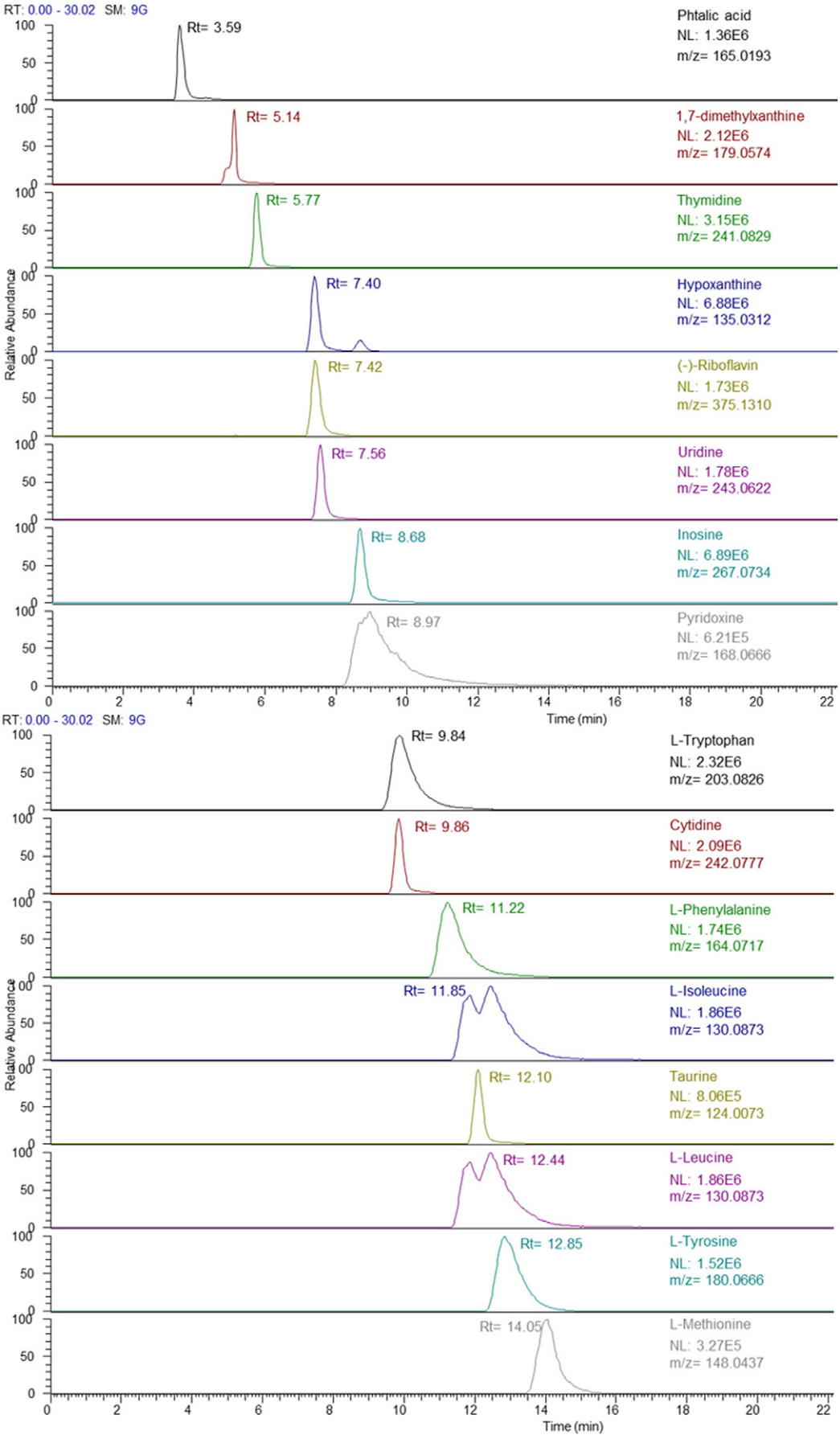

Fig. 1. LC–HRMS extracted ion chromatogram of 29 target compounds from a full scan LC-Orbitrap-MS spectrum using a 5 ppm extraction window.

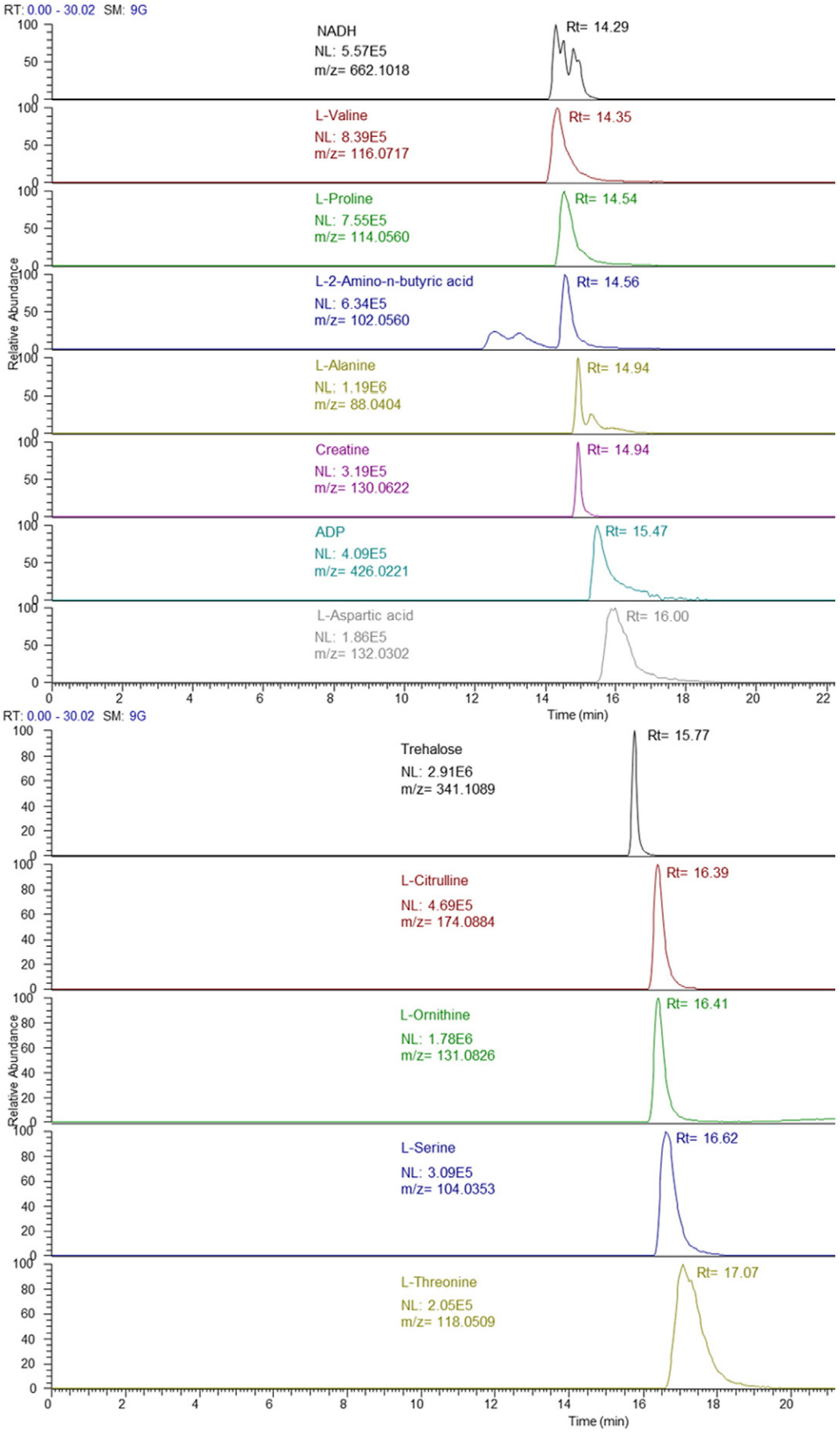

Fig. 1 (*continued*).

Table 2
Two-way ANOVA indicating *p* values for changes in metabolite concentrations based on time and dose factor. The significant changes are in bold where $p < 0.05$.

Metabolite	*p*-Value								
	Triclosan			Nimesulide			Propanolol		
	Dose factor[a]	Time factor[b]	Interaction dose × time	Dose factor[a]	Time factor[b]	Interaction Dose × Time	Dose factor[a]	Time factor[b]	Interaction dose × time
AABA	0.49	0.23	0.91	–	**3e−4**	**0.003**	–	0.24	0.32
L-Alanine	–	0.19	0.15	0.53	–	**6e−4**	–	**0.001**	**0.03**
L-Aspartic acid	0.17	0.37	0.25	**2e−4**	**0.005**	**0.004**	0.28	**0.04**	0.44
Cytidine	**0.001**	0.08	**0.02**	–	**0.02**	–	**5e−6**	**1e−5**	**1e−6**
L-Citrulline	**0.01**	0.81	0.95	**4e−6**	**2e−5**	**8e−6**	0.53	0.29	0.07
L-Isoleucine	–	**9e−4**	0.12	–	0.29	–	0.06	**3e−4**	**0.003**
L-Leucine	**0.01**	0.47	0.73	–	**0.003**	–	0.25	–	–
L-Methionine	–	0.18	**0.003**	–	0.15	**1e−4**	**0.003**	**0.005**	**0.007**
L-Ornithine hydrochloride	Not detected in *Gammarus pulex* organism								
L-Phenylalanine	–	**0.001**	**0.001**	–	0.53	**0.0001**	0.69	–	**0.001**
L-(−)-Proline	–	**0.001**	**0.01**	**4e−7**	**6e−13**	**8e−9**	–	–	**2e−4**
L-Serine	0.21	0.05	0.23	**0.04**	**0.02**	**0.03**	–	0.73	**0.01**
Taurine	–	**0.002**	0.10	–	0.58	**0.002**	**0.03**	0.05	0.75
L-Threonine	–	**0.03**	0.07	–	0.07	**0.001**	0.34	–	**0.001**
L-Tryptophan	–	0.28	0.53	–	0.08	–	**0.0012**	–	–
L-Tyrosine	–	**0.01**	0.40	**0.003**	0.97	0.12	0.70	**0.01**	0.27
L-Valine	–	**0.01**	0.05	–	0.42	–	**5e−4**	**2e−4**	–
Inosine	–	**0.01**	0.11	–	0.17	**0.03**	0.12	**0.002**	0.27
Uridine	**8e−4**	0.45	0.26	–	0.98	–	**0.002**	**6e−4**	**0.009**
ADP	0.21	0.25	0.74	**0.04**	0.14	**0.01**	**0.02**	0.87	0.64
NADH	0.05	0.41	0.31	0.49	0.72	0.12	0.52	0.58	0.83
Trehalose	**0.03**	0.11	0.08	0.07	–	–	0.21	–	–
Creatine	Not detected in *Gammarus pulex* organism								
1,7-dimethylxanthine	Not detected in *Gammarus pulex* organism								
Hypoxanthine	–	0.08	0.07	–	0.14	–	**1e−6**	**4e−5**	**8e−7**
Phtalic acid	Not detected in *Gammarus pulex* organism								
Pyridoxine (vitamin B6)	Not detected in *Gammarus pulex* organism								
(−)-Riboflavin	**0.01**	0.49	0.36	–	0.46	**0.002**	**3e−4**	0.69	**0.008**
Thymidine	–	**0.01**	0.12	–	**7e−4**	–	**4e−4**	**0.009**	**2e−4**

[a] Dose factor corresponds at the two different concentrations used for each pharmaceutical.
[b] Time factor corresponds at the different times studied (2, 6 and 24 h).

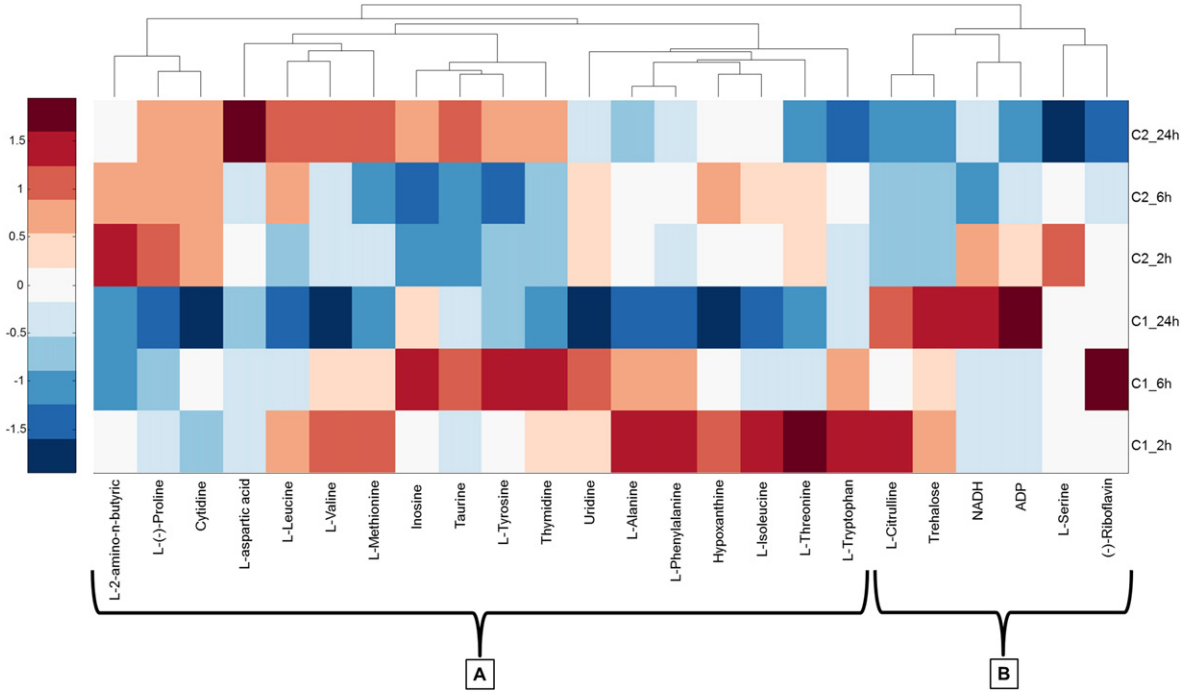

Fig. 2. Heat map of triclosan exposure representing the fold change of targeted metabolites in each exposure subgroup (C_1, C_2) relative to controls. All data have been auto scaled by column and dendrograms represent hierarchical analysis for clustering (A & B) of metabolite responses.

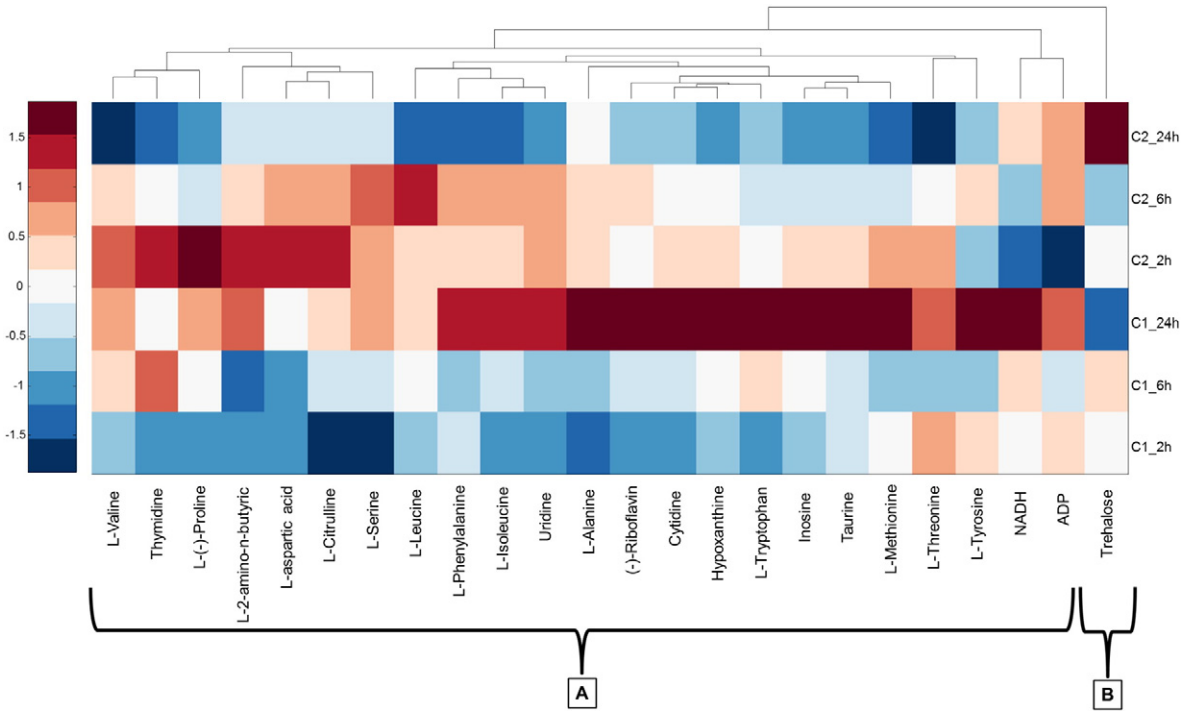

Fig. 3. Heat map of nimesulide exposure representing the fold change of targeted metabolites in each exposure subgroup (C_1, C_2) relative to controls. All data have been auto scaled by column and dendrograms represent hierarchical analysis for clustering (A & B) of metabolite responses.

3.2.3. Propranolol

Exposure to propranolol produced significant changes (based on two-way ANOVA, $p < 0.05$ analysis) in 8 out of 15 AAs (AABA, cytidine, L-methionine, L-proline, L-serine, taurine, L-tryptophan and L-valine), uridine (nucleoside), ADP (nucleotide) and others like hypoxanthine, riboflavin and thymidine (Table 2 and Fig. S6). Moreover, the exposure time affected 71% of the metabolites studied. L-alanine, L-aspartic acid, cytidine, L-isoleucine, L-leucine, L-methionine, L-phenylalanine, L-(−)-proline, L-threonine, L-tryptophan, L-tyrosine, L-valine, inosine, uridine, trehalose, hypoxanthine and thymidine displayed significant changes (p values < 0.05) across the 24 h experiments, see Table 2. Exposures at C_1, a concentration below LC_{10}, showed significant changes in the concentrations of the metabolites with respect to controls. For example, AABA increased its concentration by more than two-fold (Fig. S6). In other metabolites, decreasing metabolite concentrations were observed such as taurine, an essential amino acid for cardiovascular function and the central nervous system, or inosine, a nucleoside formed when hypoxanthine is attached to a ribose ring. Table S2 shows the concentrations of the metabolites determined from all exposures. At the higher exposure concentration, 153 mg L^{-1} (C_2), similar metabolite concentration changes occurred for AABA, taurine and inosine. Additionally, hypoxanthine and thymidine concentrations were different compared to controls (Fig. S6). In the samples exposed at C_1, all the metabolites in Cluster A (Fig. 4) had fold decreases along the 24-h exposure time. However, L-citrulline and L-tyrosine (Cluster B, Fig. 4) and ADP had fold increases at 24-h. Finally, in the samples at C_2, the general trend in Cluster A plus ADP is that the metabolites had fold increases along 24-h, with the exception of NADH and taurine. Moreover, the metabolites in Cluster B of the Fig. 4 (L-citrulline and L-tyrosine) also decreased their fold changes at 24-h exposure time.

3.3. Metabolic pathways potentially affected by selected single pharmaceutical exposures

Little or no reported metabolomics or pathway-based analysis data exists for *G. pulex* in the literature to our knowledge. However, changes in its metabolic profile following exposure to pharmaceuticals may result in processes that are suggestive of either metabolic (i.e. detoxification) or toxic responses. Firstly, and to support this, the internal concentrations were determined for the two compounds nimesulide and propranolol at the C_1 concentration at 24-h time interval. Triclosan was detected, but was unfortunately not quantifiable due to poor standard addition linearity (and similarly poor method performance as a whole). The C_1 propranolol dose resulted in measured concentrations up to 4.9 ± 0.3 mg g^{-1} (dry weight) and nimesulide reached a mean concentration of 12.2 ± 4.1 μg g^{-1} which are both significantly higher concentrations than the estimated dose required for therapeutic effects in humans. When comparing to environmental occurrence concentrations, these compounds did not exceed 36 ng g^{-1} in *G. pulex* (Miller et al., 2015) and other studies in aquatic invertebrates often report concentrations of <200 ng g^{-1} (Dodder et al., 2014; Huerta et al., 2015). However, and although the concentrations determined here are unlikely to be seen in the environment, measurement using such analytical methods enables interpretation of metabolic responses and potentially metabolic pathways indicative of adverse effects in the future for risk assessment purposes. The different responses may be elicited through numerous complex biochemical pathways such as nucleic acid expression, protein synthesis, enzymatic processes and signaling cascades. Thus, identifying and quantifying metabolite change is a useful starting point perhaps to direct metabolomics and extended pathway-based research in the future. The advantage of operating HRMS mass analysers in full-scan mode (as in the present study) is that such further qualitative meta-analysis of the data is still possible using untargeted and/or chemometric approaches at a later time (Farrés et al., 2014). The unbiased nature of non-target metabolomics would also allow the interpretation of metabolic responses in relation to known mode-of-action pathways for pharmaceuticals. Nonetheless, this was beyond the scope of this work and future work will be pursued in this direction. A general observation was that control levels of metabolites showed relatively large scatter in specific cases. During the study the organisms were collected from the same site and were of similar size, but the variances in metabolite profiles of the controls are likely to have resulted from differences between individuals

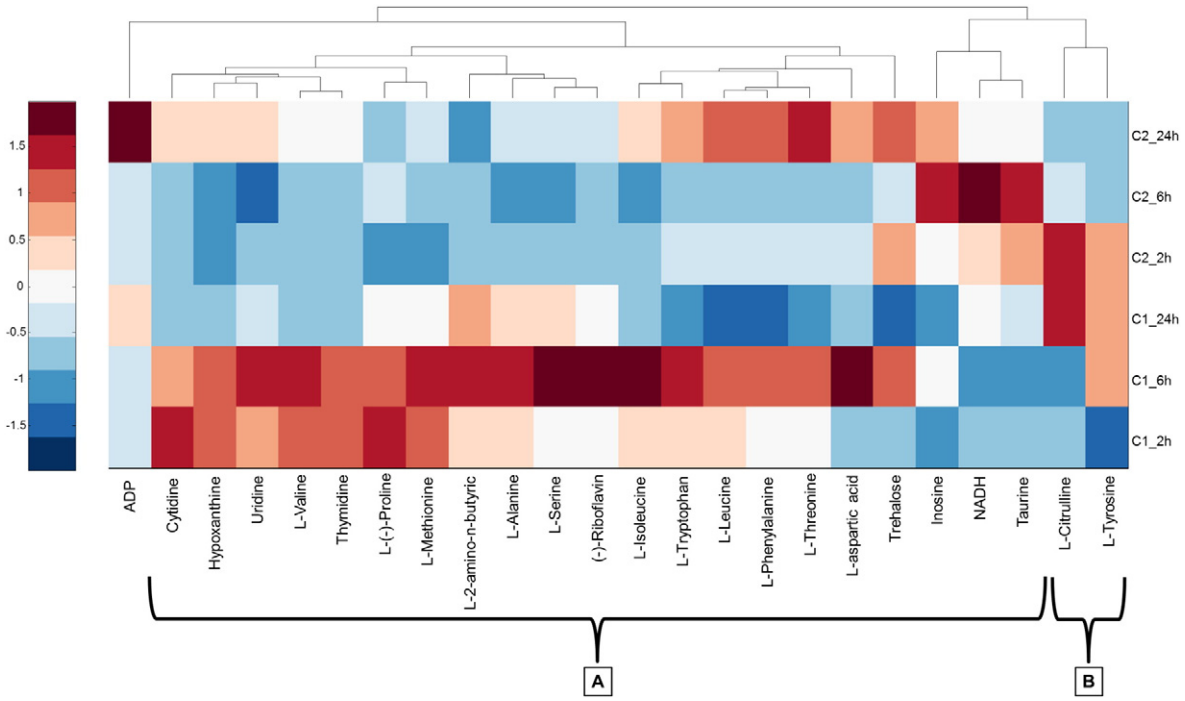

Fig. 4. Heat map of propranolol exposure representing the fold change of targeted metabolites in each exposure subgroup (C_1, C_2) relative to controls. All data have been auto scaled by column and dendrograms represent hierarchical analysis for clustering (A & B) of metabolite responses.

such as their age, moult cycle stage and gender. Furthermore, acclimatisation of mussel populations in laboratory conditions has also been demonstrated to lead to increased metabolic variability (Hines et al., 2007).

3.3.1. Protein synthesis

Exposure to all three pharmaceuticals resulted in an increase in thymidine and inosine concentrations when compared to controls. Amongst other potential reasons, their increase in concentration could be related to increases in protein synthesis as they are associated with tRNA. Cytidine concentrations varied between exposure concentrations and time points for all compounds. Triclosan had elevated cytidine concentrations at both 2 and 6-h time intervals relative to controls in the C_1 exposure. The same effect was not observed in C_2, often remaining close to the control levels except at the 6-h time interval. Cytidine in the nimesulide exposure was upregulated relative to controls at C_1, whereas C_2 showed a steady increase in cytidine concentrations over the 24-h exposure period. For propranolol, cytidine concentrations remained below controls at C_2 and were initially upregulated at C_1 before decreasing below control levels at 24 h. Uridine showed no obvious differences between controls for either exposure concentration in propranolol. Uridine was upregulated in the nimesulide C_2 exposure by 24-h whereas in the C_1 remained higher than controls at all time points. Triclosan showed increased uridine concentrations in both exposures at the 2 and 6-h intervals when compared with control levels, the C_2 uridine concentrations returned to the control level at 24-h. As uridine is absent from DNA and only present in RNA, it is plausible that together these four nucleosides are generally indicative of upregulation of protein synthesis which is potentially induced by all three pharmaceuticals. The upregulation could be considered as a general metabolic response to such xenobiotic exposure, for example, via the production of P450 enzymes (Marionnet et al., 1997; Ortiz-Delgado et al., 2008). Triclosan has also been shown to increase the P450 content of rat liver microsomes (Kanetoshi et al., 1992; Liang et al., 2013).

3.3.2. Xenometabolic pathways

The internal concentrations reached in *G. pulex* exceed the human therapeutic doses and thus are likely to induce xenometabolism by means of enzymes associated with phase I and II metabolism. It is possible that the increased content of uridine is also related to phase II metabolic processes. Uridine, when converted to a triphosphate nucleotide (UTP), is involved in the biosynthesis of uridine diphosphate glucose (UDPG) which serves as a precursor of uridine glucuronic acid, the primary substrate for phase II glucuronidation reactions catalysed by uridine 5′-diphospho-glucuronosyltransferase (UGT). Major metabolites associated with these three pharmaceuticals are glucuronide conjugates, which support this argument (Macpherson et al., 2013; Walle et al., 1985; Wu et al., 2010). Riboflavin also showed statistically significant 2–3 fold increases in concentration relative to control concentrations. This metabolite is essential for xenometabolic processes as it forms part of flavin adenine nucleotide (FAD) and flavin mononucleotide (FMN), which are essential cofactors for redox reactions involving P450 enzymes and flavin-containing monooxygenases (FMOs). These cofactors are also required for regeneration of reduced glutathione (GSH) from its oxidized form glutathione disulfide (GSSG).

At C_1 and C_2 nimesulide exposures, AABA showed a significant reduction in concentration and also decreased over the course of the experiment. This metabolite is a precursor to ophthalmic acid, which is associated with oxidative stress and the induction of ophthalmic acid pathways is shown when glutathione levels are reduced (Soga et al., 2006). As nimesulide has been shown to reduce GSH levels as well as induce oxidative stress, it is suggestive that the low levels of AABA are a result of its conversion to ophthalmic acid, but this requires confirmation (Chatterjee et al., 2006; Mingatto et al., 2002; Singh et al., 2010). It has been suggested that the physiological significance in the production of AABA is that it is a cofactor in the transport of glucuronide metabolites in the multi-drug resistance protein 1 (MRP-1) and thus required for elimination of xenobiotics (Soga et al., 2006). Lastly, perturbations in methionine concentrations may also be indicative of xenometabolic pathways. The concentrations of methionine in all exposures were

elevated relative to control with the exception of the 2 h C_2 sampling point in the propranolol exposure. Methionine acts as a precursor to S-adenosyl methionine (SAM) that is involved in methylation reactions for xenobiotic metabolism. Triclosan, for example, undergoes methylation during metabolism to methyltriclosan and therefore may explain its elevated concentrations in both triclosan exposures (Wu et al., 2010). Finally, this compound also serves as a precursor to GSH biosynthesis and therefore may be elevated even when xenobiotics are not methylated during detoxification.

3.3.3. Signaling cascade

Tryptophan was significantly expressed at increased concentrations in all three pharmaceutical exposures at both C_1 and C_2. This AA acts as a precursor to serotonin that is often released as a stress response. It is possible that the exposure to these pharmaceuticals induced a stress response. Indeed, C_2 is set at the LOAEL with mortality as the adverse effect, which upregulated the synthesis of tryptophan for which serotonin synthesis is dependent (Joseph and Kennett, 1983). Xenobiotics have been previously shown to induce the release of serotonin in rats (Yokogoshi, 1989). However, it is also possible that tryptophan is produced in response to reactive oxygen and nitrogen species (ROS/RNS) produced by the metabolism of the pharmaceuticals (Peyrot and Ducrocq, 2008). Triclosan displayed the highest concentrations of tryptophan reaching up to 142 μg g^{-1} when exposed at C_2. The higher toxicity of this compound may lead to added stress in comparison to propranolol and nimesulide. The amino acid proline also showed statistically significant changes during the three exposures. In particular, the C_1 exposures showed a decrease in proline over time until they approximately reached control levels at the 24-h time interval. The same trend is not observed in the C_2 exposures and is more variable when compared to the controls. Proline has been shown in previous studies to be important during stress responses as this amino acid has roles in preventing oxidative stress, maintenance of osmoregulation, energy production, and many other biological functions in plants and amphipods (Maity et al., 2012; Choudhary et al., 2007).

4. Conclusions

A comprehensive optimisation of a targeted multi-residue method for the quantitative determination of 29 metabolites from different biochemical classes using LC-HRMS was performed. The acute toxicity (LC_{50}) was also estimated for 26 pharmaceuticals and revealed that triclosan was the most toxic compound to *G. pulex*. However, the reliance on acute toxicity data such as LC_{50} for pharmaceutical risk assessment may ultimately not be realistic as these were at least one–two orders of magnitudes higher than concentrations typically found in the aquatic environment. Exposures performed at the NOAEL and LOAEL with three pharmaceuticals across the range of measured toxicity resulted in quantifiable changes in the metabolome in *G. pulex*. Measured internal concentrations of nimesulide and propranolol were far higher than the daily recommended doses for therapeutic effects in humans. Alterations in metabolite concentrations were observed, which could be involved in several different pathways relating to protein synthesis, oxidative stress and signaling cascades. However, further efforts are required to fully characterise and understand the effects these contaminants have on any specific pathway. In greater knowledge using such analytical methods for quantitative determinations of endogenous metabolites in aquatic organisms can now be acquired. In addition, the use of full-scan HRMS detection enables non-target meta-analysis to be performed in the future using chemometric tools that could identify biomarkers of exposure and effect for use in the environmental risk assessment of pharmaceuticals.

Role of funding source

Funding bodies played no role in the design of the study or decision to publish.

Conflict of interest

The authors declare no financial conflict of interest.

Acknowledgements

G. McEneff is acknowledged for laboratory assistance and with *G. pulex* sampling, as well as staff at the Centre for Excellence in Mass Spectrometry at King's College London for LC-HRMS support. The research leading to these results has received funding from the European Research Council under the European Union's Seventh Framework Programme (FP/2007-2013)/ERC Grant Agreement n. 320737. A JWT Jones Travelling Fellowship was also awarded to C. Gómez-Canela by the Royal Society of Chemistry for his work to be performed at KCL. T. Miller's collaboration was funded by the Biotechnology and Biological Sciences Research Council scholarship scheme (Reference BB/K501177/1).

Appendix A. Supplementary data

Supplementary data to this article can be found online at http://dx.doi.org/10.1016/j.scitotenv.2016.03.181.

References

Ashauer, R., Hintermeister, A., Potthoff, E., Escher, B.I., 2011. Acute toxicity of organic chemicals to *Gammarus pulex* correlates with sensitivity of *Daphnia magna* across most modes of action. Aquat. Toxicol. 103, 38–45.

Bourgeault, A., Ciffroy, P., Garnier, C., Cossu-Leguille, C., Masfaraud, J.F., Charlatchka, R., Garnier, J.M., 2013. Speciation and bioavailability of dissolved copper in different freshwaters: comparison of modelling, biological and chemical responses in aquatic mosses and gammarids. Sci. Total Environ. 452-453, 68–77.

Chatterjee, M., Sarkar, K., Sil, P.C., 2006. Herbal (*Phyllanthus niruri*) protein isolate protects liver from nimesulide induced oxidative stress. Pathophysiology 13, 95–102.

Choudhary, M., Jetley, U.K., Khan, M.A., Zutshi, S., Fatma, T., 2007. Effect of heavy metal stress on proline, malondialdehyde, and superoxide dismutase activity in the cyanobacterium *Spirulina platensis*-S5. Ecotoxicol. Environ. Saf. 66, 204–209.

Coulaud, R., Geffard, O., Xuereb, B., Lacaze, E., Quéau, H., Garric, J., Charles, S., Chaumot, A., 2011. In situ feeding assay with *Gammarus fossarum* (Crustacea): modelling the influence of confounding factors to improve water quality biomonitoring. Water Res. 45, 6417–6429.

Daughton, C.G., Ternes, T.A., 1999. Pharmaceuticals and personal care products in the environment: agents of subtle change? Environ. Health Perspect. 107, 907–938.

De Lange, H.J., Sperber, V., Peeters, E.T.H.M., 2006. Avoidance of polycyclic aromatic hydrocarbon-contaminated sediments by the freshwater invertebrates *Gammarus pulex* and *Asellus aquaticus*. Environ. Toxicol. Chem. 25, 452–457.

De Lange, H.J., Peeters, E.T.H.M., Lürling, M., 2009. Changes in ventilation and locomotion of *Gammarus pulex* (Crustacea, Amphipoda) in response to low concentrations of pharmaceuticals. Hum. Ecol. Risk. Assess. 15, 111–120.

Dettmer, K., Aronov, P.A., Hammock, B.D., 2007. Mass spectrometry-based metabolomics. Mass Spectrom. Rev. 26, 51–78.

Dodder, N.G., Maruya, K.A., Ferguson, P.L., Grace, R., Klosterhaus, S., La Guardia, M.J., Lauenstein, G.G., Ramirez, J., 2014. Occurrence of contaminants of emerging concern in mussels (*Mytilus* spp.) along the California coast and the influence of land use, storm water discharge, and treated wastewater effluent. Mar. Pollut. Bull. 81 (2), 340–346.

Dunn, W.B., Bailey, N.J.C., Johnson, H.E., 2005. Measuring the metabolome: current analytical technologies. Analyst 130, 606–625.

European Communities Commission, 1996. Technical guidance document in support of commission directive 93/67/EEC on risk assessment for new notified substances and commission regulation.

Evgenidou, E.N., Konstantinou, I.K., Lambropoulou, D.A., 2015. Occurrence and removal of transformation products of PPCPs and illicit drugs in wastewaters: a review. Sci. Total Environ. 505, 905–926.

Farrés, M., Piña, B., Tauler, R., 2014. Chemometric evaluation of *Saccharomyces cerevisiae* metabolic profiles using LC–MS. Metabolomics 11, 210–224.

Franquet-Griell, H., Gómez-Canela, C., Ventura, F., Lacorte, S., 2015. Predicting concentrations of cytostatic drugs in sewage effluents and surface waters of Catalonia (NE Spain). Environ. Res. 138, 161–172.

Frisvad, J.C., Filtenborg, O., 1983. Classification of Terverticillate penicillia based on profiles of mycotoxins and other secondary metabolites. Appl. Environ. Microbiol. 46, 1301–1310.

Gómez-Canela, C., Cortés-Francisco, N., Ventura, F., Caixach, J., Lacorte, S., 2013. Liquid chromatography coupled to tandem mass spectrometry and high resolution mass spectrometry as analytical tools to characterize multi-class cytostatic compounds. J. Chromatogr. A 1276, 78–94.

Gómez-Canela, C., Ventura, F., Caixach, J., Lacorte, S., 2014. Occurrence of cytostatic compounds in hospital effluents and wastewaters, determined by liquid chromatography coupled to high-resolution mass spectrometry. Anal. Bioanal. Chem. 406, 3801–3814.

Griffiths, W.J., Koal, T., Wang, Y., Kohl, M., Enot, D.P., Deigner, H.-P., 2010. Targeted metabolomics for biomarker discovery. Angew. Chem. Int. Ed. 49, 5426–5445.
Heberer, T., 2002. Occurrence, fate, and removal of pharmaceutical residues in the aquatic environment: a review of recent research data. Toxicol. Lett. 131, 5–17.
Hines, A., Oladiran, G.S., Bignell, J.P., Stentiford, G.D., Viant, M.R., 2007. Direct sampling of organisms from the field and knowledge of their phenotype: key recommendations for environmental metabolomics. Environ. Sci. Technol. 41, 3375–3381.
Horning, E.C., Horning, M.G., 1971. Human metabolic profiles obtained by GC and GC/MS. J. Chromatogr. Sci. 9, 129–140.
Huerta, B., Jakimska, A., Llorca, M., Ruhí, A., Margoutidis, G., Acuña, V., Sabater, S., Rodriguez-Mozaz, S., Barcelò, D., 2015. Development of an extraction and purification method for the determination of multi-class pharmaceuticals and endocrine disruptors in freshwater invertebrates. Talanta 132, 373–381.
Joseph, M.H., Kennett, G.A., 1983. Stress-induced release of 5-HT in the hippocampus and its dependence on increased tryptophan availability: an in vivo electrochemical study. Brain Res. 270, 251–257.
Kanetoshi, A., Katsura, E., Ogawa, H., Ohyama, T., Kaneshima, H., Miura, T., 1992. Acute toxicity, percutaneous absorption and effects on hepatic mixed function oxidase activities of 2,4,4′-trichloro-2′-hydroxydiphenyl ether (Irgasan® DP300) and its chlorinated derivatives. Arch. Environ. Contam. Toxicol. 23, 91–98.
Kim, J.W., Ishibashi, H., Yamauchi, R., Ichikawa, N., Takao, Y., Hirano, M., Koga, M., Arizono, K., 2009. Acute toxicity of pharmaceutical and personal care products on freshwater crustacean (*Thamnocephalus platyurus*) and fish (*Oryzias latipes*). J. Toxicol. Sci. 34, 227–232.
Lebrun, J.D., Perret, M., Geffard, A., Gourlay-Francé, C., 2012. Modelling copper bioaccumulation in *Gammarus pulex* and alterations of digestive metabolism. Ecotoxicology 21, 2022–2030.
Lei, Z., Huhman, D.V., Sumner, L.W., 2011. Mass spectrometry strategies in metabolomics. J. Biol. Chem. 286, 25435–25442.
Liang, X., Nie, X., Ying, G., An, T., Li, K., 2013. Assessment of toxic effects of triclosan on the swordtail fish (*Xiphophorus helleri*) by a multi-biomarker approach. Chemosphere 90, 1281–1288.
Macpherson, D., Best, S.A., Gedik, L., Hewson, A.T., KD, R., Parisi, S., 2013. The biotransformation and pharmacokinetics of 14C-nimesulide in humans following a single dose oral administration. J. Drug Metab. Toxicol.
Maity, S., Jannasch, A., Adamec, J., Nalepa, T., Höök, T.O., Sepúlveda, M., 2012. Starvation causes disturbance in amino acid and fatty acid metabolism in Diporeia. Comp. Biochem. Physiol. B Biochem. Mol. Biol. 161, 348–355.
Maltby, L., Clayton, S.A., Wood, R.M., McLoughlin, N., 2002. Evaluation of the *Gammarus pulex* in situ feeding assay as a biomonitor of water quality: robustness, responsiveness, and relevance. Environ. Toxicol. Chem. 21, 361–368.
Marionnet, D., Taysse, L., Chambras, C., Deschaux, P., 1997. 3-methylcholanthrene-induced EROD activity and cytochrome P450 in immune organs of carp (*Cyprinus carpio*). Comp. Biochem. Physiol. C Pharmacol. Toxicol. Endocrinol. 118, 165–170.
Miller, T.H., McEneff, G.L., Brown, R.J., Owen, S.F., Bury, N.R., Barron, L.P., 2015. Pharmaceuticals in the freshwater invertebrate, *Gammarus pulex*, determined using pulverised liquid extraction, solid phase extraction and liquid chromatography-tandem mass spectrometry. Sci. Total Environ. 511, 153–160.
Mingatto, F.E., Rodrigues, T., Pigoso, A.A., Uyemura, S.A., Curti, C., Santos, A.C., 2002. The critical role of mitochondrial energetic impairment in the toxicity of nimesulide to hepatocytes. J. Pharmacol. Exp. Ther. 303, 601–607.
Monteiro, S.C., Boxall, A.B.A., 2010. In: D.M., Whitacre (Ed.), Occurrence and Fate of Human Pharmaceuticals in the Environment. Rev. Environ. Contam. Toxicol.
Ortiz-Delgado, J.B., Behrens, A., Segner, H., Sarasquete, C., 2008. Tissue-specific induction of EROD activity and CYP1A protein in *Sparus aurata* exposed to B(a)P and TCDD. Ecotoxicol. Environ. Saf. 69, 80–88.
Pellet, B., Ayrault, S., Tusseau-Vuillemin, M.H., Gourlay-Francé, C., 2014. Quantifying diet-borne metal uptake in *Gammarus pulex* using stable isotope tracers. Ecotoxicol. Environ. Saf. 110, 182–189.
Peyrot, F., Ducrocq, C., 2008. Potential role of tryptophan derivatives in stress responses characterized by the generation of reactive oxygen and nitrogen species. J. Pineal Res. 45, 235–246.
Samuelsson, L.M., Förlin, L., Karlsson, G., Adolfsson-Erici, M., Larsson, D.G.J., 2006. Using NMR metabolomics to identify responses of an environmental estrogen in blood plasma of fish. Aquat. Toxicol. 78, 341–349.
Schaller, J., Brackhage, C., Mkandawire, M., Dudel, E.G., 2011. Metal/metalloid accumulation/remobilization during aquatic litter decomposition in freshwater: a review. Sci. Total Environ. 409, 4891–4898.
Singh, B.K., Tripathi, M., Pandey, P.K., Kakkar, P., 2010. Nimesulide aggravates redox imbalance and calcium dependent mitochondrial permeability transition leading to dysfunction in vitro. Toxicology 275, 1–9.
Soga, T., Baran, R., Suematsu, M., Ueno, Y., Ikeda, S., Sakurakawa, T., Kakazu, Y., Ishikawa, T., Robert, M., Nishioka, T., Tomita, M., 2006. Differential metabolomics reveals ophthalmic acid as an oxidative stress biomarker indicating hepatic glutathione consumption. J. Biol. Chem. 281, 16768–16776.
Taylor, J., King, R.D., Altmann, T., Fiehn, O., 2002. Application of metabolomics to plant genotype discrimination using statistics and machine learning. Bioinformatics 18, S241–S248.
Tweeddale, H., Notley-McRobb, L., Ferenci, T., 1998. Effect of slow growth on metabolism of *Escherichia coli*, as revealed by global metabolite pool ("metabolome") analysis. J. Bacteriol. 180, 5109–5116.
USEPA, United States Environmental Protection Agency USEPA, 2002,. Methods for measuring the acute toxicity of effluents and receiving waters to freshwater and marine organisms.
Vellinger, C., Felten, V., Sornom, P., Rousselle, P., Beisel, J.N., Usseglio-Polatera, P., 2012. Behavioural and physiological responses of *Gammarus pulex* exposed to cadmium and arsenate at three temperatures: individual and combined effects. PLoS One 7.
Viant, M.R., 2008. Recent developments in environmental metabolomics. Mol. Biol. 4, 980–986.
Viant, M.R., Sommer, U., 2013. Mass spectrometry based environmental metabolomics: a primer and review. Metabolomics 9, 144–158.
Viant, M.R., Rosenblum, E.S., Tjeerdema, R.S., 2003. NMR-based metabolomics: a powerful approach for characterizing the effects of environmental stressors on organism health. Environ. Sci. Technol. 37, 4982–4989.
Villas-Bôas, S.G., Mas, S., Åkesson, M., Smedsgaard, J., Nielsen, J., 2005. Mass spectrometry in metabolome analysis. Mass Spectrom. Rev. 24, 613–646.
Walle, T., Walle, U.K., Olanoff, L.S., 1985. Quantitative account of propranolol metabolism in urine of normal man. Drug Metab. Dispos. 13, 204–209.
Wu, J.-1., Liu, J., Cai, Z., 2010. Determination of triclosan metabolites by using in-source fragmentation from high-performance liquid chromatography/negative atmospheric pressure chemical ionization ion trap mass spectrometry. Rapid Commun. Mass Spectrom. 24, 1828–1834.
Yokogoshi, H., 1989. Effects of some xenobiotics on the disposition of brain serotonin and catecholamine in rats. Agric. Biol. Chem. 53, 1609–1615.
Zhang, A., Sun, H., Wang, P., Han, Y., Wang, X., 2012. Modern analytical techniques in metabolomics analysis. Analyst 137, 293–300.

ACS Editors' Choice

Environmental Science & Technology

Article

pubs.acs.org/est

The First Attempt at Non-Linear in Silico Prediction of Sampling Rates for Polar Organic Chemical Integrative Samplers (POCIS)

Thomas H. Miller,[†] Jose A. Baz-Lomba,[‡] Christopher Harman,[§] Malcolm J. Reid,[‡] Stewart F. Owen,[∥] Nicolas R. Bury,[⊥] Kevin V. Thomas,[‡] and Leon P. Barron*[,†]

[†]Analytical & Environmental Sciences Division, Faculty of Life Sciences and Medicine, King's College London, 150 Stamford Street, London, SE1 9NH United Kingdom

[‡]Norwegian Institute for Water Research (NIVA), Oslo, NO-0349, Norway

[§]Norwegian Institute for Water Research (NIVA), Grimstad, NO-4879, Norway

[∥]AstraZeneca, Global Environment, Alderley Park, Macclesfield, Cheshire SK10 4TF, United Kingdom

[⊥]Division of Diabetes and Nutritional Sciences, Faculty of Life Sciences and Medicine, King's College London, Franklin Wilkins Building, 150 Stamford Street, London, SE1 9NH, United Kingdom

Supporting Information

ABSTRACT: Modeling and prediction of polar organic chemical integrative sampler (POCIS) sampling rates (R_s) for 73 compounds using artificial neural networks (ANNs) is presented for the first time. Two models were constructed: the first was developed ab initio using a genetic algorithm (GSD-model) to shortlist 24 descriptors covering constitutional, topological, geometrical and physicochemical properties and the second model was adapted for R_s prediction from a previous chromatographic retention model (RTD-model). Mechanistic evaluation of descriptors showed that models did not require comprehensive a priori information to predict R_s. Average predicted errors for the verification and blind test sets were 0.03 ± 0.02 L d^{-1} (RTD-model) and 0.03 ± 0.03 L d^{-1} (GSD-model) relative to experimentally determined R_s. Prediction variability in replicated models was the same or less than for measured R_s. Networks were externally validated using a measured R_s data set of six benzodiazepines. The RTD-model performed best in comparison to the GSD-model for these compounds (average absolute errors of 0.0145 ± 0.008 L d^{-1} and 0.0437 ± 0.02 L d^{-1}, respectively). Improvements to generalizability of modeling approaches will be reliant on the need for standardized guidelines for R_s measurement. The use of in silico tools for R_s determination represents a more economical approach than laboratory calibrations.

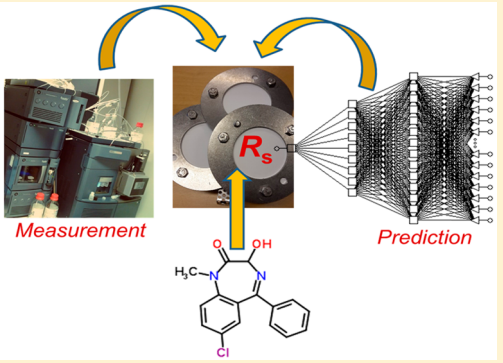

INTRODUCTION

Contamination of the aquatic environment with herbicides, pesticides, pharmaceuticals, and personal care products (PPCPs), among other contaminants, has been the focus of environmental monitoring campaigns over the last two decades. Reported concentrations and associated adverse effects of these contaminants has led to the introduction of legislative procedures to monitor and assess risk associated with pollutants, such as the EU water framework directive and the EU registration, evaluation, authorization, and restriction of chemicals (REACH).[1,2]

High frequency sampling campaigns often involve the use of grab or composite sampling, but are practically difficult and costly to manage for monitoring longer-term fluctuations in contaminant concentrations in the aquatic environment. These methods are also often labor intensive with respect to sampling and can lead to considerable cost during instrumental analysis. More recently, however, the development and use of passive sampling devices (PSDs) is increasing due to their capability for a time-integrated approach to averaging contaminant concentrations in surface waters as well as influent and effluent wastewater over extended periods.[3] PSDs minimize sample preparation and allow in situ enrichment of analytes which may potentially reduce limits of quantification in comparison to those achieved by point sampling.[4] Passive sampling devices in some fields are well-established, such as use of semipermeable membrane devices (SPMD) for organochlorines[5] and other similarly hydrophobic compounds.[6−8] However, one type of PSD which is emerging currently is the polar organic chemical integrative sampler (POCIS). These samplers have been used to determine the occurrence of a range of chemically diverse, and comparatively polar to moderately nonpolar compounds.[9−13] However, for quantitative studies, POCIS suffer from some limitations, mainly relating to the reliability of derived estimations of the sampling rates (R_s) from

Received: March 21, 2016
Revised: June 30, 2016
Accepted: July 1, 2016
Published: July 1, 2016

DOI: 10.1021/acs.est.6b01407
Environ. Sci. Technol. 2016, 50, 7973−7981

experimental measurements, as well the lack of a well-developed performance reference compound (PRC) exposure correction method.[14−16] One further hindrance is that reported sampling rate data are few and methods for their estimation vary which leads to limited transferability across other locations or studies.[17]

Given the time-intensive nature of determining R_s experimentally, it is possible that computational modeling approaches could offer a solution that would enable prediction of sampling rate data for compounds without the need for experimental determination. A previous investigation by Stephens et al.[18] evaluated the use of an empirical method (Sherwoods correlation) to determine PSD kinetic parameters for a limited number of compounds showing maximum errors of +40 and −20% for the estimation of the aqueous boundary layer mass transfer coefficient (k_f). In contrast to empirical methods for estimating specific parameters, quantitative structure−property relationship (QSPR) models are becoming more frequently used in ecotoxicology where a set of x variables are used to predict a response, y.[19] The variables are often molecular descriptors that cover constitutional, topological, geometrical, and physicochemical properties which can then be used to model a desired output. Models can vary from simple linear regression approaches to complex nonlinear functions where such models are often designed by machine learning methods. Two well-known machine learning methods are support vector machines (SVMs) and artificial neural networks (ANNs) and have been used successfully in related areas such as the prediction of bioconcentration factors (BCFs), octanol−water partition coefficients (log$P$) and biosolid/water partition coefficients (K_d), as well as for suspect compound screening via prediction of chromatographic retention time.[20−27] The use of SVMs for environmental applications is still in its infancy and substantial programming capability is required for routine application. On the other hand, ANNs are well-known and more user-friendly software has been available for many years. ANNs comprise a layered structure (normally three), each with a different purpose. The input layer contains the molecular descriptor data for each compound for training, verification and blind testing and the output layer is the response. The hidden layer sits in between and contains several nodes, and often multiple sublayers of such nodes, where linear or nonlinear functions are used to relate the descriptors to the output layer. The residual errors are monitored and reduced by using iterative algorithms which adjust weights associated with the nodes in the hidden layer. Thus, such modeling approaches could greatly increase the applicability of POCIS in environmental monitoring studies through bypassing the need for laboratory and in situ calibrations.

The aim of this work was to investigate the potential of ANNs to model and predict R_s for POCIS devices for a range of pharmaceuticals, endocrine disrupting chemicals, pesticides, herbicides and drugs of abuse. The objectives were to identify suitable analyte molecular descriptors to build, train and test a range of suitable model types and architectures and then finally to externally validate the approach for predicting R_s for several compounds which were, for comparison, determined in parallel by laboratory calibration. To the authors' knowledge, this represents the first study to draw together, harmonize and predict the published R_s data for ionizable pharmaceutical compounds on POCIS. Ultimately, where such tools can provide adequate predictions using new data generated in the future, this approach could reduce the analytical burden of laboratory estimations of R_s.

MATERIALS AND METHODS

Selection of Data Sets, Molecular Descriptors and ANN Models. A working data set derived from the literature (2007-present) was used to build, train and optimize models for R_s prediction on POCIS. A total of n = 73 compound R_s data were derived from Fauvelle et al.[28] and Morin et al.,[24] which were generated using similar experimental conditions to give the largest combined data set of all studies. Compounds included herbicides, pesticides, endocrine disrupting compounds and pharmaceuticals. Where duplicate compound R_s data existed, both values were removed entirely from the data set (six compounds). Generally, in these cases R_s differed and it was uncertain which value was correct or whether an average was appropriate for modeling. Simplified molecular input line entry system (SMILES) strings were generated from Chemspider (Royal Society of Chemistry, UK). Using these, n = 185 molecular descriptors were generated from Parameter Client freeware (Virtual Computational Chemistry Laboratory, Munich, Germany) and an additional n = 16 descriptors were from ACD laboratories Percepta software (Advanced Chemistry Development Laboratories, ON, Canada).

Two models were generated using two separate sets of descriptors covering constitutional, topological, geometrical and physicochemical properties that were investigated for their comparative prediction performance. The first subset of 24 descriptors (see Supporting Information (SI), Table S1) was generated using a genetic feature selection algorithm to produce the genetically selected descriptor model (GSD-model). Genetic feature selection algorithms follow evolutionary concepts to convert input descriptors into binary strings, in this case to prioritise descriptors for R_s prediction. Using a process similar to natural selection, prioritised strings are crossed to form a new population of strings. The generational "breeding" of strings produced an optimized selection of input variables for application to prediction. The parameters for the GA were as follows; population = 100, generation = 100, mutation rate = 0.1 and crossover rate = 1. In an alternative approach, a much simpler descriptor data set previously used to model elution from reversed-phase liquid chromatography (RPLC) stationary phases was investigated to assess any improvement (see SI Table S2).[23,25] This model is referred to as the retention time descriptor model (RTD-model). POCIS devices contain a divinylbenzene and N-vinylpyrrolidone copolymer, which enabled dual polar and nonpolar interactions for retention. As retention on reversed-phase chromatographic columns is governed predominantly by hydrophobic interactions too, it is possible that these same descriptors will also be important in passive sampling. No retention data was available for the studies by Fauvelle et al.[28] and Morin et al.[24,29] However, correlation between R_s and 21 corresponding retention times (t_R) gathered on a C_{18} stationary phase in a study by Bade et al.[30] showed a weak relationship (R = 0.472).

For both descriptor subsets, several network types were tested for predictive ability using Trajan 6.0 neural network software (Trajan Software Ltd., Lincolnshire, UK) and these included radial basis function (RBF), generalized regression neural networks (GRNNs) and multilayer perceptrons (MLPs). Following training and optimization using both data sets, the GSD- and RTD-models were produced. The GSD-model

DOI: 10.1021/acs.est.6b01407
Environ. Sci. Technol. 2016, 50, 7973−7981

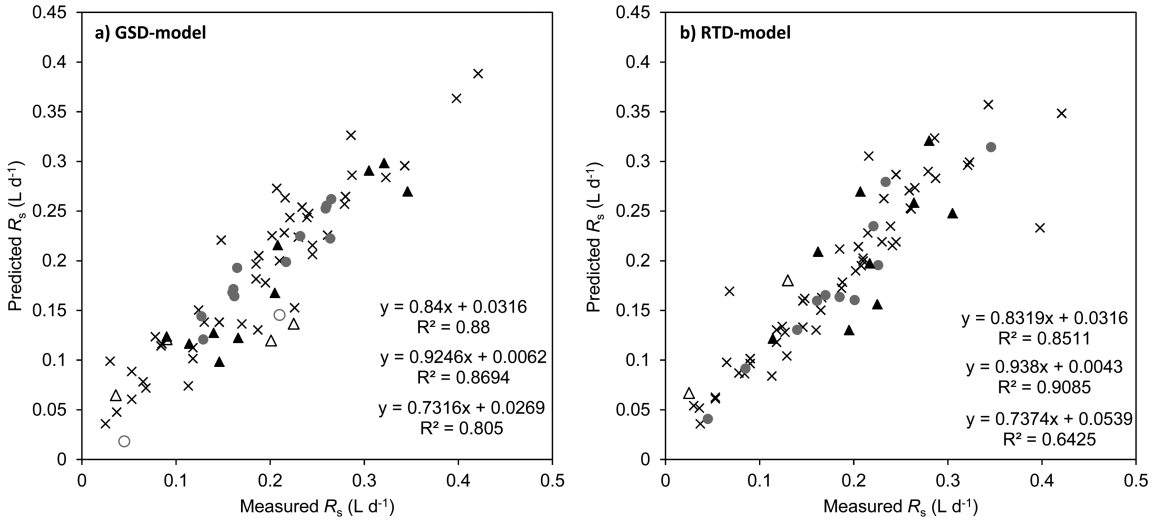

Figure 1. Measured R_s against predicted R_s for (a) the GSD-model and (b) the RTD-model. Crosses, circles and triangles are the training, verification and test subsets, respectively. Open circles and triangles indicate predicted inaccuracies of >30% of the measured value.

architecture was a four-layer MLP with 24 descriptors in the input layer (independent variables); two hidden layers containing 17 and 14 nodes and the dependent variable output layer (R_s). Training involved two types of algorithms, the first was back-propagation (BP) and the second was conjugate gradient descent (CGD). The data set was split into 45:14:14 cases for the training, verification and test subsets (optimized). The RTD-model architecture was also a four-layer MLP using both BP and CGD. The first and fourth layers were the inputs (using the set of descriptors previously used for chromatographic retention modeling) and outputs (R_s), respectively, and the second and third layers (hidden layers) contained 14 and 9 nodes, respectively. The division of cases included 51 compounds for training, 11 compounds for verification and 11 compounds for blind testing (optimized).[27] All cases were randomly selected to avoid bias. The verification data set was used to characterize network predictive performance during training and also to allow regularisation to prevent overfitting. The test set was then used to validate the model to ensure that the model generalized well to new cases. The optimized models were selected based on the lowest errors and consistency across the training, verification and test subsets.

Laboratory Calibration of Sampling Rates to Test Model Generalizability. Sampling rates (L d^{-1}) were determined using a static renewal method over a 14 day exposure period and in a similar manner to data in the literature which were used for modeling here.[28] Briefly, 3 L of high-density polyethylene vessels were filled with ultrapure water, the pH adjusted to 7.6 with 20 mg L^{-1} $NaHCO_3$ and spiked with the mixture of respective compounds to expose the POCIS. Each vessel contained three POCIS devices for exposure to an aqueous-based standard mixture of 200 ng L^{-1} of each target compound (solvent <0.001%). This standard solution was prepared and replaced daily in 3 L volumetric flasks to maintain the nominal concentration. Following this, all three POCIS were removed from each vessel at day 4, 7, and 14, rinsed with ultrapure water and frozen at −20 °C. Extraction of POCIS sorbents was performed using a wash phase of 5 mL of ultrapure water and then elution using 5 mL of MeOH. Eluate was dried under nitrogen at 35 °C for 40 min. The dried residue was then reconstituted in 0.5 mL of starting mobile phase. The analysis of the benzodiazepines was performed on an Acquity UPLC system coupled to a Xevo G2 S QTOF mass analyzer (Milford, MA) with an online Oasis HLB Direct Connect HP loading column. Analyte separation was performed on an Acquity UPLC BEH C_{18} column (1.7 μm, 50 × 2.1 mm) from Waters (Milford, MA) at 50 °C. Gradient elution (0.6 mL min^{-1}) for analyte separation was with 0.1% (v/v) formic acid in water (phase A) and 0.1% formic acid in methanol (phase B). Full method details for the laboratory calibration experiments and analysis are given in the SI.

RESULTS AND DISCUSSION

R_s Prediction Using a GSD-Model. Following genetic feature selection, a 24−17−14−1 MLP yielded the best performance using 24 input descriptors with R^2 = 0.8800, 0.8694, and 0.8050 for training, verification and blind test sets respectively (sum of squared residual errors were 0.084, 0.062, and 0.116, respectively). Therefore, this model initially seemed quite promising for application to prediction of R_s for new compounds (Figure 1a). Many shortlisted descriptors were derived from topological indices, but some others were expected to have more importance for this application, such as those that describe molecular hydrophobicity. These include the octanol−water partition coefficient (log$P$) and the distribution ratio between octanol and water (logD_{ow}). The latter takes into account the ionised proportion of a compound at a particular pH and is dependent on the log$P$ and the pK_a of all ionizable functional groups in a molecule. An investigation by Booij et al.,[31] demonstrated that uptake rates in SPMDs correlated well with log$P$ where $R_s \approx P^{-0.044}$. Correlations between log$P$ and R_s has also been observed for POCIS devices.[32−34] Assessment of the collinearity with R_s (SI Table S7) showed rather unsurprisingly for so many ionizable compounds that logD_{ow} had, by far, the highest correlation (R = 0.59), but was insufficient by itself to describe sorption to POCIS sorbents. To the authors knowledge, no previous investigations have used logD_{ow} to model R_s, although it has been weakly correlated with R_s.[35] Furthermore, interinput descriptor collinearity also existed and especially for constitutional descriptors such as the number of non-H bonds (nBO) and the sum of conventional bond orders (SCBO); as well as topological descriptors such as log Narumi simple topological

DOI: 10.1021/acs.est.6b01407
Environ. Sci. Technol. 2016, 50, 7973−7981

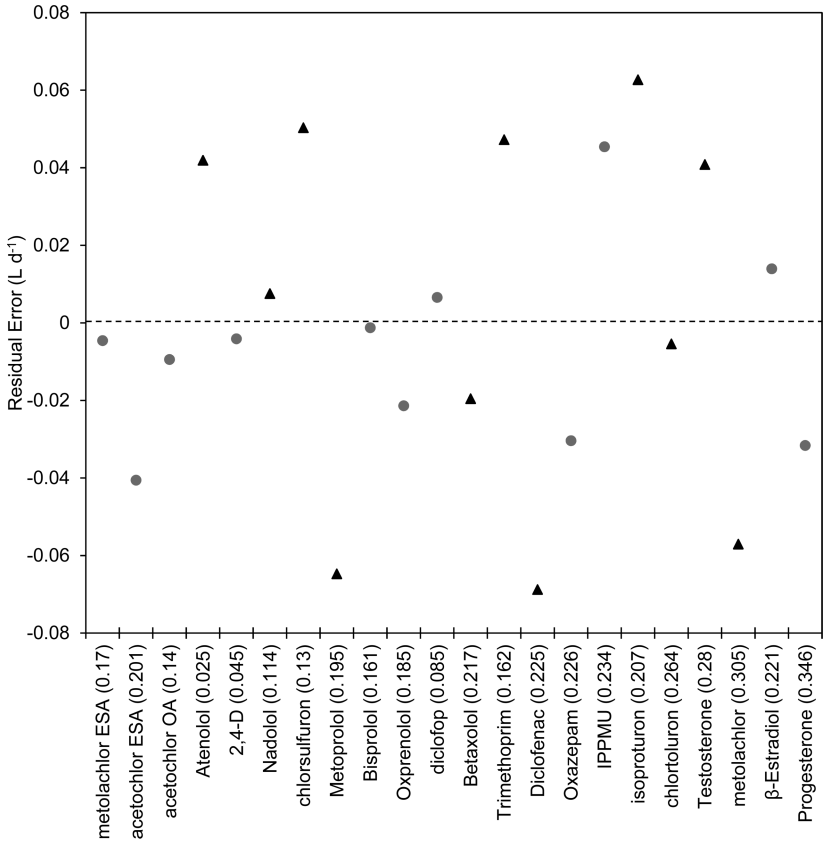

Figure 2. RTD-model residual plot of predicted R_s values for the verification and test subset only, ordered in parentheses by their ascending distribution ratio values between octanol and water ($\log D_{ow}$). Circles and triangles represent the verification and test subset, respectively. The measured R_s values are displayed in parentheses on the *x*-axis. 2,4-D (2,4-dichlorophenoxyacetic acid), ESA (ethanesulfonic acid), OA (oxanilic acid), and IPPMU (isoproturon-monodemethyl).

index (Snar), second Zagreb index (ZM2). Pearson's coefficients were ≥0.8 for these descriptors with at least eight other descriptors. Therefore, though genetic algorithms short-listed useful descriptors for potential R_s modeling here, back-interpretation of model sensitivity to descriptor data for derivation of mechanistic understanding of physicochemical POCIS uptake mechanisms would be limited. However, as a tool to predict R_s, the training set overall displayed good accuracy within 22% of the measured value on average. In comparison, the verification and test subsets were predicted on average within 19% of their measured values showing consistency across all subsets (SI, Figure S1). For particular blind test cases, however, some notably large inaccuracies were observed such as for sotalol (80% inaccuracy) where the lower hydrophobicity of this molecule may explain poorer correlation with R_s.[31] Larger errors were also recorded for acetochlor ethanesulfonic acid (40%), diclofenac (39%) and sulcotrione (38%). The verification subset contained two largely inaccurate predictions (2,4-dichlorophenoxyacetic acid at 59% and timolol at 31%), but all remaining compounds were within 20% of measured R_s. Larger inaccuracies may be related to poor learning from selected training data. For example, mesotrione had a 59% inaccuracy to the measured value in the training set which may explain the poor prediction of another structurally similar compound, sulcotrione, in the test set. Overall, inaccuracy was most prevalent for sulfonate-containing compounds where genetic selection did not sufficiently prioritise descriptors for this portion of cases for reliable R_s prediction. As the number of available cases expands, genetic selection of descriptors may improve for such compounds in the future. It is also unclear whether sulfonate bearing molecules are subject to steric and/or repulsive forces arising from the PES membrane. Furthermore, larger inaccuracies (>30%) in the full data set generally corresponded to compounds with R_s < 0.1 such as 2,4-dichlorophenoxyacetic acid, sotalol, sulcotrione and nicosulfuron. However, when predictive accuracy was plotted against R_s for all compounds, no correlation was observed for other compounds with R_s < 0.1 (SI, Figures S2 and S3).

R_s Prediction Using a RTD-Model. The correlation of predicted versus measured R_s for the RTD-model is shown in Figure 1b. The error (sum squared) for the subsets were 0.092, 0.062, and 0.121 for the training, verification and test sets, respectively. The model was, again, a four-layered MLP with a 16:14:9:1 architecture. Generally, acceptable correlations were achieved for the training, verification and blind test sets (R^2 = 0.8511, 0.9085, and 0.6425, respectively) though this model performed slightly worse (training and test) than the GSD-model. The training subset showed several larger errors which corresponded to the compounds *t*-butylphenol (149%), 2,4-dichlorphenol (41%), and simazine (41%). The compound sulfamethoxazole showed an 81% overestimation of its experimentally determined R_s. As discussed earlier, this large inaccuracy was also reflected in the GSD-model which showed an overestimation of 230% for sulfamethoxazole which also bears a sulfonate group. Overall, however, the model showed relatively good predictions of R_s (mean absolute error for training set = 15%; and for both verification and test subsets =

DOI: 10.1021/acs.est.6b01407
Environ. Sci. Technol. 2016, 50, 7973−7981

22%). The average error ± standard deviation across the verification and blind test subsets was 0.03 ± 0.02 L day^{-1} showing acceptable overall predictive accuracy for R_s. Atenolol, the compound with the lowest R_s, yielded poor prediction accuracy (predicted R_s = 0.067, measured R_s = 0.025) which was initially thought to be due its higher polarity in comparison to others selected for this study. However, no correlation was observed between predictive accuracy and logD_{ow} (Figure 2). Average predictive mean error of the verification and blind test sets both reduced to ∼15% upon removal of the atenolol datapoint. Importantly, as very polar compounds are generally not retained well by n-vinylpyrrolidone-*co*-divinylbenzene-based polymer sorbents, inaccuracy in measured R_s may be compound specific as a result, which in turn may contribute to RTD-model prediction errors. This highlights the lack of consistent measurements available for training of such models for predictive purposes. Nonetheless, considering this performance alongside the potential for inaccuracy in R_s data from different laboratory calibrations, predictions using these models were considered reasonable.

Model Interpretation and Descriptor Contribution to R_s Prediction. Given the level of multicollinearity observed for GSD-model descriptors, a sensitivity analysis could only be performed to identify the relative contribution of each descriptor to predictions in the RTD-model. This was represented as the error ratio, i.e. the ratio between the model error using all descriptors and the model error when one descriptor was removed. However, like in the GSD-model, the use of sensitivity analysis to further mechanistic understanding of sorption processes should be approached with caution if some individual descriptors display multicollinearity (please refer to SI Tables S1−S3 for full descriptor details and data). The logD_{ow}, the Moriguchi octanol−water partition coefficient (Mlog*P*), the Ghose-Crippen octanol−water partition coefficient (Alog*P*) and the number of Benzene rings (n*Bnz*) were the top four descriptors used by the RTD-model (Figure 3). This is in agreement with Bäuerlein et al., who showed that hydrophobicity and *pi-pi* interactions (e.g., via benzene rings) were important for adsorption to HLB sorbents in batch experiments[36] and which can also affect diffusion. Other important descriptors were the number of triple bonds (nTB; error ratio = 1.2165), number of five-membered rings (nR05; error ratio = 1.2041) and number of nine-membered rings (nR09; error ratio = 1.4544). The importance of the *n*-membered ring descriptors could be attributed to molecular size and flexibility thus affecting the diffusivity of molecules through the water boundary layer (WBL), PES membrane (pore = 0.1 μm) or pores of the HLB copolymer (80 Å).[37−39] A previous investigation showed that size descriptors were also important for predicting soil sorption coefficients for pesticides.[39] We also previously showed these descriptors were important for ANN-based predictions of pharmaceutical sorption to soils and sludge.[40] In addition to those mentioned above, the number of carbons (n*C*), number of oxygens (n*O*) and hydrophilic factor (*Hy*) also showed that they were important to the RTD-model. *Hy* relates to the number of hydrophilic groups in the molecule such as hydroxyls, thiols and sulfonates. As polar surface area has been previously shown to influence interactions with HLB sorbents, it is logical that hydrophilicity/polarity related descriptors would have some importance.[36] Several authors have suggested that diffusion is the main factor governing uptake rates in PSDs.[41] We have attributed the importance of the descriptors mainly to sorbent interactions so far, but it is also possible that these same descriptors could relate to diffusion processes due to the number of molecular properties that will affect it including dipole moments, polarizability, molecular size (including hydration radius) and electrostatic charge.[42] The genetic feature selection algorithm did not select some recognized diffusion-related descriptors, such as molecular weight as a simple example. However, it did select other descriptors that showed interdependencies on factors affecting diffusion such as number of atoms, number of rotatable bonds, and electrotopological states. R_s has been attributed mainly in the past to diffusion processes in partition samplers such as silicone rubbers.[41] The portion of R_s governed by diffusion in adsorption samplers using HLB-type sorbents in POCIS remains unclear especially whether sorption of analytes via hydrogen bonding, dipole−dipole, dipole−induced dipole, van der Waals and *pi-pi* interactions plays a more significant role. It is also possible that the models presented here for R_s prediction could be developed and improved further with additional or alternative descriptors, such as diffusion coefficients. However, adding such descriptors may introduce a greater uncertainty into the model as estimates can be based on several different approaches.[43−45] In addition, diffusion coefficients will be affected by numerous environmental factors and hydrodynamic conditions that would be difficult to replicate or control in situ. Inclusion of larger numbers of descriptors to cover all the processes involved will likely inhibit model generalizability. Indeed, ANNs learn more holistically, making predictions possible without the need for such comprehensive a priori information. However, such a holistic approach obviously limits deeper understanding of the precise contribution of individual mechanisms involved in POCIS.

By comparison, the GSD-model featured many more topological and geometrical descriptors than in the RTD-model. These descriptors showed multicollinearity and therefore the sensitivity analysis could not be performed reliably (Table S7). Simply adding noncollinear descriptors to the RTD-model is also disadvantageous at this point. As the number of descriptors increases, overfitting of data is more likely to occur and would require significantly more case examples for valid application.[46] Model complexity will also

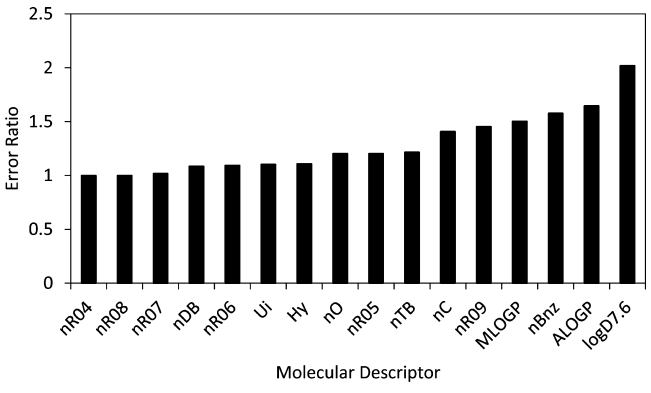

Figure 3. Sensitivity analysis of the optimized RTD-model. Acronyms: nDB/nTB = number of double/triple bonds; nC/nO = number of carbon/oxygen atoms; nR04-nR09= number of 4−9 membered rings; Ui = unsaturation index; Hy = hydrophilic factor; nBnz = number of benzene-like rings; MlogP/AlogP = Moriguchi/Ghose-Crippen logarithm of octanol−water partition coefficient; logD7.6 = logarithm of distribution ratio between octanol and water at pH 7.6.

DOI: 10.1021/acs.est.6b01407
Environ. Sci. Technol. 2016, 50, 7973−7981

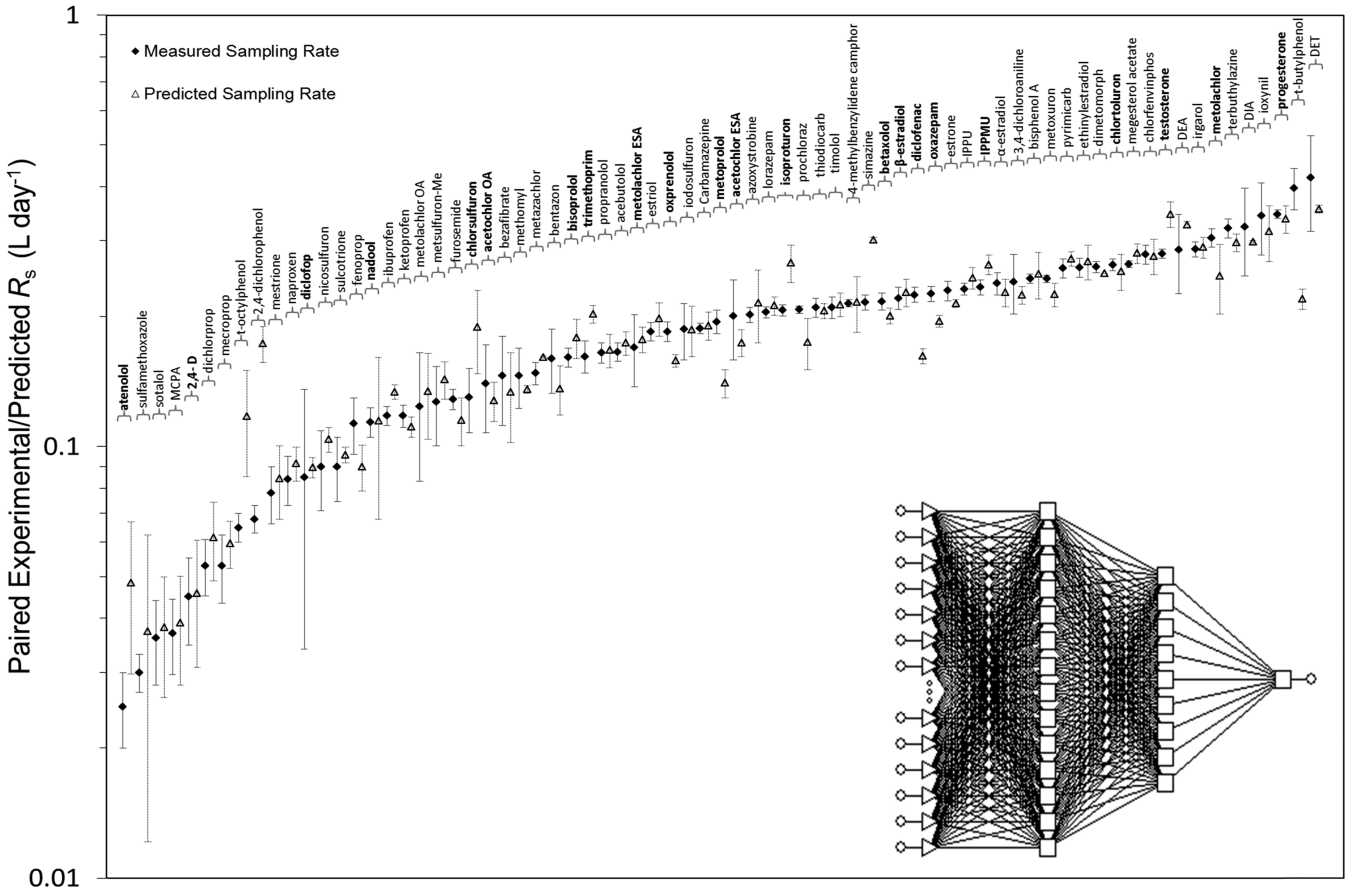

Figure 4. Comparison of the measured and predicted R_s values and their respective variances against the variance in predicted R_s (n = 73) from replicate RTD-models (n = 3). Inset: Optimized 16−14−9−1 model architecture. Compounds in bold represent the verification and blind test cases. All others were used for model training.

limit the ability of the network to generalize when predicting unknown compounds therefore a smaller number of descriptors (and nodes in the hidden layer(s)) is ultimately more beneficial.

Reproducibility of Predicted and Experimentally Determined R_s. Model performance and generalizability is limited by the quality of input data. Measured R_s can differ considerably even within calibration studies performed in the same laboratory. The largest variance in measured R_s used corresponded to diclofop which had a 60% relative standard deviation (RSD), n = 15.[28] Many of the reported R_s values vary by more than 2-fold depending on the methodology used for their estimation.[29] Although pH and temperature during collection of both sets of data used herein were similar, the type of calibration experiment applied was slightly different (flow-through and static renewal) therefore the resulting differences in the R_s estimates from each investigation could have affected the performance of a model. For the six compounds common to both calibration methods that were removed from the original data set used for model optimization, the absolute difference in R_s was 0.088 ± 0.072 L day^{-1} between measurements.

The average % RSD of measured R_s data used herein was 11% (mean deviation was ±0.017 L day^{-1}) (Figure 4). In 45% of all cases, the % RSDs of predicted R_s across triplicate network trained ab initio were better than the % RSDs of the measured data. For several specific cases, such as DET, DIA, diclofop and ioxynil, the experimental variation was relatively large when compared to the variation in predicted R_s. Such deviation in experimentally derived sampling rates can be attributed to several similar factors to those already discussed above (e.g., temperature, pH, flow rate etc.). Figure 4 shows that for cases which had poor predictive accuracy with respect to the mean true value, such as for acetochlor ESA, the standard deviation of the predicted R_s overlapped with the reported experimental variance. A review by Harman et al., suggests that literature reported R_s data should only be considered as an approximation.[47] However, in the absence of a standardized method for POCIS calibration, either in the laboratory or in the field, it would seem that R_s modeling in this way offers similar accuracy and precision without being labor or resource intensive. Calibration experiments for each compound can take several weeks, requiring a large mass of reference material for static renewal and flow through experiments, or very frequent and accurate water sampling for in situ experiments. Furthermore, given that models developed herein are derived from a very limited number of training cases, any new reported R_s data generated by similar methods to those used herein will likely enable better generalizability in the future, as was observed with retention time predictions in reversed-phase liquid chromatography.[27]

External Application to R_s Prediction. To further support the application of the optimized modeling approach, R_s data for several additional benzodiazepines were experimentally determined in our laboratory using a similar approach. In the previous sections, blind test compounds

DOI: 10.1021/acs.est.6b01407
Environ. Sci. Technol. 2016, 50, 7973−7981

were structurally diverse which is logical for testing model accuracy.[48] However, for this experiment, structural similarity was deliberately chosen to externally test its discriminative power. Despite this similarity, it was expected that measured R_s could be different on POCIS given their slight differences in chromatographic retention on C_{18} phases. The retention order of the benzodiazepines was as follows: oxazepam (3.26 min) nitrazepam (3.26 min), clonazepam (3.29 min), lorazepam (3.29 min), alprazolam (3.31 min), midazolam (3.32 min), flunitrazepam (3.37 min) and diazepam (3.58 min). As discussed previously, measurement of R_s often suffers from some imprecision. The calibration experiment performed here was not exempt from this either. Two compounds, lorazepam (R_s: 0.205 L d^{-1}) and oxazepam (R_s: 0.226 L d^{-1}), were originally present in the training set and verification set respectively during model development. The R_s values for these compounds were experimentally determined again here to characterize the variance between the selected calibration method used here and the method by Morin et al.[24] The R_s determined here varied by approximately 0.1 L d^{-1} for both compounds (lorazepam: 0.302 L d^{-1} and oxazepam: 0.327 L d^{-1}). This observation showed again that the difference in calibrations between flow-through and static renewals is not negligible and was an unavoidable limitation of the calibration experiment used here. Standard deviations for the six compounds ranged from ±0.024 to ±0.055 L day^{-1} (n = 9). Overall, the average RSD for all compounds was 20 ± 6% (flunitrazepam: 19%; clonazepam: 13%; nitrazepam: 13%; midazolam: 23%; diazepam: 23%; and alprazolam: 29%) and this variance was consistent with other studies.[29]

As shown in Figure 5, both the GSD- and RTD-models predicted R_s well to within the measured value for all six compounds. The two largest errors in the RTD-model corresponded to those substances with the highest R_s variance (diazepam and alprazolam at 16 and 17%, respectively), but the four remaining compounds showed little inaccuracy (≤5%). In terms of absolute inaccuracy of the measured R_s however, examination of the RTD-model residual errors showed that for all compounds except nitrazepam, that predictions were slightly overestimated. The GSD-model performed worse by comparison (Figure 5). The two largest errors corresponded to nitrazepam and midazolam that were 37% and 43% inaccurate, respectively. The remaining compound inaccuracies were alprazolam (28%), clonazepam (18%), diazepam (10%) and flunitrazepam (19%). The average absolute error for the GSD-model predictions was 0.0437 L d^{-1} and all compounds were predicted within ±0.075 L d^{-1}. By contrast, the RTD-model had an average absolute error of 0.0145 L d^{-1} for these benzodiazepines (and R_s for all compounds were predicted within 0.03 L day^{-1}). These predictions again demonstrated that predicted R_s were similar enough to those determined by experimental determination to be practical.

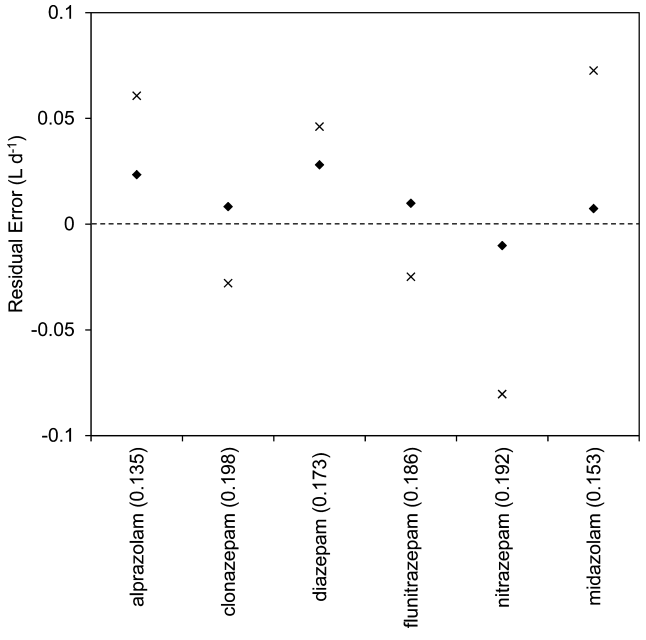

Figure 5. Residual plot of the predicted R_s values for the GSD-model (cross) and RTD-model (diamond) for external prediction validation (as a blind test application) using six additional benzodiazepines. Measured R_s values are displayed in parentheses.

Passive sampling for nonhydrophobic compounds is mainly used for screening purposes and as a semiquantitative technique. Furthermore, in situ exposures are difficult to quantify accurately as laboratory calibrations may not translate well into field R_s due to several factors such as biofouling and other matrix- or environmentally related effects on diffusion, for example. In addition, for reliable quantification the performance reference compound approach has limited availability and application for polar passive sampling due to the strong retention of analytes on HLB sorbents.[49] However, modeling approaches could potentially overcome these limitations if models were built from in situ calibration data. It is also possible that estimation of R_s by in silico approaches may offer a viable alternative for compounds where R_s data cannot be estimated by field studies due to poor correlation of concentrations in water to sample mass on the PSD.[35] Lastly, the two different approaches to the molecular descriptor selection presented show acceptable predictive accuracy for polar compound passive sampling. However, the use of descriptors derived for t_R prediction in a model for R_s prediction holds significant potential for application to new compounds based solely on their SMILES strings by simultaneously allowing preliminary identification (by t_R and high resolution m/z, for example) and estimation of R_s using the same descriptors.

■ ASSOCIATED CONTENT

Supporting Information

The Supporting Information is available free of charge on the ACS Publications website at DOI: 10.1021/acs.est.6b01407.

Additional POCIS extraction and measurement conditions; details on molecular descriptors and data; descriptor collinearity results; and predicted versus measured data for individual compounds(PDF)

■ AUTHOR INFORMATION

Corresponding Author

*Phone: +44 20 7848 3842; fax: +44 20 7848 4980; e-mail: leon.barron@kcl.ac.uk.

Notes

The authors declare no competing financial interest.

■ ACKNOWLEDGMENTS

This work was conducted under funding from the Biotechnology and Biological Sciences Research Council (BBSRC) CASE

DOI: 10.1021/acs.est.6b01407
Environ. Sci. Technol. 2016, 50, 7973−7981

industrial scholarship scheme (Reference BB/K501177/1) and AstraZeneca Global SHE research programme. AstraZeneca is a biopharmaceutical company specialising in the discovery, development, manufacturing and marketing of prescription medicines, including some products measured here. Financial support: EU International Training Network SEWPROF (Marie Curie-FP7-PEOPLE, grant number 317205). Funding bodies played no role in the design of the study or decision to publish. The authors declare no financial conflict of interest.

REFERENCES

(1) European Commission, Regulation (EC) No 1907/2006 of the European Parliament and of the Council of 18 December 2006 concerning the Registration, Evaluation, Authorisation and Restriction of Chemicals (REACH), establishing a European Chemicals Agency, amending Directive 1999/45/EC and repealing Council Regulation (EEC) No 793/93 and Commission Regulation (EC) No 1488/94 as well as Council Directive 76/769/EEC and Commission Directives 91/155/EEC, 93/67/EEC, 93/105/EC and 2000/21/EC. *OJ.* **2006**, *L396*, 1 - 849.

(2) European Commission, Directive 2000/60/EC of the European Parliament and of the Council of 23 October 2000 establishing a framework for Community action in the field of water policy *OJ.* **2000**, *L327*, 1 - 73.

(3) Vrana, B.; Allan, I. J.; Greenwood, R.; Mills, G. A.; Dominiak, E.; Svensson, K.; Knutsson, J.; Morrison, G. Passive sampling techniques for monitoring pollutants in water. *TrAC, Trends Anal. Chem.* **2005**, *24* (10), 845−868.

(4) Miège, C.; Budzinski, H.; Jacquet, R.; Soulier, C.; Pelte, T.; Coquery, M. Polar organic chemical integrative sampler (POCIS): application for monitoring organic micropollutants in wastewater effluent and surface water. *J. Environ. Monit.* **2012**, *14* (2), 626−635.

(5) Prest, H. F.; Richardson, B. J.; Jacobson, L. A.; Vedder, J.; Martin, M. Monitoring organochlorines with semi-permeable membrane devices (SPMDs) and mussels (*Mytilus edulis*) in Corio Bay, Victoria, Australia. *Mar. Pollut. Bull.* **1995**, *30* (8), 543−554.

(6) Gale, R. W. Three-compartment model for contaminant accumulation by semipermeable membrane devices. *Environ. Sci. Technol.* **1998**, *32* (15), 2292−2300.

(7) Bartkow, M. E.; Booij, K.; Kennedy, K. E.; Müller, J. F.; Hawker, D. W. Passive air sampling theory for semivolatile organic compounds. *Chemosphere* **2005**, *60* (2), 170−176.

(8) Huckins, J. N.; Petty, J. D.; Orazio, C. E.; Lebo, J. A.; Clark, R. C.; Gibson, V. L.; Gala, W. R.; Echols, K. R. Determination of uptake kinetics (sampling rates) by lipid-containing semipermeable membrane devices (spmds) for polycyclic aromatic hydrocarbons (pahs) in water. *Environ. Sci. Technol.* **1999**, *33* (21), 3918−3923.

(9) Fedorova, G.; Randak, T.; Golovko, O.; Kodes, V.; Grabicova, K.; Grabic, R. A passive sampling method for detecting analgesics, psycholeptics, antidepressants and illicit drugs in aquatic environments in the Czech Republic. *Sci. Total Environ.* **2014**, *487*, 681−687.

(10) Bailly, E.; Levi, Y.; Karolak, S. Calibration and field evaluation of polar organic chemical integrative sampler (POCIS) for monitoring pharmaceuticals in hospital wastewater. *Environ. Pollut.* **2013**, *174*, 100−105.

(11) Harman, C.; Reid, M.; Thomas, K. V. In situ calibration of a passive sampling device for selected illicit drugs and their metabolites in wastewater, and subsequent year-long assessment of community drug usage. *Environ. Sci. Technol.* **2011**, *45* (13), 5676−5682.

(12) Martínez Bueno, M. J.; Herrera, S.; Munaron, D.; Boillot, C.; Fenet, H.; Chiron, S.; Gómez, E. POCIS passive samplers as a monitoring tool for pharmaceutical residues and their transformation products in marine environment. *Environ. Sci. Pollut. Res.* **2016**, *23*, 1−11.

(13) Baz-Lomba, J. A.; Reid, M. J.; Thomas, K. V. Target and suspect screening of psychoactive substances in sewage-based samples by UHPLC-QTOF. *Anal. Chim. Acta* **2016**, *914*, 81−90.

(14) Mazzella, N.; Lissalde, S.; Moreira, S.; Delmas, F.; Mazellier, P.; Huckins, J. N. Evaluation of the use of performance reference compounds in an oasis-hlb adsorbent based passive sampler for improving water concentration estimates of polar herbicides in freshwater. *Environ. Sci. Technol.* **2010**, *44* (5), 1713−1719.

(15) Harman, C.; Allan, I. J.; Bäuerlein, P. S. The challenge of exposure correction for polar passive samplers the PRC and the POCIS. *Environ. Sci. Technol.* **2011**, *45* (21), 9120−9121.

(16) Harman, C.; Booij, K. Letter to the editor concerning the viewpoint;"Recognizing the limitations of performance reference compound (prc)-calibration technique in passive water sampling. *Environ. Sci. Technol.* **2013**, *48* (1), 3−3.

(17) Bartelt-Hunt, S. L.; Snow, D. D.; Damon-Powell, T.; Brown, D. L.; Prasai, G.; Schwarz, M.; Kolok, A. S. Quantitative evaluation of laboratory uptake rates for pesticides, pharmaceuticals, and steroid hormones using POCIS. *Environ. Toxicol. Chem.* **2011**, *30* (6), 1412−1420.

(18) Stephens, B. S.; Kapernick, A.; Eaglesham, G.; Mueller, J. Aquatic passive sampling of herbicides on naked particle loaded membranes: accelerated measurement and empirical estimation of kinetic parameters. *Environ. Sci. Technol.* **2005**, *39* (22), 8891−8897.

(19) Katritzky, A. R.; Lobanov, V. S.; Karelson, M. QSPR: the correlation and quantitative prediction of chemical and physical properties from structure. *Chem. Soc. Rev.* **1995**, *24* (4), 279−287.

(20) Toropov, A. A.; Toropova, A. P.; Lombardo, A.; Roncaglioni, A.; Benfenati, E.; Gini, G. CORAL: Building up the model for bioconcentration factor and defining it's applicability domain. *Eur. J. Med. Chem.* **2011**, *46* (4), 1400−1403.

(21) Padmanabhan, J.; Parthasarathi, R.; Subramanian, V.; Chattaraj, P. K. QSPR models for polychlorinated biphenyls: n-Octanol/water partition coefficient. *Bioorg. Med. Chem.* **2006**, *14* (4), 1021−1028.

(22) Bade, R.; Bijlsma, L.; Sancho, J. V.; Hernández, F. Critical evaluation of a simple retention time predictor based on LogKow as a complementary tool in the identification of emerging contaminants in water. *Talanta* **2015**, *139*, 143−149.

(23) Miller, T. H.; Musenga, A.; Cowan, D. A.; Barron, L. P. Prediction of chromatographic retention time in high-resolution anti-doping screening data using artificial neural networks. *Anal. Chem.* **2013**, *85* (21), 10330−10337.

(24) Morin, N.; Camilleri, J.; Cren-Olivé, C.; Coquery, M.; Miège, C. Determination of uptake kinetics and sampling rates for 56 organic micropollutants using "pharmaceutical" POCIS. *Talanta* **2013**, *109*, 61−73.

(25) Munro, K.; Miller, T. H.; Martins, C. P. B.; Edge, A. M.; Cowan, D. A.; Barron, L. P. Artificial neural network modelling of pharmaceutical residue retention times in wastewater extracts using gradient liquid chromatography-high resolution mass spectrometry data. *J. Chromatogr. A* **2015**, *1396*, 34−44.

(26) Luan, F.; Xue, C.; Zhang, R.; Zhao, C.; Liu, M.; Hu, Z.; Fan, B. Prediction of retention time of a variety of volatile organic compounds based on the heuristic method and support vector machine. *Anal. Chim. Acta* **2005**, *537* (1−2), 101−110.

(27) Barron, L.; McEneff, G. Gradient liquid chromatographic retention time prediction for suspect screening applications: A critical assessment of a generalised artificial neural network-based approach across ten multi-residue reversed-phase analytical methods. *Talanta* **2015**, *147* (147), 261−270.

(28) Fauvelle, V.; Mazzella, N.; Delmas, F.; Madarassou, K.; Eon, M.; Budzinski, H. Use of mixed-mode ion exchange sorbent for the passive sampling of organic acids by polar organic chemical integrative sampler (POCIS). *Environ. Sci. Technol.* **2012**, *46* (24), 13344−13353.

(29) Morin, N.; Miège, C.; Coquery, M.; Randon, J. Chemical calibration, performance, validation and applications of the polar organic chemical integrative sampler (POCIS) in aquatic environments. *TrAC, Trends Anal. Chem.* **2012**, *36*, 144−175.

(30) Bade, R.; Bijlsma, L.; Miller, T. H.; Barron, L. P.; Sancho, J. V.; Hernandez, F. Suspect screening of large numbers of emerging contaminants in environmental waters using artificial neural networks for chromatographic retention time prediction and high resolution

DOI: 10.1021/acs.est.6b01407
Environ. Sci. Technol. 2016, 50, 7973−7981

mass spectrometry data analysis. *Sci. Total Environ.* **2015**, *538*, 934−941.
(31) Booij, K.; Hofmans, H. E.; Fischer, C. V.; Van Weerlee, E. M. Temperature-dependent uptake rates of nonpolar organic compounds by semipermeable membrane devices and low-density polyethylene membranes. *Environ. Sci. Technol.* **2003**, *37* (2), 361−366.
(32) Mazzella, N.; Dubernet, J.-F.; Delmas, F. Determination of kinetic and equilibrium regimes in the operation of polar organic chemical integrative samplers: Application to the passive sampling of the polar herbicides in aquatic environments. *J. Chromatogr. A* **2007**, *1154* (1), 42−51.
(33) Thomatou, A.-A.; Zacharias, I.; Hela, D.; Konstantinou, I. Passive sampling of selected pesticides in aquatic environment using polar organic chemical integrative samplers. *Environ. Sci. Pollut. Res.* **2011**, *18* (7), 1222−1233.
(34) Ibrahim, I.; Togola, A.; Gonzalez, C. Polar organic chemical integrative sampler (POCIS) uptake rates for 17 polar pesticides and degradation products: laboratory calibration. *Environ. Sci. Pollut. Res.* **2013**, *20* (6), 3679−3687.
(35) Moschet, C.; Vermeirssen, E. L. M.; Singer, H.; Stamm, C.; Hollender, J. Evaluation of in-situ calibration of Chemcatcher passive samplers for 322 micropollutants in agricultural and urban affected rivers. *Water Res.* **2015**, *71*, 306−317.
(36) Bäuerlein, P. S.; Mansell, J. E.; ter Laak, T. L.; de Voogt, P. Sorption behavior of charged and neutral polar organic compounds on solid phase extraction materials: which functional group governs sorption? *Environ. Sci. Technol.* **2012**, *46* (2), 954−961.
(37) Vrana, B.; Mills, G. A.; Kotterman, M.; Leonards, P.; Booij, K.; Greenwood, R. Modelling and field application of the Chemcatcher passive sampler calibration data for the monitoring of hydrophobic organic pollutants in water. *Environ. Pollut.* **2007**, *145* (3), 895−904.
(38) Rusina, T. P.; Smedes, F.; Klanova, J.; Booij, K.; Holoubek, I. Polymer selection for passive sampling: A comparison of critical properties. *Chemosphere* **2007**, *68* (7), 1344−1351.
(39) Gramatica, P.; Corradi, M.; Consonni, V. Modelling and prediction of soil sorption coefficients of non-ionic organic pesticides by molecular descriptors. *Chemosphere* **2000**, *41* (5), 763−777.
(40) Barron, L.; Havel, J.; Purcell, M.; Szpak, M.; Kelleher, B.; Paull, B. Predicting sorption of pharmaceuticals and personal care products onto soil and digested sludge using artificial neural networks. *Analyst* **2009**, *134* (4), 663−670.
(41) Rusina, T. P.; Smedes, F.; Koblizkova, M.; Klanova, J. Calibration of silicone rubber passive samplers: Experimental and modeled relations between sampling rate and compound properties. *Environ. Sci. Technol.* **2010**, *44* (1), 362−367.
(42) Nightingale, E., Jr. Phenomenological theory of ion solvation. Effective radii of hydrated ions. *J. Phys. Chem.* **1959**, *63* (9), 1381−1387.
(43) Schramke, J. A.; Murphy, S. F.; Doucette, W. J.; Hintze, W. D. Prediction of aqueous diffusion coefficients for organic compounds at 25 C. *Chemosphere* **1999**, *38* (10), 2381−2406.
(44) La-Scalea, M. A.; Menezes, C. M. S.; Ferreira, E. I. Molecular volume calculation using AM1 semi-empirical method toward diffusion coefficients and electrophoretic mobility estimates in aqueous solution. *J. Mol. Struct.: THEOCHEM* **2005**, *730* (1), 111−120.
(45) Gharagheizi, F. Determination of diffusion coefficient of organic compounds in water using a simple molecular-based method. *Ind. Eng. Chem. Res.* **2012**, *51* (6), 2797−2803.
(46) Hawkins, D. M. The problem of overfitting. *J. Chem. Inf. Comp. Sci.* **2004**, *44* (1), 1−12.
(47) Harman, C.; Allan, I. J.; Vermeirssen, E. L. M. Calibration and use of the polar organic chemical integrative sampler—a critical review. *Environ. Toxicol. Chem.* **2012**, *31* (12), 2724−2738.
(48) Bowden, G. J.; Maier, H. R.; Dandy, G. C. Optimal division of data for neural network models in water resources applications. *Water Resour. Res.* **2002**, *38* (2), 2−1−2-11.
(49) Alvarez, D. A.; Petty, J. D.; Huckins, J. N.; Jones-Lepp, T. L.; Getting, D. T.; Goddard, J. P.; Manahan, S. E. Development of a passive, in situ, integrative sampler for hydrophilic organic contaminants in aquatic environments. *Environ. Toxicol. Chem.* **2004**, *23* (7), 1640−1648.

DOI: 10.1021/acs.est.6b01407
Environ. Sci. Technol. 2016, 50, 7973−7981

Forensic Science International: Genetics 28 (2017) 225–236

Contents lists available at ScienceDirect

Forensic Science International: Genetics

journal homepage: www.elsevier.com/locate/fsig

Research paper

DNA methylation-based forensic age prediction using artificial neural networks and next generation sequencing

Athina Vidaki[2], David Ballard[*], Anastasia Aliferi, Thomas H. Miller, Leon P. Barron[1], Denise Syndercombe Court[1]

Department of Pharmacy and Forensic Science, King's College London, Franklin-Wilkins Building, 150 Stamford Street, London, UK

ARTICLE INFO

Article history:
Received 17 November 2016
Received in revised form 7 February 2017
Accepted 16 February 2017
Available online 28 February 2017

Keywords:
Forensic epigenetics
Chronological age prediction
DNA methylation
Next generation sequencing
Artificial neural networks

ABSTRACT

The ability to estimate the age of the donor from recovered biological material at a crime scene can be of substantial value in forensic investigations. Aging can be complex and is associated with various molecular modifications in cells that accumulate over a person's lifetime including epigenetic patterns. The aim of this study was to use age-specific DNA methylation patterns to generate an accurate model for the prediction of chronological age using data from whole blood. In total, 45 age-associated CpG sites were selected based on their reported age coefficients in a previous extensive study and investigated using publicly available methylation data obtained from 1156 whole blood samples (aged 2–90 years) analysed with Illumina's genome-wide methylation platforms (27 K/450 K). Applying stepwise regression for variable selection, 23 of these CpG sites were identified that could significantly contribute to age prediction modelling and multiple regression analysis carried out with these markers provided an accurate prediction of age (R^2 = 0.92, mean absolute error (MAE) = 4.6 years). However, applying machine learning, and more specifically a generalised regression neural network model, the age prediction significantly improved (R^2 = 0.96) with a MAE = 3.3 years for the training set and 4.4 years for a blind test set of 231 cases. The machine learning approach used 16 CpG sites, located in 16 different genomic regions, with the top 3 predictors of age belonged to the genes NHLRC1, SCGN and CSNK1D. The proposed model was further tested using independent cohorts of 53 monozygotic twins (MAE = 7.1 years) and a cohort of 1011 disease state individuals (MAE = 7.2 years). Furthermore, we highlighted the age markers' potential applicability in samples other than blood by predicting age with similar accuracy in 265 saliva samples (R^2 = 0.96) with a MAE = 3.2 years (training set) and 4.0 years (blind test). In an attempt to create a sensitive and accurate age prediction test, a next generation sequencing (NGS)-based method able to quantify the methylation status of the selected 16 CpG sites was developed using the Illumina MiSeq® platform. The method was validated using DNA standards of known methylation levels and the age prediction accuracy has been initially assessed in a set of 46 whole blood samples. Although the resulted prediction accuracy using the NGS data was lower compared to the original model (MAE = 7.5 years), it is expected that future optimization of our strategy to account for technical variation as well as increasing the sample size will improve both the prediction accuracy and reproducibility.

1. Introduction

Body fluids such as blood are amongst the most important biological evidence recovered from crime scenes. Identification of the donor can be achieved through short tandem repeat (STR) profiling; nevertheless, extracting additional information regarding the donor, such as chronological age, could provide significant investigative leads and prove very useful in police investigations. For intelligence purposes, estimating the age of a recovered stain's donor could potentially narrow down the number of suspects, especially in cases where an eyewitness is not available.

Over the last decades, research has shown that aging is a very complex process influenced by various genetic, lifestyle and environmental factors. It causes a variety of molecular modifications and adjustments in tissues or organs that accumulate over an

* Corresponding author.
E-mail addresses: a.vidaki@erasmusmc.nl (A. Vidaki), david.ballard@kcl.ac.uk (D. Ballard).
[1] These authors co-led this work.
[2] Present address: Department of Genetic Identification, Erasmus MC University Medical Center Rotterdam, P.O. Box 2040, 3000 CA Rotterdam, The Netherlands.

http://dx.doi.org/10.1016/j.fsigen.2017.02.009

individual's lifetime, including chemical modifications [1], gene expression alterations [2] and variations at the DNA level [3,4]. Although there have been various approaches to estimate age at death in human remains or chronological age in living individuals [5,6], most of these attempts show limitations including low sensitivity and prediction accuracy as well as lack of standardisation, restraining their applicability in crime scene samples. Undoubtedly, developing an age prediction test is a major challenge for forensic scientists since they would need to be able to apply and validate it using minute or degraded samples consisting of a range of tissues and body fluids. As a first step, the generation of reliable age prediction models is a necessity.

It is believed that epigenetic analysis could serve as an alternative or supplementary method to existing approaches since particularly DNA methylation is well-known to be one of the mechanisms responsible for cell differentiation and the cellular response to aging [7,8]. It is generally suggested that there is an increase in global epigenetic drift with age [9] and various genome-wide methylation analyses have revealed a substantial decrease in global DNA methylation levels with advancing age [10]. Changes in DNA methylation patterns due to aging are quickly observed during the first months of an individual's life and throughout childhood [11,12]. Cumulative evidence points towards the distinct contributions of genetic [13], environmental [14,15] and stochastic factors to DNA methylation levels at single genomic areas. In order to identify specific age-associated differentially methylated CpG sites for a particular body fluid, scientists have chosen to perform genome-wide studies [7,16–20]. Interestingly, >95% of the associated sites were located within 500 bp of the transcriptional start site of the associated gene, implying a connection with regulation of gene expression [16].

From an intelligence perspective, it would be very advantageous to translate observed biological age-associated DNA methylation differences in a way that the chronological age of an individual is revealed through an age prediction model. Overall, current methodologies for methylation analysis can be divided into genome-wide or gene-specific depending on the number of CpG sites being investigated. As an example, following analysis of >650 whole blood samples from individuals aged 19–101 years using a genome-wide approach, Hannum et al. built a quantitative model using 71 highly age-predictive markers with a correlation between true and predicted age of 0.96 and an average error of 3.9 years [21]. However, it should be emphasised that each tissue or body fluid could show a different age-associated DNA methylation pattern; therefore, predicting age across a broad spectrum of human tissues and cell types could be a very challenging task. Testing 13 different cell types, Kock and Wagner [22] proposed a set of 5 CpG sites, however the precision of their model was slightly lower (mean error of 9.3 years). While the genome-wide DNA methylation arrays are considered as the best tool during the discovery phase of potential age-associated CpG sites, targeted sequencing is also required to validate any association. Replicating the detected methylation levels is necessary to confirm the utility of the selected CpG sites and assess their performance in a different dataset. From a forensic perspective, the main challenge to be faced is the low quality and quantity of forensic specimens, making it impossible to implement such age prediction models (based on hundreds of markers) in forensic casework in their current form. Therefore, developing an accurate, robust and sensitive method that can analyse the proposed CpG sites in forensic-type samples is essential.

In an attempt to narrow down the number of markers needed for accurate prediction, Weidner et al. [23] performed a comprehensive analysis of blood methylation profiles and found that the methylation levels of only 3 CpGs – located in the integrin, alpha 2b (*ITGA2B*), aspartoacylase (*ASPA*) and phosphodiesterase 4C, cAMP specific (*PDE4C*) genes – were substantial to create an epigenetic-aging-signature with a mean absolute deviation (MAD) from chronological age of 5.4 years (RMSE = 7.2 years). Within the forensic field, recent age prediction models based on a small number of CpG sites have also been studied, mainly in blood [24–30], but also in other tissues such as saliva [31], semen [32] and teeth [33]. However, most of these models are based on a limited number of individuals and some still lack validation in an independent cohort of samples. The reported mean prediction errors range between 4–8 years (especially in validation sets where available), suggesting that current tools allow for the prediction of an individual's decade (for example, the blood belongs to someone in their 30s) rather than an accurate prediction outcome. In this study, in an attempt to minimise the prediction error and increase model accuracy, the potential of artificial neural networks (ANN) was explored together with regression analysis. ANNs are a group of machine learning algorithms inspired by biological systems and have previously been used successfully to find underlying trends in complex datasets. There are various types of ANNs and the best type to be used depends on the application. Normally, ANNs consist of discrete layers; the first is the input layer, which contains the dependent variables (i.e. methylation data from age-dependent CpG sites). Each of these variables are connected to a middle layer via an optimised number of 'nodes', which, in turn, interconnect all inputs to each other and eventually to the third layer containing the designated output variable (i.e. age in years). During the learning process, ANNs generally aim to minimise the error in output estimations by systematically optimising the connective weights between the nodes within the network. Given their ability to learn holistically and often in a non-linear fashion, ANNs have been extensively studied and applied in a range of other applications [34,35].

Also, while most of these studies are based on targeted methylation detection via pyrosequencing, qPCR [36], melting curve analysis [37] and the EpiTYPER system [38,39] have also been used. Although pyrosequencing has been the gold standard for such analysis since its introduction [40,41] and shows various advantages over other methylation techniques [42], it is mainly performed as single reactions because multiplex pyrosequencing can be complex [43]. In this study we also address the question of whether a methylation assay based on benchtop next-generation sequencing (NGS) of a small number of CpG sites could not only provide focused 5-methylcytosine quantification with base resolution, but also allow for a sensitive and less costly age prediction approach with similar accuracy to genome-wide DNA methylation profiling approaches that could be applied in a forensic setting.

Towards achieving this aim, we pooled publicly available DNA methylation profiles derived from whole blood samples to investigate a subset of 45 previously reported age-associated CpGs, which belong to 45 different genomic locations/genes, in an attempt to identify those displaying the highest correlation with age. Following multivariate, linear regression and ANN analysis, we identified an epigenetic aging signature based on the methylation status of a total of 16 CpG sites. To allow for reliable age predictions, a next-generation sequencing protocol based on Illumina's MiSeq® platform was developed and optimised using commercially available DNA methylation standards. To the best of our knowledge, this is the first study that uses machine learning, via ANNs, together with an NGS-based DNA methylation detection method for forensic age prediction.

2. Materials and methods

2.1. Description of genome-wide DNA methylation data sets

Genome-wide profiling has led to a more comprehensive understanding of gene regulation epigenetic mechanisms.

Illumina's Human Methylation BeadChip technology is one of the most commonly used genome-wide methylation platforms that allows for simultaneous measurement of the methylation status of 27,578 (27 K chip) or 482,421 (450 K chip) CpG sites in the genome at single nucleotide resolution. Thousands of samples have been assayed using this platform in the literature and researchers have made some of these genome-wide methylation data available in online databases such as the National Center for Biotechnology Information Gene Expression Omnibus (GEO).

In order to build the age prediction model, data from a total of 1156 whole blood samples were collected from individuals aged between 2 and 90 years old and from various ethnic backgrounds (mean age = 44) from seven genome-wide DNA methylation studies summarised in Table S1 [12,16,17,19,21,44]. Methylation data gathered from individual blood cell types such as peripheral blood mononuclear cells (PBMCs) or CD4+ cells were avoided since the ultimate aim of this research was to predict age from whole blood stains. Samples were carefully collected so that there was an equal representation of samples for all age groups, aiming for ~100–150 samples per decade (see Fig. S1). The gathered samples were either healthy control volunteers in studies investigating DNA methylation changes of various diseases (usually above 40 years old) or were part of studies investigating epigenetic effects of aging (usually either very young or very old), hence collecting sufficient samples of 'middle' age (particularly 30–40 years old) was quite challenging. Additionally, even though the dataset included roughly equal numbers of both females and males (597 and 559 respectively), there was an uneven gender distribution within specific age groups due to the selected studies' design (Fig. S1). However, it was concluded that this should not affect age prediction since none of the sex-specific differentially methylated CpG sites previously reported in the literature, following analysis with Illumina's 27 K platform, were included in the group of selected markers in this study [44].

Following the development of age prediction models, environmental influences on age prediction were further investigated using an independent cohort of healthy blood samples comprising of 53 female monozygotic twin pairs collected from two genome-wide studies [7,45] (Table S1). Secondly, to test the robustness of the selected age-associated CpG sites when applied to body fluids other than blood, methylation data from 265 saliva samples was collected from two different studies [46,47] (Table S1). One key limitation when building a model for body fluids other than blood is the scarcity of non-blood based genome-wide studies that are both run on one of the Illumina platforms and include information regarding the volunteers' age. Finally, according to Horvath [48] the correlation between the observed and expected age in cancer/diseased tissues was generally weak as there was evidence of significant biological age acceleration in most patients included in his study (n = 5826). However, since there is usually no information regarding possible disease status in a forensic blood sample of unknown origin, it is important that the proposed age prediction model can be universally applied. To assess potential variability in age prediction, a data set including blood samples from a total of 1011 (577 females and 434 males) individuals aged 17–91 years suffering from various diseases and cancers analysed on Illumina's 27 K or 450 K platforms was analysed [8,17,19,49–52] (Table S2).

In each dataset, the DNA methylation value of each CpG site is calculated as a beta (β) value, which is interpreted as the average methylation for a particular site taking into account all cells forming a body fluid sample. Beta values can range from 0, representing the unmethylated sites to 1, corresponding to those completely methylated. Prior to analysis, genome-wide DNA methylation datasets underwent a quality control analysis to account for common experimental biases, such as batch effects using the IBM SPSS v.22 software. Therefore, we used overall mean detected methylation levels to normalise the methylation levels between different datasets, but without removing the occurring DNA methylation variation, partly explained by age. We used the normalised methylation values for age prediction analysis.

2.2. Selection of potential age-associated CpG sites

The ability to accurately predict age regardless of the tissue type would be very advantageous in criminal investigations where the identification of the tissue source of a sample is often challenging. Even if the purpose of this study was to identify age-associated CpG sites in blood, the ability to apply a potential model in other tissues with similar accuracy would save both time and resources. In an attempt to select more robust age-associated differentially-methylated markers across tissues, the study by Horvath [48] was chosen as the most appropriate. The author built an age prediction model applicable in various tissues using a total of 353 markers, which were categorised by a coefficient value (ranging from −1.719 to 3.067) that relates the CpG sites to a transformed version of age. In order to cover all potential correlations with age and maximise the chance of selecting suitable markers, 45 CpG sites from the 353 marker pool included in Hovarth's model were selected, specifically this included those displaying the highest (positive/negative) coefficients (Table S3). Their chromosomal location was confirmed using the Ensembl genome browser; most are located within or near a gene. While it has previously been demonstrated that the ELOVL2 marker can be a good predictor of chronological age in blood [24], there is an absence of genome-wide data for the relevant CpG sites, hence these sites could not be included in this study.

2.3. Statistical analysis

Statistical analysis was performed using STATISTICA software v.13.1 (StatSoft Inc., 2014, Oklahome, United States). To assess data distribution, the minimum, maximum, mean and standard deviation (SD) were calculated. Hypothesis testing was evaluated by calculating *p*-values with a significance cut-off of 0.05. Multivariate analysis was used to assess if other defined factors in the datasets (such as sex) were significantly associated with age. The degree of linear association between methylation levels and chronological age was measured by calculating the correlation coefficient (r), while a general regression model, implemented using a forward stepwise approach, was used to assess the accuracy of age prediction with the selected marker candidates. The fitted regression line explains a proportion of the variability in the dependent variable (y) and the residuals indicate the amount of unexplained variability. The proportion of the total variation explained by the model was also assessed by the goodness-of-fit of the line (R^2 value). In some cases, regression lines were linear but there were cases where the relationship between two variables was curved revealing non-linear relationships. For example, in methylation quantification by bisulfite PCR the polynomial regression was often observed either as quadratic curves ($y = ax^2 + bx + c$) or cubic curves ($y = ax^3 + bx^2 + cx + d$).

2.4. Artificial neural network (ANN) modelling

The age-specific CpG site methylation data was used to build, train and test a suitable ANN for chronological age prediction. In this study, several ANN types including 2- and 3-layer multi-layer perceptrons (MLPs), radial basis functions (RBFs), probabilistic neural networks (PNNs) and generalised regression neural networks (GRNNs) were built and their performance critically evaluated using Trajan v6 software (Trajan Software Ltd., Lincolnshire, UK). Briefly, optimisation of each ANN type and

architecture was performed in a number of stages. Firstly, all input variables (45 selected age-associated CpG sites) were included in the initial design phase to elucidate which ANN model type was likely to be most applicable to age prediction. Following this, the most promising network type (GRNN) was optimised further in a series of stages. GRNNs are a type of ANN that use a combination of a radial basis and linear functions to perform the output estimation [53]. The first optimisation stage was performed to finalise training and verification dataset proportions by assessing the performance of the mean inaccuracy of the blind test sets. Depending on the application, between 50% and 70% of the full 1156 cases were assigned as training cases with equal splitting of the remaining proportion between verification and blind test cases. This was repeated several times for each proportion value and with random assignment of cases for training, verification and testing every time. The network designer tool was set to balance GRNN verification set errors against network diversity to cover as many architectures as possible across all model types. In total, 10^8 architectures were investigated in each stage and 50 of the best GRNN networks were ranked by correlation and output error separately for the training, verification and blind test datasets. In Stage 2, advanced random sampling was applied whereby training and verification cases were assigned as per the best performing GRNN architecture from Stage 1, but blind test cases were fixed. In Stage 3, the reproducibility of ten replicates of the model was assessed by selecting the best GRNN from Stage 2 and fixing all training, verification and blind test subsets and the best model overall was then selected from this pool. The variability in age estimations for all subsets across all replicate GRNN models was then expressed as mean error ± one standard deviation. Following this, all ten networks were each subjected to a sensitivity analysis to assess the relative contribution of each CpG site input to model accuracy. The error ratio was calculated as the ratio of the observed GRNN test error using all variables to the error obtained when each variable was systematically removed. Larger error ratio values represented more network dependency on that specific CpG site variable. All input variables were also assessed for collinearity using SPSS Statistics v23 (IBM Corporation, New York, USA).

2.5. Body fluid samples and DNA preparation

A set of whole blood samples were collected to test the developed ANN model with the proposed methodology. The present study was carried out following full ethical approval by King's College London Biomedical Sciences, Dentistry, Medicine and Natural & Mathematical Sciences Research Ethics Subcommittee (BDM/13/14-30). Full informed consent was obtained from the donors or their parents in case of under-aged individuals prior to collection. Whole blood was collected from a total of 46 individuals aged 11–76 years old coming from various ethnic backgrounds. Genomic DNA was isolated from 200 μl of whole blood using the BioRobot EZ1 DNA blood kit (QIAGEN, Hilden, Germany). Following purification, samples were quantified using the Quantifiler Human DNA Quantification kit (Applied Biosystems, Foster City, United States). 500 ng of each DNA sample was used for bisulfite conversion using the MethylEdge Bisulfite Conversion system (Promega, Madison, United States) and bisulfite-treated DNA was eluted in 20 μl of elution buffer. For control and linearity analysis, a set of DNA standards of known methylation levels ranging from 0% to 100% (EpigenDx, Hopkinton, United States) were used.

2.6. Bisulfite PCRs

In this study the online Ensembl genome browser (GRCh37/hg19) genome was used to obtain the required genetic information for assay design. Primers were designed to specifically amplify bisulphite-treated DNA using the online-tool BiSearch [54] and design parameters were adjusted to account for the generally low

Table 1
Designed bisulfite PCR assays.

CpG site	Gene	Primer Sequence (5′-3′)		Amplicon Length (bp)
cg19761273	CSNK1D	F	TGTTTAGTTTGAAGATTGAG	150
		R	CCTTATTTCCTTTACAAAAA	
cg27544190	C21orf63	F	GGGTAGGATTAAAGTTGA	106
		R	CTTAAAAATAACAATCCCC	
cg03286783	CASC4	F	GTTTTAGTTAGTGGGTG	181
		R	CCCCTCCTCAAATCAAA	
cg01511567	SSRP1	F	TATTAGATTTAGTATAGGGG	132
		R	CCCACAACTATTCAAATA	
cg07158339	FXN	F	GGAATATGTTTTGTTTAAAA	122
		R	TAATTAACCTCTCTATACCT	
cg05442902	P2RXL1	F	GTATGTTTTGGTTTTTGT	109
		R	AATAACCTCTAAACTAACC	
cg24450312	RASSF5	F	GTTATTTATAGAGTTTGAG	201
		R	TCTACTACAAACCAAA	
cg17274064	ERG	F	AGGGAATAAGTATTTTTT	139
		R	CTCACAATCAAACTTCTATATAC	
cg02085507	TRIP10	F	GTTAATGGATTTGGTTTTG	186
		R	AACTCAAAAAATCCTTCCT	
cg20692569	FZD9	F	TTGTTGTTGTGGTAGT	160
		R	AACCCAACAAATTAAA	
cg04528819	KLF14	F	AATAGGTTTTGGTGTAGTT	138
		R	CAACCTCTAATAAATTCTCT	
cg08370996	NR2F2	F	GTGTTAAAGTTTATTATATAGA	187
		R	AAAAAAAAAAACACACAC	
cg04084157	VGF	F	GAGGGTGTTTGTTTTTTT	111
		R	AACATTTCATTCATTCATTC	
cg22736354	NHLRC1	F	GTTGAGTTTAGGAGTTTTAT	201
		R	CTTTAAAAAATTTAACCACC	
cg06493994	SCGN	F	GGAGAGTAAGTTAAGAAATA	150
		R	AACCTACCAAAAACCAAC	
cg02479575	C19orf30	F	GGAGGAGAATGTTATTTATT	143
		R	CTATCCAAAATTCTAAAAAC	

efficiency of bisulphite PCR and common mis-priming events due to the T-richness of the bisulphite-treated DNA sequences. A total of 16 singleplex assays were designed to investigate the selected age-associated CpG sites; each bisulfite PCR assay includes a PCR primer set (forward and reverse), none of which binds to areas containing other CpG sites to avoid potential bias (Table 1). Information on the obtained amplicons including their chromosomal location and number of included bisulfite-conversion controls and CpG sites are presented in Table S4. Although the assays were primarily designed to interrogate the 16 selected CpG sites, sequencing of the entire PCR product on the MiSeq® platform (Illumina, San Diego, United States) allowed for the co-analysis of all adjacent CpG sites included in the fragment. Briefly, PCRs were carried out in 13 μl reaction volumes containing a final concentration of 1X ZymoTaq premix (Zymo Research, Irvine, United States), 3.2 mM $MgCl_2$, 0.4 μM forward and reverse primers, with the addition of 1 μl of bisulfite DNA template. The thermocycling program used was: 95 °C for 10 min, followed by 30 cycles of 94 °C for 30 s, T_m for 30 s, 72 °C for 30 s, and a final extension step of 72 °C for 7 min. The optimised T_m was as follows: 48 °C for cg07158339, cg17274064, cg02085507, cg20692569 and cg02479575, 50 °C for cg19761273, cg27544190, cg01511567, cg24450312 and cg04528819 and 52 °C for cg03286783, cg05442902, cg08370996, cg04084157, cg22736354, cg06493994. Following amplification, the quality of PCR products was assessed on a 2% agarose gel if necessary.

2.7. Next generation sequencing using illumina MiSeq®

Singleplex PCR products were pooled together and purified using the MinElute PCR purification kit (QIAGEN) in 16 μl of DNase-free water. Prior to library preparation, all purified samples were quantified using the Qubit dsDNA HS Assay kit (Invitrogen, Carlsbad, United States) according to the manufacturer's instructions and in combination with the Qubit 2.0 Fluorometer instrument. Pooled PCR products were diluted appropriately to provide 50 ng of amplified DNA within 25 μl. Library preparation was performed using the KAPA Hyper Prep kit for Illumina (Kapa Biosystems, Wilmington, United States) with half volume reactions. Library amplification proceeded with 8 cycles while the clean-up steps were performed using the AMPure XP Beads (Beckman Coulter Genomics, Danvers, United States) and the Illumina Resuspension buffer (Illumina). To assess libraries' quantity, purified libraries were diluted 1:4000 in DNase-free water and quantified using the KAPA Library Quantification Kit for Illumina platforms (Kapa Biosystems). Indexed DNA libraries were then normalised to 4 nM using Tris-HCL 10 mM/pH 8.5 with 0.1% Tween and were pooled together to a final volume of 240 μl. Using freshly made 0.2N NaOH, 5 μl of pooled libraries were denatured and, through dilution with pre-chilled Hybridisation buffer (HT1, Illumina), a 10pM library was obtained. Finally, 13% diluted PhiX control (80 μl) was added to the library and sequencing was performed using the 300-cycle MiSeq® reagent v2 cartridge (Illumina). The preparation of the flow cell and the set-up of the instrument were performed per manufacturer's instructions. It should be noted that the instrument was set up to run a paired-end read of 150 bp of DNA sequence from both ends of the library products. Auto analysis was set up as a FASTQ-only method.

Following auto-analysis by the MiSeq® Reporter Software, which separated the millions of generated sequences into the constituent samples on the basis of the ligated adaptor tags, collated sequences were packaged in a text-based format (FASTQ files). For alignment, we used a custom bisulfite-converted reference genome containing all analysed DNA sequences, which is quicker and more user-friendly compared to available alignments using the entire genome. Sequences within these FASTQ files were aligned using a Burrows-Wheeler alignment (BWA) algorithm. This process was implemented in the BWA program [55] using the maximum entropy method (mem) algorithm that matched the sequences generated to the respective methylation marker (i.e. a sequence obtained from the PCR product of any specific marker would be most similar to the reference sequence for that marker, and hence the software would align this sequence with that marker). Therefore, the millions of sequences contained within the FASTQ file can be associated with their respective marker, giving potentially hundreds of thousands of individual sequences all aligned in parallel to a specific reference sequence/marker. At the conclusion of this alignment process, a sequence alignment/map (SAM) file was produced, which was further modified using SAMtools [56] to facilitate the conversion into a BAM file. The Genome Analysis Toolkit (GATK) [57] was subsequently used to interrogate this BAM file by targeting specific positions in these aligned sequences (i.e. each CpG site) and reporting the number of sequences containing a C and the number of sequences containing a T at this position. In this way it was possible to assess the methylation state at every studied CpG site. The unified genotyper algorithm was employed within GATK to produce these genotype data for each CpG site, which were written into a variant call format (vcf) file that could subsequently be manipulated in Excel. The Integrative Genomics Viewer software (IGV) was used for visualisation and verification of the alignment. While in most cases the bisulfite conversion rates were >99%, methylation values were 'corrected' by taking into account the mean bisulfite conversion rates per fragment calculated by the built-in conversion controls (non-CpG cytosines). The obtained methylation values for each CpG site were further normalised using the resulting equations of standard curves created from known DNA methylation standards. Lastly, to account for potential methodology-dependent differences, the NGS derived methylation values were normalised to the genome-wide data, used to build the prediction model, by applying the method previously described when normalising the different genome-wide data sets.

3. Results and discussion

3.1. Age-associated DNA methylation changes in blood

Using publicly available DNA methylation databases, normalised beta values for the selected 45 CpG sites were gathered for a total of 1156 whole blood samples from individuals 2–90 years old. Methylation fractions (zero to one) were compared against the actual age of each individual in order to investigate potential correlation between methylation levels and age (example graphs for 16 out of 45 CpGs are presented in Fig. 1). As expected, some CpG sites showed greater variation than others; for example, cg07455279 (NDUFA3) demonstrated the largest methylation range (difference between the lowest and highest detected methylation value for each marker) (0.815) while cg05442902 (P2RXL1) usually showed low methylation levels (<0.387). In general, the methylation of certain CpG sites such as cg19761273 (CSNK1D), cg01511567 (SSRP1), cg07158339 (FXN) and cg05442902 (P2RXL1) was clearly decreasing with advancing age, while others, cg20692569 (FZD9), cg04528819 (KLF14), cg04084157 (VGF) and cg22736354 (NHLRC1) to name but a few, were increasingly methylated over time. These observations align with the age relationship that Horvath reported in his study [48].

3.2. Identification of the epigenetic aging signature

The observed age-associated methylation changes for all markers were assessed for their statistical significance in an

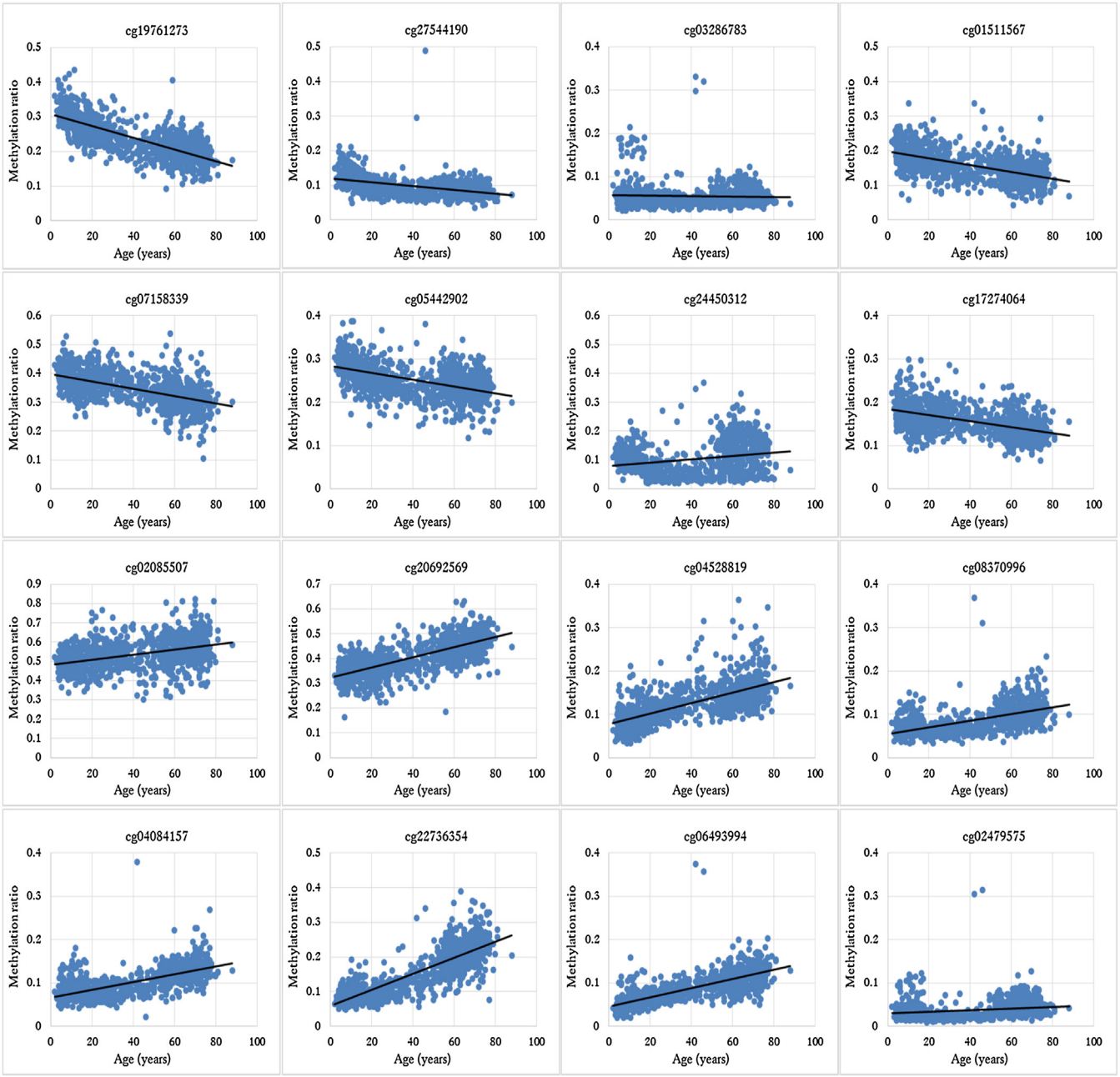

Fig. 1. Change of methylation levels over advancing age for the 16 CpG sites included in the eventual ANN model.

attempt to identify those sites that could form the proposed epigenetic-aging-signature. Firstly, using multivariate analysis and testing for the effect of gender and ethnicity on age-associated methylation, no significant correlation was determined ($p = 0.77$ and $p = 0.09$ respectively). Using linear regression analysis, a significant correlation between methylation levels and age ($p < 0.05$) was confirmed for 25 out of the 45 CpG sites (Table S5). Applying stepwise multiple linear regression for variable selection, we obtained similar results regarding the importance and order of markers (Table S6). In order to perform this type of analysis, the markers were added one by one into the age prediction model until there was no statistical improvement. As a result, the use of 23 CpG sites resulted in a value of $R^2 = 0.923$, which was not further improved with the addition of more markers. All 23 age-associated CpG sites revealed following stepwise regression are included in the set of markers identified after individual linear regression analysis. In both analyses cg22736354 (NHLRC1) was found to be the most important. Interestingly, while cg07455279 (NDUFA3) had demonstrated the higher methylation range, it did not demonstrate a statistically significant correlation with age, which mirrors the complexity and high, inter-individually variable nature of methylation patterns.

Applying multiple linear regression analysis on the methylation values of all 1156 individuals for the 23 age-associated CpG sites, the correlation between fitted and true age was strong (linear correlation, $R^2 = 0.923$), while the mean absolute age modelling error using all data was 4.61 years (standard deviation = 4.36 years) (Fig. 2a). In a brief summary, 61% (700/1156) of individuals were fitted within a ±5 year error range, while 89% (1029/1156) of samples were fitted within a ±10 year error range. Multivariate regression was mainly applied to explore the relationship between DNA methylation patterns and age, but also revealed that none of

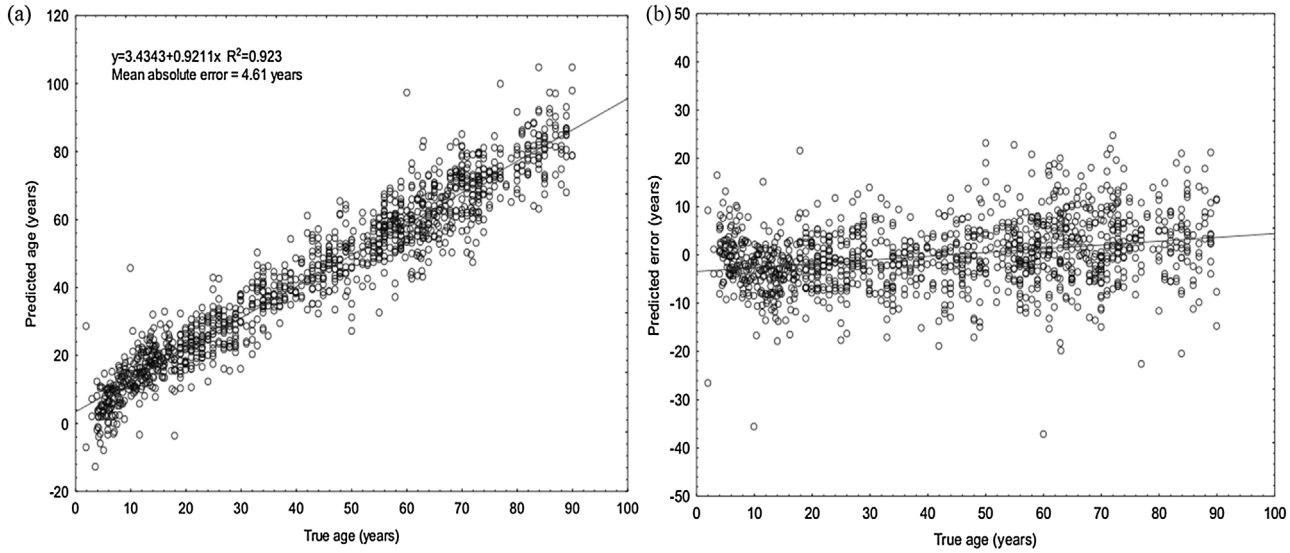

Fig. 2. Age prediction using multiple regression analysis (23 CpG sites) (a) Predicted *vs.* Chronological age (years) for all 1156 individuals used in this study (linear correlation $R^2 = 0.923$, mean absolute error = 4.61 years, standard deviation = 4.36 years), (b) Predicted error (years) over advancing age. As shown most individuals were predicted within a ±5 year error range (0.61), while 1029 out of 1156 samples were predicted within a ±10 year error range (0.89).

the available factor variables (gender, ethnicity) influenced age-associated DNA methylation patterns in a statistically significant way. While there were individuals that seemed to age fast, there were also others that were fitted as much younger (Fig. 2b). Notably, the error in older individuals (>60 years old) was higher compared to younger ones, which is not only expected as older individuals have been exposed to more environmental stress throughout their lifetime that could have potentially caused changes in DNA methylation patterns (epigenetic drift), but has also been observed before in previous models [25,33].

3.3. Age predictions from blood using artificial neural networks

Neural network models showed that the prediction accuracy could be significantly improved over multiple linear regression models. It is believed that ANN models have the ability to recognise complex patterns, which are often observed in complex traits like chronological age. The best model (Fig. 3a) was a 16-694-2-1 GRNN-type model, which was built on a 60:20:20 training, verification and blind test set dataset proportion (optimised). The average absolute errors and standard deviations in each of these subsets were 3.3 ± 3.0, 4.6 ± 3.5, and 4.4 ± 3.6 years, respectively (Fig. 3b). As a whole, a correlation between predicted and true age of $R^2 > 0.96$ was achieved across all subsets with an average absolute error of 3.8 ± 3.3 years. The correlation for the blind test set ($R^2 = 0.95$) was consistent with both the training and verification sets showing that the model could generalise very well. For the blind test set in particular, the 75th percentile of all 231 case errors lay within 6.3 years. This performance is consistent with other ANN-based applications from our research group which revealed a 3–5% average inaccuracy across predictions [58] and with a recent study reporting a percentage of prediction error of 6.3% [38].

This ANN model used data from 16 of the CpG sites, all 16 of these sites having also been identified in the stepwise multiple regression analysis: the methylation changes over time for these 16 markers are illustrated in Fig. 1. While a distinct methylation trend is observed in all cases, there are occasional samples that demonstrate an 'unusual' methylation status for a few CpG sites. This can be explained either as natural inter-individual variation or as a result of a 'unique'/personalised environment that could influence the methylation of these particular sites. Of course, technical variation cannot be excluded, however efforts were made to take this into account and normalise the data before analysis. Information regarding the genes that the CpG sites lay near or within was acquired to identify their function and potential involvement in aging. The exact chromosomal locations of the CpG sites as well as the involved genes are shown in Table 2.

As expected, all markers showing significant correlation with age belong to genes involved in age-related processes and conditions; a few examples are presented here. cg19761273 is associated with CSNK1D, which is a serine-threonine protein kinase involved in essential cell pathways including circadian rhythms and DNA repair. It is believed that CSNK1D has a role in arranging the microtubule network during mitosis to prevent DNA damage [59]. On the same theme, SSRP1 linked with cg01511567 seems to be crucial to anticancer mechanisms since it forms a transcriptional factor that interacts specifically with histones and prevents DNA damage [60]. Additionally, cg03286783 belongs to the *CASC4* gene, increased expression levels of which have been found in breast and ovarian cancers [61]. Moreover, cg05442902 is associated with the *P2RXL1* gene known for its involvement in inflammatory and immune processes, all affected by aging [62]. A recent study has also linked *TRIP10* gene (cg02085507) with the regulation of cancer cell growth; in fact differential DNA methylation of this gene has been suggested to promote cell survival or death [63]. Additionally, cg04528819 belongs to transcription factor KLF14, which is known as the 'master regulator' of obesity and other metabolic traits [64]. Lastly, the nerve growth factor VGF associated with cg04084157 has been linked with altered expression levels in the age-associated Alzheimer's disease [65]. Even though some of the genes are associated with age-related diseases, Fig. 1 demonstrates a gradual and consistent methylation increase or decrease over time at these particular CpG sites; therefore, their detected correlation with age should not be linked with effects due to these individuals being affected by age-related conditions.

The residual error obtained by the GRNN (Fig. 3b) displayed a distinct, imbalanced pattern in comparison to that obtained from multiple regression analysis (Fig. 2b), which was more randomly distributed around the mean. Residual errors obtained by the GRNN for old individuals (>60 years old) revealed a different

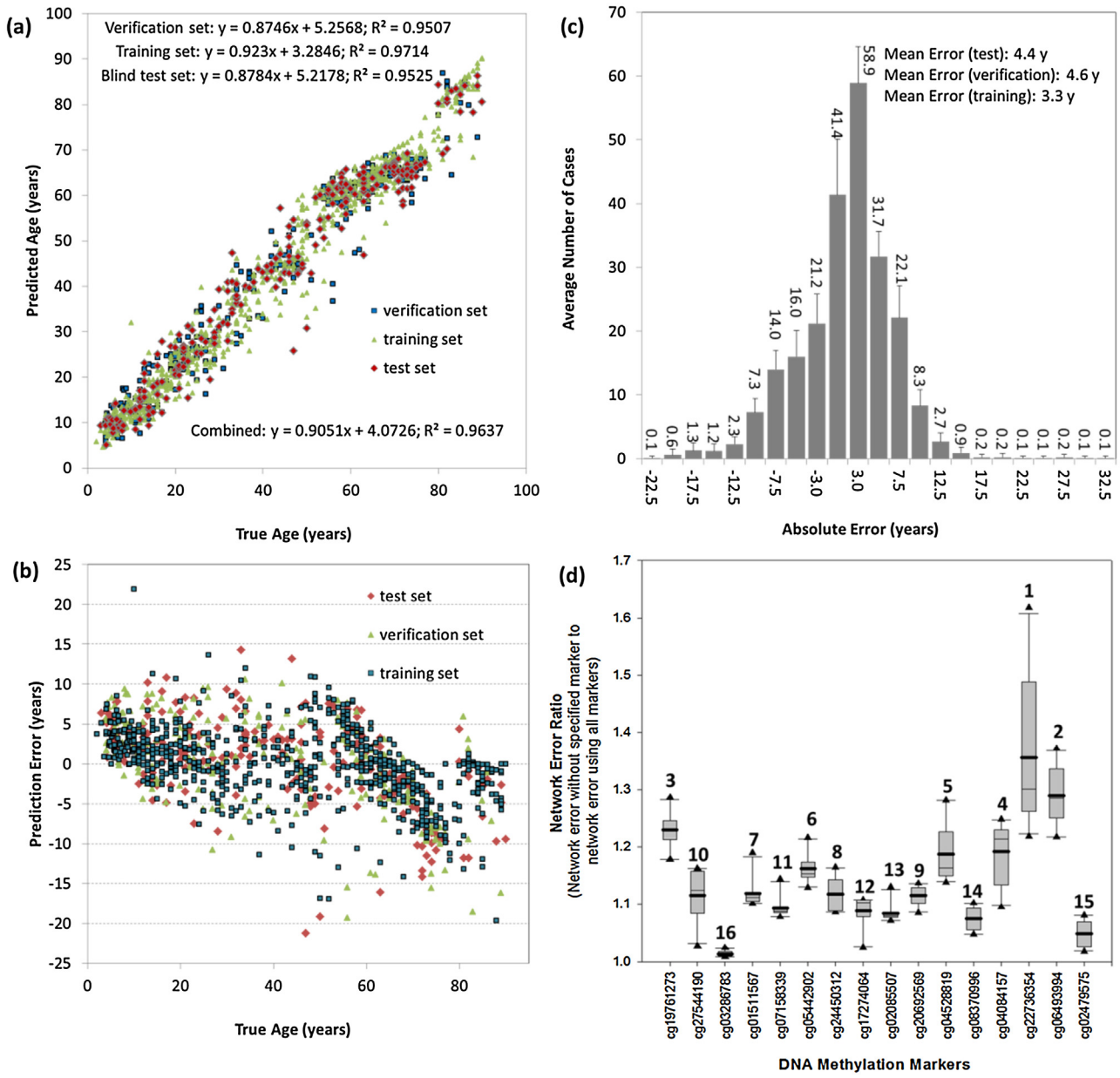

Fig. 3. Summary of ANN model for age prediction analysis. (a) Predicted *vs.* Chronological age for all 1156 individuals included in the study using the optimised 16–694-2-1 GRNN model, (b) Residual errors for the optimised model, (c) Prediction skewness for the blind test cases only using the optimised model, and (d) Sensitivity analysis and marker input consistency to age predictions across training, verification and blind test subsets. Error ratios are calculated as the ratio of the prediction inaccuracy by including all inputs to the prediction accuracy following systematic removal of each CpG site from 10 replicated GRNN networks. Boxes include data from the 25th–75th percentile as well as the median (thin line) and mean (thick line); error bars include the 5th and 95th percentile; numbers over boxes represent the rank order based on the mean.

grouping within the graph as the model tends to underestimate their age. These findings could indicate that there is a potential ANN bias in age prediction within specific age groups, that could perhaps be corrected in the future, or that there is a learning artefact due to so many different study datasets being combined. Lastly, the skewness of the blind test predictions alone showed that there was a marginal bias towards under-prediction of age using the GRNN model (Fig. 3c). In an attempt to further understand the relative contribution and consistency of each CpG site variable for age prediction, ten replicate GRNNs were generated. Sensitivity analysis showed that all error ratios lay above 1.0 meaning that they all contributed to the model positively (Fig. 3d). Most notably, cg22736354 (NHLRC1) and cg06493994 (SCGN) contributed the most to prediction, which was also true for the former in the stepwise regression analysis. Some moderate collinearity existed between these two variables and so the relative ranking of either should be considered carefully (variable inflation factors were 6.172 and 7.743 respectively, see Table S7 & S8), which has also been observed in previous models [38]. Overall, it was decided not to remove either variable from the network as predictions became worse overall, even after re-training. From the third highest ranked variable (cg19761273, CSNK1D) onwards, no severe collinearity existed and therefore these rankings were more reliable. Despite contributing to the prediction in a minor way (error ratio = 1.0127), cg03286783 (CASC4) was the lowest ranked of all 16 variables across all replicate GRNNs. Consistency of contribution across all ten GRNNs was also acceptable and in general error ratios varied $<$0.1 units for 25th–75th percentile of all data.

Considering that a similar prediction accuracy was observed when using 353 CpG sites in Horvath's study (age correlation of

Table 2
Epigenetic aging signature consisted of 16 CpG sites Information in this table includes the exact chromosomal location of the selected CpG sites (GRCh37/hg19) as well as the involved genes.

CpG sites	Chromosomal location	Gene
cg19761273	17: 80,232,096	CSNK1D – casein kinase 1; delta isoform 1
cg27544190	21: 33,785,434	C21orf63 – chromosome 21 open reading frame 63
cg03286783	15: 44,580,973	CASC4 – cancer susceptibility candidate 4 isoform a
cg01511567	11: 57,103,631	SSRP1 – structure specific recognition protein 1
cg07158339	9: 71,650,237	FXN –frataxin, mitochondrial isoform 1 preproprotein
cg05442902	22: 21,369,010	P2RXL1 – purinergic receptor P2X-like 1; orphan receptor
cg24450312	1: 206,681,158	RASSF5 – Ras association domain family 5 isoform B
cg17274064	21: 40,033,892	ERG – v-ets erythroblastosis virus E26 oncogene like isoform 2
cg02085507	19: 6,739,192	TRIP10 – thyroid hormone receptor interactor 10
cg20692569	7: 72,848,481	FZD9 – frizzled 9
cg04528819	7: 130,418,315	KLF14 – Kruppel-like factor 14
cg08370996	15: 96,874,031	NR2F2 – nuclear receptor subfamily 2; group F; member 2
cg04084157	7: 100,809,049	VGF – nerve growth factor inducible precursor
cg22736354	6: 18,122,719	NHLRC1 – malin
cg06493994	6: 25,652,602	SCGN – secretagogin precursor
cg02479575	19: 4,769,653	C19orf30 – hypothetical protein LOC284424

0.96 with a median absolute error of 3.6 years), predicting age with high accuracy using a smaller number of CpG sites (16 in our case) was possible (mean absolute error of 4.4 years in the blind test set). This is also supported by previous studies where researchers obtained mean prediction errors of 4–8 years in their validation tests, such as 5.1 years using 8 markers by Zubakov et al. [39], 6.9 years using 3 markers by Park et al. [30], 4.2 years using 7 markers by Freire-Aradas et al. [38], 3.9 years using 5 markers by Zbieć-Piekarska et al. [25], to name but a few. To the best of our knowledge, only one of the proposed 16 age-associated genes in our study has been used before in a forensic age model (more specifically, KLF14 is included in the Zbieć-Piekarska model), therefore contributing towards building a bank of potential markers. As shown before, our model sensitivity analysis revealed that there were markers contributing more to age prediction, therefore, one could propose that by replacing or adding some of the other 'strong', age-associated CpG sites reported in the literature, such as the example of *ELOVL2* locus [24], the resulting prediction accuracy can be further improved. Also, for future studies, one should also consider the combination of the best age-associated CpG markers with other age-related molecules, like mRNA, as this can also improve accuracy [39].

3.4. Validation through an independent cohort of monozygotic twins

Even though the model was applied to 231 blind test cases in the model optimisation stage, it was important to externally test model performance with an independent cohort of samples. For this reason, we evaluated the optimised model using 106 blood samples belonging to 53 monozygotic twin pairs aged 33–77 years. Monozygotic twins were chosen since they begin life with nearly identical genetic and epigenetic profile and it is the effect of various environmental factors that alters their genome-wide DNA methylation profile later in life. The methylation values of each sample for all 16 CpG sites were imported into the model as a blind test and the average mean absolute error was 7.07 ± 5.78 years. This higher prediction error could be partly explained by the fact that most twins were old (mean age of 58 years in this dataset), therefore the effect of environmental conditions and lifestyle should be considered. Interestingly, between pairs there were twins that were predicted to be either much older or much younger than their actual age, but the prediction differences within twin pairs (mean = 2.65 ± 2.37 years) were not statistically significant as obtained by paired *t*-test analysis (p-value = 0.99). These results can be interesting since they indicate some sort of systematic influence of either the twins' genetics or environment. According to Horvath, while the heritability of age acceleration was found to be 100% in new-borns, it was only 39% in older subjects suggesting that non-genetic factors become more relevant later in life [48]. Also, although all twins were volunteered as healthy controls, it would be beneficial if information regarding disease status or susceptibility was available, that could possibly partly explain these results.

3.5. Effect of disease state on age predictions

It is important to bear in mind that, in contrast with a medical setting, information regarding possible disease status is not available when trying to predict chronological age from an unknown bloodstain or sample during a criminal investigation. Consequently, it is important to build a robust age prediction model containing DNA methylation markers that would not show differential methylation patterns due to disease states. However, this might be extremely challenging to do. Therefore, although Horvath has already reported that the predicted age from cancer tissues correlated poorly with patient age in his study [48], we aimed to investigate a set of diseased samples and the effect on age prediction. For this purpose, seven datasets including diseased samples were analysed in an attempt to further validate the proposed age prediction model (Table S2). Fig. S2 shows the predicted *vs.* chronological age for all 1011 samples; combining all diseases together, a correlation of 0.74 and a mean absolute error of 7.18 years was obtained. However, when analysing separately samples suffering from blood *vs.* non-blood related diseases it becomes evident that the error is much higher for blood related diseases (error = 12.74 years). This is of course expected since the methylation data were gathered by analysing whole blood samples and therefore the potential effect is direct. In more detail, the obtained mean absolute errors for each disease were as follows: type I diabetes – 8.63 years, anaemia – 14.38 years, bone marrow disorders (including leukaemia) – 11.09 years, ovarian cancer – 7.45 years, breast cancer – 6.77 years and schizophrenia – 5.03 years.

Schizophrenia showed the lowest age prediction error, while anaemia demonstrated the lower correlation with age. While changes in expression of one of the markers included in the model – cg04084157 (VGF) – have been detected in the cerebrospinal fluid of patients with different neurological and psychiatric conditions such as schizophrenia [66], it did not seem to affect prediction in blood. It should also be noted that schizophrenia patients comprised the largest dataset; therefore a better prediction error could also be due to the greater number of samples. On the other hand, the results regarding anaemia (n = 28) come as no surprise since anaemia is one of the most common blood disorders, which

could add extra 'stress' on the body and alter DNA methylation patterns, especially in blood. Interestingly, cg07158339 is located near the *FXN* gene which has been associated with selectively and non-covalently interacting with ferric ion Fe (III) to assemble the iron-sulphur cluster [67]. Consequently, differential methylation patterns due to the disease status in blood cannot be excluded. Another example includes the *ERG* oncogene associated with cg17274064, which is an erythroblast transformation-specific transcription regulator typically mutated in myeloid leukaemia [68]. As shown, the dataset comprised by various bone marrow disorders including leukaemia demonstrated the second largest mean error (11.09 years). Thus, by testing this limited range of diseases, it seems that our model has the potential to perform quite well in disease-stressed samples unless these are blood-related, and the possibility of disease state should be taken into account when attempting predictions.

3.6. Applying the age prediction model in saliva

In Horvath's study, this set of 353 markers, which included our 16 CpG sites, were used to predict age in a wide range of other tissues. However, individual marker capabilities should not be overlooked, therefore to assess potential tissue-specific variations in age prediction, the selected markers were also tested in a set of saliva samples. Saliva is not only one of the most common types of biological evidence found at crime scenes in the form of used glasses, cigarette butts or stamps, but also was the only tissue where sufficient genome-wide methylation data was available for robust analysis. One confounding factor when analysing saliva methylation data is the variation derived from the collection method used. Depending on the method applied to collect saliva (for example by mouth wash, oral fluid swab or by 'touch' samples), the body fluid stain might contain differing proportions of various cell types (for example, buccal epithelial cells and white blood cells), which can result in detecting variable DNA methylation levels. Methylation values regarding the selected 16 CpG sites were collected from a total of 265 samples of individuals aged 21–55 years; while 159 samples were used to train a GRNN model, 53 samples were used for each of the verification and blind test sets. As shown in Fig. S3, a good correlation of 0.73 was obtained between predicted and true age, while the mean error was 3.18 years (training), 6.26 years (verification) and 4 years (blind test). The prediction accuracy was encouraging considering the size of the dataset; however, the narrow age range (21–55 years) cannot be ignored. Furthermore, saliva was collected and extracted differently between the two studies used, which could introduce further variation. The majority of saliva samples used here were collected via the Oragene DNA collection kit, which can typically result in DNA being extracted primarily from white blood cells, rather than buccal epithelial cells; which, in this case, could explain the high accuracy of obtained predictions. Again, as shown in the graph representing the age residuals, age prediction seemed to be more accurate in younger individuals, where underestimating age was not very common. Even though including more saliva-specific age-associated CpG sites could significantly improve the obtained prediction error, these results highlight the potential applicability of the proposed model in non-blood tissues.

3.7. Model validation by means of next generation sequencing

Our last goal in this study was to implement our age prediction model by using an accurate, robust and sensitive method that can analyse the proposed CpG sites in forensic-type samples. Compared to previous analog methylation methods used for age prediction analysis, we strongly believe that NGS can show great potential, as not only it can be more sensitive and accurate, but can also provide data of higher-resolution. Therefore, an NGS-based protocol capable to detect DNA methylation differences in bisulfite-converted DNA fragments was developed and adjusted using a previously published method [69]. The overall performance of the method was good including <0.05 standard deviation in methylation detection for most markers, even though we observed an imbalance between the average reads of the investigated fragments; specifically, cg24450312 (RASSF5) and cg17274064 (ERG) were the most challenging markers. This could be due to different PCR efficiencies explained by DNA sequence differences among markers, and can be improved in future experiments. Nevertheless, to ensure accurate methylation quantification, a minimum of 1000 reads per marker was set. For prediction analysis, a set of 46 blood samples from individuals aged 11–76 years old were analysed in triplicate using the proposed method and their predicted age was calculated using the average as a blind test in our age model. As a result, the age correlation taking the final normalised methylation data was 0.86 and we could predict age with a mean absolute error of 7.45 years (Fig. 4).

These results are very encouraging, and even though the age prediction accuracy is lower than that obtained in the model's blind test, for this sample set we are introducing an additional layer of variation when normalising methylation values between totally different detection systems (the NGS-derived methylation values in the samples with the microarray-derived ones used to train the model). As we aimed to investigate a representative population sample, no information regarding the individuals' health and lifestyle were collected as this information would not be available to a 'standard' forensic scenario. Since DNA methylation is known to not only be age-specific but can also be influenced by diet [70], lifestyle [71], smoking [14], ancestry [72] and other factors, we cannot exclude that these factors could have affected the methylation status of the selected sites in these individuals. However, even if efforts were made to normalise the NGS data over the genome-wide methylation data that the age prediction model uses, we cannot also ignore other potential (PCR-introduced) technical variation. Current experiments focus not only on increasing the sample size to achieve a more representative prediction accuracy, but also to analyse enough samples to re-train the model with NGS data; the latter would eliminate any methodological or technical variation. Furthermore, we are also investigating the possibility of multiplexing the bisulfite PCRs to allow for more sensitive analysis and validating the entire method using forensically relevant criteria. We understand that both the required high coverage (1000X) and triplicate analysis may be impractical in routine forensic analysis, albeit less so for blood traces where DNA is often, although not exclusively, found in relatively high quantities. Future efforts should therefore also be

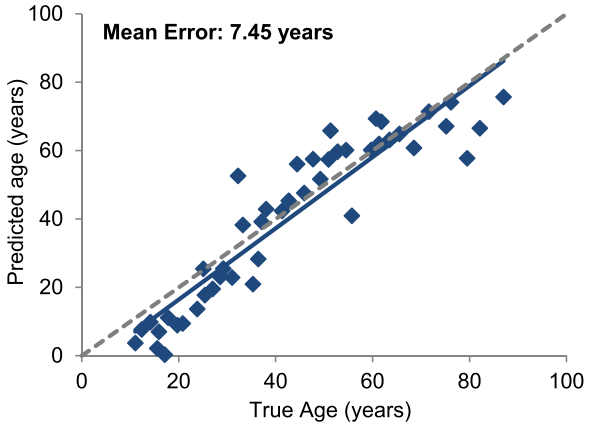

Fig. 4. Age prediction in blood using the developed MiSeq method (n = 46).

concentrated on extensively testing the sensitivity and reproducibility of the proposed NGS based method. We believe that introducing an NGS-based solution for age prediction can provide many advantages from a casework point of view, mainly due to its high sensitivity, multiplexing capabilities and the potential for merging with other DNA marker analysis. Nevertheless, all of the factors mentioned above, including the biological variation that may result from disease state and lifestyle, need to be established before such methods can be applied routinely in forensic casework.

4. Conclusions

Forensic age prediction using DNA methylation-based approaches is a fast-developing field of forensic epigenetics that has a great potential to provide accurate outcomes. Our study contributes to a range of already published prediction models, not only by providing potential age-associated markers but also by introducing a novel methodology in prediction analysis, namely machine learning by artificial neural network analysis. The proposed age prediction model does not only exhibit good prediction accuracy, but also has the potential to be applied in individuals of a very wide age range including under-aged children, individuals of various ethnic backgrounds as well as in non-blood tissues. Nevertheless, it is believed that prediction can be improved in the future by normalising for the different technologies of DNA methylation analysis used. Also, the model worked significantly less accurately in a subset of unhealthy individuals, therefore testing the markers' 'resistance' to DNA methylation alterations in disease state should be further tested. To the best of our knowledge, this is the first study that tests the ability of next generation sequencing technology to detect DNA methylation variation for age prediction in forensic samples. Following an extensive validation in future experiments it could provide the basis to an eventually combined analysis of DNA methylation and DNA sequence variation in a single streamline using an NGS platform.

Conflicts of interest

Authors declare no conflict of interest.

Acknowledgements

The authors would like to thank Dr Jon Wetton, Co-Director of the Alec Jeffreys Forensic Genomics Unit at University of Leicester and Dr Jordana Bell, Senior Lecturer in the Department for Twin Research and Genetic Epidemiology at King's College London, for reviewing this study and for their valuable comments and suggestions. The authors would also like to thank the researchers involved in the specific genome-wide DNA methylation studies used here for making their data available, without which this study would not be feasible. This research did not receive any specific grant from funding agencies in the public, commercial, or not-for-profit sectors. AV was supported by doctorate funding awarded by the Papadaki Foundation, National and Kapodistrian University of Athens. AV and DB also received financial support from the European Union Seventh Framework Programme (FP7/2007-2013) under grant agreement No. 285487 (EUROFORGEN-NoE). TM was supported by doctoral funding awarded by the Biotechnology and Biological Sciences Research Council (Reference: BB/K501177/1).

Appendix A. Supplementary data

Supplementary data associated with this article can be found, in the online version, at http://dx.doi.org/10.1016/j.fsigen.2017.02.009.

References

[1] A. Pilin, F. Pudil, V. Bencko, Changes in colour of different human tissues as a marker of age, Int. J. Legal Med. 121 (2007) 158–162.
[2] D. Glass, A. Vinuela, M.N. Davies, A. Ramasamy, L. Parts, D. Knowles, A.A. Brown, A.K. Hedman, K.S. Small, A. Buil, E. Grundberg, A.C. Nica, P. Meglio, F.O. Nestle, M. Ryten, U.K.B.E. c. the, T. c. the Mu, R. Durbin, M.I. McCarthy, P. Deloukas, E.T. Dermitzakis, M.E. Weale, V. Bataille, T.D. Spector, Gene expression changes with age in skin, adipose tissue, blood and brain, Genome Biol. 14 (7) (2013) R75.
[3] X. Ou, H. Zhao, H. Sun, Z. Yang, B. Xie, Y. Shi, X. Wu, Detection and quantification of the age-related sjTREC decline in human peripheral blood, Int. J. Legal Med. 125 (4) (2011) 603–608.
[4] A. Tsuji, A. Ishiko, T. Takasaki, N. Ikeda, Estimating age of humans based on telomere shortening, Forensic Sci. Int. 126 (2002) 197–199.
[5] C. Meissner, S. Ritz-Timme, Molecular pathology and age estimation, Forensic Sci. Int. 203 (1-3) (2010) 34–43.
[6] S.C. Zapico, D.H. Ubelaker, Applications of physiological bases of ageing to forensic sciences. Estimation of age-at-death, Ageing Res. Rev. 12 (2) (2013) 605–617.
[7] J.T. Bell, P.C. Tsai, T.P. Yang, R. Pidsley, J. Nisbet, D. Glass, M. Mangino, G. Zhai, F. Zhang, A. Valdes, S.Y. Shin, E.L. Dempster, R.M. Murray, E. Grundberg, A.K. Hedman, A. Nica, K.S. Small, T.C. Mu, E.T. Dermitzakis, M.I. McCarthy, J. Mill, T. D. Spector, P. Deloukas, Epigenome-wide scans identify differentially methylated regions for age and age-related phenotypes in a healthy ageing population, PLoS Genet. 8 (4) (2012) e1002629.
[8] K. Day, L.L. Waite, A. Thalacker-Mercer, A. West, M.M. Bamman, J.D. Brooks, R. M. Myers, D. Absher, Differential DNA methylation with age displays both common and dynamic features across human tissues that are influenced by CpG landscape, Genome Biol. 14 (9) (2013) R102.
[9] A.E. Teschendorff, J. West, S. Beck, Age-associated epigenetic drift: implications, and a case of epigenetic thrift? Hum. Mol. Genet. 22 (R1) (2013) R7–15.
[10] D. Gentilini, D. Mari, D. Castaldi, D. Remondini, G. Ogliari, R. Ostan, L. Bucci, S. M. Sirchia, S. Tabano, F. Cavagnini, D. Monti, C. Franceschi, A.M. Di Blasio, G. Vitale, Role of epigenetics in human aging and longevity: genome-wide DNA methylation profile in centenarians and centenarians' offspring, Age 35 (5) (2013) 1961–1973.
[11] D. Martino, Y.J. Loke, L. Gordon, M. Ollikainen, M.N. Cruickshank, R. Saffery, J.M. Craig, Longitudinal, genome-scale analysis of DNA methylation in twins from birth to 18 months of age reveals rapid epigenetic change in early life and pair-specific effects of discordance, Genome Biol. 14 (5) (2013) R42.
[12] R.S. Alisch, B.G. Barwick, P. Chopra, L.K. Myrick, G.A. Satten, K.N. Conneely, S.T. Warren, Age-associated DNA methylation in pediatric populations, Genome Res. 22 (4) (2012) 623–632.
[13] J.T. Bell, A.A. Pai, J.K. Pickrell, D.J. Gaffney, R. Pique-Regi, J.F. Degner, Y. Gilad, J.K. Pritchard, DNA methylation patterns associate with genetic and gene expression variation in HapMap cell lines, Genome Biol. 12 (2011) R10.
[14] K.W. Lee, Z. Pausova, Cigarette smoking and DNA methylation, Front. Genet. 4 (2013) 132.
[15] E. Gronniger, B. Weber, O. Heil, N. Peters, F. Stab, H. Wenck, B. Korn, M. Winnefeld, F. Lyko, Aging and chronic sun exposure cause distinct epigenetic changes in human skin, PLoS Genet. 6 (5) (2010) e1000971.
[16] V.K. Rakyan, T.A. Down, S. Maslau, T. Andrew, T.P. Yang, H. Beyan, P. Whittaker, O.T. McCann, S. Finer, A.M. Valdes, R.D. Leslie, P. Deloukas, T.D. Spector, Human aging-associated DNA hypermethylation occurs preferentially at bivalent chromatin domains, Genome Res. 20 (4) (2010) 434–439.
[17] S. Horvath, Y. Zhang, P. Langfelder, R.S. Kahn, M.P. Boks, K. van Eijk, L.H. van den Berg, R.A. Ophoff, Aging effects on DNA methylation modules in human brain and blood tissue, Genome Biol. 13 (10) (2012) R97.
[18] A. Zykovich, A. Hubbard, J.M. Flynn, M. Tarnopolsky, M.F. Fraga, C. Kerksick, D. Ogborn, L. MacNeil, S. Mooney, S. Melov, Genome-wide DNA methylation changes with age in disease-free human skeletal muscle, Aging Cell 13 (2014) 360–366.
[19] A.E. Teschendorff, U. Menon, A. Gentry-Maharaj, S.J. Ramus, D.J. Weisenberger, H. Shen, M. Campan, H. Noushmehr, C.G. Bell, A.P. Maxwell, D.A. Savage, E. Mueller-Holzner, C. Marth, G. Kocjan, S.A. Gayther, A. Jones, S. Beck, W. Wagner, P.W. Laird, I.J. Jacobs, M. Widschwendter, Age-dependent DNA methylation of genes that are suppressed in stem cells is a hallmark of cancer, Genome Res. 20 (4) (2010) 440–446.
[20] P. Garagnani, M.G. Bacalini, C. Pirazzini, D. Gori, C. Giuliani, D. Mari, A.M. Di Blasio, D. Gentilini, G. Vitale, S. Collino, S. Rezzi, G. Castellani, M. Capri, S. Salvioli, C. Franceschi, Methylation of ELOVL2 gene as a new epigenetic marker of age, Aging Cell 11 (2012) 1132–1134.
[21] G. Hannum, J. Guinney, L. Zhao, L. Zhang, G. Hughes, S. Sadda, B. Klotzle, M. Bibikova, J.B. Fan, Y. Gao, R. Deconde, M. Chen, I. Rajapakse, S. Friend, T. Ideker, K. Zhang, Genome-wide methylation profiles reveal quantitative views of human aging rates, Mol. Cell 49 (2) (2013) 359–367.
[22] C.M. Koch, W. Wagner, Epigenetic-aging-signature to determine age in different tissues, Aging (Milano) 3 (10) (2011) 1–10.
[23] C.I. Weidner, Q. Lin, C.M. Koch, L. Eisele, F. Beier, P. Ziegler, D.O. Bauerschlag, K. Jockel, R. Erbel, T.W. Muhleisen, M. Zenke, T.H. Brummerndorf, W. Wagner, Aging of blood can be tracked by DNA methylation changes at just three CpG sites, Genome Biol. 15 (R24) (2014) 1–11.

[24] R. Zbieć-Piekarska, M. Spólnicka, T. Kupiec, Ż. Makowska, A. Spas, A. Parys-Proszek, K. Kucharczyk, R. Płoski, W. Branicki, Examination of DNA methylation status of the ELOVL2 marker may be useful for human age prediction in forensic science, Forensic Sci. Int. Genet. 14 (2015) 161–167.
[25] R. Zbieć-Piekarska, M. Spólnicka, T. Kupiec, A. Parys-Proszek, Ż. Makowska, A. Pałeczka, K. Kucharczyk, R. Płoski, W. Branicki, Development of a forensically useful age prediction method based on DNA methylation analysis, Forensic Sci. Int. Genet. (2015).
[26] S.H. Yi, L.C. Xu, K. Mei, R.Z. Yang, D.X. Huang, Isolation and identification of age-related DNA methylation markers for forensic age-prediction, Forensic Sci. Int. Genet. 11 (2014) 117–125.
[27] S.H. Yi, Y.S. Jia, K. Mei, R.Z. Yang, D.X. Huang, Age-related DNA methylation changes for forensic age-prediction, Int. J. Legal Med. 129 (2) (2015) 237–244.
[28] Y. Huang, J. Yan, J. Hou, X. Fu, L. Li, Y. Hou, Developing a DNA methylation assay for human age prediction in blood and bloodstain, Forensic Sci. Int. Genet. 17 (2015) 129–136.
[29] C. Xu, H. Qu, G. Wang, B. Xie, Y. Shi, Y. Yang, Z. Zhao, L. Hu, X. Fang, J. Yan, L. Feng, A novel strategy for forensic age prediction by DNA methylation and support vector regression model, Sci. Rep. 5 (2015) 17788.
[30] J.L. Park, J.H. Kim, E. Seo, D.H. Bae, K.S.Y.H.C. Lee, K.M. Woo, Y.S. Kim, Identification and evaluation of age-correlated DNA methylation markers for forensic use, Forensic Sci. Int. Genet. 23 (2016) 64–70.
[31] D. Soares Bispo Santos Silva, J. Antunes, K. Balamurugan, G. Duncan, C. Sampaio Alho, B. McCord, Evaluation of DNA methylation markers and their potential to predict human aging, Electrophoresis 36 (15) (2015) 1775–1780.
[32] H.Y. Lee, S.E. Jung, Y.N. Oh, A. Choi, W.I. Yang, K.J. Shin, Epigenetic age signatures in the forensically relevant body fluid of semen: a preliminary study: forensic science international, Genetics 19 (2015) 28–34.
[33] B. Bekaert, A. Kamalandua, S.C. Zapico, W. Van de Voorde, R. Decorte, Improved age determination of blood and teeth samples using a selected set of DNA methylation markers, Epigenetics 10 (10) (2015) 922–930.
[34] M. Amiri, K. Derakhshandeh, Applied Artificial Neural Networks: from Associative Memories to Biomedical Applications, InTech, 2011.
[35] T.R. Gaunt, H.A. Shihab, G. Hemani, J.L. Min, G. Woodward, O. Lyttleton, J. Zheng, A. Duggirala, W.L. McArdle, K. Ho, S.M. Ring, D.M. Evans, G. Davey Smith, C.L. Relton, Systematic identification of genetic influences on methylation across the human life course, Genome Biol. 17 (2016) 61.
[36] S.K. Mawlood, L. Dennany, N. Watson, B.S. Pickard, The EpiTect Methyl qPCR Assay as novel age estimation method in forensic biology, Forensic Sci. Int. 264 (2016) 132–138.
[37] Y. Hamano, S. Manabe, C. Morimoto, S. Fujimoto, M. Ozeki, K. Tamaki, Forensic age prediction for dead or living samples by use of methylation-sensitive high resolution melting, Leg. Med. 21 (2016) 5–10.
[38] A. Freire-Aradas, C. Phillips, A. Mosquera-Miguel, L. Girón-Santamaría, A. Gómez-Tato, M. Casares de Cal, J. Álvarez-Dios, J. Ansede-Bermejo, M. Torres-Español, P.M. Schneider, E. Pospiech, W. Branicki, A. Carracedo, M.V. Lareu, Development of a methylation marker set for forensic age estimation using analysis of public methylationd data and the Agena Bioscience EpiTYPER system, Forensic Sci. Int. Genet. 24 (2016) 65–74.
[39] D. Zubakov, F. Liu, I. Kokmeijer, Y. Choi, J.B.J. van Meurs, W.F.J. van, I. Jcken, A.G. Uitterlinden, A. Hofman, L. Broer, C.M. Van Duijn, J. Lewin, M. Kayser, Human age estimation from blood using mRNA, DNA, methylation, DNA rearrangement, and telomere length, Forensic Sci. Int. Genet. 24 (2016) 33–43.
[40] M. Ronaghi, Pyrosequencing sheds light on DNA sequencing, Genome Res. 11 (2001) 3–11.
[41] E. Dejeux, H. El abdalaoui, I.G. Gut, J. Tost, in: J. Tost (Ed.), Identification and Quantification of Differentially Methylated Loci by the Pyrosequencing Technology, umana Press, 2009, pp. 189–205.
[42] K. Reed, M.L. Poulin, L. Yan, A.M. Parissenti, Comparison of bisulfite sequencing PCR with pyrosequencing for measuring differences in DNA methylation, Anal. Biochem. 397 (1) (2010) 96–106.
[43] N. Pourmand, E. Elahi, R.W. Davis, M. Ronaghi, Multiplex pyrosequencing, Nucleic Acids Res. 30 (7) (2002) 1–5.
[44] Y.A. Chen, S. Choufani, J.C. Ferreira, D. Grafodatskaya, D.T. Butcher, R. Weksberg, Sequence overlap between autosomal and sex-linked probes on the Illumina HumanMethylation27 microarray, Genomics 97 (4) (2011) 214–222.
[45] J.T. Bell, A.K. Loomis, L.M. Butcher, F. Gao, B. Zhang, C.L. Hyde, J. Sun, H. Wu, K. Ward, J. Harris, S. Scollen, M.N. Davies, L.C. Schalkwyk, J. Mill, T.C. Mu, F.M. Williams, N. Li, P. Deloukas, S. Beck, S.B. McMahon, J. Wang, S.L. John, T.D. Spector, Differential methylation of the TRPA1 promoter in pain sensitivity, Nat. Commun. 5 (2014) 2978.
[46] S. Bocklandt, W. Lin, M.E. Sehl, F.J. Sanchez, J.S. Sinsheimer, S. Horvath, E. Vilain, Epigenetic predictor of age, PLoS One 6 (6) (2011) 1–6.
[47] J. Liu, M. Morgan, K. Hutchison, V.D. Calhoun, A study of the influence of sex on genome wide methylation, PLoS One 5 (4) (2010) 1–8.
[48] S. Horvath, DNA methylation age of human tissues and cell types, Genome Biol. 14 (R115) (2013) 1–19.
[49] C.G. Bell, A.E. Teschendorff, V.K. Rakyan, A.P. Maxwell, S. Beck, D.A. Savage, Genome-wide DNA methylation analysis for diabetic nephropathy in type 1 diabetes mellitus, BMC Med. Genomics 3 (2010) 33.
[50] C. Perez, M. Pascual, J.I. Martin-Subero, B. Bellosillo, V. Segura, E. Delabesse, S. Alvarez, M.J. Larrayoz, J. Rifon, J.C. Cigudosa, C. Besses, M.J. Calasanz, N.C. Cross, F. Prosper, X. Agirre, Aberrant DNA methylation profile of chronic and transformed classic Philadelphia-negative myeloproliferative neoplasms, Haematologica 98 (9) (2013) 1414–1420.
[51] J. Zhuang, A. Jones, S.H. Lee, E. Ng, H. Fiegl, M. Zikan, D. Cibula, A. Sargent, H.B. Salvesen, I.J. Jacobs, H.C. Kitchener, A.E. Teschendorff, M. Widschwendter, The dynamics and prognostic potential of DNA methylation changes at stem cell gene loci in women's cancer, PLoS Genet. 8 (2) (2012) e1002517.
[52] S. Anjum, E.-O. Fourkala, M. Zikan, A. Wong, A. Gentry-Maharaj, A. Jones, R. Hardy, D. Cibula, D. Kuh, I.J. Jacobs, A.E. Teschendorff, U. Menon, M. Widschwendter, A BRCA1-mutation associated DNA methylation signature in blood cells predicts sporadic breast cancer incidence and survival, Genome Med. 6 (6) (2014) 47.
[53] K. Zhong, L.C. Karssen, M. Kayser, F. Liu, CollpsABEL – an R library for detecting compound heterozygote alleles in genome-wide association studies, BMC Bioinf. 17 (2016) 156.
[54] G.E. Tusnady, I. Simon, A. Varadi, T. Aranyi, BiSearch: primer-design and search tool for PCR on bisulfite-treated genomes, Nucleic Acids Res. 33 (1) (2005) e9.
[55] H. Li, R. Durbin, Fast and accurate long-read alignment with Burrows-Wheeler transform, Bioinformatics 26 (5) (2010) 589–595.
[56] H. Li, B. Handsaker, A. Wysoker, T. Fennel, J. Ruan, N. Homer, G. Marth, G. Abecasis, R. Durbin, G.P.D.P. Subroup, The sequence alignment/map format and SAMtools, Bioinformatics 25 (16) (2009) 2078–2079.
[57] A. McKenna, M. Hanna, E. Banks, A. Sivanchenko, K. Cibulskis, A. Kernytsky, K. Garimella, D. Altshuler, S. Gabriel, M. Daly, M.A. DePristo, The genome analysis Toolkit: a MapReduce framework for analyzing next-generation DNA sequencing data, Genome Res. 20 (9) (2010) 1297–1303.
[58] L.P. Barron, G.L. McEneff, Gradient liquid chromatographic retention time prediction for suspect screening applications: a critical assessment of a generalised artificial neural network-based approach across 10 multi-residue reversed-phase analytical methods, Talanta 147 (2016) 261–270.
[59] L. Behrend, M. Stoter, M. Kurth, G. Rutter, J. Heukeshoven, W. Deppert, U. Knippschild, Interaction of casein kinase 1 delta (CK1delta) with post-Golgi structures, microtubules and the spindle apparatus, Eur. J. Cell Biol. 79 (4) (2000) 240–251.
[60] A.T. Yarnell, S. Oh, D. Reinberg, S.J. Lippard, Interaction of FACT, SSRP1, and the high mobility group (HMG) domain of SSRP1 with DNA damaged by the anticancer drug cisplatin, J. Biol. Chem. 276 (28) (2001) 25736–25741.
[61] J.J. Oh, D.R. Grosshans, S.G. Wong, D.J. Slamon, Identification of differentially expressed genes associated with HER-2/neu overexpression in human breast cancer cells, Nucleic Acids Res. 27 (20) (1999) 4008–4017.
[62] T. Kendall Harden, J.L. Boyer, R.A. Nicholas, P2-PURINERGIC RECEPTORS: subtype-associated signaling responses and structure, Annu. Rev. Pharmacol. Toxicol. 35 (1995) 541–579.
[63] C.C. Hsu, Y.W. Leu, M.J. Tseng, K.D. Lee, T.Y. Kuo, J.Y. Yen, Y.L. Laui, Y.C. Hung, W. S. Sun, C.M. Chen, P.Y. Chu, K.T. Yeh, P.S. Yan, Y.S. Chang, T.H. Huang, S.H. Hsiao, Functional characterization of Trip10 in cancer cell growth and survival, J. Biomed. Sci. 18 (1) (2011) 12.
[64] K.S. Small, A.K. Hedman, E. Grundberg, A.C. Nica, G. Thorleifsson, A. Kong, U. Thorsteindottir, S.Y. Shin, H.B. Richards, G. Consortium, M. Investigators, D. Consortium, N. Soranzo, K.R. Ahmadi, C.M. Lindgren, K. Stefansson, E.T. Dermitzakis, P. Deloukas, T.D. Spector, M.I. McCarthy, T.C. Mu, Identification of an imprinted master trans regulator at the KLF14 locus related to multiple metabolic phenotypes, Nat. Genet. 43 (6) (2011) 561–564.
[65] O. Carrette, I. Demalte, A. Scherl, O. Yalkinoglu, G. Corthals, P. Burkhard, D.F. Hockstrasser, J.C. Sanchez, A panel of cerebrospinal fluid potential biomarkers for the diagnosis of Alzheimer's disease, Proteomics 3 (8) (2003) 1486–1494.
[66] J.T. Huang, F.M. Leweke, D. Oxley, L. Wang, N. Harris, D. Koethe, C.W. Gerth, B.M. Nolden, S. Gross, D. Schreiber, B. Reed, S. Bahn, Disease biomarkers in cerebrospinal fluid of patients with first-onset psychosis, PLoS Med. 3 (11) (2006) e428.
[67] L.E. Gentry, M.A. Thacker, R. Doughty, R. Timkovich, L.S. Busenlehner, His86 from the N-terminus of frataxin coordinates iron and is required for Fe-S cluster synthesis, Biochemistry 52 (35) (2013) 6085–6096.
[68] H. Yi, Y. Fujimura, M. Ouchida, D.D. Prasad, V.N. Rao, E.S. Reddy, Inhibition of apoptosis by normal and aberrant Fli-1 and erg proteins involved in human solid tumors and leukemias, Oncogene 14 (11) (1997) 1259–1268.
[69] D.R. Masser, A.S. Berg, W.M. Freeman, Focused, high accuracy 5-methylcytosine quantitation with base resolution by benchtop next-generation sequencing, Epigenet. Chromatin 61–12 (2013) 33.
[70] J.C. Jimenez-Chillaron, R. Diaz, D. Martinez, T. Pentinat, M. Ramon-Krauel, S. Ribo, T. Plosch, The role of nutrition on epigenetic modifications and their implications on health, Biochimie 94 (11) (2012) 2242–2263.
[71] B.M.L. Baselmans, J. van Dongen, M.G. Nivard, B.D. Lin, B. Consortium, N.R. Zilhao, D.I. Boomsma, M. Bartels, Epigenome-wide association study of wellbeing, Twin Res. Hum. Genet. 18 (6) (2015) 710–719.
[72] H. Heyn, S. Moran, I. Hernando-Herraez, S. Sayols, A. Gomez, J. Sandoval, D. Monk, K. Hata, T. Marques-Bonet, L. Wang, M. Esteller, DNA methylation contributes to natural human variation, Genome Res. 23 (2013) 1363–1372.

Chemosphere 183 (2017) 389–400

Contents lists available at ScienceDirect

Chemosphere

journal homepage: www.elsevier.com/locate/chemosphere

Uptake, biotransformation and elimination of selected pharmaceuticals in a freshwater invertebrate measured using liquid chromatography tandem mass spectrometry

Thomas H. Miller [a], Nicolas R. Bury [b], Stewart F. Owen [c], Leon P. Barron [a, *]

[a] Analytical & Environmental Sciences Division, Faculty of Life Sciences and Medicine, King's College London, 150 Stamford Street, London, SE1 9NH, United Kingdom
[b] Division of Diabetes and Nutritional Sciences, Faculty of Life Sciences and Medicine, King's College London, Franklin Wilkins Building, 150 Stamford Street, London, SE1 9NH, United Kingdom
[c] AstraZeneca, Global Environment, Alderley Park, Macclesfield, Cheshire, SK10 4TF, United Kingdom

HIGHLIGHTS

- Bioconcentration factors of 9 pharmaceuticals in *G. pulex* ranged from 0 to 73 L kg^{-1}
- *G. pulex* are capable of pharmaceutical biotransformation.
- Five pharmaceutical metabolites were determined up to 94.5 ng g^{-1}
- Biotransformation can affect BCF_{total} estimates if metabolites are not accounted for.

GRAPHICAL ABSTRACT

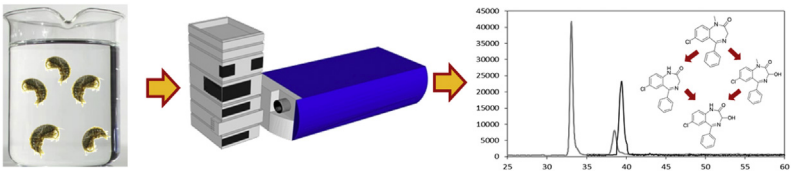

ARTICLE INFO

Article history:
Received 15 December 2016
Received in revised form
28 April 2017
Accepted 13 May 2017
Available online 13 May 2017

Handling Editor: Frederic Leusch

Keywords:
Biotransformation
Pharmaceuticals
Gammarus pulex
Bioconcentration

ABSTRACT

Methods were developed to assess uptake and elimination kinetics in *Gammarus pulex* of nine pharmaceuticals (sulfamethazine, carbamazepine, diazepam, temazepam, trimethoprim, warfarin, metoprolol, nifedipine and propranolol) using targeted LC-MS/MS to determine bioconcentration factors (BCFs) using a 96 h toxicokinetic exposure and depuration period. The derived BCFs for these pharmaceuticals did not trigger any regulatory thresholds and ranged from 0 to 73 L kg^{-1} (sulfamethazine showed no bioconcentration). Metabolism of chemicals can affect accurate BCF determination through parameterisation of the kinetic models. The added selectivity of LC-MS/MS allowed us to develop confirmatory methods to monitor the biotransformation of propranolol, carbamazepine and diazepam in *G. pulex*. Varying concentrations of the biotransformed products; 4-hydroxypropranolol sulphate, carbamazepine-10,11-epoxide, nordiazepam, oxazepam and temazepam were measured following exposure of the precursor compounds. For diazepam, the biotransformation product nordiazepam was present at higher concentrations than the parent compound at 94 ng g^{-1} dw. Overall, the results indicate that pharmaceutical accumulation is low in these freshwater amphipods, which can potentially be explained by the rapid biotransformation and excretion.

1. Introduction

Extensive research into organic environmental micropollutants has enabled the elucidation of the mechanisms for the uptake and

* Corresponding author.
E-mail address: leon.barron@kcl.ac.uk (L.P. Barron).

http://dx.doi.org/10.1016/j.chemosphere.2017.05.083

accumulation in biota (Barber et al., 1988, 1991; Mackay and Fraser, 2000). Uptake was mainly considered to occur by passive diffusion across cellular membranes and traditional models relied heavily on physico-chemical properties such as octanol-water partition coefficients (log*P*) to describe and predict xenobiotic concentrations in biota (Kanazawa, 1981; Neely et al., 1974; Veith et al., 1979). Such earlier works often focussed on neutral compounds (Fu et al., 2009; Klosterhaus et al., 2013; Wu et al., 2013), but more recently identified micropollutant classes, such as pharmaceuticals, are somewhat different in that they are often ionisable and have a wider range of molecular polarity. Additional mechanisms such as ion trapping, carrier mediated transport and partitioning to non-lipid components (protein binding) could also influence the accumulation of pharmaceutical residues in the environment (Fu et al., 2009; Klosterhaus et al., 2013; Stott et al., 2015). As most of the reported work has focussed on vertebrates such as fish (Gobas et al., 1986; Kanazawa, 1981; Spacie and Hamelink, 1982; Veith et al., 1979), the bioaccumulation of compounds in invertebrates is not well understood.

The OECD 305 guidelines are widely used for estimating the bioconcentration factor (BCF) or bioaccumulation factor (BAF) in fish and have also been applied to invertebrates, such as bivalves and amphipods (Ashauer et al., 2006, 2010; Meredith-Williams et al., 2012; OECD; Sordet et al., 2016). Estimations using these guidelines can be determined using steady-state or kinetic measurements. Kinetic measurement estimates are based on non-linear regression to generate uptake (k_1) and elimination rate constants (k_2) and used together to estimate BCF/BAF. Models assume that rate constants do not change. However, recent investigations in our laboratory showed that the OECD model led to significant lack-of-fits for measured data in invertebrates (Miller et al., 2016). The lack-of-fits were shown to arise from a potentially decreasing k_1 trend over time for a proportion of compounds tested. This finding was significant as such models could lead to under/over estimation of BCF/BAFs during risk assessment of chemicals in invertebrates. Possible causes for the decreases in k_1 could be related to several factors such as growth, metabolism and sorption processes. Metabolism in particular, is generally not considered in bioconcentration studies. Many analytical methods rely on measurement of total radioactivity of a labelled compound using liquid scintillation counting (LSC) (Arnot and Gobas, 2006) as an alternative to confirmatory analytical tools based on liquid chromatography (LC) or gas chromatography (GC) coupled to mass spectrometry (MS). However for small freshwater invertebrates, only a few published LC or GC-MS-based methods exist for parent compound determination (Grabicova et al., 2015; Inostroza et al., 2016; Miller et al., 2015; Sordet et al., 2016). A reason for the small number of published methods is that sensitivity at environmentally relevant concentrations is often challenging due to their small size. Similarly, simply increasing the sample mass to be extracted (via pooling of individuals) is often undesirable due to extra MS signal suppression or enhancement effects caused by the matrix. Therefore, a delicate balance is required to ensure sufficient MS sensitivity and that reliable quantifications can be performed. In the absence of confirmatory analytical methods, biotransformation during the exposure period could have a significant effect on invertebrate BCF/BAF estimation using scintillation counting methods (de Wolf et al., 1992; Oliver and Niimi, 1985; Opperhuizen and Sijm, 1990). Xenobiotics can also induce or inhibit their own metabolism or the metabolism of other compounds that will affect the clearance rate and hence the BCF/BAF (Golan et al., 2011). Moreover, as standardised methods to measure metabolic products and the kinetics of biotransformation currently do not exist, it is difficult to assess the influence of biotransformation in accumulation (Cowan-Ellsberry et al., 2008). Several authors have applied *in vitro* intrinsic clearance rates to extrapolate to whole body biotransformation rates for predictive BCF modelling (Arnot et al., 2008; Nichols et al., 2013). However, these extrapolations measure only the loss of parent compound to predict whole body biotransformation. Thus, *in vitro* clearance rates may not reliably reflect whole body metabolic rates (Nichols et al., 2006).

To date only three studies have measured biotransformation products and their associated toxicokinetics in invertebrates (Ashauer et al., 2012; Jeon et al., 2013b; Rösch et al., 2016). Two of these works used LC coupled to high resolution MS (HRMS) or LC with a radioactivity detector to model the uptake and elimination profiles of organic micropollutants and their biotransformation products in *G. pulex* (Ashauer et al., 2012; Rösch et al., 2016). Ashauer et al. showed that the measurement of biotransformation improved the accuracy of BCF estimates when compared to estimates using total radioactivity counts (Ashauer et al., 2012). A further constraint to the study of xenometabolism is that *a priori* knowledge of biotransformation products in aquatic organisms is lacking leading to difficulty when developing targeted analytical methods (Celiz et al., 2009). Current methods have focussed on the determination of organic pollutants in fish, with little attention given to invertebrates or pharmaceutical biotransformation. Therefore, it is essential that methods are developed that can determine pharmaceutical biotransformation products to more reliably assess the affect metabolism has on bioconcentration models.

The aim of this work was to assess the bioconcentration of a selection of nine pharmaceuticals in *G. pulex* using targeted LC-MS/MS methods described in (Miller et al., 2015). In this regard, the method developed for pharmaceutical occurrence was used for the determination of selected known pharmaceutical biotransformation products of carbamazepine, diazepam and propranolol. The method showed good performance in terms of linearity, recovery, precision and robustness. In particular, BCFs were estimated using the OECD 305 guidelines and kinetic parameters were checked for constancy over time. Finally, the optimised LC-MS/MS method was used for the identification and determination of biotransformation products of propranolol, carbamazepine and diazepam. As few published works have studied pharmaceutical bioconcentration and biotransformation, the work presented herein addresses the knowledge gaps concerning their bioaccumulation and biotransformation in invertebrates at environmentally relevant concentrations using a minimised test design.

2. Materials and methods

2.1. Reagents, chemicals and consumables

HPLC grade methanol, acetonitrile, acetone, ethyl acetate, dichloromethane and dimethyldichlorosiloxane were purchased from Fischer Scientific (Loughborough, UK). Analytical grade ammonium acetate was sourced from Sigma-Aldrich (Dorset, UK). Propranolol hydrochloride, warfarin, sulfamethazine, carbamazepine, nimesulide, (±)-metoprolol (+)-tartrate salt, temazepam, diazepam, nifedipine, oxazepam, nordiazepam, carbamazepine-10,11-epoxide, and sulfamethazine were all obtained from Sigma-Aldrich (Steinheim, Germany). Trimethoprim, was ordered from Fluka (Buchs, Switzerland). Stable isotope-labelled standards including carbamazepine-d_{10}, propranolol-d_7, temazepam-d_5 and diazepam-d_5 were ordered from Sigma-Aldrich. Sulfamethazine-d_4, nifedipine-d_4, metoprolol-d_7, trimethoprim-d_3 and warfarin-d_5 were ordered from QMX Laboratories (Essex, UK). The propranolol biotransformation products; 4-hydroxypropranolol, 4-hydroxypropranolol sulphate and 4-hydroxypropranolol glucuronide were sourced from Santa Cruz Biotechnology (Heidelberg,

Germany). All pharmaceuticals were of a purity of ≥97%. Analytical grade salts (>99%) including sodium hydrogen carbonate, magnesium sulphate, calcium sulphate, potassium chloride were purchased from Sigma. Ultra-pure water was obtained from a Millipore Milli-Q water purification system with a specific resistance of 18.2 MΩ cm or greater (Millipore, Bedford, MA, USA).

2.2. Sample collection and culture maintenance

Gammarus pulex were collected by kick-sampling from the River Cray, South-East London, UK, 51°23′09.5″N 0°06′32.4″E. This site was previously shown to have low pharmaceutical contamination in both collected surface water and animal samples (Miller et al., 2015). The populations were transported to the laboratory in 500 mL Nalgene™ flasks filled with surface water from the sample collection site. Populations were rinsed with artificial freshwater (AFW) and then acclimatised to laboratory conditions (as specified below) for a minimum of 7 days before any exposure experiments were performed. AFW was prepared from 1.15 mM of $NaHCO_3$, 0.50 mM $MgSO_4$, 0.44 mM $CaSO_4$ and 0.05 mM of KCl dissolved in 20 L of ultra-pure water. This water was subsequently aerated for several hours to remove dissolved carbonic acid and maximise the dissolved oxygen concentrations. Each culture tank (n = 8) was filled with 2.5 L of AFW and animals were fed with either alder or horse chestnut leaves obtained from the sampling site and conditioned by submersion in surface water for two days prior to use.

2.3. Toxicokinetic exposure and conditions

Toxicokinetic experiments were performed separately for each pharmaceutical for a total of 96 h which included a 48 h uptake phase followed by a 48 h depuration period as per (Miller et al., 2016). Individual adult organisms (n = 25), both male and female (>5 mg wet weight) were placed in Pyrex glass beakers. *G. pulex* were carefully transferred to beakers using blunt forceps to avoid any harm to the organisms before exposure. Each beaker contained 25 organisms in 200 mL of exposure media (AFW and test compound). *G. pulex* were exposed to individual pharmaceuticals at a concentration of 1 μg L^{-1}, except for propranolol and warfarin which were exposed at 10 μg L^{-1}. All exposure media contained <0.001% of organic solvent (methanol). A total of 300 organisms were used per compound exposure and were sampled for n = 3 per time-point. Samples were taken at 6, 24, 48 and 96 h across the toxicokinetic experiments. Negative control exposures were set up and also sampled at the 96 h time interval. These were subsequently analysed for background contamination. The exposure media was replaced daily and water samples (n = 3) were analysed at 0 and 24 h after exposure to ensure concentrations of the compounds remained constant in the AFW. Each animal specimen was rinsed with ultra-pure water and then frozen at −20 °C. The light cycle was 12 h light followed by 12 h dark without a dusk/dawn transition period. All experiments were performed in a temperature controlled room at 15 °C (±2 °C) and water pH was also monitored across each experiment and measured at an average of 8.19 ± 0.05.

2.4. Sample preparation

Water samples collected from exposure experiments were filtered using Whatman filters (0.2 μM) and directly injected onto the LC-MS/MS for analysis. For *G. pulex*, A mass of 50 mg of lyophilised and ground material was extracted by glass bead pulverisation in 5 mL of acetonitrile and diluted with 100 mL of ammonium acetate buffer (10 mM) for loading onto Waters HLB solid phase extraction (SPE) cartridges (6 cc, 200 mg sorbent). After loading, samples were eluted using a mixture of ethyl acetate:acetone (50:50 v/v) which was subsequently evaporated under nitrogen (99% purity) and reconstituted in 250 μL of starting LC mobile phase (90:10 v/v, 10 mM ammonium acetate buffer: acetonitrile).

2.5. Instrumental analysis

Full instrumental conditions were used as per (Miller et al., 2015). Briefly, separations were performed on an Agilent HP1100 LC system configured with a Waters SunFire reversed-phase C_{18} column (150 mm × 2.1 mm, 2.5 μM particle size). Following injection (20 μL), elution followed a gradient profile (totalling 75 min including a 12.5-min re-equilibration time) using a mixture of acetonitrile and ultra-pure water with 10 mM ammonium acetate. Detection was performed using a Waters Quattro triple quadrupole mass spectrometer with electrospray ionisation operated in positive and negative polarity switching mode. Quantification of analytes was performed using 3-point internal standard matrix-matched calibration using the peak area ratio of non-labelled analyte (precursor range: 50–300 ng g^{-1}, biotransformation product range: 50–150 ng g^{-1}) to the stable isotope labelled internal standard (SIL-IS) (100 ng g^{-1}). The exception to this was in the temazepam exposure where quantification was performed against a SIL-IS calibrant concentration (100 ng g^{-1}) by comparing the response ratio of SIL-IS:unlabelled temazepam. The compounds (4-hydroxypropranolol sulphate and carbamazepine-10,11-epoxide) were quantified using 3-point external matrix-matched calibration curves due to unavailability of SIL-IS standards.

2.6. Modelling bioconcentration factors

Parameter estimation of uptake rate constant (k_1) and depuration rate constant (k_2) was performed using a curve fitting algorithm via Minitab statistical software (Minitab Ltd., Coventry UK) and as outlined in the OECD 305 Fish Bioconcentration Guidelines (OECD). Full details of parameter estimation can be found in (Miller et al., 2016). Herein, the authors define BCF_{total} as the summation of the BCF of both parent/precursor and biotransformation products (i.e. the total body burden). Whereas, BCF_{parent} will be used to describe the BCF determined for the parent compound alone.

3. Results and discussion

3.1. Analytical performance and minimised test design evaluation

The previously described analytical method required a sample mass of 100 mg dw, which corresponded to approximately 40 animals per measurement (Miller et al., 2015). This presented feasibility issues for sampling, maintaining cultures and the scale of exposure experiments. To mitigate this, 50 mg was used instead and the reconstitution volume of solvent (post-SPE) was also scaled down (to 250 μL) to maintain sensitivity. Analytical method performance was reassessed for 10 pharmaceuticals (See SI, Fig. S1 and Table S1). In general, imprecision increased with decreasing sample mass extracted. The use of SIL-IS has been shown to offer improved precision during analytical method development (Stokvis et al., 2005). The corresponding SIL-IS for each analyte here also resulted in markedly improved precision for all compounds with % RSDs ranging from 1 to 11%. Linearity also improved using SIL-IS in comparison to matrix-matched calibration curves (R^2 ≥0.9897). Therefore, for precise analysis of biota like *G. pulex* for trace pharmaceutical residue determination, it is recommended that SIL-IS be used with LC-MS/MS to overcome precision problems relating to the limited sample mass available and to enable the number of

specimens to be minimised.

In addition to the reduction in the number of organisms, a reduction in the number of sampling time intervals was also considered. Time points were selected at 6, 24, 48 and 96 h so that the uptake phase had three time points and the elimination phase contained two intervals. The additional time point in the uptake phase was selected so that any losses in k_1 constancy could be highlighted as identified previously (Miller et al., 2016). The potential limitation when using a small number of time intervals is that the data may not reflect reliably the ability of a compound to concentrate as modelling is limited to a few data points. The OECD 305 guidelines do propose a minimised test design with two time intervals in the uptake and elimination phase, respectively (e.g. day 14, 28, 35 & 42). This minimised study design was evaluated independently in the literature and it was concluded that the test was valuable and offered reliable BCF estimation for regulatory purposes (Carter et al., 2014). Springer et al. proposed a second minimised test design involving only two sampling time intervals in a 14 d depuration period (Springer et al., 2008). They also found that minimised test designs were a viable alternative to a full study design. Given that our experiments here focused on a non-standard invertebrate species and much shorter uptake and depuration phases, re-evaluation of the uptake and elimination data from (Miller et al., 2016) was performed to assess the suitability of a minimised test design for simultaneous and sequential methods of BCF estimation in *G. pulex* (Table S3). An ANOVA was performed for each method of estimation and resulted in *p*-values of 0.95 for comparison of simultaneous BCF_{total}, 0.43 for sequential BCF_{total} and 0.45 for sequential BCF_{total} determined using linear regression in the elimination phase data. All three *p*-values were >0.05 indicating that there were no statistically significant differences between the BCFs estimated by the full study design nor the minimised design. Therefore, going forward all non-radiolabelled exposures were performed using the minimised design.

3.2. Toxicokinetic modelling of eight selected pharmaceuticals

Aqueous pharmaceutical concentrations remained stable across the exposure period for carbamazepine, diazepam, temazepam, sulfamethazine, metoprolol and trimethoprim (Table 1). Propranolol showed stable aqueous concentrations over the first 24 h, but declined by 29% to an average of 6.41 μg L^{-1} thereafter. Nifedipine showed an average decrease of 39% across both days of the uptake phase. It is possible that sorption was the cause in the reduction of nifedipine in the exposure media or could also be attributed to other transformation processes.

For pharmaceuticals in *G. pulex*, maximal concentrations after the uptake phase were observed for propranolol and likely due to its higher exposure concentration at 10 μg L^{-1} (due to a relatively high LOQ value (61 ng g^{-1} dw). In this exposure, internal concentrations reached 519 ± 143 ng g^{-1} with a mean value of 210 ± 9 ng g^{-1} at the end of the uptake period. Warfarin also showed relatively higher concentrations in *G. pulex* which again was likely explained by the higher exposure concentration. In contrast to the other studied compounds, the data for warfarin suggested that it did not reach/approach steady state in the uptake period as no plateau was observed in the toxicokinetic profile. The remaining pharmaceuticals carbamazepine, diazepam, metoprolol, nifedipine, trimethoprim and temazepam exposed at 1 μg L^{-1} showed internal concentrations of ≤51 ng g^{-1} at the end of the uptake phase. These internal concentrations showed rapid elimination and were reduced to ≤ LOQ/LOD. The rapid turnover of all pharmaceuticals suggested that bioaccumulation could be less relevant for these types of ionisable compounds. BCFs were generated using both simultaneous and sequential modelling presented in Table 2. The BCF_{parent} generated for each compound was in the order of trimethoprim and nifedipine < metoprolol < warfarin < carbamazepine < propranolol < temazepam < diazepam. The highest BCF_{parent} generated by the simultaneous method was 41 L kg^{-1} for diazepam and the lowest estimation was 16 L kg^{-1} for both trimethoprim and nifedipine. These values remain significantly lower than any regulatory threshold to be considered bioaccumulative or very bioaccumulative (European Commission, 2006). The BCF_{parent} values for propranolol and metoprolol were also compared with the BCF_{total} generated previously (Miller et al., 2016). Propranolol BCF_{total} was estimated to be 32 L kg^{-1} and metoprolol BCF_{total} was 16 L kg^{-1}, which showed very good agreement with the BCF_{parent} values of 28 and 17 determined by LC-MS/MS here. Sulfamethazine was not detected in any sample and therefore indicated that no accumulation in *G. pulex* had occurred. Interestingly, exposure to nifedipine (log*P* = 3.45) resulted in a low BCF despite it being less polar and was similar to that of trimethoprim (log*P* = 1.12). This further suggested that log*P* was not a reliable indicator for BCF of pharmaceuticals and the degree of ionisation may also play an important role in uptake and bioconcentration mechanisms. Uptake models have usually been based on neutral organic micropollutants and is the reason that log*P* can be a good indicator of bioconcentration for these compounds especially when log*P* is < 6. The log*P*, log*D* and predominant form of each pharmaceutical exposed to *G. pulex* is shown in Table S4. Temazepam, diazepam and carbamazepine remain neutral, but their respective BCF_{parent} do not follow any specific trend when directly compared to their log*P*. However, the selection of pharmaceuticals here is limited and therefore discernible trends may not be apparent. A plot of log*D*/*P* versus estimated BCF showed that there were no identifiable trends (Fig. S2). Consideration of the complexity of biological

Table 1
Pharmaceutical concentrations in exposure media during the uptake phase. 24 h and 48 h represent the concentration after 24 h of exposure with solutions used on either Day 1 or Day 2.

Compound	Concentration (μg L^{-1})						
	Day 1 (n = 3)	SD	24 h (n = 3)	SD	Day 2 (n = 2)	48 h (n = 3)	SD
Carbamazepine	1.12	0.03	1.01	0.05	1.08	1.07	0.02
Diazepam	1.02	0.03	0.86	0.05	1.04	0.89	0.11
Temazepam	0.96	0.03	0.85	0.03	1.17	1.03	0
Nifedipine	0.94	0.09	0.59	0.06	0.82	0.49	0.18
Sulfamethazine	1.06	0.07	0.99	0.17	0.89	0.71	0.15
Trimethoprim	1.09	0.04	1.01	0.11	0.99	0.97	0.04
Metoprolol	0.77	0.18	0.72	0.15	0.86	0.87	0.21
Propranolol	9.22	0.5	8.92	0.29	8.98	6.41[a]	–

Day 1- initial pharmaceutical concentration on day 1.
Day 2- initial pharmaceutical concentration on day 2.
[a] n = 2

Table 2
Determination of BCFs using either simultaneous or sequential parametrisation of k_1 and k_2.

Compound	Simultaneous						Sequential[a]						Sequential[b]					
	k_1	SE	k_2	SE	p-value	BCF_{parent}	k_1	SE	k_2	SE	p-value	BCF_{parent}	k_1	SE	k_2	r^2	p-value	BCF_{parent}
Carbamazepine	0.5307	0.115	0.0214	0.008	0.049	25	0.4418	0.054	0.014	0.007	0.07	32	0.4643	0.056	0.0158	0.534	0.08	29
Diazepam	9.5942	2.126	0.2349	0.058	0.028	41	2.6469	0.265	0.046	0.011	0	58	3.0917	0.28	0.0582	0.953	0.001	53
Temazepam	4.3326	0.556	0.1186	0.018	0.131	37	2.8514	0.116	0.0702	0.027	0.022	41	2.751	0.117	0.0669	0.9965	0.016	41
Trimethoprim	2.325	0.916	0.1488	0.066	0.376	16	0.8451	0.105	0.0402	0.017	0.066	21	0.837	0.105	0.0396	0.8468	0.064	21
Nifedipine	4677.31	n/a	295.66	n/a	n/a	16	0.7802	0.146	0.0248	0.001	0	31	0.7802	0.146	0.0248	0.9967	0	31
Warfarin[c]	0.2242	0.022	0.0119	0.003	0.043	19	0.2091	0.012	0.0096	0.003	0.066	22	0.2118	0.012	0.01	0.6989	0.072	21
Metoprolol	0.4413	0.135	0.0259	0.015	0.005	17	0.2788	0.046	0.0071	0.006	0.005	39	0.2855	0.047	0.0078	0.39	0.006	37
Propranolol[c]	6.596	5.797	0.2348	0.221	0.027	28	0.8059	0.181	0.0111	0.002	0.006	73	0.8116	0.182	0.0113	0.8543	0.006	72

SE — Standard Error.
[a] Determined using Levenberg-Marquardt algorithm.
[b] Determined using linear regression on elimination data.
[c] Exposed at 10 μg L^{-1}.

systems and the unique characteristics of pharmaceuticals, it may be expected that uptake and bioconcentration is a much more complex process than can be predicted by a single or small number of physicochemical properties. Many factors have been proposed and reported to influence the bioconcentration of pharmaceuticals including hydrophobicity, biotransformation, bioavailability, environmental exposure scenarios, and carrier mediated uptake (Barron, 1990). A particularly important factor is the environmental exposure as the complexity of environmental matrices on BCFs may well increase or decrease predicted BCFs or measured BCFs from *in vivo* laboratory exposures. Surface water temperature, pH, concentrations in sediment and the composition of other components in the surface water (e.g. complex mixtures including other pharmaceuticals, colloids, surfactants, organic chemicals etc.) may directly or indirectly affect the accumulation potential of a compound (Brown et al., 2007; Chen et al., 2017; Nichols et al., 2015).

Few data or reported studies exist on the uptake of pharmaceuticals in invertebrates. However, comparison of the BCF_{parent} estimated here showed good agreement with a study on *G. pulex* by Meredith-Williams et al. for two compounds, carbamazepine and diazepam, (Meredith-Williams et al., 2012). Sordet et al., reported carbamazepine BCF of 5 L kg^{-1} in *Gammarus fossarum* which was ~5-fold lower than the BCF determined here (Sordet et al., 2016). Another study also reported a similar BCF of 51 L kg^{-1} for diazepam in a marine mussel, *Mytilus galloprovincialis* (E. Gomez et al., 2012). In *Daphnia magna*, BCFs of between 18 and 83 L kg^{-1} for propranolol were reported, but the estimated value varied with exposure concentration (Ding et al., 2016). A review of fish data generally revealed low level bioconcentration of the selected pharmaceuticals herein. For example, diazepam BCF in fish (*Ictalurus punctatus*) ranged from 2 to 146 L kg^{-1} depending on the tissue type (Overturf et al., 2016); sulfamethazine BCF in sturgeons was shown to be 1 L kg^{-1} (Hou et al., 2003); carbamazepine BCF in two species of fish (*Pimephales notatus* and *I. punctatus*) was <7 L kg^{-1} depending on tissue (Garcia et al., 2012); and propranolol was also estimated to have a BCF of <1 L kg^{-1} in *Oncorhynchus mykiss* and *I. punctatus* (C. F. Gomez et al., 2010). These data further support the results herein and indicate that the selected pharmaceuticals are likely to have a low potential for bioconcentration in aquatic species.

The model fits of simultaneous and sequential BCF_{parent} estimation showed a significant lack-of-fit for several pharmaceuticals (Fig. 1). Lack-of-fits may arise from a large scatter in the data. However, the advantage of pooling organisms through LC-MS/MS measurements is that it reduces scatter of measured internal concentrations from single organisms that arises from inter-individual variability. The lack-of-fit observed seemed to arise from the uptake phase data and therefore the rate constant was estimated over each time interval during the uptake period. This revealed that there was a decreasing trend in the k_1 rate constant which again did not obey the model's assumptions. Lack-of-fits were observed in the simultaneous method of estimation for five compounds (carbamazepine, propranolol, metoprolol, warfarin and diazepam) with two compounds showing no significant lack-of-fits (temazepam and trimethoprim). Lack-of-fit for the final compound nifedipine was not possible to estimate due to line that was fit (Fig. 1(d)). As several significant lack-of-fits were observed, the k_1 rate constant was recalculated over the time intervals for the uptake phase data (Fig. 2). Again, k_1 was observed to decrease over time. These decreases again are potentially the cause of the lack-of-fits, as suggested previously (Miller et al., 2016). The reason for the decrease in k_1 over time could be attributed to either sorption on to the cuticle of the animal during the uptake phase, toxicodynamic effects where the pharmaceuticals are reducing the ability of the organism to eliminate the compound or growth dilution of the animal. However, preliminary evidence in (Miller et al., 2016) and the larger

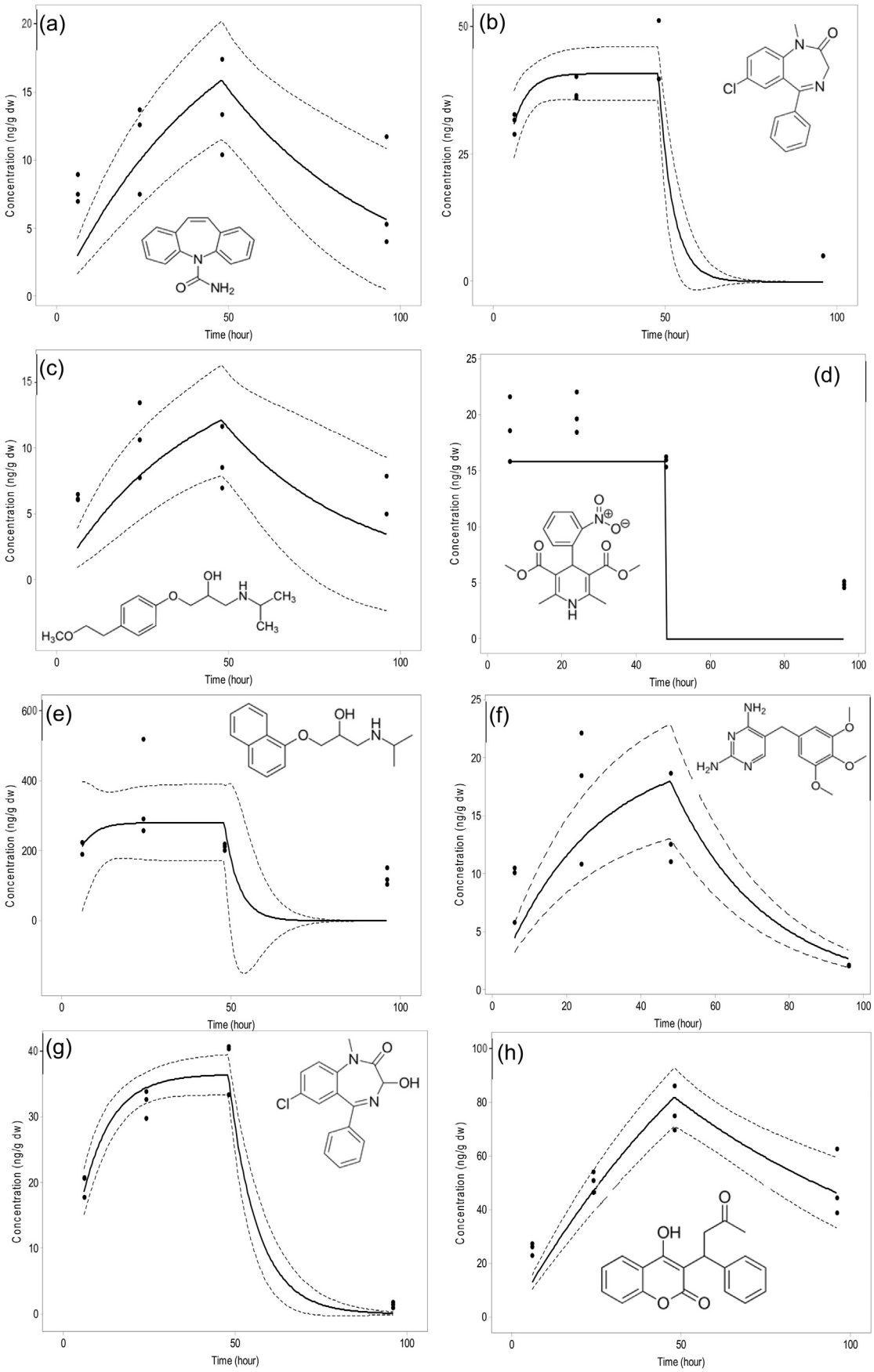

Fig. 1. Toxicokinetic profiles of selected pharmaceuticals in *G. pulex* measured using LC-MS/MS. Solid line represents model fit, dashed lines represent 95% confidence interval. (a) carbamazepine, (b) diazepam, (c) metoprolol, (d) nifedipine, (e) propranolol, (f) trimethoprim, (g) temazepam and (h) warfarin.

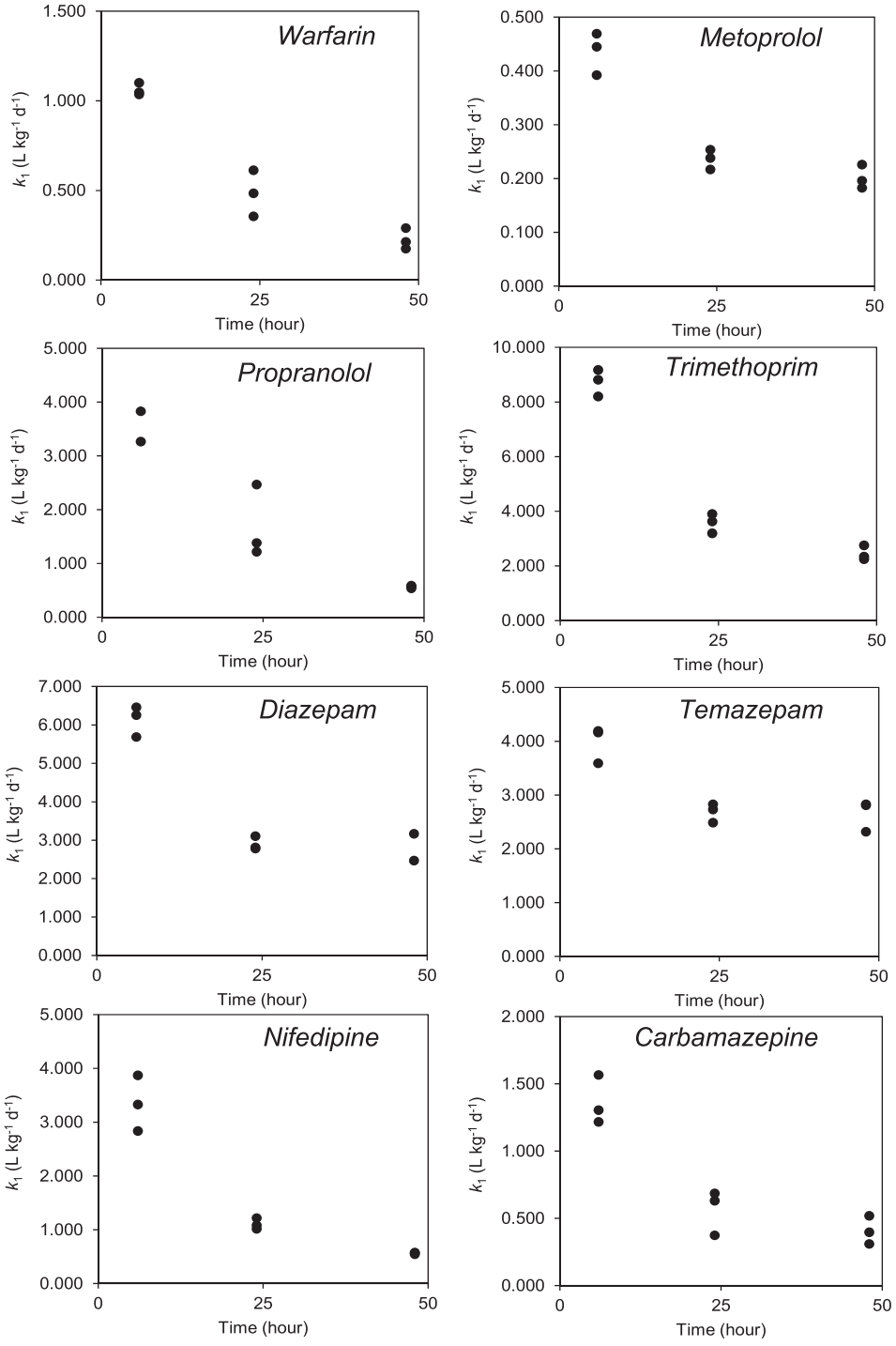

Fig. 2. Plots of k_1 over time for the selected eight pharmaceuticals.

decreases in k_1 at the earlier time interval (this study) suggest that sorption might be a significant cause of the decreases in k_1 over time. In the cases of warfarin, carbamazepine, diazepam and temazepam an apparent plateau had been reached indicating k_1 constancy and it was possible to use this value to estimate the BCF_{parent}. The average of the k_1 over the 48 h time interval for these compounds resulted in a BCF_{parent} of 20, 26, 40 and 48 L kg^{-1} for warfarin, carbamazepine, temazepam and diazepam, respectively. These values showed good agreement between the BCFs generated by the simultaneous method indicating this could provide an alternative method for BCF estimation when k_1 values are found to decrease over time. However, it is also possible that steady-state measurements are more appropriate over kinetic measurements when estimating pharmaceutical BCFs. Behaviour of pharmaceuticals is also different to more traditional organic pollutants (PAHs, PCBs, etc.), it appears they often reach steady-state within a relatively short timeframe (~2–3 days) (Meredith-Williams et al., 2012; Miller et al., 2016). Thus, determination of BCFs using kinetic parameterisation offers no advantage over the time requirements for steady-state BCF estimates. Furthermore, steady-state

measurements would also be less resource intensive as they do not require a depuration period. In addition, the inconsistencies of kinetic data as demonstrated here and in (Miller et al., 2016) might not provide a reliable estimate of BCFs.

3.3. Biotransformation of carbamazepine, diazepam and propranolol by G. pulex

In addition to their medium to low log*P*, pharmaceuticals are designed to be metabolised and excreted to minimise accumulation (Kumar and Surapaneni, 2001). As the data suggests, factors other than hydrophobicity may be important in accumulation, such as biotransformation, which could also partly explain the variability in BCFs. Authors have demonstrated that *G. pulex* are able to metabolise a range of organic micropollutants (Ashauer et al., 2012; Jeon et al., 2013b; Rösch et al., 2016). Conservation of cytochrome P450 enzymes has also been observed in invertebrates (Snyder, 2000) and pharmaceuticals have been shown to undergo oxidative and conjugation reactions (Jeon et al., 2013b). As the targeted LC-MS/MS method only determines the amount of parent compound, the BCF_{parent} values presented above (Table 2) do not take into account the accumulation of any biotransformation products. The biotransformation product half-lives in the body can be longer or shorter than the parent compound as they are modified by biotransformation processes and potentially may lead to increased or decreased accumulation (Jeon et al., 2013a) and thus will not be accounted for by estimations of BCF_{parent}.

Selected pharmaceuticals with readily available biotransformation product reference standards (propranolol, carbamazepine and diazepam) were used in biotransformation studies and several transformation products were targeted in the analytical method including 4-hydroxypropranolol, 4-hydroxypropranolol sulphate, 4-hydroxypropranolol glucuronide, carbamazepine-10,11-epoxide, oxazepam and nordiazepam and temazepam, the latter of which was already included in analytical method. A matrix effect and recovery experiment was performed for these additional analytes before exposures were performed (SI Table S5). Unfortunately, poor stability in solution made the matrix effect or recovery assessment for 4-hydroxypropranolol impossible. This has been reported previously (Pritchard et al., 1979) and samples required additives (sodium metabisulfite and sodium bisulfite) to maintain stability. Overall, matrix effects were relatively minor for most biotransformation products ranging from 4% suppression to 9% enhancement. However the exception was nordiazepam which showed 31% signal suppression. biotransformation products showed acceptable absolute recoveries ranging 82–103% (≤13% RSD) with the exception of 4-hydroxypropranolol sulphate (34% recovery and 20% RSD) and 4-hydroxypropranolol glucuronide (no recovery). The lower recoveries and precision of these polar conjugates are likely to arise from poor affinity to the SPE sorbents (HLB) used during sample preparation. The lower recoveries and precision of these polar conjugates are likely to arise from poorer affinity to these SPE sorbents. The use of alternative chemistries including mixed-mode ion exchangers or dipole bearing polymers may improve the selectivity for such polar compounds.

Carbamazepine exposures resulted in the detection of carbamazepine-10,11-epoxide at 24 h and 48 h in *G. pulex*. Control organisms (exposed to AFW only) also showed no detectable peaks for carbamazepine-10,11-epoxide. This was identified by a single *m*/*z* transition (253 → 235) and chromatographic retention time (within 0.4%). Unfortunately, carbamazepine-10,11-epoxide was not quantifiable as signals were below a signal to noise ratio of 10:1 (Fig. 3). Carbamazepine-10,11-epoxide was not detected at 96 h suggesting that the biotransformation product may have been eliminated from the organism by this point. Elimination may either

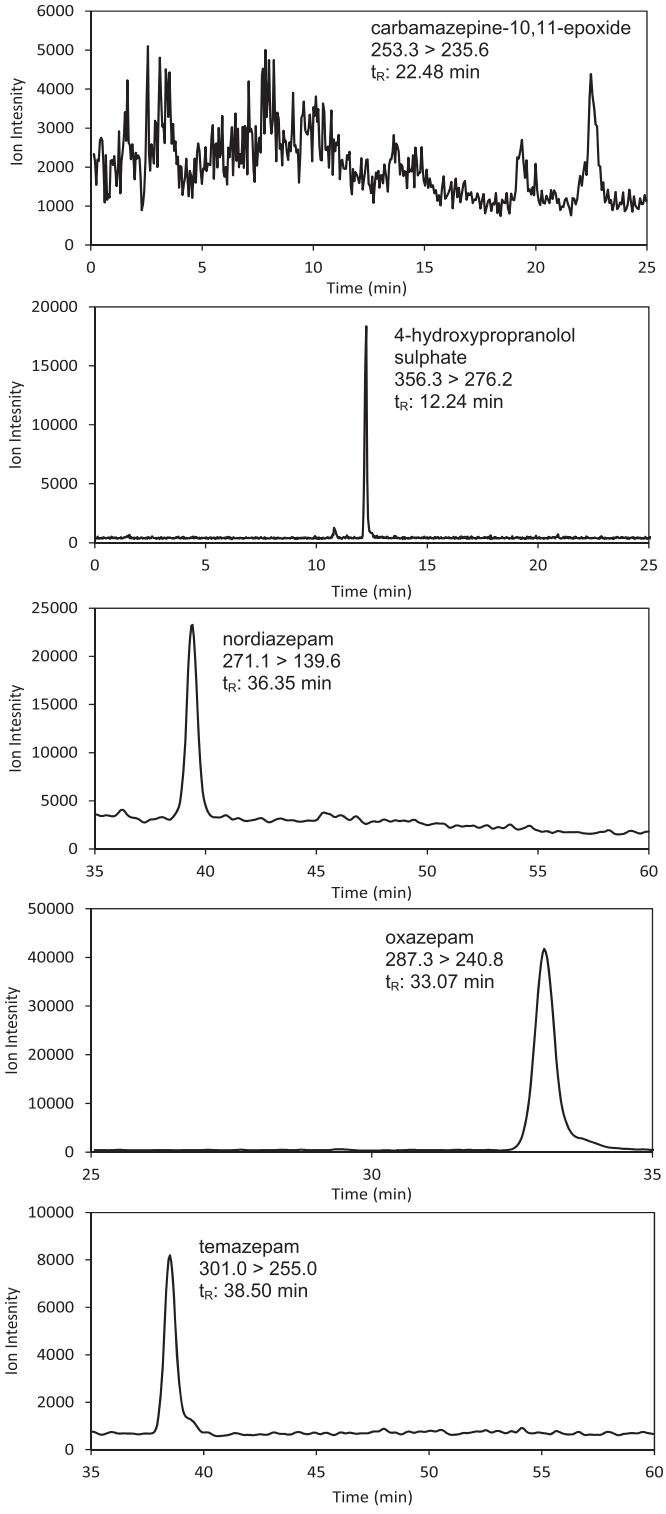

Fig. 3. SRM transitions for the detected biotransformed products during toxicokinetic exposures.

be via excretion or further biotransformation, e.g. carbamazepine-10,11–diol is excreted in its free form or as a glucuronic acid conjugate in humans (Kudriakova et al., 1992). However, limited data is available for biotransformation of xenobiotics in invertebrates. A previous study identified that carbamazepine was converted to carbamazepine-10,11-epoxide and was the main metabolic

pathway in the mussel, *Mytilus galloprovincialis* (Boillot et al., 2015). Fish exposed to carbamazepine have also shown the presence of two carbamazepine biotransformation products, carbamazepine-10,11-epoxide and 2-hydroxycarbamazepine (Boillot et al., 2015).

For propranolol exposures, 4-hydroxypropranolol sulphate was confirmed with a single peak transition (356.3 → 276.2) and chromatographic retention time (within 0.25%) (Fig. 3). HP-SULPH reached a mean concentration of 75 ± 17 ng g^{-1} dw by the end of the uptake phase (Fig. 4(a)). The elimination phase showed no decreases in the concentration 4-hydroxypropranolol sulphate which was measured at a mean concentration of 84 ± 4 ng g^{-1} dw at 96 h. Determination of the parent compound propranolol showed a peak at the 24 h time interval which decreased by 48 h. Decreases of internal concentrations during the uptake phase are indicative of active metabolic pathways (Crookes and Brooke, 2011). To the authors' knowledge, no propranolol biotransformation products have previously been specifically identified using LC-MS/MS in either fish or invertebrates. However, from the induced P450 activity of trout *in vivo* and *in vitro* propranolol was suggested to likely induce its metabolism and it was hypothesised that biotransformation products may be identified (Bartram et al., 2012). More recently trout gill cells have been shown to be capable of propranolol transport and biotransformation (Stott et al., 2015), and in carp a range of biotransformation products were tentatively identified *in vivo* using UV methods (Ding et al., 2015). Furthermore, sulphate conjugates of pharmaceuticals have not been previously detected in invertebrates. However, previous works have detected sulphate and glucose conjugates of pyrene in *Daphnia magna* (Ikenaka et al., 2006, 2007) and sulphate conjugates of aldicarb, carbaryl and dichlorophenols in *G. pulex* (Ashauer et al., 2012). For biocides (algicides), glutathione conjugates have been detected in *G. pulex* and *D. magna* (Jeon et al., 2013b). Finally, *G. pulex* have also been shown to biotransform azole fungicides into sulphate, glutathione and glucose-sulphate conjugates (Rösch et al., 2016). Human trials show that the major biotransformation products of propranolol were HP and napthoxylactic acid (Walle and Gaffney, 1972). The relative importance of this sulphate conjugation pathway in *G. pulex* is not known as the napthoxylactic acid and the glucuronide conjugate could not be determined. However, some authors have suggested that sulphate and glucoside conjugation is the major metabolic process in invertebrates for the metabolism of aryl group containing compounds such as propranolol (Ikenaka et al., 2007; Livingstone, 1998).

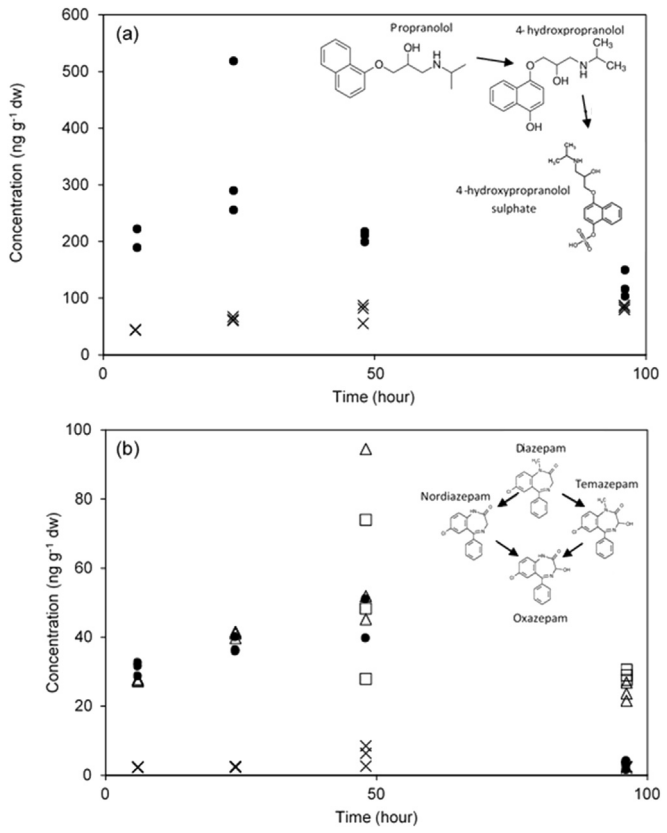

Fig. 4. Determination of biotransformation products (a) Concentration-time profile for propranolol (solid circles) and 4-hydroxypropranolol sulphate (crosses) in *G. pulex*. (b) Concentration-time profile for diazepam (solid circles), nordiazepam (triangles), oxazepam (squares) and temazepam (crosses) in *G. pulex*.

The final exposure was performed with diazepam and all three selected biotransformation products were detected and quantified (Fig. 4(b)). Nordiazepam showed concentrations that reached a mean concentration of 64 ± 27 ng g^{-1} dw in contrast to temazepam that reached a maximum mean concentration of 6 ± 3 ng g^{-1} dw at 48 h. The 10-fold difference in concentrations suggested that the biotransformation of diazepam to nordiazepam is the major metabolic pathway in contrast to the conversion of diazepam to temazepam. This agrees with mammalian data that shows the demethylation of diazepam to nordiazepam is the primary metabolic pathway (Umezawa et al., 2008). Temazepam was not detectable by the 96 h time interval, suggesting this compound had been either excreted or further biotransformed to oxazepam. The k_2 was determined at 0.0194 d^{-1} which is 3-fold lower than the k_2 of diazepam. The estimated half-lives of diazepam and nordiazepam were 12 h and 36 h, respectively. The difference observed is also in agreement with the reported half-lives, as nordiazepam has a longer half-life (50–120 h) than its parent compound diazepam (44 h) (Umezawa et al., 2008). The k_2 of temazepam was estimated at 0.016 d^{-1}, approximately 4-fold lower than the k_2 of temazepam when exposed to *G. pulex* as a parent compound. The lower k_2 may be explained by the apparent preferential metabolism of diazepam to nordiazepam. Thus, enzymes involved in the temazepam pathway may be less active.

The final biotransformation product oxazepam was not detectable until 48 h reaching a mean concentration of 50 ± 23 ng g^{-1} dw. The biotransformation of diazepam to either nordiazepam or temazepam and further conversion to oxazepam would be rate liming steps leading to the apparent lag phase in the detection of oxazepam. The k_2 estimated for oxazepam was 0.009 d^{-1}, with mean internal concentrations reduced by 21 ng g^{-1} dw over the 48 h depuration period. The half-life determined for oxazepam was 70 h which is much greater than the reported single or multiple dose half-life in humans (9–11.6 h) (Greenblatt, 1981). The difference in half-lives could be due to the continued conversion of nordiazepam or temazepam to oxazepam after the uptake phase ended giving an apparent longer half-life. Furthermore, oxazepam is primarily excreted by conjugation with glucuronide moieties indicating that *G. pulex* may not readily metabolise oxazepam as well as in humans. The degree of accumulation of each biotransformation product is in agreement with Overturf et al., whom generally found higher concentrations of nordiazepam and oxazepam in comparison to temazepam dependent on the tissue type (Overturf et al., 2016).

Metabolite enrichment factors (MEFs) can be determined for biotransformation products (Ashauer et al., 2012). The MEFs can be likened to a 'pseudo-BCF' and further indicate that these biotransformation products were not accumulative. However, nordiazepam and oxazepam reached higher internal concentrations relative to the parent compound diazepam. The BCF of

oxazepam has been reported at 22 L kg^{-1} in *G. fossarum* indicating that this compound is not accumulative (Sordet et al., 2016). Furthermore, the summation of the BCF_{parent} and MEFs can give a BCF that would be comparable to those determined by total radioactivity counts (i.e. BCF_{total}) (Ashauer et al., 2012). For example, the BCF_{parent} of diazepam ranged from 41 to 58 L kg^{-1} whereas summation of the diazepam BCF and the MEFs would give a BCF_{total} estimate of 165 L kg^{-1}. However, it should be considered that targeted methods will likely only show a small window of the biotransformation pathways involved with xenobiotic detoxification (as in this work). Secondly, targeted methods may not focus on the important biotransformation products in terms of accumulation, toxicity and elimination. Therefore, untargeted analytical techniques such as high resolution mass spectrometry (HRMS) could potentially offer a much greater insight into biotransformation pathways involved with xenobiotic detoxification or identification of new compounds (Ashauer et al., 2012; Munro et al., 2015). However, the quantitative application of LC-HRMS to toxicokinetic profiling needs to be considered carefully, especially where reference materials for biotransformation products are not available as discussed previously (Jeon et al., 2013a; Rösch et al., 2016). Furthermore, studies that only monitor the parent compound by non-specific methods should be cautious when reporting BCFs, especially if there is a high potential for biotransformation. Comparison of the total BCF (BCF_{parent} + MEF) to BCFs determined by LSC was not possible here. However, Ashauer et al. (2012) reported that comparison of total BAF and BAF by LSC gave values that were within a single order of magnitude. However, the differentiation between biotransformation products and their respective parents gave better accuracy in parameter estimates (k_1/k_2) compared to radioactivity measurements (Ashauer et al., 2012). The reason for this is that radioactivity measurements can over or underestimate elimination if biotransformation is not taken into account. As a final consideration, the data presented show that at environmentally relevant exposure concentrations, pharmaceuticals remain at very low level concentrations. Furthermore, for the selected compounds herein, they do not show any significant accumulation which has also been evidenced in the literature by several authors (Boillot et al., 2015; Meredith-Williams et al., 2012; Miller et al., 2016; Paterson and Metcalfe, 2008; Sordet et al., 2016). Thus, biotransformation studies will be key in highlighting the behaviour of these contaminants inside the animal and reveal the role of metabolic clearance for regulating accumulation. In addition, whilst the accumulation potential of pharmaceuticals is low, it must now be considered how these innately low level concentrations of precursor and biotransformed products will affect the organisms that are exposed to them. Thus, future work should aim to link accumulation data to effect data for more comprehensive understanding of the potential for adverse outcomes of these emerging contaminants.

4. Conclusions

As an alternative to traditional LSC approaches, LC-MS/MS was shown as a suitable technique for the measurement of uptake and elimination kinetics. The simultaneous BCF estimates ranged from 16 to 41 L kg^{-1} for eight compounds (diazepam, temazepam, nifedipine, propranolol, metoprolol, carbamazepine, warfarin and trimethoprim) using the simultaneous model method. Sequential parameterisation resulted in BCFs of 21–72 L kg^{-1} showing overestimates compared to the simultaneous method. Sulfamethazine showed no bioconcentration in the animals, as no peaks were detected upon exposure. Models were shown to have significant lack-of-fits for six of the eight pharmaceuticals. The lack-of-fits also coincided with decreases in the uptake rate constant over time suggesting that poor model fits may have resulted from this trend. No trends in bioconcentration were observed with log*D* or log*P*, suggesting factors other than compound hydrophobicity were important in bioconcentration. The role of metabolism was investigated for three selected pharmaceuticals (carbamazepine, propranolol and diazepam). *G. pulex* were shown to metabolise all three pharmaceuticals into several different biotransformation products, indicating the conservation of cytochrome P450 enzymes in this species. Furthermore, detection of 4-hydroxpropranolol sulphate indicates the presence of transferases. The ability of *G. pulex* to readily metabolise these xenobiotics may explain, in part, the relatively low BCFs determined for pharmaceuticals in this work and the literature. Biotransformation pathways and products were found to be the same between vertebrate data. However, differences between half-lives were observed for the benzodiazepine compounds (diazepam = 12 h, nordiazepam = 36 h) suggesting that rates of metabolism and elimination are different. Whilst, kinetics may differ, the same metabolic pathways involved in elimination mean that human pharmacokinetic data is valuable for consideration of pharmaceuticals in environmental risk assessment. Analytical methods that only target and determine the parent compound in toxicokinetic studies do not measure a BCF_{total}. As MEFs for the diazepam biotransformation products, nordiazepam and oxazepam, showed that some compounds may be more accumulative than the parent and could potentially be more toxic. Therefore, it is advisable that targeted MS methods account for biotransformed products when estimating BCFs.

Acknowledgements

This work was conducted under funding from the Biotechnology and Biological Sciences Research Council (BBSRC) CASE industrial scholarship scheme (Reference BB/K501177/1) and AstraZeneca Global SHE research programme. AstraZeneca is a biopharmaceutical company specialising in the discovery, development, manufacturing and marketing of prescription medicines, including some products measured here. Funding bodies played no role in the design of the study or decision to publish. The authors declare no financial conflict of interest.

Appendix A. Supplementary data

Supplementary data related to this article can be found at http://dx.doi.org/10.1016/j.chemosphere.2017.05.083.

References

Arnot, J.A., Gobas, F.A.P.C., 2006. A review of bioconcentration factor (BCF) and bioaccumulation factor (BAF) assessments for organic chemicals in aquatic organisms. Environ. Rev. 14 (4), 257–297. http://dx.doi.org/10.1139/a06-005.

Arnot, J.A., Mackay, D., Bonnell, M., 2008. Estimating metabolic biotransformation rates in fish from laboratory data. Environ. Toxicol. Chem. 27 (2), 341–351. http://dx.doi.org/10.1897/07-310r.1.

Ashauer, R., Boxall, A., Brown, C., 2006. Uptake and elimination of chlorpyrifos and pentachlorophenol into the freshwater amphipod Gammarus pulex. Arch. Environ. Contam. Toxicol. 51 (4), 542–548. http://dx.doi.org/10.1007/s00244-005-0317-z.

Ashauer, R., Caravatti, I., Hintermeister, A., Escher, B.I., 2010. Bioaccumulation kinetics of organic xenobiotic pollutants in the freshwater invertebrate Gammarus pulex modeled with prediction intervals. Environ. Toxicol. Chem. 29 (7), 1625–1636. http://dx.doi.org/10.1002/etc.175.

Ashauer, R., Hintermeister, A., O'Connor, I., Elumelu, M., Hollender, J., Escher, B.I., 2012. Significance of xenobiotic metabolism for bioaccumulation kinetics of organic chemicals in Gammarus pulex. Environ. Sci. Technol. 46 (6), 3498–3508. http://dx.doi.org/10.1021/es204611h.

Barber, M.C., Suárez, L.A., Lassiter, R.R., 1991. Modelling bioaccumulation of organic pollutants in fish with an application to PCBs in lake ontario salmonids. Can. J. Fish. Aquatic Sci. 48 (2), 318–337. http://dx.doi.org/10.1139/f91-044.

Barber, M.C., Suérez, L.A., Lassiter, R.R., 1988. Modeling bioconcentration of nonpolar organic pollutants by fish. Environ. Toxicol. Chem. 7 (7), 545–558. http://

dx.doi.org/10.1002/etc.5620070703.
Barron, M.G., 1990. Bioconcentration. Will water-borne organic chemicals accumulate in aquatic animals? Environ. Sci. Technol. 24 (11), 1612–1618. http://dx.doi.org/10.1021/es00081a001.
Bartram, A.E., Winter, M.J., Huggett, D.B., McCormack, P., Constantine, L.A., Hetheridge, M.J., Sumpter, J.P., 2012. In vivo and in vitro liver and gill EROD activity in rainbow trout (Oncorhynchus mykiss) exposed to the beta-blocker propranolol. Environ. Toxicol. 27 (10), 573–582.
Boillot, C., Martinez Bueno, M.J., Munaron, D., Le Dreau, M., Mathieu, O., David, A., Gomez, E., 2015. In vivo exposure of marine mussels to carbamazepine and 10-hydroxy-10,11-dihydro-carbamazepine: bioconcentration and metabolization. Sci. Total Environ. 532, 564–570. http://dx.doi.org/10.1016/j.scitotenv.2015.05.067.
Brown, J.N., Paxéus, N., Förlin, L., Larsson, D.G.J., 2007. Variations in bioconcentration of human pharmaceuticals from sewage effluents into fish blood plasma. Environ. Toxicol. Pharmacol. 24 (3), 267–274. http://dx.doi.org/10.1016/j.etap.2007.06.005.
Carter, L.J., Ashauer, R., Ryan, J.J., Boxall, A.B.A., 2014. Minimised bioconcentration tests: a useful tool for assessing chemical uptake into terrestrial and aquatic invertebrates? Environ. Sci. Technol. 48 (22), 13497–13503. http://dx.doi.org/10.1021/es5031992.
Celiz, M.D., Tso, J., Aga, D.S., 2009. Pharmaceutical metabolites in the environment: analytical challenges and ecological risks. Environ. Toxicol. Chem. 28 (12), 2473–2484. http://dx.doi.org/10.1897/09-173.1.
Chen, Y., Zhou, J.L., Cheng, L., Zheng, Y.Y., Xu, J., 2017. Sediment and salinity effects on the bioaccumulation of sulfamethoxazole in zebrafish (Danio rerio). Chemosphere 180, 467–475. http://dx.doi.org/10.1016/j.chemosphere.2017.04.055.
European Commission, 2006. Regulation (EC) No 1907/2006 of the european parliament and of the Council of 18 december 2006 concerning the registration, evaluation, authorisation and restriction of chemicals (REACH), establishing a european chemicals agency, amending directive 1999/45/EC and repealing Council regulation (EEC) No 793/93 and commission regulation (EC) No 1488/94 as well as Council directive 76/769/EEC and commission directives 91/155/EEC, 93/67/EEC, 93/105/EC and 2000/21/EC. Off. J. Eur. Union L 396, 1–520.
Cowan-Ellsberry, C.E., Dyer, S.D., Erhardt, S., Bernhard, M.J., Roe, A.L., Dowty, M.E., Weisbrod, A.V., 2008. Approach for extrapolating in vitro metabolism data to refine bioconcentration factor estimates. Chemosphere 70 (10), 1804–1817. http://dx.doi.org/10.1016/j.chemosphere.2007.08.030.
Crookes, M.J., Brooke, D.N., 2011. Estimation of Fish Bioconcentration Factor (BCF) from Depuration Data Bristol. Environment Agency. Retrieved from. http://publications.environment-agency.gov.uk.
de Wolf, W., de Bruijn, J.H.M., Seinen, W., Hermens, J.L.M., 1992. Influence of biotransformation on the relationship between bioconcentration factors and octanol-water partition coefficients. Environ. Sci. Technol. 26 (6), 1197–1201. http://dx.doi.org/10.1021/es50002a608.
Ding, J., Lu, G., Li, S., Nie, Y., Liu, J., 2015. Biological fate and effects of propranolol in an experimental aquatic food chain. Sci. Total Environ. 532, 31–39.
Ding, J., Lu, G., Liu, J., Yang, H., Li, Y., 2016. Uptake, depuration, and bioconcentration of two pharmaceuticals, roxithromycin and propranolol, in Daphnia magna. Ecotoxicol. Environ. Saf. 126, 85–93. http://dx.doi.org/10.1016/j.ecoenv.2015.12.020.
Fu, W., Franco, A., Trapp, S., 2009. Methods for estimating the bioconcentration factor of ionizable organic chemicals. Environ. Toxicol. Chem. 28 (7), 1372–1379. http://dx.doi.org/10.1897/08-233.1.
Garcia, S.N., Foster, M., Constantine, L.A., Huggett, D.B., 2012. Field and laboratory fish tissue accumulation of the anti-convulsant drug carbamazepine. Ecotoxicol. Environ. Saf. 84, 207–211. http://dx.doi.org/10.1016/j.ecoenv.2012.07.013.
Gobas, F.A., Opperhuizen, A., Hutzinger, O., 1986. Bioconcentration of hydrophobic chemicals in fish: relationship with membrane permeation. Environ. Toxicol. Chem. 5 (7), 637–646.
Golan, D.E., Tashjian, A.H., Armstrong, E.J., 2011. Principles of Pharmacology: the Pathophysiologic Basis of Drug Therapy. Lippincott Williams & Wilkins.
Gomez, C.F., Constantine, L., Huggett, D.B., 2010. The influence of gill and liver metabolism on the predicted bioconcentration of three pharmaceuticals in fish. Chemosphere 81 (10), 1189–1195. http://dx.doi.org/10.1016/j.chemosphere.2010.09.043.
Gomez, E., Bachelot, M., Boillot, C., Munaron, D., Chiron, S., Casellas, C., Fenet, H., 2012. Bioconcentration of two pharmaceuticals (benzodiazepines) and two personal care products (UV filters) in marine mussels (Mytilus galloprovincialis) under controlled laboratory conditions. Environ. Sci. Pollut. Res. 19 (7), 2561–2569. http://dx.doi.org/10.1007/s11356-012-0964-3.
Grabicova, K., Grabic, R., Blaha, M., Kumar, V., Cerveny, D., Fedorova, G., Randak, T., 2015. Presence of pharmaceuticals in benthic fauna living in a small stream affected by effluent from a municipal sewage treatment plant. Water Res. 72, 145–153.
Greenblatt, D.J., 1981. Clinical pharmacokinetics of oxazepam and lorazepam. Clin. Pharmacokinet. 6 (2), 89–105.
Hou, X., Shen, J., Zhang, S., Jiang, H., Coats, J.R., 2003. Bioconcentration and elimination of sulfamethazine and its main metabolite in sturgeon (Acipenser schrenkii). J. Agric. Food Chem. 51 (26), 7725–7729. http://dx.doi.org/10.1021/jf030492+.
Ikenaka, Y., Eun, H., Ishizaka, M., Miyabara, Y., 2006. Metabolism of pyrene by aquatic crustacean, Daphnia magna. Aquat. Toxicol. 80 (2), 158–165.
Ikenaka, Y., Ishizaka, M., Eun, H., Miyabara, Y., 2007. Glucose–sulfate conjugates as a new phase II metabolite formed by aquatic crustaceans. Biochem. Biophysical Res. Commun. 360 (2), 490–495. http://dx.doi.org/10.1016/j.bbrc.2007.06.086.
Inostroza, P.A., Wicht, A.-J., Huber, T., Nagy, C., Brack, W., Krauss, M., 2016. Body burden of pesticides and wastewater-derived pollutants on freshwater invertebrates: method development and application in the Danube River. Environ. Pollut. 214, 77–85.
Jeon, J., Kurth, D., Ashauer, R., Hollender, J., 2013a. Comparative toxicokinetics of organic micropollutants in freshwater crustaceans. Environ. Sci. Technol. 47 (15), 8809–8817.
Jeon, J., Kurth, D., Hollender, J., 2013b. Biotransformation pathways of biocides and pharmaceuticals in freshwater Crustaceans based on structure elucidation of metabolites using high resolution mass spectrometry. Chem. Res. Toxicol. 26 (3), 313–324. http://dx.doi.org/10.1021/tx300457f.
Kanazawa, J., 1981. Measurement of the bioconcentration factors of pesticides by freshwater fish and their correlation with physicochemical properties or acute toxicities. Pesticide Sci. 12 (4), 417–424. http://dx.doi.org/10.1002/ps.2780120408.
Klosterhaus, S.L., Grace, R., Hamilton, M.C., Yee, D., 2013. Method validation and reconnaissance of pharmaceuticals, personal care products, and alkylphenols in surface waters, sediments, and mussels in an urban estuary. Environ. Int. 54, 92–99. http://dx.doi.org/10.1016/j.envint.2013.01.009.
Kudriakova, T.B., Sirota, L.A., Rozova, G.I., Gorkov, V.A., 1992. Autoinduction and steady-state pharmacokinetics of carbamazepine and its major metabolites. Br. J. Clin. Pharmacol. 33 (6), 611–615. http://dx.doi.org/10.1111/j.1365-2125.1992.tb04089.x.
Kumar, G.N., Surapaneni, S., 2001. Role of drug metabolism in drug discovery and development. Med. Res. Rev. 21 (5), 397–411. http://dx.doi.org/10.1002/med.1016.
Livingstone, D.R., 1998. The fate of organic xenobiotics in aquatic ecosystems: quantitative and qualitative differences in biotransformation by invertebrates and fish. Comp. Biochem. Physiol. Part A: Mol. Integr. Physiol. 120 (1), 43–49. http://dx.doi.org/10.1016/S1095-6433(98)10008-9.
Mackay, D., Fraser, A., 2000. Bioaccumulation of persistent organic chemicals: mechanisms and models. Environ. Pollut. 110 (3), 375–391. http://dx.doi.org/10.1016/S0269-7491(00)00162-7.
Meredith-Williams, M., Carter, L.J., Fussell, R., Raffaelli, D., Ashauer, R., Boxall, A.B.A., 2012. Uptake and depuration of pharmaceuticals in aquatic invertebrates. Environ. Pollut. 165, 250–258. http://dx.doi.org/10.1016/j.envpol.2011.11.029.
Miller, T.H., McEneff, G.L., Brown, R.J., Owen, S.F., Bury, N.R., Barron, L.P., 2015. Pharmaceuticals in the freshwater invertebrate, Gammarus pulex, determined using pulverised liquid extraction, solid phase extraction and liquid chromatography–tandem mass spectrometry. Sci. Total Environ. 511, 153–160. http://dx.doi.org/10.1016/j.scitotenv.2014.12.034.
Miller, T.H., McEneff, G.L., Stott, L.C., Owen, S.F., Bury, N.R., Barron, L.P., 2016. Assessing the reliability of uptake and elimination kinetics modelling approaches for estimating bioconcentration factors in the freshwater invertebrate, Gammarus pulex. Sci. Total Environ. 547, 396–404. http://dx.doi.org/10.1016/j.scitotenv.2015.12.145.
Munro, K., Miller, T.H., Martins, C.P.B., Edge, A.M., Cowan, D.A., Barron, L.P., 2015. Artificial neural network modelling of pharmaceutical residue retention times in wastewater extracts using gradient liquid chromatography-high resolution mass spectrometry data. J. Chromatogr. A 1396, 34–44. http://dx.doi.org/10.1016/j.chroma.2015.03.063.
Neely, W.B., Branson, D.R., Blau, G.E., 1974. Partition coefficient to measure bioconcentration potential of organic chemicals in fish. Environ. Sci. Technol. 8 (13), 1113–1115. http://dx.doi.org/10.1021/es60098a008.
Nichols, J.W., Du, B., Berninger, J.P., Connors, K.A., Chambliss, C.K., Erickson, R.J., Brooks, B.W., 2015. Observed and modeled effects of pH on bioconcentration of diphenhydramine, a weakly basic pharmaceutical, in fathead minnows. Environ. Toxicol. Chem. 34 (6), 1425–1435.
Nichols, J.W., Huggett, D.B., Arnot, J.A., Fitzsimmons, P.N., Cowan-Ellsberry, C.E., 2013. Toward improved models for predicting bioconcentration of well-metabolized compounds by rainbow trout using measured rates of in vitro intrinsic clearance. Environ. Toxicol. Chem. 32 (7), 1611–1622. http://dx.doi.org/10.1002/etc.2219.
Nichols, J.W., Schultz, I.R., Fitzsimmons, P.N., 2006. In vitro–in vivo extrapolation of quantitative hepatic biotransformation data for fish: I. A review of methods, and strategies for incorporating intrinsic clearance estimates into chemical kinetic models. Aquat. Toxicol. 78 (1), 74–90. http://dx.doi.org/10.1016/j.aquatox.2006.01.017.
OECD. Test No. 305: Bioaccumulation in Fish: Aqueous and Dietary Exposure: OECD Publishing.
Oliver, B.G., Niimi, A.J., 1985. Bioconcentration factors of some halogenated organics for rainbow trout: limitations in their use for prediction of environmental residues. Environ. Sci. Technol. 19 (9), 842–849. http://dx.doi.org/10.1021/es00139a013.
Opperhuizen, A., Sijm, D.T.H.M., 1990. Bioaccumulation and biotransformation of polychlorinated dibenzo-p-dioxins and dibenzofurans in fish. Environ. Toxicol. Chem. 9 (2), 175–186. http://dx.doi.org/10.1002/etc.5620090207.
Overturf, C.L., Overturf, M.D., Huggett, D.B., 2016. Bioconcentration and endocrine disruption effects of diazepam in channel catfish, Ictalurus punctatus. Comp. Biochem. Physiol. Part C Toxicol. Pharmacol. 183–184, 46–52. http://dx.doi.org/10.1016/j.cbpc.2016.02.001.
Paterson, G., Metcalfe, C.D., 2008. Uptake and depuration of the anti-depressant fluoxetine by the Japanese medaka (Oryzias latipes). Chemosphere 74 (1), 125–130. http://dx.doi.org/10.1016/j.chemosphere.2008.08.022.

Pritchard, J.F., Schneck, D.W., Hayes, A.H., 1979. Determination of propranolol and six metabolites in human urine by high-pressure liquid chromatography. J. Chromatogr. B Biomed. Sci. Appl. 162 (1), 47–58. http://dx.doi.org/10.1016/S0378-4347(00)82062-9.

Rösch, A., Anliker, S., Hollender, J., 2016. How biotransformation influences toxicokinetics of azole fungicides in the aquatic invertebrate Gammarus pulex. Environ. Sci. Technol. 50 (13), 7175–7188. http://dx.doi.org/10.1021/acs.est.6b01301.

Snyder, M.J., 2000. Cytochrome P450 enzymes in aquatic invertebrates: recent advances and future directions. Aquat. Toxicol. 48 (4), 529–547. http://dx.doi.org/10.1016/S0166-445X(00)00085-0.

Sordet, M., Berlioz-Barbier, A., Buleté, A., Garric, J., Vulliet, E., 2016. Quantification of emerging micropollutants in an amphipod crustacean by nanoliquid chromatography coupled to mass spectrometry using multiple reaction monitoring cubed mode. J. Chromatogr. A 1456, 217–225.

Spacie, A., Hamelink, J.L., 1982. Alternative models for describing the bioconcentration of organics in fish. Environ. Toxicol. Chem. 1 (4), 309–320.

Springer, T.A., Guiney, P.D., Krueger, H.O., Jaber, M.J., 2008. Assessment of an approach to estimating aquatic bioconcentration factors using reduced sampling. Environ. Toxicol. Chem. 27 (11), 2271–2280. http://dx.doi.org/10.1897/07-514.1.

Stokvis, E., Rosing, H., Beijnen, J.H., 2005. Stable isotopically labeled internal standards in quantitative bioanalysis using liquid chromatography/mass spectrometry: necessity or not? Rapid Commun. Mass Spectrom. 19 (3), 401–407. http://dx.doi.org/10.1002/rcm.1790.

Stott, L.C., Schnell, S., Hogstrand, C., Owen, S.F., Bury, N.R., 2015. A primary fish gill cell culture model to assess pharmaceutical uptake and efflux: evidence for passive and facilitated transport. Aquat. Toxicol. 159, 127–137. http://dx.doi.org/10.1016/j.aquatox.2014.12.007.

Umezawa, H., Lee, X.-P., Arima, Y., Hasegawa, C., Marumo, A., Kumazawa, T., Sato, K., 2008. Determination of diazepam and its metabolites in human urine by liquid chromatography/tandem mass spectrometry using a hydrophilic polymer column. Rapid Commun. Mass Spectrom. 22 (15), 2333–2341. http://dx.doi.org/10.1002/rcm.3613.

Veith, G.D., DeFoe, D.L., Bergstedt, B.V., 1979. Measuring and estimating the bioconcentration factor of chemicals in fish. J. Fish. Board Can. 36 (9), 1040–1048.

Walle, T., Gaffney, T.E., 1972. Propranolol metabolism in man and dog: mass spectrometric identification of six new metabolites. J. Pharmacol. Exp. Ther. 182 (1), 83–92.

Wu, X., Ernst, F., Conkle, J.L., Gan, J., 2013. Comparative uptake and translocation of pharmaceutical and personal care products (PPCPs) by common vegetables. Environ. Int. 60, 15–22. http://dx.doi.org/10.1016/j.envint.2013.07.015.